Synthesis of fused heterocyclic aromatic compounds as potential antiplasmodial agents

by
Leon Jacobs

Dissertation presented for the degree of
Doctor of Philosophy in Chemistry
in the
Faculty of Science at
Stellenbosch University

Supervisor: Dr M.A.L. Blackie

Co-supervisor: Dr S.C. Pelly

December 2017

Declaration

By submitting this thesis/dissertation electronically, I declare that the entirety of the work contained therein is my own, original work, that I am the sole author thereof (save to the extent explicitly otherwise stated), that reproduction and publication thereof by Stellenbosch University will not infringe any third party rights and that I have not previously in its entirety or in part submitted it for obtaining any qualification.

Date: December 2017

Summary

3-Methyl benzofuran antiplasmodial compounds have been described in literature and and synthesis of heterocyclic derivatives forms the basis of this project. These benzofuran compounds were synthesized with the primary role as effective inhibitors of the enzyme *Plasmodium falciparum N*-Myristoyl transferase (PfNMT). PfNMT plays an important enzymatic function in the majority of all living organisms, facilitating the myristoylation of *N*-terminal glycine residues of proteins that serve many functions *in vivo*, and is considered vital to the viability of not only most organisms, but *P. falciparum* too. The rationale behind the key features of these antiplasmodial compounds include the heterocyclic scaffold that induces π – π stacking with amino acid residues at the active site of PfNMT, aromatic amide and ester groups also necessary for π – π stacking and a piperidinium salt coupled to the heterocycle, providing a salt-bridge interaction with neighboring amino acid residues.

Five different heterocycles were synthesized with the primary function of replacing the benzofuran moiety in order to ascertain which heterocyclic system is the most efficacious. We synthesized indole, 3-methyl indole, 1-methyl benzimidazole, benzoxazole and benzothiophene scaffolds, each containing an ester group at the C2-position necessary for transesterification and amidation reactions, as well as a phenolic group at the C4-position (C7-position for the benzimidazole scaffold) required for the introduction of a piperidine group. The Boc-protected piperidine group was introduced first, followed by esterification reactions with 2-phenylethanol, benzyl alcohol and 1-naphthalenemethanol. Amidation reactions were also carried out with 2-phenethylamine, benzylamine, 1-naphthylmethylamine and 4-(aminomethyl)pyridine. The synthesis of each series of heterocyclic antiplasmodials was realized after the final Boc-deprotection step, providing all the compounds in salt form.

These compounds were sent for whole-cell testing against a *P. falciparum* chloroquine sensitive strain (NF54) with the intention to prove which heterocycle and aromatic ester or amide substituent improves the efficacy the most, and validate the importance of a methyl group on the 3-methyl indole and 1-methyl benzimidazole scaffold when comparing the efficacy of analogous esters and amides.

The results indicated that the benzoxazole series of compounds were inactive and the 3-methyl indole series are the most active which returned IC_{50} values of 0.56 – 6.1 µM respectively, but is trailed closely in efficacy by the indole (IC_{50} values of 0.83 – 6.5 µM) and benzothiophene (IC_{50} values of 0.71 – 5.9 µM) series of compounds. The 1-methyl benzimidazole series of compounds were the least active with IC_{50} values between 7.4 – 13.3 µM apart from one compound indicating an IC_{50} value of 1.1 µM.

Opsomming

‘n Versameling van 3-metiel bensofuraan verbindings was ontdek na ‘n literatuur studie uitegrig is, en vorm deel van die doel van die projek wat insluit die sintese van alternatiewe analogiese heterosiekliese verbindinge wat struktureel eenders as die bensofuraan kern molekuul. Die oorpronklike bensofuraan verbindings was gesintetiseer met die doel om ‘n ensiem, *Plasmodium falciparum N*-myristoïel transferase (PfNMT) te inhibeer. Die funksie van PfNMT is beskou as belangrik en noodsaaklik vir die lewensvatbaarheid van die meerderheid van lewendige organismes, asook vir die parasiet *Plasmodium*. Die rol van PfNMT sluit in die miristoïelasie van *N*-terminale glisien aminosuur residue en is beskoou as ‘n goeie teiken vir ensiem inhibisie.

Die chemiese redes agter die ontwerp van die vebindings wat gebaseer is op die bensofuraan reeks sluit in die aanwesigheid van die heterosiekliese kern molekuul wat π – π interaksies het met die naasliggende aminosuur residue in die aktiewe setel, die armoatiese ester en amied in C2-posisie wat ook π – π interaksies toon met naasliggende aminosuur residue, en laastens ‘n piperidinium groep wat ‘n sout-brig interaksie vorm met aminosuur residue in die aktiewe setel.

Vyf verskillende heteroskikliese verbindings was gesintetiseer wat isostrutureel is met die oorspronklike bensofuraan kern, indool, 3-metiel indool, 1-metiel bensimidasool, bensoksasool asook bensotiofaan. Elke heterosikliese verbinding het n ester groep op die C2-posisie, met die doel om transesterifikasie en amidasie reaksies uit te rig, asook ‘n suurstof atoom by die C4-posisie (C7-posisie op die bensimidasool) wat onderandere gebruik was vir die koppeling met die verkose piperidien groep.

Die verbinding van die piperidien groep aan die vyf heterosikliese verbindings was eerste uit gevoer, en gevolg deur die transesterifikasie reaksies met 2-fenieletanol, bensiel alkohol and 1-naftaleenmetanol. Amidasie reaksies was uitevoer met 2-fenieletielamien, bensielamien, 1-naftaleenmetielamien and 4-(aminometiel)piridien. Die finale verbindings van elke heterosikliese reeks was bereik deur middel van ‘n Boc-verwydering op die piperidien groep, wat elke molekuul in soutform los.

Die vyf reekse molekules was ingestuur om getoets te word vir aktiwiteit teenoor n chloroquine sensitiewe stam van *Plasmodium falciparum* (NF54) om te kan onderskei wat se reeks is die mees aktiefste, asook om te onderskei waste aromatiese ester of amied lei na beter aktiwiteit, en laaste, om potensieel te kan bewys dat die metiel groepe aanwesig in die 3-metiel indool en 1-metiel bensimidasool is inderdaad nodig om a verskil in aktiwiteit te toon as analogiese esters en amiede met mekaar vergekyk word.

Die resulate het aangetoon dat die bensoksasool reeks van verbindings was onaktief gewees, waarby die 3-metiel indool reeks die mees aktiefste was deur dat dit aktiwiteite tussen 0.56 – 6.1 µM vertoon het. Naaste aan die aktiwiteit van die 3-metiel indool reeks was die indool reeks (IC_{50} waardes tussen 0.83 – 6.5 µM) en die bensotiofaan (IC_{50} waardes tussen 0.71 – 5.9 µM). Die 1-metiel bensimidasool reeks het die laagste aktiwitiet betoon met IC_{50} waardes tussen 0.71 – 5.9 µM behlawe vir een verbinding wat wel n hoe aktiwiteit betoon het van 1.1 µM.

Acknowledgements

A PhD degree is a project that cannot be taken lightly and requires dedication, hard work, many hours in the lab and sacrifice. It is filled with ups and downs, good and bad results, but due to this project, one major contribution to my life was made: I learned a lot. And for that I want to thank Stellenbosch University and all the lecturers involved in my undergraduate and honours degrees that taught me chemistry. Without a good chemical foundation, postgrad would have been much tougher. But I never learned as much as I did in my postgraduate life.

Therefore, I want to thank Dr. Margaret Blackie who took me in as her student in 2010. Thank you for all the effort you have put in through the years regarding the research I had to carry out. I also want to thank you for letting me have a large degree of freedom when it comes to synthetic routes I want to pursue, even though some of them did not work out! The freedom to pursue different routes and to synthesize different unplanned compounds were always welcomed and supported by you and in doing so, became the catalyst for me to learn a lot about chemistry and realize what I can achieve in the lab.

I want to thank my co-supervisor, Dr. Steve Pelly, for also helping me a lot with technical synthetic difficulties, the molecular modeling and also giving me motivation with my project when I was experiencing some slow progress. It was most welcomed. Thank you for the group get-togethers at Craft and Hudson's we had, it was fun and really relaxing. Beer relaxes me and you know this!

A major contributor to the chemistry knowledge that I have obtained during the past four years of my PhD, and the years before that, was Dr. Gareth Arnott. Thank you for all the research advice and the help you provided with solving problems that seemed difficult at the time until you tackled them. You were always a dependable source of chemistry knowledge and helped me till the end of my project, even though I was not you student.

To Prof. Willem van Otterlo, thank you for listening to my quick questions I have regarding synthesis and problems I have, even though you are a busy man and always on the go somewhere else! Thank you for your contribution to my thesis and the valuable suggestions I received from you.

I also want to thank the people in the GOMOC group for help whenever it was needed and to each individual who played their part in keeping the group run smoothly.

The best years of my university career were during my postgraduate life and it was made fun by all my wonderful friends. I can't name them all, but I have to particularly say thank you to Derik and Luke, for all the good times. And we truly had many good times.

If there is one person that I need to thank the most, it would have to be my smart, beautiful and lovely girlfriend Nicole. The support I received from you during the last two years of my project was just phenomenal. I can't imagine how difficult the last two years would have been for me without your love and input. Apart from being my wonderful liefie, you are also an amazing organic chemist who I could always come to talk to regarding work when times are tough, but even better when times are wonderful, always having a celebratory attitude towards my success. Now I can finally stop constantly talking about work and writing up! You are my best friend and my partner in crime. I love you.

My family played an indescribable roll in my postgraduate life. To my father and mother, thank you for giving me the opportunity to study and supporting me throughout everything that has happened since day one. Thank you for the faith you had in me, but also for the hard talks we had every now and then, helping me to realign my priorities and perspectives. I love you and only wish to make you proud.

Additional acknowledgements,

1. Stellenbosch University,
2. Elsa Malherbe and Dr. Jaco Brand and for assistance with the NMR analysis. Thank you for the time, effort and help whenever I needed it, as well as all the interesting discussions!
3. Dr. Vincent Smith, Monica Clements and Dawie de Villers, Supramolecular group, Stellenbosch, for their help with obtaining crystal structures.
4. Sunel de Kock and Bernard Dippenaar for the ESP calculations.
5. CAF for the HRMS analysis.
6. Dr. Dale Taylor and Carmen de Kock at the University of Cape Town, Pharmacology Department, for whole cell testing.
7. National Research Foundation and the Harry Crossley Foundation for funding.

I am truly going to miss the Stellenbosch life.

List of Abbreviations

ITN – insecticide-treated bed nets

QN – quinine

CQ – chloroquine

MQ – mefloquine

AQ – amodiaquine

CQS – chloroquine sensitive strain

ACTs – artemisinin-combination therapies

LU – lumefantrine

PfNMT – *Plasmodium falciparum N*-myristoyl transferase

PvNMT – *Plasmodium vivax N*-myristoyl transferase

HsNMT1 – Human type-I *N*-myristoyltransferase

HsNMT2 – Human type-2 *N*-myristoyltransferase

EC_{50} – Half maximal effective concentration

IC_{50} – Half maximal inhibitory concentration

IH – code for indole final compounds

IM – code for 3-methyl indole final compounds

BI – code for 1-methyl benzimidazole final compounds

BO – code for benzoxazole final compounds

BT – code for benzothiophene final compounds

ETFA – ethyl trifluoroacetate

TLC – thin layer chromatography

NMR- nuclear magnetic resonance

CDI – carbonyl diimidazole

Pd/C – palladium on carbon

DEAD – diethyl azodicarboxylate

DIAD – diisopropyl azodicarboxylate

DBAD – di-*tert*-butyl azodicarboxylate

ADDM – azodicarbonyldimorpholide

PPh_3 – triphenyl phosphine

Boc_2O – di-*tert*-butyl dicarbonate

COSY – correlated spectroscopy

HSQC – Heteronuclear Single Quantum Coherence Spectroscopy

HMBC – Heteronuclear Multiple Bond Correlation

NOESY – Nuclear Overhauser Effect Spectroscopy

HRMS – High Resolution Mass Spectrometry

LiTMP – lithium tetramethylpiperidine

*p*TsOH – tosylic acid

TFA – trifluoroacetic acid

ESP – electrostatic potential

DFT – density functional theory

Chapter 1

1.1 Introduction

The starting point for this project was the desire to synthesize novel compounds as potential antiplasmodial agents. This thesis describes the development of the concept and the process of designing the proposed series of compounds, the various methods utilized to synthesize each series of compounds, as well as the rational explanation of the efficacy of each compound within each series. The results from the biological testing will in turn provide us with possible structure-activity relationships - valuable information used in the search for novel antimalarial agents.

1.2 History of malaria

The earliest record describing the symptoms related to malaria dates back to 2700 BC, documented in the NeiChing, an ancient Chinese medical text.[1] Throughout history many civilizations have documented the devastating effects of the disease i.e. the Mesopotamians (2000 BC), Egyptians (1570 BC) and Indians describing it in their Hindu texts (600 BC).[2] The infection rate of the disease increased proportionate to the higher rate of human settlements being established, in conjunction with the progression of agricultural technology.[3] The disease is attributed to the great loss of life to the troops of the Roman Empire, playing a significant role in the decline of the Empire itself.[4] The disease has been referred to as “marsh fever” through its connection to swamps and marshes. The origin of the word malaria comes from the Italian word “*mala aria*” which directly translates to “bad air”.[5]

Historically, it was described as one of the most deadly diseases to humans and postulated to have been the cause of death of half of all the people who have ever lived.[6] Research conducted by Louis Pasteur and Robert Koch resulted in the development of the germ theory of infection, which increased the desire and the need to discover the cause for malaria.[7] This ultimately led to the discovery of the existence of the parasite by the French physician Charles Louis Alphonse Laveran in 1880 while stationed in Algeria.[8] The Italian physician Giovanni Battista Grassi conducted extensive research in the field of malariology. He discovered that the parasite responsible for human malaria is only transmitted by the female *Anopheles* mosquito.[2] The parasite resides in the saliva of the female *Anopheles* mosquito - the transmission vector. Thus,

infection is caused when the mosquito has a blood meal causing the parasite to be released into the bloodstream.[9]

The disease is caused by the parasite belonging to the genus *Plasmodium*, of which the species *Plasmodium falciparum* is the most dangerous regarding human infection and mortality rates.[10] There are three other species of *Plasmodium* which are well known to cause human malaria: *P. ovale, P, malariae and P. vivax*. For the most part, malaria infections from these parasites are not as common as *P. falciparum* infections and less dangerous.[10] *P. knowlesi* is a species found in pig-tailed and long-tailed macaques, however, in Sarawak, Malaysian Borneo, a large human infection rate was reported in 2004, thus *P. knowlesi* is now considered the fifth *Plasmodium* species that causes human malaria.[11]

1.3 Worldwide risk and prevention

According to the Center of Disease Control and Prevention USA, approximately 3.2 billion people are living in areas where they are at risk of contracting malaria, most of whom live in developing countries that are situated in Sub-Saharan Africa, South America and Asia.[8] The 2016 WHO world malaria report indicates that in 2015 there were an estimated 212 million cases of malaria infection, of which 90% were living in the WHO African region and 114 million in Sub-Saharan Africa.[12] It is estimated that between 429 000 and 438 000 people died of malaria in 2015, of which 99% of deaths were due to *P. falciparum* infection.[12] Children under the age of five account for roughly 306 000 malaria deaths in 2015, which is approximately 70% of the global fatalities for malarial infection, making it the second biggest killer of this age group after pneumonia.[13] The disease has a devastating effect on the heath and development of a foetus in the womb, which facilitate the onset of placental parasitaemia and maternal anaemia. These health factors contribute to low birth weight in infants, which in turn contributes to infant mortality.[8,12]

Since 2000 a global effort has been launched to combat malaria infection and deaths.[14] The use of insecticide-treated nets (ITN) as well as artemisinin combination therapy (ACT) has had a major impact on reducing infection rates, as the amount of people sleeping under ITN's have increased from 37% in 2010 to 57% in 2015, of which 53% reside in sub-Saharan Africa.[12] Between 2000 and 2015 it was calculated that there has been a tremendous decrease in incident and death rate worldwide, as there has been a 42% decline in incidents and a 66% decline in deaths in Africa.[12] This is illustrated in **Figure 1**.

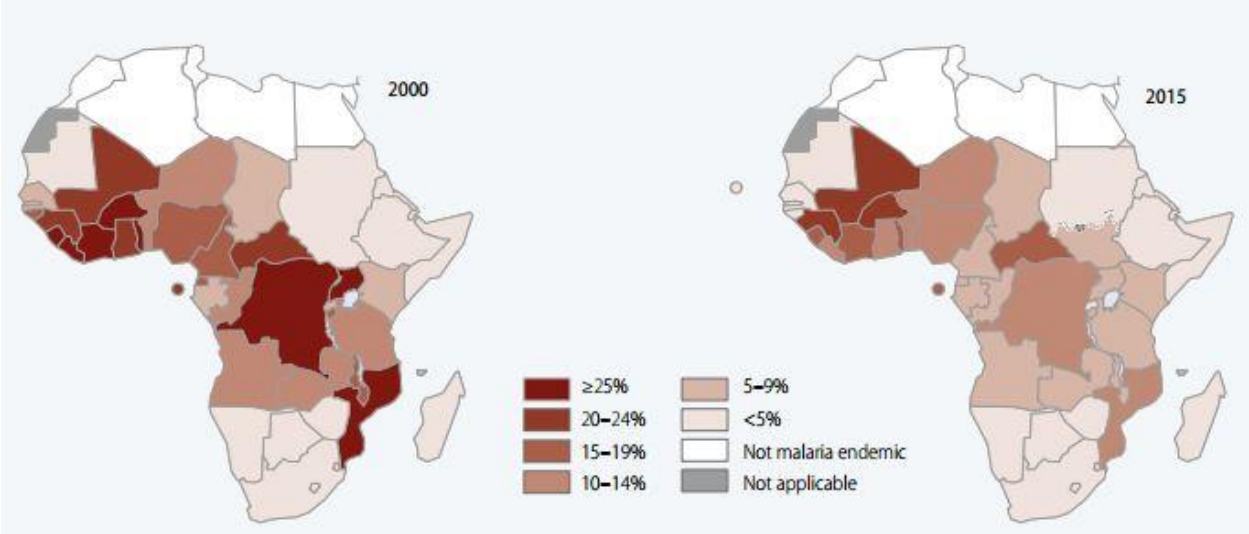

Figure 1: Comparative maps of malaria deaths of children under five between 2000 and 2015[15]

1.4 Life cycle of the parasite

The parasite requires two hosts in order to survive, the mosquito which is the primary host and humans which are the secondary host. The life cycle of the parasite has multiple stages that can only be achieved inside the human body. **Figure 2** illustrates the life cycle of the parasite inside the human host. Infection occurs when an infected female *Anopheles* mosquito has a blood meal, which results in the injection of sporozoites into the bloodstream. The sporozoites travel to the liver via the bloodstream and then invade the liver cells or hepatocytes. The sporozoites continue to multiply inside the hepatocytes, which is known as the pre-erythrocytic development phase.[16] This is a silent infectious phase that is asymptomatic, lasting between 6 – 8 days for *P. falciparum*.[16] The exoerythrocytic merozoites are then released from the hepatocytes into the bloodstream, which subsequently invade the erythrocytes and begin to multiply asexually. This is known as the blood stage of the parasite life cycle. Due to the rapid asexual multiplication of merozoites inside erythrocytes, the erythrocytes become ridged and prone to adhere to a variety of different cell types. The sudden change in the red blood cell structure and loss of primary function induces symptoms like fever, lactic acidosis, coma and death.[17]

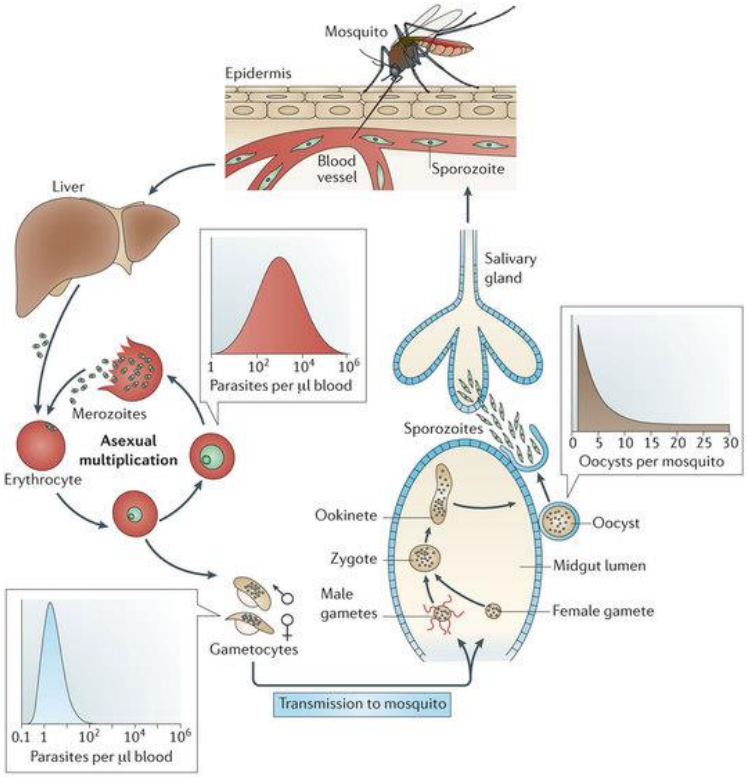

Figure 2: Life cycle of the *Plasmodium* parasite[16]

A small percentage of the merozoites transform into sexual gametocytes. This is the only form of the parasite that can achieve successful and sustainable transmission from humans to mosquito (ingestion of sporozoites by the mosquito results in the death of the sporozoites in the mosquito gut).[18] Immature gametocytes have five stages of maturation, stage I to stage V, of which the immature stages II to IV are sequestered in the spleen and bone marrow for maturation, which lasts for 10 – 12 days.[19] Only mature gametocytes (stage V) are released in the bloodstream with an average circulation time of 3 – 6 days which allows for transmission to occur.[16] Due to the fact that most antimalarials target the asexual stages of the parasite life cycle - and have no effect on the transmissible stages - this is an important field of research.[18] Upon ingestion of the gametocytes into the gut of the mosquito, each gametocyte develops into either a single female macrogamete or multiple male microgametes (up to eight male microgametes). This is the start of the sexual reproduction stage called sporogony and lasts between 9 – 10 days. The fusion of the female and male gametes results in the formation of a zygote. Zygotes then develop into motile ookinetes which have the ability to penetrate the midgut wall of the mosquito, forming oocysts. The enlargement of the oocysts results in the rupture of the oocysts after 8 – 15 days releasing sporozoites which migrate to the salivary gland of the mosquito. During the infected

mosquito's subsequent blood meal, sporozoites are released into the bloodstream which results in the renewal of the life cycle.[16]

The most common symptom induced due to infection is paroxysm, which entails the onset of sudden coldness and shivering followed by an intense fever and sweating, occurring in a two day cycle.[20] Malaria is classified as an acute febrile illness, meaning that it is a disease that induces a sudden onset of fever. The activation of the immune response by the cytokine cascade is what causes the symptoms of malaria infection. Malaria infection can be divided into two categories, uncomplicated and complicated malaria.[20] The difference between uncomplicated and complicated malaria is due to the immune response of the infected person. The general symptoms of fever and sweating followed by shivering and coldness, vomiting, headaches and anaemia can all be attributed to uncomplicated malaria. Complicated malaria usually is attributed to an infected person who has an immunity that is compromised or absent (non-immune subjects), such as people who have HIV/AIDS. Symptoms of infection are usually related to the pulmonary, renal, central nervous and haematopoietic systems, which can lead to respiratory and acute renal failure, cerebral malaria and severe anaemia.[20]

1.5 Treatment of malaria

The first documented treatment for malaria spans back to the end of the Middle Ages where Spanish missionaries in Peru discovered that the native Peruvians treated severe fevers with Peruvian bark, bark originating from multiple trees that belongs to the genus *Chinchona*.[21] Exporting Peruvian bark became a lucrative market, but due to adulteration issues and problems faced with quality control, it was necessary to isolate the active ingredient as this would increase the efficacy of treatments. Two French chemists, Pierre Joseph Pelletier and Jean Bienaime Caventou, managed to isolate the active ingredient, an alkaloid which they named quinine, shown in **Figure 3**.[21] Within a year, French physicians were using quinine for the treatment of malaria.[22]

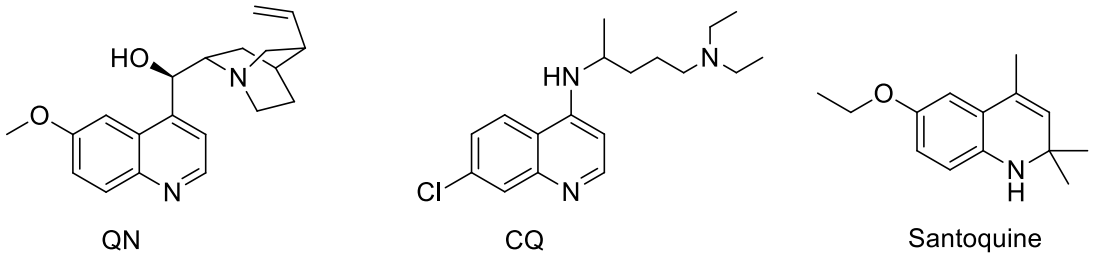

Figure 3: Structure of quinine (QN), chloroquine (CQ) and santoquine

The Second World War initiated the development of alternative antimalarials by the Americans as the supply of quinine was cut off by the Japanese as a result of their invasion of Java.[21] This resulted in the development and clinical trials of various derivatives of santoquine (**Figure 3**), an antimalarial developed by German chemists. The compound that indicated the most promise was called chloroquine (CQ, **Figure 3**), displaying great efficacy, few side effects and an easy synthetic method.[23] In 1947 CQ was introduced into clinical practice and became the most widespread antimalarial drug. Due to mass drug administrations of monotherapeutic CQ and the inevitable lack of patient compliance, the onset of *P. falciparum* CQ resistance was documented in the late 1950's in Colombia and at the Cambodia-Thailand border.[24] CQ resistance is prominent in *P. falciparum* and *P. vivax* treatment, and has spread to most of the areas in the world where *P. falciparum* infections are frequent.[8] Resistance to CQ is attributed to polymorphisms of the *Plasmodium falciparum* chloroquine resistance transporter (*pfcrt*) gene, and evidence suggests that polymorphism of the *P. falciparum* multidrug resistance 1 (*pfmdr1*) gene is also linked to resistance.[25] Polymorphism is defined as the condition or quality of being polymorphic, i.e. a mutation had occurred and the result is a difference in polymorphic genes.[26] CQ resistance is defined as the reduced accumulation of active drug molecules at a high affinity target. *Plasmodium falciparum* chloroquine resistance transporter protein (PfCRT) is a transporter protein that is embedded in the membrane of the digestive food vacuole of the parasite which actively pumps quinoline based drugs like CQ and amodiaquine (AQ) out of the digestive food vacuole.[27,28] *P. falciparum* multidrug resistance protein 1 (PfMDR1) forms part of a superfamily of ATP-binding cassette transporters and has the ability to transport various substrates across membranes. The ability of PfMDR1 to transport xenobiotic substrates (foreign chemicals substances) across membranes gave rise to the drug resistance towards mefloquine (MQ) and lumefantrine (LU).[27] In comparison to QN, drugs like CQ, AQ, MQ and LU (**Figure 4**) are all antimalarials with the same mechanism of action. These drugs inhibit the process of haemozoin biomineralization, a haem detoxification process necessary for the viability of the parasite.[29]

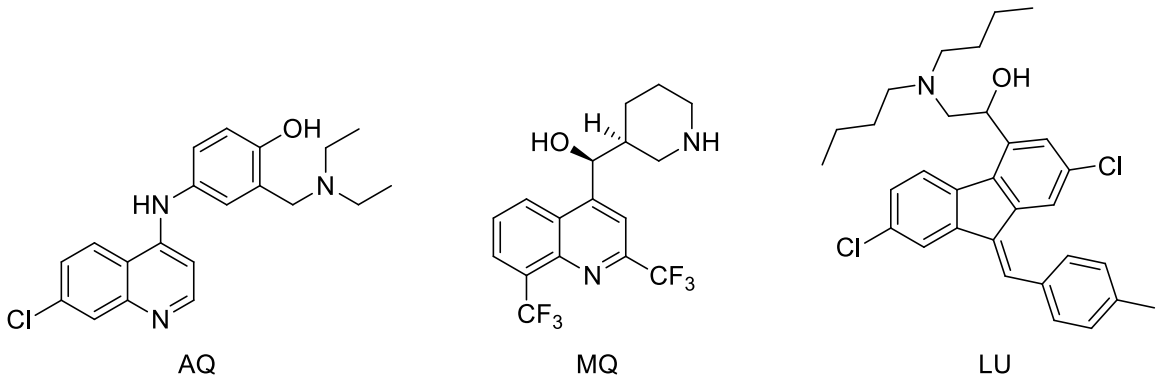

Figure 4: Molecular structures of AQ, MQ and LU

In the same way that Peruvians used Peruvian bark as their method to treat malaria, so did the Chinese use the leaves of the sweet wormwood tree to cure malaria, documented to be in use from as early as 1596 AD.[30] The active ingredient in the sweet wormwood leaves was identified in the early 1970's by Tu Youyou, and was called artemisinin.[31] Artemisinin proved a potent antimalarial, but was also found to be unstable *in vivo*. Hence two derivates were synthesized that possessed better stability - artemether which is a methyl ether derivative and artesunate which is water soluble.[31] (**Figure 5**)

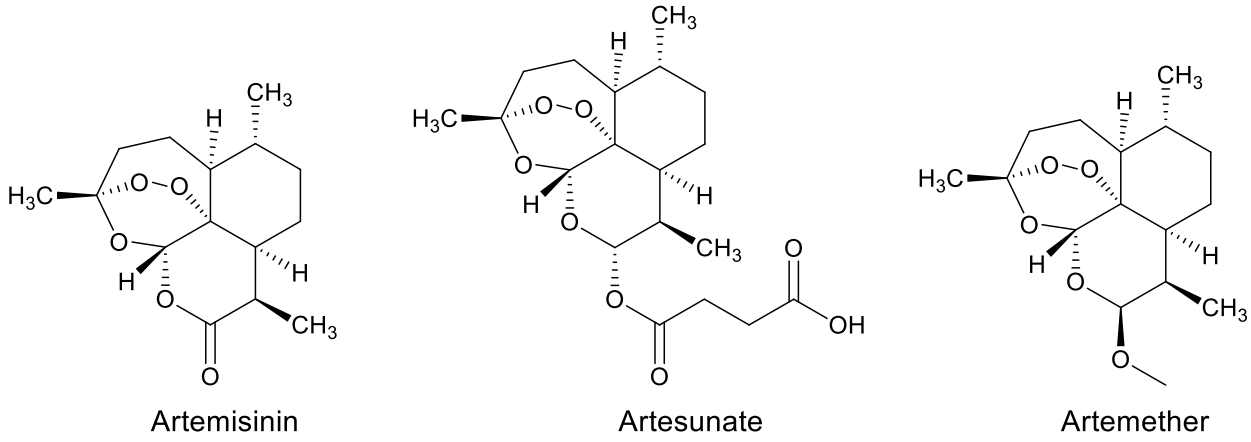

Figure 5: Molecular structures of artemisinin, artesunate and artemether

In order to combat the emerging onset of resistance, artemisinin-based combination therapies (ACTs) were implemented. The use of ACTs has been proven to be an effective method of treatment against uncomplicated malaria of all species. It has been endorsed by the World Health Organization (WHO) as the recommended treatment for malaria,[32] and as such has been implemented worldwide as the standard antimalarial treatment. The use of ACTs has the benefit that it decreases the probability of the onset of drug resistance as the different antimalarial drugs

used in ACTs have different modes of action in the parasite.[33] It is believed that the peroxide bridge present in artemisinin and the respective derivatives play a key role in its efficacy, as structurally similar compounds that do not contain a peroxide bride exhibited no antimalarial activity.[34] Although the true mechanism of action of artemisinin is still contested, it has been found that it selectively targets the mitochondria of *P. berghei* due to its effect on the reduction of membrane potential across the mitochondrial membrane.[34]

Resistance to artemisinin in *P.falciparum* due to monotherapy has been discovered and is prevalent across mainland South-East Asia.[35] Research has indicated that polymorphism in the kelch domain–carrying protein K13 is indicative of delayed parasite clearance and thus is associated with resistance.[36,37] This is cause for concern as delayed parasite clearance implies that medication is administered over an increased time period, lengthening the time period that the ACT partner drug is in contact with the parasite. This in turn could lead to drug resistance to the partner drug.[37]

1.6 Alternative enzymatic targets

Although ACTs are still effective in the majority of cases - provided that no drug resistance to the partner drug exists in the geographical area that the ACTs are administered - the notion of artemisinin resistance becoming prevalent is alarming. The preferential use of ACT over monotherapy is, however, a significant improvement to the way that malaria is being treated. As previously stated, this is due to more than one target being essential to the viability of the parasite. The search for new targets and potential antimalarial chemotherapeutic agents is essential, as new antimalarial drugs would delay the onset of resistance. Drug resistance is also increased due to the emergence of cross resistance. Resistance towards a certain drug i.e. CQ also results in resistance forming towards other drugs that have the same pharmacophore or belongs to the same chemical family. This is known as cross resistance. Examples include amodiaquine and/or quinine and/or mefloquine, which share the same mode of action.[38] The incorporation of pharmacophores and moieties that are known to cause resistance must be altered or completely changed, or different biological targets or processes of *Plasmodium* have to be targeted with novel chemotherapeutic antimalarials. Under current legislation any novel therapy would have to be incorporated in combination with a second therapeutic agent to be registered and approved as a malaria therapy. Our project would focus on this issue by identifying a druggable target that does not possess any resistance, as this is part of the solution to combat the emergence of resistance.

Research conducted by G.J. Crowther *et al*.[39] have tested the antiplasmodial activity of a large number of non-propriety compounds developed by The Genomics Institute of the Novartis Research Foundation (GNF). They identified a subset of 5655 compounds that displayed potent activity against drug resistant strains of *P. falciparum* (W2 and 3D7 strains) and retained those compounds that indicated an EC_{50} value of <1.25 µM.

Table 1: Selection of promising drug targets for biochemical screens[39]

Enzyme name (PlasmoDB ID)	**Essentiality**	**Druggability score**
Adenylosuccinate synthase (PF13 0287)	Part of purine salvage pathway, which should be essential because *Plasmodium* cannot synthesize purines *de novo*.[40]	0.8
Choline kinase (PF14 0020)	Chemical validation of the Kennedy pathway for phosphatidyl-choline synthesis is suggested by the work of Henri Vial.[41]	0.6
dUTPase (PF11 0282)	dUTPase is most likely essential because it prevents the buildup of dUTP and makes dUMP for dTTP synthesis.[42]	0.6
Farnesyl pyrophosphate synthase (PVX 092040)	Since protein farnesyl transferase is a valid drug target in *Plasmodium*, FPPS should be as well because it supplies the substrate for PFT. A recent paper reported an ability to predict cell-killing activity from bisphosphonates' inhibition of FPPS.[43]	0.8
Glutamate dehydrogenase (PF14 0164)	Thought to be a major source of NADPH for glutathione reductase, which is thought to be essential.[44] This is based in part on the fact that *Plasmodium* is "exposed to multiple oxidative stress due to its high metabolicrate, the degradation of heme and reactive oxygen species imposed by the host immune system".[45]	0.8
Guanylate kinase (PVX 099895)	Based on metabolic maps, guanylate kinase appeared to be the only route by which *Plasmodium* can convert GMP to GDP or dGMP to dGDP. (A possible bypass is noted in the text.) Also, expression during liver stage suggests importance in that stage.[46]	0.2
N-myristoyl-transferase (PF14 0127)	As argued by Gelb *et al*.[47], "Genetic studies have shown that the NMT gene is essential for viability in a range of species, including *Drosophila melanogaster*, *S.cerevisiae* and *Candida albicans* and *Cryptococcus neoformans*."	0.8
OMP decarboxylase (PF10 0225)	Part of the *de novo* pyrimidine synthesis pathway, which should be essential in *Plasmodium* because it does not have a pyrimidine salvage pathway. Also, chemical validation of the *de novo* pyrimidine pathway comes from studies of dihydroorotate dehydrogenase.[48]	N/A
S-adenosyl-homocysteine hydrolase (PFE1050w)	Part of a methylation cycle whose blockage should be fatal.[49]	0.8

Those compounds were tested against a variety of enzymatic targets known to be essential to the viability of the parasite. **Table 1** is an excerpt from the article "Identification of inhibitors for putative malaria drug targets among novel antimalarial compounds" by Crowther *et al*.[39] indicating the enzymatic target, the essentiality of the target to the viability of the parasite, and the druggability of that enzymatic target. They considered certain important criteria in order to select

the enzymatic targets they used for the screening. The criteria were i) was the enzyme required for the survival of the parasite, ii) does the enzyme have a binding site that can be inhibited by a small molecule, inhibiting the function of the enzyme, iii) is there a big enough difference between the human and parasitic enzymes which would lower adverse effects of the inhibitory drug on humans, iv) is the enzyme related to recombinant expression and v) could a high-throughput screening assay be used to indicate enzymatic activity. The targetable enzymes and druggability scores were obtained from TDRtargets.org.[50]

Enzymatic inhibition of each enzyme with compounds that indicated an EC_{50} value of <1.25 µM was carried out in order to obtain hit compounds that indicated good activity. **Table 2** indicates the number of hits each enzymatic assay indicated, the activity range of those compounds in the enzymatic assay, as well as the efficacy against the 3D7 strain of *P. falciparum*. They also performed a counterscreen of the hit compounds identified against the Huh7 human hepatocellular carcinoma cell line (indicating cytotoxicity) as well as fluorescence quencher assessment (compounds that quenched fluorescence were excluded). The enzymatic assays that indicate n/a indicate that the hits were also inhibitors of the counterscreens.

Table 2: Biochemical results for enzymatic and antiplasmodialscreens[39]

Enzyme	**# hits**	**enzyme reconfirmation (IC_{50}, µM)**	***P. falciparum* 3D7 (EC_{50}, µM)**
Pf Choline kinase	69	2.9–19.0	0.04–0.7
Pf dUTPase	95	n/a	n/a
Pf OMP decarboxylase	26	2.4–58.0	0.093–6.0
Pf *S*-adenosyl-homocysteine hydrolase	38	0.1–9.1	0.9–7.6
Pf glutamate dehydrogenase	164	n/a	n/a
Pv Guanylate kinas	17	2.9–4.0	0.092–3.4
Pf Adenylosuccinate synthase	9	1.7–22.9	0.2–1.6
Pf *N*-Myristoyltransferase	6	1.4–8.6	0.04–2.6
Pf Farnesyl pyrophosphate synthase	6	n/a	n/a

With the results in mind, we decided to follow up on exploring research devoted to Pf *N*-myristoyl transferase (PfNMT) inhibition. The reasoning behind this decision was that PfNMT indicated a druggability score of 0.8 which is significant, giving scope to the development of novel inhibitors that could provide effective inhibition. PfNMT only indicated 6 hits, thus we came to the conclusion that the synthesis of novel PfNMT inhibitors as potential antimalarial chemotherapeutic agents is a favourable choice as the amount of inhibitors are low. A co-crystal structure of *Plasmodium*

vivax *N*-myristoyl transferase (PvNMT) with a ligand in the active site has been published, enabling us to follow a rational design of new inhibitors.[51] PvNMT and PfNMT share an 81% sequence identity with each other, whereby only two of 23 residues differ within a 5Å radius of the ligand.[51]

1.7 *N*-Myristoyl transferase as a viable enzymatic target

N-Myristoyltransferase (NMT) is a monomeric enzyme that is ubiquitous in all eukaryotic cells, and catalyzes the irreversible *N*-myristoylation of proteins.[51] *N*-myristoylation involves the coupling of a 14-carbon fatty acid, tetradecanoic acid or myristic acid, to the *N*-terminal glycine residues of proteins, and occurs mainly co-translationally, meaning that *N*-myristoylation occurs while the peptide is still attached to the ribosome.[52] **Figure 6** illustrates the pathway that is followed for *N*-myristoylation.

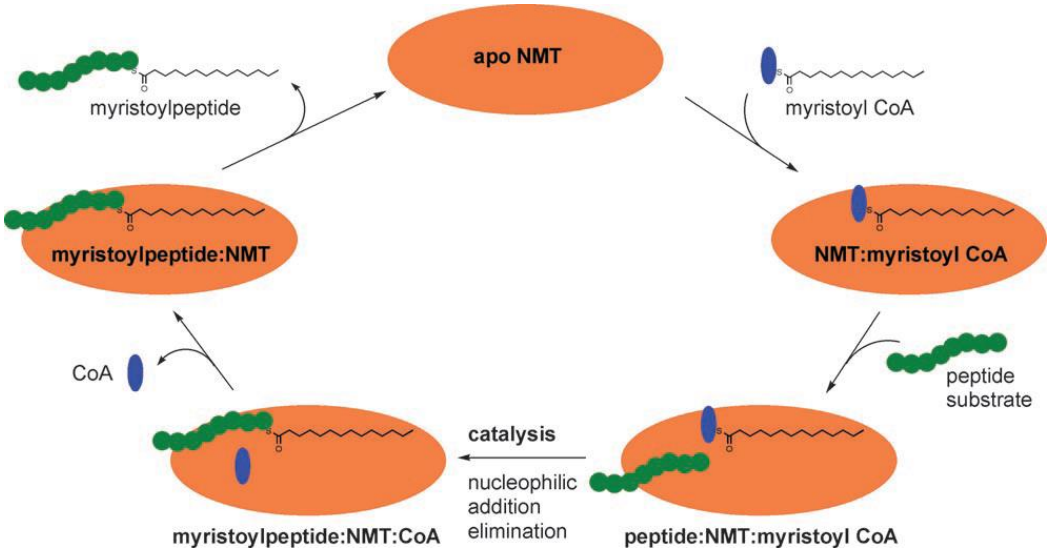

Figure 6: Myristoylation pathway involving myristoyl CoA, the peptide to be *N*-myristoylated and release of the myristoylated peptide.[53]

N-myristoylation occurs through a Bi-Bi reaction mechanism, where the binding of myristoyl-CoA (MyrCoA) and NMT creates the opening of a second binding pocket, which facilitates the binding of the peptide substrate to the pocket.[53] Transfer of the myristate group from MyrCoA to the *N*-terminal glycine residue of the NMT-bonded peptide occurs via a nucleophilic addition-elimination reaction, whereby the glycine ammonium group is neutralized by a close-by leucine carboxylate, producing the freebase amine form of glycine, which is now nucleophilic. Subsequently,

nucleophilic attack of the amine at the thioester of MyrCoA, followed by the release of CoA as the leaving group results in *N*-myristoylation.[54]

Genetic knockdown of NMT in *P. berghei* proved an acute dependency of the enzyme during the parasite life cycle.[51] Research conducted by Wright *et al*.[52] has proven that *N*-myristoylation was essential for the viability of the parasite, whereby effective inhibition of NMT resulted in the irreversible failure of the ability of the parasite to assemble the inner membrane complex, a critical sub-cellular organelle. They followed a direct detection method of tagged proteins. Cultured parasites (schizonts) in the blood phase of their life cycle were exposed to tetradec-13-ynoic acid (YnMyr), an analogue to myristate that contains a terminal alkyne. Incorporation of YnMyr *in vivo*, resulted in the biosynthesis of YnMyr-CoA, which facilitated the coupling of YnMyr to the *N*-terminal glycine residues of peptides, synonymous to myristoylation. The *N*-YnMyr coupled proteins were isolated, and through a copper catalyzed Huisgen 1,3-dipolar cycloaddition, or "click" reaction, was reacted with azido-TAMRA-PEG-biotin, to form the *N*-Myrtriazole-TAMRA-PEG-biotin coupled protein (**Figure 7**).

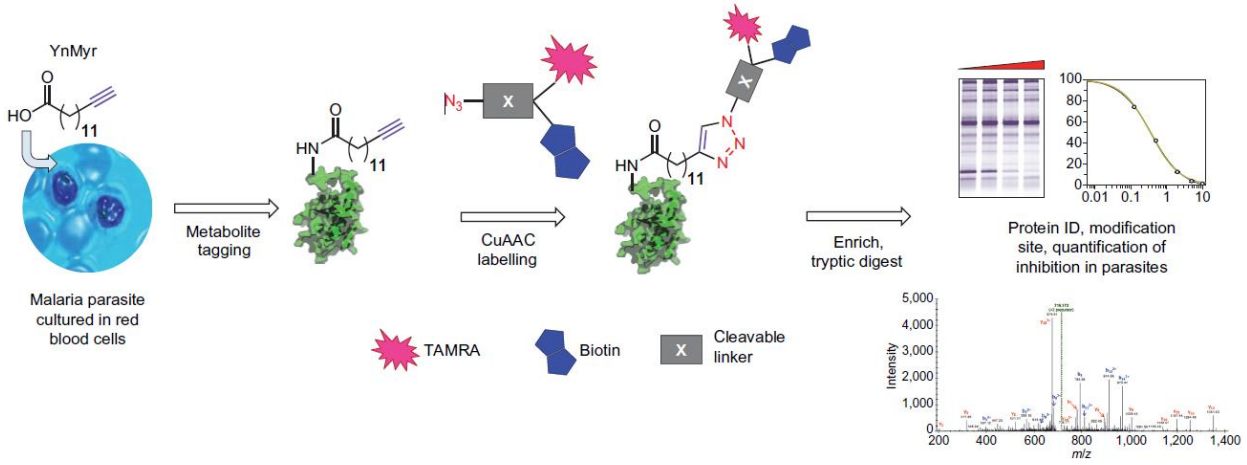

Figure 7: *N*-YnMyristoylation of proteins, and coupling of azido-TAMRA-PEG-biotin to produce fluorescent marker[52]

This enabled direct in-gel fluorescence detection of the proteins that are myristoylated under natural circumstances. They deduced that NMT is involved in the myristoylation of more than 30 proteins which are involved with biological processes like organelle biosynthesis, parasitic motility, ion channel regulation, inner-membrane complex proteins and protein homeostasis.[52]

Targeting both *P. falciparum* and *P. vivax* NMT is also possible as it has been determined that the PfNMT and PvNMT share an 81% sequence identity as previously stated. Compounds

synthesized for PfNMT inhibition could potentially inhibit the function of PvNMT with a high degree of certainty.[52] This is of great interest as *P. vivax* is the second most prevalent form of malaria. Thus we could produce a drug which is active towards both *P. falciparum* and *P. vivax*, a dual species drug. Apart from evidence supporting the importance of PfNMT as an essential enzyme for the livelihood of the parasite, the other aspect of enzymatic targeting involves the similarity between PfNMT and the human counterpart enzyme that performs the same enzymatic function. Human cells have two NMT isoforms, HsNMT1 and HsNMT2.[55] In order to selectively target PfNMT, there must be a sufficient difference between PfNMT and HsNMT1/HsNMT2 at the active site so that PfNMT inhibitors do not inhibit the function of HsNMT1/HsNMT2. The sequence identity between HsNMT1 and HsNMT2 relative to PfNMT are both 52%, whereas the sequence similarity between HsNMT1 and HsNMT2 relative to PfNMT is 70% and 71% respectively.[55] Sequence identity is the exact match of characters (amino acids in this case) between two different enzyme sequences, whereas sequence similarity is the degree of resemblance between two sequences, essentially indicating the extent to which amino acids are aligned.[56] Due to the fact that the sequence similarity is relatively high, there is cause for concern regarding the potential selectivity between PfNMT and HsNMT1/HsNMT2.

1.8 Previously synthesized PfNMT inhibitors

Having established that NMT plays a critical role in the normal functioning and health of the parasite, we had sufficient reason to pursue PfNMT as a viable focus for this project. So, the next step in the project was to establish the work that had previously been done in the synthesis of PfNMT inhibitors. Yu *et al*.[51] have developed novel PvNMT inhibitors by identifying an active PvNMT inhibitor by a “piggy back” approach, essentially screening known chemotherapeutic compounds that are inhibitors of *Candida albicans* NMT (CaNMT) and *Trypanosoma brucei* NMT (TbNMT) in a PvNMT inhibition assay to obtain active compounds. They identified a hit compound (RO-09-4609) that was developed by Roche[57] that contains a 3-methyl benzofuran heterocycle connected to a pyridine ring via a linker, as seen in **Figure 8**. RO-09-4609 indicated moderate inhibition towards PvNMT (IC_{50}: 51 µM), but had good selectivity over HsNMT1 (IC_{50}: >1000 µM).

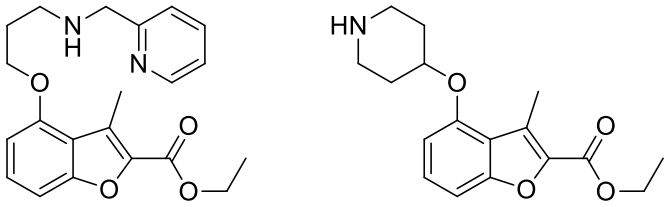

RO-09-4609 **2**

Figure 8: Compound RO-09-4609 and compound **2**[51]

They developed a series of derivatives of RO-09-4609 in order to increase the efficacy towards PvNMT inhibition but retain the selectivity towards HsNMT1. They followed a chemistry-driven approach in optimizing RO-09-4609 by varying the substituents at the C2- and C4-positions. 24 Analogues containing different derivatives of the side chain at the C4-position confirmed that a trimethylene side chain length is optimal and a secondary amine is preferable. 4-Piperidinol was the most promising substituent at that position and of the compounds synthesized compound **2** showed the most promise (**Figure 8**). Compound **2** exhibited an increased PvNMT inhibition at 16.5 µM but retained a good selectivity over HsNMT1 with >200 µM. Derivatization of the C2-ester was carried out to determine the most effective substituent at that position. Various phenethyl, benzyl and 1-methylnaphthyl esters and amides were synthesized. Overall, the analogues bearing either a naphthylic ester or amide exhibited the best inhibition of PvNMT with IC_{50} values of 1.4 and 2.3 µM respectively, were the naphthylic amide had an EC_{50} value of 2.4 µM against *P. falciparum* 3D7 line. The benzylic ester and amide had IC_{50} values of 0.27 and 13.0 µM (PvNMT), and the ester had an EC_{50} value of 1.2 µM (3D7). The phenethyl ester had an IC_{50} of 4.1 µM (PvNMT) and an EC_{50} of 4.0 µM (3D7). A 3-methoxybenzyl ester, compound **26** (**Figure 9**), indicated the highest inhibition with an IC_{50} of 0.60 µM (PvNMT).[51]

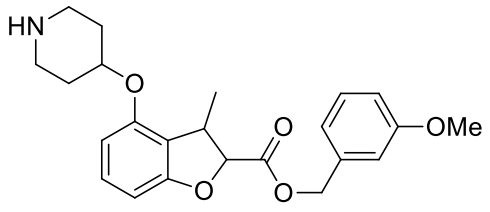

26

Figure 9: Benzofuran with a 3-methoxybenzyl ester indicating a PvNMT IC_{50} value of 0.60 µM[51]

A crystal structure of **26** co-crystallized with PvNMT (PDB code 4B14) was obtained, which indicated the important interactions of the amino acid residues with compound **26**, as seen in **Figure 10**.

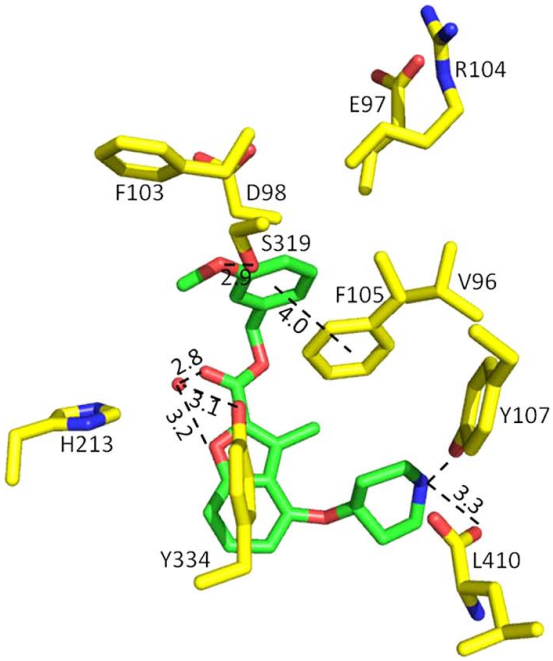

Figure 10: Crystal structure of **26** co-crystallized with PvNMT, PDB code 4B14.[58]

26 Occupied the peptide binding pocket of PvNMT, the active site. As indicated, a prominent salt-bride interaction of the piperidine amine with a tyrosine residue Y107' and a leucine residue L410 is observed. Furthermore, a pi-pi interaction was observed between the 3-methoxybenzyl group and a phenylalanine residue F105. An interaction between a water molecule and the ester carbonyl, benzofuran oxygen and the phenolic group of a tyrosine residue Y334 is also observed. These favorable interactions are indicative why compound **26** is more active than **2**. According to Yu *et al*,[51] inclusion of a methyl group at the C3-position would induce an effect on the orientation of the ester carbonyl versus the secondary amide carbonyl, explaining that the amide proton would be in close proximity to the C3-methyl group, thus forcing the orientation of the carbonyl oxygen to be "*syn*" to the methyl. This results in a different spatial location of the ester versus the amide aromatic substituent, which explains the overall efficacy traits of the ester analogues being more active than the amide analogues.

There is no crystal structure of PfNMT available, but due to the fact that PvNMT and PfNMT share 81% sequence identity, any rational drug design approach using PvNMT as enzyme would mean that those potential inhibitors could also inhibit PfNMT.

1.9 Isostructural heterocycles

Compound **26** exhibited good PvNMT inhibition, which is due to the salt-bride formation of the piperidine ring and pi-pi stacking of the aromatic ester to a phenylalanine residue. We suggested that the activity of selected benzofuran analogues could potentially be increased by changing the benzofuran heterocycle to various other isostructural heterocycles.

1.9.1 Indoles

Indoles is considered a privileged structure and is one of the most important heterocycles in drug discovery. The inclusion of indoles in various drugs on the market has proven its importance.[59] Fluvastatin, an indole based member of the statin family, is used for treating hypercholesterolemia inhibiting the enzyme HMG-CoA reductase, an important enzyme in the mevalonate pathway that produces cholesterol.[60] Tadalafil is a phosphodiesterase (PDE) inhibitor that is used for congestive heart failure, hypertension and the treatment of male erectile dysfunction.[61] The indole scaffold is also present in various biologically important compounds such as tryptophan, tryptamine, serotonin and melatonin, which play crucial roles in numerous biochemical pathways.[62]

Sheng *et al*.[63] have replaced the benzofuran scaffold of RO-09-4609 with an indole scaffold and derivatized the ester group to various other amides, thioethers and ethers, in an attempt to increase the inhibitory effect on NMT enzymes of *Candida* spp., *Cryptococcus neoformans* and *Aspergillus fumigates*. However, the indole scaffold showed poor activity relative to RO-09-4609 against all types of fungal NMT enzymes. For our own comparative study we have decided to include this moiety.

1.9.2 Benzimidazoles

Benzimidazoles form part of many bioactive compounds with many clinical and biological applications. To name a few, Albendazole is an anthelmintic agent for the treatment of various parasitic worm infections,[64] Bendamustine is an anti-cancer agent used in chemotherapy for the treatment of non-Hodgkin's lymphoma, chronic lymphocytic leukemia and multiple myeloma[65] and Telmisartan is an antihypertensive drug for the treatment of high blood pressure,[66] all containing a benzimidazole scaffold.

Our search for NMT inhibitors with a benzimidazole scaffold provided us with no results, although we did locate an article by Kawasaki *et al*.[67] that derivatized RO-09-4609 by incorporating a 2-(1-methyl benzimidazolyl) ketone substituent at the C2-position, which indicated good inhibition against *Candida albicans* and *Aspergillus fumigatus* NMT.[68]

1.9.3 Benzoxazoles

Benzoxazoles are also a structurally important moiety found in nature and various drugs. Calcimycin is an antibiotic that acts against fungi and Gram-positive bacteria, but is also used in the study of the role divalent cations play in biological systems as it binds to calcium, and facilitates the transport of calcium over membranes.[68,69] Benzoxomycin A and B are antibiotics produced by an Actinomycetes strain and are active against Gram-positive bacteria like *Streptococcus pyogenes*, *Mycobacterium smegmatis*, *Clostridium difficile* and *Bacterioides fragilis*.[70]

Sheng *et al*.[63] have also replaced the benzofuran heterocycle of RO-09-4609 with a benzoxazole scaffold, in which some compounds synthesized indicated a greater efficacy against *Candida tropicalis* than RO-09-4609, and indicated a greater efficacy than the indole analogues.

1.9.4 Benzothiophenes

Benzothiophenes are also included in a number of biologically active drugs, like relaxifene which is used to treat and prevent osteoporosis, as well as treatment to reduce the risk of breast cancer in postmenopausal women.[71] Zileuton is used as an inhibitor of 5-lipoxygenase, thus used for the treatment of chronic asthma.[72] Sertaconazole is used as a fungicidal drug and used to treat athlete's foot, caused by species of *Trichophyton* which are susceptible to Sertaconazole.[73]

Rackham *et al*.[74] have synthesized various benzothiophene PfNMT and PvNMT inhibitors, which showed great efficacy in enzymatic inhibition. Inhibition of PfNMT and PvNMT was at 8 and 2 nM, and had an EC_{50} value of 302 nM against the 3D7 strain of *P. falciparum in vitro*.

1.10 Aims and objectives

All the above mentioned heterocycles have been found in literature with the purpose of NMT inhibition of various fungi and parasites. We envisioned changing the benzofuran scaffold of

compound **26** to the various heterocycles mentioned *i.e*. indoles, 3-methyl indoles, 1-methyl benzimidazoles, benzoxazoles and benzothiophenes. As mentioned earlier, Yu *et al*. also derivatized the ester at the C2-position to various aromatic esters and amides. We envisioned synthesizing the above mentioned heterocycles, each containing an ester at the C2-position which would be derivatized to produce benzyl, 1-methylnaphthyl and phenethyl esters and amides, as well as a 4-methylpyridine amide. Each heterocycle would also contain a derivatizable oxygen atom at the C4-position (C7-position for benzimidazole) with the intent on installing a piperidine ring on that position. The differences in the heterocycles together with the different ester and amide substituents at the C2-position would give us valuable insight into structure-activity relationships for these compounds.

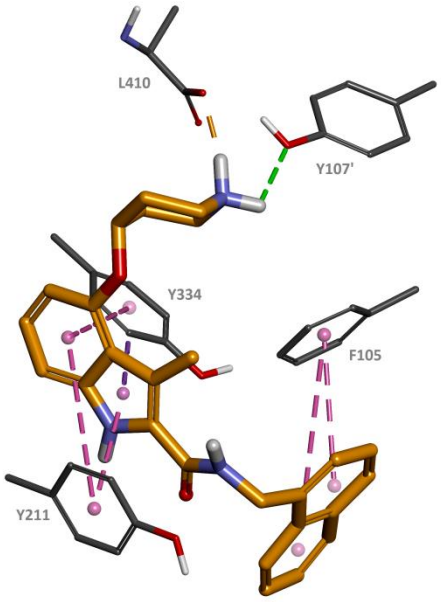

Figure 11: Docking of 3-methyl indole scaffold with 1-methylnaphthyl amide and piperidine ether indicating the various interactions.

We docked the proposed compounds we envisioned synthesizing into the crystal structure of PvNMT, as illustrated in **Figure 10**. Most of the compounds had a similar orientation when docked as a ligand in the crystal structure, as expected. The most favorable interactions were seen by the 3-methyl indole compounds we planned to synthesize and the least favorable were the benzoxazole series of compounds. **Figure 11** illustrated the most favorable interaction in the docking studies, a 3-methyl indole compound containing a 1-methylnaphthyl amide. Of particular interest is the favorable double pi-pi stacking observed between the naphthyl group and the phenylalanine residue F105, as well as pi-pi stacking between two tyrosine residues Y211 and Y334 and the indole scaffold. It was also observed that the interaction between the piperidine ring

with the neighboring tyrosine Y107' and leucine L410 residues were more favorable if the piperidine ring was in the salt form, thus a piperidinium ring.

The 3-methyl indole scaffold would be compared to the 3-methyl benzofuran analogue, and the indole scaffold would be compared to the 3-methyl indole scaffold to confirm the importance of a methyl group at the C3-position. The 1-methyl benzimidazole scaffold would be compared to the 3-methyl indole and benzofuran scaffold to determine which heterocycle displays the largest inhibitory effect. The benzoxazole and benzothiophene compounds would be compared with the indole scaffold in order to see which is the most effective; since those three heterocycles will not have a methyl group at the C3-position. **Figure 12** illustrates the proposed heterocycles connected to the various aromatic esters and amides we envisaged to synthesize.

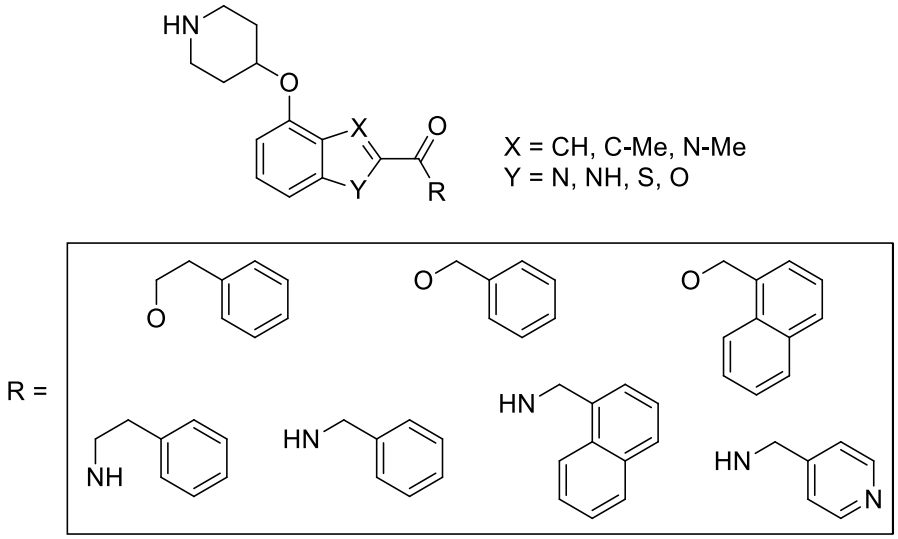

Figure 12: Indole, 3-methyl indole, 1-methyl benzimidazole, benzoxazole and benzothiophene heterocycles to be synthesized, indicating the aromatic esters and amides

The main objectives of this project were to synthesize each of the heterocyclic scaffolds, each of those initially containing an ester group at the C2-position that would subsequently be transesterified and amidated to produce the desired aromatic esters and amides. Secondly the inclusion of a piperidine ring at the C4-position of the indoles, benzoxazole and benzothiophene scaffold and at the C7-position of the benzimidazole was necessary in order to compare the activity of the benzofuran analogues. The third objective was to synthesize 3-methyl indole and 1-methyl benzimidazole scaffolds. This would be the main focus of activity for this project as the presence of a methyl group at those respected positions would potentially have a significant effect on the efficacy of the 3-methyl indole and 1-methyl benzimidazole libraries, as well as give insight

if the aromatic esters are more active than the analogous amides. All of this requires an exploration of the underlying synthetic chemistry.

The second chapter focuses on the various methods used to synthesize the indole scaffold with the desired substitution pattern, and the methods used to facilitate the substitution at the desired positions. Different methodologies regarding the synthesis and functionalization are explained, giving experimental insight into the effectiveness of different synthetic procedures. Spectroscopic data is explained to assure the formation of the precursors. The chapter focuses on the use of the Knoevenagel-condensation reaction to produce an azido acrylate which, after thermolysis, produced the required indole scaffold in a Hemetsberger indolisation reaction. The chapter concludes with the synthesis of the desired final compounds abbreviated **IH**, which is shorthand for **I**ndole 3-**H**.

The third chapter involves the methods used to introduce a methyl group at the C3-position of the indole scaffold and explains the trial and error involved in the methods used. Reasons to why various attempts to synthesize the 3-methyl analogues failed are discussed, whereby any byproducts formed that were of interest were characterized and their formation explained. The chapter attempts to explain observed regioselectivity differences, and leads to the synthesis of the desired 3-methyl indole scaffold via the selective bromination followed by methylation via a Suzuki–Miyaura reaction. The chapter concludes with the synthesis of the desired final compounds, abbreviated **IM**, shorthand for **I**ndole 3-**M**ethyl.

The fourth chapter involves the synthesis of the 1-methyl benzimidazole scaffold, and the functionalization of the benzimidazole scaffold to synthesize the analogues to the **IM** series of compounds. Focus is placed on the derivatization of the C2-position in order to introduce an ester group at that position, which is realized by a versatile oxidative esterification reaction from an aldehyde. The chapter concludes with the synthesis of the desired final compounds abbreviated **BI**, for **B**enz**I**midazole.

The fifth chapter involves the synthesis of the benzoxazole library and explains the different methodologies involved regarding benzoxazoles. Two distinctly different approaches were followed regarding the synthesis of benzoxazoles. The main focus of the chapter is the one-pot synthesis of a benzoxazole scaffold via a Mitsunobu mediated cyclodehydration reaction, resulting in the formation of the desired heterocycle with the required substitutions needed. The subsequent steps include the direct functionalization of the 4-phenoxy groups with alternative

Mitsunobu reagents, as well as functionalization of the ester group to produce the desired final compounds abbreviated as **BO**, for **B**enz**O**xazole.

The sixth chapter describes the formation of the benzothiophene heterocycles that are analogous to the **IH** series of compounds. The chapter focuses on the Duff reaction, a key formylation reaction, and the subsequent one-pot *ipso*-nucleophilic substitution and dehydration reaction sequence to produce the desired benzothiophene. The chapter concludes with the synthesis of the final compounds, abbreviated **BT** for **B**enzo**T**hiophene.

In the seventh chapter we discuss the biological results obtained regarding activity against *P. falciparum* as well as the effects that the different heterocycles, esters and amides have on efficacy.

The eighth chapter includes a computational study regarding the reactivity of the ester group of each heterocycle, with the aim of explaining the differences in electrophilicity.

The ninth chapter summarises the most important conclusions regarding the work carried out in this thesis as well as gives an outline for future work in this field.

The tenth chapter is the general experimental section.

1.11 References

1. Neghina, R.; Neghina, A. M.; Marincu, I.; Iacobiciu, I. *Am. J. Med. Sci.* **2010**, *340,* 492.

2. Cox, F. E. G. *Parasit. Vectors*, **2010**, *3,* 5.

3. Harper, K.; Armelagos, G. *Int. J. Environ. Res. Public Health.* **2010**, 7*(2)*, 675.

4. Hanson, A. E. *J. Hist. Med. Allied Sci.* **2005**, *60,* 102.

5. Reiter, P. *Emerg. Infect. Diseases.* **2000**, *6,* 1.

6. Wells, T. N.; van Huijsduijnen, R. H.; Van Voorhis, W. C. *Nat. Rev. Drug Discov*. **2015**, *14,* 424.

7. Smith, K. A. *Front. Immunol.* **2012**, *3,* 68.

8. Center for Disease Control, USA , *Dec 29, 2016*.

9. Stone, C. M.; Jackson, B. T.; Foster, W. A. *Am. J. Trop. Med. Hyg.* **2012**, *87,* 727.

10. Carter, R.; Mendis, K. *Clin. Microbiol. Rev.* **2002**, *15,* 564.

11. Singh, B.; Daneshvar, C. *Clin. Microbiol. Rev.* **2013**, *26,* 165.

12. World Health Organization **2016**.

13. UNICEF **2016**, *2017,* 1.

14. Bhatt, S.; Weiss, D.; Cameron, E.; Bisanzio, D.; Mappin, B.; Dalrymple, U.; Battle, K.; Moyes, C.; Henry, A.; Eckhoff, P. *Nature* **2015**, *526,* 207.

15. World Health Organization **2015**.

16. Bousema, T.; Okell, L.; Felger, I.; Drakeley, C. *Nature Rev. Microbiol.* **2014**, *12,* 833.

17. Cowman, A. F.; Berry, D.; Baum, J. *J. Cell Biol.* **2012**, *198,* 961.

18. Baker, D. A. *Mol. Biochem. Parasitol.* **2010**, *172,* 57.

19. Eichner, M.; Diebner, H. H.; Molineaux, L.; Collins, W. E.; Jeffery, G. M.; Dietz, K. *Trans. R. Soc. Trop. Med. Hyg.* **2001**, *95,* 497.

20. Bartoloni, A.; Zammarchi, L. *Mediterr. J. Hematol. Infect. Dis.* **2012**, *4,* 1.

21. Butler, A. R.; Khan, S.; Ferguson, E. *J. R. Coll. Physicians. Edinb.* **2010**, *40,* 172.

22. Meshnick, S. R.; Dobson, M. J. *Antimalarial chemotherapy* **2001**, 15.

23. Surrey, A. R.; Hammer, H. F. *J. Am. Chem. Soc.* **1946**, *68,* 113.

24. Wellems, T. E.; Plowe, C. V. *J. Infect. Dis.* **2001**, *184,* 770.

25. Setthaudom, C.; Tan-ariya, P.; Sitthichot, N.; Khositnithikul, R.; Suwandittakul, N.; Leelayoova, S.; Mungthin, M. *Am. J. Trop. Med. Hyg.* **2011**, *85,* 606.

26. Karki, R.; Pandya, D.; Elston, R. C.; Ferlini, C. *BMC Med Genomics*. **2015**, *8,* 1.

27. Eyase, F. L.; Akala, H. M.; Ingasia, L.; Cheruiyot, A.; Omondi, A.; Okudo, C.; Juma, D.; Yeda, R.; Andagalu, B.; Wanja, E. *Plos one* **2013**, *8,* e64299.

28. Juge, N.; Moriyama, S.; Miyaji, T.; Kawakami, M.; Iwai, H.; Fukui, T.; Nelson, N.; Omote, H.; Moriyama, Y. *Proc. Natl. Acad. Sci. U. S. A.* **2015**, *112,* 3356.

29. Egan, T. J. *Targets* **2003**, *2,* 115.

30. Brown, G. *Educ. Chem.* **2006**, *43,* 97.

31. Faurant, C. *Parasite* **2011**, *18,* 215.

32. Kuhn, T.; Wang, Y. *Prog. Drug Res.* **2008**, *66,* 383.

33. Mutabingwa, T. K. *Acta Trop.* **2005**, *95,* 305.

34. Wang, J.; Huang, L.; Li, J.; Fan, Q.; Long, Y.; Li, Y.; Zhou, B. *Plos one* **2010**, *5,* e9582.

35. Ashley, E. A.; Dhorda, M.; Fairhurst, R. M.; Amaratunga, C.; Lim, P.; Suon, S.; Sreng, S.; Anderson, J. M.; Mao, S.; Sam, B. *N. Engl. J. Med.* **2014**, *371,* 411.

36. Mok, S.; Ashley, E. A.; Ferreira, P. E.; Zhu, L.; Lin, Z.; Yeo, T.; Chotivanich, K.; Imwong, M.; Pukrittayakamee, S.; Dhorda, M.; Nguon, C.; Lim, P.; Amaratunga, C.; Suon, S.; Hien, T. T.; Htut, Y.; Faiz, M. A.; Onyamboko, M. A.; Mayxay, M.; Newton, P. N.; Tripura, R.; Woodrow, C. J.; Miotto, O.; Kwiatkowski, D. P.; Nosten, F.; Day, N. P.; Preiser, P. R.; White, N. J.; Dondorp, A. M.; Fairhurst, R. M.; Bozdech, Z. *Science* **2015**, *347,* 431.

37. World Health Organization *Geneva: World Health Organization* **2015**.

38. Smrkovski, L. L.; Buck, R. L.; Alcantara, A. K.; Rodriguez, C. S.; Uylangco, C. V. *Trans. R. Soc. Trop. Med. Hyg.* **1985**, *79,* 37.

39. Crowther, G. J.; Napuli, A. J.; Gilligan, J. H.; Gagaring, K.; Borboa, R.; Francek, C.; Chen, Z.; Dagostino, E. F.; Stockmyer, J. B.; Wang, Y.; Rodenbough, P. P.; Castaneda, L. J.; Leibly, D. J.; Bhandari, J.; Gelb, M. H.; Brinker, A.; Engels, I. H.; Taylor, J.; Chatterjee, A. K.; Fantauzzi, P.; Glynne, R. J.; Van Voorhis, W. C.; Kuhen, K. L. *Mol. Biochem. Parasitol.* **2011**, *175,* 21.

40. Hyde, J. E. *Curr. Drug Targets* **2007**, *8,* 31.

41. Vial, H. J.; Wein, S.; Farenc, C.; Kocken, C.; Nicolas, O.; Ancelin, M. L.; Bressolle, F.; Thomas, A.; Calas, M. *Proc. Natl. Acad. Sci. U. S. A.* **2004**, *101,* 15458.

42. Nguyen, C.; Kasinathan, G.; Leal-Cortijo, I.; Musso-Buendia, A.; Kaiser, M.; Brun, R.; Ruiz-Pérez, L. M.; Johansson, N. G.; González-Pacanowska, D.; Gilbert, I. H. *J. Med. Chem.* **2005**, *48,* 5942.

43. Mukkamala, D.; No, J. H.; Cass, L. M.; Chang, T.; Oldfield, E. *J. Med. Chem.* **2008**, *51,* 7827.

44. Jarzynak, R.; Lenarcik, E.; Brya, J. *Pharmacol. Res*. **1997**, *35,* 79.

45. Werner, C.; Stubbs, M. T.; Krauth-Siegel, R. L.; Klebe, G. *J. Mol. Biol.* **2005**, *349,* 597.

46. Tarun, A. S.; Peng, X.; Dumpit, R. F.; Ogata, Y.; Silva-Rivera, H.; Camargo, N.; Daly, T. M.; Bergman, L. W.; Kappe, S. H. *Proc. Natl. Acad. Sci. U. S. A.* **2008**, *105,* 305.

47. Gelb, M. H.; Van Voorhis, W. C.; Buckner, F. S.; Yokoyama, K.; Eastman, R.; Carpenter, E. P.; Panethymitaki, C.; Brown, K. A.; Smith, D. F. *Mol. Biochem. Parasitol.* **2003**, *126,* 155.

48. Gujjar, R.; Marwaha, A.; El Mazouni, F.; White, J.; White, K. L.; Creason, S.; Shackleford, D. M.; Baldwin, J.; Charman, W. N.; Buckner, F. S. *J. Med. Chem.* **2009**, *52,* 1864.

49. Tanaka, N.; Nakanishi, M.; Kusakabe, Y.; Shiraiwa, K.; Yabe, S.; Ito, Y.; Kitade, Y.; Nakamura, K. T. *J. Mol. Biol.* **2004**, *343,* 1007.

50. Agüero, F.; Al-Lazikani, B.; Aslett, M.; Berriman, M.; Buckner, F. S.; Campbell, R. K.; Carmona, S.; Carruthers, I. M.; Chan, A. E.; Chen, F. *Nat. Rev. Drug Discov.* **2008**, *7,* 900.

51. Yu, Z.; Brannigan, J. A.; Moss, D. K.; Brzozowski, A. M.; Wilkinson, A. J.; Holder, A. A.; Tate, E. W.; Leatherbarrow, R. J. *J. Med. Chem.* **2012**, *55,* 8879.

52. Wright, M. H.; Clough, B.; Rackham, M. D.; Rangachari, K.; Brannigan, J. A.; Grainger, M.; Moss, D. K.; Bottrill, A. R.; Heal, W. P.; Broncel, M. *Nature Chem.* **2014**, *6,* 112.

53. Bowyer, P. W.; Tate, E. W.; Leatherbarrow, R. J.; Holder, A. A.; Smith, D. F.; Brown, K. A. *ChemMedChem* **2008**, *3,* 402.

54. Rudnick, D. A.; McWherter, C. A.; Rocque, W. J.; Lennon, P. J.; Getman, D. P.; Gordon, J. I. *J. Biol. Chem.* **1991**, *266,* 9732.

55. Bell, A. S.; Mills, J. E.; Williams, G. P.; Brannigan, J. A.; Wilkinson, A. J.; Parkinson, T.; Leatherbarrow, R. J.; Tate, E. W.; Holder, A. A.; Smith, D. F. *PLoS Negl. Trop. Dis.* **2012,** *6,* e1625.

56. Fassler, J.; Cooper, P. BLAST glossary, **2011**.

57. Masubuchi, M.; Kawasaki, K.; Ebiike, H.; Ikeda, Y.; Tsujii, S.; Sogabe, S.; Fujii, T.; Sakata, K.; Shiratori, Y.; Aoki, Y.; Ohtsuka, T.; Shimma, N. *Bioorg. Med. Chem. Lett.* **2001,** *11,* 1833.

58. Yu, Z.; Brannigan, J. A.; Moss, D. K.; Brzozowski, A. M.; Wilkinson, A. J.; Holder, A. A.; Tate, E. W.; Leatherbarrow, R. J. *J. Med. Chem.*, **2012**, *55* (20), 8879.

59. de Sa, A.; Fernando, R.; Barreiro, E. J.; Fraga, M.; Alberto, C.*Mini. Rev. Med. Chem.* **2009**, *9,* 782.

60. Herd, J. A.; Ballantyne, C. M.; Farmer, J. A.; Ferguson III, J. J.; Jones, P. H.; West, M. S.; Gould, K. L.; Gotto Jr., A. M. *Am. J. Cardiol.* **1997**, *80,* 278.

61. Daugan, A.; Grondin, P.; Ruault, C.; Le Monnier de Gouville, Anne-Charlotte; Coste, H.; Linget, J. M.; Kirilovsky, J.; Hyafil, F.; Labaudinière, R. *J. Med. Chem.* **2003**, *46,* 4533.

62. Kaushik, N. K.; Kaushik, N.; Attri, P.; Kumar, N.; Kim, C. H.; Verma, A. K.; Choi, E. H. *Molecules* **2013**, *18,* 6620.

63. Sheng, C.; Xu, H.; Wang, W.; Cao, Y.; Dong, G.; Wang, S.; Che, X.; Ji, H.; Miao, Z.; Yao, J.; Zhang, W. *Eur. J. Med. Chem.* **2010**, *45,* 3531.

64. Adams, E. J.; Stephenson, L. S.; Latham, M. C.; Kinoti, S. N. *J. Nutr.* **1994**, *124,* 1199.

65. Elefante, A.; Czuczman, M. S. *Am. J. Health. Syst. Pharm.* **2010**, *67*.

66. Lacourciere, Y.; Krzesinski, J. M.; White, W. B.; Davidai, G.; Schumacher, H. *Blood Press. Monit.* **2004**, *9,* 203.

67. Kawasaki, K.; Masubuchi, M.; Morikami, K.; Sogabe, S.; Aoyama, T.; Ebiike, H.; Niizuma, S.; Hayase, M.; Fujii, T.; Sakata, K. *Bioorg. Med. Chem. Lett.* **2003**, *13,* 87.

68. Abbott, B. J.; Fukuda, D. S.; Dorman, D. E.; Occolowitz, J. L.; Debono, M.; Farhner, L. *Antimicrob. Agents Chemother.* **1979**, *16,* 808.

69. Chaney, M. O.; Demarco, P. V.; Jones, N. D.; Occolowitz, J. L. *J. Am. Chem. Soc.* **1974**, *96,* 1932.

70. Kusumi, T.; Ooi, T.; Walchli, M. R.; Kakisawa, H. *J. Am. Chem. Soc.* **1988**, *110,* 2954.

71. Muchmore, D. B. *Oncologist.* **2000**, *5,* 388.

72. Israel, E.; Cohn, J.; Dubé, L.; Drazen, J. M.; Ratner, P.; Pleskow, W.; DeGraff, A.; Chervinsky, P.; Wasserman, S.; Nelson, H. *JAMA* **1996**, *275,* 931.

73. Palacin, C.; Sacristan, A.; Ortiz, J. A. *Arzneimittelforschung* **1992**, *42,* 711.

74. Rackham, M. D.; Brannigan, J. A.; Rangachari, K.; Meister, S.; Wilkinson, A. J.; Holder, A. A.; Leatherbarrow, R. J.; Tate, E. W. *J. Med. Chem.* **2014**, *57,* 2773.

Chapter 2: Synthesis of indoles

2.1 Introduction

As described in Chapter 1, the proposed heterocyclic inhibitors should contain structurally important moieties and substituents that are theoretically essential for the inhibition of the peptide binding cavity of the enzyme *Pv*NMT. These substituents and their relative position on the heterocyclic core are important as these compounds have to fit into the pocket in such a manner as to have favorable interactions with the nearby amino acid residues.

Figure 13 illustrates the seven proposed indole-based compounds that we envisioned synthesizing. In order to synthesize these compounds, an ester group in the C2-position and an oxygen atom at the C4-position (phenoxy group) was needed with the intention of further derivatization to obtain the desired final compounds.

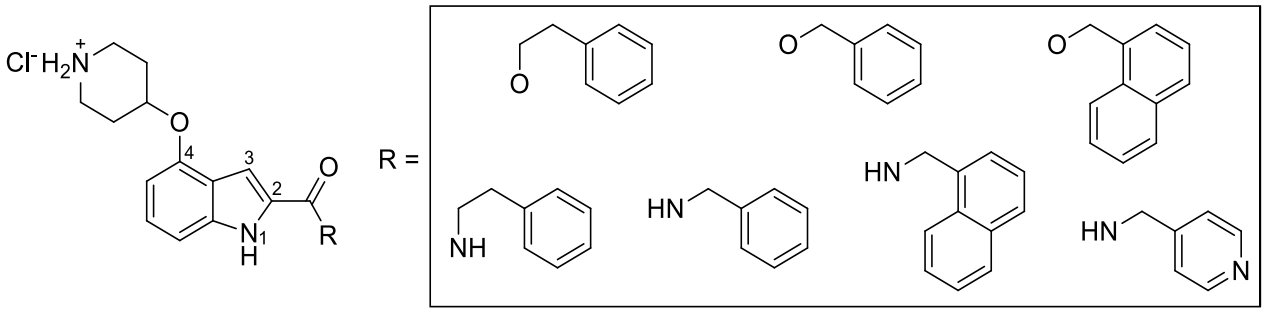

Figure 13: Proposed indole based compounds with various amides and esters to be synthesized

The ester group on the C2-position provides the necessary reactivity required to perform transesterification and amidation reactions that would deliver the desired libraries for each heterocyclic core. In addition, the oxygen at the C4-position of the indole provides a means to install a piperidinium chloride moiety.

This chapter will discuss the various methods used in order to achieve the most efficient route to synthesize the indole heterocyclic core given the particular challenges of working in geographically remote location (with respect to chemical delivery) and a reasonably restricted budget. Subsequently the multiple ways used for the required functional group transformations will be discussed, followed by the final deprotection step to obtain the final compounds to make up this library.

2.2 Synthesis of the indole scaffold

The synthesis of indoles can be divided into two distinct reaction types.[1] The first type revolves around intermolecular bond formation between an *ortho*-substituted aryl system and a second reactant to form the indole heterocycle. The coupling of *ortho*-substituted aryl systems to form indoles can also be subdivided into two broader categories; the first category employs the use of a transition-metal catalyst to facilitate ring closure while the second category uses more classical methods employing a base- or acid-catalyzed ring closure. Indole formation by way of a transition-metal catalyst includes the Larock,[2] Hegedus,[3] Mori-Ban,[4] Castro,[5] Ma[6] and Cacchi[7] indole syntheses which results in regiospecific ring closure. Classical synthesis includes the Madelung,[8] Reissert,[7] Furstner[9] and the Leimgruber–Batcho[8] indole syntheses.

The second type of indole construction involves the intramolecular bond formation of a mono-substituted aryl system. In this instance the ring closure is a result of direct bond formation between the aryl ring and the substituent. The most notable reactions includes the Fischer,[10] Bischler,[11] Bartolli,[12] Nenitzescu[13] and Hemetsberger-Knittel[14] indole syntheses. With these reactions, regioselectivity upon ring closure is controlled through the presence of an *ortho* or *para* substituent on the aryl ring. Due to the fact that the indole scaffold we proposed to synthesize had a tri-substituted aryl ring, we envisaged that synthesis of the indole scaffold by way of the second type of indole synthesis using intramolecular bond formation would be preferred.

Of the reactions listed above, it was decided that the Hemetsberger-Knittel indole synthesis would provide the best route to synthesize the desired indole scaffold containing a derivatizable oxygen atom at the C4-position and an ester group on the C2-position. The synthesis of 2-azido-3-arylacrylate for the use of indolization was first reported by Hemetsberger and Knittel in 1969.[15] The Hemetsberger indole synthesis was an attractive synthetic route as the formation of the indole scaffold occurred with the addition of thermal energy and therefore required no expensive catalysts. Furthermore, the Hemetsberger indole synthesis could be carried out in short reaction times. In order to utilize the Hemetsberger indolization reaction, the necessary 2-azido-3-aryl acrylate precursor had to first be synthesized. Once synthesized the acrylate could then undergo thermolysis leading to an intramolecular cyclization generating the indole scaffold, as shown in **Scheme 1**. When both proposed mechanisms were studied, it became evident that the azide-acrylate double bond had to be in the *Z*-configuration in order to facilitate ring closure to form the pyrrole ring. The mechanism for the Hemetsberger indolization is not entirely clear, but

it was postulated that it proceeds either via an azirine intermediate (Mechanism 1, **Scheme 1**) or an electrophilic nitrene species (Mechanism 2, **Scheme 1**).

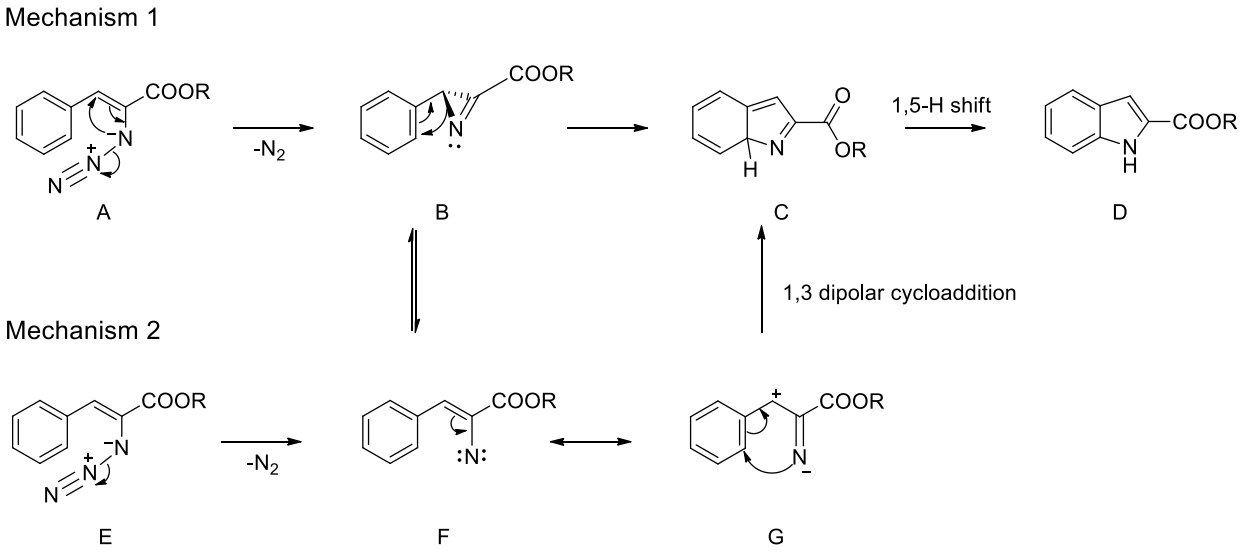

Scheme 1: The two proposed mechanisms involved in the Hemetsberger-Knittel indolisation reaction[15,16]

The first mechanism, postulated by Hemetsberger,[15,16] involves the formation of an azirine intermediate **B** by way of the thermal decomposition of the vinyl azide group **A** expelling nitrogen gas as byproduct. Due to the highly strained azirine ring, nucleophilic aromatic substitution occurs after which a 1,5-H shift results in rearomatization of the aryl ring to form the desired indole heterocycle **D**. The second mechanism involved the direct formation of a nitrene species in the singlet state **F** via the thermal cleavage of the azide group to form the electrophilic nitrene intermediate. Tautomerization of the vinyl π-electrons produce the ideneamide intermediate **G** after which a 1,3-dipolar cycloaddition produces intermediate **C** that undergoes the same 1,5-H shift to form the desired indole heterocycle **D**. It was postulated that the azirine **B** and nitrene **F** species could exist in an equilibrium.[17]

Two methodologies were followed to synthesize the desired α-azido-β-arylacrylate, these are:

1. The radical-mediated addition-elimination reaction of (*E*)-ethyl 3-(2-(benzyloxy)phenyl) acrylate with cerium ammonium nitrate and sodium azide, followed by a sodium acetate mediated elimination.
2. A base-promoted Knoevenagel condensation reaction between (2-benzyloxy) benzaldehyde with ethyl azidoacetate.

2.3 Cerium ammonium nitrate/sodium azide mediated azido-β-arylacrylate synthesis

Research conducted by Trahanovsky and co-workers[17] has shown that the reaction of olefins with sodium azide and cerium ammonium nitrate produced an α-azido-β-nitrato product. This work was then taken further by Nair *et al.* by converting various cinnamic esters to the corresponding α-azido-β-nitrato addition product, followed by a base-mediated elimination reaction which resulted in the formation of vinyl azides.[18]

This methodology was an attractive choice as the procedure allowed for the synthesis of the necessary α-azido-β-arylacrylate in order to obtain the indole scaffold via the Hemetsberger indolization. This required us to synthesize a cinnamic ester containing a protected oxygen on the aryl ring, which would in turn be converted into the analogous α-azido-β-aryl acrylate **B**. This would subsequently be subjected to thermolysis to produce the indole heterocycle **A**. **Scheme 2** illustrates the retrosynthetic approach with disconnection to synthesize the required indole scaffold.

The vinyl azide that has to be in the Z-configuration as stated earlier, would be synthesized from (*E*)-ethyl 3-(2-(benzyloxy)phenyl)acrylate, the ethyl cinnamate **C**, utilizing the CAN/NaN_3/base-mediated addition-elimination sequence. The ethyl cinnamate in turn would be synthesized from benzyl-protected salicylaldehyde **D** by means of a Horner-Wadsworth-Emmons reaction with the phosphonate **E**, ethyl 2-(diethoxyphosphoryl)acetate, to predominantly produce the required *E*-cinnamate. Benzylation was chosen as the preferred protection method for salicylaldehyde as it is an easy protecting group to introduce and remove using Pd/C in the presence of hydrogen gas.

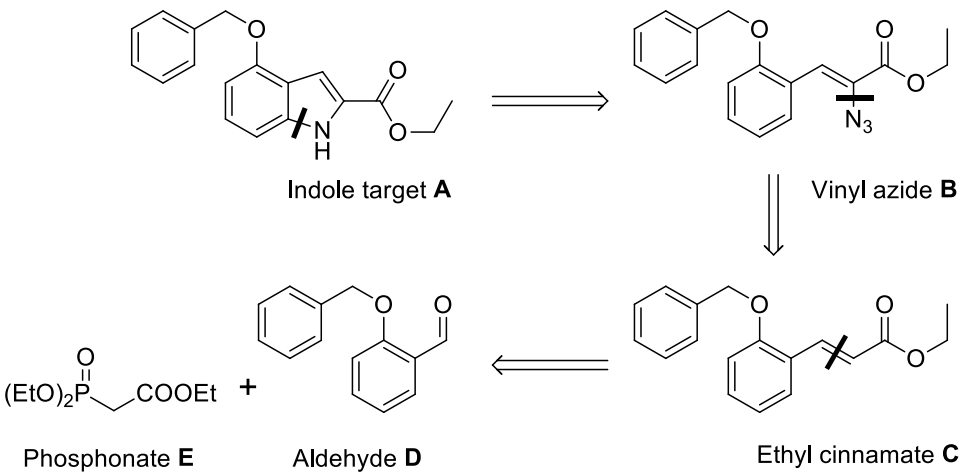

Scheme 2: Retrosynthesis of the indole target to the aldehyde starting compound

2.3.1 Horner-Wadsworth-Emmons olefination

The Horner-Wadsworth-Emmons reaction is the reaction between an aldehyde or a ketone with a phosphonate-stabilized carbanion that produces mainly alkenes with an *E*-configuration.[19] Phosphonates that contain an electron-withdrawing substituent α to the phosphonate group are stabilized phosphonates, as deprotonation of any α-CH protons results in the delocalization of the negative charge through the electron-withdrawing group, as well as the phosphonate. The phosphonate that we used was triethyl phosphonoacetate (ethyl 2-(diethoxyphosphoryl)acetate, (**Scheme 3**), a widely used phosphonate for the synthesis of *E*-ethyl cinnamates and substituted *E*-ethyl acrylates).[20,21] Triethyl phosphonoacetate **(4)** was synthesized by way of the Michaelis-Arbuzov reaction[22] between triethyl phosphite **(1)** and ethyl chloroacetate **(2)** in a 1:1 ratio by heating both components to 120 °C for 3 hours, and then at 170 °C overnight. **Scheme 3** shows the mechanism of the formation of **(4)**.

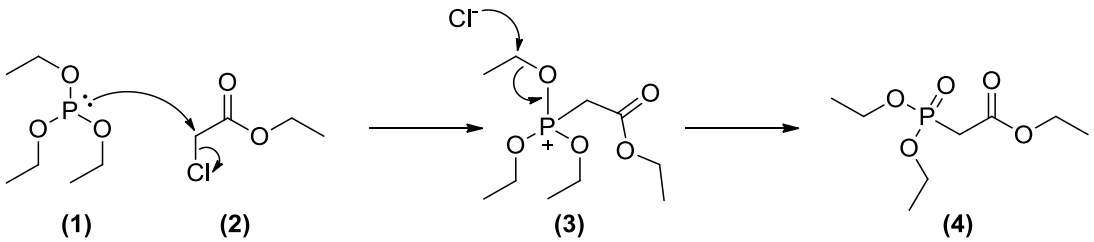

Scheme 3: Mechanism for the formation of triethyl phosphonoacetate **(4)** with triethyl phosphite **(1)** and ethyl chloroacetate **(2)**

Purification was achieved by distilling off **(1)** (boiling point: 156 °C) and **(2)** (boiling point: 143 °C) to obtain the phosphonate ester in a 35% yield. ^{1}H-NMR spectroscopy confirmed the formation of the phosphonate by the presence of a characteristic doublet appearing as a result of the ^{1}H-^{31}P coupling, measuring 21.6 Hz at 2.86 ppm. The spectral data corresponded well with data from literature.[23] Subsequently, salicylaldehyde **(5)** was reacted with benzyl bromide **(6)** in DMF, with K_2CO_3 as the base, to benzylate the phenolic hydroxyl group in a classical Williamson ether synthesis as shown in **Scheme 4**.

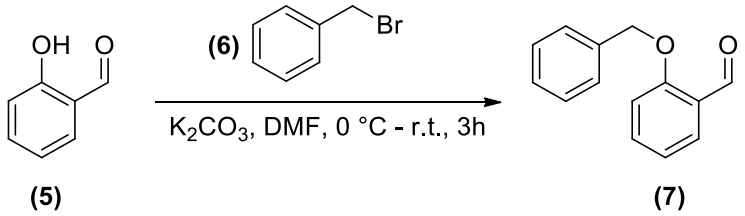

Scheme 4: Benzyl protection of salicylaldehyde **(5)** to afford **(7)**

DMF proved to be the superior solvent for this reaction with fast reaction times resulting in a high conversion, as yields ranged from 80% – quantitative. Initially, THF was used as a solvent and Na_2CO_3 as the base, but yields were consistently below 60%. With the method for benzylation optimized, we attempted to scale the reaction up. However, on a large scale (7g and up), column chromatography was not an effective method of purification. Purification of **(7)** was achieved through crystallization followed by washing the crystals with sufficient volumes of hexane to remove any traces of benzyl bromide. The ^{1}H-NMR spectrum of (2-benzyloxy)benzaldehyde indicated the distinctive aldehyde signal at 10.59 ppm and the benzyl methylene protons at 5.21 ppm confirming the protection of the phenolic hydroxyl group.

The Horner-Wadsworth-Emmons reaction between triethyl phosphonoacetate **(4)** and (2-benzyloxy)benzaldehyde **(7)** to form the required ethyl cinnamate, was performed in THF at 0 °C. The reaction mechanism is illustrated in **Scheme 5**.

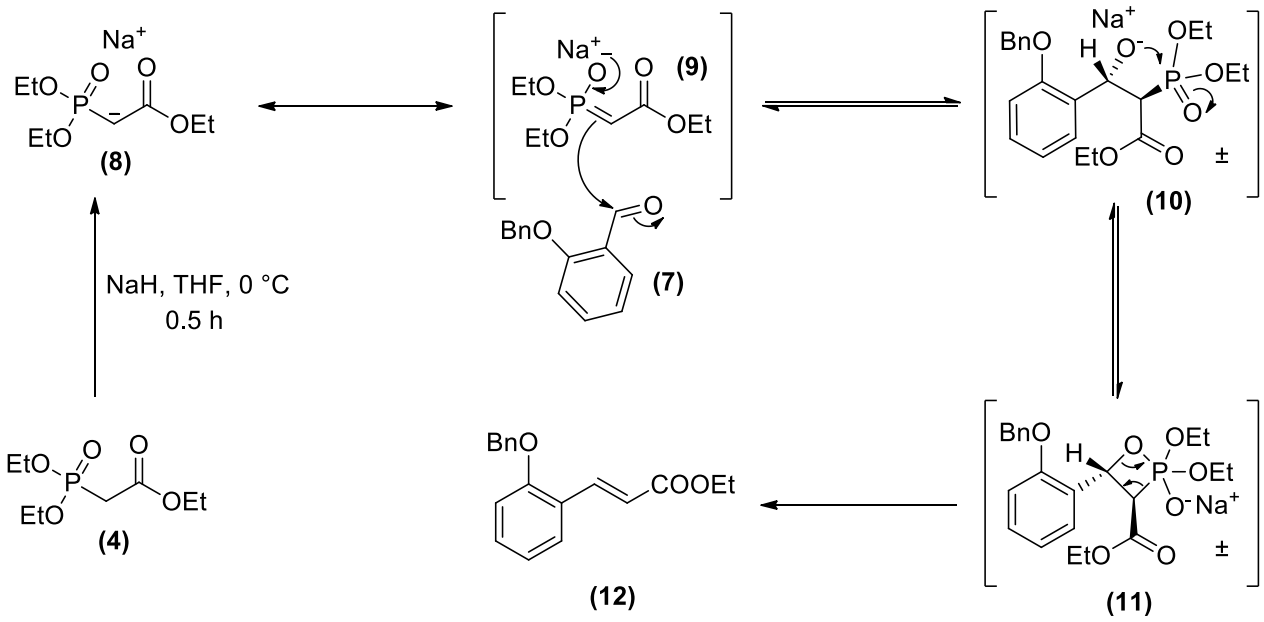

Scheme 5: Mechanism for the formation of (*E*)-ethyl 3-(2-(benzyloxy)phenyl)acrylate **(12)**

Sodium hydride was used as the irreversible base to form the triethyl phosphonoacetate carbanion **(8)** and **(9)** *in situ,* after which **(7)** was added, producing the newly C–C bonded intermediate **(10)**. The stereochemistry of **(10)** is due to steric approach control, where the aldehyde proton eclipses the bulky phosphonate group. Intramolecular nucleophilic attack of the alkoxide onto the phosphonate produced oxaphosphetane **(11)** which decomposes by a syn-cycloreversion process producing **(12)**. **(12)** And **(7)** had the same R_f value on TLC, thus it was difficult to determine whether the reaction had gone to completion. After leaving the reaction overnight followed by purification, it was evident that there was a full conversion of **(7)** to the desired ethyl cinnamate. ^{1}H-NMR spectroscopy confirmed the absence of any aldehyde signals, and the presence of the benzyl methylene signal which integrated for two protons, and the quartet and triplet, corresponding to the ethyl ester, which integrated for two and three protons respectively. The configuration of the *E*-double bond was confirmed when observing the ^{1}H-NMR spectrum as seen in **Figure 14**, where two distinct doublets are observed at 6.56 ppm and 8.11 ppm, indicated in the red rectangles. Both doublets had a ^{1}H-C – ^{1}H-C ^3J – coupling constant of 16.2 Hz, falling into the range of 12 – 18 Hz which is the typical coupling constant range of *trans*-alkenes.[24]

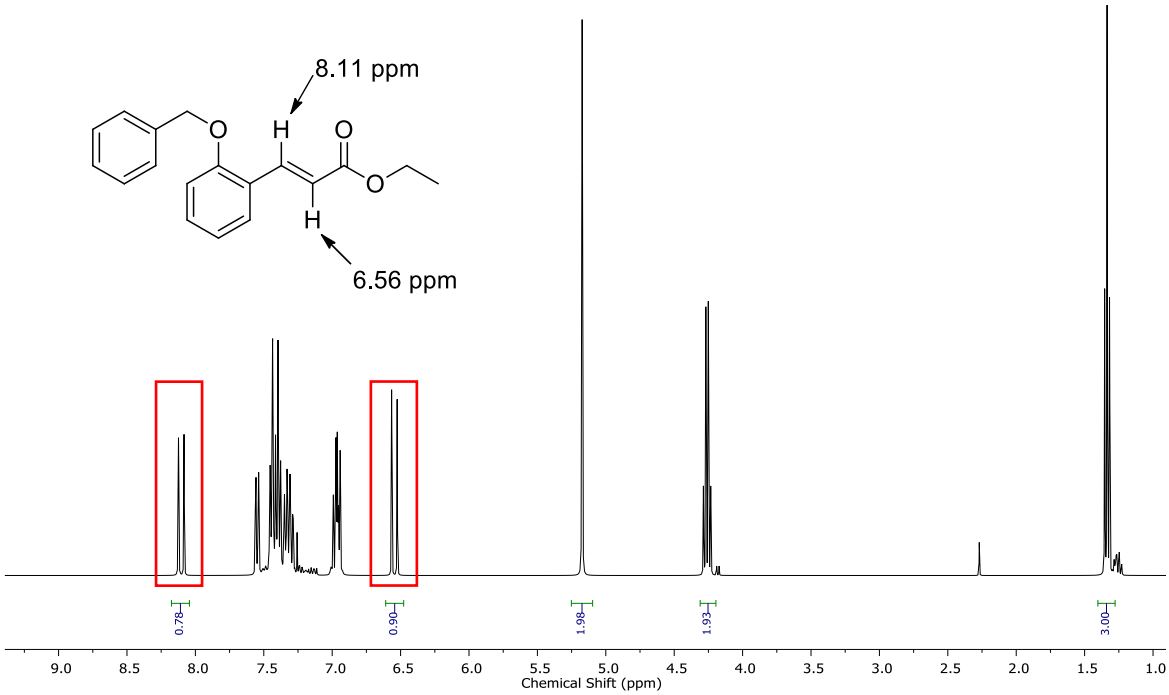

Figure 14: ^{1}H-NMR spectrum of (*E*)-ethyl 3-(2-(benzyloxy)phenyl)acrylate **(12)** in $CDCl_3$ indicating two doublets with coupling constants of 16.0 Hz at 6.65 ppm and 8.11 ppm.

2.3.2 CAN/NaN_3 addition, NaOAc mediated elimination

The reaction of cerium ammonium nitrate (CAN) and sodium azide (NaN_3) with aromatic acrylate esters to produce the desired α-azido-β-arylacrylate after treatment with sodium acetate has been widely reported in literature.[18,25,26] **Scheme 6** illustrates the reaction sequence to produce the desired α-azido-β-arylacrylate **(18)**. A solution of CAN in acetonitrile was added to a mixture of **(12)** and NaN_3 in acetonitrile under a nitrogen atmosphere at 0 °C and stirred for 12 hours. After workup the crude residue was dissolved in acetone and anhydrous sodium acetate was added to promote the elimination reaction. The formed azide cinnamate was purified and isolated giving a low yield of 22%.

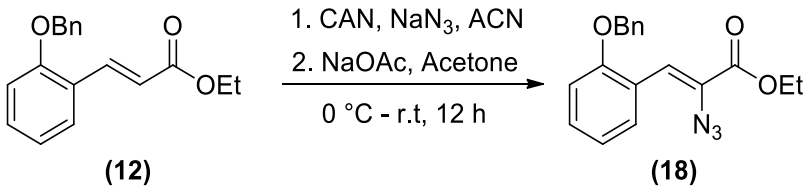

(12) **(18)**

Scheme 6: CAN/NaN_3/NaOAc mediated synthesis of **(18)**

^{1}H-NMR spectroscopy provided conclusive evidence for the formation of **(18)**. The characteristic doublets observed in **Figure 14** had disappeared, thus ^{1}H-C – ^{1}H-C ^3J – coupling was no longer observed. In addition, a new singlet at 7.55 ppm was observed, accounting for the vinylic proton *trans* to the azide. Only a single vinyl hydrogen was observed in the ^{1}H-NMR spectrum which confirmed that only one stereoisomer had been synthesized. **Figure 15** illustrates the ^{1}H-NMR spectrum of **(18)** indicating the vinyl proton in red and corresponding singlet in a red rectangle.

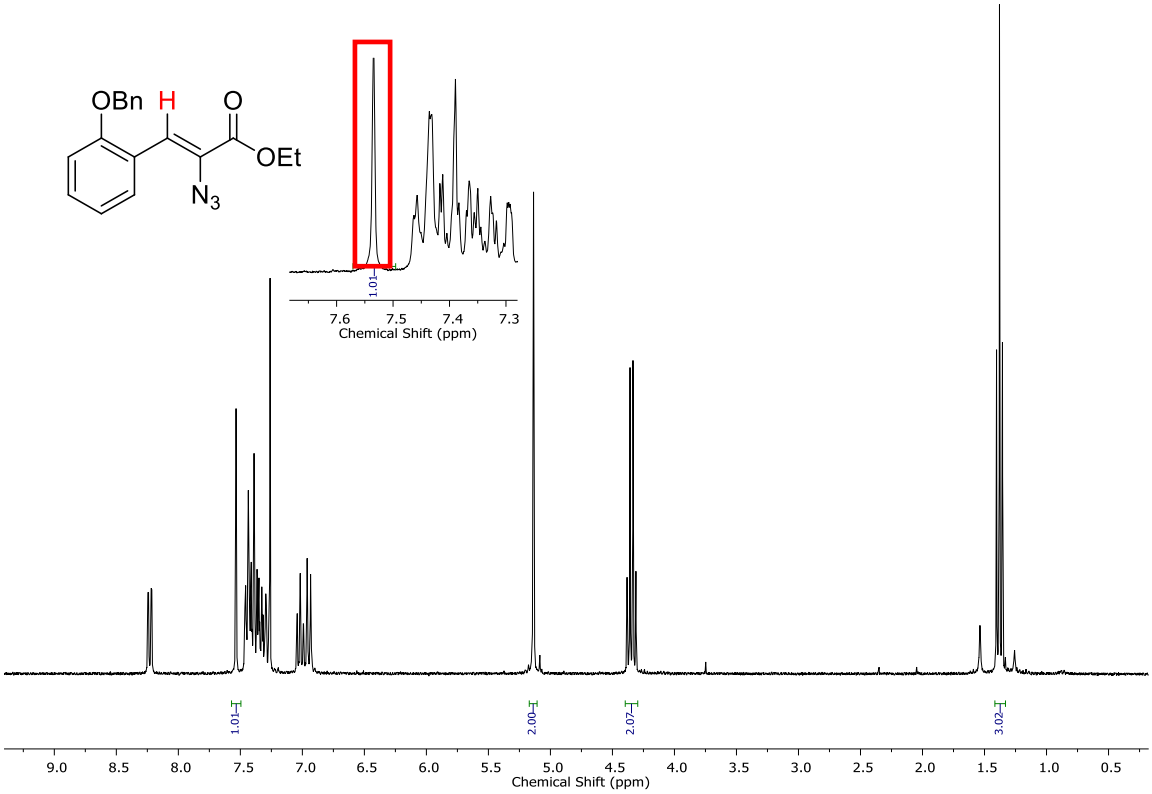

Figure 15: ^{1}H-NMR spectrum of (*Z*)-ethyl 2-azido-3-(2-(benzyloxy)phenyl)acrylate **(18)**

Scheme 7 illustrates the proposed mechanism for the radical-mediated addition of an azide and nitrato group to a model cinnamic ester.[18] CAN, a strong one electron oxidizing agent,[27] produced an azide radical **(14)** from an azide anion while being reduced from Ce(IV) to Ce(III) **(13)**. The addition of **(14)** to the double bond of **(12)** produced the azide bonded benzylic radical species **(15)**. CAN initiated the formation of a nitrato radical **(16)** which reacted with **(15)** to produce anti- and syn-addition α-azido-β-nitrato product **(17)**. An E1cB elimination facilitated by sodium acetate produced **(18)**.

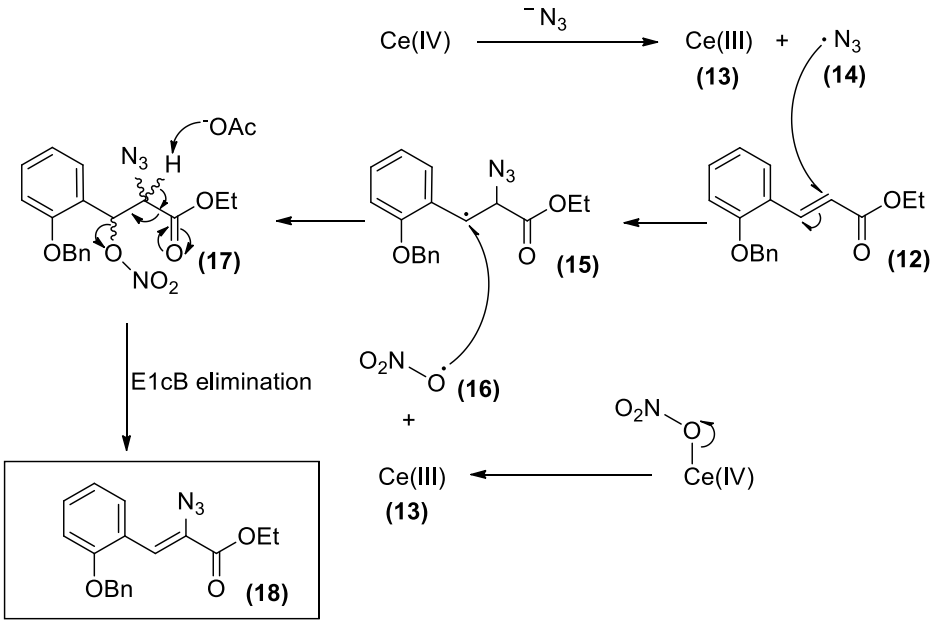

Scheme 7: Reaction mechanism for the radical-mediated addition of an azide/nitrato group, followed by the base promoted elimination to produce **(18)**

2.4 Knoevenagel condensation to produce the α-azido-β-arylacrylate

Due to the low yielding nature of the cerium ammonium nitrate/sodium azide mediated α-azido-β-arylacrylate synthesis, we decided to pursue other methods for synthesizing **(18)**. Furthermore, the reaction setup was tedious and the reaction times were long.

The Knoevenagel condensation reaction, discovered by Emil Knoevenagel[28] involved the coupling reaction of an aldehyde or ketone with an enolizable group, i.e. an ester, carboxylic acid or malonic derivative to produce a newly formed carbon–carbon double bond.[29] Due to the fact that the reaction was performed in basic media, dehydration occurred and therefore the final product

was an α,β-unsaturated carbonyl (**Scheme 8**). We discovered numerous examples in the literature where the Knoevenagel condensation reaction was employed in order to obtain α-azido-β-arylacrylates using an alkyl azidoacetate.[30-34] The main drawback of this synthetic procedure as a means to produce indoles was the reported inconsistent and low yields obtained during the Knoevenagel condensation. The reaction was usually performed in ethanol (or methanol) as the solvent, with sodium ethoxide (or sodium methoxide) as the base, to promote enolization of the alkyl azidoacetate to facilitate nucleophilic attack on the aldehyde or ketone respectively. **Scheme 8** illustrates the reaction mechanism for the condensation between **(7)** and ethyl azidoacetate **(19)** to produce **(18)**. For simplicity, the sodium counterion has been omitted.

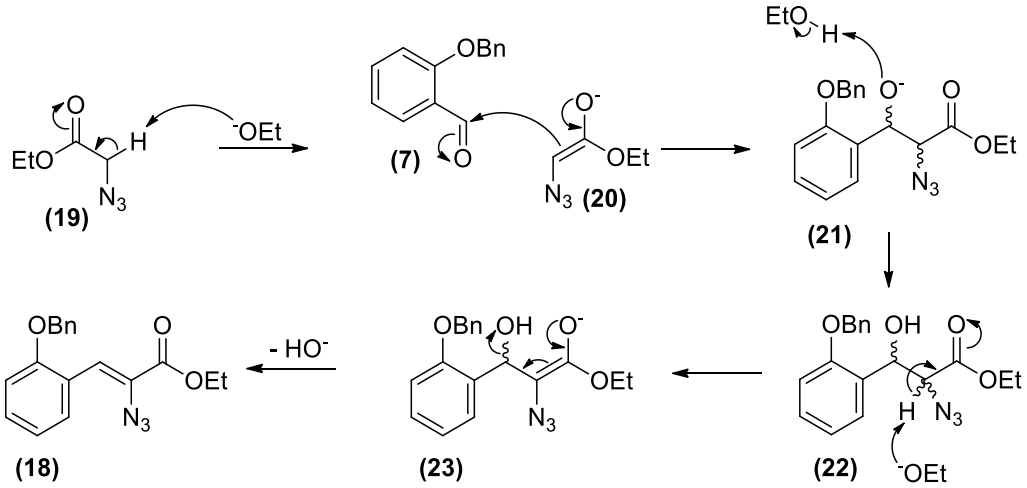

Scheme 8: Mechanism of the Knoevenagel condensation to produce **(18)**

Sodium ethoxide facilitated enolization of **(19)** to form enolate **(20)**, which reacted with **(7)** to produce the azido alkoxide intermediate **(21)**. Protonation of **(21)** resulted in the formation of the azido alcohol **(22).** The subsequent dehydration step, an E1cB elimination, involved the deprotonation of **(22)** to produce the vinyl azide intermediate **(23)**, which after dehydroxylation afforded **(18)** and sodium hydroxide as a byproduct. As stated previously, low yields have been reported for the Knoevenagel condensation reaction with alkyl azidoacetates to synthesize α-azido-β-arylacrylates. The low yield can be explained by the presence of the free hydroxide ion in solution which has the ability to hydrolyze the ester groups of **(19)**, the intermediate vicinal azido alcohol **(22)** as well as the product **(18)**. Research conducted by Liotta and co-workers[35] found a route to overcome this issue with the addition of a reactive sacrificial electrophile, ethyl trifluoroacetate (ETFA). This is illustrated in **Scheme 9**. The *Z*-stereoselectivity of the reaction could be explained by density functional theory calculations carried out by Liotta and co-workers.

They have confirmed that the energy of the transition state that results in the formation of the *Z*-isomer is lower than that of the *E*-isomer, and that the thermodynamic stability of the Z-isomer differs by 6.86 kcal/mole compared to the *E*-isomer.

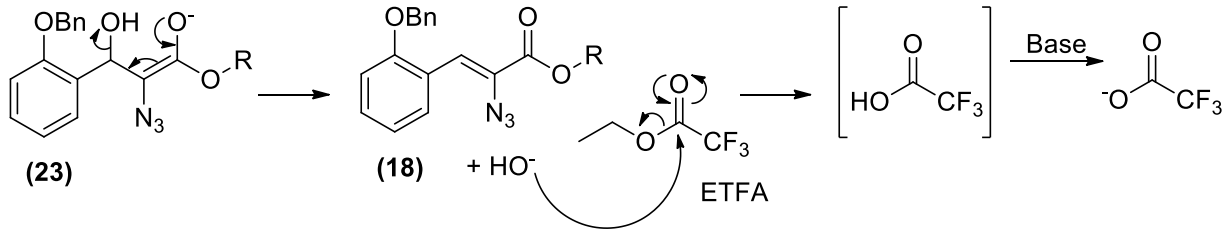

Scheme 9: Ethyltrifluoroacetate (ETFA) acting as sacrificial electrophile

The addition of a sacrificial electrophile reacts with the free hydroxide ion in solution, thereby hindering the formation of byproducts. The hydrolysis of ethyl trifluoroacetate in solution by way of the hydroxide ion facilitates the release of sodium ethoxide, the base used in the reaction. We decided to employ the improved method described by Liotta to synthesize **(18)** as illustrated in **Scheme 10**.

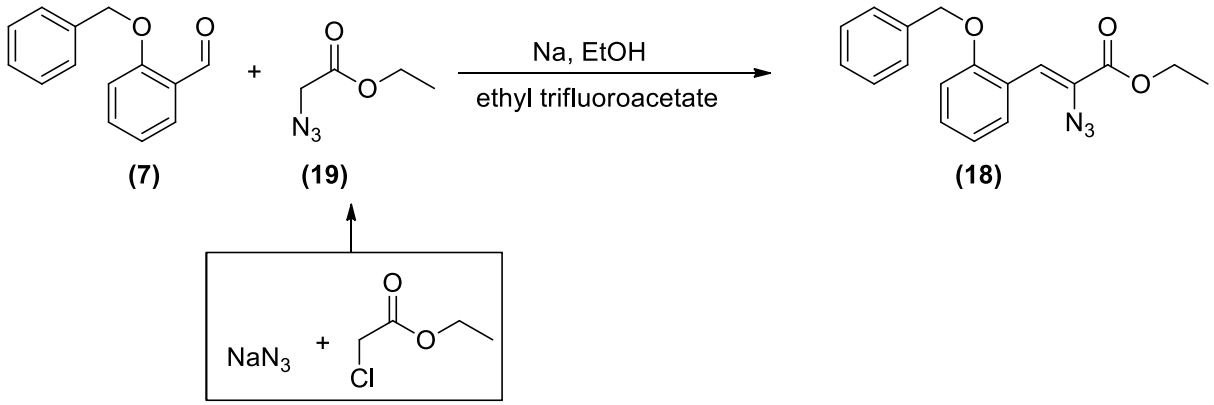

Scheme 10: Knoevenagel condensation to produce **(18)**

Ethyl azido acetate **(19)** was synthesized by reacting ethyl chloroacetate with sodium azide (shown in box) in a solution of water/acetone for 24 hours to produce **(19)** in a 55% yield after workup. The purity of **(19)** was determined by ^{1}H-NMR spectroscopy to ascertain whether any ethyl chloroacetate was still present in the product. A singlet at 3.81 ppm was observed integrating for two protons, confirming the complete substitution of the chloro group to an azide; in addition, there was no singlet present at 4.07 ppm that corresponded to the methylene bridge of ethyl chloroacetate.

The Knoevenagel condensation was carried out in anhydrous ethanol that was freshly distilled from iodine and magnesium turnings under nitrogen. 1.5 Equivalents of sodium metal was then added to the ethanol. The modified procedure[35] required that all the reactants be added in one aliquot to the sodium ethoxide solution at 0 °C, using 1.5 equivalents of ethyl trifluoroacetate and ethyl azidoacetate as well as 1.0 equivalent of **(7)**. When the reaction was carried out according to the literature procedure, we observed a low conversion of **(7)** into what was suspected to be **(18)**. After workup with EtOAc and ammonium chloride, the crude product was purified using column chromatography. Unfortunately **(18)** and **(7)** both had similar R_f values which made purification over silica gel difficult. However, the synthesis of **(18)** was achieved and confirmed by ^{1}H- and^{13}C-NMR spectroscopy. The NMR spectral data corresponded well with previous NMR spectra obtained when carrying out the CAN/NaN_3/NaOAc mediated synthesis of **(18)**. Disappointingly, the improved reaction procedure reported by Liotta afforded **(18)** in a low yield of 33%.

A slight adjustment to the procedure proved to be beneficial as we were able to obtain higher yields of the desired product. The initial procedure called for the addition of all the reagents in one aliquot; however, keeping the equivalents of the reagents the same, we decided to add the ethyl azidoacetate last to the solution of sodium ethoxide, trifluoro ethylacetate and **(18)** at -10 °C, where the final concentration of sodium ethoxide was 1.34 M. This caused a slight precipitate to form in the solution shortly after the addition of ethyl azidoacetate. It was essential to keep the reaction between -10°C – 0 °C, as higher temperatures caused the yellow solution to turn red, which indicated that decomposition of the product had occurred. The precipitate proved to be the product **(18),** and monitoring the reaction by TLC analysis revealed a full conversion of **(7)** to **(18)** in as little as 2 hours. The product was filtered off and dried under vacuum to produce **(18)** in analytically pure form. With this adjusted method a maximum of 66% yield was obtained – approximately double the yield of the previous methods.

The more reasonable yield obtained indicated that the mother liquor of the Knoevenagel condensation reaction still contained a sizable amount of **(18)** as the filtered off product yield ranged between 55% – 66%, despite a full conversion having been observed by TLC. Extraction of the remaining product with EtOAc and ammonium chloride solution proved to cause degradation as multiple spots on TLC were visible afterwards. Purification by way of column chromatography also proved to be difficult as **(18)** co-eluted with one of the degradation byproducts. The byproduct was collected and ^{1}H-NMR spectroscopy indicated that it was

compound **(7)**, which suggested that **(18)** was not chemically stable in aqueous media and hydrolyzed back to the aldehyde.

We also attempted to purify **(18)** on silica gel using column chromatography without carrying out the workup mentioned previously. However, the formation of **(7)** was also observed in the columned fractions, as observed via NMR spectrsoscopy. Hence the Knoevenagel condensation reaction proved to be very efficient in the formation of **(18)** in relatively quick reaction times, but degradation to the aldehyde **(7)** was observed when treated with aqueous media or purification over silica gel.

2.4.1 Hemetsberger indolization

The Hemetsberger indolization reaction (**Scheme 11**) was carried out by adding **(18)** to toluene under reflux to produce the desired indole **(24)** in a 70% yield, as reported in the literature.[36,37]

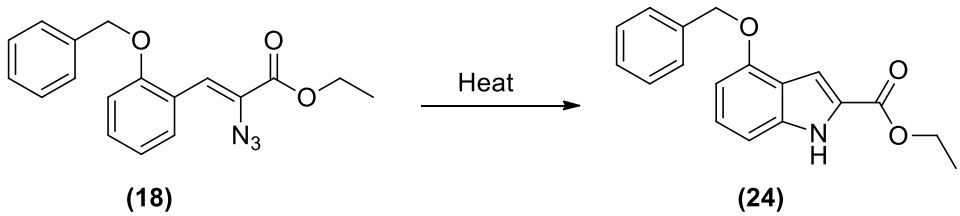

(18) **(24)**

Scheme 11: Hemetsberger indolization of **(18)** to form the indole heterocycle **(24)**

Despite a yield of 70%, the formation of byproducts was still observed. DSC experiments carried out by Liotta and co-workers[35] on a multitude of synthesized α-azido-β-arylacrylates have indicated two distinct exothermic events. The first exothermic event at temperatures ranging between 129.0 °C – 139.4 °C was associated with the formation of the azirine intermediate (or potentially the formation of the nitrene intermediate as previously discussed). The second exothermic event, at temperatures ranging between 154.6 °C – 166.3 °C, was due to cyclization leading to the formation of the indole heterocycle. The reaction was optimized by changing the solvent to 1,3-dichlorobenzene, and increasing the temperature to 160 °C. The dropwise addition of **(18)**, dissolved in 1,3-dichlorobenzene, to 1,3-dichlorobenzene preheated to 160 °C, caused the immediate evolution of nitrogen gas in the reaction mixture. The conversion of **(18)** to **(24)** was rapid, as the formation of the indole product was completed in less than 5 minutes after the addition of **(18)** when monitored by TLC. The reaction conditions using 1,3-dichlorobenzene proved superior to refluxing toluene as, in this instance, the formation of byproducts was not

observed and a full conversion of **(18)** to **(24)** was indicated via TLC analysis. As a result, yields ranged between 87% and 95%. The formation of **(24)** was confirmed by ^{1}H- and^{13}C-NMR spectroscopy in addition to HRMS which confirmed the molecular ion as calculated. In addition, IR spectroscopy indicated a strong band at 3321 cm^{-1}, indicative of the indole N-H stretching frequency, and notably the absence of a band at 2118 cm^{-1} that would have corresponded to an azide stretch.

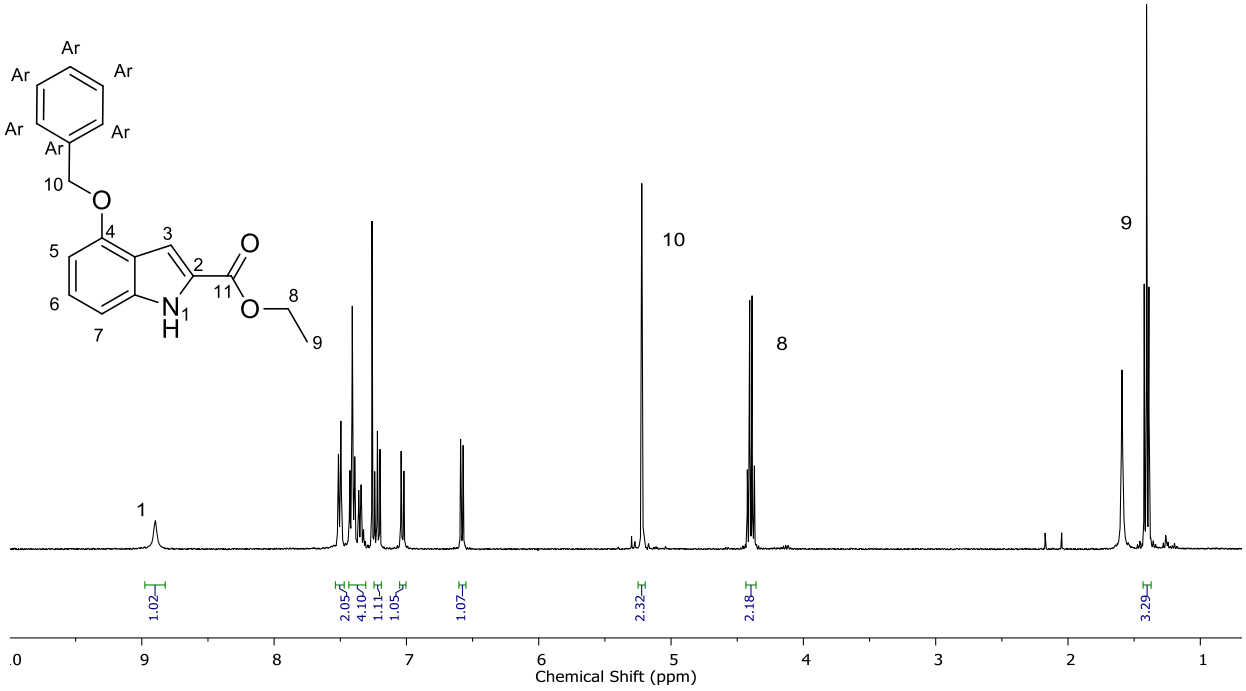

Figure 16:^{1}H-NMR spectrum of **(24)** in $CDCl_3$

The ^{1}H-NMR spectrum of **(24)** is illustrated in **Figure 16**. The characteristic indole N-H proton can be observed as a broad signal at 8.95 ppm. The ethyl ester could unambiguously be assigned by the expected triplet **9** at 1.41 ppm, which integrated for three protons, and a quartet **8** at 4.41 ppm, which integrated for two protons (**Figure 16**). The benzylic methylene protons **10** appeared at 5.22 ppm as a singlet, and integrated for two protons. **Figure 17** illustrates the aromatic proton signals.

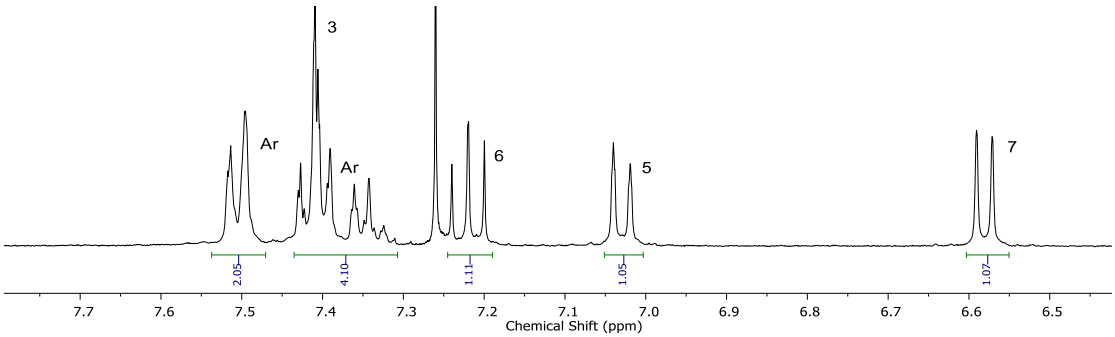

Figure 17: ^{1}H-NMR spectrum of the aromatic region of **(24)**

We suspected that the doublet between 6.57 – 6.61 ppm could be assigned to proton **7**, since the indole N-H is *ortho* to carbon **7** which due to the resonance effect of the nitrogen lone pairs, would increase electron density on carbon **7**. This would cause a greater shielding effect on proton **7**, resulting in the upfield appearance of the doublet. The doublet between 7.01 – 7.04 ppm could subsequently be assigned to proton **5**. The same deshielding effect of the oxygen atom *ortho* to carbon **5** would also result in the doublet appearing more upfield, but in a lesser extent compared to **7** as the resonance effect of the indole N-H would be more prominent. The doublet of doublets (appearing as a triplet) between 7.20 – 7.24 ppm could unambiguously be assigned as proton **6**. The remainder of the aromatic signals, annotated as Ar, integrated for six protons, which included the five aromatic protons belonging to the benzyl group, as well as proton **3**. It is suspected that proton **3** is at 7.41 ppm.

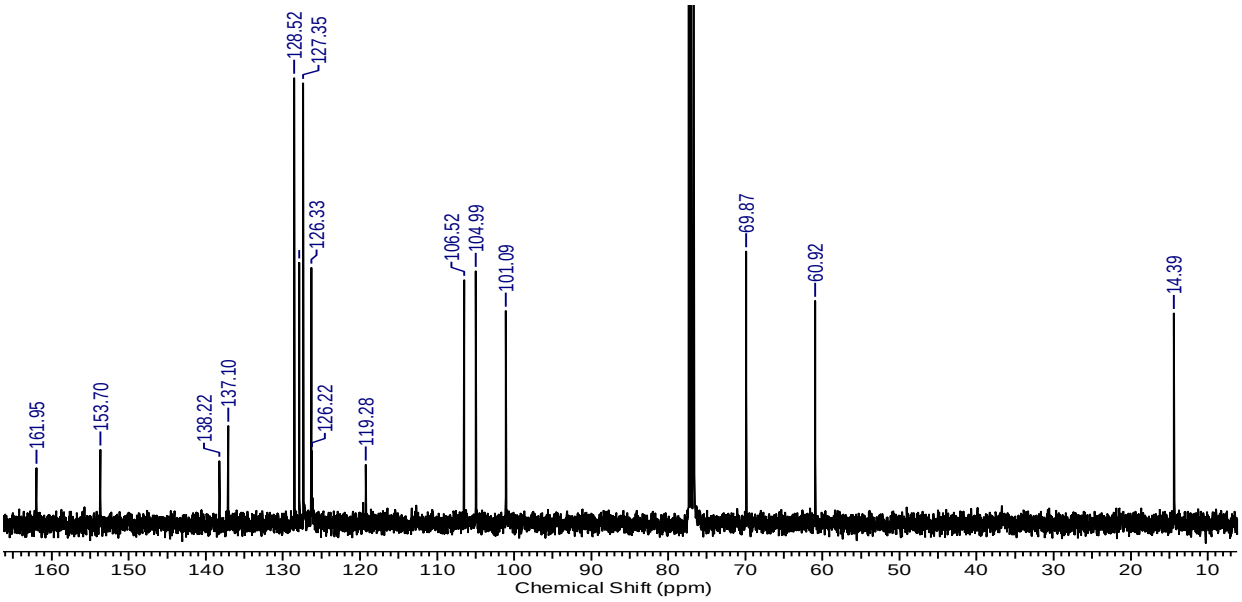

Figure 18: ^{13}C-NMR spectrum of **(24)**

Figure 18 illustrates the ^{13}C-NMR spectrum of **(24)**. The spectrum indicated that all the expected carbons were accounted for. The expected aliphatic carbons associated with the ethyl ester, **8** and **9**, and benzylic methylene **10** appeared at 14.4 ppm, 60.9 ppm and 69.9 ppm. The signals at 101.1 ppm, 105.0 ppm and 106.5 ppm could be assigned to carbons **7**, **5** and **3** respectively. The shifts are attributed to the resonance effect of the oxygen atom *para* and the indole nitrogen *ortho* to **7**, as well as the oxygen atom *ortho* and the indole nitrogen *para* to **5**. The chemical shift of **3** could be explained by the resonance effect of the indole nitrogen through the pyrrole ring. The signal at 162.0 ppm could be assigned to carbon **11**, and the signal at 153.7 ppm to carbon **4**. Due to the increased intensity of the signals at 127.4 ppm and 128.5 ppm, it was possible to deduce that each signal corresponded to the two pairs of chemically equivalent carbons on the benzyl group.

2.5 Derivatization of ethyl 4-(benzyloxy)-1*H*-indole-2-carboxylate (24)

2.5.1 Derivatization of the ester functional group

We envisaged that derivatization of the ester at the C2-position to the various proposed benzylic esters and amides could be facilitated via a carbonyldiimidazole (CDI) coupling reaction. CDI is a versatile coupling reagent, providing the effective coupling of alcohols and amines to various nucleophiles such as amines, alcohols and carboxylic acids to produce esters, amides, ureas and mixed or symmetrical anhydrides.[38] Our proposed synthetic strategy, as seen in **Scheme 12,** was to hydrolyze the ester to the corresponding carboxylic acid, which would subsequently be reacted with CDI to produce the imidazole acid derivative. Imidazole is a good leaving group with a pKa of 7.05 for the conjugate acid,[39] thus any nucleophilic attack of an alcohol or amine on the electrophilic imidazoyl carbonyl would favour the formation of either the ester or the amide respectively.

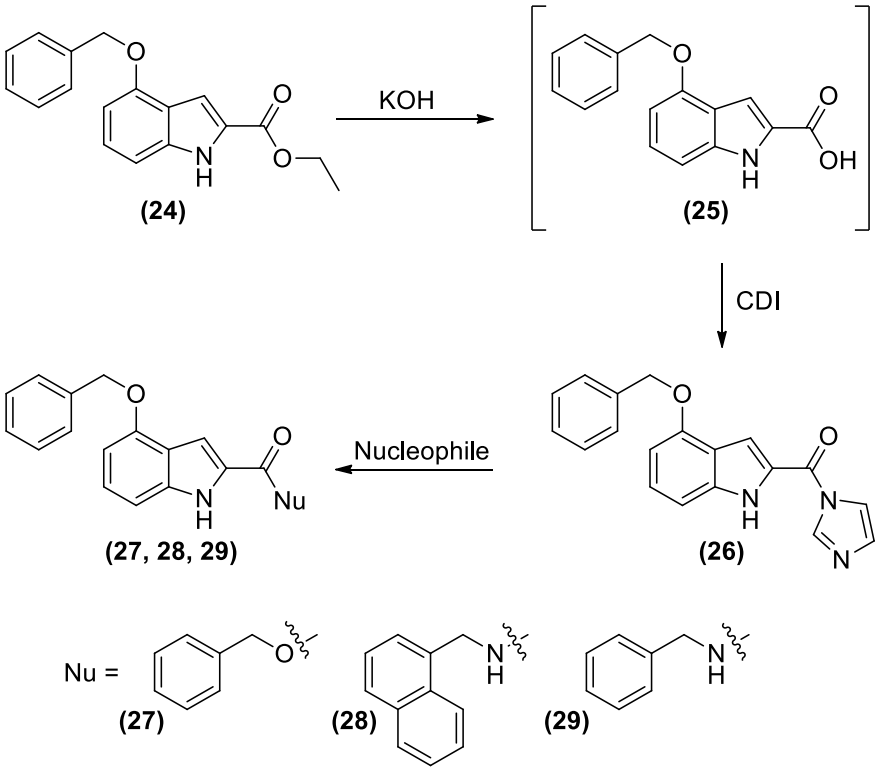

Scheme 12: CDI-mediated coupling of nucleophiles to **(26)**

This provided an effective method to synthesize the various amides and esters envisioned as seen in **Figure 13**. Hydrolysis of **(24)** to the corresponding acid was carried out in ethanol with the addition of four equivalents of KOH and was heated to 70 °C for two hours. After acidification, the product was extracted and concentrated to provide the carboxylic acid. The intermediate indole acid was dissolved in THF to which was added CDI, pre-dissolved in THF. The evolution of a gas was observed, indicating that the acid was reacting with CDI producing CO_2, as illustrated by the mechanism in **Scheme 13.** Monitoring the reaction by means of TLC showed the carboxylic acid **(25)** on the baseline diminishing and **(26)** forming. Purification and subsequent ^{1}H- and ^{13}C-NMR spectroscopy together with HRMS analysis proved the formation of **(26)**. Three extra singlets in the aromatic region at 7.23 ppm, 7.75 ppm and 8.45 ppm was observed, confirming the addition of an *N*-substituted imidazole group proving that the acid was converted into **(26)**.

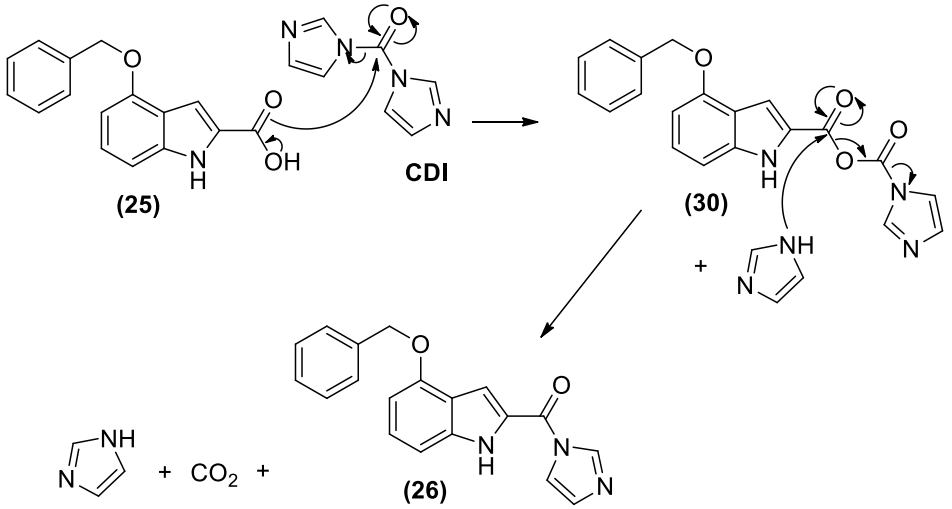

Scheme 13: Abbreviated mechanism for the formation of **(26)**

The reaction of **(26)** with benzyl alcohol in THF to produce the benzoate ester was attempted first. The nucleophilicity of benzyl alcohol proved to be less than desirable as the coupling between **(26)** and benzyl alcohol was slow, even at elevated temperatures. Converting benzyl alcohol into sodium benzyloxide with NaH in THF proved to increase the nucleophilicity. The desired benzoate ester **(27)** was isolated in a 40% yield. The reaction of **(26)** with 1-naphthyl methylamine and benzylamine to produce amides **(28)** and **(29)** proved to be more successful as the amidation reaction occurred readily at room temperature without the aid of a strong base to increase the nucleophilicity of the amines. **(28)** And **(29)** were isolated in 68% and 76% yields respectively and **(27)**, **(28)**, and **(29)** were fully characterized. The appearance of two benzyl methylene peaks at 5.21 ppm and 5.39 ppm was confirmation of the esterification of **(7)** to **(27)**, in addition, the aromatic signals integrated for 14 protons. The formation of **(28)** was confirmed by ^{1}H-NMR spectroscopy due to the amide N-H proton appearing as a broad triplet at 6.39 ppm with a coupling constant of 5.1 Hz. This was due to the amide proton coupling to the benzylic methylene protons. The appearance of a doublet at 5.14 ppm, which integrated for 2 protons with a coupling constant 5.5 Hz, was indicative of the benzylic methylene protons coupling to the amide proton. Similar signals were observed for compound **(29)**, with a doublet at 4.69 ppm (benzyl methylene protons) and a broad triplet at 6.44 ppm (amide N-H proton).

2.5.2 Derivatization of the 4-phenoxyposition on the indole

We foresaw a logistical problem in derivatizing the ester group first followed by derivatization of the 4-phenoxy group. We required the insertion of 1-Boc-4-hydroxypiperidine at the C4-position throughout the series of compounds we wanted to make. Derivatizing the ester group first, followed by debenzylation and subsequent coupling of 1-Boc-4-hydroxypiperidine at the C4-position would increase the number of reactions threefold. We decided to derivatize the phenol group first, followed by derivatization of the ester. **Scheme 14** illustrates the synthetic route that was followed to synthesize the *N*-Boc piperidine coupled indole **(33)**.

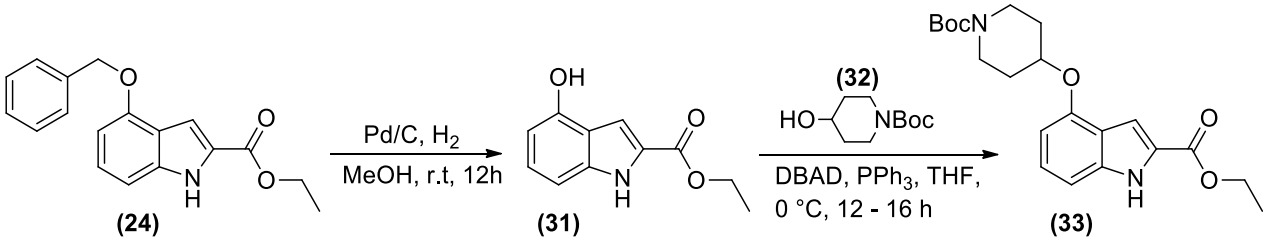

Scheme 14: Debenzylation of **(24)** and Mitsunobu coupling of **(31)** to produce **(33)**

The debenzylation of **(24)** with carried out with 10% Pd/C under 1 atmosphere of hydrogen gas in methanol. The conversion of **(24)** into the indole phenol **(31)** was obtained in an 87% yield after purification. Analysis of the ^{1}H-NMR spectrum displayed the absence of the benzyl methylene signals; in addition, only four aromatic signals were observed, each integrating for one proton relative to the ethyl protons. A broad signal at 5.23 ppm was indicative of a phenolic proton.

A Mitsunobu reaction was carried out in order to couple **(31)** with 1-Boc-4-hydroxypiperidine **(32)**. The Mitsunobu reaction was a coupling reaction discovered by Mitsunobu and Yamada[40] that involved the dehydrative coupling of an alcohol with various pro-nucleophiles. Suitable pro-nucleophiles include carboxylic acids, phenols, thiocarboxylic acids, thiophenols, sulfonamides and imides, resulting in the formation of esters, phenolic ethers, their respected thio counterparts or alkylated sulfonamides and imides.[40,41,42] The Mitsunobu reagents necessary for the reaction are triphenylphosphine and various dialkyl azodicarboxylates which include diethyl azodicarboxylate (DEAD), diisopropyl azodicarboxylate (DIAD) and di*tert*-butyl azodicarboxylate (DBAD).[42] In the case of coupling chiral secondary and occasionally tertiary alcohols, complete inversion of stereochemistry is observed.[42,44] As seen in **Scheme 15**, all the steps involved in the mechanism are reversible, except the final irreversible step involving the oxidation of triphenylphosphine to triphenylphosphine oxide.

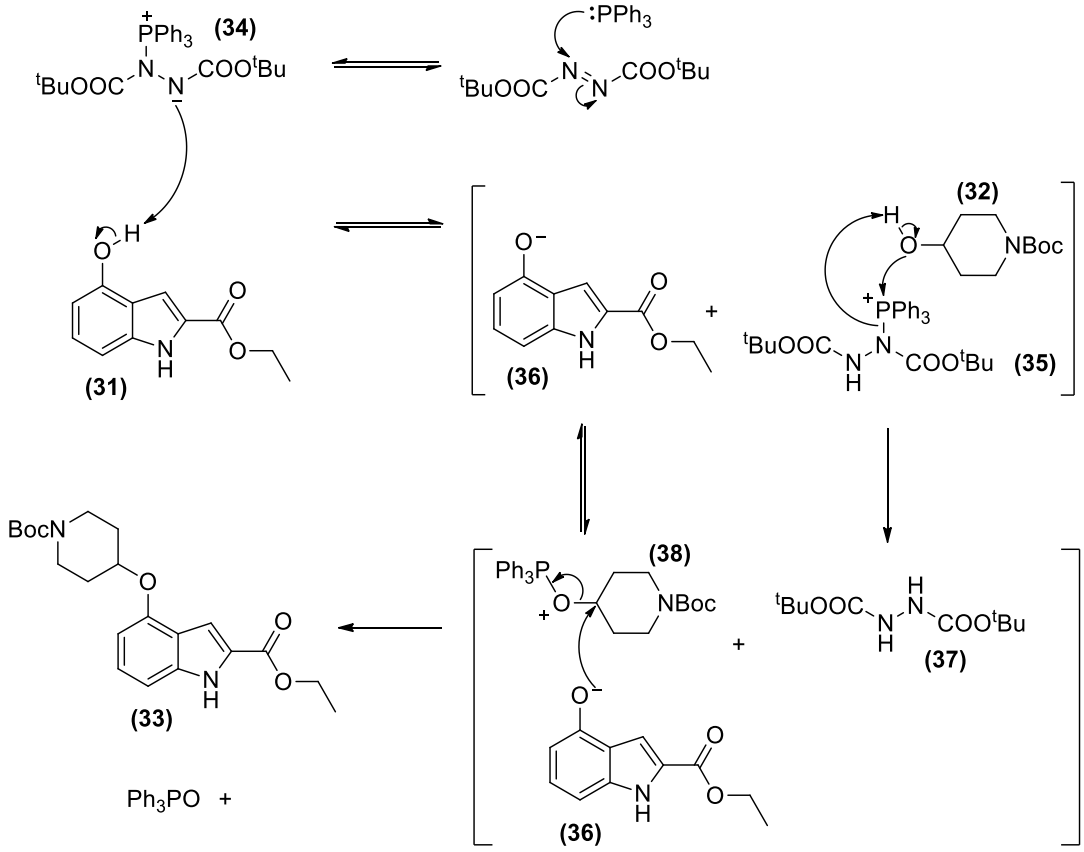

Scheme 15: Mechanism for the formation of **(33)** via the Mitsunobu reaction

The first step involved the nucleophilic attack of the phosphine lone pair on the electrophilic azo group of DBAD. This resulted in the formation of the betaine intermediate **(34)**, which facilitated the deprotonation of the phenolic proton of **(31)** due to the basicity of the resulting negative charge, to produce phenoxide **(36)**. Phosphonium intermediate **(35)** was subsequently attacked by **(32)** to produce the oxyphosphonium intermediate **(38)**. The nucleophilic attack of **(36)** on **(38)** lead to the oxidation of the oxyphosphonium species, producing triphenylphosphine oxide and resulted in the final coupled product **(33)**.

The initial procedure that we followed reported by Leatherbarrow and co-workers[43] used 2.5 molar equivalents of DBAD, PPh_3 and **(32)** relative to the phenolic compound. We attempted these conditions at first, and due to the efficiency of the Mitsunobu reaction, complete conversion of **(31)** to **(33)** was observed when monitored by TLC analysis. We however decided to decrease the molar equivalents of DBAD, PPh_3 and 1-Boc-4-hydroxypiperidine to a minimum of 1.5 equivalents, due to the fact that 2.5 molar equivalents is considerably less atom efficient. 1.5

Molar equivalents however increased the reaction time, but a full conversion was still achieved within 12 – 16 h.

Purification of **(33)** proved problematic as the R_f values of **(33)** and the hydrazine byproduct **(37)** were quite similar. This posed a problem as repeated purification steps of co-eluted fractions by column chromatography diminished the overall yield. As a way around this problem we proposed altering the R_f value of **(33)** by carrying out a Boc-protection of the indole nitrogen, as seen in **Scheme 16**. This decreased the polarity significantly, which altered the R_f value allowing effective purification of compound **(39)** by way of column chromatography.

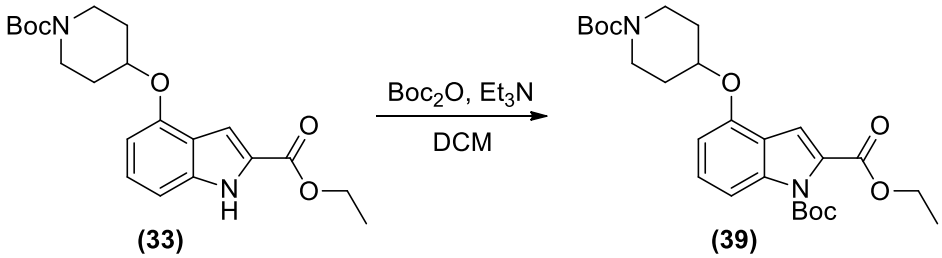

Scheme 16: Boc-protection of **(33)** to form **(39)**

Subsequent reactions to synthesize **(39)** were carried out by carrying out the Mitsunobu reaction until complete conversion of **(33)** was observed via TLC, followed by a pseudo purification step utilizing column chromatography to isolate **(33)**, as well as the co-eluted hydrazine byproduct. The mixture was then treated with Boc_2O in DCM and triethylamine to produce **(39)** in 95% yield over two steps. This high yield could be explained by the fact that the Mitsunobu and Boc-protection reactions are effective and frequently quantitative in nature. ^{1}H-NMR spectroscopy of **(39)** confirmed the successful conversion of **(31)** into **(39)** as seen in **Figure 19.**

The ^{1}H-NMR spectrum of **(39)** provided conclusive proof of the successful Mitsunobu coupling reaction with 1-Boc-4-hydroxypiperidine, as well as the addition of a Boc-group on the indole nitrogen. The two *tert*-butyl signals at 1.47 ppm and 1.61 ppm were observed which corresponded to the presence of both Boc-groups.The absence of the broad signal indicative of the indole N-H previously appearing at 8.95 ppm also confirmed the addition of the Boc-group, while the absence of the phenolic broad signal at 5.23 ppm was confirmation that the Mitsunobu reaction was successful. Interestingly, a multiplet a 4.65 ppm appearing as a septet was anomalous. The proton on the tertiary carbon of the piperidine ring was expected to have the multiplicity of a quintet, yet appeared as a septet. It is plausible that the proton is in different chemical

environments accounting for the greater multiplicity. It is important to note that this cannot be a true septet. The piperidine ring has a bulky Boc group on the nitrogen, and a bulky

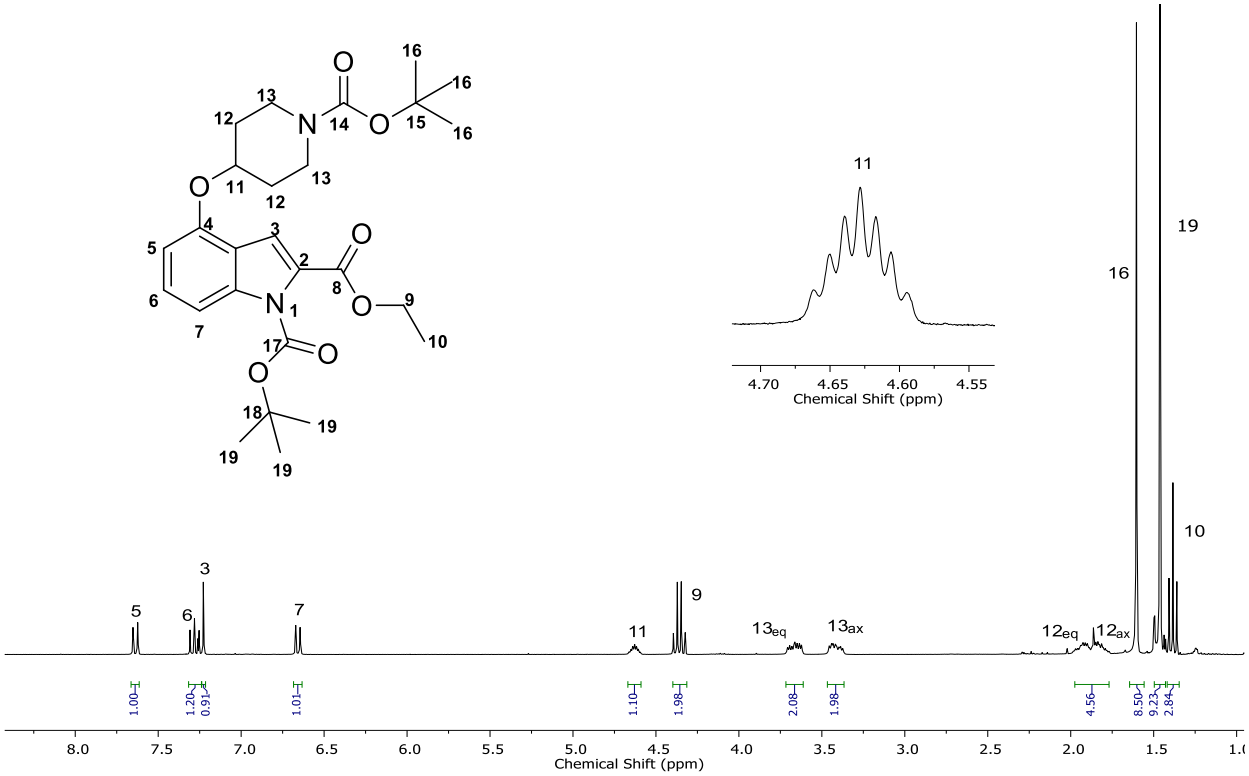

Figure 19: Assigned ^{1}H-NMR spectrum of **(39)** indicating the multiplet corresponding to the methine proton

4-phenoxy indole "*para*" to it. Big and bulky substituents on a 6-membered ring prefer an equatorial or pseudo-equatorial position. In this case, the piperidine ring had two bulky substituents, an aromatic ring and a Boc-group. Due to the two distinct chair conformations as seen in **Scheme 17**, the methine proton (coloured in red) is either in an axial or equatorial position, thus there are two distinct species of **(39)** in solution whose signals are partly coalesced, producing the multiplet observed.

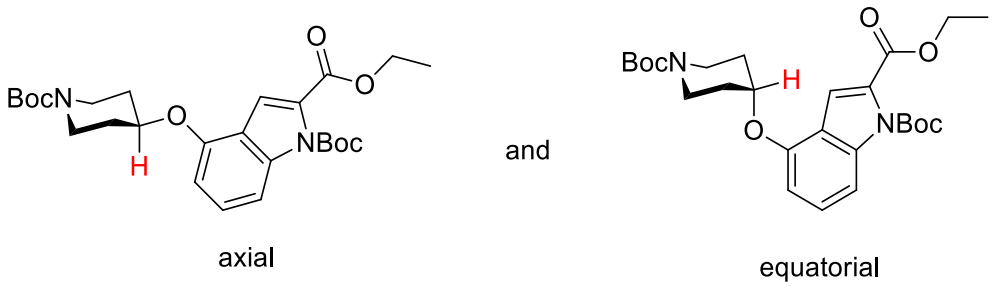

Scheme 17: Different conformations of the *N*-Boc piperidine ring of **(39)** indicating the axial and equatorial position of the methine proton (coloured in red)

Analysis of the ^{13}C-NMR spectrum confirmed the correct number of carbon signals expected as seen in **Figure 20**. One of the signals correlating to the chemically equivalent carbons of the piperidine ring however, displayed an interesting anomaly. The signal appeared as an unresolved broad signal at 40.5 ppm. We suspect that due to the bulky nature of the *N*-Boc group, there was minimal conformational change around the two methylene carbons (position **13**, **Figure 19**) which was most likely slow on the NMR timescale, therefore the two *N*-methylene carbons have multiple chemical environments. The broad peak is in fact multiple signals of the same two carbons. **Figure 20** illustrates the broad peak indicated in the purple box, which corresponded with the two *N*-methylene carbons (position **13**, **Figure 19**), as well as two O-CH-methylene carbons (position **12**, **Figure 19**) corresponding to the signal in the green box.

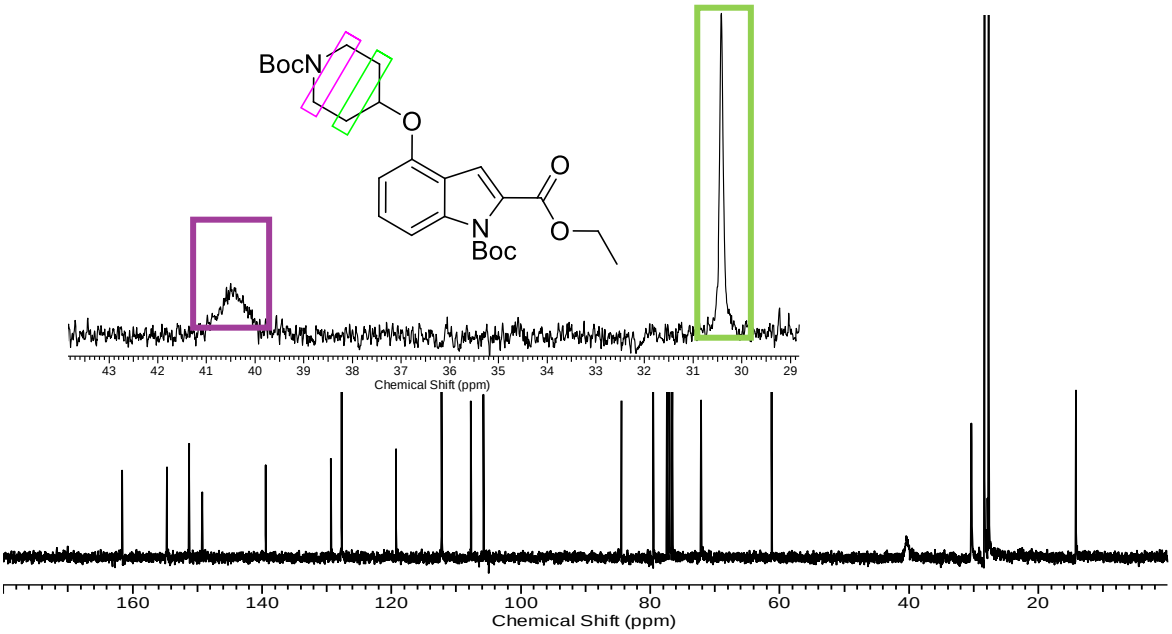

Figure 20:^{13}C-NMR spectrum of **(39)** in $CDCl_3$ indicating a broad signal at 40.5 ppm

A COSY spectrum of compound **(39)** in *d*-DMSO was acquired in order to verify the expected coupling interactions between protons, as seen in **Figure 21**.

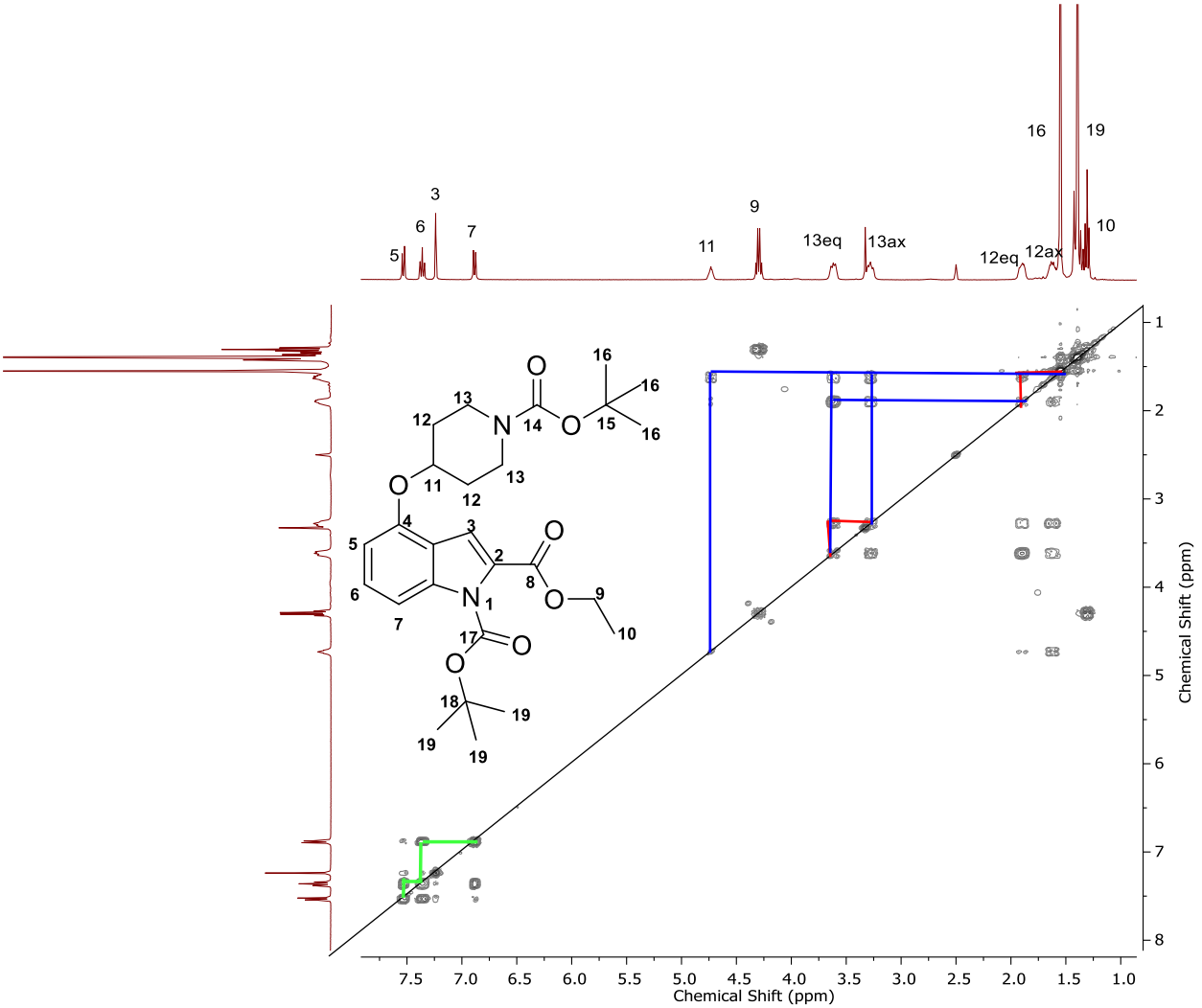

Figure 21: COSY spectrum of **(39)**

The ethyl ester has as expected the triplet at 1.39 ppm which is coupled to the quartet at 4.37 ppm. The two *tert*-butyl groups do not couple with any protons as expected. Analogous to the cyclohexyl rings, the axial and equatorial protons of the piperidine ring exhibit different chemical environments. Axial protons are more shielded than equatorial protons,[47] thus an axial proton would appear more upfield relative to the equatorial proton on the same methylene carbon. The multiplet which appeared at 4.64 ppm coincided with the proton on the tertiary carbon of the piperidine ring annotated at position **11**. Analysis of the COSY spectrum confirmed the coupling to the two multiplets between 1.77 – 1.89 ppm and 1.89 – 2.00 ppm, thus at position **12,** the axial protons appeared between 1.77 – 1.89 ppm and the equatorial protons appeared between 1.89–

2.00 ppm. It was also observed that the two multiplets which appeared at 3.38 – 3.49 ppm and 3.63 – 3.74 ppm were coupled to the axial and equatorial protons at position **12**, therefore those protons were axial protons between 3.38 – 3.49 ppm and equatorial protons between 3.63 – 3.74 ppm at position **13**. The multiplet at 4.63 ppm corresponded to the methine proton at position **11** and was coupled to the axial and equatorial protons at position **12**. The aromatic region indicated a singlet at 7.24 ppm which corresponded to the proton on the indole at position **3**. The doublet of doublets at 7.30 ppm corresponded to the proton on position **6**. The doublets at 6.68 ppm and 7.66 ppm were both coupled to the proton at position **6** but could not be assigned unambiguously as the protons at position **5** and **7**. We did not acquire a NOESY spectrum to unambiguously assign protons **5** and **7** but suspect that proton **7** appears at 6.68 ppm and proton **5** at 7.66 ppm due to the fact that **7** is *ortho* to the indole nitrogen and therefore would cause a greater shielding effect on the proton at **7** than would the oxygen atom at position **4** on the proton at position **5**. **Figure 22** illustrates the HSQC spectrum of **(39)**.

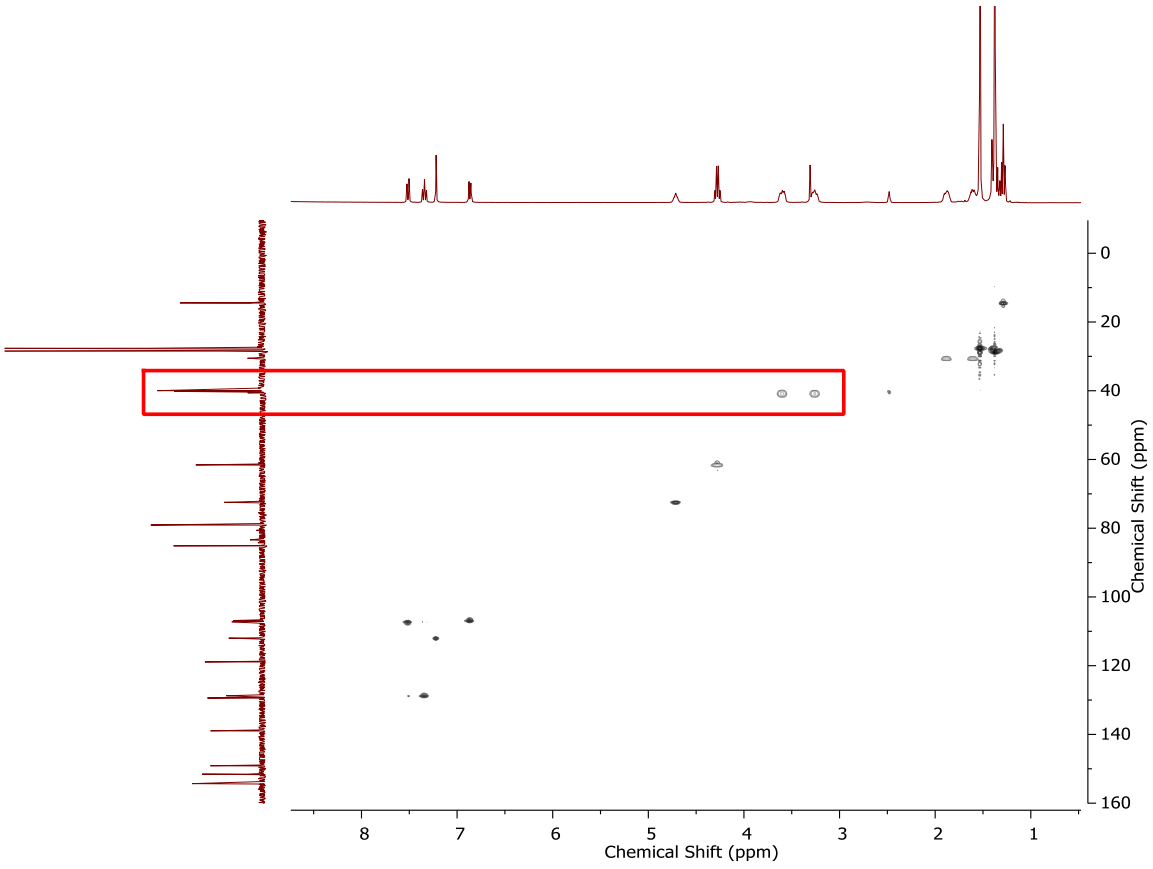

Figure 22: HSQC spectrum of **(39)**

It must be noted that the carbon signals at position **(13)** are not distinct the ^{13}C-NMR spectrum, but analysis of the HSQC spectrum has shown that the signals appear behind the *d*-DMSO solvent peak, as shown in the red rectangle.

2.5.3 Derivatization of the 2-ethyl ester

2.5.3.1 Transesterification of (39)

Transesterification is the process of substituting an initial *O*-alkyl group of one ester into a different *O*-alkyl group. This process is brought on by the reaction of an ester group with an alcohol, and can be either base-catalyzed (Lewis base or Brønsted base), performed under neutral conditions, amine-catalyzed or acid-catalyzed (Lewis acid or Brønsted acid) usually at elevated temperatures.[46]

Transesterification is also in equilibrium between the newly formed transesterified ester and the alcohol of the initial ester. Due to the fact that **(39)** had two acid labile *N*-Boc groups present, Brønsted acid catalyzed transesterification was not a viable route. Brønsted acid-catalyzed *N*-Boc deprotection of the piperidine ring would have resulted in the formation of the expected ammonium intermediate. This would have created problems as amidation of the ester by the ammonium salt of another molecule of **(39)** could have been possible, especially if the reaction temperature was high enough. For our first attempt at transesterification of the C2-position ethyl ester we utilized a Lewis acid/Lewis base-catalyzed transesterification using LiCl and 1,8-diazabicyclo[5.4.0]undec-7-ene (DBU)[49] as seen in **Scheme 18**.

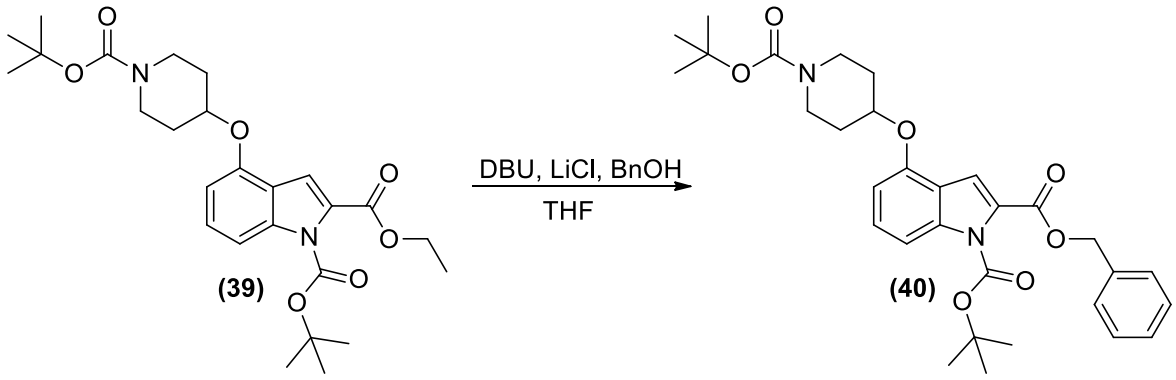

Scheme 18: DBU/LiCl-catalyzed transesterification of **(39)**

Lithium chloride acted as the Lewis acid, where the lithium ion coordinated to the ester carbonyl group resulting in increased electrophilicity. The role of DBU was to act as a non-nucleophilic

amine base, and facilitate with deprotonation of the transesterification intermediate. The first reaction attempted was between **(39)** and benzyl alcohol.

The reaction was carried out at room temperature and under an atmosphere of nitrogen due to the highly hygroscopic nature of LiCl. The reaction did not produce any product, but resulted in the partial *N*-Boc deprotection of the indole nitrogen, as the characteristic indole N-H peak at 8.95 ppm was observed in the ^{1}H-NMR spectrum. The potential mechanism for *N*-Boc deprotection is given in **Scheme 19**. The chelation of the lithium cation of the carbamate carbonyl oxygen increases the electrophilicity. This in turn would cause a greater polarized effect on the carbonyl group, which resulted in the simultaneous decarboxylation of the carbamate group as well as formation of a *tert*-butyl cationic species. The *tert*-butyl cationic species reacted with the chloride to form *tert*-butyl chloride **(44)**. The resulting negatively charged indole nitrogen **(43)** deprotonates **(44)**, which produces isobutene and the protonated indole nitrogen **(45)**.

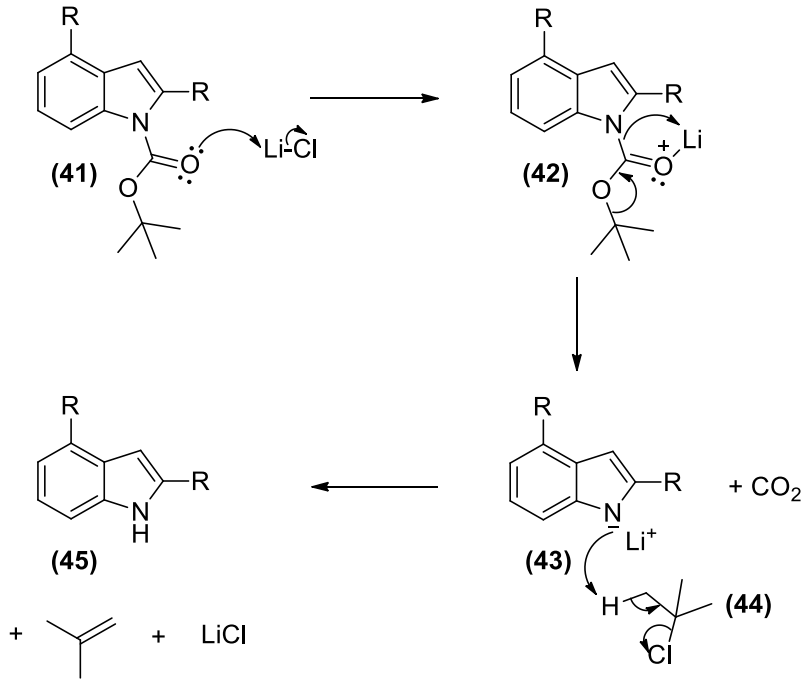

Scheme 19: Potential indole *N*-Boc deprotection mechanism

Compound **(39)** has two Boc-protected nitrogen atoms, one on the pyrrole ring of the indole and another on the amine of the piperidine ring. This selective Boc-cleavage of the pyrrole ring could be rationalized by the fact that the negative charge that resides on the pyrrole nitrogen was stabilized by the aromaticity of the indole, plus the added stabilizing nature of the ester on the C2-position. **Figure 23** illustrates the delocalization of the negative charge between **(46)** and **(47)**.

The Boc-protected amine of the piperidine ring does not possess any stabilization and therefore does not undergo cleavage.

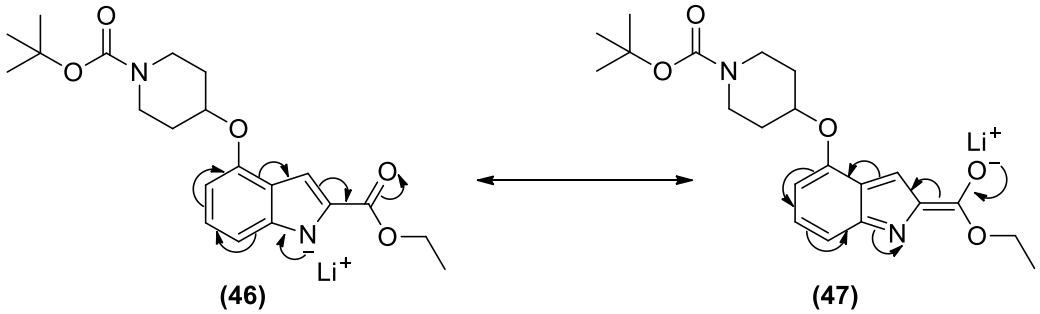

(46) **(47)**

Figure 23: Resonance effect on the negatively charged indole system

Due to the decreased reactivity of the ester using LiCl/DBU as catalysts, we focused on base-promoted transesterification. Base-promoted transesterification is a popular method for transesterification of esters, where transesterification is facilitated by a nucleophilic acyl substitution of alkoxides, making use of sodium or potassium alkoxide.[48] **Scheme 12** shown earlier in the chapter illustrated the synthesis of compound **(26)** by way of the hydrolysis of **(24)** with KOH in water and ethanol. This reaction was carried out at two different temperatures. The hydrolysis of **(24)** at 70 °C provided the indole carboxylic acid in a short period of 3 hours, while room temperature required stirring overnight to afford the carboxylic acid in a high yield. Brønsted base-mediated ester hydrolysis and transesterification are similar in that the nucleophile is a metal hydroxide and metal alkoxide respectively. The pKa value of sodium hydroxide is 15.7 and that of sodium or metal alkoxides range between 13 –18. Thus, it stands to reason, that if the stable and seemingly unreactive ester hydrolyzes at room temperature overnight, it is possible that an alkoxide may follow the same reactivity, in other words, transesterify. Potassium *tert*-butoxide is a non-nucleophilic base that has a high pKa value of 18, and thus would be able to deprotonate primary alcohols with a lower pKa value. We added potassium *tert*-butoxide and **(39)** together with benzyl alcohol, and stirred the mixture at room temperature in order to verify whether the non-nucleophilic base would create enough potassium benzyloxide to facilitate transesterification. Unfortunately, TLC analysis showed the formation of little to no product. We did not repeat the reaction at elevated temperatures because even though potassium *tert*-butoxide is considered non-nucleophilic, at high temperatures it could be reactive enough to be nucleophilic and facilitate transesterification.[50]

The use of potassium phosphate as a basic catalyst for the esterification of glycerides and plant oils has been reported in literature.[51] We proceeded with reacting **(39)** with 20 equivalents of

benzyl alcohol in THF together with three equivalents of K_3PO_4 at 80 °C in a microwave vial overnight, and noticed the appearance of two different spots on TLC with the starting material consumed. After purification and analysis by NMR spectroscopy, it was confirmed that signals due to the indole *N*-H of two compounds were present. Compound **(49)** was obtained and the other product was confirmed to be compound **(33)**, the *N*-Boc deprotected staring material (**Scheme 16**). Increasing the temperature to 110 °C and utilizing benzyl alcohol as the solvent and reactant, decreased the reaction time significantly as transesterification to produce **(49)** was completed in 3 hours. However, only a yield of 45% was obtained. Transesterification of **(39)** with 2-phenylethanol produced the corresponding ester **(48)** in 39% yield. **Scheme 20** illustrates the transesterification of **(39)** and indicates the ester substituents.

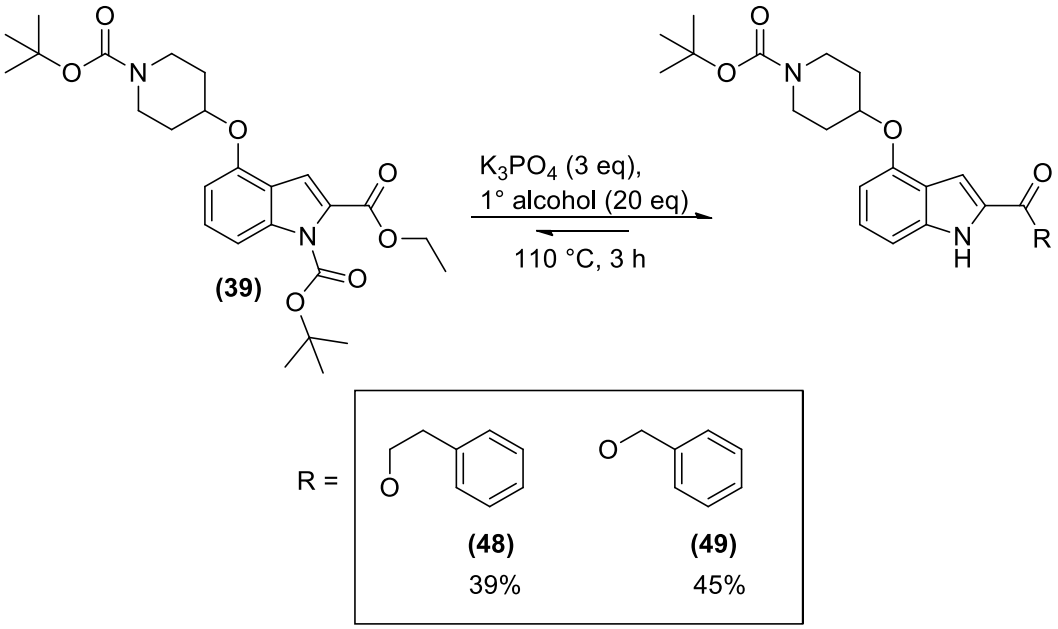

Scheme 20: Transesterification of **(39)** with K_3PO_4 as base

The synthesis of compounds **(48)** and **(49)** was confirmed by ^{1}H- and^{13}C-NMR spectroscopy and HRMS. Analysis of the ^{1}H-NMR spectrum of **(49)** confirmed the absence of a triplet and quartet in the aliphatic region corresponding to the ethyl ester of **(39)**, as well as the absence of a singlet at 1.61 ppm corresponding to the indole *tert*-butyl group of the *N*-Boc. In addition, the appearance of a singlet at 5.42 ppm was observed, integrating for two protons which corresponded to the benzylic methylene protons. The aromatic region contained additional signals that integrated for five protons, associated with the newly added phenyl ring. The ^{13}C-NMR spectrum indicated 20

signals as expected, taking into account the chemically equivalent carbons of the phenyl ring. Analyzing the ^{1}H-NMR spectrum of **(48)**, the same additional aromatic and absent ethyl signals could be observed as were evident in the ^{1}H-NMR spectrum of **(49)**.The ethylene chain present in the ester corresponded to two triplets in the aliphatic region at 3.15 ppm and 4.61 ppm, both integrating for two protons and having a coupling constant of 7.0 Hz.

2.5.3.2 Amidation of (39)

Due to the fact that transesterification was achieved at high temperatures, we decided to carry out the necessary amidation reactions at elevated temperatures as well. **Scheme 21** illustrates the performed amidation reactions on compound **(39)**, together with the amide substituents.

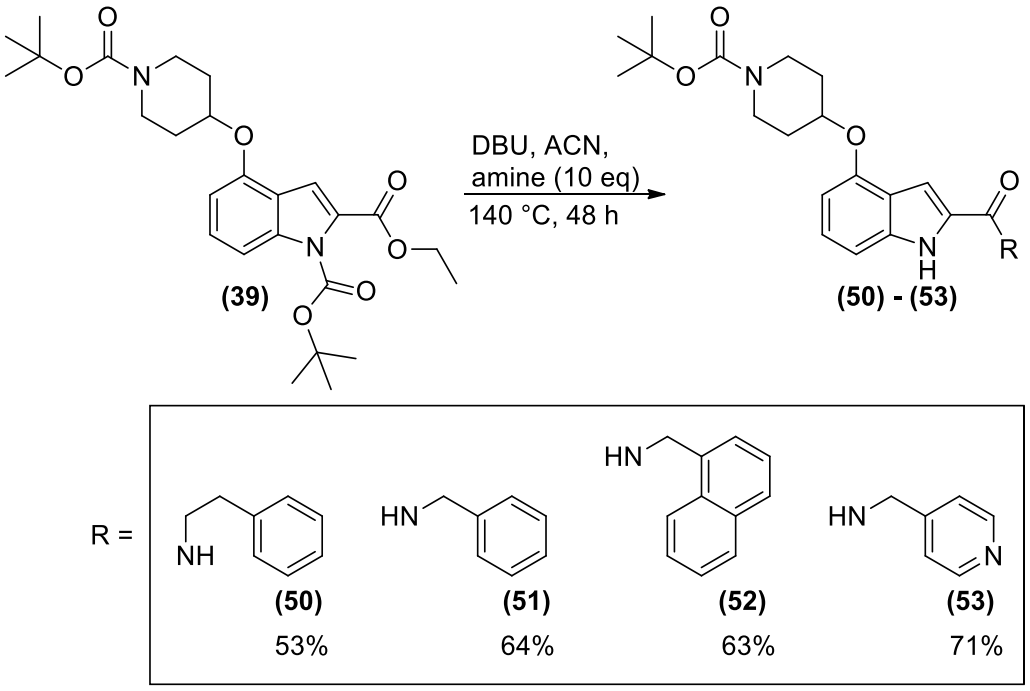

Scheme 21: Amidation of **(39)** to produce compounds **(50)**–**(53)**

A test reaction with **(39)** and 10 equivalents of 2-phenylethylamine was carried out in acetonitrile with 0.5 equivalents of DBU as a base catalyst. Initially the reaction was set at 80 °C, but TLC indicated only the quantitative removal of the Boc group on the indole nitrogen. The temperature was increased to 100 °C, upon which a more polar product was formed when monitored via TLC. After 12 hours at 100 °C, starting material was still present, thus the temperature was increased

to 140 °C and stirred for 2 days, after which it was observed that the presence of staring material had decreased significantly and the newly formed product spot was more prominent on TLC. In the same manner, the reaction of **(39)** with 2-phenylethylamine, benzyl amine, 1-naphthylmethylamine and (4-pyridylmethyl)amine was done at 140 °C for 2 days before purification.

The synthesis of compounds **(50)** – **(53)** was confirmed by ^{1}H- and ^{13}C-NMR spectroscopy and HRMS. Analysis of the ^{1}H-NMR spectrum of **(50)** – **(53)** indicated the absence of a triplet and quartet relating to the ethyl ester of **(39)**, as well as the absence of a singlet at 1.61 ppm corresponding to the *tert*-butyl group of the indole *N*-Boc. ^{13}C-NMR spectroscopy indicated the correct number of signals expected for **(50)** – **(53)**; in addition, HRMS confirmed the molecular weight of each compound as calculated. Inspection of the ^{1}H-NMR spectrum of compound **(50)** confirmed the presence of a secondary amide due to the appearance of a broad signal appearing as a triplet at 6.20 ppm. This was due to the coupling of the amide proton to the adjacent methylene of the phenethyl substituent. Thus the quartet that is visible at 3.75 ppm was due to the methylene coupling to the adjacent methylene and the amide proton. The addition of extra aromatic signals integrating for five protons confirmed the addition of 2-phenylethylamine to **(39)**. Inspection of the ^{1}H-NMR spectrum of compound **(51)** indicated a similar broad signal due to the amide proton appearing as a triplet at 6.87 ppm which is coupling to the benzyl methylene which in turn appeared as a doublet. **Figure 24** illustrates the ^{1}H-NMR spectrum of compound **(51)** which shows the amide proton signal in a red box and the methylene proton signal in a blue box.

Inspection of the ^{1}H-NMR spectrum of compound **(52)** indicated a similar broad triplet of the amide proton at 6.39 ppm, coupled to the naphthalic methylene which appeared as a doublet at 5.15 ppm. The aromatic region has extra signals that integrate for seven protons, thus confirming the addition of the 1-naphthylmethylamine to **(39)**. The ^{1}H-NMR spectrum of compound **(53)** indicated a broad triplet at 7.91 ppm due to the amide proton, as well as a doublet at 4.65 ppm due to the benzylic methylene. The aromatic region has two doublets at 7.28 ppm and 8.52 ppm, due to the chemically equivalent protons of the 4-substituted pyridine ring.

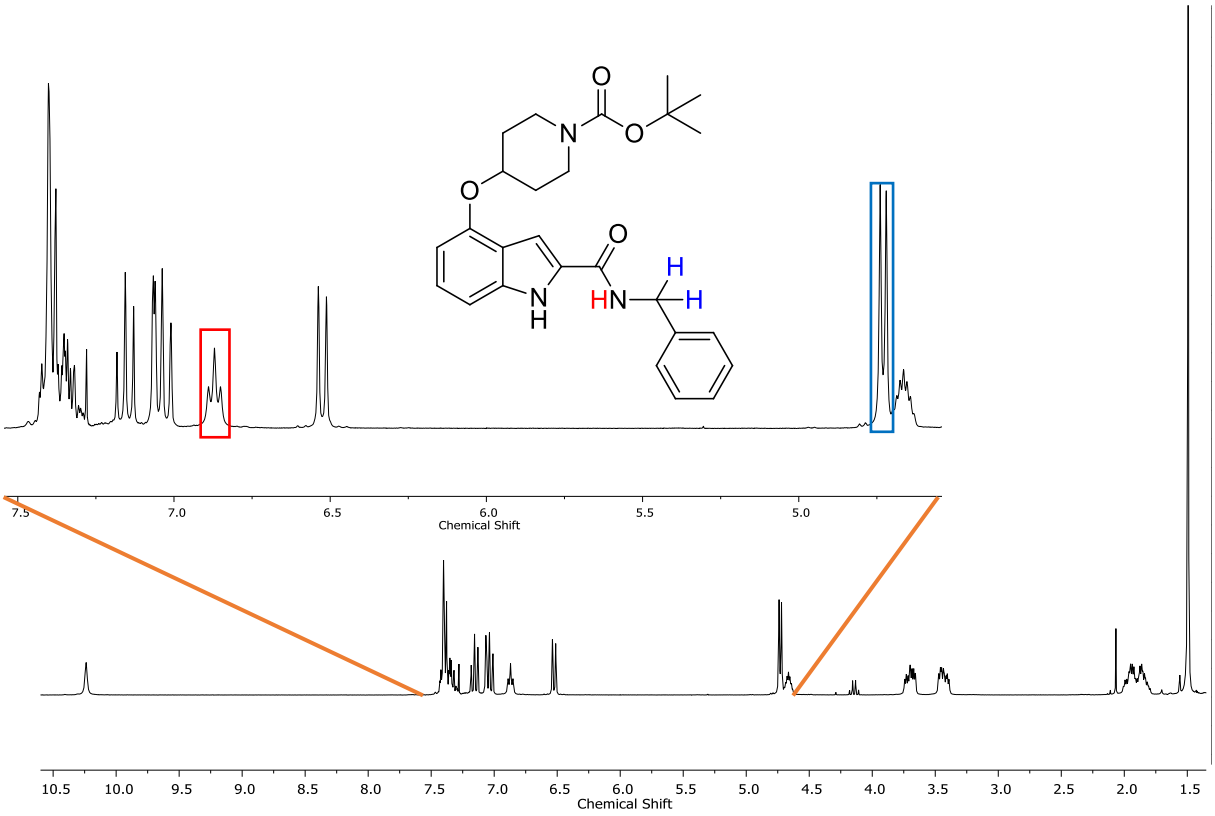

Figure 24: ^{1}H-NMR spectrum of **(51)** in $CDCl_3$, indicating the benzylic methylene protons (blue) and the amide proton (red)

2.6 Studies on the thermal stability of (39)

During the transesterification and amidation steps, it was observed that the *N*-Boc group on the indole was being removed. This, however, was not problematic, as the removal of the *N*-Boc group would have no effect on subsequent steps involving the synthesis of our required final compounds. Literature reported that a protic solvent, with or without the addition of a carbonate or phosphate base at high temperatures facilitates the removal of indole *N*-Boc groups.[48,49, 50]

We obtained variable temperature NMR spectroscopic data that indicated that neither the base nor the protic solvent is necessary for indole *N*-Boc deprotection, and that the process is in fact thermally induced.

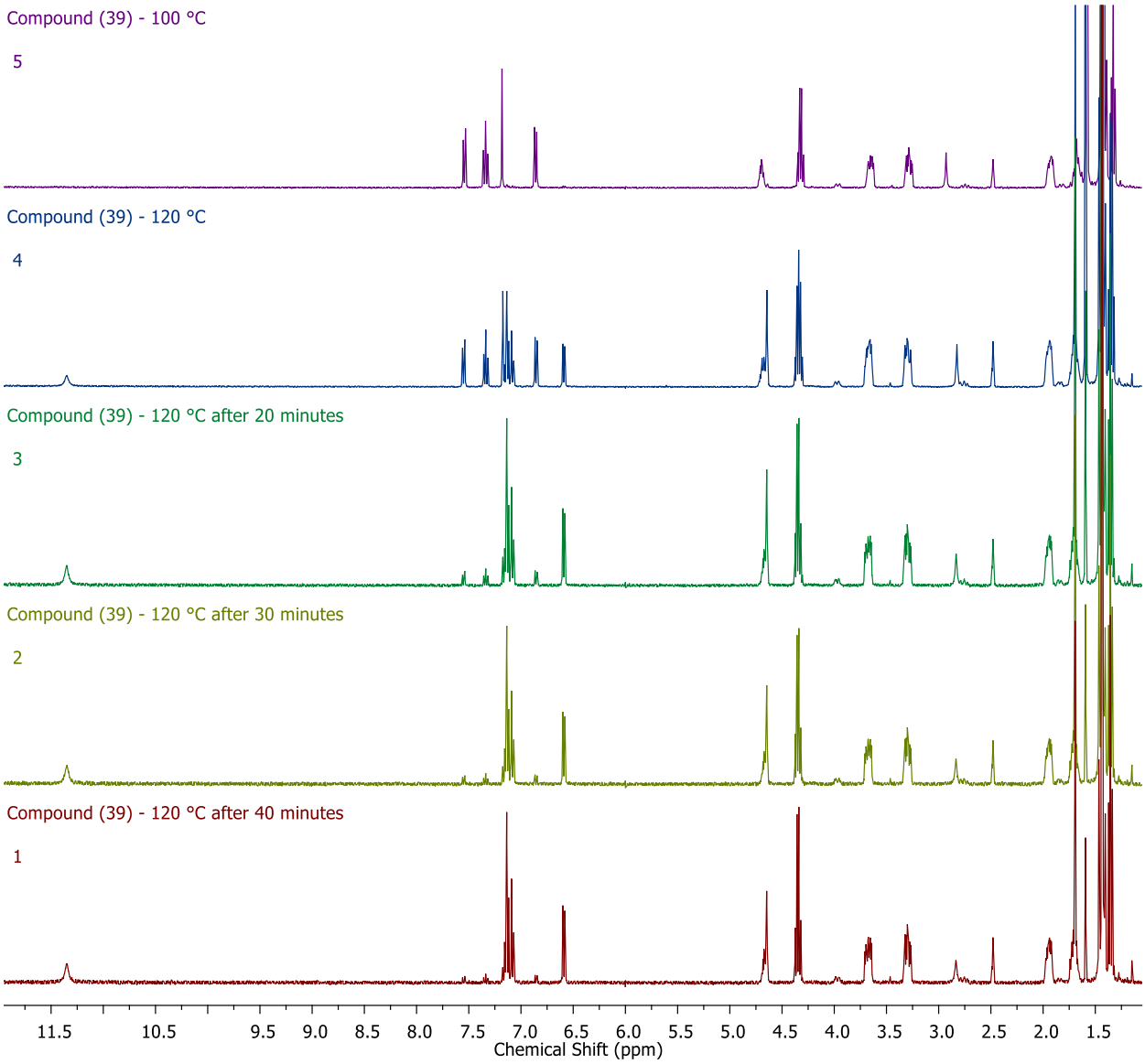

Figure 25: Variable temperature and time ^{1}H-NMR spectra of **(39)** in *d*-DMSO

^{1}H-NMR spectra of **(39)** was acquired at 25 °C, 50 °C, 100 °C and 120 °C in *d*-DMSO. As can be seen in **Figure 25**, compound **(39)** underwent structural changes above 100 °C, whereas between 25 °C and 100 °C no changes in the spectra were observed. At 120 °C extra signals in the aromatic region and aliphatic region appeared, as well as a broad signal at 11.37 ppm. This is due to the removal of the indole *N*-Boc group, concluding the presence of two indole species in solution as well as the byproducts of Boc-deprotection. Three extra aromatic signals were also observed associated with the *N*-Boc deprotected indole **(33)**. By the time the probe was heated to 120 °C and the spectrum was acquired, integration of the aromatic signals indicate that 50% of **(39)** had been *N*-Boc deprotected as all six signals integrated the same amount of protons relative

to another. We acquired spectra 20, 30 and 40 minutes after the initially acquired spectrum at 120 °C, whereby observing that the aromatic signals of **(39)** had almost completely diminished. The signal corresponding to the methylene protons of isobutene, the byproduct of *N*-Boc deprotection, can be seen forming at 4.67 ppm.

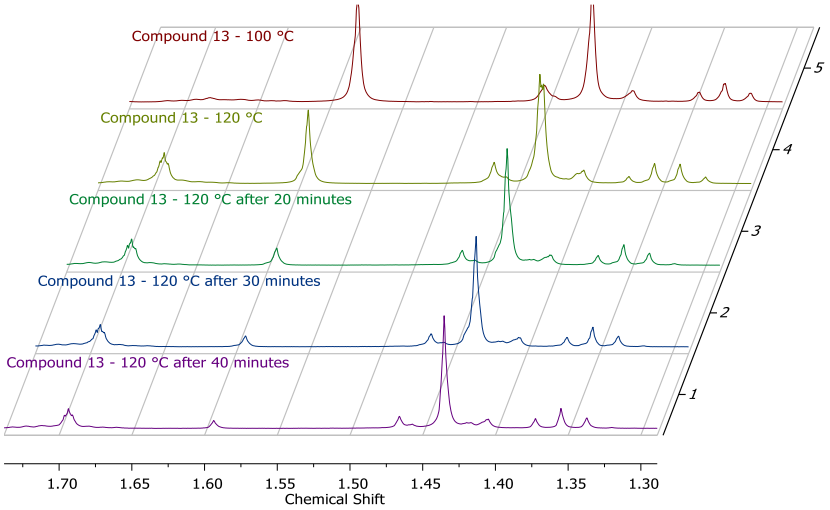

Figure 26: Stacked section of the aliphatic region

When observing **Figure 26** it is clear that the *tert*-butyl signal at 1.59 ppm was diminishing, with an increase in signal strength of the dimethyl protons of isobutene at 1.69 ppm. Thus we have concluded that indole *N*-Boc deprotection is not dependent on the use of protic solvents and base but is thermal in nature. The mechanism of thermally induced Boc deprotection is proposed to be similar to that of **Scheme 19**, but without the aid of a Lewis acid to facilitate decarboxylation and carbocation formation. We propose that due to the high thermal energy at 120 °C, carbocation formation is proposed to occur readily and is stabilized by the DMSO molecules, as can be seen in **Scheme 22**.

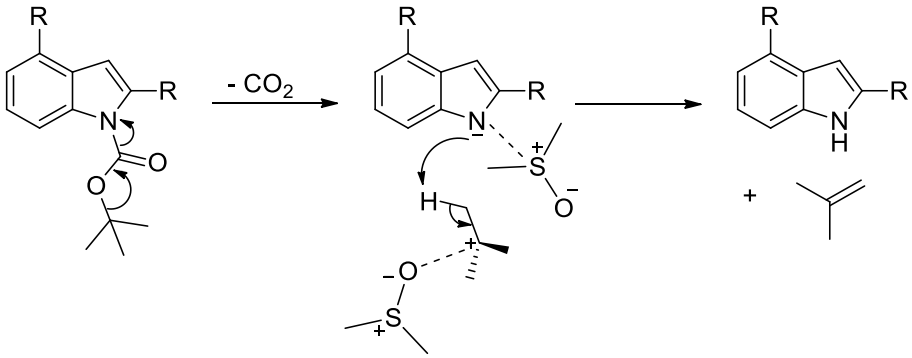

Scheme 22: Proposed mechanism for indole *N*-Boc thermolysis

2.7 Deprotection of the *N*-Boc piperidine ring

The final step in the synthesis of the 3-H indole series involved the deprotection of the *N*-Boc piperidine ring. We had decided to use 4M HCl in dioxane as the preferred method for the deprotection step, as subsequent purification would be minimal. Compounds **(48)** – **(53)** each were dissolved in 1mL DCM to which was added 1mL 4M HCl in dioxane and the reaction was carried out for 1 – 2 hours, after which a full conversion of **(48)** – **(53)** into the respected piperidinium hydrochloride salts was observed (**Scheme 23**). No starting material was observed when the reaction was monitored using TLC analysis.

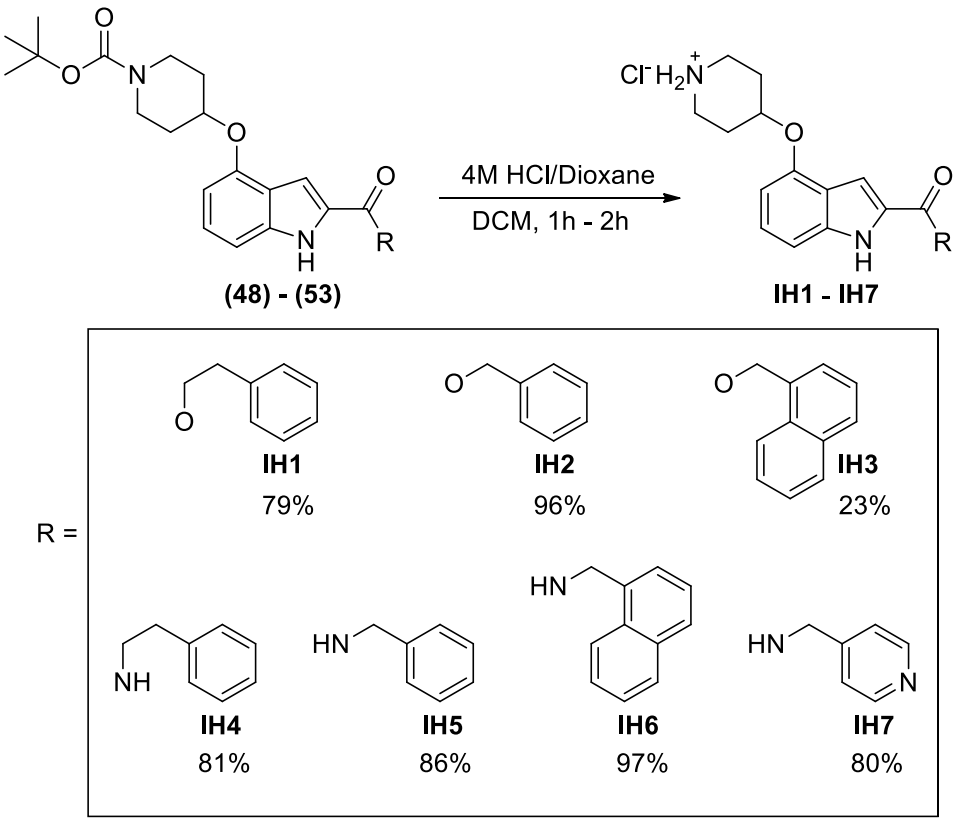

Scheme 23: *N*-Boc deprotection of **(48)** – **(53)** via HCl in dioxane to produce **IH1 – IH7**. Compound **IH7** isolated as pyridinium HCl salt.

The synthesis of compounds **IH1**, **IH2**, **IH4** - **IH7** was successful and was completed in a short period of time ranging between 1 and 2 hours. Compound **IH3** was synthesized via the transesterification of **(39)** with 1-naphthyl methanol and K_3PO_4 as seen in **Scheme 20**, and followed directly by *N*-Boc deprotection. Reasons for direct deprotection of the piperidine *N*-Boc group after transesterification was due to purification issues. The transesterified naphthyl ester

had a similar R_f value to 1-naphthyl methanol, and thus co-eluted during purification with column chromatography. It was not possible to remove 1-naphthyl methanol via evaporation as the boiling point is between 300–302 °C. After *N*-Boc deprotection, due to the increased polarity of the ammonium salts, purification was readily achieved, as column chromatography with DCM as eluent provided the required separation of **IH3** and 1-naphthyl methanol after which the eluent polarity was increased to 90% DCM:10% MeOH to obtain **IH3** in a 23% yield over two steps. The low yield can be explained by the fact that multiple purifications via column chromatography were attempted before deciding on deprotection of the *N*-Boc group. Analysis of the ^{1}H-NMR spectrum of **IH3**, as seen in **Figure 27**, indicated the absence of the *tert*-butyl signal, usually between 1.5 – 1.6 ppm, as well as the two signals of the resulting ammonium chloride salt formed on the deprotected nitrogen of the piperidine ring, appearing at 8.78 and 8.99 ppm.

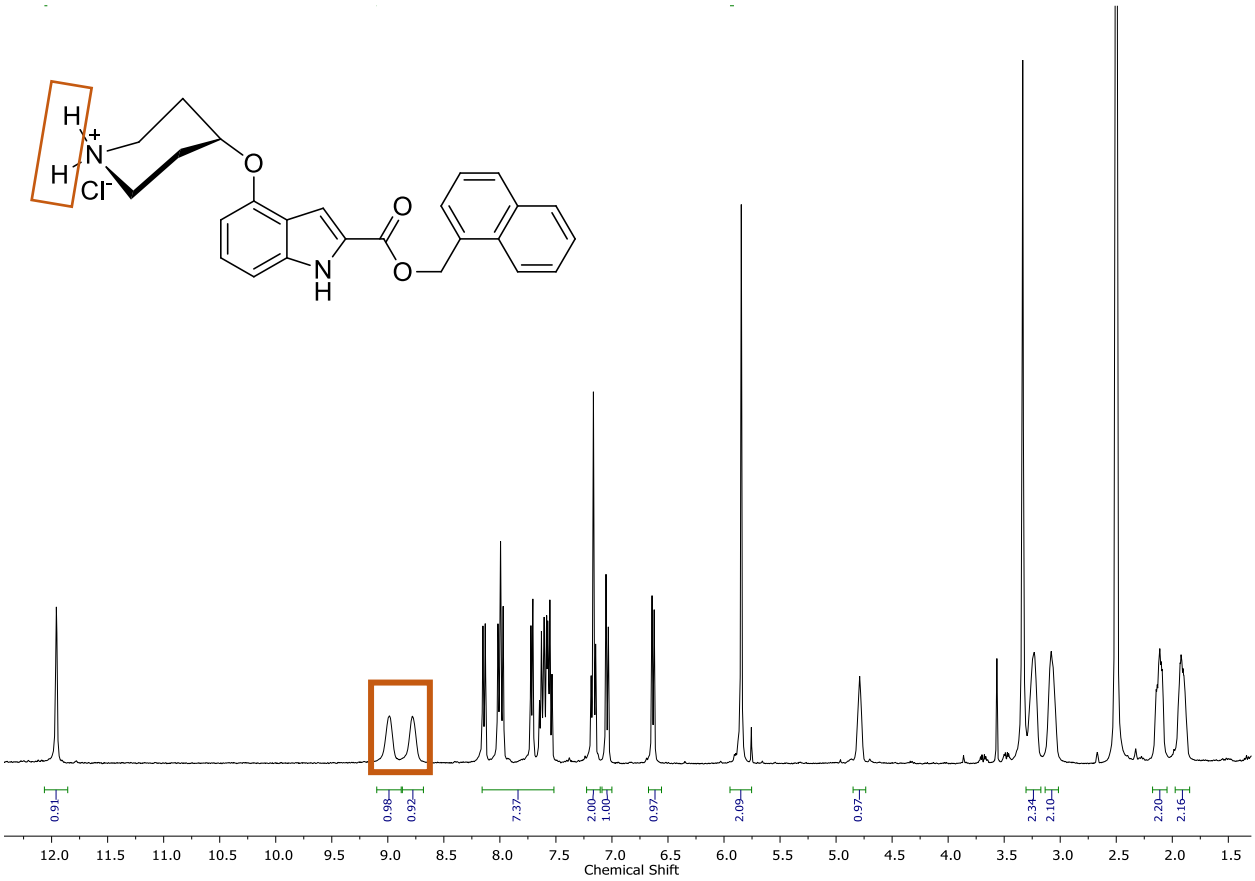

Figure 27: ^{1}H-NMR spectrum of **IH3** indicating the protons of the ammonium salt as well as the removal of the piperidine *N*-Boc group. Note: a dioxane and water impurity is observed.

The two signals were indicative of the ammonium protons in their respective axial and equatorial position, which resulted in two different chemical shifts. They are visualized in a brown rectangle on **Figure 27**.

Compounds **IH1 – IH7** all have been characterized through ^{1}H- and ^{13}C-NMR spectroscopy, infrared spectroscopy and HRMS and the purity was obtained of the final compounds. The ^{1}H-NMR and ^{13}C-NMR spectroscopy data corresponded with the correct amount of protons and carbon signals expected and the HRMS data correlated with the calculated values of each compound.

The HRMS data also confirmed the doubly protonated **IH7** containing the piperidinium chloride and pyridinium chloride salts. The m/z value of 176.0954 is observed, which corresponds to the $[M + 2H]^{2+}$ /2 value expected of the double protonated species (calculated for 176.0950). The m/z value for the singly charged species was also observed as the $[M + H]^{+}$ value of 351.1830 (calculated for 351.1821)

2.8 Conclusion

In this chapter we have described the successful synthesis of an indole scaffold via firstly having to synthesize an α-azido-β-arylacrylate, the vinyl azide precursor of the desired indole scaffold. Due to the required substitution pattern on the desired indole, the α-azido-β-arylacrylate also had to contain the correct substitution. The α-azido-β-arylacrylate was initially synthesized via a CAN/NaN_3 addition, NaOAc mediated elimination reaction on a benzyloxy substituted ethyl cinnamate precursor. The cinnamate was synthesized via a Horner-Wadsworth-Emmons reaction with 2-(benzyloxy)benzaldehyde and a stabilized ylid formed from triethyl phosphonoacetate. Due to the low yield obtained in synthesizing the desired vinyl azide we decided to pursue another method. The Knoevenagel reaction provided the necessary tools to synthesize the desired vinyl azide by means of the condensation reaction of 2-(benzyloxy)benzaldehyde and ethyl azidoacetate, and proved to produce higher yields than the CAN/NaN_3 addition elimination reaction.

The subsequent step involved thermolysis of the α-azido-β-arylacrylate via the Hemetsberger indolization reaction whereby changes in the reaction temperature and solvent proved to produce nearly quantitative conversion of the acrylate to indole. The indole contained the desired substitution pattern, i.e. an ester in the C2-position and a phenoxy group at the C4-position.

Deprotection of the 4-benzyloxy group was followed by a successful Mitsunobu coupling of 1-Boc-4-hydroxypiperidine. Due to purification issues, the indole nitrogen was Boc-protected which resulted in a change in polarity, aiding in the purification step of the precursor compound necessary for the required transesterification and amidation steps.

Amidation and transesterification proved to be difficult due to the increased stability of the ester group. These reactions could only be performed at elevated temperatures in order for amidation and transesterification to be achieved. High heat also proved to be the catalyst for indole *N*-Boc deprotection. Studies on the thermal stability of the *N*-Boc indole proved that indole *N*-Boc deprotection is possible and probable due to elevated temperatures, occurring in neutral conditions such as DMSO. The final step involved the *N*-Boc deprotection of the *N*-Boc piperidine ring to produce the final compounds labeled **IM1 – IM7**.

2.9 References

1. Inman, M.; Moody, C. J. *Chemical Science* **2013**, *4,* 29.

2. Larock, R. C.; Yum, E. K. *J. Am. Chem. Soc.* **1991**, *113,* 6689.

3. Harrington, P. J.; Hegedus, L. S. *J. Org. Chem.* **1984**, *49,* 2657.

4. Mori, M.; Chiba, K.; Ban, Y. *Tetrahedron Lett.* **1977**, *18,* 1037.

5. Castro, C.; Gaughan, E.; Owsley, D. *J. Org. Chem.* **1966**, *31,* 4071.

6. Ezquerra, J.; Pedregal, C.; Lamas, C.; Barluenga, J.; Pérez, M.; García-Martín, M. A.; González, J. M. *J. Org. Chem.* **1996**, *61,* 5804.

7. Cacchi, S.; Fabrizi, G. *Chem. Rev.* **2005**, *105,* 2873.

8. Gribble, G. W. *Indole Ring Synthesis: From Natural Products to Drug Discovery,* p583, John Wiley & Sons.

9. Banini, S. R. *Palladium-Catalyzed Syntheses of Indoles, Pyrroloindoles, Quinolines; a Base-Mediated Formation of N-Alkoxyindoles, and Progress Toward the First Total Synthesis of Echinosulfone A.* ProQuest, p6, 2008.

10. Robinson, B. *Chem. Rev.* **1963**, *63,* 373.

11. Bischler, A. *Ber. Dtsch. Chem. Ges.***1892**, *25,* 2860.

12. Bartoli, G.; Palmieri, G.; Bosco, M.; Dalpozzo, R. *Tetrahedron Lett.* **1989**, *30,* 2129.

13. Nenitzescu, C. *Bull.Soc.Chim.Romania* **1929**, *11,* 37.

14. Hemetsberger, H.; Knittel, D. *Monatsh. Chem.* **1972**, *103,* 194.

15. Hemetsberger, H.; Knittel, D.; Weidmann, H. *Monatsh. Chem.***1969**, *100,* 1599.

16. Hemetsberger, H.; Knittel, D.; Weidmann, H. *Monatsh. Chem*.**1970**, *101,* 161.

17. Trahanovsky, W. S.; Robbins, M. D. *J. Am. Chem. Soc.* **1971**, *93,* 5256.

18. Nair, V.; George, T. G. *Tetrahedron Lett.* **2000**, *41,* 3199.

19. Wadsworth, W. S. *Org. React.* **1977**, *25*, 73.

20. Borg, T.; Danielsson, J.; Mohiti, M.; Restorp, P.; Somfai, P. *Adv. Synth. Catal.* **2011**, *353,* 2022.

21. Ando, K.; Yamada, K. *Tetrahedron Lett.* **2010**, *51,* 3297.

22. Michaelis, A.; Kaehne, R. *Ber. Dtsch. Chem. Ges.* **1898**, *31,* 1048.

23. Kiddle, J.; Gurley, A. *Phosphorus Sulfur Silicon Relat. Elem.* **2000**, *160,* 195.

24. Speed, T. J.; McIntyre, J. P.; Thamattoor, D. M. *J. Chem. Educ.* **2004**, *81,* 1355.

25. Chang, M.; Lin, C.; Sun, P. *J. Chin. Chem. Soc.* **2005**, *52,* 1061.

26. Hu, M.; He, X.; Niu, Z.; Yan, Z.; Zhou, F.; Shang, Y. *Synthesis* **2014**, *46,* 510.

27. Sastri, V. R.; Perumareddi, J.; Rao, V. R.; Rayudu, G.; Bünzli, J. *Modern Aspects of Rare Earths and their Complexes;* Elsevier, 554, 2003.

28. Knoevenagel, E. *Ber. Dtsch. Chem. Ges.* **1898**, *31,* 2596.

29. Jones, G. *Organic Reactions, Chapter 2, 222,* **1967**

30. Chen, W.; Shao, J.; Li, Z.; Giulianotti, M. A.; Yu, Y. *Can. J. Chem.* **2011**, *90,* 214.

31. Chen, W.; Hu, M.; Wu, J.; Zou, H.; Yu, Y. *Org. Lett.* **2010**, *12,* 3863.

32. Wang, R.; Shi, H.; Zhao, J.; He, Y.; Zhang, H.; Liu, J. *Bioorg. Med. Chem. Lett.* **2013**, *23,* 1760.

33. Arques, A.; Molina, P.; Auñón, D.; Vilaplana, M. J.; Velasco, M. D.; Martínez, F.; Bautista, D.; Lahoz, F. J. *J. Organomet. Chem.* **2000**, *598,* 329.

34. Cananzi, S.; Merlini, L.; Artali, R.; Beretta, G. L.; Zaffaroni, N.; Dallavalle, S. *Bioorg. Med. Chem.* **2011**, *19,* 4971.

35. Heaner, W. L.; Gelbaum, C. S.; Gelbaum, L.; Pollet, P.; Richman, K. W.; DuBay, W.; Butler, J. D.; Wells, G.; Liotta, C. L. *RSC Advances* **2013**, *3,* 13232.

36. Moody, C. J. *J. Chem. Soc. Perkin Trans. I* **1984**, 1333.

37. Gray, N. M.; Dappen, M. S.; Cheng, B. K.; Cordi, A. A.; Biesterfeldt, J. P.; Hood, W. F.; Monahan, J. B. *J. Med. Chem.* **1991**, *34,* 1283.

38. Staab, v. H. *Angew. Chem., Int. Ed.* **1962**, *1,* 351.

39. WI, H.; Isensee, R. W. *J. Org. Chem.* **1961**, *26,* 2789.

40. Mitsunobu, O.; Yamada, M. *Bull. Chem. Soc. Jpn.* **1967**, *40,* 2380.

41. Mitsunobu, O. *Synthesis* **1981**, *1981,* 1.

42. Fletcher, S. *Org. Chem. Front.* **2015**, *2,* 739.

43. Yu, Z.; Brannigan, J. A.; Moss, D. K.; Brzozowski, A. M.; Wilkinson, A. J.; Holder, A. A.; Tate, E. W.; Leatherbarrow, R. J. *J. Med. Chem.* **2012**, *55,* 8879.

44. Lemieux, R.; Kullnig, R.; Bernstein, H.; Schneider, W. *J. Am. Chem. Soc.* **1958**, *80,* 6098.

45. Nickon, A.; Castle, M. A.; Harada, R.; Berkoff, C. E.; Williams, R. O. *J. Am. Chem. Soc.* **1963**, *85,* 2185.

46. Otera, J. *Chem. Rev.* **1993**, *93,* 1449.

47. Guan, G.; Kusakabe, K.; Yamasaki, S. *Fuel Process Technol.* **2009**, *90,* 520.

48. Wang, J.; Liang, Y.; Qu, J. *Chem. Commun.* **2009**, 5144.

49. Dandepally, S. R.; Williams, A. L. *Tetrahedron Lett.* **2009**, *50,* 1071.

50. Ravindranath, N.; Ramesh, C.; Ravinder Reddy, M.; Das, B. *Adv. Synth. Catal.* **2003**, *345,* 1207.

Chapter 3: Synthesis of 3-methyl indoles

3.1 Introduction

As described in Chapter 1, the introduction of a methyl group at the C3-position of the benzofuran model compound had an effect on the efficacy of aromatic amides versus their analogous aromatic esters. This is due to the fact that a steric clash between the C3-methyl and the proton on the amide resulted in a conformational change of the amide. This in turn decreased the PvNMT inhibition IC_{50} values of the amides relative to the analogous esters by a factor of 1.6 (benzyl amide vs benzyl ester) to as much as 48. Hence, our proposal was to form an analogous 3-methyl indole scaffold to test the theory that a methyl at the C3-position would have an influence on the efficacy compared to the indole analogues of Chapter 2. Thus building on the indole based compounds synthesized in Chapter 2, this chapter discusses the different procedures undertaken to synthesize the required 3-methyl indole scaffold, and the subsequent functionalization of the 3-methyl indole scaffold to synthesize the target compounds, as illustrated in **Figure 28**.

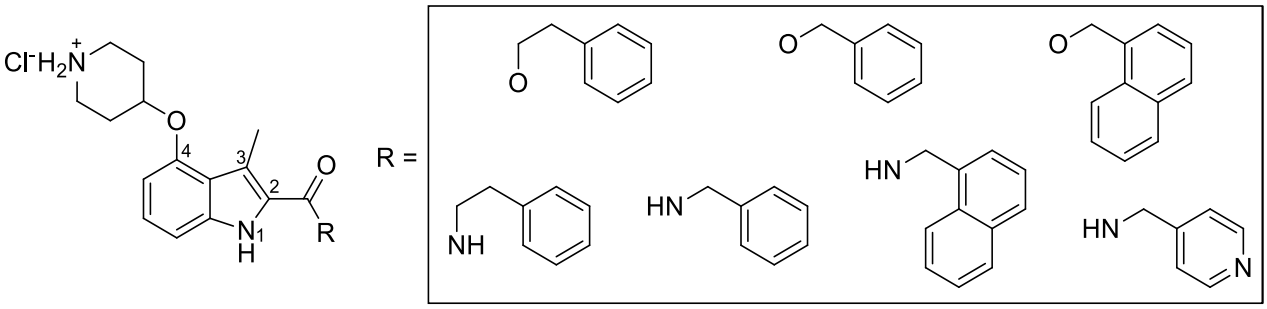

Figure 28: Proposed 3-methyl indole based compounds with various amides and esters to be synthesized

In this chapter four different methodologies for the synthesis of the 3-methyl analogue of compound **(24)** are described, these are:

1. The Vilsmeier-Haack formylation followed by a Mozingo reduction
2. A ligand-free copper-catalyzed coupling of ethyl isocyanoacetate and 2-bromo acetophenone
3. The Larock indole synthesis
4. Bromination followed by Suzuki-Miyaura coupling

3.2 Vilsmeier-Haack formylation followed by a Mozingo reduction

The Vilsmeier-Haack formylation is a versatile reaction utilized to introduce an aldehyde group onto electron rich aryl systems.[1] Regioselective formylation of a 2-ester indole system at the C3-position through the use of the Vilsmeier-Haack formylation has been well documented in literature.[2,3,4,5] Formylation of the indole system at the C3-position has the added benefit of introducing a functionalizable carbon atom at that position. For the purposes of this project this is advantageous as the aim is to introduce a methyl group at that position. **Scheme 24** illustrates the proposed synthetic strategy to convert indole **(24)** to 3-methyl indole **(56)**. Formylation of **(24)** to yield **(54)** would be followed by the formation of dithioacetal **(55)**, and subsequent desulfurization to produce **(56)**.

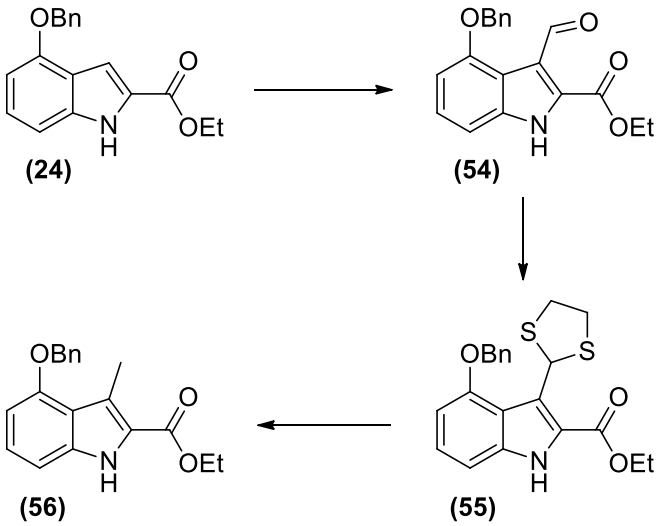

Scheme 24: Vilsmeier-Haack formylation and Mozingo reduction to produce compound **(56)**

The indole ring is the most nucleophilic at the C3-position,[6,7] due to the fact that the indole nitrogen lone pairs can delocalize through the pyrrole ring acting like a nucleophilic enamine. Therefore the addition of a potent electrophile results in the regioselective nucleophilic aromatic substitution of the indole ring at the C3-position. **Scheme 25** illustrates the mechanism involved in the formylation of **(24)**.The initial step of the Vilsmeier-Haack formylation is the addition of phosphoryl chloride to DMF to produce a chloroiminium ion **(57)** *in situ*, also known as the Vilsmeier reagent. Addition of indole compound **(24)** to **(57)** leads to the formation of addition product **(58)**, which subsequently re-aromatizes to **(59)** after which the iminium intermediate **(60)** forms. An acidic aqueous workup leads to the formation of product **(54)**. In our hands, the aldehyde was obtained

in a 62% yield after purification. ^{1}H-NMR spectroscopy confirmed the formation of an aldehyde due to the presence of a singlet at 9.94 ppm, as well as the integration of the aromatic signals accounting for eight protons as opposed to nine. The ^{13}C-NMR spectrum indicated 17 signals, of which the signal at 190.4 ppm was verification of the formation of the aldehyde. HRMS ESI+ indicated that the molecular ion was 324.1222 g/mol, comparable to the calculated value of 324.1236 g/mol.

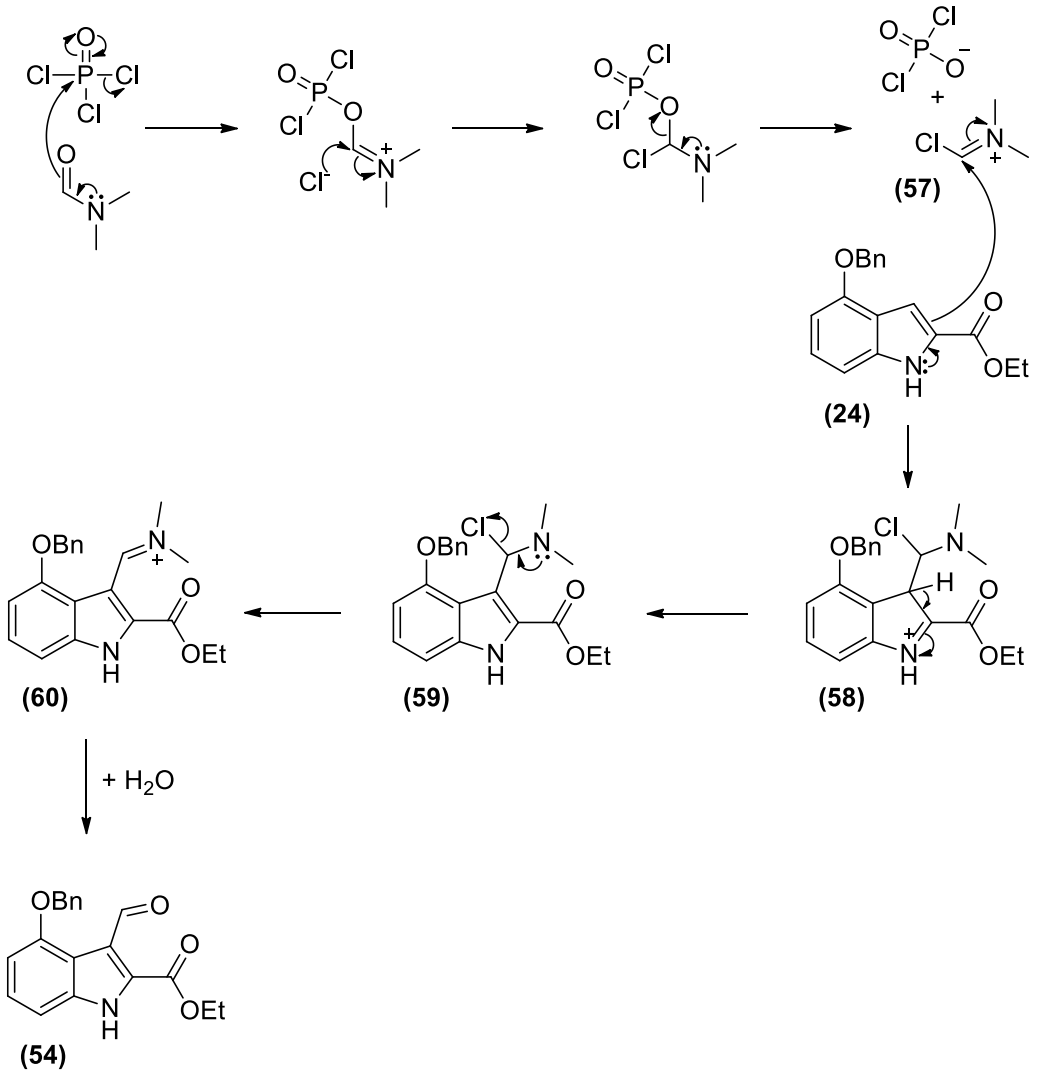

Scheme 25: Mechanism for the formation of the Vilsmeier reagent and the electrophilic aromatic substitution of **(24)**

The formation of a dithioacetal from the aldehyde (**Scheme 24**) was relatively straight forward. A catalytic amount of *p*-toluenesulfonic acid and ethane-1,2-dithiol was added to the aldehyde in THF while stirring overnight at 40 °C to produce a dithioacetal in a yield of 88%. The ^{1}H-NMR

spectrum indicated two multiplets between 3.37– 3.47 ppm and 3.55– 3.66 ppm corresponding to the axial and equatorial protons of the dithioacetal ring as well as a singlet at 5.95 ppm corresponding to the methine proton of the dithioacetal ring. ^{13}C-NMR spectroscopy and HRMS indicated the correct amount of carbon signals as well as the correct molecular weight which corresponded with the calculated value. **Figure 29** illustrates the ^{1}H-NMR spectra of the indole carbaldehyde (top) with the aldehyde signal at 9.95 ppm (shown in a green rectangle) and the dithioacetal (bottom), with the axial and equatorial methylene signals of the dithioacetal ring between 3.37– 3.47 ppm and 3.55– 3.66 ppm as well the methine proton signal at 5.94 ppm (indicated with a red rectangle). A signal observed at 1.56 ppm indicated that H_2O was present as an impurity.

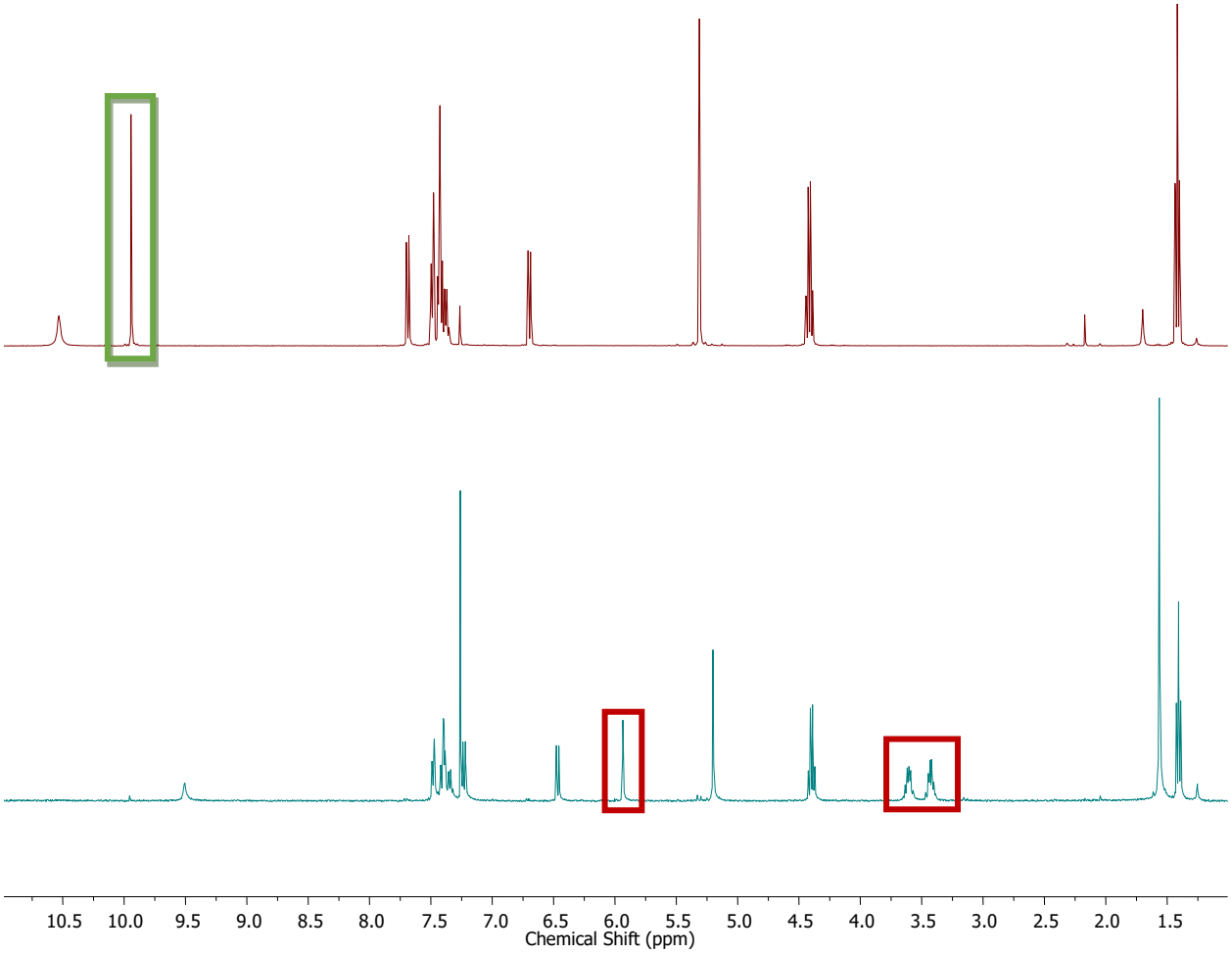

Figure 29: ^{1}H-NMR spectra of aldehyde at the top and dithioacetal at the bottom in $CDCl_3$

With the dithioacetal in hand the next step was to carry out the Mozingo reduction in order to obtain the desired 3-methyl indole. Desulfurization was achieved by reacting the dithioacetal with freshly prepared Raney nickel. **Figure 30** illustrates the ^{1}H-NMR spectra of the product isolated from this reaction.

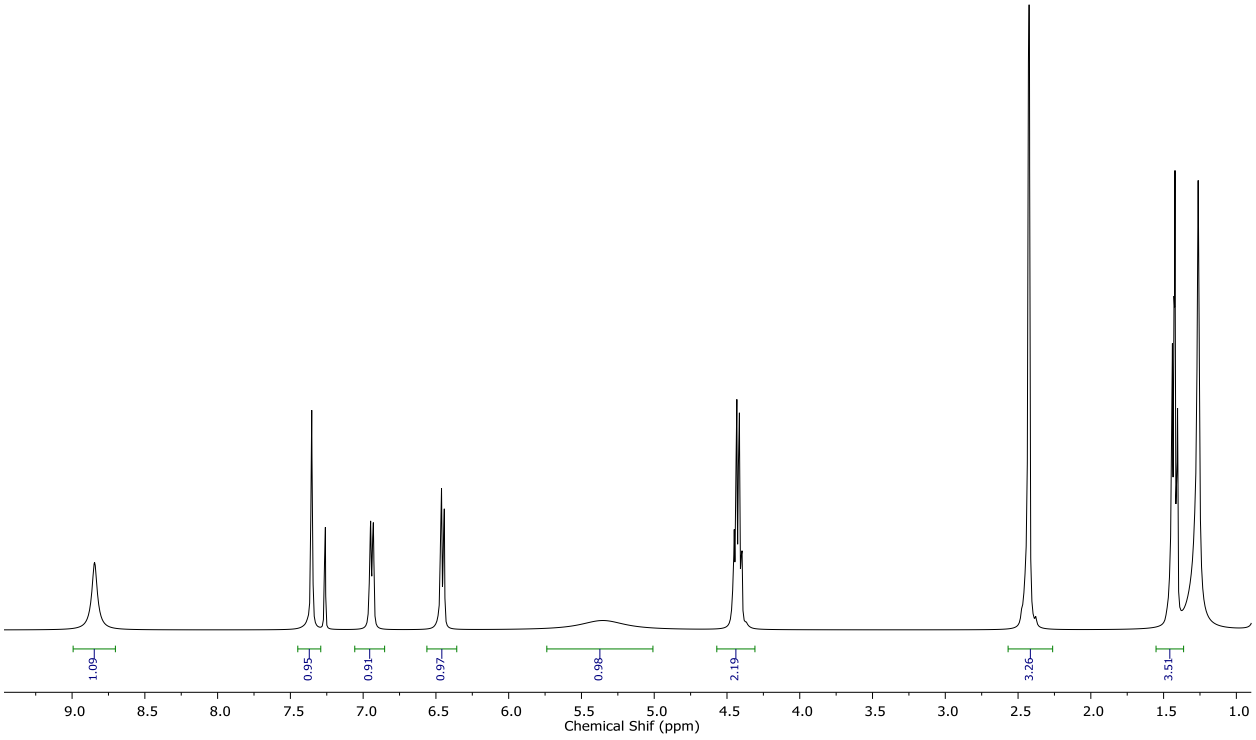

Figure 30: ^{1}H-NMR spectra of the product isolated from Raney Nickel reduction

Three important observations were made when interpreting the ^{1}H-NMR spectra of the obtained product. The first observation was that the desulfurization had occurred successfully due to the absence of the signals indicative of the dithioacetal ring, and the appearance of the expected methyl signal at 2.42 ppm integrating for three protons. The second observation was the absence of the signals corresponding to the benzyl group, and the presence of a broad phenolic proton signal at 5.36 ppm. The third observation was that the splitting pattern of the aromatic signals was not what was expected for the desired 3-methyl indole. Two doublets at 6.46 ppm and 6.94 ppm and a singlet at 7.35 ppm was observed, opposed to the expected doublet of doublets (potentially appearing as a triplet) and two doublets. This indicated that the formylation reaction had occurred at the wrong position on the indole ring, forming the undesired regioisomer. It was difficult to identify the unexpected splitting pattern in the ^{1}H-NMR spectra of the fromylated and dithioacetal indoles due to the overlapping proton signals of the benzyl protecting group. The Vilsmeier-Haack formylation was carried out a second time with the aim of isolating the 7-formylated indole in order

to obtain a crystal structure to determine the actual position of the aldehyde on the indole. The reaction was carried out with the same conditions as the initial reaction, but in this instance inexplicably an additional product was observed when the reaction was monitored by TLC. Isolation of the second product and subsequent ^{1}H-NMR spectroscopy confirmed the formation of the desired product, formylated in the C3-position. A yield of 13% was obtained indicating that the undesired product was still the major product. **Figure 31** illustrates the ^{1}H-NMR spectrum of the newly formed product.

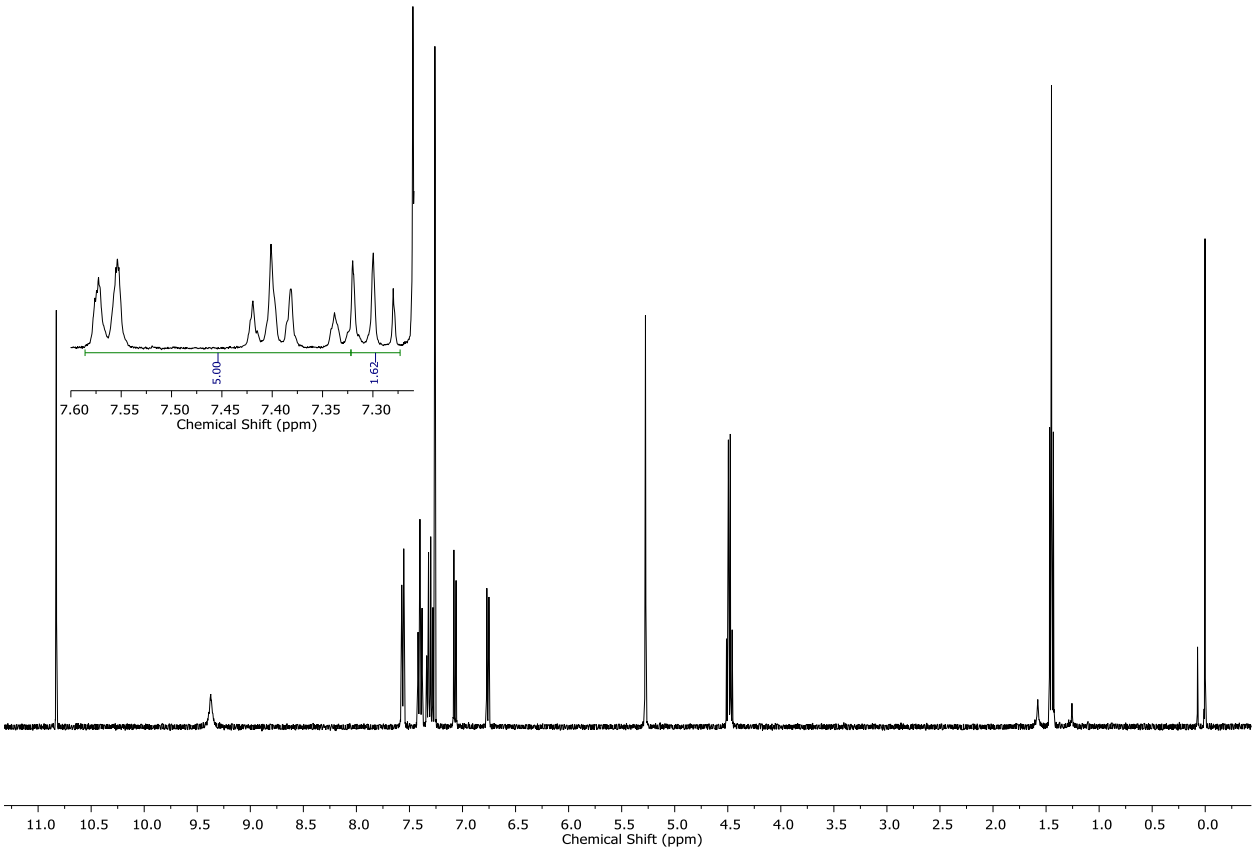

Figure 31: ^{1}H-NMR spectrum of formylated byproduct indicating the doublet of doublets at 7.30 ppm

Inspection of the aromatic region showed the expected two doublets at 6.77 ppm and 7.08 ppm as well as a doublet of doublets (appearing as a triplet) at 7.30 pm. Integration of the doublet of doublets does give a higher than expected integration value of 1.62, but this is due to the overlap of the benzyl aromatic signals. Integration of the benzyl aromatic signals and the doublet of doublets however give an integration of 6 protons. The absence of a singlet confirms that the

substitution had occurred at the C3-position. The structures depicted in **Scheme 24** were amended and the corrected scheme is shown below (**Scheme 26**).

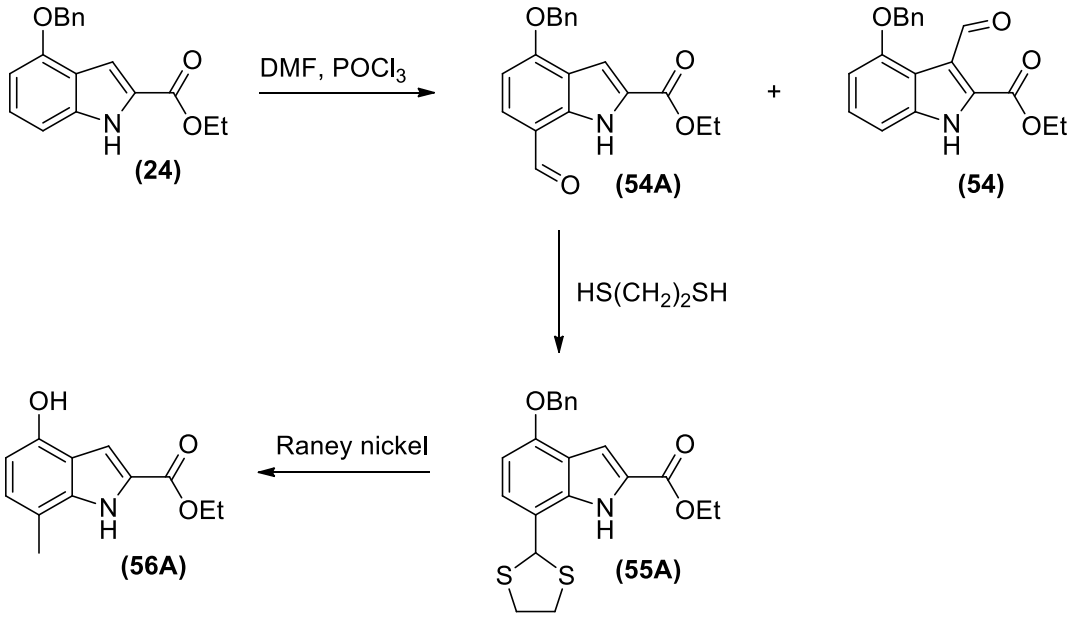

Scheme 26: Amended molecular structures of **Scheme 24**.

The regioselectivity obtained when carrying out the Vilsmeier-Haack formylation on **(24)** could be explained by the fact that the indole nitrogen is *ortho* and *para* directing, and the oxygen of the benzyl ether is also *ortho* and *para* directing. Thus the C5- and C7-position of the indole ring are nucleophilic and can undergo electrophilic aromatic substitution. It is possible that the steric hindrance of the benzyl group prohibits nucleophilic attack at the C5-position, and due to the increased reactivity of the C3-position relative to the C5-position, only a small amount of C3-formylated product was formed. Thus the C7-position is the most unhindered reactive site and formylation readily occurred at that position. The absence of a phenoxy group at the C4-position would make the Vilsmeier-Haack formylation – Mozingo reduction sequence a viable method for the methylation for the C3-position.

A crystal structure of **(54A)** was obtained to confirm the position of the aldehyde on the indole. **Figure 32** confirms the structure of **(54A)**. The crystal structure obtained confirms the presence of an aldehyde at the C7-position of the indole scaffold as opposed to the desired C3-position.This observation coincides with previously obtained spectroscopic data (**Figure 30**). The oxygen atom of the aldehyde is directed towards the proton of the indole nitrogen. Due to the bond length between the proton and the aldehyde oxygen reaching 2.89 Å, this indicated a moderate hydrogen bond of a mostly electrostatic nature.[8]

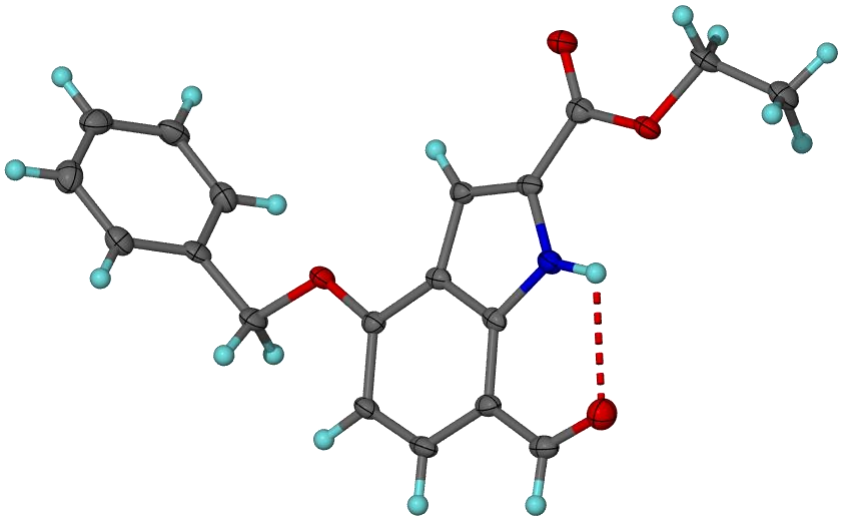

Figure 32: Molecular structure of **(54A)**. Thermal ellipsoids are shown at 50% probability. The intramolecular hydrogen bond is indicated as a dashed red line. (N–H---OHC, 2.89 Å, 113.3°)

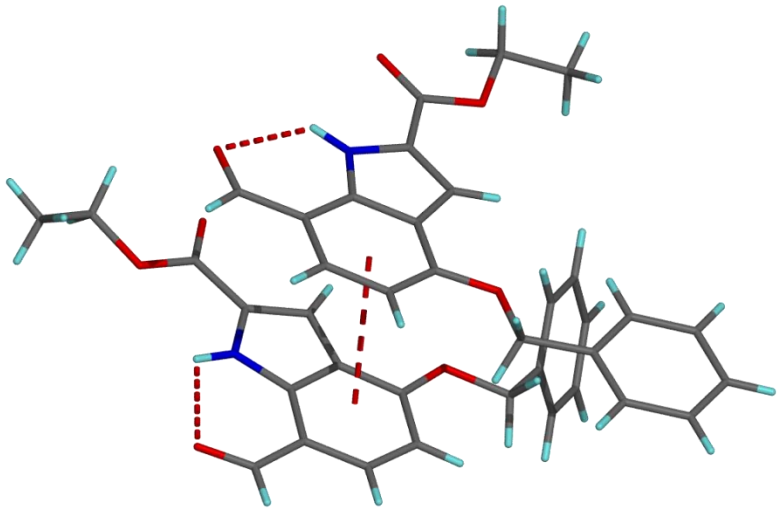

Figure 33: Parallel displaced pi-pi stacking between to indole rings of **(54A)**

The unit cell indicated two molecules of **(54A)** with different configurations. As seen in **Figure 33**, the benzyl group of one molecule is flat and in the plane of that molecule, while the benzyl group of the other molecule is rotated at an angle. A parallel displaced pi-pi stacking is also seen between the two indole rings, indicated by a red dashed line.

3.3 A ligand-free copper-catalyzed coupling of ethyl isocyanoacetate and 2-bromo acetophenones

Due to the fact that the formylation of **(24)** was not as regioselective as initially thought due to the increased reactivity of the indole heterocycle, we decided to explore another method to synthesize the required 3-methylated indole heterocycle. Research conducted by Ding *et al*.[9] described a simple transformation of substituted 2-halo benzaldehydes and aryl ketones to indoles utilizing a copper catalyzed condensation/coupling/deformylation cascade reaction sequence with ethyl isocyanoacetate, as illustrated in **Scheme 27**.

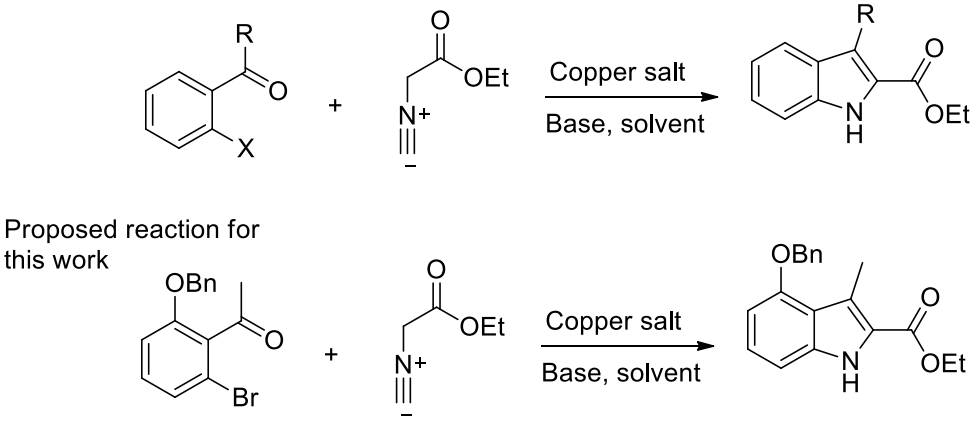

Scheme 27: Coupling of 2-halo aryl ketones and aldehydes with ethyl isocyanoacetate

We envisioned following up on this reaction sequence by synthesizing the required 2-bromo-6-benzyloxy acetophenone precursor necessary to produce the desired 3-methyl substituted indole scaffold, as seen in **Scheme 27**. Chloro and iodo substituted aryl rings are also feasible precursors for the cascade reaction to produce the desired indole. Our first attempt to synthesize 1-(2-bromo-6-hydroxyphenyl)ethanone was to follow the procedure described by a patent.[10] The procedure utilized a Fries rearrangement using $AlCl_3$ to obtain the desired substituted 2-halo benzaldehyde, as seen in **Scheme 28**.

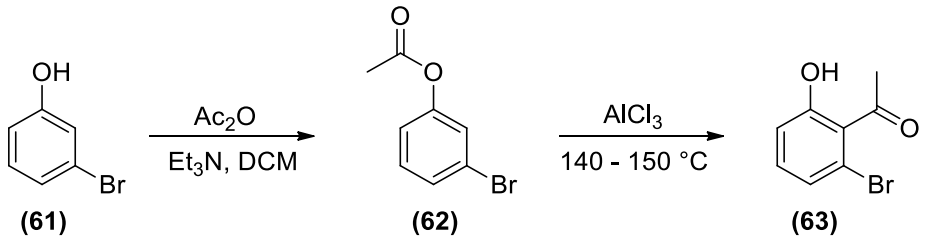

Scheme 28: Proposed reaction sequence to produce **(63)**

The Fries rearrangement involves the conversion of a phenyl acetate derivative to either an *ortho*- or *para*-acetylated phenolic derivative. The regioselectivity is governed by temperature control. *Ortho*-acetylation occurs at elevated temperatures while *para*-acetylation occurs at room temperature.[11] 3-Bromophenol **(61)** was acetylated using acetic anhydride to produce 3-bromophenyl acetate **(62)** in nearly quantitative yield. The subsequent Fries rearrangement of 3-bromophenyl acetate with $AlCl_3$ at 140 – 150 °C to synthesize 1-(2-bromo-6-hydroxyphenyl) ethanone **(63)** however produced the undesired regioisomer 1-(4-bromo-2-hydroxyphenyl) ethanone **(64)**, as seen in **Scheme 29**. This was confirmed by analysis of the ^{1}H-NMR spectrum. The substitution pattern on the aryl ring was not indicative of a 1,2,3-substituted aryl system, as the aromatic signals were all doublets. Further searching of the literature indicated that the synthesis of **(64)** via the Fries rearrangement of **(62)** has been well documented.[12,13,14]

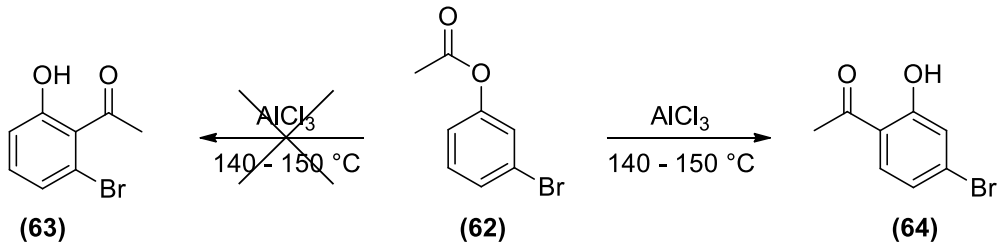

Scheme 29: Fries rearrangement of **(62)** producing **(64)**

We shifted our focus on trying to change the acetyl group to a formyl group, by carrying out a Reimer–Tiemann formylation[15] which is an ortho-formylation reaction. We reasoned that we could convert the aldehyde to a secondary alcohol via the reaction of methyl lithium, and then oxidize the secondary alcohol to the methyl ketone as seen in **Scheme 30**.

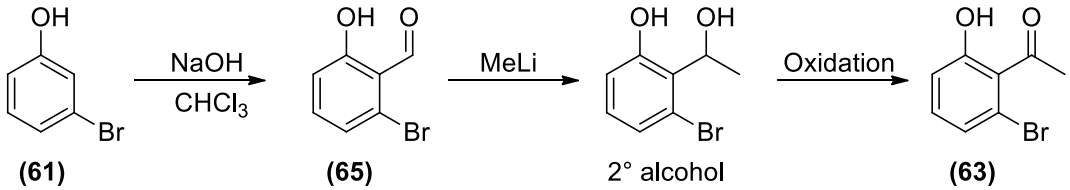

Scheme 30: Reimer–Tiemann formylation of **(61)** to yield **(65)** and proposed subsequent steps to synthesize **(63)**

The formylation however followed the same regioselectivity as that of the Fries rearrangement, producing **(66)** instead of the desired **(65)** as seen in **Scheme 31**. The ^{1}H-NMR spectrum confirmed the substitution pattern, as two doublets and a singlet in the aromatic region were observed.

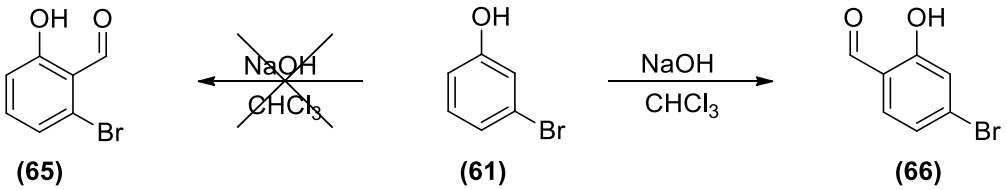

Scheme 31: Reimer–Tiemann formylation of **(61)** to yield **(66)**

Due to the fact that the Fries rearrangement and the Reimer–Tiemann formylation resulted in the undesired substitution on the 3-bromophenol ring, we decided to attempt a more direct substitution utilizing *ortho*-metalation followed by the reaction with a suitable electrophile to produce the desired aromatic ketone. We followed the procedure of a patent[16] in which they described the use of a methoxymethyl (MOM) group to facilitate *ortho*-lithiation followed by the introduction of acetic anhydride as the electrophile to produce **(68)**. **Scheme 32** illustrates this synthetic route.

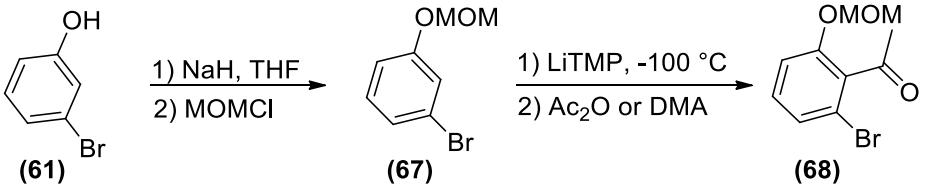

Scheme 32: MOM protection of **(61)** and subsequent *ortho*-lithiation to produce **(68)** using Ac_2O or DMA as electrophile.

MOM protection of **(61)** was carried out with MOMCl in the presence of NaH in THF to produce **(67)** in 39% yield. All the aromatic and aliphatic signals in the ^{1}H- and ^{13}C-NMR spectra were accounted for. The subsequent synthesis of **(68)** was carried out at -100 °C in THF using LiTMP as the base to facilitate deprotonation. When acetic anhydride (Ac_2O) was introduced as the electrophile, we observed the formation of a product when the reaction was monitored via TLC. ^{1}H-NMR spectroscopy however proved that the acquired product was not the desired product **(68)** but an unknown product. The reaction was carried out again using the same conditions, but this time *N,N*-dimethyl acetamide (DMA) was used as the electrophile. Interestingly, the ^{1}H-NMR spectra of both products were identical. In order to determine the identity of the unknown product, numbered **(69)**, a number of spectroscopic experiments were carried out.

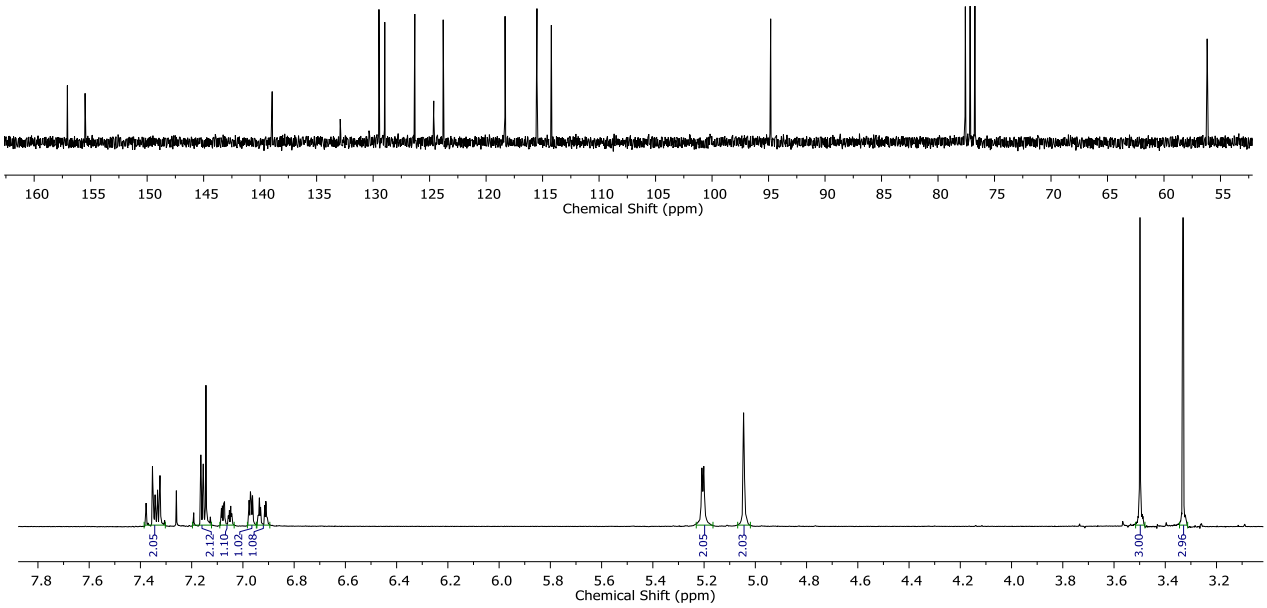

Figure 34: ^{1}H- and ^{13}C-NMR spectra of unknown compound **(69)** after *o*-lithiation and Ac_2O quench in $CDCl_3$

Figure 34 illustrates the ^{1}H-NMR and ^{13}C-NMR spectra of the unknown compound formed by the reaction with Ac_2O, and **Figure 35** shows the superimposed ^{1}H-NMR spectra of both products obtained after *ortho*-lithiation and quenching with Ac_2O as well as DMA. As mentioned, both products obtained after quenching with Ac_2O or DMA are identical with regards to their respective ^{1}H- and ^{13}C-NMR spectra.

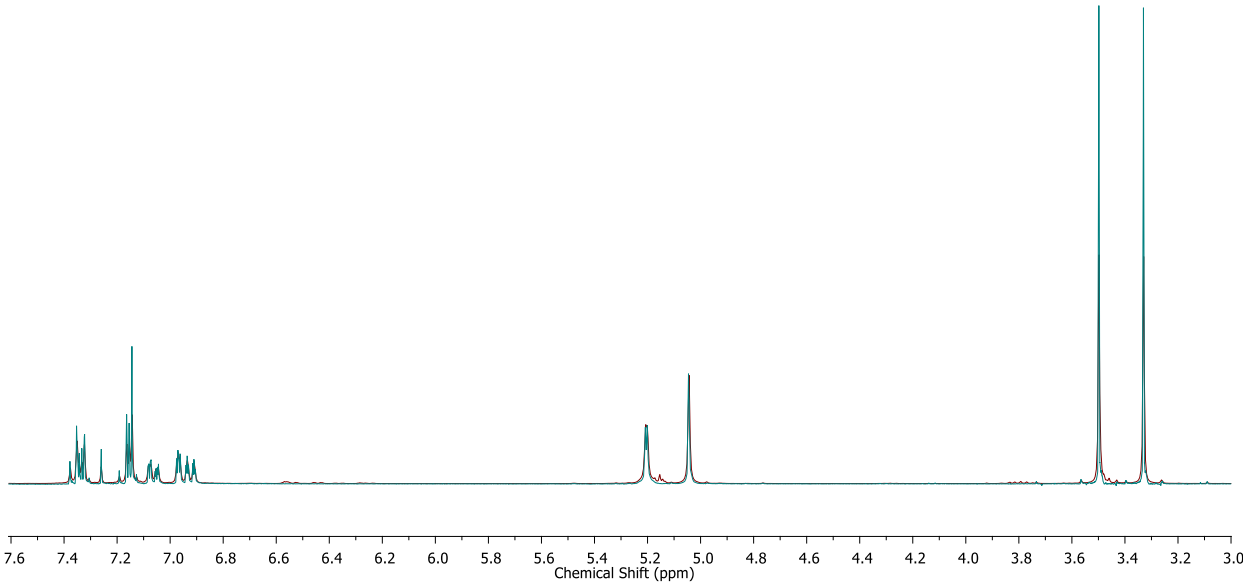

Figure 35: Superimposed ^{1}H-NMR spectra of the unknown compound formed in both reactions

Analysis of the ^{1}H-NMR spectrum shown in **Figure 34** suggested that the unknown product **(69)** has two MOM groups evident by the appearance of two signals at 5.04 ppm and 5.21 ppm, integrating for two protons each and two singlets at 3.33 ppm and 3.50 ppm integrating for three protons respectively. The aromatic signals integrate for a total of seven protons. The ^{13}C-NMR spectrum indicated a total of 16 signals, 12 in the aromatic region and four in the aliphatic region indicative of the carbons of the MOM group. The HRMS of the **(69)** was obtained which can be seen in **Figure 36**. Analysis of the MS data shows a molecular ion of 294.2006 m/z as the most abundant mass. Furthermore it was speculated that since the starting reagent **(67)** contained a bromine atom, the molecular ions at 323.0035 m/z and 372.0556 m/z could be closely related to the actual unknown compound mass, due to the nearly 50/50 abundance of both isotopes of ^{79}Br and ^{81}Br resulting in the double signals observed.

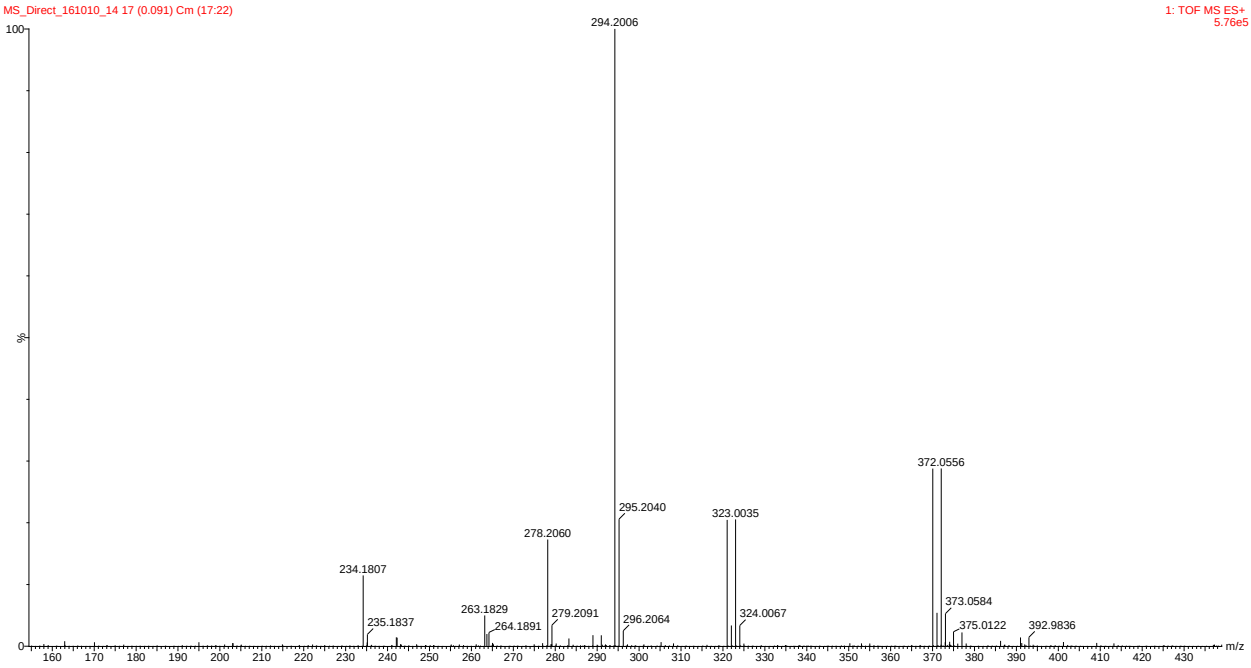

Figure 36: HRMS of unknown compound

Due to the fact that two MOM-groups as well as seven protons in the aromatic region were observed from the ^{1}H-NMR spectrum and in addition twelve aromatic signals were identified in the ^{13}C-NMR spectrum it was speculated that the unknown product **(69)** contains two aryl rings. Additionally the MS data suggested that at least one of the aryl rings contains a bromine substituent. The degree of unsaturation for **(69)** was calculated with the idea that **(69)** only contains one bromine substituent. A degree of unsaturation number of 8 was calculated, this result was further indicative of two aryl rings. Seven protons, two aryl MOM groups and at least one

aromatic bromine gives reason to believe that the aryl rings are directly connected. Since the same unknown compound was obtained regardless of the quenching with DMA or Ac_2O as the electrophile, it was postulated that the unknown product was pre-formed *in situ* and that as a result neither DMA nor Ac_2O played a role in the formation of **(69)**. Further spectroscopic data was required in an attempt to identify **(69)**. As a result a COSY spectrum was obtained to determine the coupling pattern between the aromatic signals. **Figure 37** indicates the enlarged aromatic region with drawn lines indicating proton signals that couple to each other.

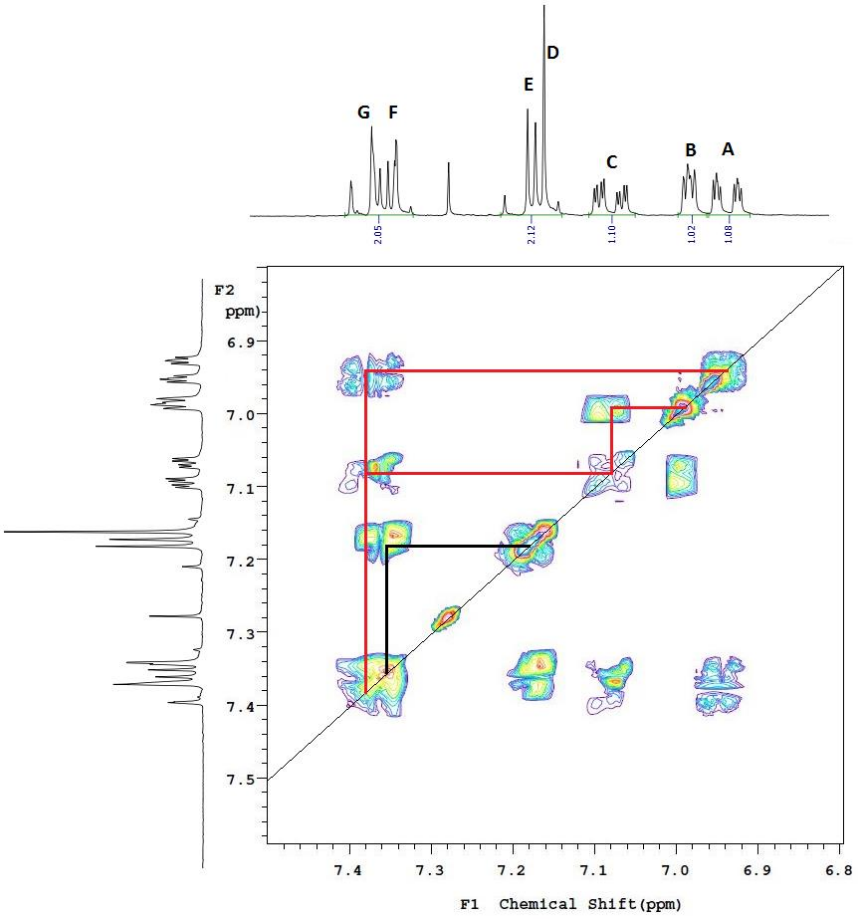

Figure 37: COSY spectrum of **(69)** Indicating the proton signals that couple to each other.

As can be seen in **Figure 37**, proton **A** is coupled to a proton in the multiplet at 7.30 – 7.38 ppm annotated as **G**, proton **B** is coupled to proton **C**, which also coupled to proton **G**. Since **G** is coupled to both **A** and **C**, **G** would have to be *ortho* to **A** and **C**. A multiplet at 7.12 – 7.19 ppm integrates for two protons, thus both protons annotated as **D** and **E** couple to a proton in the multiplet at 7.30 – 7.38 ppm annotated as **F** shown by the black lines in **Figure 37.** The COSY spectrum indicates that one aryl ring has four protons (**A**, **B**, **C**, **G**) which are separated by the

neighboring aryl ring containing three protons (**D**, **E**, **F**). **Figure 38** illustrates the HSQC spectrum of **(69)**, illustrating the entire spectrum (top) as well as an enlarged version of the aromatic region (below).

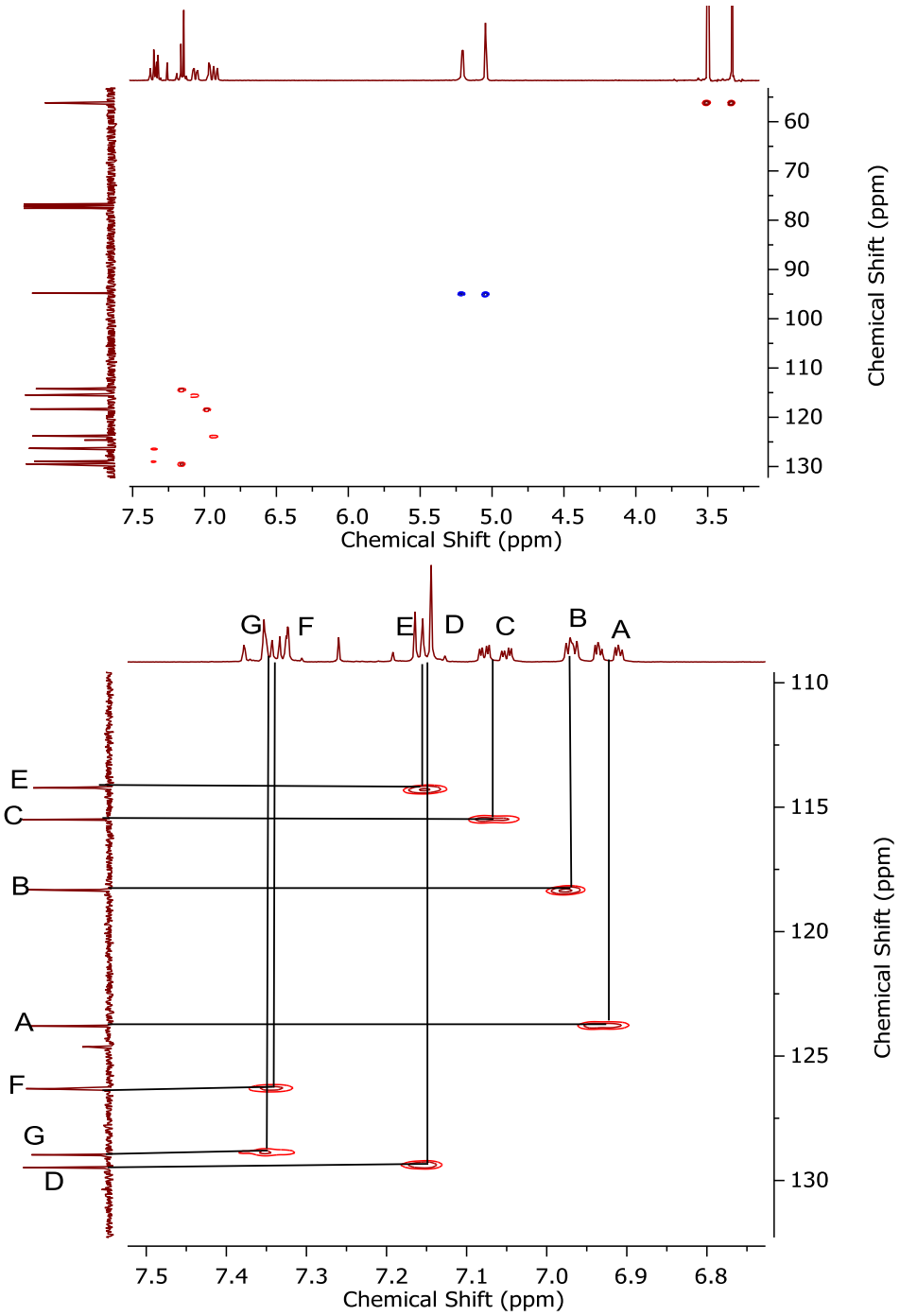

Figure 38: HSQC spectra of **(69)**, the full spectrum is at the top and the enlarged aromatic region at the bottom.

The HSQC spectrum shown at the top of **Figure 38** illustrates that the two MOM groups are in fact present due to the fact that a HSQC spectrum indicates methylene groups in blue, while methyl and tertiary carbon groups are indicated in red. It also gives us an indication which carbons are coupled to certain protons. The carbons that are coupled to protons **A** – **G** are annotated in the spectrum.

A NOESY spectrum (**Figure 39**) of **(69)** was acquired in order to obtain information regarding protons which correlate due to being in a close proximity through space. This could potentially indicate on which aryl ring each MOM group is situated, provided that the MOM groups are adjacent to a protonated carbon. The methyl and methylene groups of the MOM groups would have an interaction through space with each other as we see in the green box, where methyl **H** has a correlation with methylene **J**, and methyl **I** has a correlation with methylene **K**. The methylene in turn would have correlations with protons on the aryl rings.

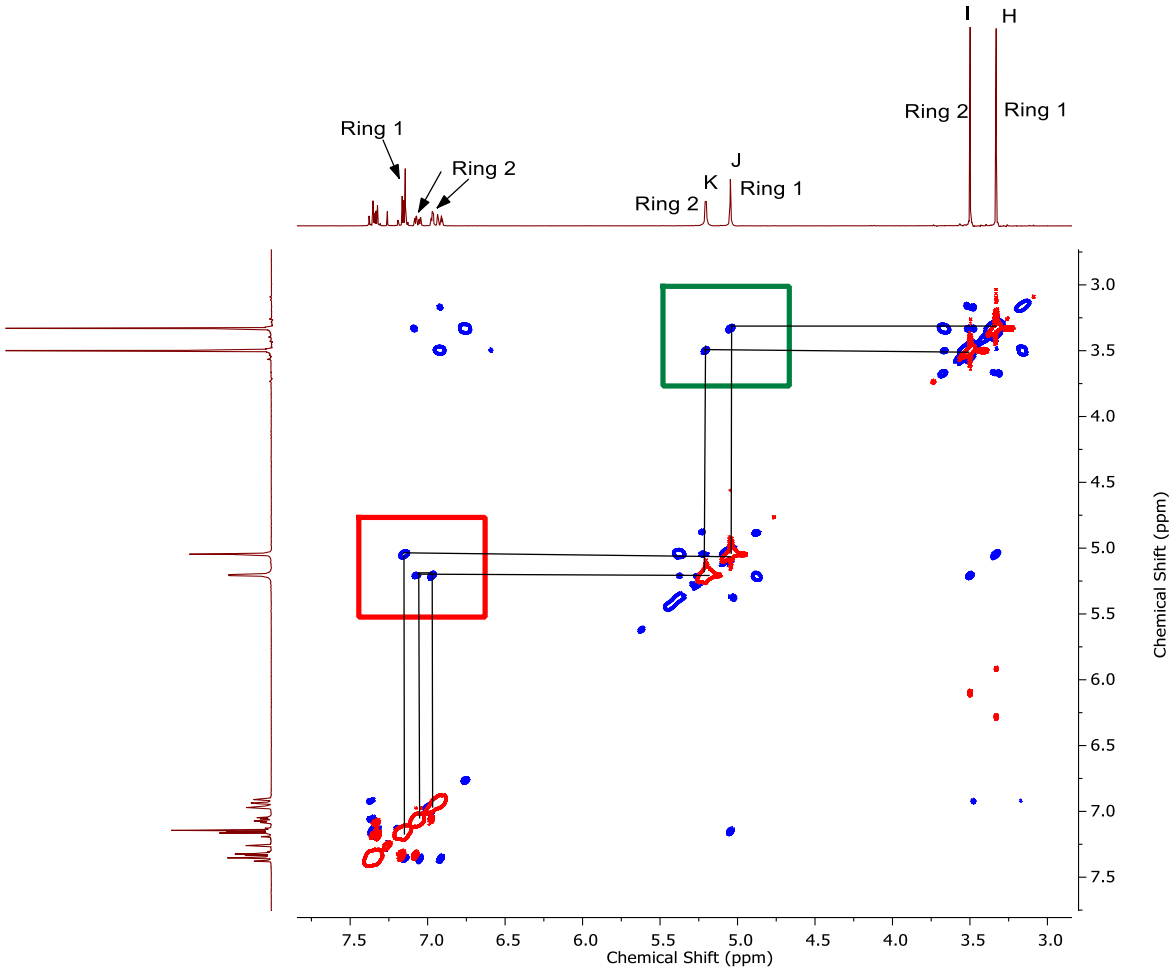

Figure 39: NOESY spectrum of **(69)**

Methylene **J** has a correlation with either proton **D** or **E** (red box), which has been shown by the COSY spectrum to be on the same aryl ring. Methylene **K** has two separate interactions with protons **B** and **C** respectively. This suggests that protons **B** and **C** are both *ortho* to the MOM group of that aryl ring. The aryl rings are titled Ring 1 and Ring 2. Ring 1 contains the MOM groups with protons **H** and **J** as well as aromatic protons **D**, **E** and **F**. Ring 2 contains the MOM groups with protons **I** and **K** as well as aromatic protons **A**, **B, C** and **G**. Analysis of the COSY spectrum enabled us to determine that protons **A** and **C** are most likely *ortho* to proton **G**, yet proton **B** couples to **C** as well. Through analysis of the NOESY spectrum it was determined that proton **B** has no protons *ortho* to it. Proton B appears as a doublet of doublets in the ^{1}H-NMR spectrum, with coupling constants of J = 2.5 and 1.6 Hz. The small coupling constants indicates long range coupling and further adds to the observation that proton **B** has no protons *ortho* to it.

To finalize the structure elucidation we obtained an HMBC spectrum to indicate ^{3}J – couplings between protons and carbons. This in turn provides a method to assign the carbon signals to either Ring 1 or Ring 2. The HMBC spectrum is illustrated in **Figure 40** and the enlarged aromatic region in **Figure 41**.

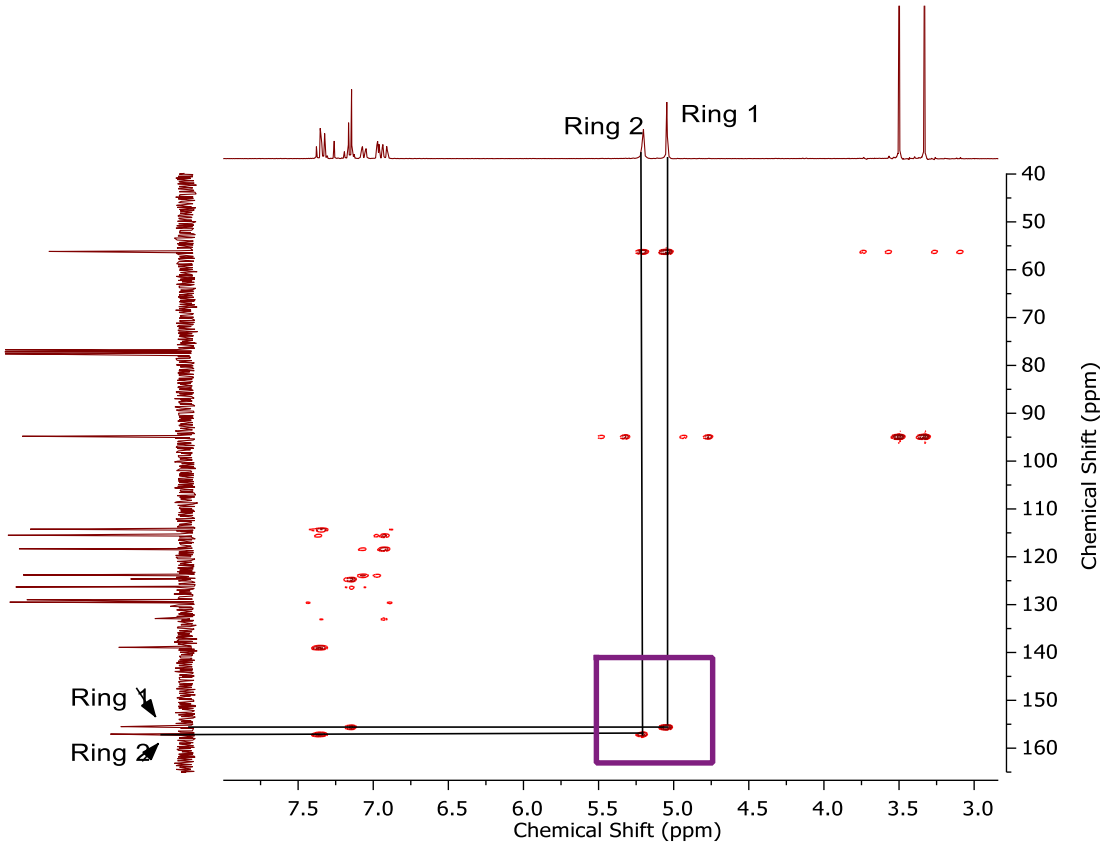

Figure 40: HMBC spectrum of **(69)**

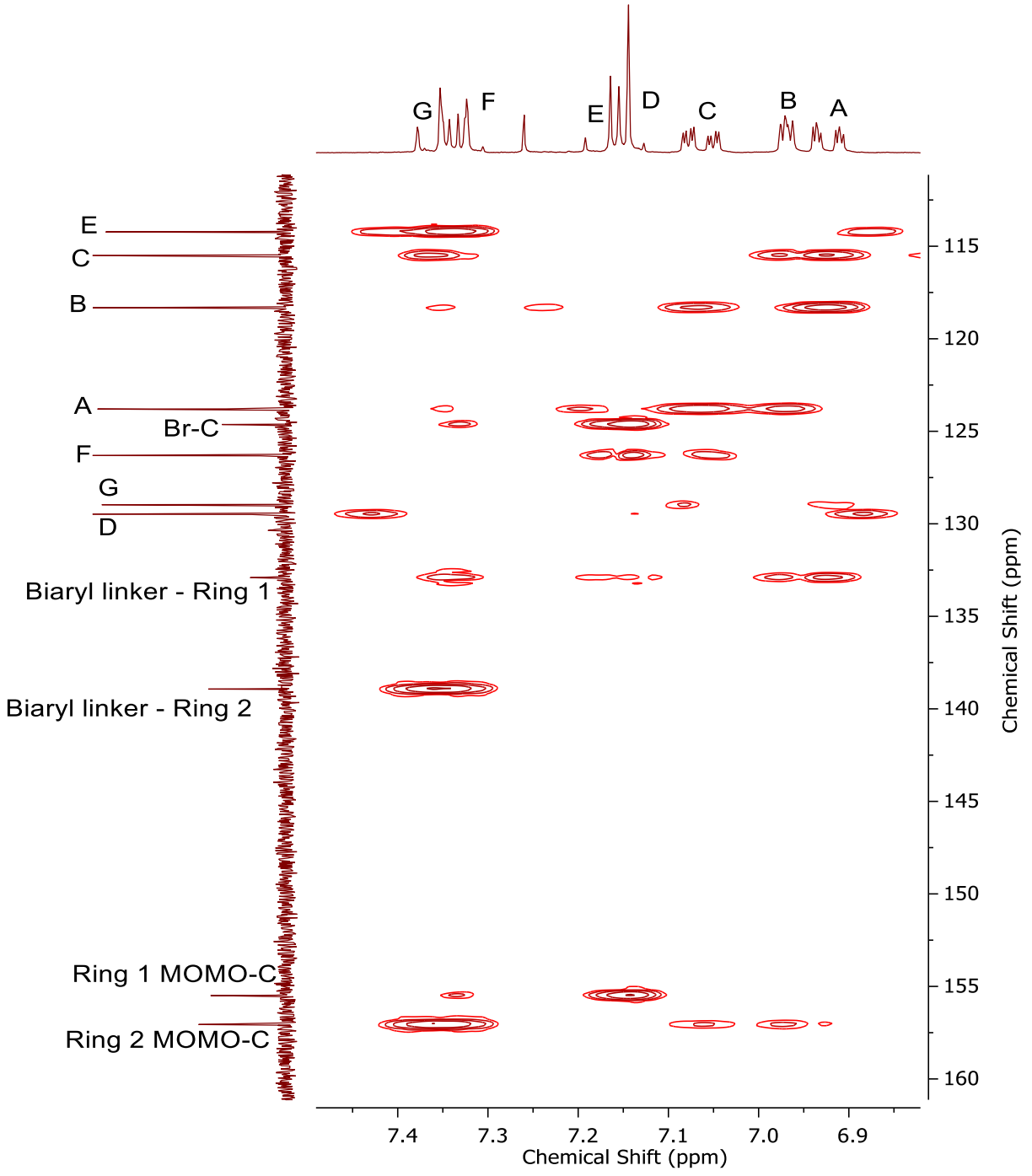

Figure 41: Aromatic section of the HMBC spectrum of **(69)**

As previously determined, Ring 1 contains the MOM groups with protons **H** and **J** as well as aromatic protons **D**, **E** and **F**. Ring 2 contains the MOM groups with protons **I** and **K** as well as aromatic protons **A**, **B, C** and **G.** Proton **G** ^{3}J – couples to the carbon at 157.1 ppm, thus *meta* to

the -OMOM group situated on Ring 2, but also couples to the quaternary carbon (4ºcarbon) at 139.0 ppm thus *meta* to the carbon that bonds the two aryl rings, thus that carbon is on Ring 2. Proton **A** and **B** ^{3}J – couples to carbon **C**, thus proton **A** and **B** are *meta* to proton **C**. Proton **A** ^{3}J – couples to 4º carbon at 132.9 ppm, and since there are only two 4º carbons on Ring 2, one of which is the carbon connected to the OMOM, it is speculated that the 4º carbon on Ring 1 bonds the two aryl rings. Proton **D** is ^{3}J – coupling to the OMOM carbon at 155.5 ppm on Ring 1, thus *meta* to that carbon, but also coupling to the 4º carbon at 124.6 ppm therefore the carbon at 124.6 ppm must contain the bromine atom as substituent. This observation further confirms that protons **E** and **F** are both *ortho* to proton **D**. We also observe ^{2}J – and ^{4}J – coupling of protons **E** and **F** to the carbon with the bromine substituent. Proton **F** is coupling to the 4º carbon at 132.9 pm thus it is *meta* to that carbon.

Considering all the data we suspect that the unknown compound **(69)** has the molecular structure shown in **Figure 42**.

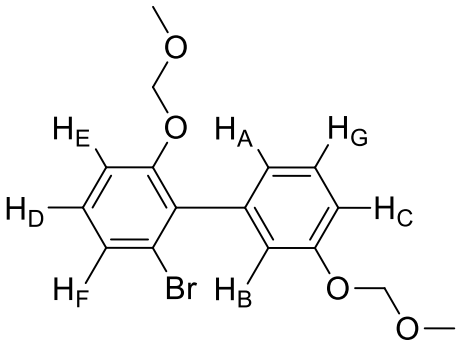

Figure 42: Proposed molecular structure of **(69)**

The molecular ions obtained from the HRMS results as seen in **Figure 36** could not be explained by possible adducts and selective fragments. The m/z 370.0576 and m/z 372.0556 values corresponded to the molecular ion of the compound bonded with the Br^{79} and Br^{81} isotopes respectively, as well as the observed m/z 321.0055 and m/z 323.0035 values. The calculated mass $[M+H]^{+}$ for **(69)** would be m/z 353.0389 and m/z 355.0368 for both isotopes. We could however not calculate the correct fragmentation pattern and possible adducts for the two sets of m/z values that would give a mass accuracy of less than 5 ppm. Despite this we were confident that the various analysis techniques used were effective to accurately elucidate the unknown structure. The mechanism by which **(69)** was formed could be explained by the formation of a benzyne intermediate. The use of bromobenzene derivatives for benzyne formation have been well documented in the literature[17,18] and pose a versatile method for functionalization on aryl

systems. Benzyne formation requires a leaving group on an aromatic system, usually a halogen *ortho* to a hydrogen, as well as the use of strong bases like butyllithium and amide bases *i.e*. LiTMP and LDA. Deprotonation of the proton *ortho* to the leaving group results in the formation of a lithiated aryl carbanion, after which the newly formed negative charge facilitates the elimination of the leaving group. The reaction mechanism is shown in **Scheme 33.**

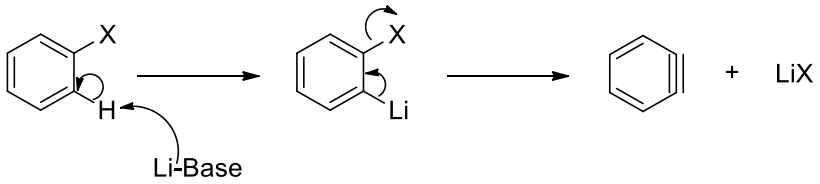

Scheme 33: Mechanism for the formation of a benzyne species

The regiochemistry of benzyne formation is affected by the electronic nature of the substituents on the aryl ring.[19] On *para* and *ortho* di-substituted aryl systems where one of the substituents is the leaving group, benzyne formation results in the formation of only one regioisomer. *Meta* di-substituted systems however have two regioisomers that can form due to the two deprotonatable protons *ortho* to the leaving group. If the substituent is electron withdrawing, it acidifies the adjacent proton promoting deprotonation between the substituent and the leaving group, whereas if the substituent is electron donating, a mixture of benzyne regioisomers is formed. The regiochemistry of the benzyne triple bond has an effect on the position of nucleophilic attack of a given nucleophile, as mixtures of regioisomers can form. Due to the fact that the ^{13}C-NMR spectrum only indicates 16 carbons, **(69)** is not a mixture of products. As a result it can be assumed there was regiocontrol in the formation of **(69)**.

We suspected that the presence of the OMOM group is the reason for the observed regiocontrol. Methoxymethyl ethers are excellent *ortho*-metalation directing groups.[20] The acidification of the proton *ortho* to the bromine and OMOM group on **(67)** due to the electron withdrawing nature of the bromine substituent alongside the added *ortho*-directing nature of the -OMOM group results in the formation of only one regioisomer of the benzyne intermediate.

The formation of **(69)** could be explained via the formation of a benzyne intermediate as well as the regiospecific nucleophilic attack of a lithiated species of **(67)**. The formation of **(69)** is illustrated in **Scheme 34**.

Formation of benzyne intermediate

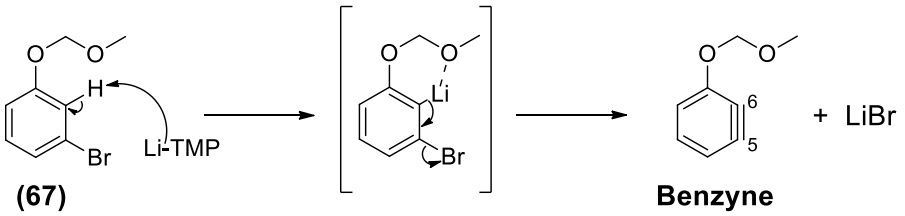

(67) **Benzyne**

Ortho lithiation of **(67)**

(67) **Nucleophile**

Nucleophilic attack on benzyne

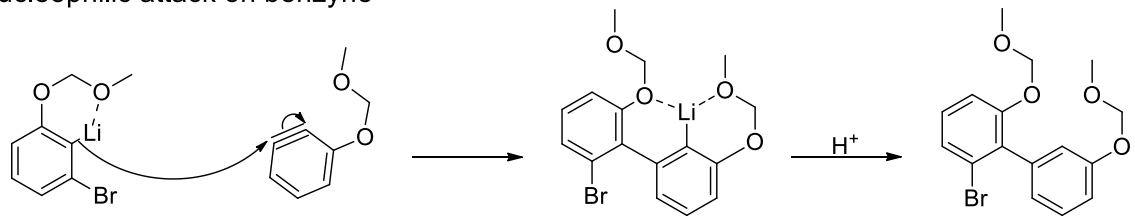

Nucleophile **Benzyne** **Stabilized Bi-Aryl** **(69)**

Scheme 34: Benzyne formation of **(67)** and subsequent nucleophilic attack to produce **(69)**

LiTMP deprotonates the acidic proton *ortho* to the bromine and the OMOM group. The newly formed carbocation then undergoes benzyne formation upon which another newly formed carbocation acts as a nucleophile and attacks the benzyne at the C5-position. This results in the formation of a lithiated bi-aryl species which is stabilized by two OMOM groups in close proximity. We suggest that the stabilization of the two OMOM groups is what drives the regiospecific nucleophilic addition.

Although the results were unexpected but interesting to say the least, this route to produce the desired compound **(68)** was not successful and thus this route could not be used to synthesize the desired 3-methyl indole scaffold.

3.4 Larock indole synthesis

Due to the difficulty in forming the 2-bromoacetophenones, that method to form the 3-methyl indole scaffold was abandoned. Through an extensive search through the literature we came across the Larock indole synthesis, also known as the Larock heteroannulation reaction. The Larock indole synthesis is a palladium catalyzed heteroannulation reaction involving the coupling of an *ortho*-iodo aniline with internal alkynes to produce 2,3–substituted indoles[21,22] as seen in **Scheme 35**. The use of unsymmetrical alkynes has an overall effect on the regioselectivity of the substituents on the indole ring. It was shown that the largest substituent R_L on the alkyne prefers to be situated on the C3-position of the indole ring and thus the smallest substituent R_S on the C2-position.

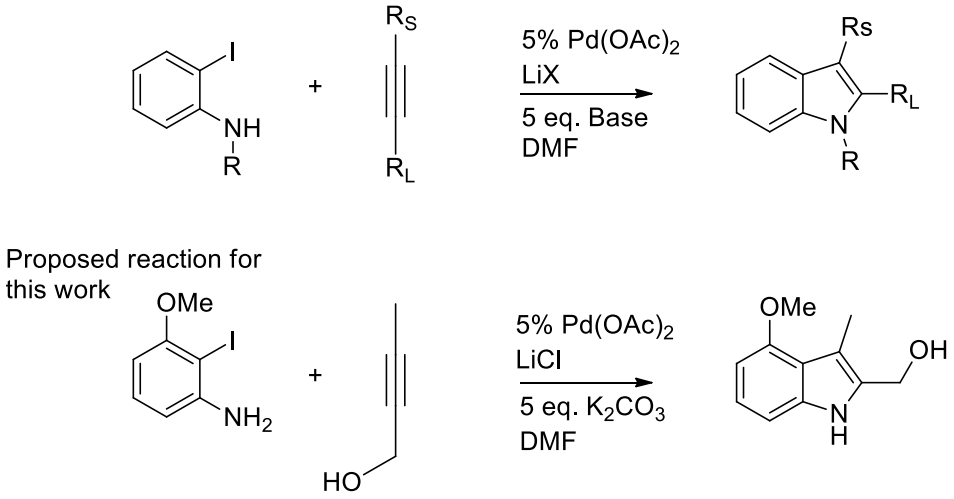

Scheme 35: Larock heteroannulation indicating the regioselectivity due to alkyne substituent sizes, as well as proposed reaction to synthesize the desired 3-methyl indole scaffold

We envisioned that using this reaction procedure would be a plausible method by which to synthesize the desired 3-methyl indole scaffold. In order for us to synthesize the desired indole containing an ester in the C2-position it was proposed that a methanol substituent in the C2-position would be required which could be further derivatized to obtain the desired ester group. Due to the nature of the Larock, the presence of the ester group on the alkyne would result in the undesired regioselectivity. It was envisioned that the Larock synthesis could be accomplished using but-2-yn-1-ol as the unsymmetrical alkyne. Larock and co-workers described that alcohol containing alkynes exhibit complete regioselectivity resulting in the alcoholic substituent being placed on the C2-position exclusively, hence regioselective formation of the indole ring would occur.[22]

In order to obtain the desired 3-methyl indole scaffold the necessary *ortho*-iodo aniline had to be synthesized. We envisaged that this could be achieved starting with 2-amino-3-nitrophenol **(70)**, and **Scheme 36** illustrates the reaction scheme followed in order to synthesize the required 2-iodo aniline derivative **(74)**. As it was necessary to protect the phenol to avoid competing side reactions we decided on utilizing a methoxy as protecting group for the initial heteroannulation reaction. This is due to the fact that a protecting group such as a benzyl group could crowd the aromatic region of the ^{1}H-NMR spectra and as a result hinder the ability to ascertain whether the correct product had been formed. We planned on exchanging the methoxy with a benzyloxy when we have successfully confirmed the synthesis of the desired 3-methyl indole scaffold due to the fact that the benzyl group is easier to remove.

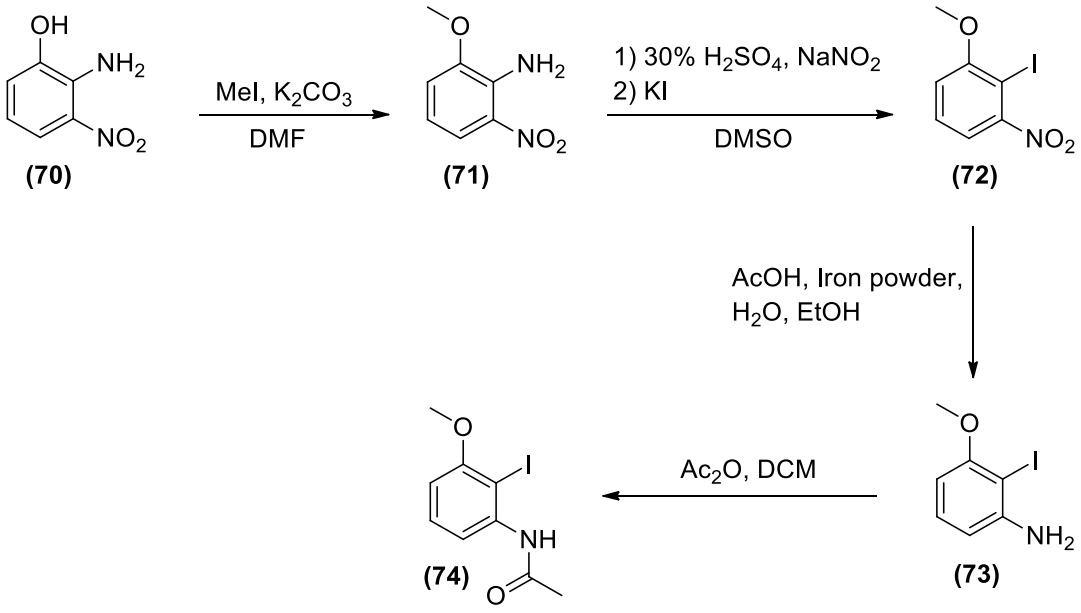

Scheme 36: Synthesis of iodo aniline **(73)** and iodo acetanilide **(74)**

The first step involved the methylation of 2-amino-3-nitrophenol **(70)** with methyl iodide in DMF with K_2CO_3 as base, producing **(71)** in a 97% yield after purification. *O*-Methylation on the phenol was observed and little to no *N*-methylation, due to the decreased nucleophilicity of the amine *ortho* to the nitro substituent. ^{1}H-NMR spectroscopy provided sufficient evidence for the successful *O*-methylation. The conversion of **(71)** via the Sandmeyer reaction to the corresponding 2-iodo-1-methoxy-3-nitrobenzene **(72)** was carried out following a procedure reported by Dai and co-workers[23] to produce **(72)** in 81% yield. ^{1}H-NMR spectroscopy proved the absence of the amine protons, but the presence of an iodine on the aryl ring was determined by ^{13}C-NMR spectroscopy due to a carbon signal appearing at 79.9 ppm, corresponding to the

aromatic carbon bonded to the iodine. **(73)** Was obtained through the reduction of **(72)** with acetic acid and iron powder. The procedure for the reduction of **(72)** was reported by Gamble and co-workers.[24] They describe carrying out the reduction using sonication instead of classical stirring and/or reflux conditions. This proved to be a mild and effective nitro reduction method as we obtained **(73)** in a 94% yield. In the publication of Larock and co-workers,[22] it was noted that they also acetylate the aniline nitrogen as a measure to increase the reactivity of the amine. We subsequently acetylated **(73)** with Ac_2O to obtain **(74)** in a 58% yield.

With compounds **(73)** and **(74)** in hand we attempted to carry out the heteroannulation reactions of **(73)** and **(74)** with but-2-yn-1-ol using $Pd(OAc)_2$, K_2CO_3 and LiCl in DMF at 100 °C. Disappointinly, we did not manage to isolate any products from either heteroannulation reactions of **(73)** or **(74)** as the conditions resulted in the formation of a multitude of products when analyzed via TLC. We did not pursue optimizing the conditions to produce the desired indole in **Scheme 35** as at the time we had discovered another more effective method for the synthesis of the desired 3-methyl indole.

3.5 Bromination followed by Suzuki-Miyaura coupling

As illustrated in **Scheme 25**, indole systems have an increased nucleophilicity at the C3-position due to delocalization of the indole nitrogen lone pair into the pyrrole ring, activating the C3-position. Research conducted by Tani *et al*.[25] have devised different methodologies regarding the regioselective bromination of substituted ethyl indole-2-carboxylates. Depending on the substituents on the aryl ring of the ethyl indole-2-carboxylate and depending on the use of NBS or bromine in acetic acid as bromonium source, electrophilic aromatic substitution on either the aryl or pyrrole rings of the indole heterocycle could be controlled. As part of their study they carried out bromination reactions on ethyl 4-methoxy-1*H*-indole-2-carboxylate, the 4-methoxy analogue of compound **(24)**. The reaction of ethyl 4-methoxy-1*H*-indole-2-carboxylate and NBS in DMF at 0 °C resulted in bromination on the C3-position in a 76% yield and 3,7-dibromination in a 14% yield. In light of the regioselectivity observed by means of the Vilsmeier-Haack formylation where electrophilic aromatic substitution occurred predominantly on the 7-position, this was a promising result as it increased the probability that we could get the desired regioselectivity on compound **(24)**.

Research conducted by Kimber[26] reported having managed to convert a 3-bromo ethyl-1*H*-indole-2-carboxylate to the corresponding 3-methylated indole derivative using trimethylboroxine (TMB) in a Suzuki-Miyaura coupling. The use of TMB to effectively methylate aryl halides has been studied in the literature.[27] We envisaged using both procedures as a means to methylate **(24)** at the C3-position. **Scheme 37** illustrates the route we followed.

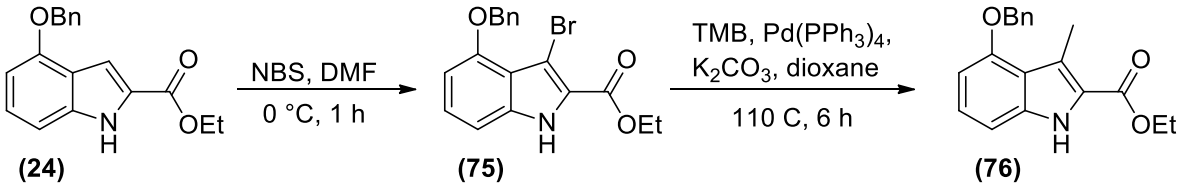

Scheme 37: Bromination of **(24)** and methylation of **(75)** by means of a Suzuki coupling

Bromination was carried out by adding 1.1 equivalents of NBS dissolved in DMF to a solution of **(24)** in DMF at 0 °C after which the reaction was completed within a period of 40 minutes to one hour. The reaction was monitored via TLC and complete consumption of starting material was observed, while two distinct product spots appeared to have formed. The two products were purified after which ^{1}H-NMR spectroscopy confirmed the formation of **(75)** as the major product in an 80% yield. This was due to the aromatic signals integrating for eight protons altogether. The appearance of two doublets at 6.62 ppm (J = 7.8 Hz) and 7.02 ppm (J = 8.4 Hz) and a doublet of doublets at 7.25 ppm (J = 8.4, 7.8 Hz) confirms that no substitution had occurred on the aryl ring of **(24)**. HRMS confirmed the mass to be that of the calculated mass.

The byproduct was isolated in a 14% yield and fully characterized. The ^{1}H-NMR spectrum confirmed that di-bromination had occurred due to the aromatic signals integrating for seven protons overall. The presence of two doublets having a coupling constant of J = 8.4 Hz and the absence of a doublet of doublets (appearing a triplet) indicates bromination on the aryl ring. HRMS confirmed the molecular ion of a di-brominated indole. A 1D NOESY experiment was performed to confirm the position of substitution on the aryl ring in order to verify the results reported by Tani. **Figure 43** indicates the two positions that possible bromination could have occurred.

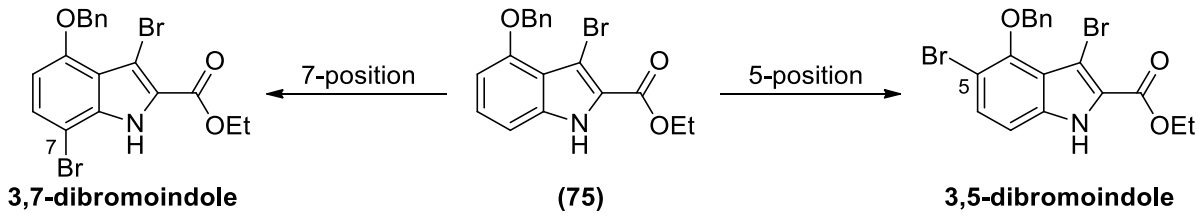

3,7-dibromoindole **(75)** **3,5-dibromoindole**

Figure 43: Possible positions for bromination

Figure 44 indicates the aromatic region of the byproduct as well as the two doublets in question shown in red rectangles. In order to elucidate the position of the bromine atom we irradiated the methylene protons of the benzyl group and the proton of the indole nitrogen. A proton at the 5-position could potentially exhibit an NOE effect with the methylene protons, but a proton on the 7-position would not due to the long distance. The indole N-H would also potentially exhibit an NOE effect with a proton at the 7-position and not at the 5-postion. **Figure 45** illustrates the 1D NOESY experiment, with the top spectrum in maroon indicating the methylene protons irradiated, with a positive NOE effect on the proton on the indole ring appearing as a doublet at 6.39 ppm and the benzyl doublet at 7.47 ppm. Irradiation of the indole N-H proton (blue) however exhibits no NOE effect on nearby protons. This is indicative that the bromine is on the 7-position and is therefore the 3,7-dibromo indole.

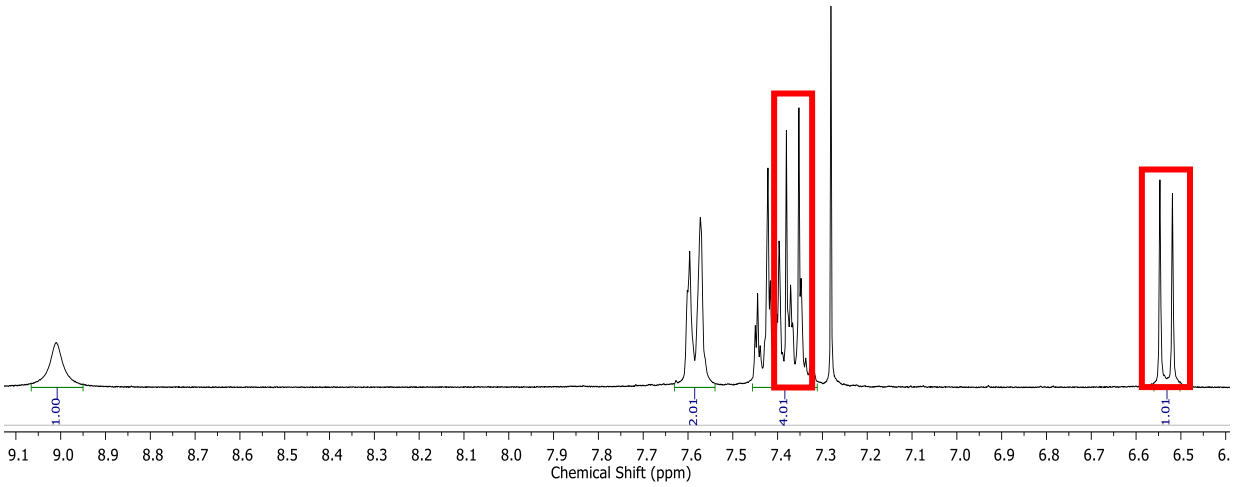

Figure 44: ^{1}H-NMR spectrum of the aromatic section of the 3,7-dibrominated byproduct in $CDCl_3$

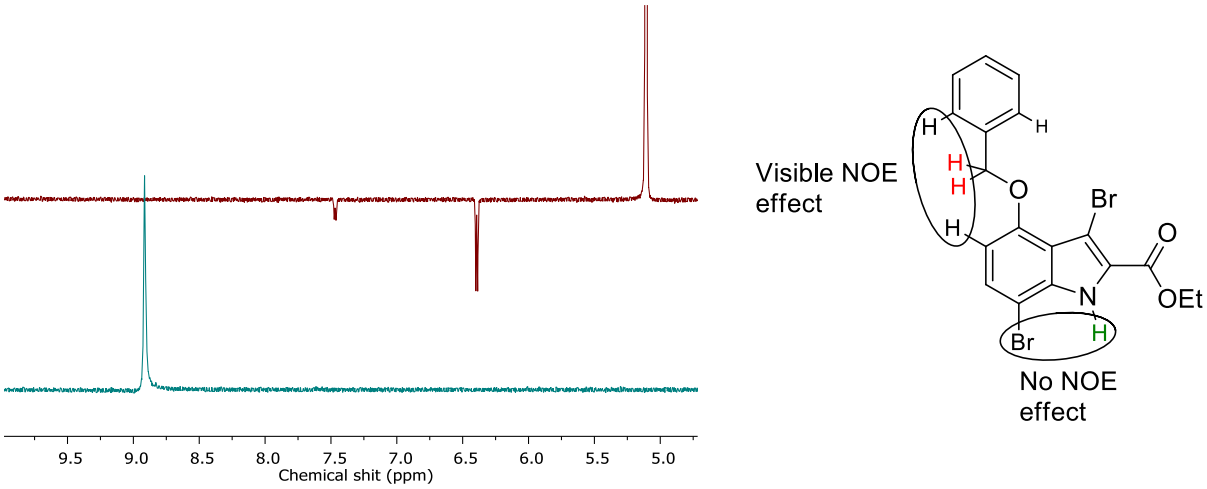

Figure 45: 1D NOESY of the 3,7-dibrominated indole irradiating benzyl methylene protons (top) and indole N-H (bottom)

The reason as to why the Vilsmeier-Haack formylation would be regioselective for formylation on the 7-position and bromination regioselective on the C3-position could possibly be explained by the solvent effects of each reaction. The Vilsmeier-Haack formylation was carried out in THF, and although polar in nature, does not have the charge stabilization properties as that of DMF in which the bromination step was carried out. Both electrophiles are small but considering the size, NBS is larger. It stands to reason that the nucleophilicity of the C3-position is significantly affected by the solvent used, as the delocalization of the indole N-H through the pyrrole ring is stabilized by the DMF molecules, in turn activating the C3-position to a greater extent even though NBS is larger and the benzyl group has a steric factor. This explanation is only speculative in nature, as the same argument could also be held for the stabilization of the *para*-directing *O*-benzyl group and the *ortho*-directing indole N-H group.

With compound **(75)** in hand we carried out the Suzuki-Miyaura coupling to synthesize **(76)**. Suzuki-Miyaura coupling, commonly referred to as the Suzuki coupling, is the palladium catalyzed cross-coupling reaction of an aryl halide with an aryl or aliphatic boronic acid. The palladium source for the Suzuki coupling was tetrakis(triphenylphosphine)palladium(0) ($Pd(PPh_3)_4$) and K_2CO_3 was the base involved in the formation of methyl boronic acid from TMB *in situ*. Monitoring the reaction via TLC had shown the appearance of another spot with a blue hue. This was indicative that the reaction had worked, as under UV light, **(24)** had a blue hue, **(75)** did not and the newly formed product did. The product was purified and ^{1}H-NMR spectroscopy **Figure 46** confirmed the formation of **(76)**.

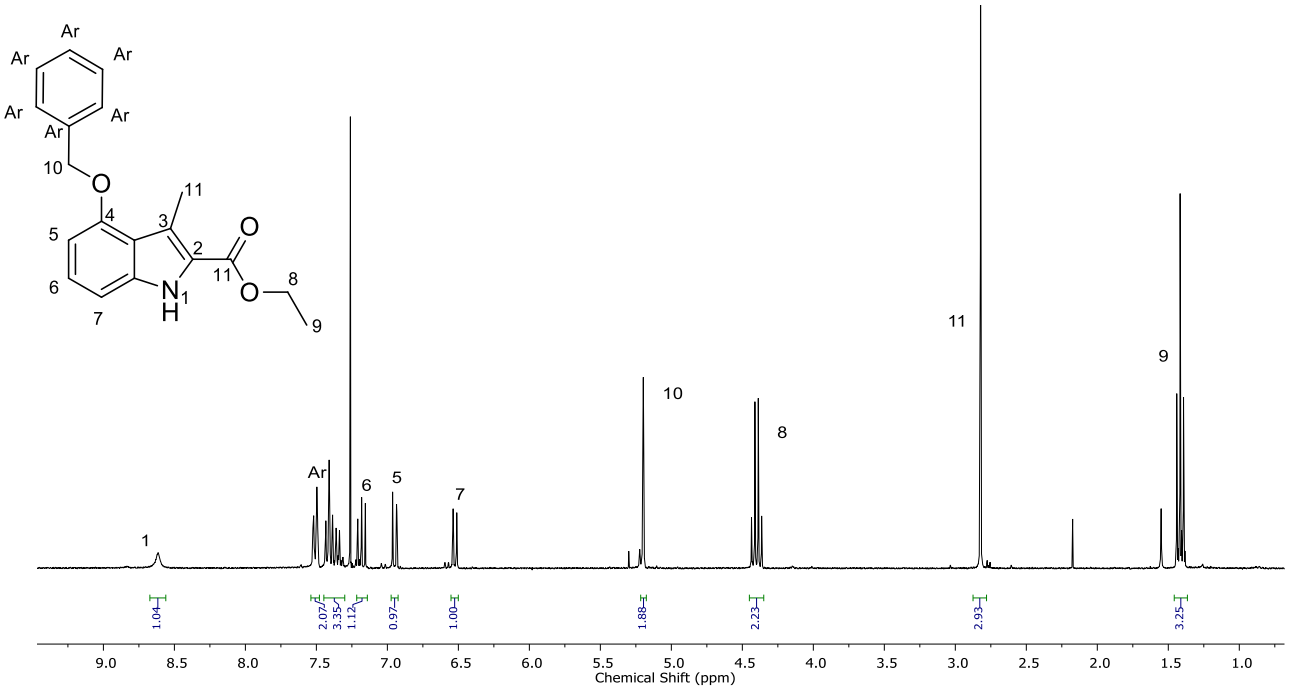

Figure 46: ^{1}H-NMR spectrum of **(76)** in $CDCl_3$

The most notable indication that **(76)** had formed was the appearance of a singlet at 2.84 ppm integrating for 3 protons. In addition the aromatic protons consisting of two doublets, a doublet of doublets (appearing as a triplet) and the benzyl protons integrate for eight protons, thus also confirming that the C3-position does not contain a proton and is substituted with a methyl group. HRMS confirmed the expected molecular weight which corresponded with the calculated value.

3.6 Derivatization of the 4-phenoxy position

With **(76)** in hand the subsequent reactions involved *N*-Boc protection, then debenzylation followed by a Mitsunobu coupling of 1-Boc-4-hydroxypiperidine **(32)** as seen in **Scheme 38**. Due to the similarity between compound **(76)** and compound **(24)** (Chapter 2) we decided to *N*-Boc protect **(76)** before the final Mitsunobu coupling in order to avoid co-elution of **(79)** with the hydrazine byproduct, as we suspected that we would face a similar problem with purification as that with the synthesis of compound **(33)** in Chapter 2. *N*-Boc protection of **(76)** was carried out successfully generating **(77)** in quantitative yield. ^{1}H- and ^{13}C-NMR spectroscopy confirmed the synthesis of **(77)**. Subsequent debenzylation with 10% Pd/C/H_2 was surprisingly low yielding as **(78)** was obtained in a low yield of 36%.

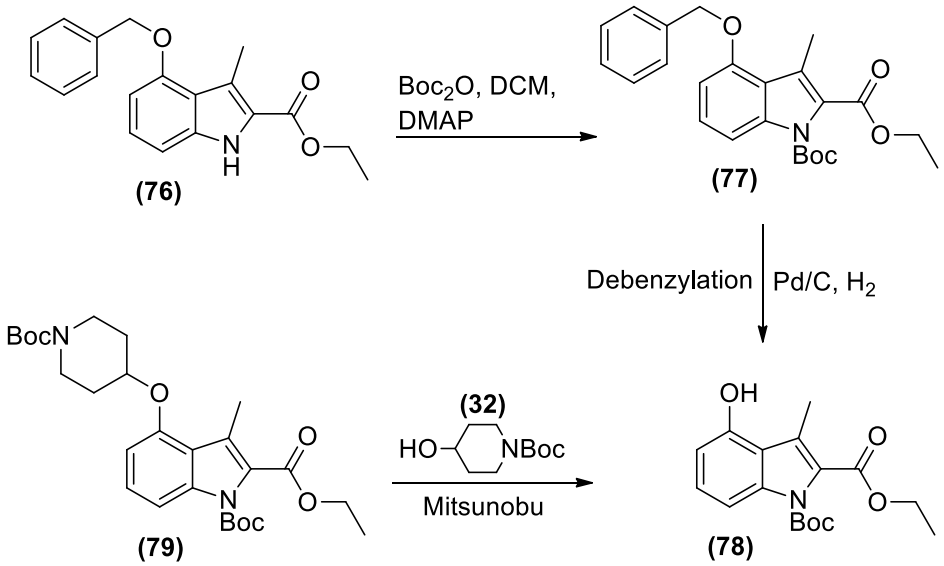

Scheme 38: Debenzylation of **(77)** and Mitsunobu coupling of **(78)** to produce **(79)**

Furthermore, monitoring the reaction with TLC revealed the presence of multiple byproducts. We did not isolate these byproducts. The ^{1}H-NMR spectrum of **(78)** revealed the presence of a *tert*-butyl signal at 1.62 ppm and a singlet corresponding to the phenolic proton at 6.73 ppm, while the ^{13}C-NMR spectrum indicated 15 carbon signals as expected.

Due to the low yield obtained, it was decided that the synthetic route should be altered by debenzylating **(76)** prior to *N*-Boc protection. In this instance a product was formed in nearly quantitative yield, however the product formed was not the desired debenzylated indole derivative. **Figure 47** illustrates the ^{1}H-NMR spectrum of the byproduct. Analysis of the spectrum revealed a number of expected signals such as the broad signal at 10.29 ppm, presumably the NH of the indole pyrrole, as well as a triplet and quartet observed at 1.35 ppm and 4.31 ppm respectively indicative of the ethyl chain of the ester. However, three unexpected additional aliphatic signals were observed, integrating for two protons each. Due to the electron rich nature of indoles, plus the added inductive effect that the 3-methyl group could exhibit, we postulated that the aryl ring of the indole had been hydrogenated as seen in **Scheme 39**.

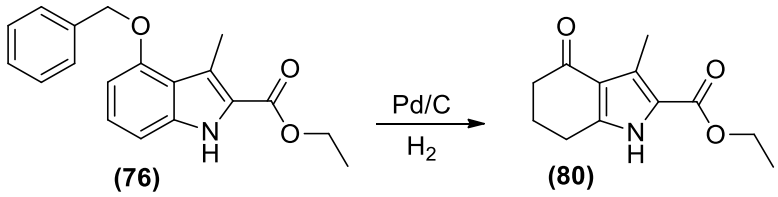

Scheme 39: Hydrogenation of **(76)** to produce **(80)**

This hypothesis was further justified by analysis of the ^{13}C-NMR spectrum. The ^{13}C-NMR spectrum indicated six aliphatic carbon signals and only six aromatic signals as opposed to the expected nine aromatic signals. In addition, a signal at 195.6 ppm indicated in a red rectangle in the ^{13}C-NMR spectrum of **Figure 47** suggested the presence of a carbonyl. The expected mass of compound **(80)** was confirmed by HRMS. The ^{1}H-NMR spectrum of **(80)** indicated three signals between 6.85 and 7.30 ppm, which suggests to be the aromatic protons of the debenzylated indole precursor.

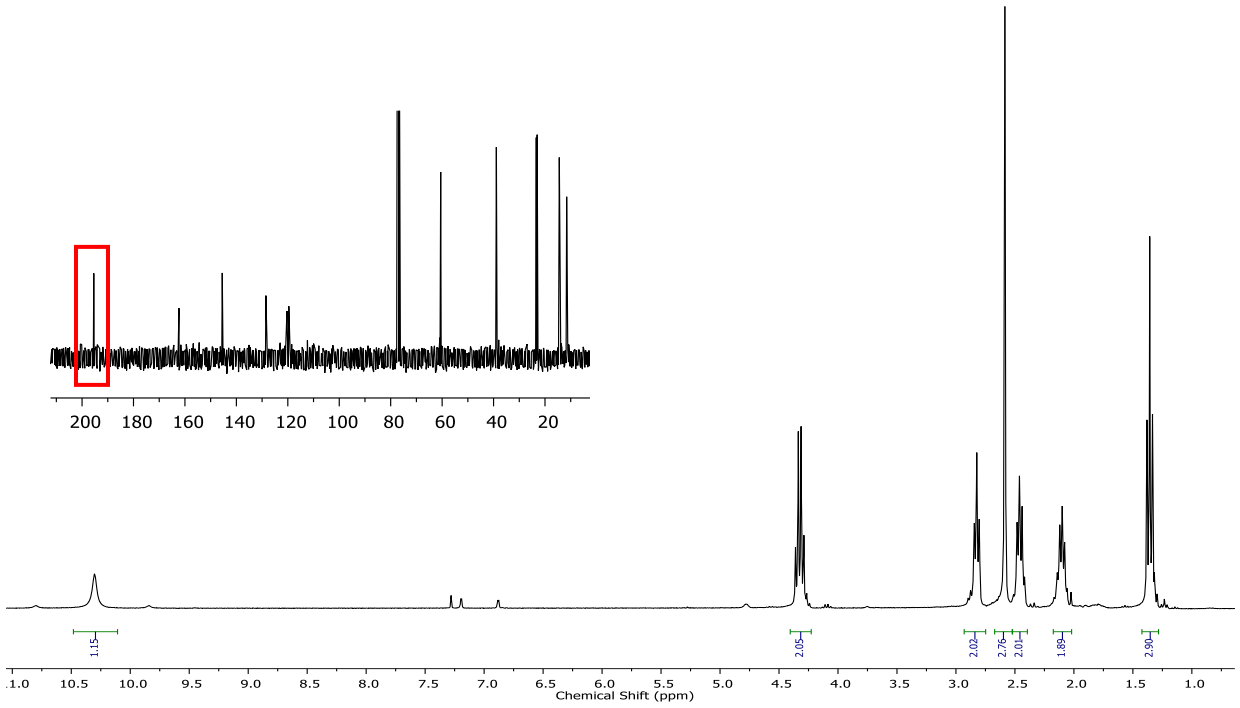

Figure 47: ^{1}H-NMR and ^{13}C-NMR spectrum of **(80)** in $CDCl_3$

Due to the formation of **(80)** as the sole product for the debenzylation of **(76)** we decided to the follow the initial synthetic route of debenzylation of *N*-Boc protected **(77)**. Despite the low yield of this route the amount of compound **(78)** that was obtained was enough to carry out the subsequent Mitsunobu reaction.

The coupling of **(78)** to **(32)** via the Mitsunobu reaction to form **(79) (Scheme 38)** was carried out successfully and **(79)** was obtained in a 94% yield. ^{1}H- and ^{13}C-NMR spectroscopy of **(79)** together with HRMS confirmed the formation of the desired product. **Figure 48** illustrates the ^{1}H-NMR spectrum of **(79)**. The unambiguous assignment of the proton signals can be achieved by extrapolation due to the assignment of compound **(39)** (Chapter 2). The 3-methyl peak at 2.58 ppm was assigned to position **20** (**Figure 48**) together with the two *tert*-butyl peaks at

1.45 ppm and 1.59 ppm assigned at positions **19** and **16** respectively. The absence of the indole N-H signal roughly between 8 – 9 ppm and phenolic proton roughly between 5.5 – 6.5 ppm was indicative of the fact that the Mitsunobu reaction had been successful and both Boc groups were still present. The triplet and quartet is that of the methyl **10** and methylene **9** of the ethyl ester respectively. Positions **13** and **12** correspond to the axial and equatorial protons of the methylene carbons of the piperidine ring, of which the axial protons appear upfield relative to the equatorial protons. Position **11** corresponded to the methine proton of the piperidine ring.

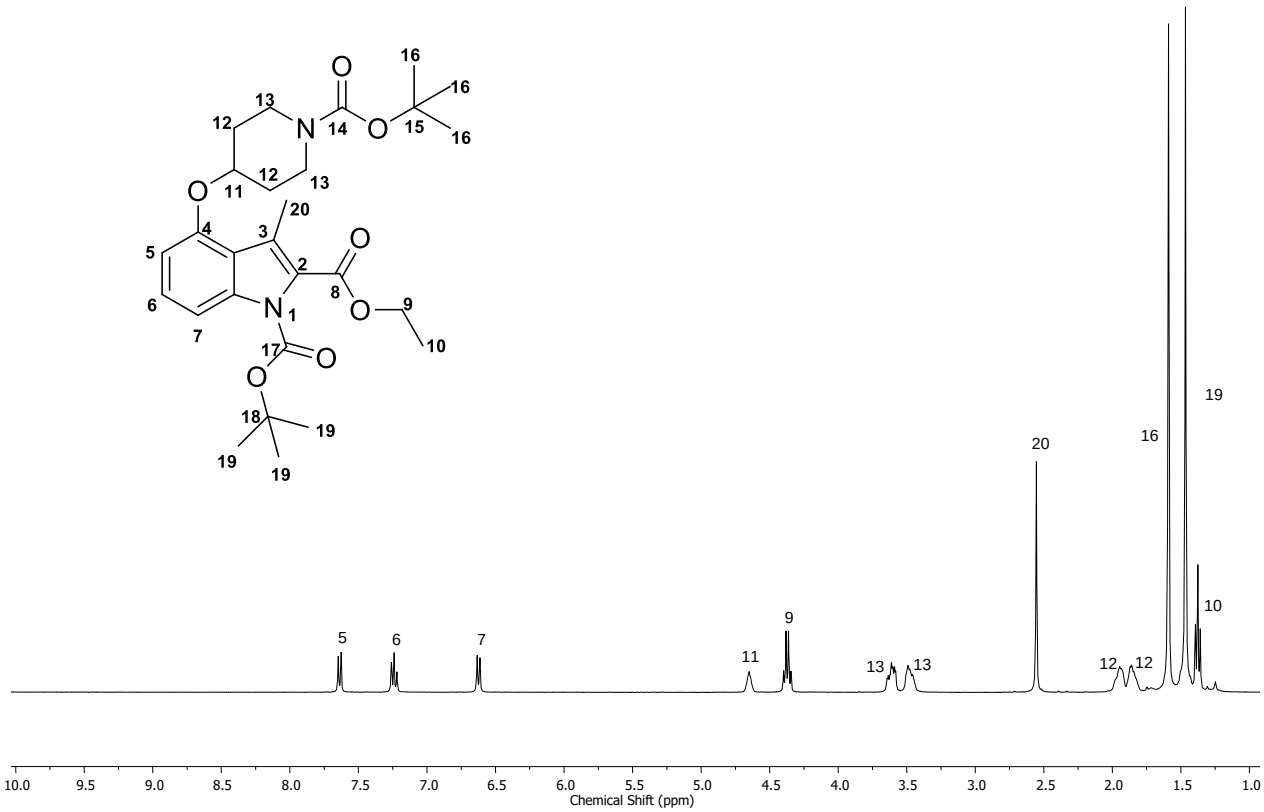

Figure 48: ^{1}H-NMR spectrum of **(79)** in $CDCl_3$

A COSY spectrum was acquired to unambiguously assign each proton signal, as seen in **Figure 49**.

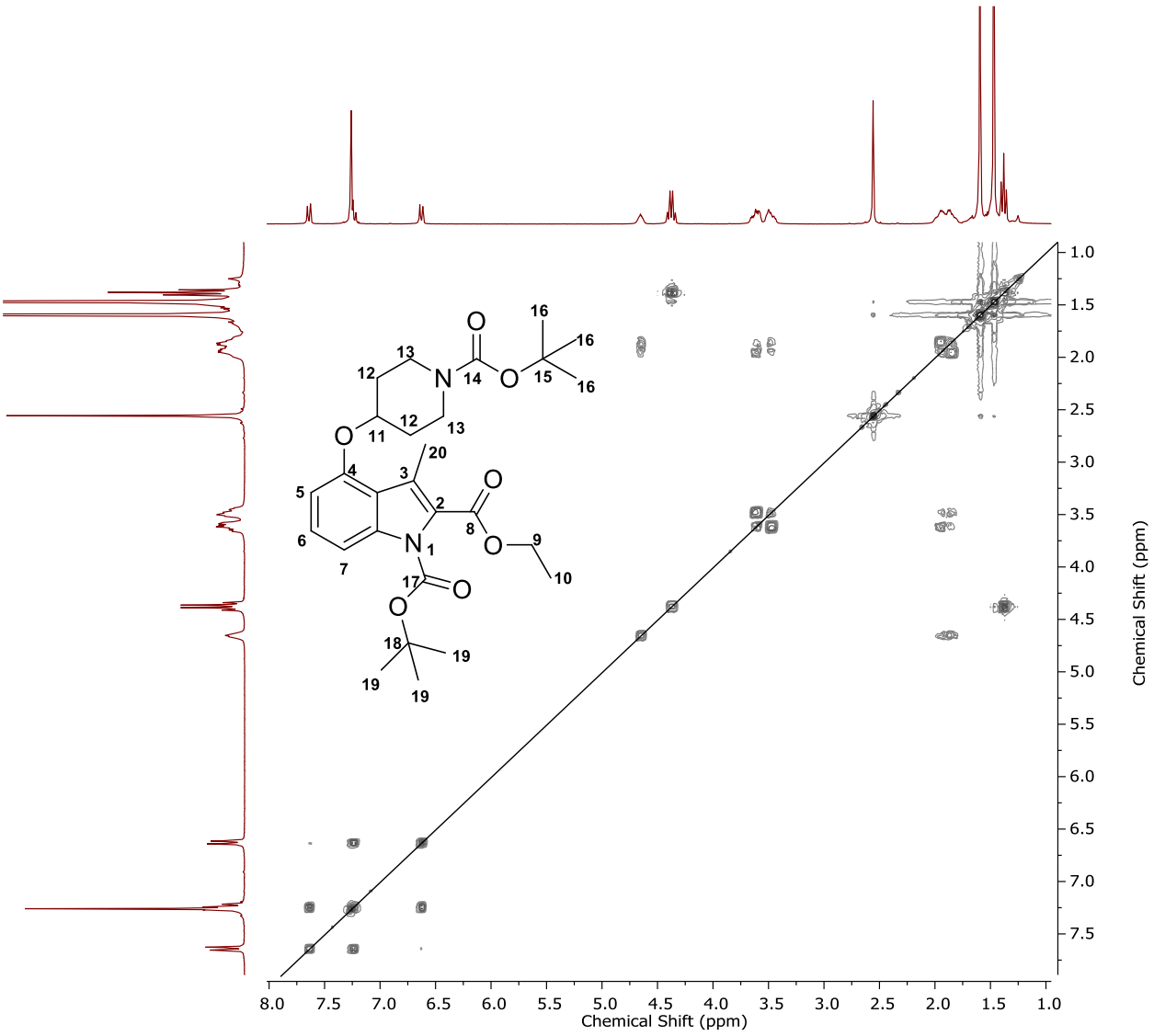

Figure 49: COSY spectrum of **(79)** in $CDCl_3$

The COSY spectrum indicated that the methine proton **11** at 4.65 ppm coupled to the axial and equatorial methylene protons **12** at 1.79 – 1.90 ppm and 1.90 – 2.01 ppm, whereas **12** coupled to the axial and equatorial methylene protons **13** at 3.43 – 3.53 ppm and 3.55 – 3.66 ppm respectively. The coupling of the aromatic signals exhibited the same trend as the COSY spectrum of **(39)** in that the doublet of doublets **6** (appearing as a triplet) at 7.25 coupled to both doublets **5** and **7** at 7.64 ppm and 6.62 ppm respectively. We were, however, unable to unambiguously assign protons **5** and **7**. The proton coupling is analogous to the coupling with the COSY spectrum of **(39)** (Chapter 2). A HSQC spectrum of **(79)** was obtained in order to show the coupling of important protons to significant carbons. **Figure 50** illustrates the HSQC spectrum of **(79)**.

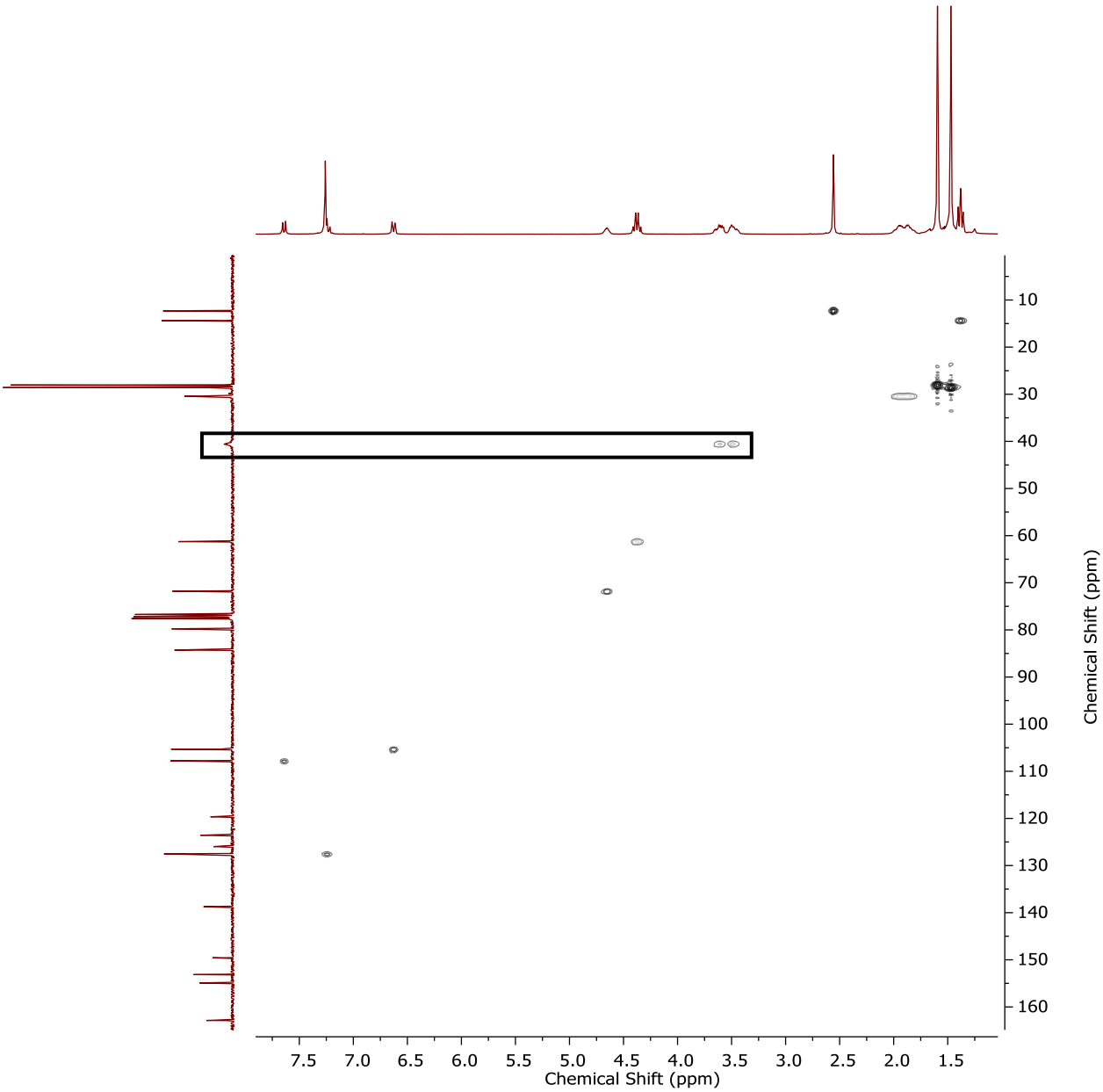

Figure 50: HSQC spectrum of **(79)** in $CDCl_3$

The ^{13}C-NMR spectrum of **(79)** indicated an undefined broad peak at 40.5 ppm, this however is now evident to be the methylene carbons on position **13**, and the correlation is indicated with a rectangle on the spectrum.

3.7 Transesterification of (79) followed by *N*-Boc deprotection

With **(79)** in hand we could derivatize the ester functionality at the 2-position of the indole. Transesterification was carried out utilizing the same procedure reported for the transesterification of **(39)** discussed in Chapter 2. Transesterification was achieved by the neat reaction of **(79)** with benzyl alcohol, 2-phenylethanol and 1-naphthylmethanol respectively using K_3PO_4 at 110 – 120 °C. The reaction was monitored by TLC until it was observed that the starting material **(79)** had disappeared. Despite the complete consumption of starting material compound **(81)** was isolated in a yield of 38%. This low yield could be attributed to some degradation occurring during the transesterification step. **Scheme 40** illustrates the transesterification step of **(79)** with 2-phenylethanol, benzyl alcohol and 1-naphthylmethanol. In the case of 2-phenylethanol and 1-naphthylmethanol, purification of the respective transesterified products proved difficult as the R_f values of the two transesterified products were very similar to 2-phenylethanol and 1-naphthylmethanol respectively.

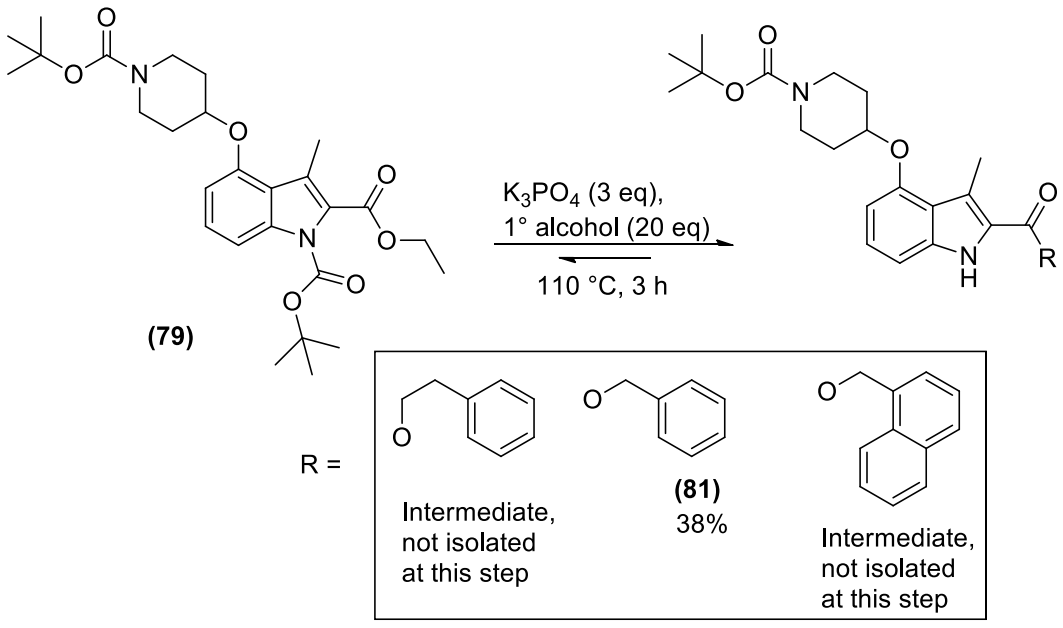

Scheme 40: Transesterification of **(79)** with 2-phenylethanol, benzyl alcohol and 1-naphthylmethanol

We decided to abandon attempts to isolate the transesterified products of **(79)** with 2-phenylethanol and 1-naphthylmethanol and instead use the crude mixture of the transesterified products to continue with the final deprotection of the piperidine *N*-Boc group (**Scheme 41**). This method proved to be successful and we were able to isolate the *N*-Boc deprotected products **IM1**

and **IM3** in yields of 19% and 49% over two steps respectively. The *N*-Boc deprotection of **(81)** using 4M HCl in dioxane generated **IM2** in 83% yield.

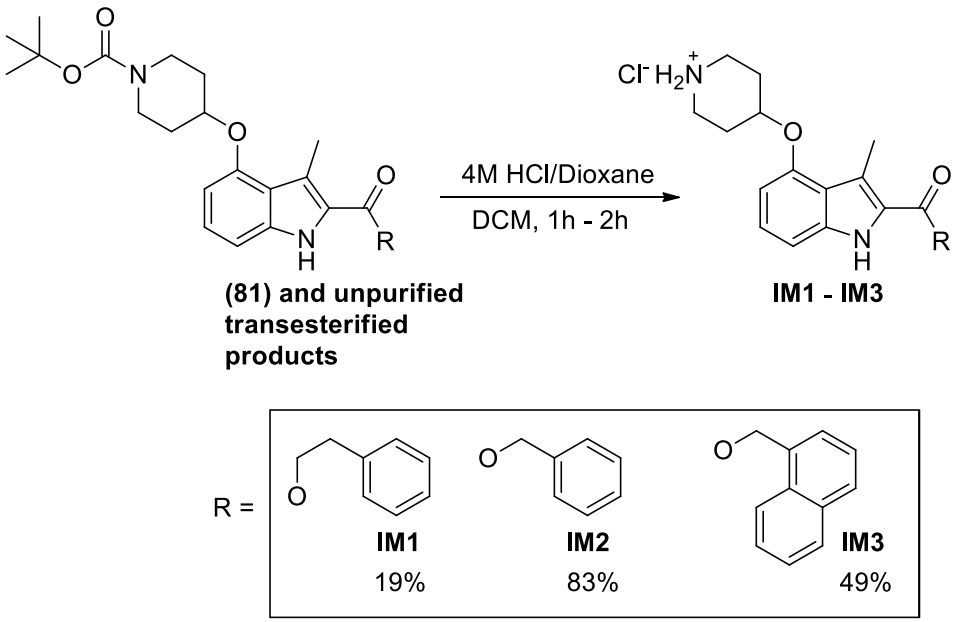

Scheme 41: *N*-Boc deprotection of **(81)** and the crude phenethyl and naphthylmethyl esters via HCl in dioxane to produce **IM1** – **IM3**

Figure 51 illustrates the ^{1}H-NMR spectrum of **IM2**. The spectrum clearly shows the absence of both *tert*-butyl signals belonging to the *N*-Boc groups on the piperidine ring and the indole nitrogen. Instead, two multiplet signals at 9.04 ppm and 9.27 ppm corresponding to the axial and equatorial protons of the piperidinium chloride (R_2NH_2Cl) group are observed, in addition to a singlet at 11.48 ppm corresponding to the indole *N*-H proton. Furthermore, the absence of the triplet and quartet of the ethyl ester and the appearance of a singlet at 5.35 ppm integrating for two protons, as well as the multiplets in the aromatic region integrating for five protons indicate that the transesterification of the ethyl ester to the benzyl ester at the 2-position had been carried out successfully. The ^{1}H-NMR spectra of **IM1** and **IM3** showed similar changes to those observed in the ^{1}H-NMR spectrum of **IM2.** The only differences in the ^{1}H-NMR spectra of **IM1** – **IM3** were due to the different ester substituents. For the ^{1}H-NMR spectrum of **IM1** the appearance of two triplets at 3.06 ppm and 4.50 ppm corresponding to the two methylene protons of the 2-phenylethoxy ester substituent were observed. In the case of the ^{1}H-NMR spectrum of **IM3** the aromatic region showed that seven additional protons were present which confirmed the presence of the naphthyl group. Furthermore, a singlet at 5.83 ppm corresponded with the methylene protons of the 1-naphthylmethyl ester substituent.

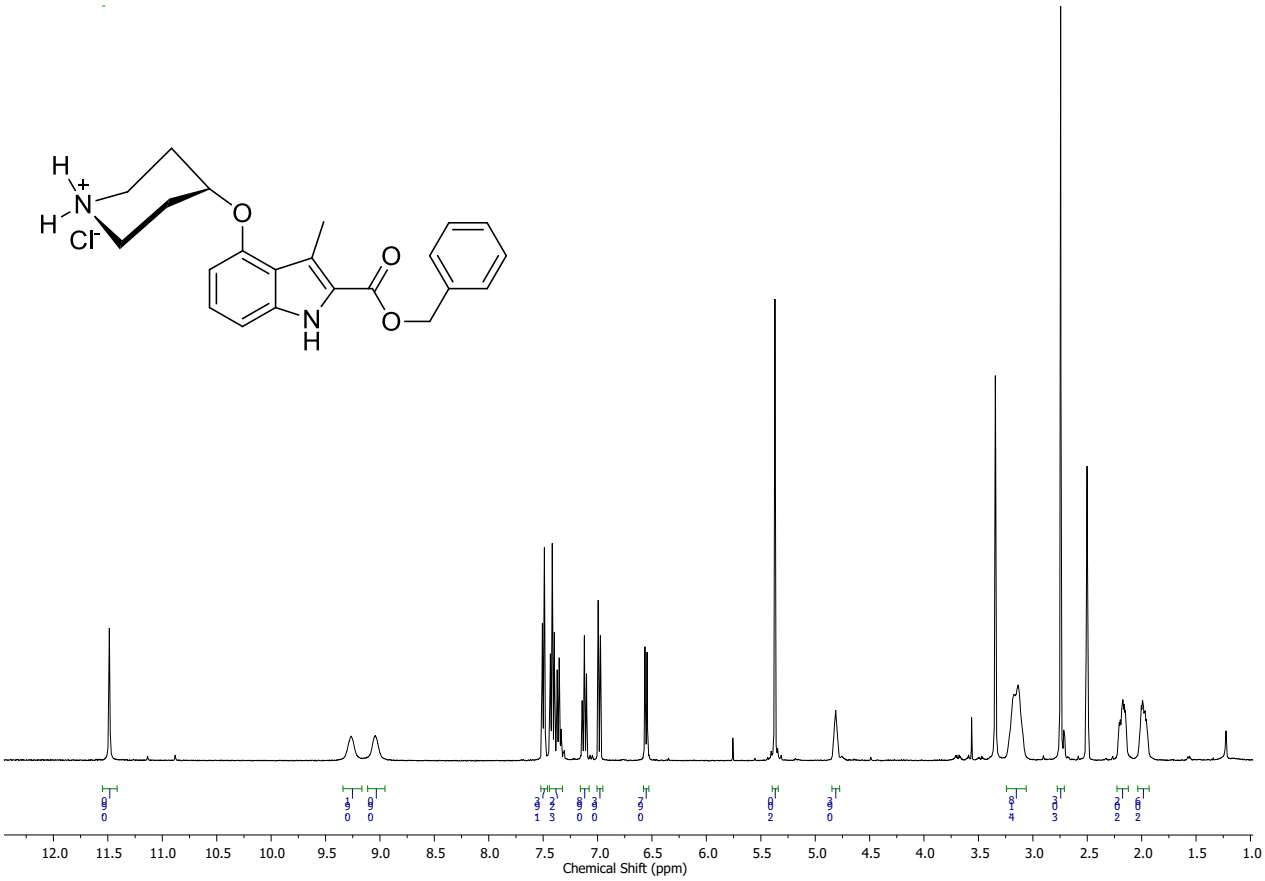

Figure 51: ^{1}H-NMR spectrum of **IM2** indicating the protons of the ammonium salt as well as the removal of the piperidine *N*-Boc group. It must be noted, a dioxane and water impurity is observed.

3.8 Amidation of (79) followed by *N*-Boc deprotection

With the esters in hand we turned our attention to the synthesis of the respective amides. Amidation was carried out by utilizing the same procedure for the amidation of **(39)** discussed in Chapter 2. Compound **(79)** was added to 20 – 30 equivalents of amine which acted as both the reagent and the solvent to yield compounds **(82)** – **(85)** (**Scheme 42**). In comparison to the amidation reactions with **(39)** the amidation reactions with **(79)** proceeded at a much slower rate and gave lower yields. Attempts at heating the reaction mixture to 140 °C and stirring the reaction for a longer period of time such as for 2 – 3 days did little to improve the yields.

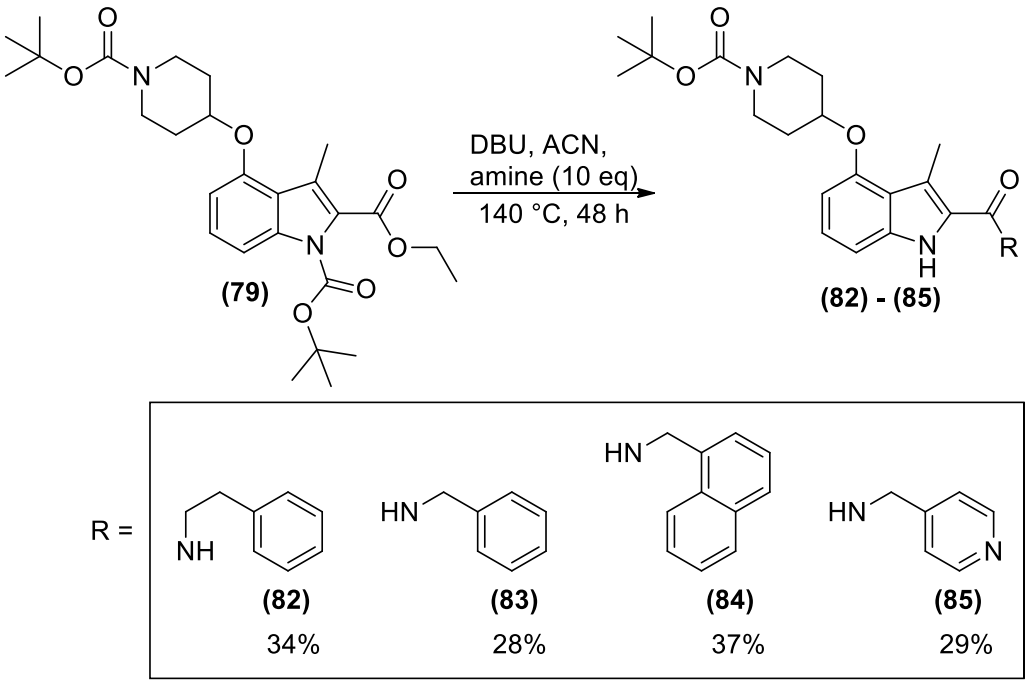

Scheme 42: Amidation of **(79)** to produce compounds **(82)**–**(85)**

It was postulated that the low yields obtained for compounds **(82)** – **(85)** could be due to the fact that the reactivity of the ester group on **(79)** was significantly less than that of **(39)**, which could be attributed to the addition of a methyl group on the C3-position. This could be explained by the fact that the methyl group had a positive inductive effect on the indole ring which would increase the electron density of the indole system as well as that of the ester. This in turn would decrease the electrophilicity of the ester group.

Analysis of the ^{1}H-NMR spectra of compounds **(82)**–**(85)** indicated that in all cases a broad triplet - indicative of the amide *N*-H proton coupling to the neighboring methylene protons - was observed. The ^{1}H-NMR spectrum of **(82)** indicated that all the expected protons were accounted for. The signals in the aromatic region integrated for eight protons. The aliphatic region consists of the methine and methylene protons of the piperidine ring, as well as a quartet and triplet indicative of the methylene protons of the 2-phenethyl amide substituent. Finally the singlet of the 3-methyl group and that of the *tert*-butyl group of the piperidine *N*-Boc are observed. The ^{13}C-NMR spectrum showed the expected 22 signals, and HRMS confirmed the molecular weight. Compounds **(83)** – **(85)** were also fully characterized by ^{1}H- and ^{13}C-NMR spectroscopy as well as HRMS.

3.9 *N*-Boc deprotection of (82) – (85)

Piperidine *N*-Boc deprotection on compounds **(82)** – **(85)** was carried out using 4M HCl in dioxane to generate final compounds **IM4** – **IM7** in moderate to high yields. (**Scheme 43**).

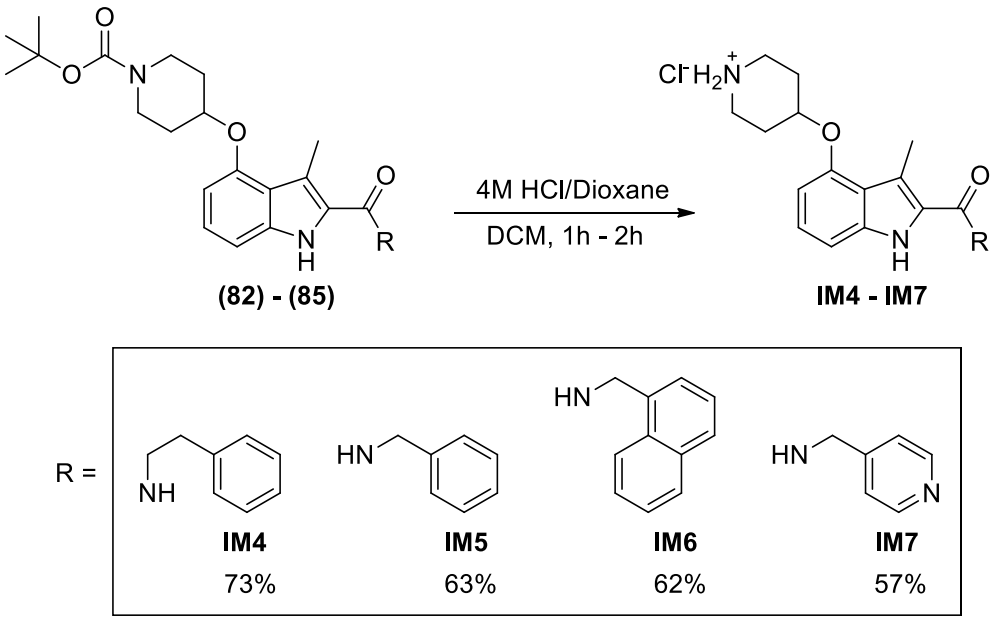

Scheme 43: *N*-Boc deprotection of **(82)** – **(85)** via HCl in dioxane to produce **IM4** – **IM7**. **IM7** was isolated as the pyridinium chloride salt.

^{1}H- and ^{13}C-NMR spectroscopy plus HRMS confirmed the successful synthesis of **IM4 – IM7**. The ^{1}H-NMR spectra of compounds **IM4** – **IM7** were analogous to the spectra of compounds **IH4 – IH7** described in Chapter 2. The only differences were the appearance of the 3-methyl signal and that the aromatic region integrated for one less proton. In the ^{1}H-NMR spectrum of **IM6** as an example two broad piperidinium N*H*$_2$Cl signals were observed in addition to the indole N-H signal and the amide N-H proton appearing as a broad triplet (**Figure 52**).

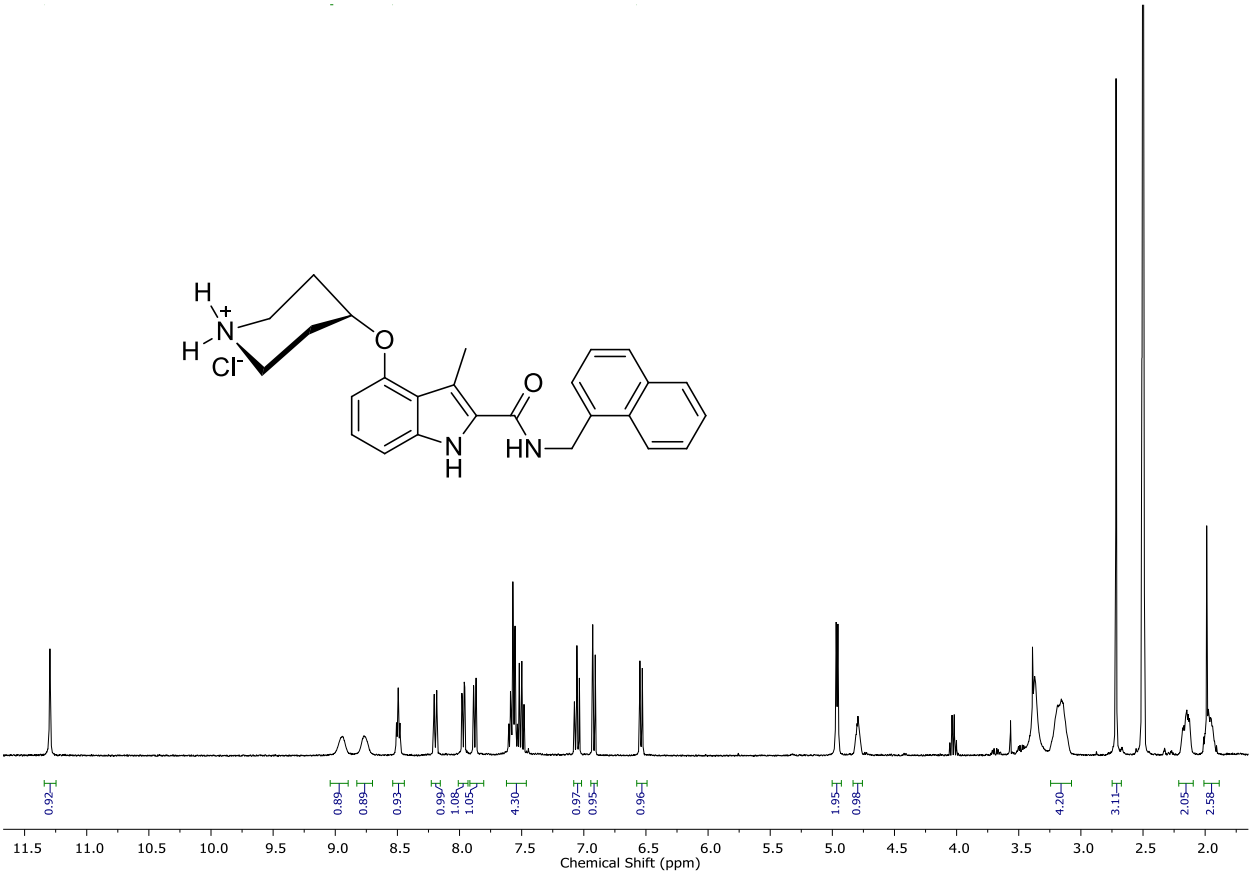

Figure 52: ^{1}H-NMR spectrum of **IM6** (Note: an EtOAc and water impurity is observed)

3.10 Conclusion

This chapter described the process of synthesizing a 3-methyl indole system, analogous to the indoles synthesized in Chapter 2. It was postulated by Yu *et al*.[28] that the presence of a methyl group at the 3-position would have an effect on the efficacy of the aromatic amides vs. aromatic esters at the C2-position, due to the steric clash between the methyl group and the proton of the secondary amide. The first attempt at introducing a methyl group at the C3-position involved regioselective formylation at the C3-position via a Vilsmeier-Haack formylation, followed by a Mozingo reduction which involve the synthesis of a dithioacetal followed by desulfurization of the dithioacetal to a methyl with Raney Nickel. Although the Vilsmeier-Haack formylation and Mozingo reduction was successful, the regioselectivity of the Vilsmeier-Haack formylation was undesired due to formylation occurring primarily at the 7-position, producing the C3-formylated product in a low yield. The regioselectivity was only realized after the desulfurization reaction, which apart

from producing the desired methyl group, also facilitated debenzylation. The aromatic signals of the 7-methyl indole were visible and due to the multiplicity observed, the position at which formylation had occurred could be postulated. This was confirmed by the crystal structure.

We decided to follow another procedure which involved a ligand-free copper-catalyzed coupling of ethyl isocyanoacetate and substituted 2-bromo acetophenones to produce the desired 3-methyl indole. Due to the fact that 1,2,3-trisubstituted aromatic systems are expensive and not widely available, we decided to synthesize the 2-bromo acetophenone via a regioselective acetylation reaction on 1-bromo-3-(methoxymethoxy)benzene using LiTMP as base and acetic anhydride and dimethylacetamide as the source of the acyl-group. We however did not produce the desired acetophenone derivative but instead produced the same byproduct when using acetic anhydride and dimethylacetamide as electrophile. Various 2D NMR experiments were carried out to elucidate the unknown structure, which was eventually solved. A bi-aryl system was being formed during the course of the reaction, which we speculate formed due to the formation of an electrophilic benzyne intermediate which underwent nucleophilic attack of the deprotonated aryl system. This was not a viable method for the synthesis of the desired acetophenone.

We focused our attention towards the Larock indole synthesis, which could theoretically assemble the desired 3-methyl indole scaffold via a palladium catalyzed heteroannulation reaction which involves the coupling of an *ortho*-iodo aniline with internal alkynes to produce 2,3–substituted indoles. We synthesized the required 3-(benzyloxy)-2-iodoaniline via the benzylation of 2-amino-3-nitrophenol, followed by a Sandmeyer reaction converting the aniline to the corresponding aryl iodide and subsequent reduction of the nitro group to the corresponding aniline. The reaction with 3-(benzyloxy)-2-iodoaniline and but-2-yn-1-ol under the required conditions did however not produce any indole products. Acetylation of the aniline NH_2 were also carried out due to research suggesting that reactivity would be increased, but again no indole product was formed.

The final attempt to produce the desired 3-methyl indole proved to be successful, as research has show that methylation of aryl bromides could be achieved using a Suzuki-Miyaura coupling with trimethylboroxine. Regioselective C3-bromination could be achieved on the indole system that we had already synthesized using the Hemetsberger indolization reaction. Subsequent methylation under Suzuki-coupling conditions was successful and thus we succeeded in synthesizing the required 3-methyl indole scaffold.

The sunsequent reactions followed the same direction as that of the indole compounds discussed in Chapter 2, involving indole *N*-Boc protection, debenzylation, Mitsunobu coupling using 1-Boc-

4-hydroxypiperidine, amidation and transesterification with the specified aromatic amines and alcohols, and finally *N*-Boc deprotection. We decided to Boc-protect the indole nitrogen before benzyl deprotection to facilitate purification steps during the Mitsunobu coupling. Unfortunately the debenzylation reaction using Pd/C and hydrogen resulted in the formation of byproducts and a low yield for the debenzylated indole. Attempts to debenzylate the 3-methyl indole scaffold first resulted in hydrogenation of the indole aryl ring. Subsequent Mitsunobu coupling of the previously isolated debenzylated indole however provided the necessary starting material for the subsequent amidation and transesterification reactions.

3.11 References

1. Vilsmeier, A.; Haack, A. *Ber. Dtsch. Chem. Ges. (A and B Series)* **1927,** *60,* 119.

2. Hickman, Z. L.; Sturino, C. F.; Lachance, N. *Tetrahedron Lett.* **2000,** *41,* 8217.

3. Pagire, H. S.; Chun, H.; Bae, M. A.; Ahn, J. H. *Tetrahedron* **2013,** *69,* 3039.

4. Köse, M.; Ritter, K.; Thiemke, K.; Gillard, M.; Kostenis, E.; Müller, C. E. *ACS Med. Chem. Lett*. **2014,** *5,* 326.

5. Skibo, E. B.; Xing, C.; Dorr, R. T. *J. Med. Chem.* **2001,** *44,* 3545.

6. Bandini, M.; Eichholzer, A. *Angew. Chem., Int. Ed.* **2009,** *48,* 9608.

7. Bandini, M. *Org. Biomol. Chem.* **2013,** *11,* 5206.

8. Jeffrey, G. A.; Jeffrey, G. A. *An Introduction to Hydrogen Bonding;* Oxford university press New York, **1997**.

9. Cai, Q.; Li, Z.; Wei, J.; Ha, C.; Pei, D.; Ding, K. *Chem. Commun.* **2009,** 7581.

10. Butler, T. W.; Wager, T. T.; Patent, Publication number: WO2007088450 A2, **2007**

11. Blatt, A. *Chem. Rev.* **1940,** *27,* 413.

12. Wang, C.; Dong, J.; Zhang, Y.; Wang, F.; Gao, H.; Li, P.; Wang, S.; Zhang, J. *MedChemComm* **2013,** *4,* 1434.

13. Doble, M.; Karthikeyan, S.; Padmaswar, P. A.; Akamanchi, K. G. *Bioorg. Med. Chem.* **2005,** *13,* 5996.

14. Gao, H.; Su, P.; Shi, Y.; Shen, X.; Zhang, Y.; Dong, J.; Zhang, J. *Eur. J. Med. Chem.* **2015,** *90,* 232.

15. Reimer, K.; Tiemann, F. *Ber. Dtsch. Chem. Ges.***1876,** *9,* 1268.

16. Leclerc, J. P.; Li, C. S.; Moradei, O. M.; Patent, Publication number: WO2011011872 A1, **2011**

17. Diemer, V.; Begaud, M.; Leroux, F. R.; Colobert, F. *Eur. J. Org. Chem.* **2011,** *2011,* 341.

18. García-López, J.; Greaney, M. F. *Chem. Soc. Rev.* **2016,** *45,* 6766.

19. Anslyn, E. V.; Dougherty, D. A. *Modern Physical Organic Chemistry;* University Science Books, 614, **2006**.

20. Clayden, J. *Organolithiums: Selectivity for Synthesis;* Elsevier, p 36, 55. **2002**.

21. Larock, R. C.; Yum, E. K. *J. Am. Chem. Soc.* **1991,** *113,* 6689.

22. Larock, R.; Yum, E.; Refvik, M. *J. Org. Chem.* **1998,** *63,* 7652.

23. Dai, W.; Lai, K. W. *Tetrahedron Lett.* **2002,** *43,* 9377.

24. Gamble, A. B.; Garner, J.; Gordon, C. P.; O'Conner, S. M. J.; Keller, P. A. *Synth. Commun.* **2007,** *37,* 2777.

25. Tani, M.; Ikegami, H.; Tashiro, M.; Hiura, T.; Tsukioka, H.; Kaneko, C.; Notoya, T.; Shimizu, M.; Uchida, M.; Aida, Y. *Heterocycles* **1992,** *34,* 2349.

26. Kimber, M. C.; Moody, C. J. *Chem. Commun.* **2008,** 591.

27. Gray, M.; Andrews, I. P.; Hook, D. F.; Kitteringham, J.; Voyle, M. *Tetrahedron Lett.* **2000,** *41,* 6237.

28. Yu, Z.; Brannigan, J. A.; Moss, D. K.; Brzozowski, A. M.; Wilkinson, A. J.; Holder, A. A.; Tate, E. W.; Leatherbarrow, R. J. *J. Med. Chem.* **2012,** *55,* 8879.

Chapter 4: Synthesis of benzimidazoles

4.1 Introduction

As mentioned in Chapter 1 we envisioned synthesizing isostructural analogues of the indole methyl (**IM)** series of compounds, by replacing the core indole scaffold with 1-methyl benzimidazole as shown in **Figure 53**.

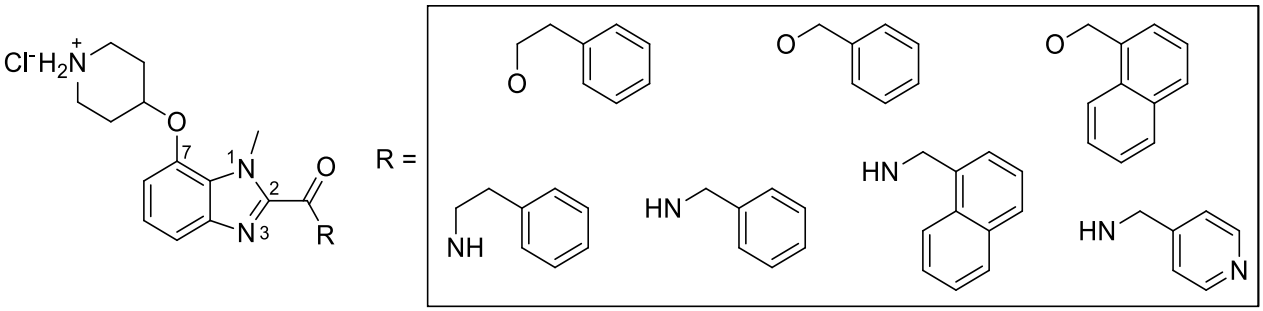

Figure 53: Proposed 1-methyl benzimidazole based compounds with various amides and esters to be synthesized

This chapter will focus on the method used to synthesize the desired 1-methyl benzimidazole scaffold as well as the various methods attempted to functionalize the C2-position as a means to introduce the necessary carboxylic acid derivative.

4.2 Synthesis of the benzimidazole heterocycle

Literature reports numerous methods for the synthesis of substituted and unsubstituted benzimidazoles. The most predominant method makes useof *ortho*-phenylene diamines which undergo a cyclization reaction with carboxylic acids[1,2] aldehydes[3,4] and orthoesters[5,6] to produce 2-substituted and unsubstituted benzimidazoles (**Scheme 44**). The objective was to synthesize a benzimidazole heterocycle with a methyl group at the C1-position, an ester group at the C2-position, and a derivatizable oxygen atom at the C7-position similar to the indole compounds discussed in Chapter 3. The disadvantage of the methods shown in **Scheme 44** for the synthesis of the benzimidazole scaffold is that the desired ester group at the C2-position cannot be directly installed using this method. However, benzimidazole scaffolds with a proton at the C2-position

can be readily synthesized and subsequently functionalized. The functionalization and derivatization of the C2-position will be discussed later in this chapter.

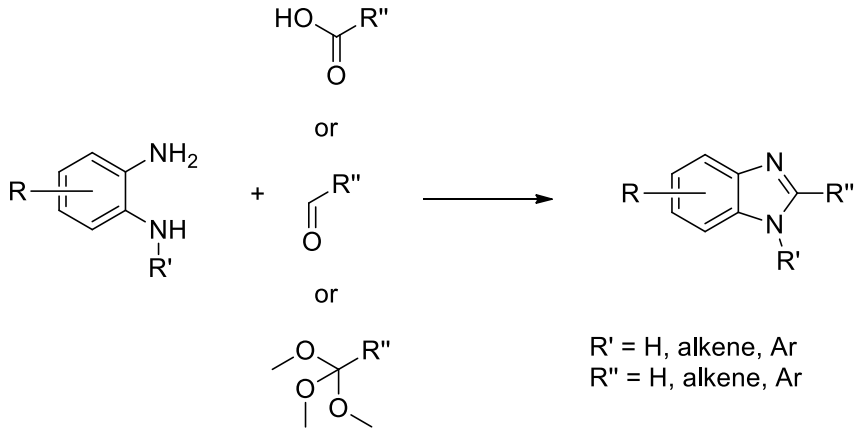

Scheme 44: Formation of substituted and unsubstituted benzimidazoles through the cyclization of *o*-phenylene diamines with carboxylic acids, aldehydes and orthoesters

In order to synthesize the benzimidazole scaffold with the desired substitution pattern illustrated in **Figure 53** the appropriate *o*-phenylene diamine had to first be synthesized. We envisaged that we could synthesize the required diamine using commercially available 2-amino-3-nitrophenol **(70)** as a starting point as this would introduce the oxygen atom at the C7-position of the benzimidazole (**Scheme 45**).

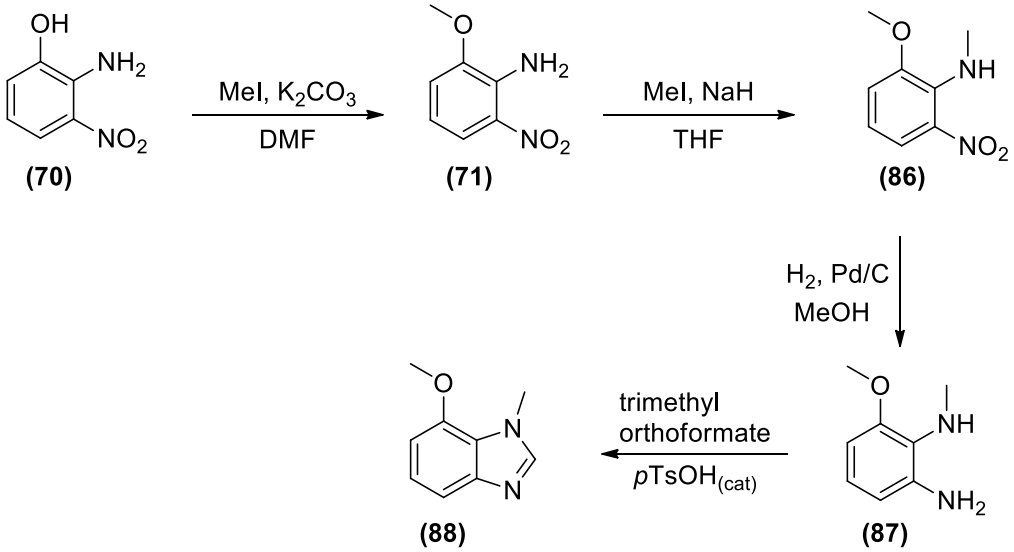

Scheme 45: Synthesis of benzimidazole **(88)**

In a synthetic route described by Zhou *et al.*[7], 7-methoxy-1-methyl-benzimidazole **(88)** was successfully synthesized from **(70)**. The synthetic strategy described by Zhou *et al.* is illustrated in **Scheme 45**. The first step involved the methylation of the hydroxy group of **(70)** with methyl iodide and K_2CO_3 as the base. In our hands this gave **(71)** in a 97% yield. Subsequent methylation of the amine with NaH and MeI in THF produced **(86)** in a 58% yield. Methylation of 2-methoxy-6-nitroaniline **(71)** proceeded slowly due to the low nucleophilicity of *ortho*-nitro anilines. The ^{1}H-NMR spectrum of **(86)** indicated the presence of two singlets, confirming that methyl groups were present on the hydroxy group and the amine. In the procedure described by Zhou *et al.* methylation of the hydroxy group and the amine was carried out simultaneously to yield **(86)** directly from **(70)**, however, in our hands only methylation of the hydroxy group occurred and so **(86)** had to be synthesized over two steps.

The following step in the synthesis involved the nitro reduction of **(86)** with Pd/C and hydrogen which afforded *o*-phenylene diamine **(87)** in a 98% yield. The ^{1}H-NMR spectrum of **(87)** showed a broad peak integrating for three protons, corresponding to the three protons on both amines. The characterization data obtained from the first three steps are in accordance with the literature.[7] The formation of benzimidazole **(88)** was carried out through a neat reaction between **(87)** and triethyl orthoformate with a catalytic amount of tosylic acid at 115 °C. Monitoring the reaction by TLC indicated that a spot-to-spot conversion of **(87)** to **(88)** had occurred after a period of 40 minutes. The product spot had a blue hue under UV light that provided proof that the cyclization had occurred and a heterocycle had been formed. The product was isolated in a yield of 82%. **Figure 54**: illustrates the ^{1}H-NMR spectrum of **(88)**.

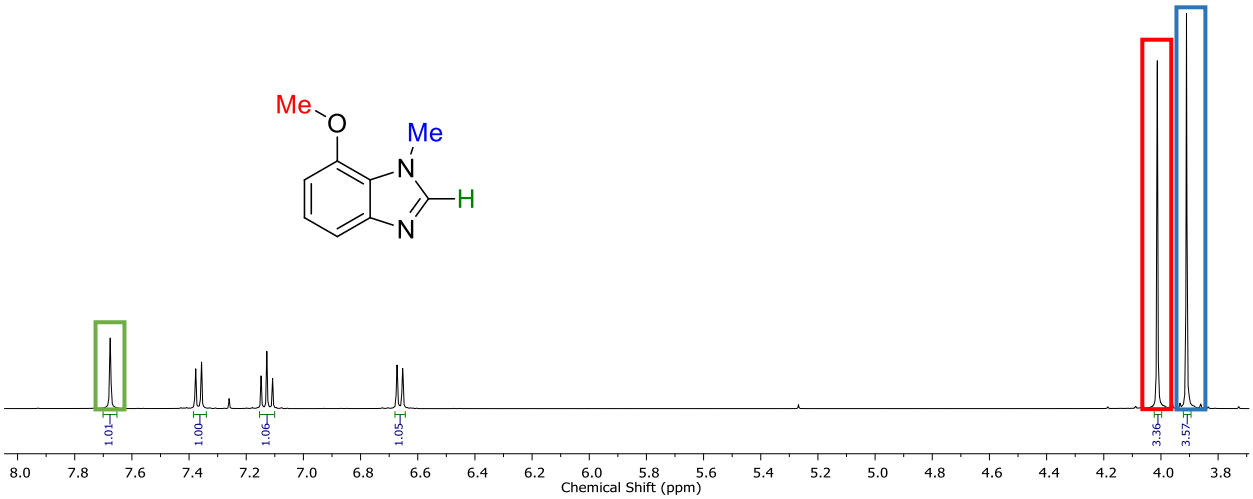

Figure 54: ^{1}H-NMR spectrum of **(88)** in $CDCl_3$

The absence of any amine proton signals as well as the presence of a singlet in the aromatic region at 7.69 ppm corresponding to the proton at the C2-position of the structure indicated that the expected cyclization had occurred. With compound **(88)** in hand, the following steps in the synthesis as illustrated in **Scheme 46** would include demethylation of the 7-methoxy group to produce the 7-hydroxy-1-methylbenzimidazole **(89)**, after which a Mitsunobu reaction would be carried out coupling **(89)** to 1-Boc-4-hydroxypiperidine **(32)** to yield **(90)**.

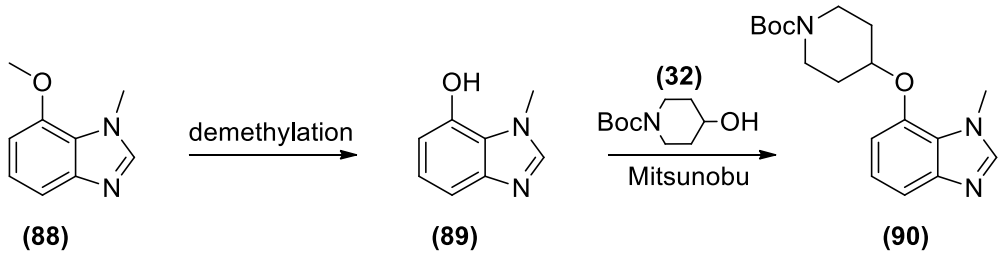

Scheme 46: Demethylation of **(88)** and subsequent Mitsunobu coupling with **(32)**

Various methods were used to promote demethylation of **(88)**, but in our hands all of the methods were unsuccessful. The first method was the use of boron tribromide in DCM, which is considered a classical method for demethylation.[8] The use of $AlCl_3$ with pyridine or thioethane as a means of demethylation has also been reported in the literature[9,10]. Both of these procedures were attempted but were unsuccessful in producing **(89)**, instead **(88)** was fully recovered. The use of concentrated 47% hydrobromic acid has also been used as a demethylating reagent,[11] but demethylation of **(88)** with HBr (47%) was also unsuccessful. Due to the difficulties faced demethylating benzimidazole **(88)**, we decided to change the choice of protecting group to a benzyl group as benzyl groups, as shown in previous chapters, are easier to introduce as well as remove. **Scheme 47** illustrates the newly devised route to synthesize **(90)**.

Benzylation of **(70)** was carried out in DMF with K_2CO_3. Temperature control played an important role in preventing di-benzylation of **(70)**. The *O*,*N*-di-benzylated product was notoriously difficult to separate from **(91)** since both compounds had similar polarities as seen by TLC analysis. Keeping the reaction temperature at -10 – 0 °C was an effective method in preventing the formation of the *O,N*-di-benzylated product and **(91)** was synthesized in a yield of 98%. ^{1}H-NMR spectroscopy confirmed the formation **(91)**. A singlet at 5.13 ppm integrating for two and multiplets in the aromatic region integrating for five protons was observed, together with the presence of three doublet of doublets at 6.59, 6.97 and 7.75 ppm. Subsequent *N*-methylation was carried out using the same method reported in **Scheme 45** and **(92)** was obtained in a yield of 97%.^{1}H-NMR

spectroscopy of **(92)** indicated the presence of a singlet at 3.15 ppm integrating for three protons which corresponded to the addition of the methyl group.

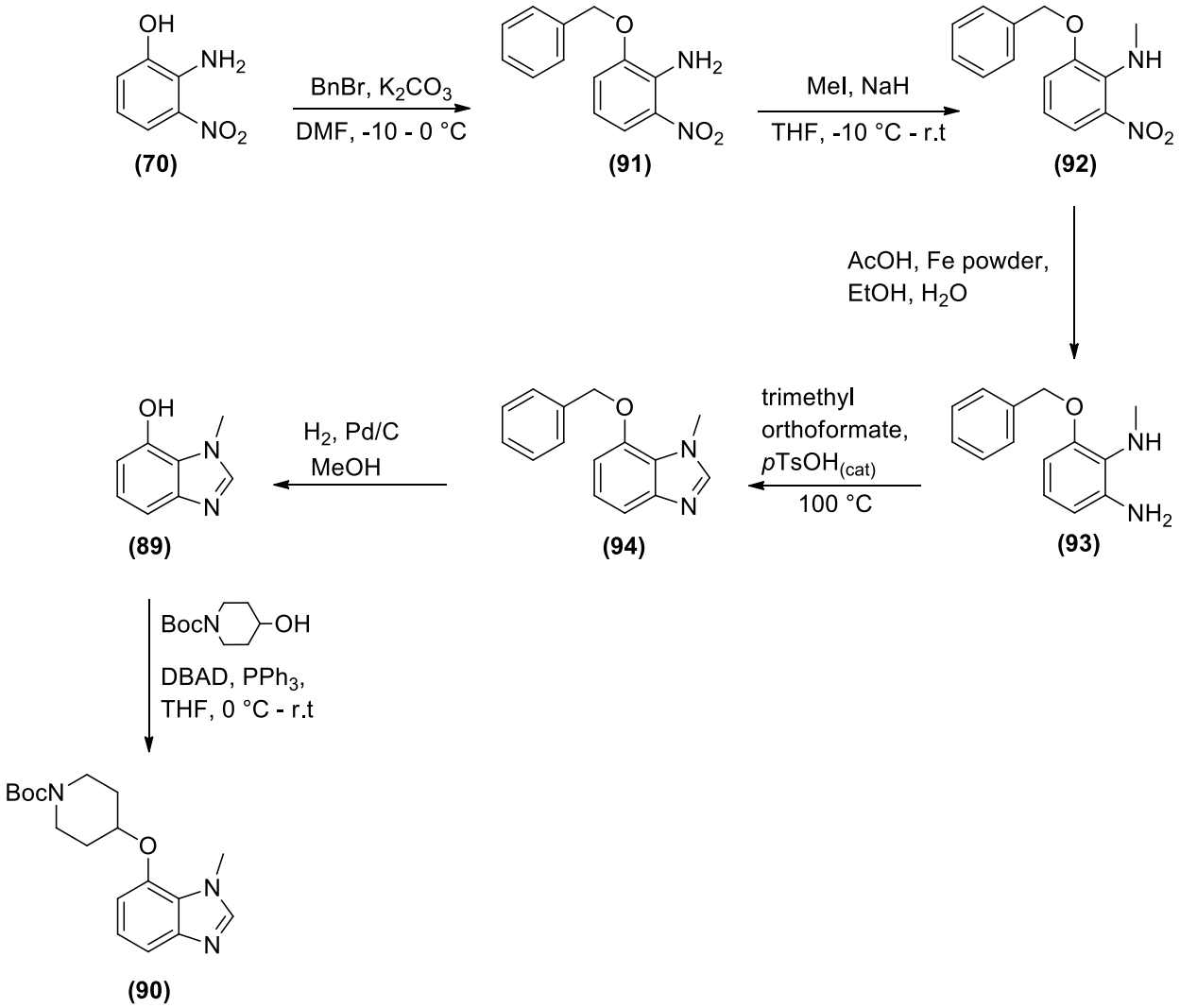

Scheme 47: New synthetic route to synthesize **(90)**

Due to the fact that compound **(92)** contained a benzyl ether, we had to find an alternative method to reduce the nitro group to that used previously. Reduction of the nitro group using hydrogen and palladium on carbon would result in the removal of the benzyl group in addition to the reduction of the nitro group. We resorted to the same nitro reduction method described by Gamble *et al*.[12] which we had used for the synthesis of **(73)** described in Chapter 3. Using this method **(93)** was obtained in a 72% yield, and its synthesis was confirmed by full spectroscopic characterization.

The cyclization step to produce the desired benzimidazole was performed using the same procedure for the synthesis of **(88)** as seen in **Scheme 45**. The reaction was carried out in neat

conditions using trimethylorthoformate and a catalytic amount of tosylic acid at 100 °C to produce **(94)** in a yield of 97%. ^{1}H-, ^{13}C-NMR spectroscopy and HRMS analysis confirmed the formation of **(94)**. Subsequent debenzylation with hydrogen and palladium on carbon provided 7-hydroxy-1-methylbenzimidazole **(89)** in a 65% yield. The ^{1}H-NMR spectrum of **(89)** is shown in **Figure 55**.

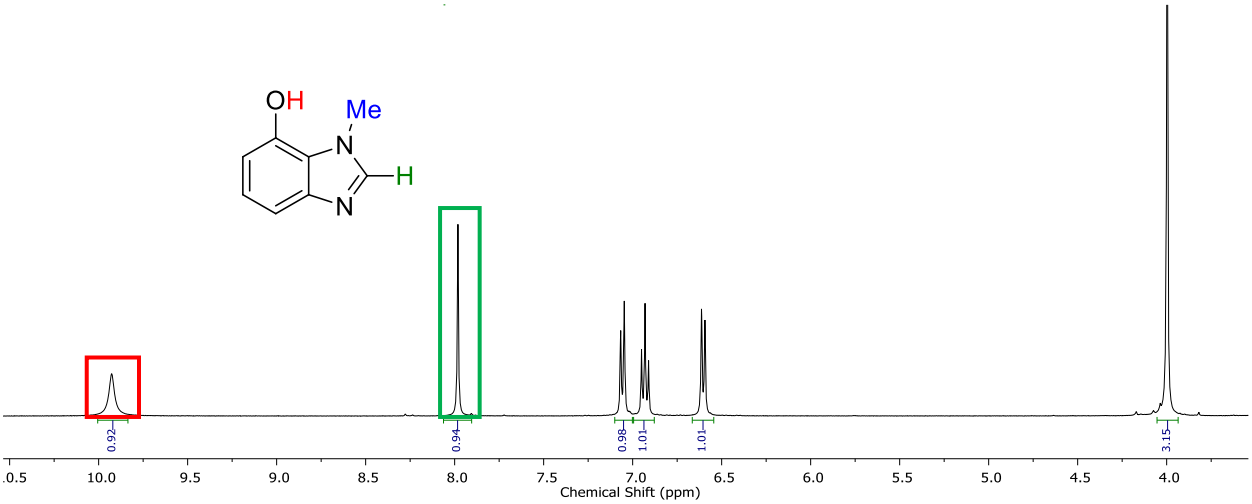

Figure 55: ^{1}H-NMR spectrum of **(89)** in *d*-DMSO

The phenolic proton signal appeared at 9.93 ppm and confirmed that debenzylation had occurred successfully. The phenolic proton is shown in red and is indicated by a red square on the ^{1}H-NMR spectrum. The proton at the C2-position is shown in green and indicated by a green rectangle on the spectrum and the 1-methyl group by a blue rectangle on the spectrum.

Having successfully deprotected **(94)** to obtain desired benzimidazole **(89)** we could carry out the Mitsunobu reaction to synthesize **(90)**. The Mitsunobu reaction was carried out by coupling **(89)** with **(32)** in the presence of DBAD and PPh_3. The reaction afforded the coupled product **(90)** in a 98% yield. Purification was difficult at first as **(90)** was a highly polar compound. TLC analysis with 100% EtOAc as eluent indicated that **(90)** and triphenylphosphine oxide, the byproduct of the Mitsunobu reaction, had the same R_f value. In an attempt to overcome this problem the eluent was changed to 20% acetone:80% DCM. In this instance the R_f value of **(90)** was significantly greater than that of triphenylphosphine oxide and so purification of **(90)** could be readily achieved through column chromatography. ^{1}H- and ^{13}C-NMR spectroscopy with HRMS analysis confirmed the formation of **(90)**. The ^{1}H-NMR spectrum indicated the characteristic axial and equatorial methylene proton signals of the *N*-Boc piperidine ring as well as the methine proton signal appearing as a septet. The absence of the phenolic proton gave further evidence that the coupling reaction did occur.

4.3 Functionalization of the C2-position

In order to carry out the necessary transesterification and amidation reactions for the synthesis of the desired final benzimidazole compounds as seen in **Figure 53**, we needed to introduce an ester group at the C2-position. In order to do so we had to consider the reactivity of the C2-position of the benzimidazole scaffold. The pKa value of the C-H bond at the C2-position of 1-methylbenzimidazole in DMSO was reported as 37.3.[13] As a result, the use of strong bases with a higher pKa value such as bultyllithiums and lithium amides would deprotonate the C2-position readily, creating a nucleophilic aryl anion. Therefore it would be possible to functionalize the C2-position by adding an appropriate electrophile. **Scheme 48** illustrates the different methods attempted to functionalize this position. The aim was to introduce an ester group either directly or through subsequent functional group transformations.

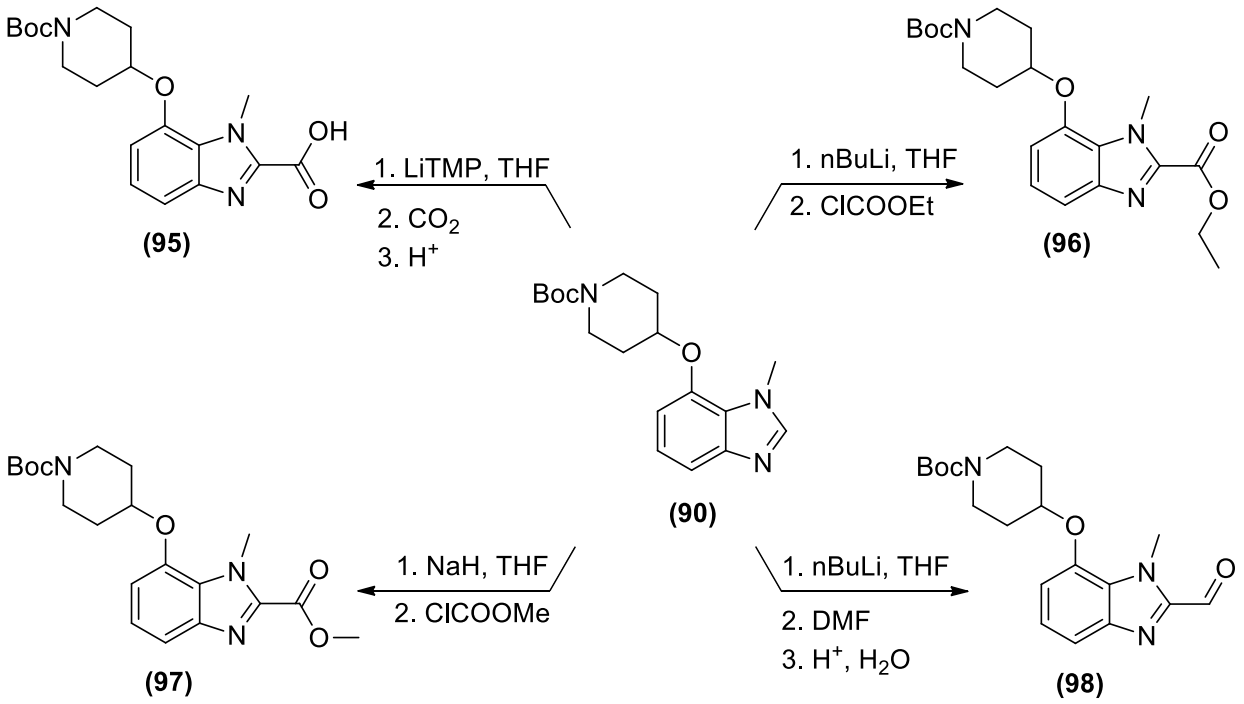

Scheme 48: Various methods attempted to functionalize the C2-position

Our first attempt at functionalizing the C2-position involved the introduction of a carboxylic acid at the 2-position **(95)** which would enable us to either convert the acid directly to an ester or, if that failed, to perform coupling reactions with reagents like CDI, various carbodiimides and 1-hydroxy-aryltriazoles to form the desired ester, which was described in Chapter 2. The synthesis of

benzimidazole **(95)** was attempted by deprotonating the C2-proton of **(90)** with LiTMP, followed by bubbling CO_2 gas through the solution. The reaction in our hands however was unsuccessful.

The second attempt involved the direct carboethoxylation of the C2-position of **(90)** using ethyl chloroformate to form **(96)**. We wanted to avoid the use of LiTMP and use *n*-BuLi directly to ensure deprotonation of the C2-position. *n*-BuLi was added to a solution of **(90)** in THF, after which the electrophile ethyl chloroformate was introduced to the reaction mixture. Unfortunately, TLC analysis showed that multiple products had formed, none of which we were able to isolate and identify. Despite numerous attempts at this reaction we were unable to synthesize **(96)**. It was speculated that the reason for the formation of a number of byproducts could be attributed to numerous factors such as the nucleophilic attack of *n*BuLi to the *N*-Boc group as well as acylation of the benzimidazole nitrogens leading to the formation of *N*-acyl salts.

In our third attempt we endeavored to synthesize the methyl ester benzimidazole **(97)** using sodium hydride, an irreversible, non-nucleophilic base and methyl chloroformate as the electrophile. However, carbomethoxylation was unsuccessful and the desired product was not formed in this instance either.

Our final endeavor to functionalize the C2-positon of **(90)** involved attempted formylation at the C2-position using *n*-BuLi and DMF to yield **(98)**. Formylation of 1-methyl benzimidazoles at the C2-position through deprotonation and subsequent quenching with DMF have been widely reported in the literature.[14,15,16] The introduction of an aldehyde at the C2-position would allow for functional group transformations such as oxidation to the carboxylic acid or oxidative transesterification whereby the ester is formed directly from the aldehyde. Deprotonation of **(90)** followed by a DMF quench and aqueous workup produced **(98)** in a 54% yield. ^{1}H- and ^{13}C-NMR analysis provided evidence for the formation of **(98)**. **Figure 56** illustrates the ^{1}H-NMR of **(98)**. The presence of a singlet at 10.06 ppm was indicative of the formation of an aldehyde (indicated by the red rectangle), while the absence of a singlet in the aromatic region belonging to the C2 proton provided further proof that **(98)** had been synthesized.

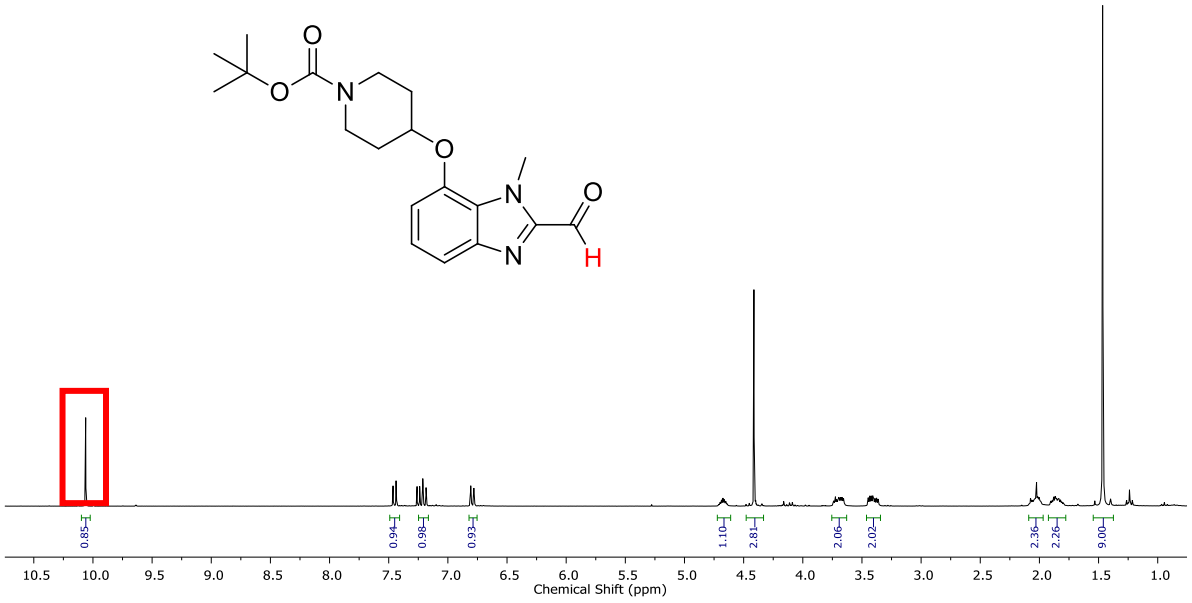

Figure 56: ^{1}H-NMR spectrum of **(98)** indicating the presence of an aldehyde signal at 10.06 ppm.

4.4 Alternative route for the synthesis of an ester at C2-position

The synthesis of **(98)** proved that formylation at the C2-position was possible, however we were unable to isolate **(98)** in a yield higher than 54%. We decided to change our synthetic strategy at this point by carrying out the formylation step at an earlier stage of the synthetic route before the Mitsunobu coupling of **(32)** and **(89)** (**Scheme 47**). We decided to carry out the formylation on benzimidazole **(94)** in the hope that by carrying out the formylation on a less reactive benzimidazole we would be able to improve the yield. **Scheme 49** illustrates the alternative synthetic strategy to synthesize **(110)**, starting with the formylation of **(94)** to produce **(99)** followed by oxidative esterification to yield **(110)** which will be discussed further on in this chapter.

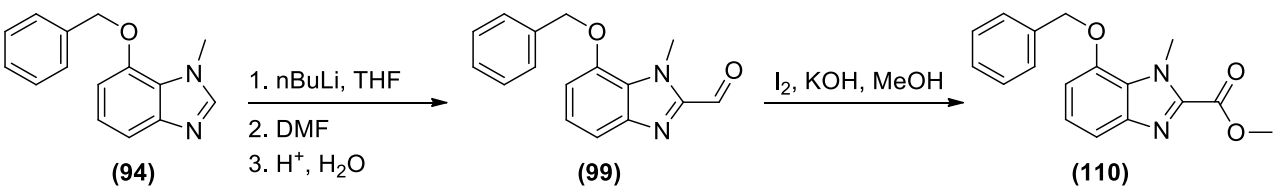

Scheme 49: Synthesis of **(110)** which includes formylation and oxidative esterification

4.4.1 Formylation of (94)

Benzimidazole **(94)** was formylated at the C2-position using the same procedure for the synthesis of **(98)** to produce **(99)** in a 69% yield. This was a marked improvement of the yield in comparison with the 54% obtained when formylation was carried out on **(90)**. The ^{1}H-NMR spectrum of **(99)** was similar to that of **(98)** in that a singlet at 10.09 ppm corresponding to the aldehyde was observed and the singlet in the aromatic region corresponding to the C2-proton was absent.

It was interesting to note that during the aqueous workup of the formylation reaction we noticed the formation of a byproduct **(107)** which was isolated and subsequently characterized. **Figure 57** illustrates the ^{1}H-NMR spectrum of this byproduct. The ^{1}H-NMR spectrum indicated a singlet at 9.66 ppm, indicative of the presence of an aldehyde, however the aromatic signals integrated for nine protons and not the expected eight protons found for **(99)** due to the addition of an unexpected singlet at 7.11 ppm. The aliphatic region contained the expected singlets relating to the benzyl methylene and *N*-methyl group, however a number of additional signals in the aliphatic region were also observed. These include a multiplet at 3.05 ppm which integrated for two protons, a multiplet at 1.55 ppm which integrated for two protons as well as a triplet at 0.97 ppm which integrated for three protons.

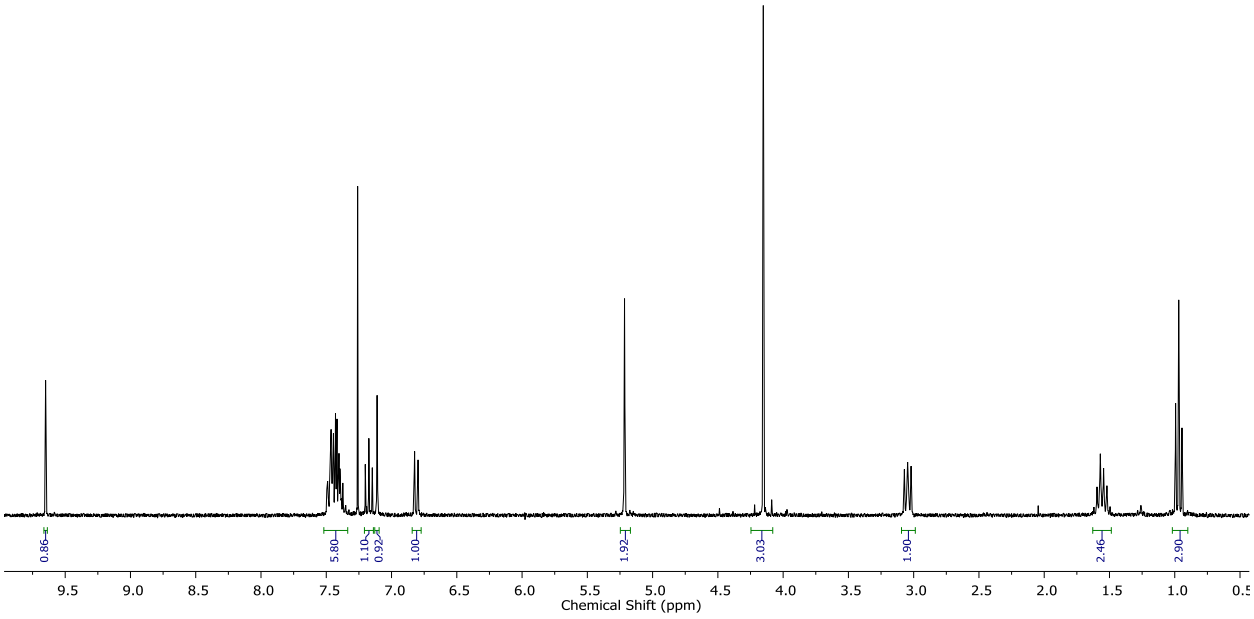

Figure 57: ^{1}H-NMR spectrum of unknown byproduct **(107)** in $CDCl_3$

We were unable to determine the structure of the unknown from the NMR spectroscopy data alone and therefore decided to obtain a crystal structure. The crystal structure indicated that the

formylation of the benzimidazole at the C2-position had occurred however the aldehyde had evidently reacted further to give **(107)** as shown in **Figure 58** below, and draw out in **Figure 59**. Having obtained a crystal structure it was now evident that the additional aliphatic signals observed at 3.05 ppm, 1.55 ppm and 0.97 ppm in the ^{1}H-NMR spectrum corresponded to the propyl chain annotated as carbons C(19), C(20) and C(21) in the crystal structure. Furthermore the additional signal observed at 7.11 ppm in the aromatic region was not aromatic but rather corresponded to the singlet at C(16) due to the double bond between carbons C(16) and C(17).

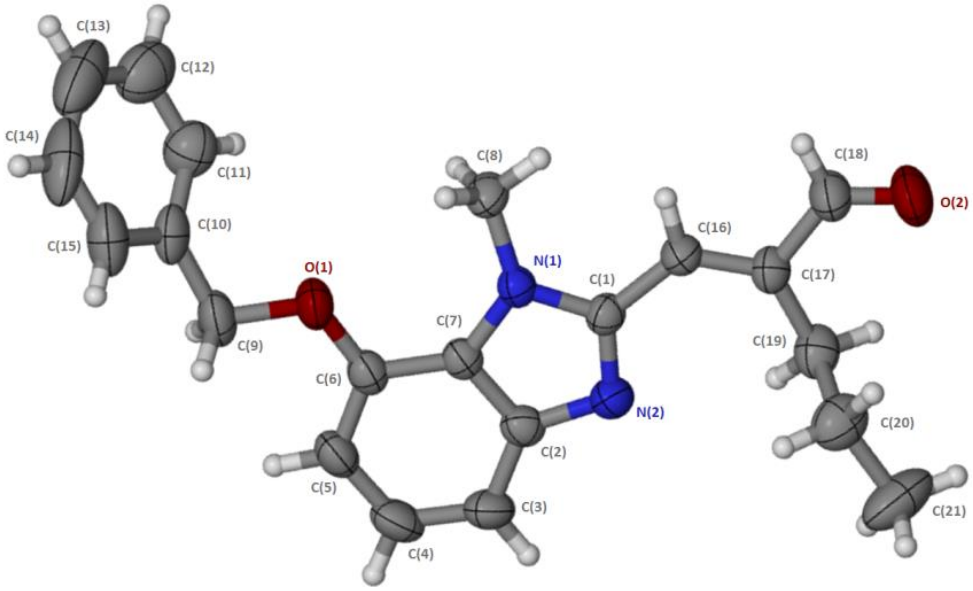

Figure 58: Molecular structure of unknown byproduct **(107)**. Thermal ellipsoids are shown at 50% probability. Crystallographic information is available in Chapter 10.

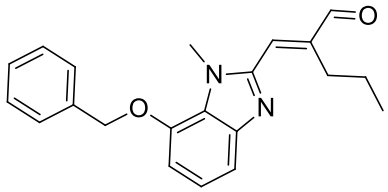

Figure 59: Skeletal structure of byproduct **(107)**

The mechanism by which formation of **(107)** had occurred is explained by **Scheme 50**. The first step involved the deprotonation of **(94)** by *n*-BuLi **(101)** to create the lithium benzimidazolyl species **(100)**. The following step involved the addition of DMF in an excess of 1.3 equivalents,

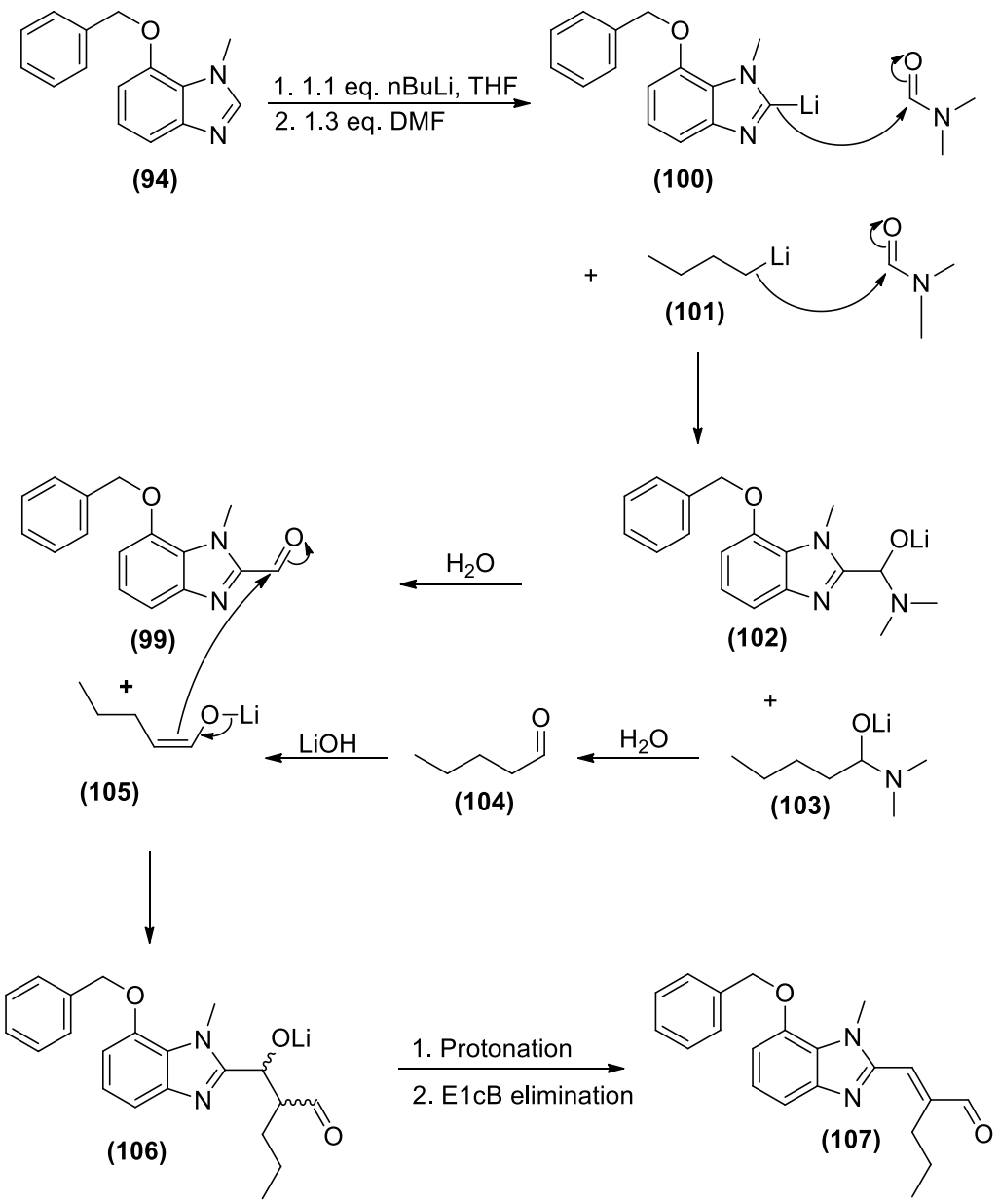

Scheme 50: Proposed mechanism for the formation of **(107)**

which acted as the electrophile to produce the lithium hemiaminolate species **(102)**. However, due to the fact that we used a slight excess of *n*-BuLi to ensure complete deprotonation of **(94)**, a small amount of *n*-BuLi reacted with the excess DMF to produce lithium 1-(dimethylamino)pentan-1-olate **(103)**. The final step which involved the hydrolysis of lithium hemiaminolate species **(102)** to produce the product **(99)** would also result in the hydrolysis of the small amount of **(103)** formed to produce pentanal **(104)**. LiOH and dimethylamine are the byproducts for the hydrolysis of **(102)** and **(103)**. The presence of LiOH facilitated enolization of

(104), resulting in the formation of *cis*-enolate **(105)**. As a result, subsequent aldol reaction between **(105)** and **(99)** would have occurred to produce the intermediate **(106)**, which after protonation of the lithium alkoxide followed by E1cB elimination would afford byproduct **(107)**.

Due to the fact that the addition of water resulted in the formation of **(107)**, the synthesis of **(99)** was attempted again, whereby saturated aqueous $NaHCO_3$ solution was used to facilitate hydrolysis of the hemiaminolate, preventing the formation of LiOH. In this instance no byproduct was formed and **(99)** was obtained in an 81% yield.

4.4.2 Oxidative esterification of (99)

Having successfully installed the aldehyde at the C2-position of the benzimidazole in higher yields we could focus on transforming the aldehyde to the desired ester through oxidative esterification. Oxidative esterification involves the direct conversion of alcohols and aldehydes to their ester counterpart in a one-pot process.

In order to convert **(99)** to the desired ester **(110)** as depicted in **Scheme 49**, we decided to follow a procedure developed by Yamada and co-workers.[17] They reported the use of molecular iodine, KOH and a relevant alcohol for the transformation of an aldehyde to an ester. The advantage of utilizing the procedure developed by Yamada is that it requires mild reaction conditions, inexpensive reagents and the conversion is generally high yielding. Furthermore, this transformation method eliminates the need for a two-step process whereby oxidization of the aldehyde to the carboxylic acid is required prior to esterification. Avoiding this process is advantageous as oxidative reagents are generally difficult to work with and can often promote the formation of various byproducts. **Scheme 51** illustrates the mechanism by which this transformation occurs. The first step involves the formation of potassium methoxide (KOMe) by dissolving KOH in methanol. A nucleophilic attack of KOMe on an aldehyde, in this case **(99)**, results in the formation of the potassium hemiacetalate **(108)**, which then reacts with molecular iodine to form the methoxy hypoiodite **(109)**. The final oxidative step involved deprotonation of the methoxy hypoiodite proton which resulted in the elimination of the iodide and subsequent formation of the desired ester **(110)**.

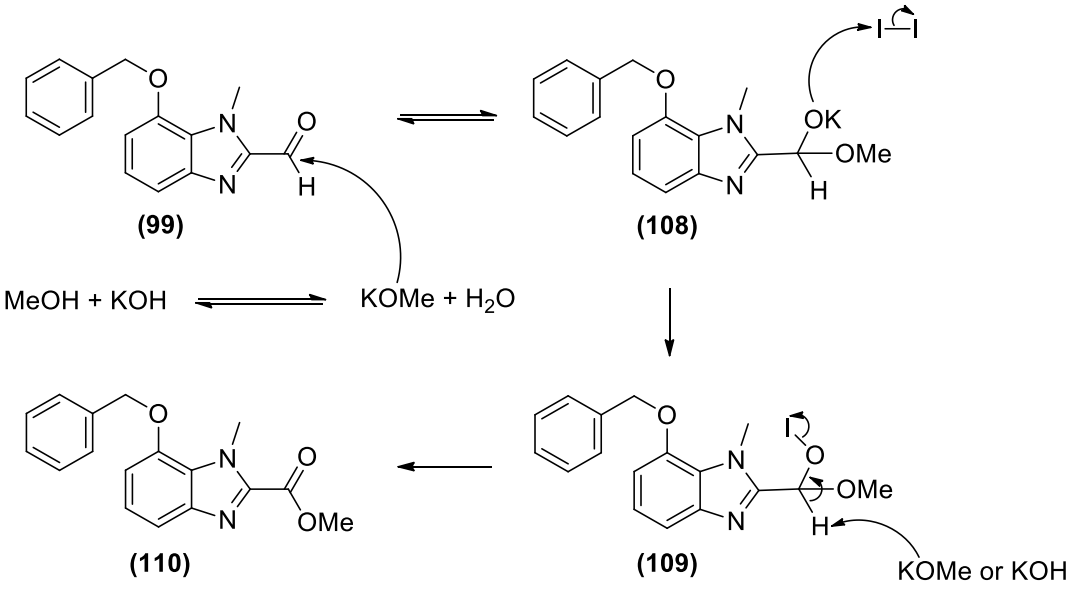

Scheme 51: Mechanism for the oxidative esterification of **(99)** to produce **(110)**

Using this method we were able to obtain **(110)** in a 79% yield. Analysis of the ^{1}H-NMR spectrum of **(110)** (**Figure 60**) revealed the presence of two singlets, both integrating for three protons. The singlet at 4.02 ppm corresponded to the *N*-methyl protons indicated by the red rectangle, while the singlet at 4.42 ppm corresponds to the methyl ester protons, indicated by the blue rectangle.

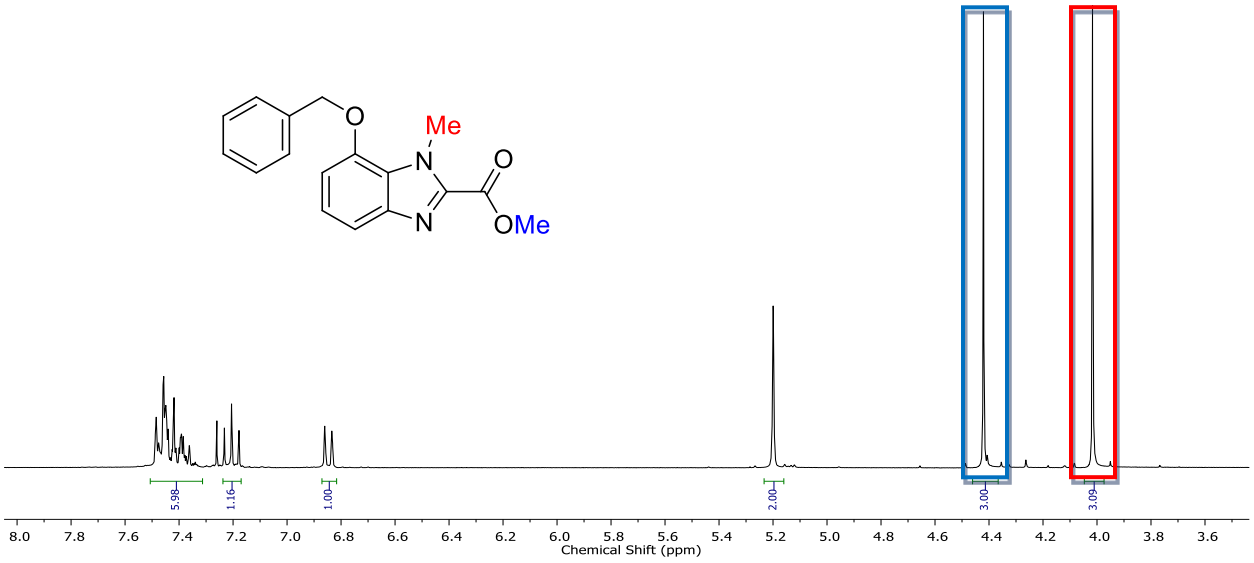

Figure 60: ^{1}H-NMR spectrum of **(110)** in $CDCl_3$

4.5 Debenzylation and Mitsunobu reaction

Having successfully synthesized the desired 2-methyl ester benzimidazole scaffold **(110)** we could continue with the subsequent debenzylation step to produce **(111)** followed by the Mitsunobu reaction to couple **(111)** with 1-Boc-4-hydroxypiperidine **(32)** as seen in

Scheme 52.

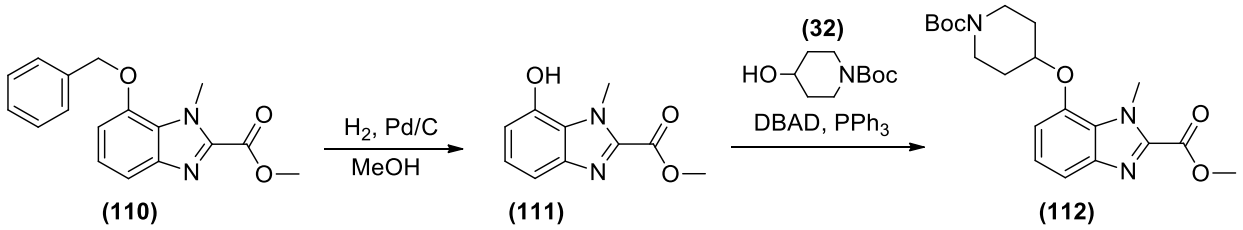

Scheme 52: Debenzylation of **(110)** and subsequent Mitsunobu reaction to afford **(112)**

Debenzylation was carried out using the same procedure for the synthesis of **(94)** with Pd/C and hydrogen which afforded **(111)** in a 92% yield. The synthesis of **(111)** was verified by ^{1}H-, ^{13}C-NMR spectroscopy as well as HRMS. The Mitsunobu reaction resulted in the successful coupling of **(111)** with **(32)** to produce **(112)** in a 76% yield. **Figure 61** illustrates the ^{1}H-NMR spectra of **(111)** (top) and **(112)** (bottom).

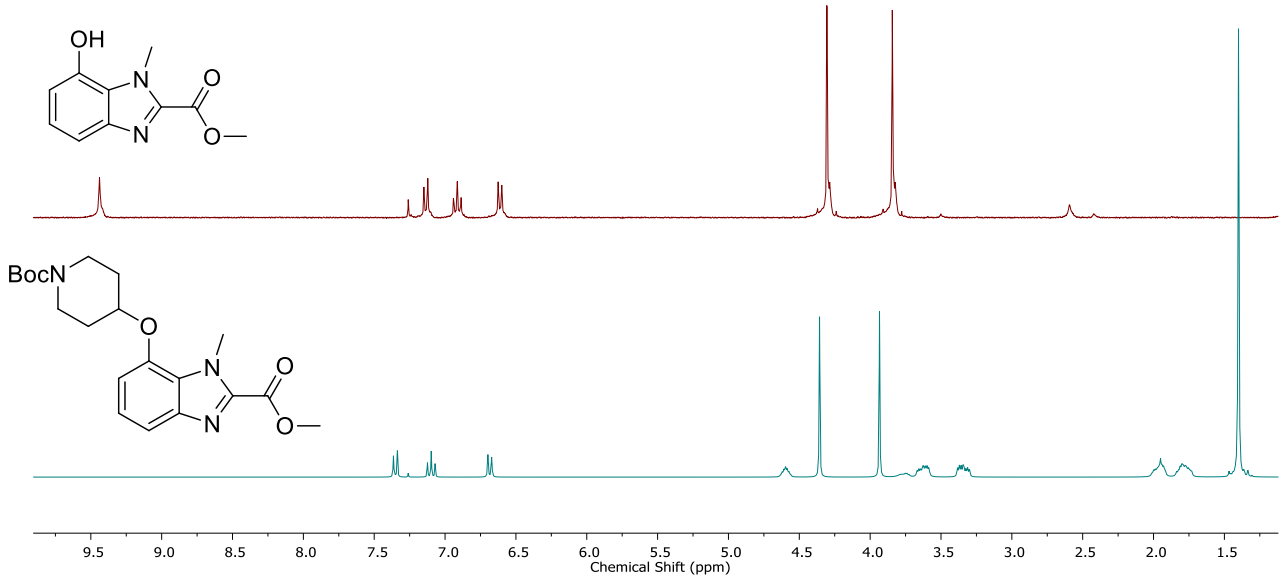

Figure 61: Stacked ^{1}H-NMR spectra of **(111)** at the top and **(112)** at the bottom in $CDCl_3$

For **(111)** the phenolic proton signal can be observed at 9.45 ppm, however for **(112)** this signal is absent. For the ^{1}H-NMR spectrum of **(112)** the methine and methylene proton signals corresponding to the coupled *N*-Boc piperidine are observed in the aliphatic region. Interestingly, a byproduct was formed during the Mitsunobu reaction of the benzimidazole **(111)** with **(32)** a phenomenon which was not observed in the case of the indole scaffolds described in Chapters 2 and 3. NMR spectroscopy and HRMS analysis confirmed that the byproduct formed was a result of transesterification between **(112)** and 1-Boc-4-hydroxypiperidine **(32)**. The byproduct **(113)** can be seen in **Scheme 53**.

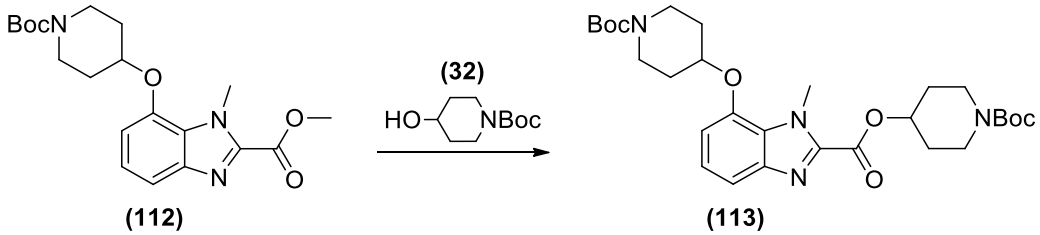

Scheme 53: Transesterification of **(112)** to form **(113)**

Figure 62 illustrates the ^{1}H-NMR spectrum of **(113)**. Analysis of the ^{1}H-NMR spectrum revealed that additional methine proton signals (blue rectangle) and methylene proton signals (red rectangle) were present.

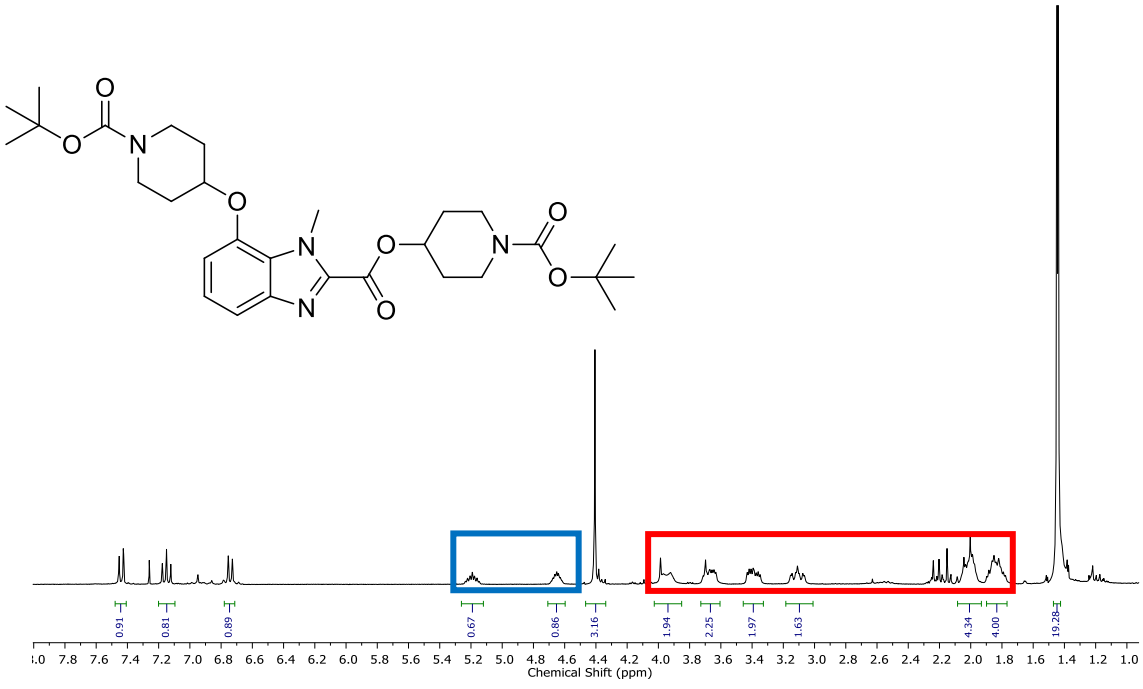

Figure 62: ^{1}H-NMR spectrum of **(113)** in $CDCl_3$

The fact that transesterification occurred during the Mitsunobu reaction was noteworthy. In comparison to the high temperatures (100°C) required for transesterification of the indole compounds described in Chapters 2 and 3, the Mitsunobu reaction was carried out at temperatures ranging from 0 °C to room temperature. The fact that transesterification of the benzimidazole ester had occurred under such mild conditions implied that the electrophilicity of the benzimidazole ester was significantly higher than that of the indole ester. Furthermore, the greater electrophilicity of the benzimidazole ester allowed for transesterification to occur with the 1-Boc-piperidine alkoxide which we believe may have formed as a result of the deprotonation of **(32)** by the betaine species **(34)** (Chapter 2, **Scheme 15**). Although we could not find the true pKa value for the betaine species, it was estimated that the betaine species had a $pKa_{(DMSO)}$ value that ranged between 12 – 17 which would be basic enough to deprotonate **(32)** or facilitate proton transfer during the transesterification process.[18]

4.6 Transesterification of (112)

The formation of **(113)** at room temperature lead to the conclusion that the transesterification of **(112)** with 2-phenylethanol, benzyl alcohol and 1-naphthylmethanol need not be carried out at the high temperatures reported in Chapters 2 and 3.

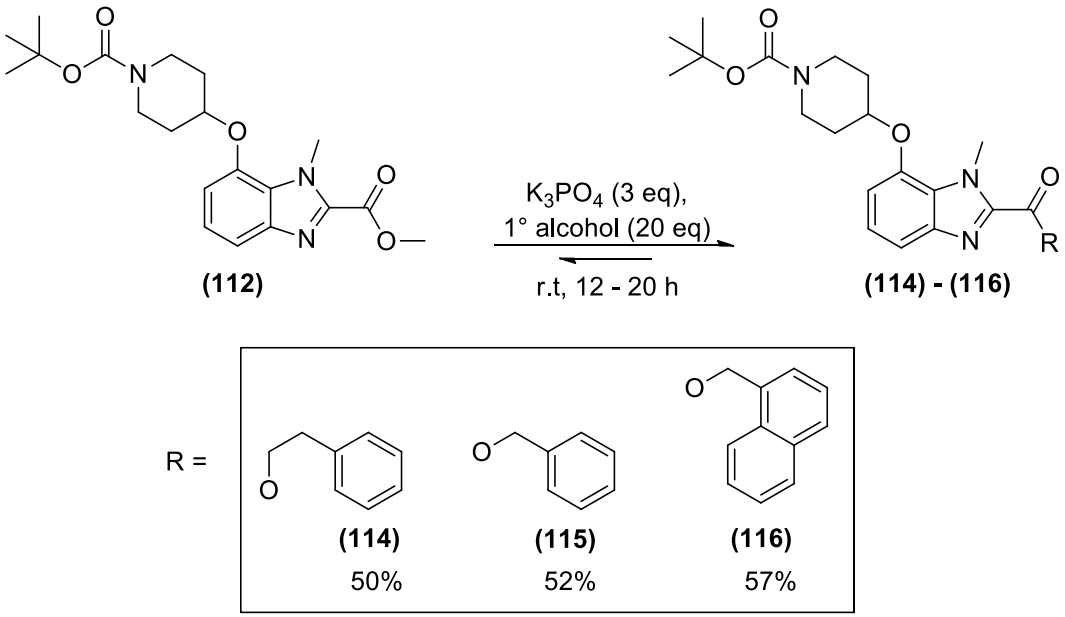

Scheme 54: Transesterification of **(112)** with 2-phenylethanol, benzyl alcohol and 1-naphthylmethanol. Yields are indicated.

As a result, the transesterification reaction between **(112)** and the three alcohols listed previously was carried out at room temperature using K_3PO_4 as the base (**Scheme 54**). In the case of 1-naphthylmethanol, which is a solid at room temperature, the reaction was taken up in a small amount of THF to dissolve **(112)** and 1-naphthylmethanol. 2-Phenylethanol and benzyl alcohol were used as the reagent and the solvent. Transesterified benzimidazole compounds **(114)** – **(116)** were isolated and characterized by ^{1}H-, ^{13}C-NMR spectroscopy as well as HRMS. Analysis of the ^{1}H-NMR spectrum of **(114)** revealed that the methyl ester proton signal at 3.93 ppm observed in the ^{1}H-NMR spectrum of compound **(112)** was absent. In addition, two clear triplets at 3.17 ppm and 4.62 ppm was observed, integrating for two protons each, which corresponded to the methylene protons of the phenethyl ester. The aromatic region displayed a set of multiplets that integrated for eight protons, which corresponded with the aromatic signals of the benzimidazole and phenethyl aromatic protons of **(114)**.

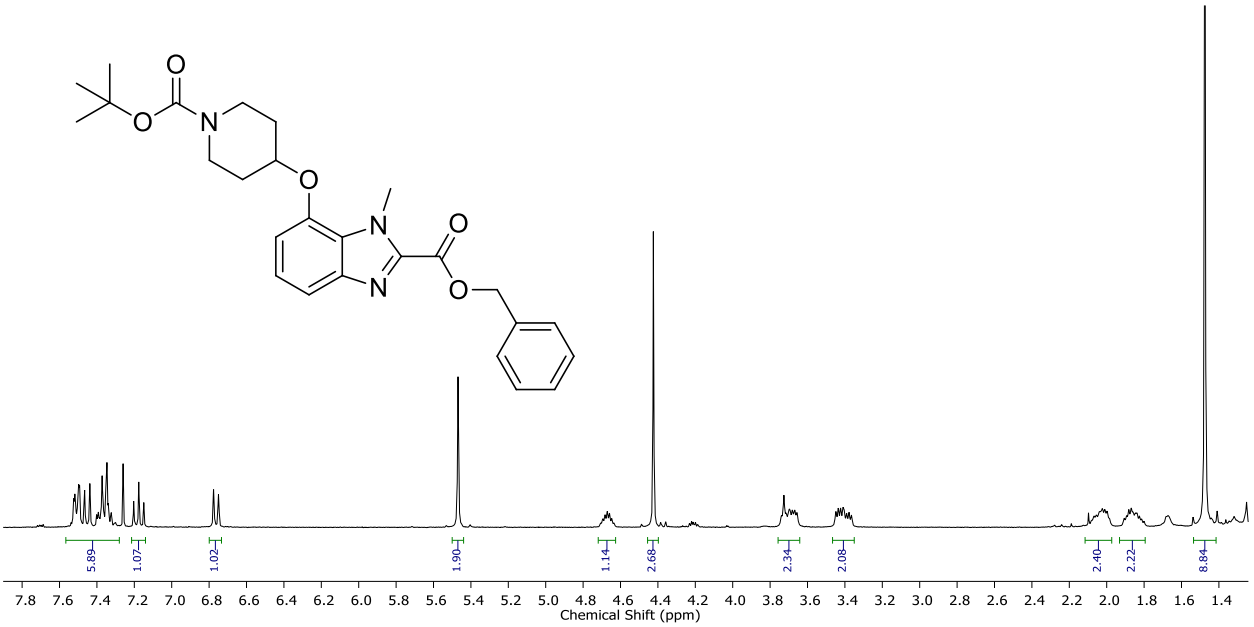

Figure 63: ^{1}H-NMR spectrum of **(115)** in $CDCl_3$

The ^{1}H-NMR spectrum of **(115)** also indicated the absence of the methyl ester proton signal at 3.93 ppm (**Figure 63**). However, ^{1}H-NMR analysis revealed the presence of a singlet at 5.47 ppm which corresponded to the methylene protons of the benzyl ester and the signals in the aromatic region integrated for eight protons corresponding to the aromatic protons of **(115)**.

The same absence of the methyl ester proton signal was observed in the^{1}H-NMR spectrum of **(116)**. Analysis revealed the presence of the naphthalic methylene proton appearing at 5.95 ppm

and the naphthyl and benzimidazole protons, which integrated for ten protons, in the aromatic region.

4.7 Amidation of (112)

Due to the increased reactivity of the methyl ester which enabled us to carry out the transesterification reaction at room temperature, we concluded that amidation of **(112)** with 2-phenylethylamine, benzyl amine, 1-naphthylmethylamine and 4-(aminomethyl)pyridine could also be carried out at room temperature to yield the desired amides **(117)** – **(120)** (**Scheme 55**). Benzimidazole **(112)** and ten equivalents of the respective amine was dissolved in THF and stirred at room temperature for 12 – 20 hours. TLC analysis of each reaction indicated the formation of a polar compound, indicative of the formation of an amide functional group. The synthesis of compounds **(117)** – **(120)** was verified by ^{1}H-, ^{13}C-NMR spectroscopy and HRMS. Analysis of the ^{1}H-NMR spectra of **(117)** – **(120)**, revealed that, in all cases, the methyl ester singlet at 3.93 ppm was absent. Furthermore, a broad triplet indicative of the amide proton coupling to the neighboring methylene protons was observed in each ^{1}H-NMR spectrum of **(117)** – **(120)**, in the region between 7.88 ppm and 8.36 ppm.

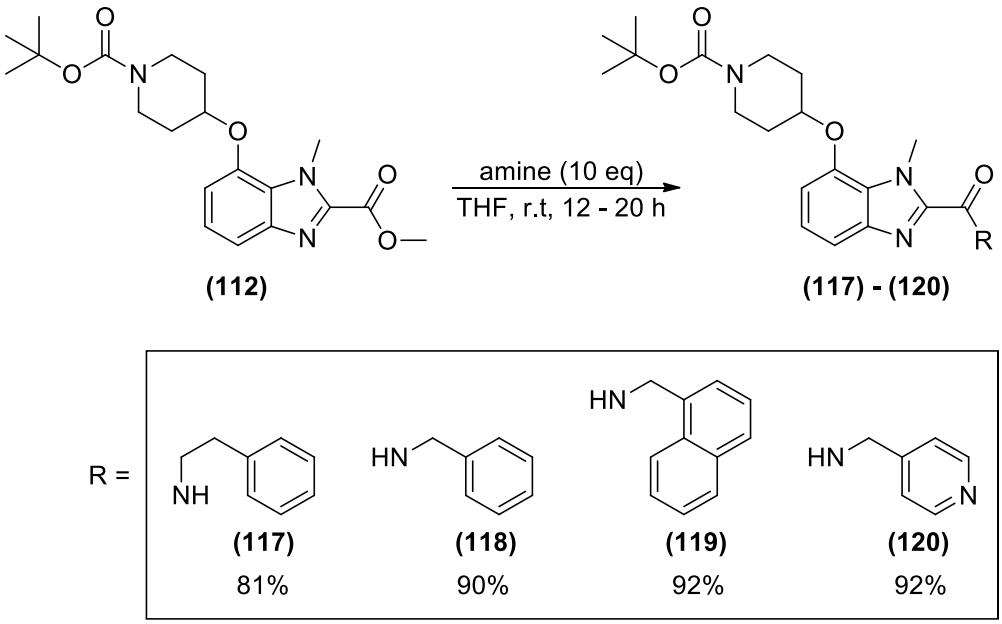

Scheme 55: Amidation of **(112)** with 2-phenylethylamine, benzyl amine, 1-naphthylmethylamine and 4-(aminomethyl)pyridine. Analysis of the ^{1}H-NMR spectrum of **(117)** indicated the

appearance of a quartet at 3.71 ppm which corresponded to the methylene protons of the phenethyl chain coupled to the amide proton and the neighboring methylene proton. The quartet overlapped with the multiplet corresponding to the axial protons of the piperidine ring. The quartet together with the multiplet integrated for four protons. A triplet at 2.96 ppm which integrated for two protons was also observed which corresponded to the other methylene on the phenethyl chain. The aromatic region integrated for eight protons.

Analysis of the ^{1}H-NMR spectrum of **(118)** revealed a visible doublet at 4.64 ppm which corresponded to the methylene protons of the benzyl group coupled to the amide proton. The aromatic region integrated for a total of eight protons. **Figure 64** illustrates the ^{1}H-NMR spectrum of **(118)** where the broad triplet of the amide can be observed at 8.16 ppm.

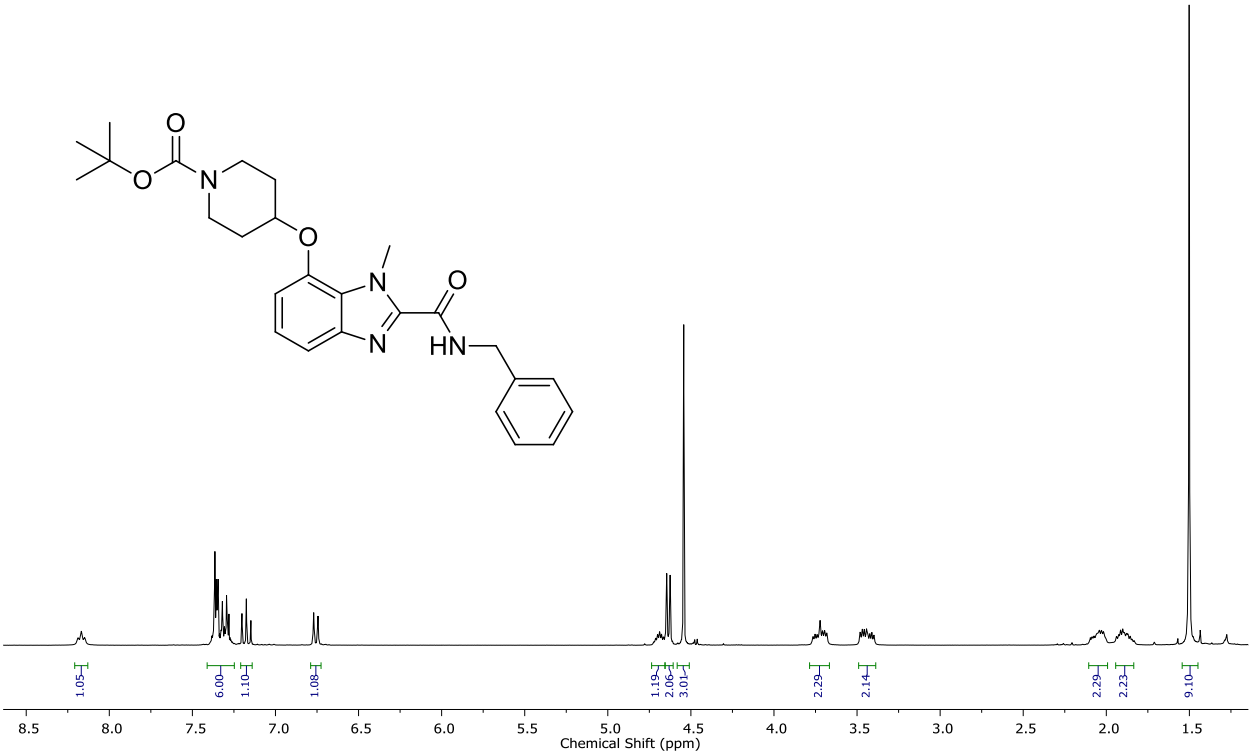

Figure 64: ^{1}H-NMR spectrum of **(118)** in $CDCl_3$

The ^{1}H-NMR spectra of **(119)** indicated the expected doublet which corresponded to the methylene protons at 5.10 ppm. The aromatic region integrated for a total of ten protons which corresponded to the presence of the naphthyl group. Finally, the ^{1}H-NMR spectrum of **(120)** indicated a visible doublet corresponding to the methylene protons of the 4-methylpyridine group at 4.64 ppm, as well as two aromatic signals at 7.27 ppm and 8.56 ppm integrating for two protons each.

4.8 *N*-Boc deprotection of (114) – (120)

Piperidine *N*-Boc deprotection was carried out using 4M HCl in dioxane, the same procedure used in the synthesis of the indole compounds described in Chapters 2 and 3. **Scheme 56** illustrates the *N*-Boc deprotection of compounds **(114)** – **(120)** to produce **BI1** – **BI7**.

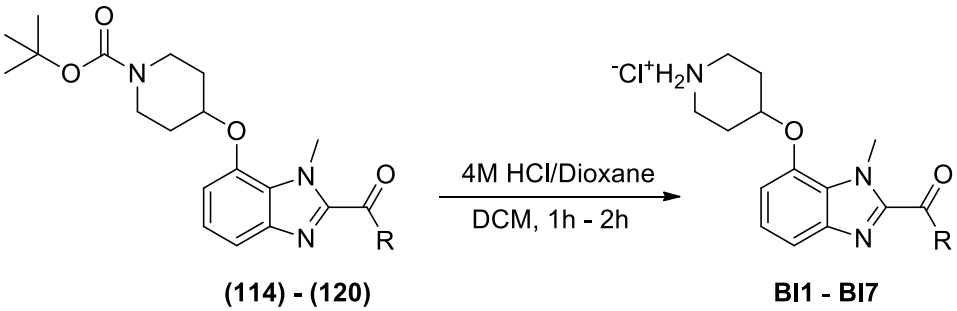

R =

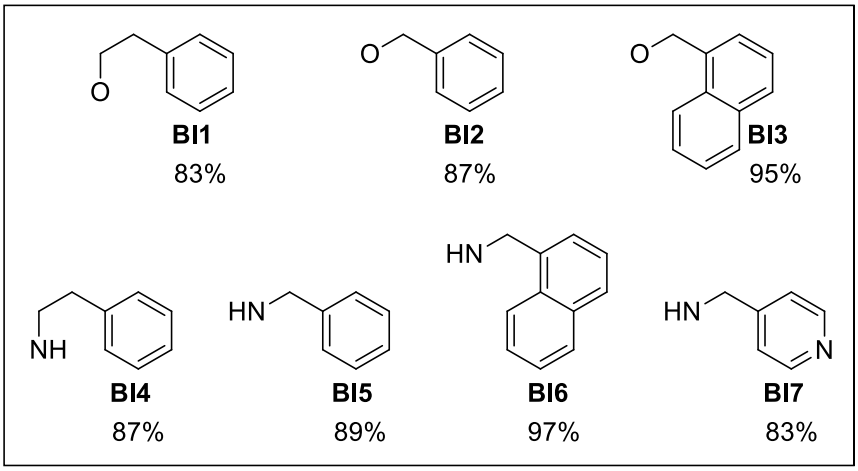

Scheme 56: *N*-Boc deprotection of **(114)** – **(120)** via HCl in dioxane to produce **BI1 – BI7**. **BI7** was isolated as the pyridinium HCl salt.

Successful *N*-Boc deprotection of compounds **BI1**– **BI7** was confirmed through characterization using ^{1}H-, ^{13}C-NMR spectroscopy and HRMS. **Figure 65** illustrates the ^{1}H-NMR spectrum of **BI1**, where the absence of the *tert*-butyl group of the *N*-Boc confirmed that deprotection was effective. The axial and equatorial protons which correspond with the piperidinium chloride group are visible at 9.25 ppm and 9.44 ppm and both signals integrate for one proton. The broad signal observed at 6.23 ppm corresponded to the water peak in the *d*-DMSO solution which had shifted from the usual position at 3.33 ppm due to the presence of the piperidinium chloride salt. The ^{1}H-NMR spectra of **BI1 – BI7** all indicated the presence of the axial and equatorial protons of the piperidinium chloride.

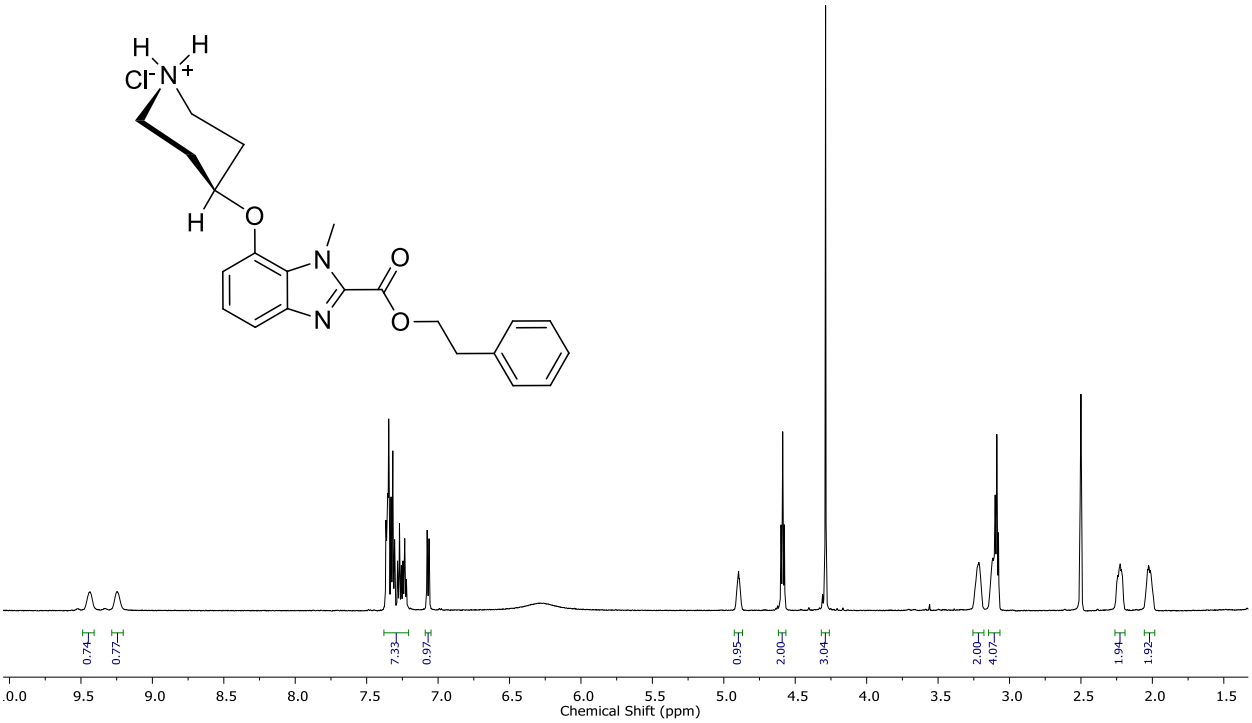

Figure 65: ^{1}H-NMR spectrum of **BI1** in *d*-DMSO

4.9 Conclusion

In this chapter we described the synthesis of a 1-methyl-4-benzyloxy-benzimidazole scaffold, which is isostructural to the 3-methyl indoles synthesized in Chapter 3. This was done to validate which heterocycle is the most active antimalarial agent, and to ascertain whether the methyl group indeed has an effect on the activity when comparing the efficacy of the analogous aromatic amides and esters.

Initially we synthesized the benzimidazole scaffold utilizing a well known literature procedure by reacting an *o*-phenylenediamine derivative with trimethyl orthoformate. We needed a derivatizable oxygen atom at the 7-position and a methyl at the 1-position of the benzimidazole scaffold. We selectively *O*-methylated 2-amino-3-nitrophenol, followed by mono-methylation of the amine, then reduction of the nitro group which produced the necessary substituted *o*-phenylenediamine 6-methoxy-*N*1-methylbenzene-1,2-diamine. Synthesis of the 7-OMe benzimidazole was achieved in a high yield with trimethyl orthoformate and catalytic tosylic acid.

The reasoning behind initial *O*-methylation as –OH protection was due to numerous literature methods known for the demethylation step that were seemingly faster than benzyl deprotection as well as the fact that nitro reduction could be achieved using Pd/C and hydrogen. However demethylation was not achieved after multiple failed attempts using various demethylation techniques. We duplicated the synthesis of the 7-methoxy-benzimidazole but in stead of O-methylation, we selectively *O*-benzylated, *N*-methylated, reduced the nitro group followed by ring closure to produce the 7-*O*Bn-benzimidazole heterocycle.

The next step was functionalizing the C2-position in order to introduce an ester at that position. Different unsuccessful routes were taken in order to attempt functionalization of the C2-position. Evidently, we managed to formylate at the C2-position using *n*-BuLi to deprotonate the C2-proton, and using DMF to formylate. It was also observed that the formylation reaction is sensitive to the workup procedure, as a byproduct formed during the aqueous workup as a result of the 2-carbaldehyde benzimidazole being involved in an aldol condensation reaction. A crystal structure was obtained to unambiguously confirm the structure of the previously unknown byproduct. We converted the aldehyde directly to an ester through an I_2/KOH/MeOH mediated oxidative esterification reaction. After benzyl deprotection was carried out, subsequent Mitsunobu coupling with 1-Boc-4-hydroxypiperidine was achieved. Transesterification/amidation reactions proceeded at room temperature and were generally high yielding. Boc deprotection of the *N*-Boc piperidine ring produced the final compounds **BI1** – **BI7**.

4.10 References

1. Yu, H.; Kawanishi, H.; Koshima, H. *J. Photochem. Photobiol. A.* **2006,** *178,* 62.

2. Lim, C. J.; Kim, N.; Lee, E. K.; Lee, B. H.; Oh, K.; Yoo, S.; Yi, K. Y. *Bioorg. Med. Chem. Lett.* **2011,** *21,* 2309.

3. Secci, D.; Bolasco, A.; D'Ascenzio, M.; della Sala, F.; Yáñez, M.; Carradori, S. *J. Heterocycl. Chem.* **2012,** *49,* 1187.

4. Maleki, A.; Ghamari, N.; Kamalzare, M. *RSC Advances* **2014,** *4,* 9416.

5. Zhang, Z.; Li, J.; Gao, Y.; Liu, Y. *J. Heterocycl. Chem.* **2007,** *44,* 1509.

6. Lim, C. J.; Kim, N.; Lee, E. K.; Lee, B. H.; Oh, K.; Yoo, S.; Yi, K. Y. *Bioorg. Med. Chem. Lett.* **2011,** *21,* 2309.

7. Zhou, J.; Jin, J.; Zhang, Y.; Yin, Y.; Chen, X.; Xu, B. *Eur. J. Med. Chem.* **2013,** *68,* 222.

8. McOmie, J.; Watts, M.; West, D. *Tetrahedron* **1968,** *24,* 2289.

9. Lange, R. G. *J. Org. Chem.* **1962,** *27,* 2037.

10. Node, M.; Nishide, K.; Fuji, K.; Fujita, E. *J. Org. Chem.* **1980,** *45,* 4275.

11. Burger, M.; Ni, Z. J.; Pecchi, S.; Atallah, G.; Bartulis, S.; Frazier, K.; Smith, A.; Verhagen, J.; Zhang, Y.; Wagman, A. Patent, Publication number; US8563549 B2, **2007**

12. Gamble, A. B.; Garner, J.; Gordon, C. P.; O'Conner, S. M. J.; Keller, P. A. *Synth. Commun.* **2007,** *37,* 2777.

13. Shen, K.; Fu, Y.; Li, J.; Liu, L.; Guo, Q. *Tetrahedron* **2007,** *63,* 1568.

14. Plater, M. J.; Barnes, P.; McDonald, L. K.; Wallace, S.; Archer, N.; Gelbrich, T.; Horton, P. N.; Hursthouse, M. B. *Org. Biomol. Chem.* **2009,** *7,* 1633.

15. Zhou, Y.; Gong, Y. *Eur. J. Org. Chem.* **2011,** *2011,* 6092.

16. Kannappan, R.; Nicholas, K. *ACS. Comb. Sci.* **2013,** *15,* 90.

17. Yamada, S.; Morizono, D.; Yamamoto, K. *Tetrahedron Lett.* **1992,** *33,* 4329.

18. Ragnarsson, U.; Grehn, L.; Koppel, J.; Loog, O.; Tšubrik, O.; Bredikhin, A.; Mäeorg, U.; Koppel, I. *J. Org. Chem.* **2005,** *70,* 5916.

Chapter 5: Synthesis of benzoxazoles

5.1 Introduction

This chapter describes the synthesis of a series of benzoxazole analogues that are isostructural to the **IH**, **IM** and **BI** series of compounds synthesized in Chapters 2, 3 and 4. Like the indole and benzimidazole scaffolds the benzoxazole heterocycle should contain a derivatizable oxygen atom at the 4-position and an ester group at the 2-position. The oxygen atom at the 4-position would be derivatized via the Mitsunobu reaction with 1-Boc-4-hydroxypiperidine in order to couple the necessary piperidine ring at the 4-position. Transesterification and amidation reactions of the ester group with various benzylic alcohols and amines would deliver the desired ester and amide substituents. **Figure 67** illustrates the benzoxazole library that was synthesized.

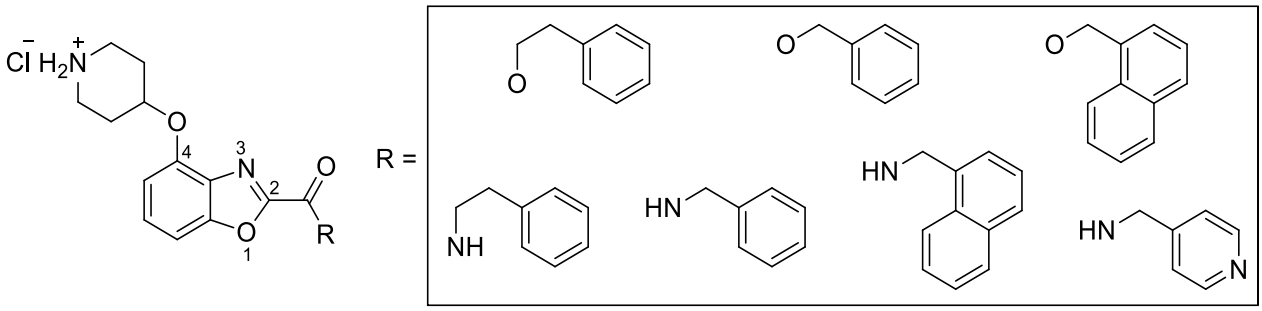

Figure 67: Proposed benzoxazole based compounds with various amides and esters to be synthesized

5.2 Synthesis of the benzimidazole heterocycle

For the synthesis of the benzoxazole series of compounds a similar synthetic strategy employed for the synthesis of benzimidazoles, discussed in Chapter 4, could be followed. As in the case of the *o*-phenylene diamines discussed in Chapter 4, 2-aminophenol derivatives cyclize with carboxylic acids[1,2] aldehydes[3,4] and orthoformates[5-7] under acid-catalyzed conditions to produce benzoxazole derivatives containing either an alkyl, aryl or a proton as substituent at the 2-position (**Scheme 57**).

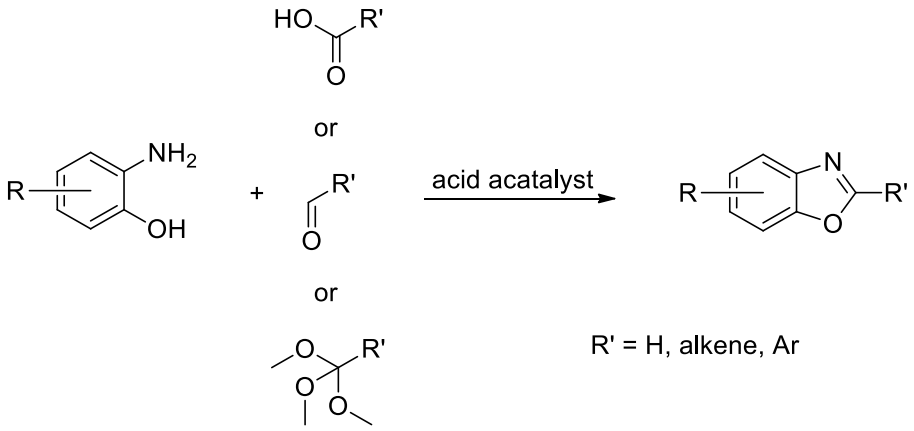

Scheme 57: Formation of substituted and unsubstituted benzoxazoles via the cyclization of 2-aminophenol with carboxylic acids, aldehydes and orthoesters

Our first objective was to synthesize the 4-(benzyloxy)benzoxazole **(125)** which contained a benzyl protected oxygen atom at the 4 position, as seen in **Scheme 58**. In order to synthesize **(125)** the appropriate 2-aminophenol had to be synthesized first. We envisaged that this could be achieved starting with commercially available resorcinol **(121)** which could be nitrated at the 2-position to yield **(122)** and then subsequently reduced to yield the desired 2-aminophenol **(123)**.

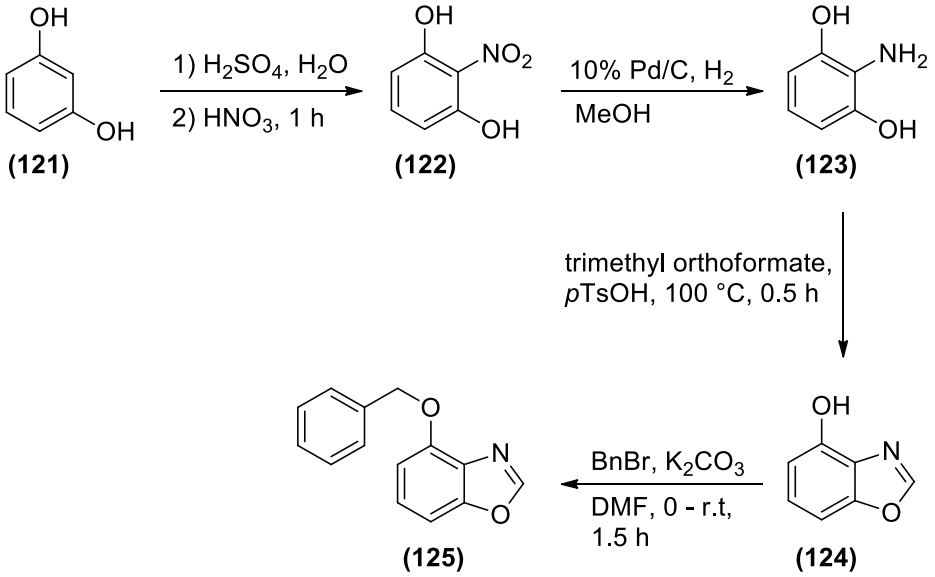

Scheme 58: Synthetic route to synthesize **(125)**

2-Nitroresorcinol **(122)** was synthesized according to a procedure reported by Cozza *et al*.[8] which involved the regioselective nitration of **(121)** with H_2SO_4 and HNO_3. Regioselective nitration was observed due to the fact that aromatic sulfonation with H_2SO_4 occurred through electrophilic

aromatic substitution on the 4- and 6-positions of **(121)**. Positions 4 and 6 of resorcinol **(121)** are activated due to the *ortho*- and *para*-directing hydroxyl groups on the 1- and 3-positions on the aromatic ring. The *meta*-directing sulfonic acid groups in addition to the *ortho*-directing groups of the hydroxyls activated the 2-position, thus facilitating regioselective nitration at the 2-position. A yield of 16% was obtained, partly due to the insufficient purification step which involves steam distillation to isolate **(122)**, as well as the requirement of high temperatures during isolation causing significant degradation. ^{1}H-NMR spectroscopy indicated that nitration had occurred due to the presence of a doublet at 6.62 ppm integrating for two protons, and a triplet at 7.44 ppm, integrating for one proton. The signals observed were in accordance with the literature.[8] 2-Aminoresorcinol **(123)** was synthesized by way of a nitro reduction of **(122)** with 10% Pd/C and hydrogen. **(123)** was obtained in an 87% yield.

The cyclization step which lead to the synthesis of **(124)** was carried out according to a procedure reported by Musser *et al*.[9] **(123)** was reacted with trimethyl orthoformate in the presence of catalytic tosylic acid to facilitate cyclization, which afforded **(124)** in an 88% yield after purification. The reaction was carried out neat. **Figure 68** illustrates the ^{1}H-NMR spectrum of **(124)**.

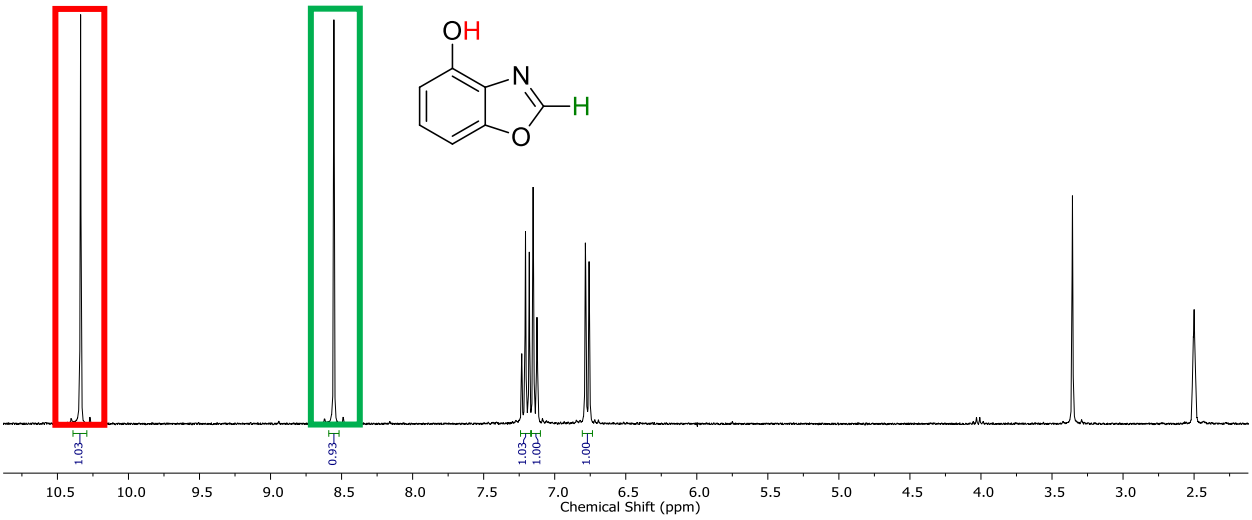

Figure 68: ^{1}H-NMR spectrum of **(124)** in *d*-DMSO indicating the phenolic proton (coloured in red) and the C2-proton (coloured in green)

^{1}H-NMR spectroscopy confirmed the formation of **(124)** due to the presence of a singlet at 8.55 ppm, which corresponded to the proton at the C2-position of the benzoxazole. The phenolic proton signal which appeared at 10.34 ppm integrating for one proton was observed in addition to two doublets at 6.77 ppm and 7.14 ppm and multiplet that appears as a triplet at 7.20 ppm

which correspond to the three protons on the aryl ring. The final protection step with benzyl bromide in DMF with K_2CO_3 afforded the benzyl protected product **(125)** in a quantitative yield. Having readily synthesized the desired benzoxazole **(125)** we could focus on the functionalization of the C2-position.

5.3 Carbomethoxylation at the C2-position

Due to the fact that an ester group was required at the C2-position, we envisioned employing a synthetic route which would involve the carbomethoxylation at the C2-position of the benzoxazole scaffold using methyl chloroformate as the electrophile and *n*-BuLi as base. **Scheme 59** illustrates this proposed synthetic strategy.

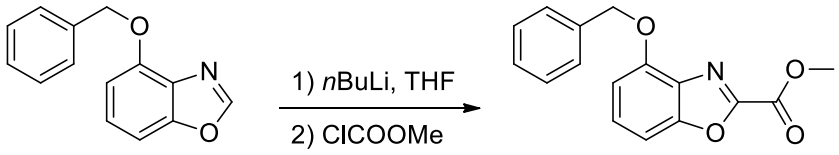

(125) **(126)**

Scheme 59: Acylation of **(125)** to produce **(126)**

The reaction was attempted but no product was obtained. An extensive search of the literature revealed the reason the reaction had been unsuccessful. A review on the metalation of oxazoles and benzoxazoles by Fu[10] revealed that lithiation of the C2-position induces a structural change of oxazoles and benzoxazoles.

Scheme 60 illustrates the ring opening mechanism of **(125)**. Lithiation of **(125)** resulted in the formation of the 2-lithio benzoxazole species **(127)** which lead to a ring opening of **(127)** to form the lithium 2-isocyanophenolate species **(128)**.

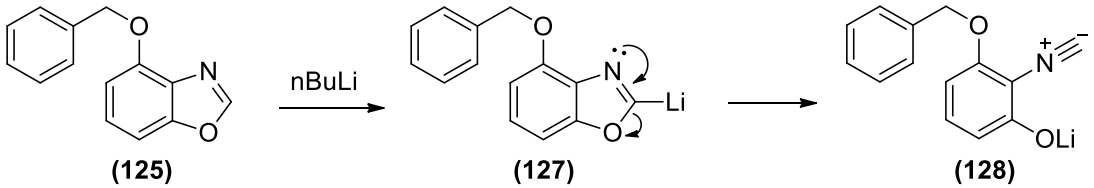

(125) (127) (128)

Scheme 60: Ring opening of **(125)** via lithiation

Due to the difficulty of direct carbomethoxylation at the C2-position, we shifted our focus to alternative methods regarding functionalization at the C2-position of the benzoxazole.

5.4 Intra- and intermolecular cyclization of (123)

Another extensive literature search was carried out in order to ascertain if there were any reactions which would allow for a one pot cyclization of 2-aminophenol derivatives that would produce the benzoxazole scaffold with the ester at the C2-position already installed. Fortuitously three methodologies were discovered that reported the formation of alkyl benzoxazole-2-carboxylates from 2-aminophenol. The methodologies reported are listed below.

1. Cyclization with methyl trimethoxyacetate,
2. Acylation/cyclization with ethyl chlorooxoacetate in pyridine,
3. Acylation/cyclization with ethyl chlorooxoacetate under Mitsunobu reaction conditions.

5.4.1 Cyclization of (123) with methyl trimethoxyacetate

Papers by Musser[11] and Boyle[12] reported that 2-aminophenols could undergo a cyclization reaction with commercially available methyl trimethoxyacetate in the presence of an acid catalyst to afford methyl benzoxazole-2-carboxylates. We attempted the cyclization reaction of **(123)** with methyl trimethoxyacetate **(129)** to produce methyl ester benzoxazole **(130)**, as seen in **Scheme 61**.

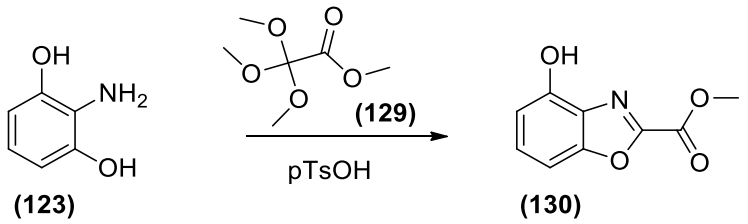

Scheme 61: Reaction of **(123)** with methyl trimethoxyacetate to produce **(130)**

The reaction between **(123)** and **(129)** was similar to the reaction between **(123)** and trimethylorthoformate for the synthesis of **(124)**. Due to the similarity and the fact that the synthesis of **(124)** resulted in high yields, the same reaction conditions were employed for the synthesis of **(130)**. Unfortunately, in this instance the reaction produced a number of products when monitored by way of TLC analysis and we were unable to isolate or identify **(130)**. We did not attempt to optimize this reaction as methyl trimethoxyacetate is an expensive reagent and would not be feasible to use for large scale synthesis of **(130)**.

5.4.2 Acylation/cyclodehydration with ethyl chlorooxoacetate in pyridine

Research conducted by Teno *et al*.[13] described the successful conversion of a 2-aminophenol derivative into the ethyl benzoxazole-2-carboxylate derivative by way of a one pot acylation/cyclodehydration reaction. The method involved the acylation of the respective 2-aminophenol with ethyl chlorooxoacetate **(131)** in pyridine and stirred overnight at 100 °C to produce the benzoxazole in a 25% yield after purification. The *in situ* formation of pyridinium chloride acts as the necessary acid catalyst for cyclization to occur. We decided to employ this methodology with the aim of synthesizing **(130)** through acylation of **(123)** with ethyl chlorooxoacetate **(131)** and subsequent cyclization at 100 °C (**Scheme 62**).

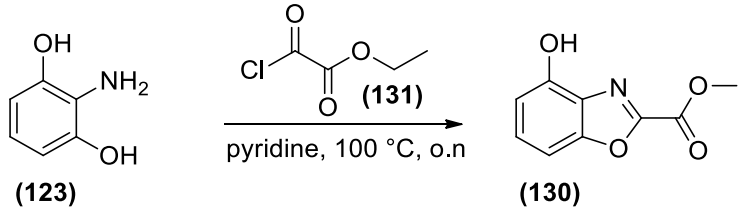

Scheme 62: Acylation/cyclodehydration reaction of **(123)** to produce **(130)**

TLC analysis indicated the formation of a product spot, after which the reaction was stopped and the formed product was isolated. Unfortunately **(130)** was obtained in a poor yield of 25%. ^{1}H-, ^{13}C-NMR spectroscopy and HRMS analysis confirmed the formation of **(130)**. The ^{1}H-NMR spectrum of **(130)** is shown in **Figure 69**.

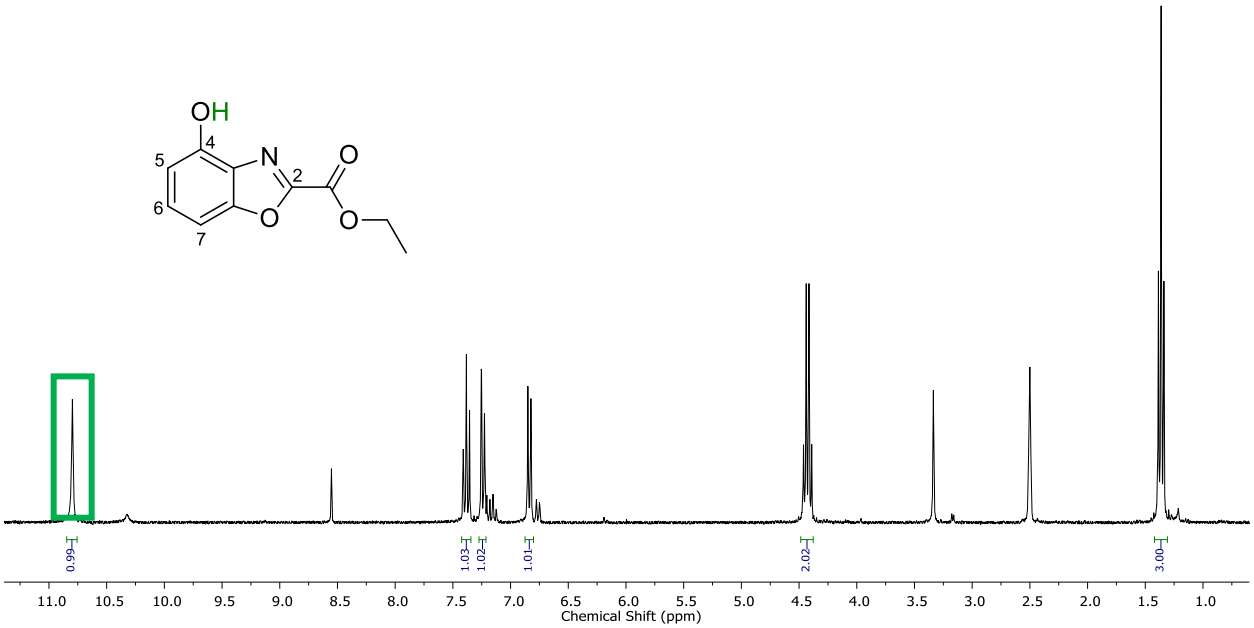

Figure 69: ^{1}H-NMR spectrum of **(130)** in *d*-DMSO

Analysis of the ^{1}H-NMR spectrum of **(130)** revealed the presence of a broad singlet at 10.80 ppm which integrated for one proton, indicative of the phenolic proton. This signal is shown in a green rectangle. A triplet at 1.37 ppm, which integrated for three protons and a quartet at 4.43 ppm, which integrated for two protons was observed and was indicative that the expected ethyl ester was present. The doublets at 6.84 ppm and 7.25 ppm in addition to the doublet of doublets at 7.39 ppm (appearing as a triplet) corresponded to the protons at the 5-, 6- and 7-position of **(130)**.

Although we were able to synthesize **(130)** using the one-pot method of acylation and subsequent cyclodehydration with ethyl chlorooxoacetate, the yield obtained was unsatisfactorily poor. As a result, we decided to explore the third and final method which involved acylation and subsequent cyclization with ethyl chlorooxoacetate under Mitsunobu reaction conditions

5.4.3 Acylation/cyclization with ethyl chlorooxoacetate under Mitsunobu reaction conditions

The synthesis of oxazoles and benzoxazoles by way of an intramolecular cyclodehydration under Mitsunobu reaction conditions has been well documented in the literature.[14,15] The advantage of using Mitsunobu conditions for the synthesis of 2-substituted benzoxazoles is that the reaction conditions are mild and product formation is generally reported as being high yielding. The only potential disadvantage would be during the purification step. The mixture of staring materials, byproducts and product could pose a challenging purification step in some cases.

This synthetic method involves the formation of a 2-hydroxyanilide derivative which subsequently undergoes a ring closing reaction under Mitsunobu conditions. Any substituent that is adjacent to the anilide carbonyl would in turn become the substituent on the C2-position of the benzoxazole, as depicted with the R-group in **Scheme 63**. This method would provide an efficient synthetic strategy to functionalize the C2-position during the formation of the benzoxazole. A search of the literature revealed that benzoxazoles synthesized by this method have had various substituents at the C2-position, most notably functionalized alkanes[16,17] and substituted amines.[15] This gave credence to the versatility of this method.

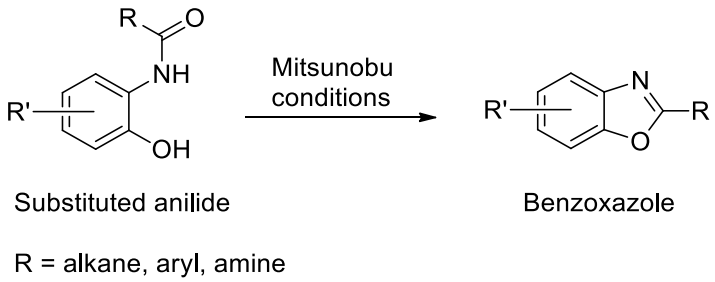

Scheme 63: Cyclodehydration of a substituted anilide to produce a substituted benzoxazole

Our main focus was to introduce an ester at the C2-position and, as a result, we had to synthesize an alkyl oxamate derivative to acylate the required 2-aminophenol. To our knowledge, a patent was the only literature source for the formation of 2-alkyl ester benzoxazoles.[18] The patent described the synthesis of various methyl benzoxazole-2-carboxylates by means of acylation of 2-aminophenol with methyl chlorooxoacetate, and subsequent cyclodehydration under Mitsunobu conditions with di-2-methoxyethyl azodicarboxylate (DMEAD®) and PPh_3.

We envisioned that we could employ the same procedure for the synthesis of **(130)**, but exchanging DMEAD® for either DBAD (di-tert-butyl azodicarboxylate) or DEAD (di-ethyl

azodicarboxylate) and acylating 2-aminoresorcinol **(123)** with ethyl chlorooxoacetate **(131)** (**Scheme 64**).

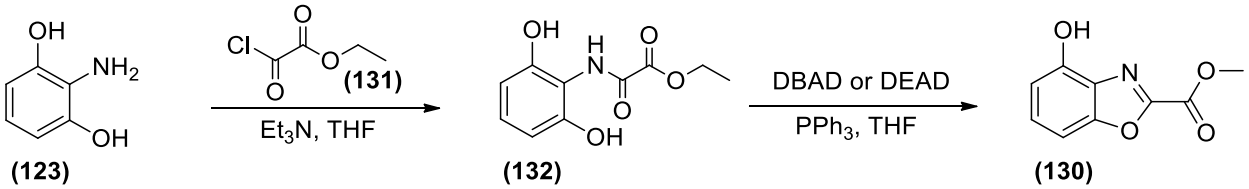

Scheme 64: Synthesis of **(130)** via acylation of **(123)** and subsequent cyclodehydration

(123) was chemoselectively acylated with **(131)** in THF to produce the 2-hydroxyanilide **(132)**. TLC analysis revealed full consumption of the starting material and the formation of a single product. However, isolation of **(132)** was problematic as workup with aqeous NH_4Cl and purification by way of column chromatography resulted in degradation and a loss of recoverable product. Workup with aqeous NH_4Cl resulted in the amidation of the oxoester **(132)** to the primary oxalamide. ^{1}H-NMR spectroscopy confirmed the formation of the primary oxalamide. **(132)** was isolated in a 12% yield, and confirmed by ^{1}H-NMR spectroscopy. The expected aromatic triplet and doublet was observed, as well as quartet and triplet in the aliphatic region correlating to the ethyl group of the ethyl oxamate.

Due to the fact that purification by way of column chromatography resulted in significant degradation of **(132)** we decided to omit the purification step and carry out the ensuing cyclization step with crude **(132)** obtained after aqueous workup.

In order to promote intramolecular cyclodehydration, the Mitsunobu reaction was carried out at a dilution of 15 mL THF per 1 mmol of compound **(132)**. This dilution of the reactants would prevent dimerization reactions from occurring. Initially we attempted the Mitsunobu cyclization reaction on **(132)** following a literature procedure[14] that suggested using five equivalents of PPh_3 and DEAD, as these equivalents would have ensured that cyclodehydration would occur readily. However, utilizing these equivalents we were unable to produce **(130)**. We re-attempted the Mitsunobu reaction but used 1.1 equivalents of DEAD since theoretically only one equivalent of the Mitsunobu reagent (DBAD, DIAD, DEAD etc.) is required for the coupling of an alcohol to a pro-nucleophile. In this instance, the reaction was stirred for six hours until TLC analysis confirmed full conversion of **(132)** to **(130)**. Purification of **(130)** by column chromatography however was challenging as **(130)** had a similar R_f value to the hydrazine byproduct formed from DEAD during the Mitsunobu reaction. To overcome this issue, crude **(130)** was benzylated to produce the 4-benzyloxy derivative **(133)** as seen in **Scheme 65**.This resulted in a decrease of the polarity and

therefore an increase in the R_f value of **(133)** thus enabling almost effortless purification of **(133)** which was isolated in a 46% yield over two steps. Debenzylation of **(133)** was readily achieved with Pd/C and hydrogen and 98% of **(130)** was recovered (**Scheme 65**).

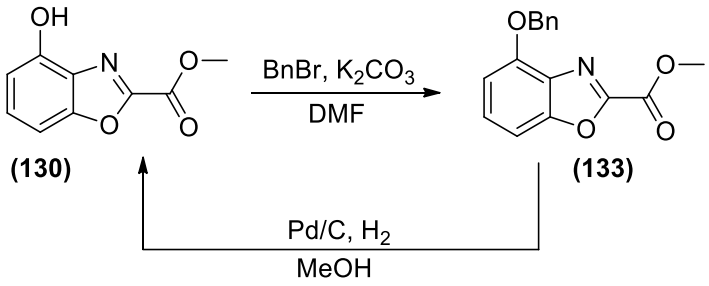

Scheme 65: Benzylation of **(130)** to produce **(133)**

We decided to optimize the reaction conditions as the overall yield for the synthesis of **(130)** was too low. As both the acylation reaction and the Mitsunobu reaction were carried out in THF we wondered if it would be possible to synthesize **(130)** in a one-pot process as opposed to over two steps. Acylation of **(123)** with ethyl chlorooxoacetate **(131)** and Et_3N was carried out at -10 °C. After two hours, TLC analysis indicated a full conversion of **(123)** to **(132)**. The reaction was then diluted with THF and PPh_3 was added followed by the dropwise addition of 1.1 equivalents of DEAD at -10 °C. After three hours, TLC analysis again indicated full conversion of **(132)** to **(130)**. Compound **(130)** was obtained in an 84% yield over two steps. Surprisingly purification in this instance was not problematic as the hydrazine byproduct of DEAD did not co-elute with **(130)**. The proposed reaction mechanism for the one-pot formation of **(130)** is illustrated in **Scheme 66**. The mechanism is an adaptation of a intramolecular Mitsunobu reaction mechanism illustrated in the article “First cascade Mitsunobu reactions for the synthesis of 2-benzoxazole-*N*-phenyl and 2-benzimidazole-*N*-phenyl derivatives” by Yu and co-workers,[15] describing the synthesis of 2-amino benzoxazoles via the cyclodehydration of 1-(2-hydroxyphenyl)urea derivatives.

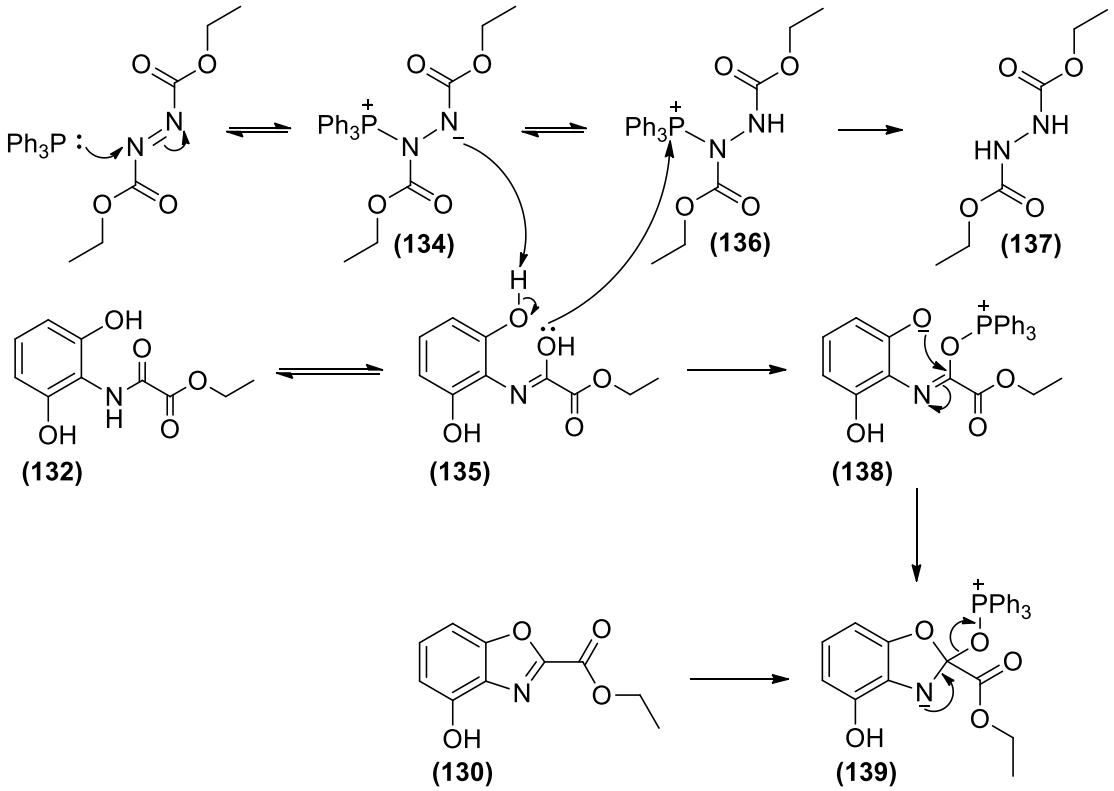

Scheme 66: Proposedmechanism for the formation of **(130)** via Mitsunobu reaction conditions

The first step was the formation of the betaine intermediate **(134)** which acted as a base and deprotonated the phenolic proton of **(135)** resulting in the formation of the phosphonium intermediate **(136)**. **(135)** is the tautomer of anilide **(132)**, an imidic acid. **(135)** acted as a nucleophile and attacked **(136)** at the phosphonium cation, subsequently producing the hydrazine byproduct **(137)** and the imino triphenylphosphonium intermediate **(138)**. The phenoxide anion then acted as a nucleophile, reacting at the electrophilic imino carbon **(138)** which tautomerized to form the amide phosphonium intermediate **(139)**. Subsequent aromatization along with the oxidation of the triphenylphosphonium substituent to triphenylphosphine oxide produced **(130)**. The fundamental difference between this mechanism and the mechanism for the Mitsunobu reaction described in Chapter 2 (**Scheme 15**) was that the oxygen atom that facilitated the oxidation of triphenylphosphine to triphenylphosphine oxide originated from the imidic acid, which acted as the alcohol counterpart of 1-Boc-4-hydroxypiperidine **(32)**.

A crystal structure of **(130)** was obtained as seen in **Figure 70**. The crystal structure in addition to spectroscopic data confirmed that **(130)** had indeed been synthesized. The crystal structure reveals that two molecules of **(130)** link by means of hydrogen bonding between the hydroxyl group annotated as O(2) of one molecule of **(130)** and the carbonyl oxygen atom annotated as

O(7) of a second molecule. No significant π-π stacking interactions between the molecules of **(130)** were observed.

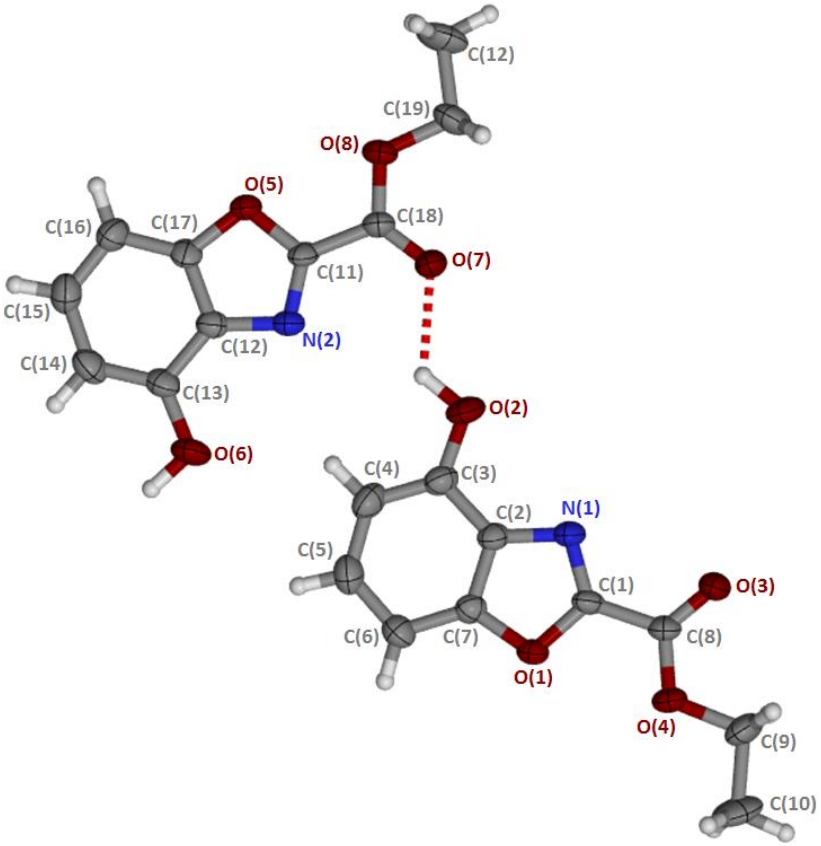

Figure 70: Asymmetric unit of **(130)**. Thermal ellipsoids are shown at 50% probability. The intramolecular hydrogen bond is indicated as a dashed red line. Crystallographic information is available in Chapter 10.

5.5 Mitsunobu coupling of (130) with 1-Boc-4-hydroxypiperidine (32)

The Mitsunobu coupling of **(32)** with various phenolic heterocycles has been discussed extensively in this dissertation. The Mitsunobu reaction between **(130)** and **(32)** was carried out in the same manner reported in Chapters 2 to 4 with PPh_3 and DBAD to produce **(140)** (**Scheme 67**). The reaction was carried out until TLC analysis confirmed the full conversion of **(130)** to **(140)** within 30 minutes.

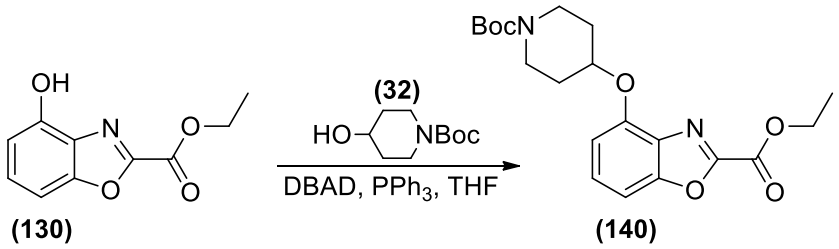

Scheme 67: Mitsunobu coupling of **(130)** with **(32)** to produce **(140)**

However, once again, purification was found to be challenging as **(140)** had the same R_f value as the hydrazine byproduct of DBAD. In order to overcome this obstacle once and for all, we looked at other variations of the Mitsunobu reagent.

Research conducted by Lanning[19] reported the development of a water soluble azo derivative, azodicarbonyldimorpholide (ADDM) as an alternative to DIAD in the coupling of various alcohols with different phenolic substrates to produce the desired phenolic ethers in high yields.

The synthesis of ADDM was readily achieved. As seen in **Scheme 68**, DEAD was reacted with morpholine in diethyl ether at 0 °C, which produced ADDM in 89% yield. Purification was effortless as the product precipitated out of solution as it formed and could therefore be filtered off and washed with diethyl ether to remove any traces of starting material. The ^{1}H-NMR spectrum was not conclusive proof that the synthesis of ADDM was successful, however, the ^{13}C-NMR spectrum provided the evidence. The morpholide group is essentially a urea derivative and has tertiary amide characteristics, thus the morpholide group is a rotamer. This means that the methylene carbons adjacent to the morpholine nitrogen are in different chemical environments and would have different chemical shifts. The ^{13}C-NMR spectrum indicated the presence of the urea carbonyl at 159.7 ppm, but two signals at 45.2 ppm and 43.7 ppm indicative of the methylene carbons adjacent to the morpholine nitrogen, and two close signals at 66.4 ppm and 66.5 ppm, indicative of the methylene carbons adjacent to the morpholine oxygen.

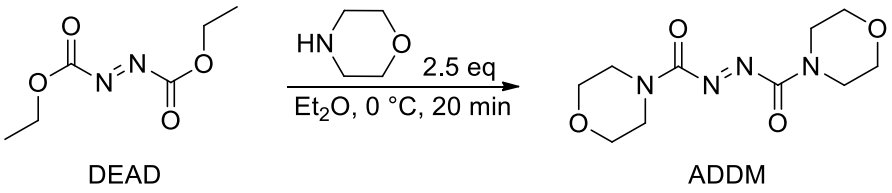

DEAD ADDM

Scheme 68: The formation of ADDM via the reaction of DEAD and morpholine

We attempted the Mitsunobu coupling of **(130)** with 1-Boc-4-hydroxypiperidine **(32)** in THF with PPh_3 and the newly synthesized ADDM. The reaction proceeded slowly due to the low solubility of ADDM in THF. However, the addition of DCM to the reaction solution dissolved the ADDM, which sped up the reaction. Using ADDM instead of DEAD or DBAD proved to be a successful means to overcome issues with purification as ADDM and the hydrazine byproduct of ADDM were significantly more polar than benzoxazole **(140)**. We were able to obtain **(140)** in a 79% yield. The synthesis of **(140)** was confirmed NMR spectroscopy and HRMS. **Figure 71** illustrates the ^{1}H-NMR spectrum of **(140)**.

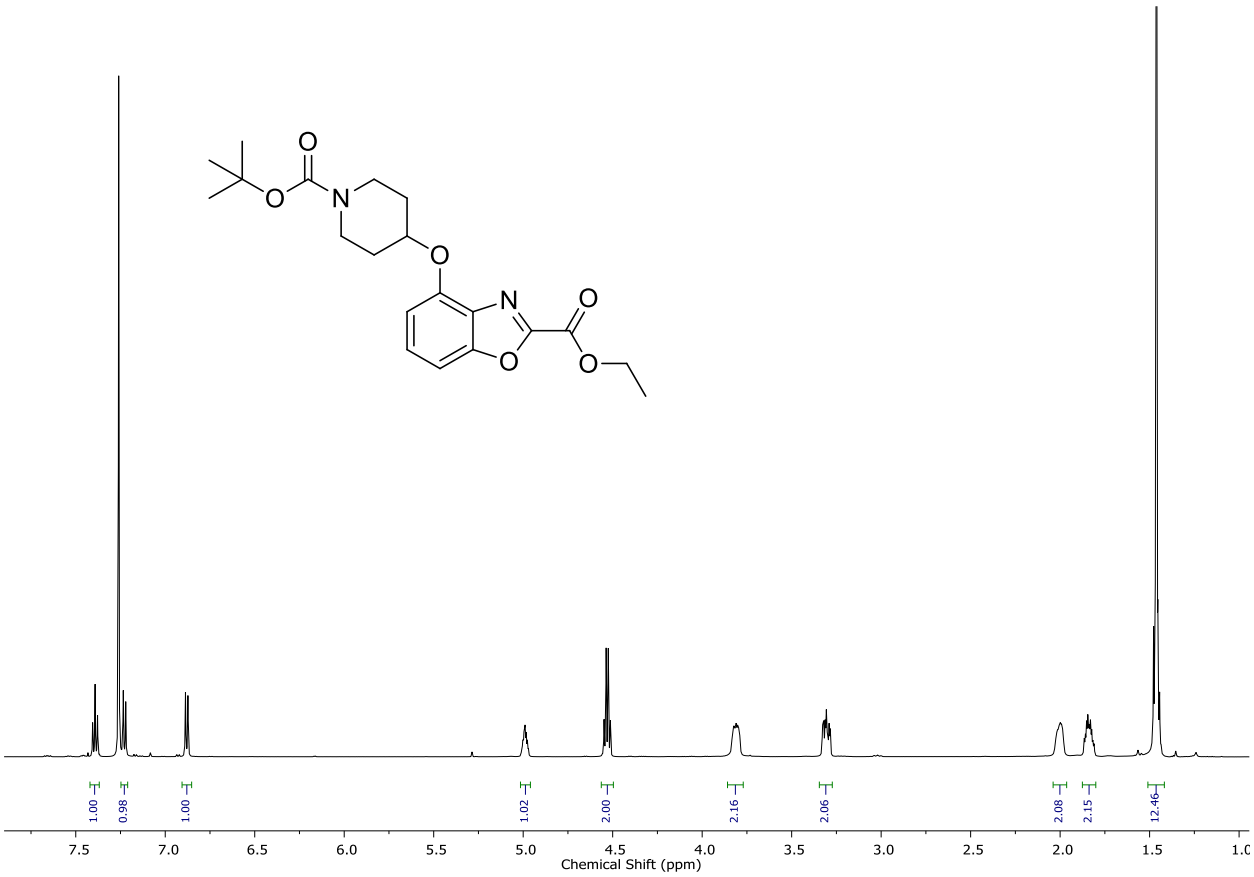

Figure 71: ^{1}H-NMR spectrum of **(140)** in $CDCl_3$

The ^{1}H-NMR spectrum of **(140)** indicates that the Mitsunobu reaction was successful in coupling **(130)** to **(32)** as the phenolic proton signal is absent and the presence of the methine, methylene and *tert*-butyl signals, indicating the 1-Boc-piperidine ring. The quartet at 4.56 ppm is indicative of the methylene of carboethoxy but the triplet of the methyl is masked by the large *tert*-butyl signal.

5.6 Transesterification of (140)

The transesterification of **(140)** with 2-phenylethanol, benzyl alcohol and 1-naphthylmethanol as seen in **Scheme 69** was carried out using the same procedure reported for the transesterification of **(112)** in Chapter 4 (**Scheme 54**).

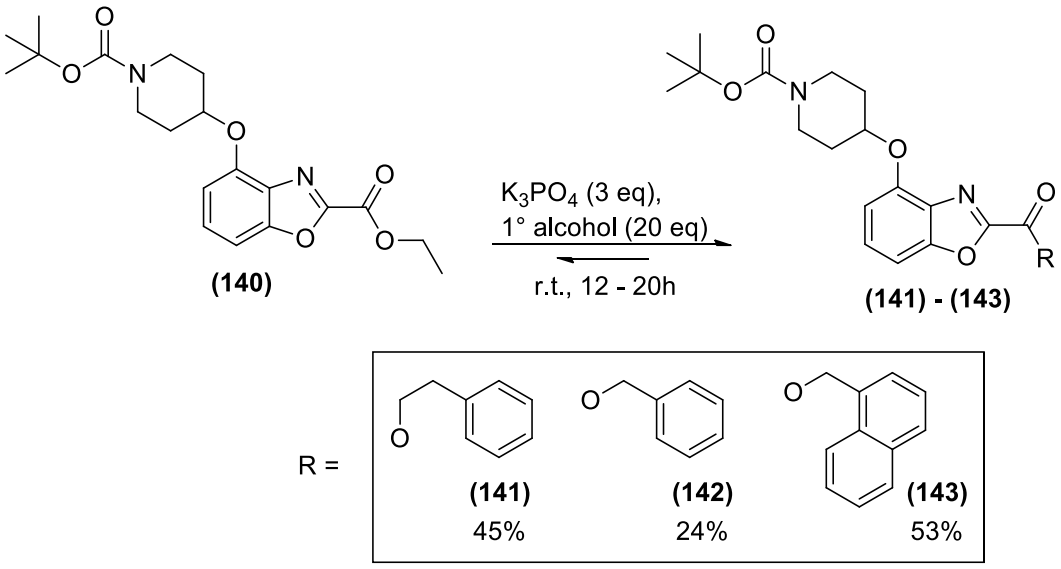

Scheme 69: Transesterification of **(140)** to produce **(141) – (143)**

The transesterification reaction was carried out at room temperature to produce compounds **(141)** – **(143)**. TLC analysis of the reaction indicated that each reaction had successfully converted **(140)** to the respective transesterified product. Due to the fact that **(140)** had an R_f value similar to that of **(141)** – **(143)** as well as the respective alcohols used for transesterification, purification was challenging. We attempted a number of purifications by means of column chromatography using different ratios of EtOAc:hexane as the mobile phase. This system, however proved to be ineffective in the purification of compounds **(141)** – **(143)**. On the other hand, a solvent system which consisted of 5% EtOAc:95% DCM increased the difference in R_f value dramatically and as a result purification of compounds **(141)** – **(143)** was readily accomplished. Interestingly, column chromatography with this solvent system reversed the polarity of the transesterified products **(141)** – **(143)** with respect to their respective alcohols. Compounds **(141)** – **(143)** were characterized by ^{1}H-, ^{13}C-NMR spectroscopy and HRMS. **Figure 72** illustrates the ^{1}H-NMR spectrum of benzoxazole **(141)**.

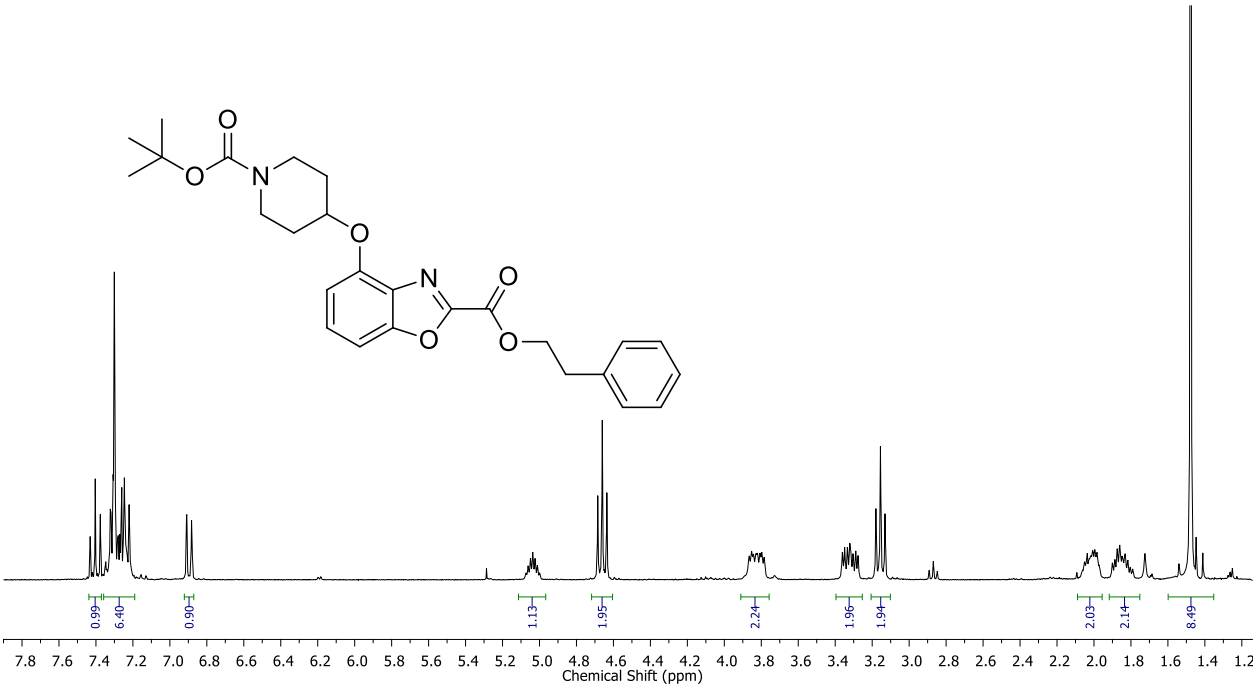

Figure 72: ^{1}H-NMR spectrum of **(141)** in $CDCl_3$

The ^{1}H-NMR spectrum of **(141)** revealed the presence of two triplets at 4.66 ppm and 3.15 ppm, which corresponded to the methylene protons of the phenylethyl ester. The aromatic region integrated for eight protons, which confirmed that transesterification with 2-phenlyethanol had occurred. ^{1}H-NMR analysis of compounds **(142)** and **(143)** revealed the expected signals in the aliphatic region coinciding with their respective aryl esters and all signals in the aromatic region were accounted for.

5.7 Amidation of (140)

The amidation of **(140)** with 2-phenylethylamine, benzylamine, 1-naphthylmethylamine and 4-(aminomethyl)pyridine as seen in **Scheme 70** was carried out using the same procedure for the amidation of **(112)** reported in Chapter 4 (**Scheme 55**). The amidation of **(140)** was carried out at room temperature using 10 equivalents of the respective amine in THF. TLC analysis of the reaction after 12 hours indicated a full conversion of **(140)** to the respective amide products **(144)** – **(147)**.

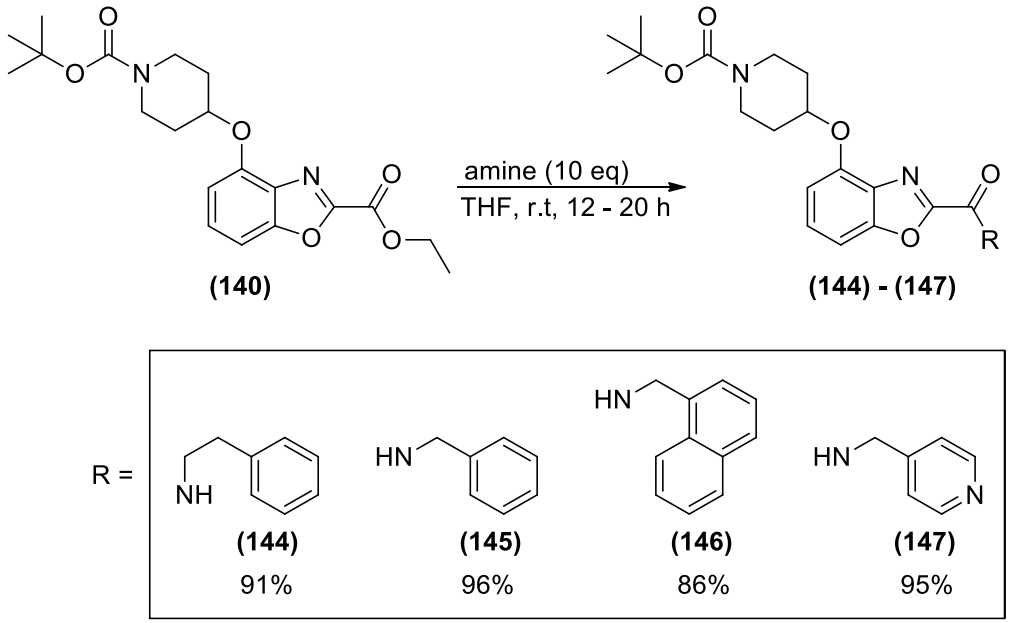

Scheme 70: Amidation of **(140)** to produce **(144)** – **(147)**

Compounds **(144)** – **(147)** were characterized by ^{1}H-, ^{13}C-NMR spectroscopy and HRMS. **Figure 73** illustrates the ^{1}H-NMR spectrum of benzoxazole **(146)**. The doublet observed at 5.14 ppm was indicative of the methylene protons of the naphthyl methyl ester which coupled to the amide proton. The aromatic signals all integrated for 10 protons.

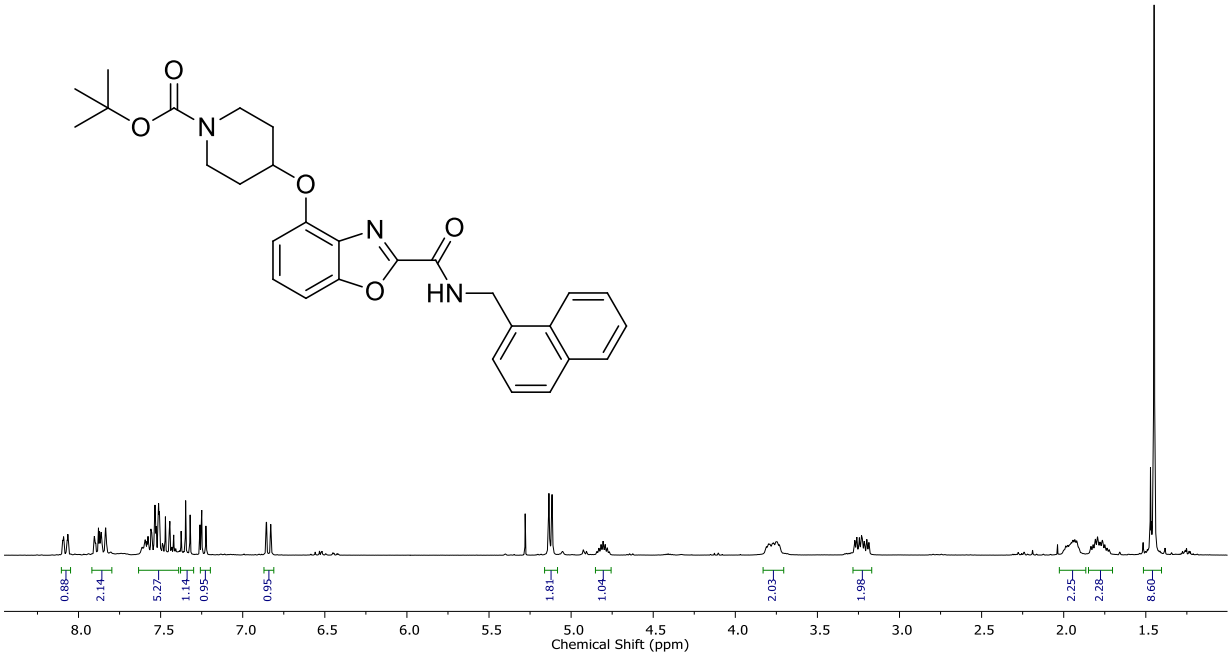

Figure 73: ^{1}H-NMR spectrum of **(146)** in $CDCl_3$.

5.8 *N*-Boc deprotection of (141) – (147)

Piperidine *N*-Boc deprotection was carried out using 4M HCl in dioxane, the same procedure reported for the synthesis of **IM1** – **IM7** in Chapter 3. **Scheme 71** illustrates the *N*-Boc deprotection of compounds **(141)** – **(147)** to produce final compounds **BO1** – **BO7**.

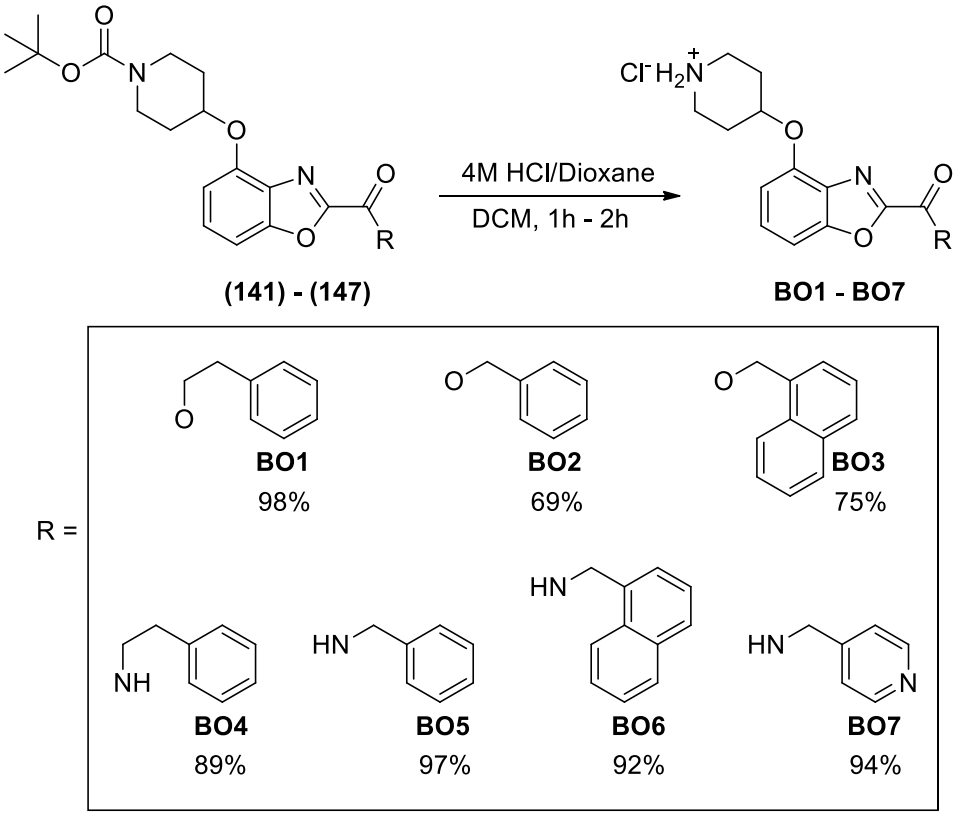

Scheme 71: *N*-Boc deprotection of **(141)** – **(147)** to produce **BO1** – **BO7**. **BO7** was isolated as the pyridinium HCl salt.

Characterization by ^{1}H- , ^{13}C-NMR spectroscopy and HRMS confirmed the successful *N*-Boc deprotection of **(141)** – **(147)** to afford **BO1** –**BO7**. The ^{1}H-NMR spectra of compounds **BO1 – BO7** all indicated the absence of the *tert*-butyl signal of the deprotected *N*-Boc group and the presence of two broad signals between 9.10 ppm and 9.64 indicating the axial and equatorial protons of the piperidinium chloride salt. **Figure 74** illustrates the ^{1}H-NMR spectrum of **BO7**, clearly indicating that the N-Boc deprotection step was successful due to the presence of the piperidinium protons appearing at 9.64 ppm and 9.40 ppm.

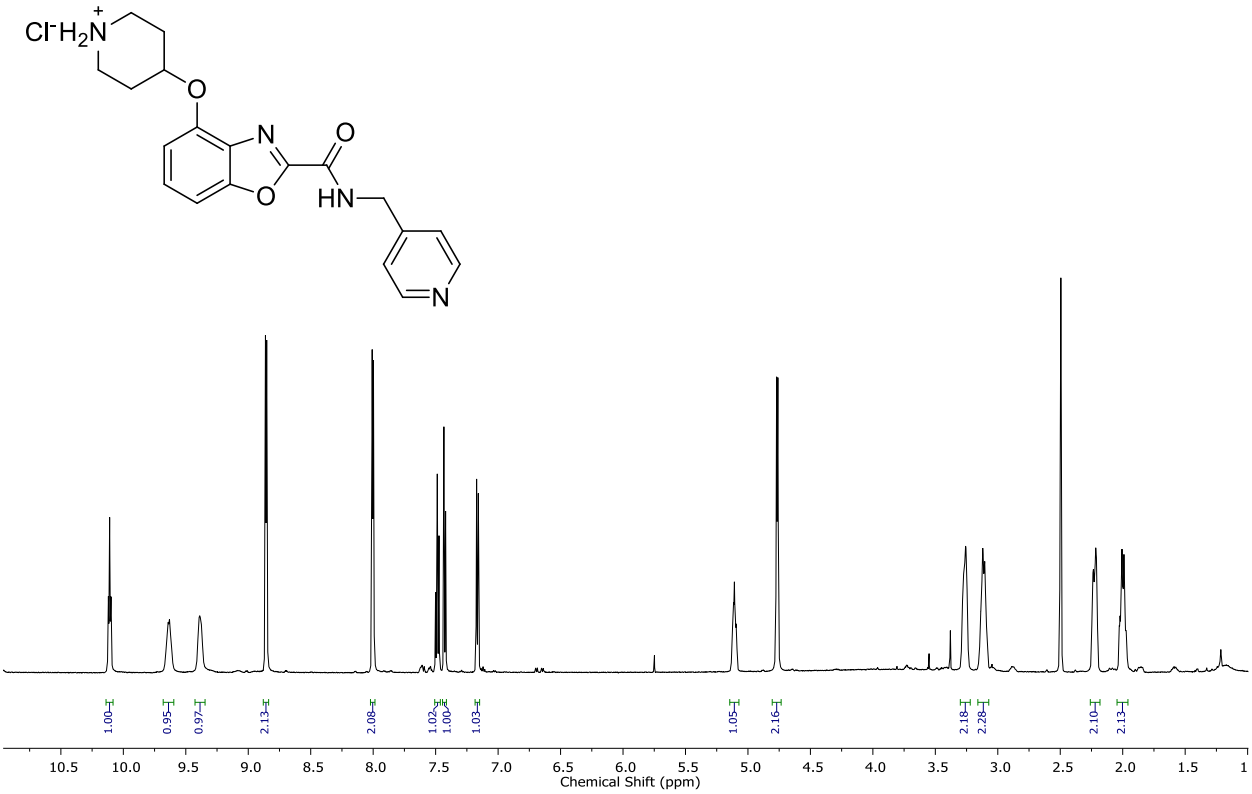

Figure 74: ^{1}H-NMR spectrum of **BO7** in *d*-DMSO

5.9 Conclusion

In this chapter we described the synthesis of benzoxazole derivatives that are analogous to the indoles synthesized in Chapter 2. The initial synthetic route was to follow a similar procedure as that of the synthesis of the 2-carbomethoxy benzimidazole described in Chapter 4 which involved synthesizing the core (4-benzyloxy)benzoxazole heterocycle via trimethylorthoformate, followed by deprotonation of the C2-proton with *n*-BuLi to quench with methyl chloroformate. Regioselective nitration of resorcinol produced 2-nitroresorcinol, which after nitro reduction produced 2-aminoresorcinol, the required starting material for cyclization with trimethylorthoformate to produce 4-hydroxybenzoxazole. This was subsequently benzylated to protect the –OH since the follow up step involved *n*-BuLi. C2-deprotonation followed by the reaction with methyl chloroformate however did not produce the desired 2-carbomethoxy benzoxazole as it was discovered through a literature search that the reactivity of C2-

deprotonated benzoxazoles and benzimidazoles are not the same and that benzoxazoles undergo ring opening upon deprotonation.

A literature search provided methods for the direct synthesis of 2-carboalkoxy benzoxazoles via a cyclodehydration reaction which involved the acylation of 2-aminophenols with ethyl chlorooxoacetate in pyridine, producing the corresponding 2-hydroxyanilide which underwent thermal cyclization. We attempted the reaction with 2-aminoresorcinol and ethyl chlorooxoacetate, and although the reaction was successful, a low yield was obtained. To increase the yield, we attempted and succeeded in synthesizing the desired 4-phenoxy-2-carboethoxy benzoxazole via a one-pot acylation with ethyl chlorooxoacetate followed by an intramolecular cyclodehydration reaction under Mitsunobu conditions. Using DEAD as the Mitsunobu reagent, we managed to produce ethyl 4-hydroxybenzoxazole-2-carboxylate in an 84% yield. A crystal structure was obtained from the product produced by the one-pot acylation/cyclodehydration reaction for absolute confirmation of the product synthesized. The advantage was that no debenzylation reaction was required afterwards. The subsequent Mitsunobu reaction involving the coupling of 1-Boc-4-hydroxypiperidine was firstly carried out with DBAD as the Mitsunobu reagent but due to unavoidable purification issues involving the hydrazine byproduct, a modified Mitsunobu reagent, ADDM, was synthesized due to it being more polar in nature, thus producing the coupled product without any purification issues. The subsequent amidation and transesterification reactions were efficient and high yielding, as amidation and transesterification proceeded at room temperature. The amidated and transesterified products were *N*-Boc deprotected to produce the final compounds **BO1** – **BO7**.

5.10 References

1. Terashima, M.; Ishii, M.; Kanaoka, Y. *Synthesis* **1982**, *1982,* 484.

2. Chen, T. *J. Organomet. Chem.* **2008**, *693,* 3117.

3. Reyes, H.; Beltran, H. I.; Rivera-Becerril, E. *Tetrahedron Lett.* **2011**, *52,* 308.

4. Blacker, A. J.; Farah, M. M.; Hall, M. I.; Marsden, S. P.; Saidi, O.; Williams, J. M. *Org. Lett.* **2009**, *11,* 2039.

5. Boyle, K. E.; MacMillan, K. S.; Ellis, D. A.; Lajiness, J. P.; Robertson, W. M.; Boger, D. L. *Bioorg. Med. Chem. Lett.* **2010**, *20,* 1854.

6. McElhinny, C. J.; Lewin, A. H.; Mascarella, S. W.; Runyon, S.; Brieaddy, L.; Carroll, F. I. *Bioorg. Med. Chem. Lett.* **2012**, *22,* 6661.

7. Bastug, G.; Eviolitte, C.; Markó, I. E. *Org. Lett.* **2012**, *14,* 3502.

8. Cozza, G.; Gianoncelli, A.; Bonvini, P.; Zorzi, E.; Pasquale, R.; Rosolen, A.; Pinna, L. A.; Meggio, F.; Zagotto, G.; Moro, S. *ChemMedChem* **2011**, *6,* 2273.

9. Musser, J. H.; Chakraborty, U.; Bailey, K.; Sciortino, S.; Whyzmuzis, C.; Amin, D.; Sutherland, C. A. *J. Med. Chem.* **1987**, *30,* 62.

10. Fu, L. *Metalation of Azoles and Related Five-Membered Ring Heterocycles;* Anonymous Springer, **2012**, pp 103-154.

11. Musser, J.; Hudec, T.; Bailey, K. *Synth. Commun.* **1984**, *14,* 947.

12. Boyle, K. E.; MacMillan, K. S.; Ellis, D. A.; Lajiness, J. P.; Robertson, W. M.; Boger, D. L. *Bioorg. Med. Chem. Lett.* **2010**, *20,* 1854.

13. Teno, N.; Gohda, K.; Wanaka, K.; Tsuda, Y.; Akagawa, M.; Akiduki, E.; Araki, M.; Masuda, A.; Otsubo, T.; Yamashita, Y. *Bioorg. Med. Chem.* **2015**, *23,* 3696.

14. Wipf, P.; Fritch, P. C. *J. Am. Chem. Soc.* **1996**, *118,* 12358.

15. Yan, Y.; Zhong, Q.; Zhao, N.; Liu, G. *Mol. Divers.* **2012**, *16,* 157.

16. Wang, F.; Hauske, J. R. *Tetrahedron Lett.* **1997**, *38,* 6529.

17. Jiao, P.; Xu, J.; Zhang, Q.; Choi, M. C.; Chan, A. S. *Tetrahedron: Asymmetry* **2001**, *12,* 3081.

18. Mukumoto, F.; Tamaki, H.; Iwakoshi, M.; Kusaka, S. Patent, Publication number: US9119396 B2, **2014**.

19. Lanning, M. E.; Fletcher, S. *Tetrahedron Lett.* 2013, *54,* 4624.

Chapter 6: Synthesis of benzothiophenes

6.1 Introduction

In this chapter we describe the synthesis of substituted benzothiophenes as our final heterocyclic series. As described in Chapters 2 – 5, all the synthesized heterocycles contained an ester at the C2-position and an oxygen atom at the C4-position. (**Figure 75**)

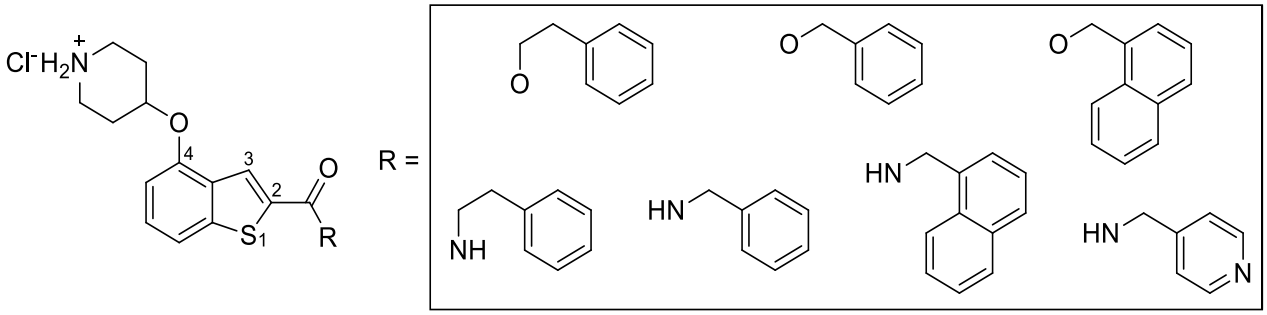

Figure 75: Proposed benzothiophene based compounds with various amides and esters to be synthesized

6.2 Synthesis of the benzothiophene heterocycle

A search of the literature revealed a high yielding synthetic route for the synthesis of substituted and unsubstituted alkyl 2-benzothiophene carboxylates, as illustrated in **Scheme 72**. The thiolation of 2-fluoro, -chloro, -bromo and -nitro substituted benzaldehydes **(148)** with an alkylmercaptoglycolate **(149)** resulted in the *ipso*-nucleophilic substitutionof the 2-substituted halogen or nitro group to produce an aromatic thioether **(150)**.[1,2,3,4]

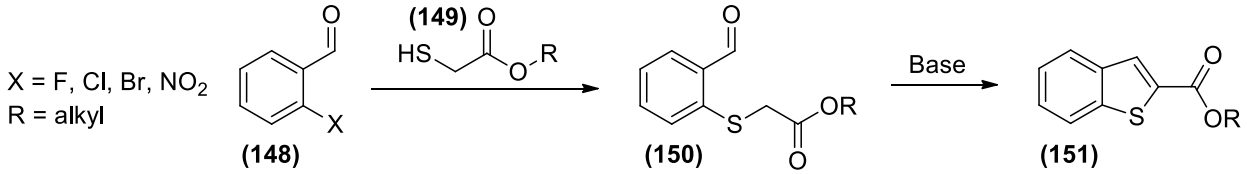

Scheme 72: Nucleophilic aromatic substitution of an alkyl mercaptoglycolate and subsequent base-promoted ring closure to produce benzothiophene **(151)**

Subsequent base promoted condensation of **(150)** resulted in the formation of the desired thiophene **(151)**. The most widely used base and solvent for the condensation respectively is K_2CO_3 and DMF.[1,5,6] As illustrated in **Scheme 73**, the first step involved the formylation of 3-nitrophenol **(152)** by way of the Duff reaction to afford **(160)**, followed by benzyl protection to afford **(161)**. **(160)** was benzyl protected because the subsequent thiolation and condensation step with **(162)** to produce **(163)** was base-mediated.

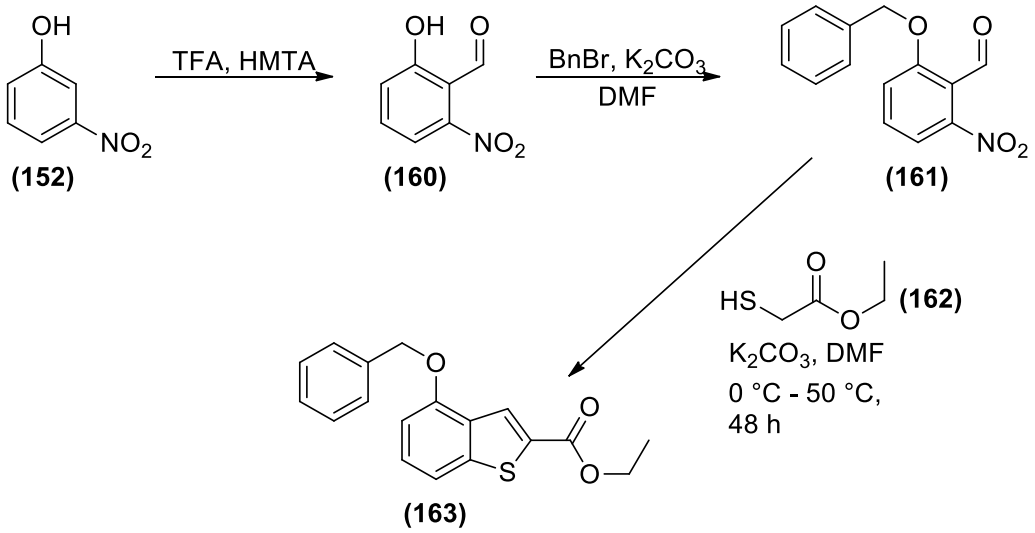

Scheme 73: Synthesis of **(163)** by means of the Duff reaction and benzylation followed by base mediated substitution and condensation

In order for us to synthesize the 4-phenoxy benzothiophene containing an ester at the C2-position, we were required to synthesize a 1,2,3-tri-substituted salicylaldehyde derivative containing either a halogen or a nitro group at the 6-position, *ortho* to the aldehyde. Although 1,2,3-tri-substituted salicylaldehyde derivatives are commercially available they are extremely expensive and as a result we had to synthesize the desired 1,2,3-tri-substituted salicylaldehyde derivative **(160)**.

Normally, the synthesis of these salicylaldehyde derivatives is challenging due to problems associated with regioselectivity, however we came across a method for the synthesis of a 6-halo or 6-nitro salicylaldehyde derivative by way of the Duff reaction starting from 3-nitrophenol **(152)**.[7,8] The Duff reaction is described as a Mannich-type *ortho*-formylation reaction between hexamethylenetetramine (HMTA) and any electron rich aromatic ring system, such as phenolic and aniline derivatives, carried out in strongly acidic conditions at temperatures above 90 °C.[6,9]

Formylation of **(152)** by way of the Duff reaction to produce the desired 1,2,3-trisubstituted salicylaldehyde **(160)** was first carried out in acetic acid as a cheaper alternative to TFA, the acid

most commonly used in the Duff formylation. However, with acetic acid no product was formed. The reaction was then carried out using TFA, proving to be an effective acid catalyst for the formylation step as we were able to synthesize **(160)** in a 29% yield. **Scheme 74** illustrates the proposed mechanism for the formation of **(160)** via the Duff reaction using TFA as the acid catalyst.[10]

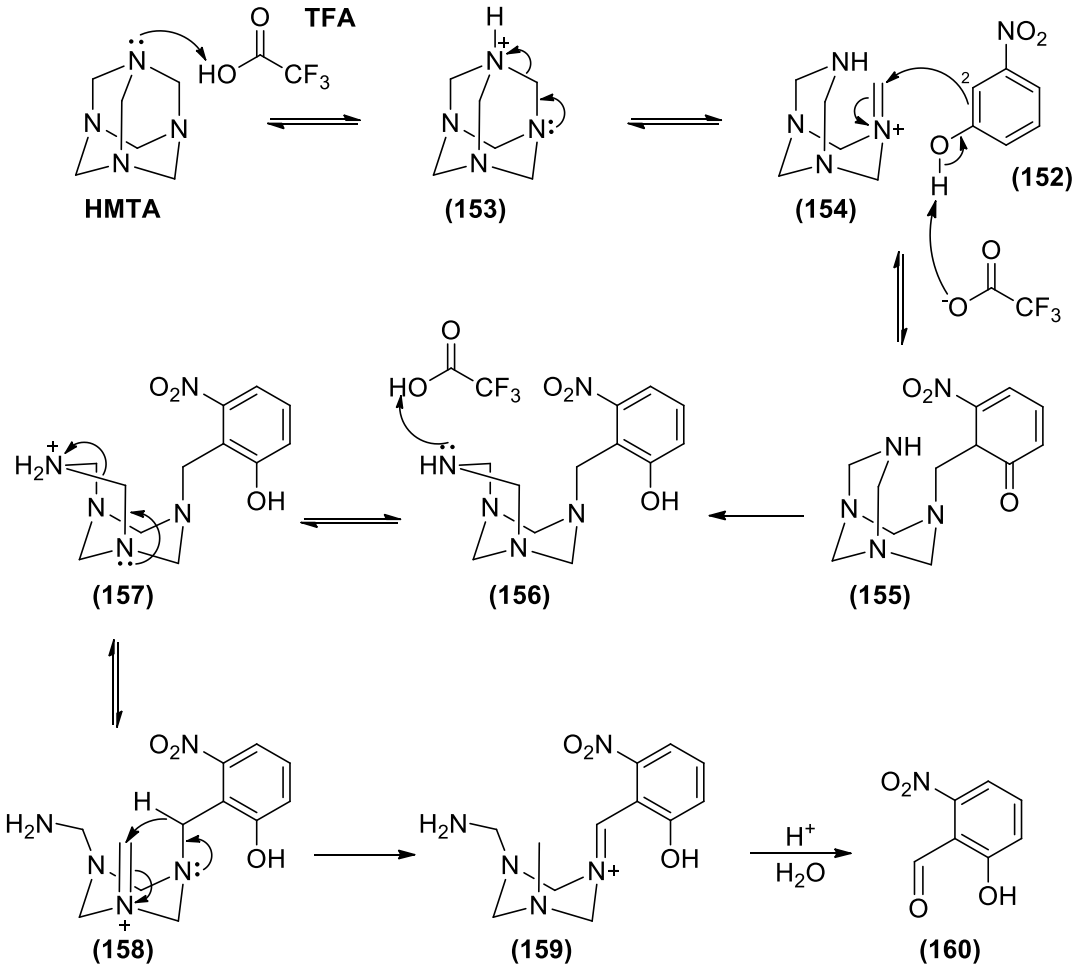

Scheme 74: Proposed mechanism for the formation of **(160)**

The first step involves the protonation of HMTA with TFA to produce the ammonium species **(153)**, followed by the lone pair of electrons of a neighboring amine facilitating iminium formation producing **(154)**. Deprotonation of **(152)** with a trifluoroacetate anion results in a reaction with **(154)** by way of an electrophilic aromatic substitution reaction, producing the ketone **(155)** which subsequently aromatizes to the phenol **(156)**. Protonation of **(156)** with TFA produces the second ammonium species **(157)** which forms the iminium **(158)** in a similar fashion to the formation of **(154)**. A redox reaction ensued to from **(159)**, as the lone pair of electrons of the benzylic amine

facilitates the formation of the benziminium species, made possible by a hydride-shift of a benzylic proton effectively reducing the iminium to the amine. An acid-mediated hydrolysis of **(159)** results in the formation of **(160)**.

The low yield obtained for the synthesis of **(160)** could be explained by considering the C–C bond formation step between **(154)** and **(152)** to form **(155)**. **(154)** is a sizable electrophilic species, and the nucleophilic carbon of **(152)** (annotated as position 2) has two substituents in the *ortho*-position, increasing the steric effect of that position. Thus, the initial approach of both electrophilic and nucleophilic species is unfavorable, affecting the regioselectivity of the reaction and thus resulting in formation of the regioisomer of **(160)** as well. Although we did see the formation of the regioisomer when monitoring the reaction through TLC, we did not isolate the product for full characterization. ^{1}H-NMR spectroscopy confirmed the formation of **(153)**. The aromatic substitution pattern was verified by the presence of two doublet of doublets at 7.55 ppm and 7.33 ppm as well as a doublet of doublets appearing as a triplet at 7.63 ppm. The aldehyde signal appears at 10.32 ppm confirming that the formylation had taken place. **Figure 76** illustrates the ^{1}H-NMR of **(160)** as well as the expanded section of the aromatic region.

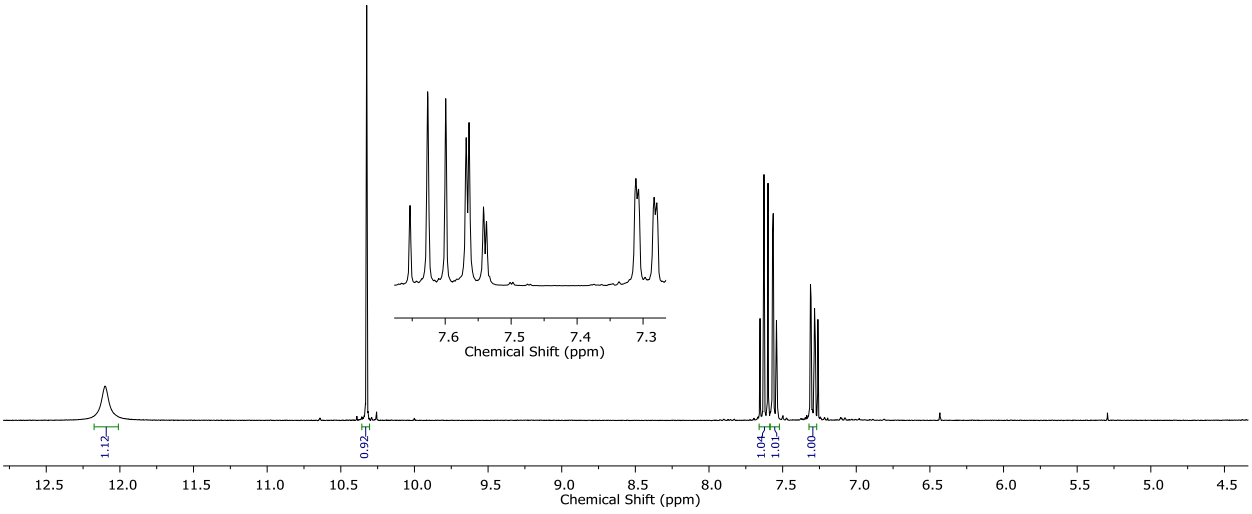

Figure 76: ^{1}H-NMR spectrum of **(160)**

Benzylation of **(160)** with benzyl bromide produced **(161)** in a quantitative yield (**Scheme 73**). With the desired 1,2,3-trisubstituted salicylaldehyde in hand we could carry out the *ipso*-nucleophilic substitution/condensation reaction with ethyl thioglycolate **(162)** to yield the desired benzothiophene **(163)**. We followed the procedure by Kolasa and co-workers[11] for the synthesis of **(163)**. The reaction with ethyl thioglycolate **(162)** and **(161)** in DMF with K_2CO_3 as the base was stirred for 48 hours, after which **(163)** was isolated in a 95% yield after purification. The formation

of **(163)** was confirmed by ^{1}H-, ^{13}C-NMR spectroscopy and HRMS. **Figure 77** illustrates the ^{1}H-NMR spectrum of **(163)**.

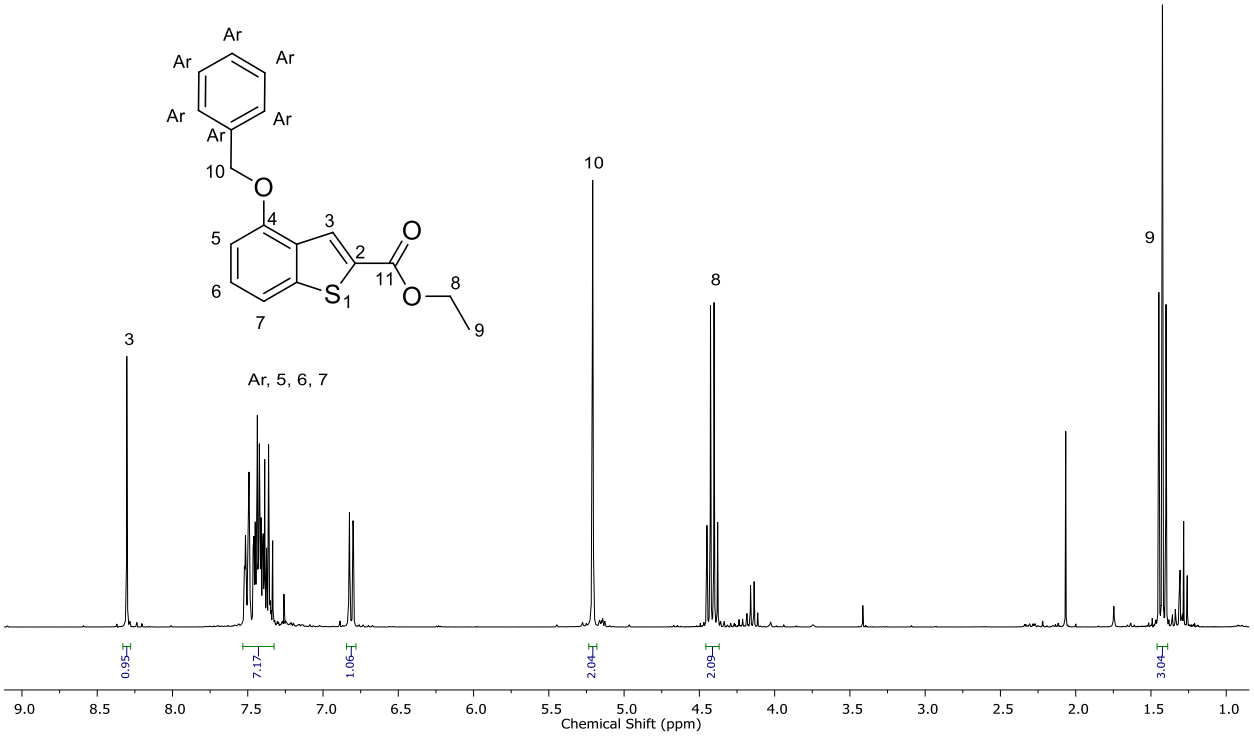

Figure 77:^{1}H-NMR spectrum of **(163)** in $CDCl_3$. An EtOAc impurity is also observed.

Analysis of the ^{1}H-NMR spectrum of **(163)** revealed the presence of a singlet at 8.31 ppm which corresponds to the proton annotated **3** on the benzothiophene ring. The aromatic signals annotated as **3, Ar, 5, 6, 7** integrated for nine protons as expected. The quartet **8** at 4.42 ppm and the triplet **9** at 1.43 ppm are indicative of the desired carboethoxy group at the C2-position.

6.3 Debenzylation and Mitsunobu reaction

With compound **(163)** in hand we could carry out debenzylation to yield the phenolic benzothiophene **(164)** which would enable us to carry out the subsequent Mitsunobu reaction with **(32)** to yield precursor **(165)** (**Scheme 75**).

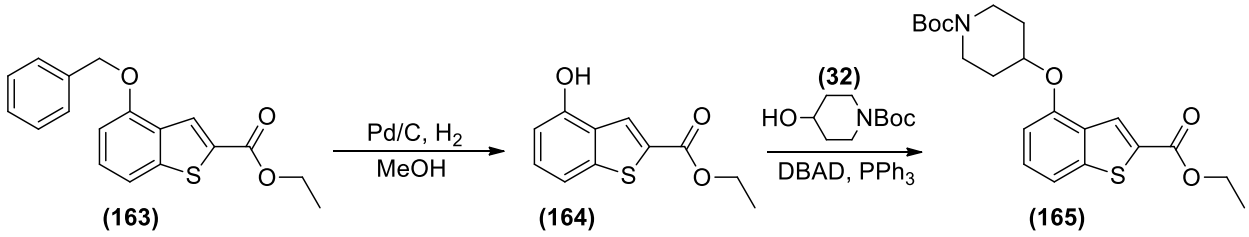

Scheme 75: Debenzylation of **(163)** followed by Mitsunobu coupling to produce **(165)**

Debenzylation with Pd/C and hydrogen afforded **(164)** in a 68% yield. The formation of **(164)** was confirmed by ^{1}H-, ^{13}C-NMR spectroscopy and HRMS. ^{1}H-NMR spectroscopy indicated the absence of the aromatic signals of the benzyl group, and revealed a broad signal at 5.72 ppm, indicative of the phenolic proton of **(164)**. The subsequent Mitsunobu reaction of **(164)** with 1-Boc-4-hydroxypiperidine **(32)** using DBAD and PPh_3 as the Mitsunobu reagents afforded **(165)** in a 99% yield after purification. The synthesis of **(165)** was confirmed by ^{1}H-, ^{13}C-NMR spectroscopy and HRMS. **Figure 78** illustrates the ^{1}H NMR spectrum of **(165)**.

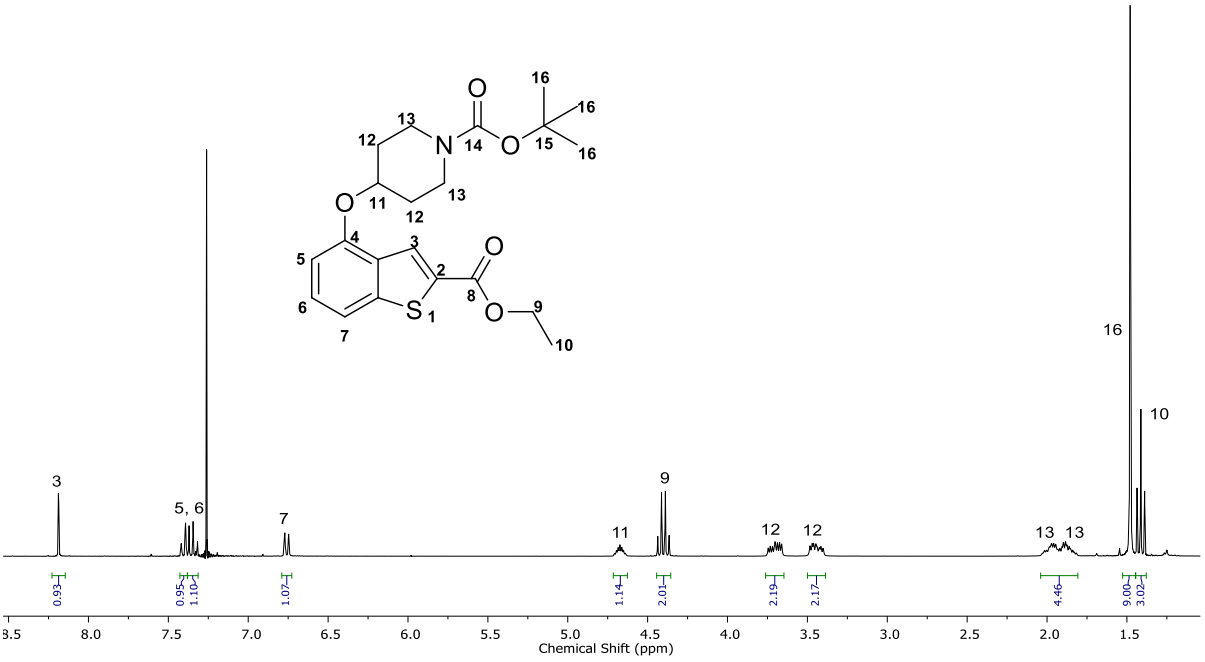

Figure 78: ^{1}H-NMR spectrum of **(165)** in $CDCl_3$

Analysis of the ^{1}H-NMR spectrum of **(165)** revealed the presence of the methine and methylene signals of the *N*-Boc piperidine ring (annotated as **11**, **12** and **13**), in addition to the *tert*-butyl signal **16** at 1.48 ppm.

6.4 Transesterification of (165)

As shown in **Scheme 76,** the transesterification of **(165)** with 2-phenylethanol, benzyl alcohol and 1-naphthylmethanol to yield compounds **(166)** – **(168)** was carried out with 26 equivalents of the respective alcohol and 3 equivalents K_3PO_4 at 70 °C for 12 – 20 hours. Initially we carried out a test reaction between **(165)** and 2-phenylethanol to ascertain what temperature is necessary for transesterification to proceed. After 12 hours of reaction time at room temperature there was no sign of product formation when monitoring the reaction via TLC. The temperature was increased to 45 °C, but no product formation was observed after a day of stirring. Increasing the temperature to 70 °C proved to be a suitable reaction temperature as TLC analysis indicated a full conversion of **(165)** to **(166)**.

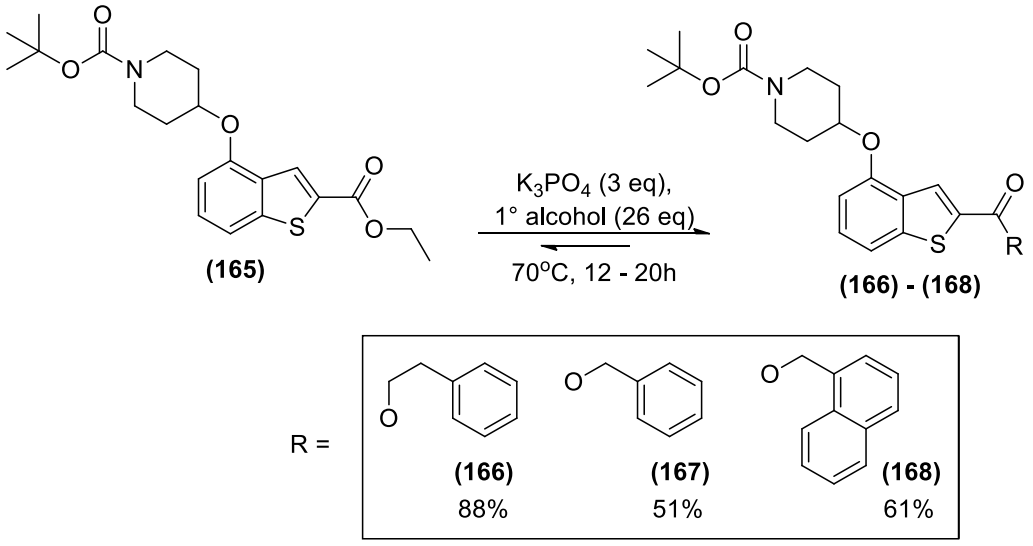

Scheme 76: Transesterification of **(165)** to afford **(166)** – **(168)**

The yields obtained for the transesterification of **(165)** were significantly higher than the yields for the transesterification reactions carried out on the indole, benzimidazole and benzoxazole heterocycles. The successful synthesis of compounds **(166)** – **(168)** was confirmed by ^{1}H-, ^{13}C-NMR spectroscopy and HRMS. The ^{1}H-NMR spectrum of **(167)** is illustrated in **Figure 79**.

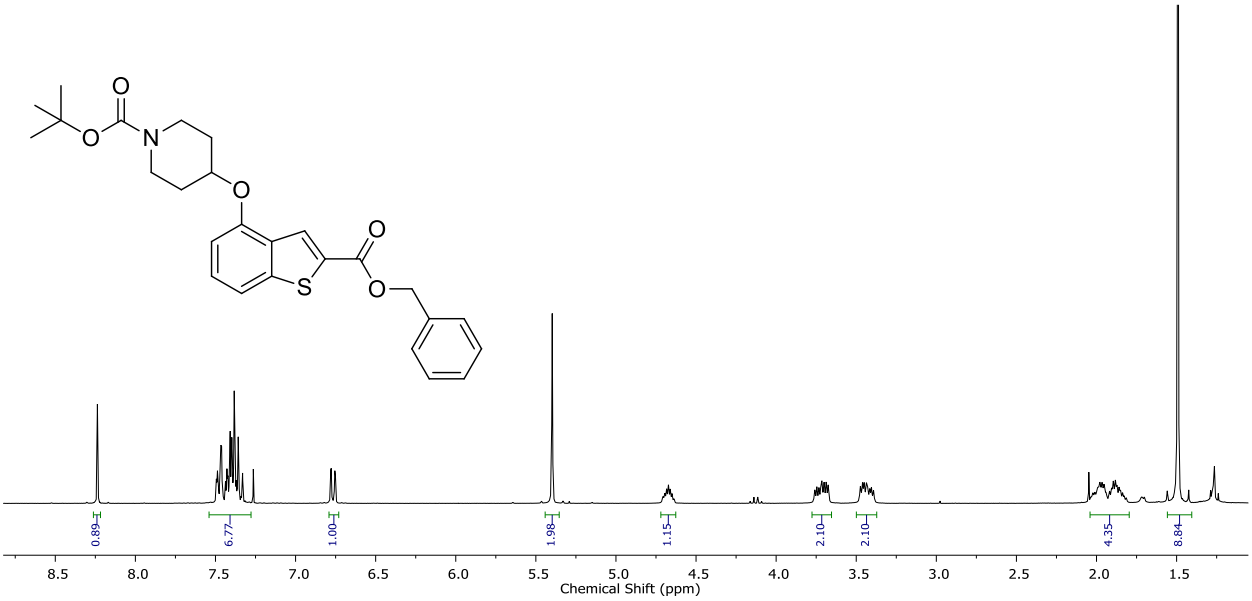

Figure 79: The ^{1}H-NMR spectrum of **(167)** in $CDCl_3$

Analysis of the ^{1}H-NMR spectrum of **(167)** revealed a total of nine protons in the aromatic region which corresponded to the presence of the benzyl and benzothiophene aromatic rings. The absence of a triplet and doublet corresponding to the protons of the ethyl ester of **(165)** and the presence of a methylene signal belonging to the benzylic ester was a clear indication that the ester had been successfully transesterified. The same observations that confirmed the successful transesterification of **(165)** with benzyl alcohol were present in the ^{1}H-NMR spectra of **(166)** and **(168)**.

6.5 Amidation of (165)

Scheme 77 illustrates the amidation of **(165)** with 2-phenylethylamine, benzylamine, 1-naphthylmethylamine and 4-(aminomethyl)pyridine to yield compounds **(169)** – **(172)**. The reaction was carried out using the same procedure for the amidation of **(39)** illustrated in Chapter 2, **Scheme 20.** The amidation reaction of **(165)** with benzylamine was carried out first as a test reaction. Initially the reaction temperature was set to 100 °C and the reaction was stirred overnight.

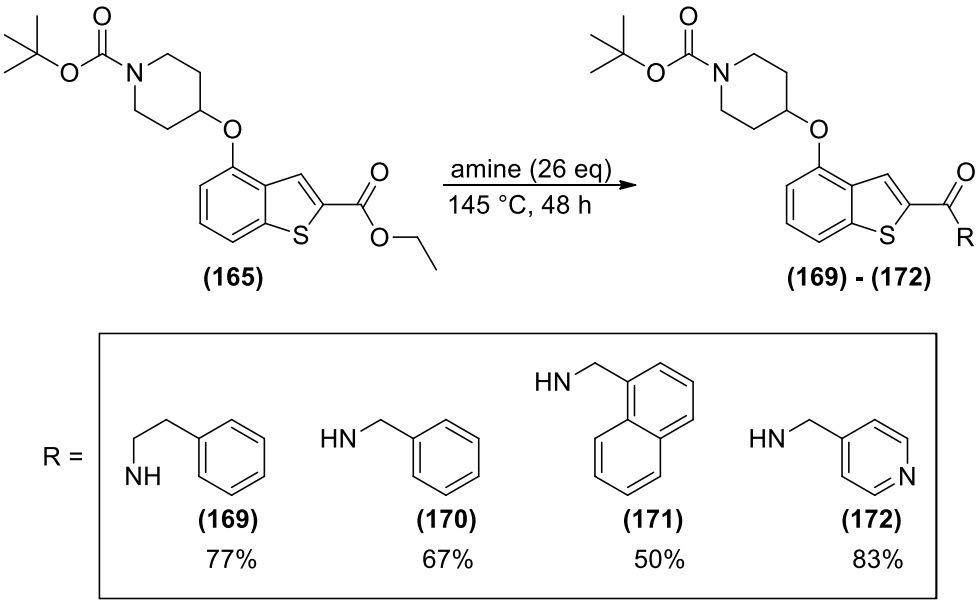

Scheme 77: Amidation of **(165)** to produce **(169) – (172)**

TLC analysis the following day indicated that a small amount of the desired amide **(170)** had formed. The reaction temperature was increased to 145 °C, and the reaction was monitored by TLC. After 48 hours the reaction was stopped and although full consumption of **(165)** had not been observed by means of TLC analysis a moderate yield of 67% of the product was obtained. An incomplete conversion was also observed for the formation of **(171)** which was obtained in a yield of 50%. Interestingly, full consumption of **(165)** was observed for the amidation reactions to produce **(169)** and **(172)**. The products were purified and the formation of **(169) – (172)** was confirmed by ^{1}H-, ^{13}C-NMR spectroscopy and HRMS. **Figure 80** illustrates the ^{1}H-NMR spectrum of **(170)**.

As expected, the signals corresponding to the protons of ethyl ester were not observed in the ^{1}H-NMR spectra of **(169)** – **(172)**, and the appearance of a broad triplet was observed indicative of the amide proton. Analysis of the ^{1}H-NMR spectrum of (**170**) revealed a broad triplet at 6.52 ppm corresponding to the mide proton, as well as the overlapped signals of the benzylic methylene and the methine protons at 4.68 ppm.

In comparison to the transesterification and amidation reactions on the indole scaffolds, it would appear that the electrophilicity of the benzothiophene ester is relatively on par with that of the indole analogue, more electrophilic than that of the 3-methyl indole analogue and less electrophilic than the benzimidazole and benzoxazole analogues.

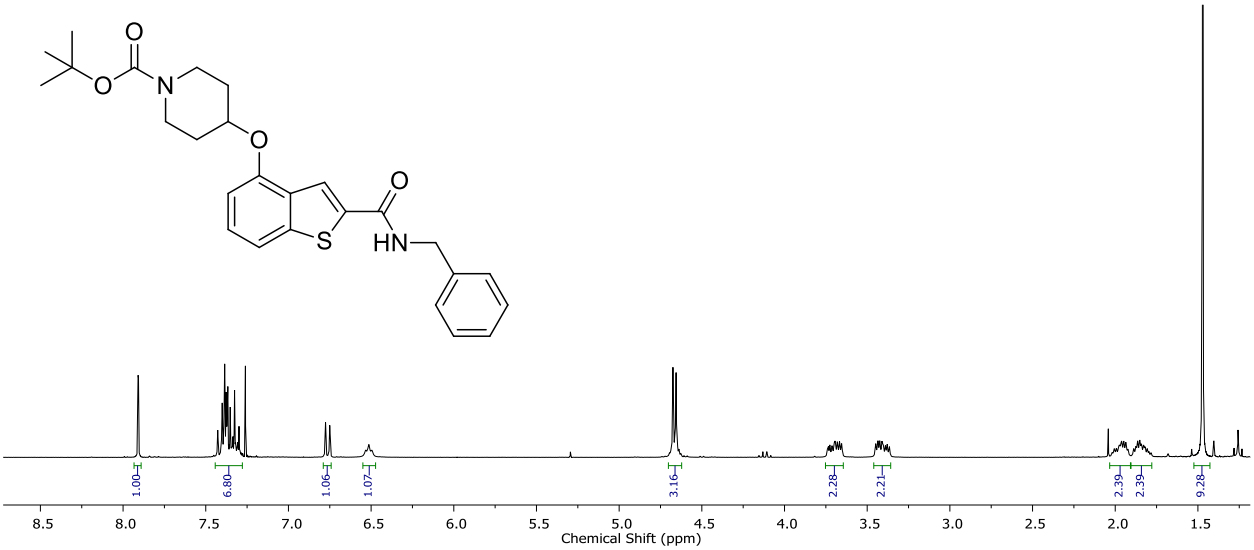

Figure 80: The ^{1}H-NMR spectrum of **(170)** in $CDCl_3$

6.6 Deprotection of the *N*-Boc piperidine ring

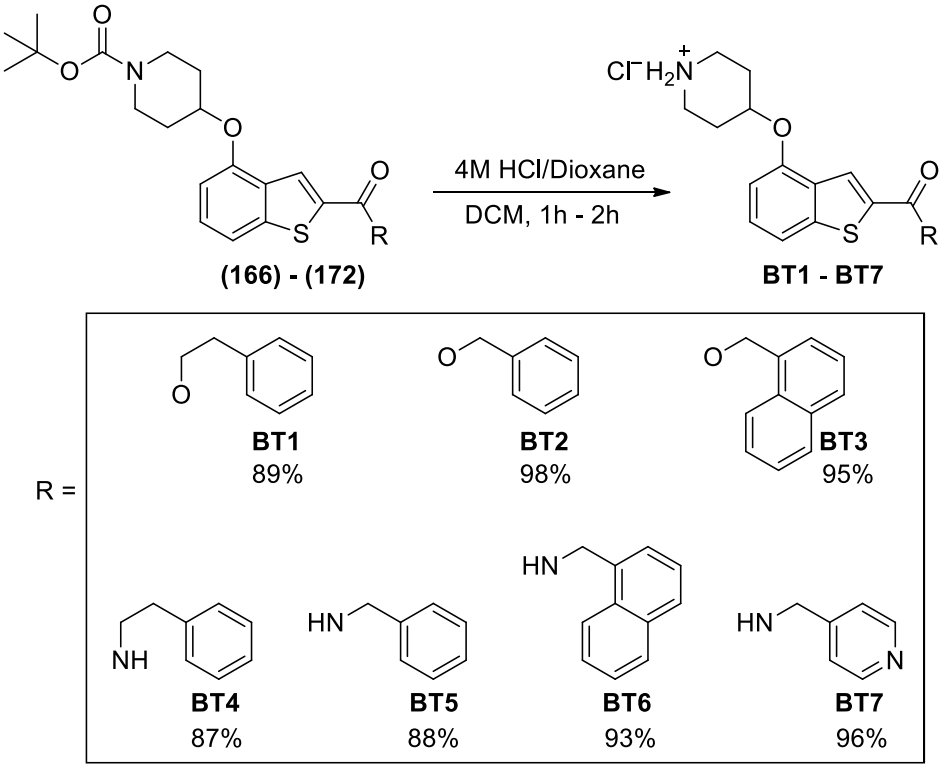

Scheme 78: *N*-Boc deprotection of **(166)** – **(172)** via HCl in dioxane to produce **BT1 – BT7**

The final step in the synthesis of the desired benzothiophene final compounds as shown **Scheme 78** was the N-Boc deprotection of the piperidine ring with 4M HCl and dioxane. The reaction conditions were described in Chapters 2 to 5. The deprotection of compounds **(166) – (172)** was completed in 1 – 2 hours after TLC analysis indicated that no starting material was visible.

The synthesis of compounds **BT1 – BT7** was confirmed by ^{1}H-, ^{13}C-NMR spectroscopy and HRMS. The expected absence of the *tert*-butyl signal and the appearance of the broad signals indicative of the piperidinium chloride salt confirmed that the *N*-Boc deprotection had been successful. **Figure 81** illustrates the ^{1}H-NMR spectrum of **BT2**.

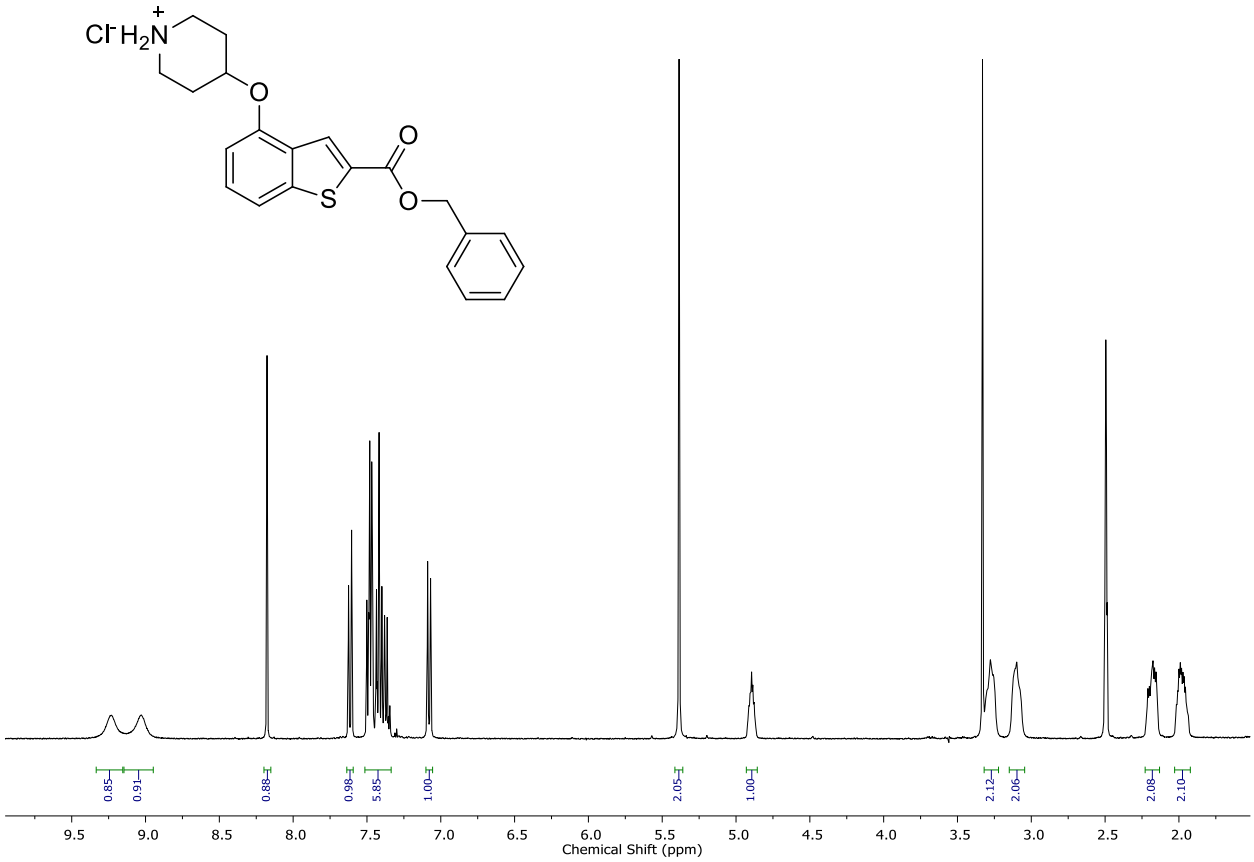

Figure 81: ^{1}H-NMR spectrum of **BT2** in *d*-DMSO. A water impurity is observed at 3.30 ppm.

6.7 Conclusions

This chapter describes the synthesis of benzothiophenes analogous to the indole series of compounds synthesized in Chapter 2. A literature search provided a quick and efficient synthesis of 2-carboalkoxy benzothiophenes via the base promoted *ipso*-nucleophilic substitution reaction of 2-nitrobenzaldehydes with ethyl thioglycolate, followed by a cyclodehydration reaction. Due to the fact that we need an oxygen atom at the C4-position of the heterocycle to couple 1-Boc-4-hydroxypiperidine, we had to synthesize the starting material, 2-hydroxy-6-nitrobenzaldehyde. The Duff reaction facilitated the formylation of 3-nitrophenol to produce the desired minor-product 2-hydroxy-6-nitrobenzaldehyde which was subsequently benzylated. The follow-up base promoted *ipso*-nucleophilic substitution/cyclodehydration reaction produced ethyl 4-(benzyloxy)benzothiophene-2-carboxylate in a 95% yield. Subsequent debenzylation, Mitsunobu coupling with 1-Boc-4-hydroxypiperidine followed by amidation/ transesterification and ultimately *N*-Boc deprotection formed the final compounds **BT1 –BT7**.

6.8 References

1. Lee, S.; Lee, H.; Yi, K. Y.; Lee, B. H.; Yoo, S.; Lee, K.; Cho, N. S. *Bioorg. Med. Chem. Lett.* **2005,** *15,* 2998.

2. Cai, J.; Zhang, S.; Zheng, M.; Wu, X.; Chen, J.; Ji, M. *Bioorg. Med. Chem. Lett.* **2012,** *22,* 806.

3. Zhou, P.; Zhang, Z.; Li, Y.; Chen, X.; Qin, J. *Chem. Mater.* **2014,** *26,* 3495.

4. Beck, J. R. *J. Org. Chem.* **1972,** *37,* 3224.

5. Ji, P.; Xu, X.; Ma, S.; Fan, J.; Zhou, Q.; Mao, X.; Qiao, C. *ACS Med. Chem. Lett.* **2015,** *6,* 1010.

6. Deng, H.; Fang, Y. *ACS Med. Chem. Lett.* **2012,** *3,* 550.

7. Miranda, L. P.; Meutermans, W. D.; Smythe, M. L.; Alewood, P. F. *J. Org. Chem.* **2000,** *65,* 5460.

8. Harayama, T.; Nakatsuka, K.; Nishioka, H.; Murakami, K.; Ohmori, Y.; Takeuchi, Y.; Ishii, H.; Kenmotsu, K. *Heterocycles* **1994,** *38,* 2729.

9. Duff, J.; Bills, E. *J. Chem. Soc. (Resumed)* **1932,** 1987.

10. Wang, Z. In *Comprehensive Organic Name Reactions and Reagents;* John Wiley & Sons, Inc., 2009; Vol. 202, pp 943.

11. Kolasa, T.; Brooks, D. W. *Syn. Commun.* **1993,** *23,* 743.

Chapter 7: Biological results and discussion

7.1 Introduction

In this chapter we evaluate the biological data obtained from the whole cell *P. falciparum* assay carried out on compounds belonging to series **IM**, **IH**, **BO**, **BT** and **BI**. The aim of this chapter is to attempt to rationalize any structure activity relationship between each series, regarding the difference in efficacy related to the varying heterocyclic core, the aromatic substituent and the ester and amide functional group. An explanation of the difference in efficacy between the two heterocycles with a methyl group (**IM** and **BI**) would also be attempted.

Compounds belonging to series **IM** had a methyl group at the C3-position, and the synthesis of series **IM** was the main focus of the project to ascertain if a C3-methyl indole heterocycle has better, similar or worse activity relative to the analogous benzofuran compounds synthesized by Yu *et al*.[1]

An indole series **IH** which does not have a methyl group in the C3-position was also synthesized in order to provide insight into the importance of a methyl in the C3-position.

An isostructural series of the **IM** series, the 1-methyl benzimidazole series **BI** was synthesized to be directly compared to the **IM** series in order to provide insight into which methylated heterocycle exhibits the most potent activity.

A benzothiophene **BT** and benzoxazole **BO** series of compounds were also synthesized to compare their respected efficacy against the **IH** series of compounds.

We did not test these compounds in a PfNMT inhibition assay, since initial efficacy against *P. falciparum* was necessary to ascertain if these compounds indicated any whole-cell inhibition.

7.2 Whole cell testing results

The compounds of series **IM**, **IH**, **BO**, **BT** and **BI** were tested against the chloroquine sensitive (CQS) NF54 strain of *P. falciparum*, and the EC_{50} values corresponding to each compound is summarized in **Table 3**. All the compounds were tested at the Pharmacology Department of the University of Cape Town, with the help of Dr. Dale Taylor and Carmen de Kock.

Table 3: *In vitro* activity of series **IH**, **BT**, **BI**, **BO** and **IM** against *P. falciparum* (NF54)

Series	Compound	NF54 EC_{50} (µM)
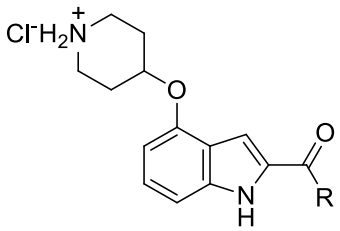	**IH1**	6.5
	IH2	3.4
	IH3	0.83
	IH4	3.1
	IH5	3.7
	IH6	0.90
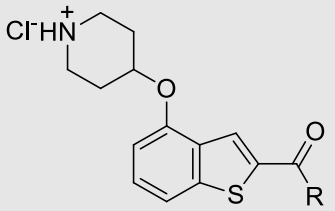	**BT1**	5.9
	BT2	5.7
	BT3	1.9
	BT4	3.0
	BT5	3.5
	BT6	0.71
	BT7	2.7
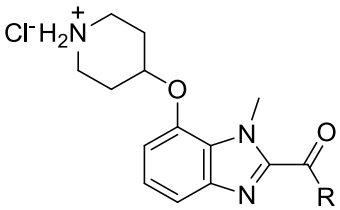	**BI1**	11.0
	BI2	13.3
	BI3	7.4
	BI4	8.7
	BI5	8.8
	BI6	1.2
	BI7	n.a[a]
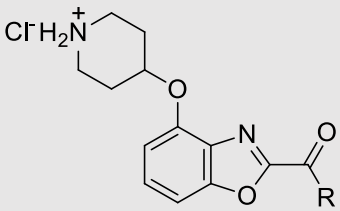	**BO1**	n.a
	BO2	n.a
	BO3	n.a
	BO4	n.a
	BO5	n.a
	BO6	2.0
	BO7	n.a
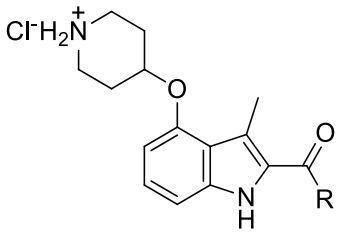	**IM1**	3.9
	IM2	0.56
	IM3	0.74
	IM4	3.4
	IM5	6.1
	IM6	0.74
	IM7	20.0
	Chloroquine	13 nM
	Artesunate	9.4 nM

R = 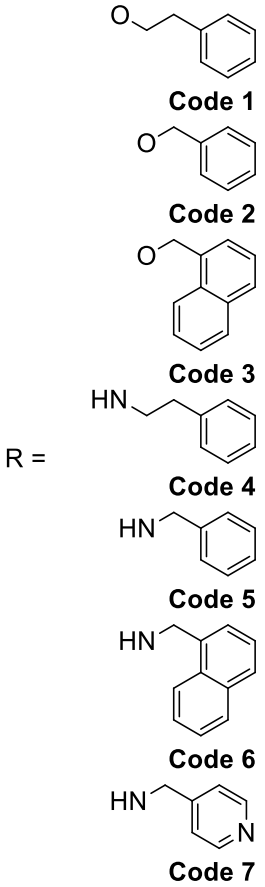

IH7 was not tested, [a]n.a = not active

BO1 – BO5 and **BO7** were not active in inhibiting *P. falciparum* growth, and thus it was clear that the use of a benzoxazole as a heterocyclic core containing a carbonyl in the C2-position and a piperidinium group at the C4-position was ineffectual as *P. falciparum* antiplasmodials. It was however very interesting to note that **BO6** indicated a relatively potent inhibition of 2.0 µM. This superior activity relative to the rest of the compounds of the **BO** series is inexplicable, however, the stability of the ester functional group could be brought into question. During the LC/MS analysis of all the final compounds synthesized, it was discovered that the purity of the aromatic ester benzoxazoles were low due to the formation of another compound that could be seen in the spectrum. Interestingly, in the LC/MS spectra of all three esters the same molecular ion was observed corresponding to the formed byproduct. **Figure 82** illustrates the LC/MS spectrum of **BO3** indicating the two major peaks which corresponds to the product **BO3** with an m/z = 403.2, and the unknown product with an m/z = 277.12. The purity was initially determined to be 26.8%. Due to the fact that we have experimentally observed the highly electrophilic properties of the ethyl ester at the C2-position, and considering that the LC/MS samples were prepared with methanol, we deduced that the aromatic ester did indeed undergo transesterification with methanol to produce the methyl ester, which has an exact mass m/z = 277.12.

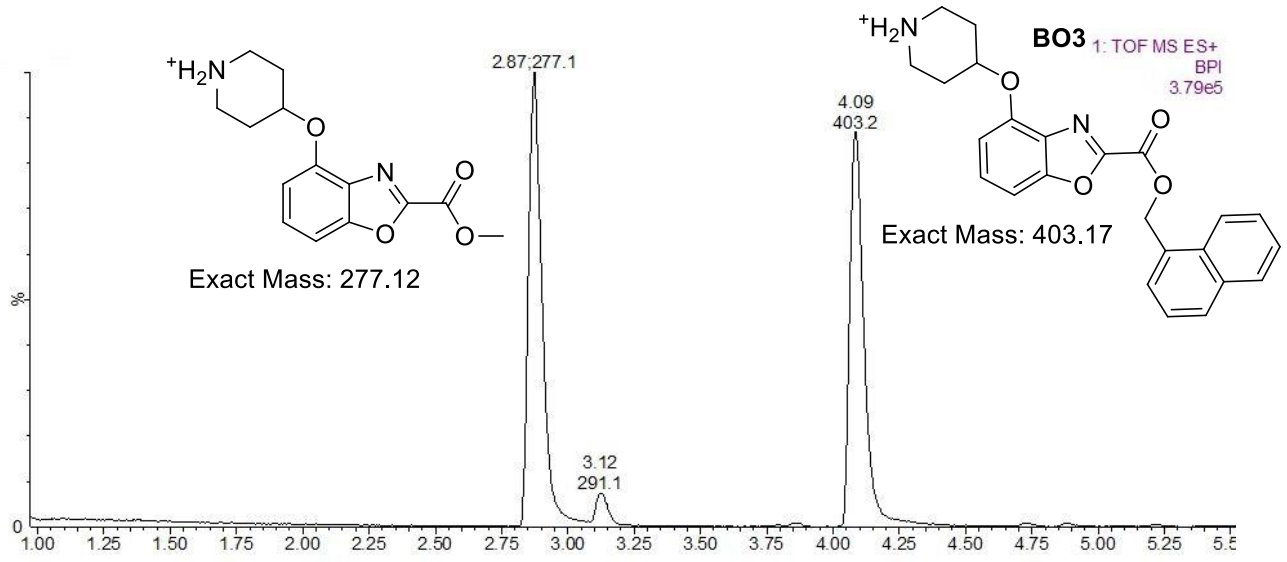

Figure 82: The LC/MS spectrum indicating the two signals observed due to transesterification of **BO3** with methanol

Due to the fact that methanol readily transesterified the aromatic ester at room temperature without the aid of any acid or base catalyst, the same principle could hold if water was hydrolyzing the ester to the corresponding carboxylic acid. This would render the antiplasmodial ineffectual

due to the loss of the aryl ring that was involved in important π – π interactions. This hypothesis however does not explain the inactivity of the benzoxazole amides as the amides would not hydrolyze that readily, especially at physiological temperature. We however did not find any literature sources providing evidence for a similar type of hydrolysis of the amides to explain the efficacy observed.

When we compared the activity of the **IM** series with the **IH** series, no trend could be observed to indicate that one series was more active than the other. **IM1 – IM3** and **IM6** indicated an increased activity relative to the analogous **IH1 – IH3** and **IH6** but **IM4** and **IM5** wad similar activity in comparison to **IH4** and **IH5**. Thus the addition of the methyl at the C3-position in the **IM** series proved to not be as crucial regarding whole-cell activity.

The **BT** series relative to the **IM** series showed an interesting trend. The **BT1** – **BT3** esters were less active than the analogous **IM1 – IM3** esters but the **BT4** – **BT6** amides had comparable activity with the **IM4** – **IM6** amides.

The isostructural **BI** series in relation to the **IM** series proved to be less active, even though they both contained a methyl in the same structural position. The **BI1** – **BI3** esters were significantly less active than the **IM1** – **IM3** esters. The decreased activity of the **BI4** – **BI6** amides relative to the **IM4** – **IM6** amides were minor, except for **IM4** being 2.5 times more active than **BI4**. No significant difference in efficacy was observed between the activity of the esters and the analogous amides in the **IM** and **BI** series respectively. Thus it stands to reason if the methyl group does in fact increase the activity of the ester analogues in comparison to the amides. However, this assumption could only be verified with a PfNMT assay to determine the significance of the methyl group of both **IM** and **BI** compounds.

The **BT** and **IH** series of compounds seems to have similar activities except for the **BT2** and **BT3** vs. **IH2** and **IH3**.

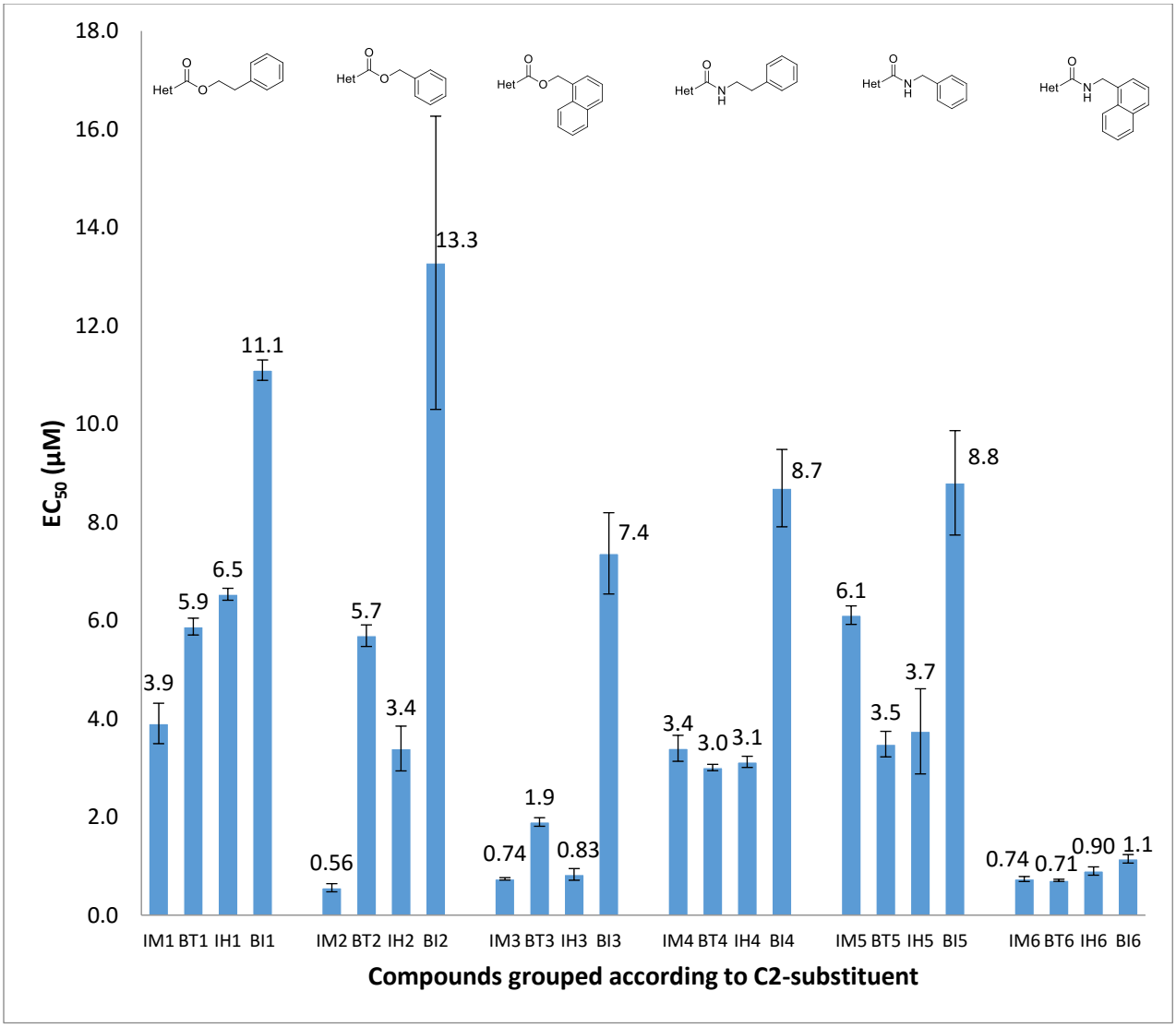

Figure 83: EC_{50} (µM) of compounds grouped according to C2-substituent

The most notable trend is the effect of the aromatic ester and amide substituents on the efficacy of each compound. Compounds containing the naphthylmethyl ester and amide substituent were significantly more effective than the other aromatic ester and amides, (except **BI3**), whereby **BO6** also indicated a low EC_{50} of 2.0 µM. The naphthylmethyl amides **IM6**, **BT6**, **IH6** and **BI6** indicated that a naphthyl methyl amide was in fact the most preferred substituent for high activity, with a narrow range of activities ranging between 0.71 – 1.1 µM, regardless of the heterocycle. The most active compound was **IM2** which exhibited an EC_{50} value of 0.56 µM.

It must be acknowledged here that we ran into a significant problem with respect to evaluating these compounds against PfNMT itself. Obviously this would have been ideal in order to see whether there was any direct correlation between the modeled binding energy, the enzyme inhibition activity and the whole cell inhibition. The only path we could see through this difficulty would have required a significant investment of both time and financial resources. Given that these compounds only show moderate activity and therefore are highly unlikely to make it in their current form into any kind of drug development, the expenditure was deemed too great.

7.3 Conclusions

The whole cell assay results against the CQS *P. falciparum* NF54 line determined that the majority of the compounds, with the exception of the **BO** series and most of the 4-methylpyridine amides, proved to be active in the low micromolar to sub-micromolar range, with activities ranging between 13.3 µM to 0.56 µM. The low efficacy of the pyridine amide substituents could be attributed to the fact that they are protonated, thus the pyridinium salts. This could have an effect on the bioavailability of those compounds as the doubly charged compounds would struggle to cross intercellular membranes.

It should be noted that these results are not directly comparable to the benzofuran analogues developed by Yu *et al.* since the whole cell data they have obtained is from the *P. falciparum* 3D7 line, nonetheless it does appear that we have managed to achieve an improvement in efficacy by an order of magnitude in some cases. None of the benzofuran derivatives synthesized by Yu *et al*. exhibited sub-micromolar activity in the whole cell assay. This suggests that we have managed to make moderate, but significant, gains in efficacy through rational design. The results indicate that our initial rational design of potentially active compounds was justified due to the fact that the compounds did in fact show efficacy against *P. falciparum* (CQS). The incorporation of different heterocycles with the piperidinium group at the C4-position of each heterocycle (C7-position of the benzimidazole) and the introduction of aromatic esters and amides at the C2-position did in fact exhibit similar to better activity than the benzofuran analogues developed by Yu *et al*.

In this thesis we have managed to successfully synthesize four different benzazole series and a benzothiophene series of compounds, with the intention of increasing the activity relative to the already published benzofuran analogues, as well as determining which heterocycle is the most active and which aromatic ester or amide is the most preferable. The **BO** series of compounds

were not active, followed by the **BI** series, followed by the **BT** and **IH** series, leading to the **IM** series being the most active.

7.4 References

1. Yu, Z.; Brannigan, J. A.; Moss, D. K.; Brzozowski, A. M.; Wilkinson, A. J.; Holder, A. A.; Tate, E. W.; Leatherbarrow, R. J. *J. Med. Chem.* **2012,** *55,* 8879.

Chapter 8: ESP calculations to determine electrophilicity

8.1 Introduction

The amidation and transesterification reaction carried out on the five different 2-carboalkoxy-heterocycles proceeded at different temperatures and reaction rates. The amidation and transesterification of the 2-carboethoxy-indole and -3-methyl indole proceeded at temperatures of 100 °C and above for the transesterification and 140 °C and above for the amidation reactions, and lasted between 2 to 3 days. Amidation and transesterification of the 2-carboethoxy-benzothiophene proceeded at a lower temperature for the transesterification reactions (70 °C) but a high temperature for the amidation reaction (145 °C). Both the 2-carbomethoxy-benzimidazole and 2-carboethoxy-benzoxazole heterocycles were significantly more reactive then the indole and benzothiophene analogues as amidation and transesterification proceeded at room temperature. We wanted to explain this trend in reactivity.

Utilizing molecular electrostatic potential (ESP) to identify possible electrophilic sites which exhibit reactivity towards nucleophiles is not as straight forward as identifying nucleophilic sites. The most electrophilic site would indicate a positive ESP energy value, but the positive maxima are located on the nucleus of each atom in the molecule.[1] Since the electrophilic site is the anti-bonding orbital of a functional group e.g. an ester, and is not situated near the nucleus, the problem could be solved by generating ESP values at the surface of the molecule at a set distance. ESP energy values are calculated by introducing a positively charged elementary particle close to the nucleus and calculating the electrostatic potential energies of that particle as it moves away from the nucleus, generating a maximum (close to the nucleus) and minimum (a distance away from the nucleus) ESP energy value. Thus, ESP energy values indicated the charge distribution of atoms in molecules in three dimensions, and thus gives a better indication of where there is a greater electron density i.e. a potential nucleophilic site. This is indicated by a negative ESP energy value (favorable due to the positively charged elementary particle), and where there is a deficiency of electron density, thus giving rise to a positive ESP energy value which in turn indicate the sites that are most susceptible to nucleophilic attack.

In order to quantify the electrophilicity of each ester, we envisioned generating ESP maps of each heterocycle, which would in turn also provide us with energy values of each atom, particularly the energy values of the carbonyl group of the ester on each of the different heterocycles. The

differences in these energy values would potentially give us a rationale for the trend in the reactivity seen experimentally. We have observed that the reactivity increases as follows:

3-methyl indole< indole <benzothiophene< benzimidazole ≈ benzoxazole

An interesting aspect of these 2-carboalkoxy-4-methoxy (7-methoxy for benzimidazole) heterocycles are the two different resonance structures that can be illustrated for each one (except that 1-methyl benzimidazole has only one resonance structure) which results in the formation of the same alkoxy-enolate resonance structure at the C2-position. This could explain the low reactivity of the indole and the benzothiophene esters but this does not explain the increased electrophilicity of the benzoxazole and benzimidazole ester groups. **Figure 84** illustrates the resonance structures of each of the five heterocycles.

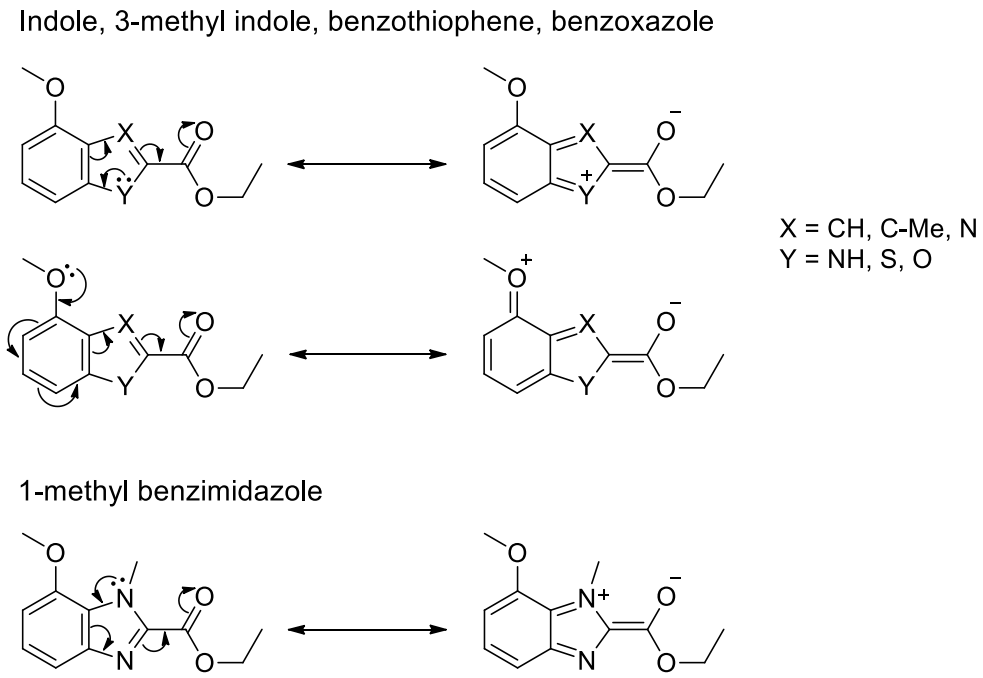

Figure 84: Resonance structures of the five heterocycles

8.2 Method for ESP calculations

The computational work was carried out by fellow research students Sunel de Kock and Bernard Dippenaar who works at the physical chemistry department at the University of Stellenbosch, supervised by Prof. Catherine Esterhuysen.

The first step was to geometrically optimize the heterocycles by using the program Gaussian, specifically Gaussian 09 revision D.01,[2] and to generate the wave function file that would be used in the subsequent step. The ESP properties of each heterocycle wascalculated using the AIMAII software package,[3] which by default calculated the ESP at an electron density of 0.001 e/bohr^3.This parameter was used for the calculation of the ESP properties, and was also used in the mapping of the function to an isosurface to generate the desired ESP maps. The ranges of the colour scales were kept constant in order to be able to directly compare the ESP properties of each heterocycle. All the quantum chemical calculations were carried out using density functional theory (DFT) with the B3LYP functional and Def2-TZVP as the basis set. Within the theory of AIM (Atoms in Molecules), electron density is partitioned into individual atomic basins. With AIMAII it is possible to assign portions of the isosurface to individual atoms. We can therefore determine the maximum, minimum and average electrostatic potential of each atom.

Initially the ESP calculations of each *N*-Boc piperidine coupled heterocycle was attempted but due to the high number of degrees of freedom inherent to the piperidine ring, calculations were computationally expensive and time consuming. It is reasonable to assume that replacing the *N*-Boc piperidine ring by a methyl group would have little to no effect on the relative reactivity of the ester groups, thus we decided to reduce the molecular size of the five different heterocycles by making this substitution in order to shorten calculation times, as seen in **Figure 85**.

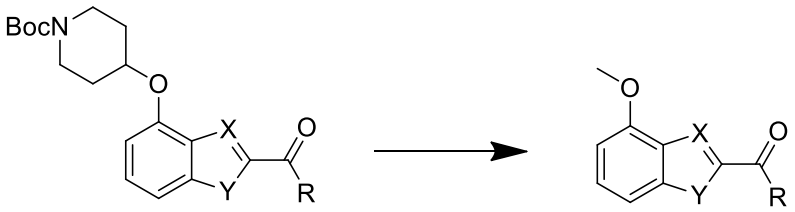

X = CH, C-Me, N-Me, N
Y = N, NH, S, O
R = OEt, OMe

Figure 85: Exchange of *N*-Boc piperidine ring with a methyl group

8.3 ESP maps of the five simplified heterocycles

Below are the ESP maps generated for the five different heterocycles alongside the corresponding molecular structure. (**Figure 86**). Red indicates a negative ESP energy value and blue a positive ESP energy value.

4-OMe IM

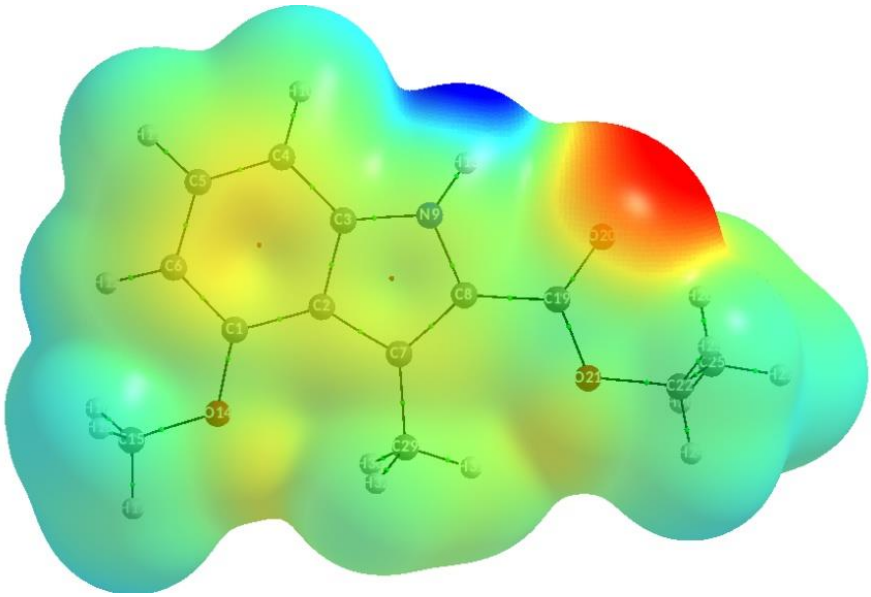

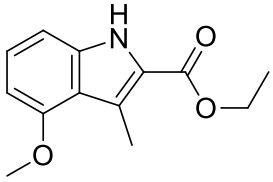

4-OMe IH

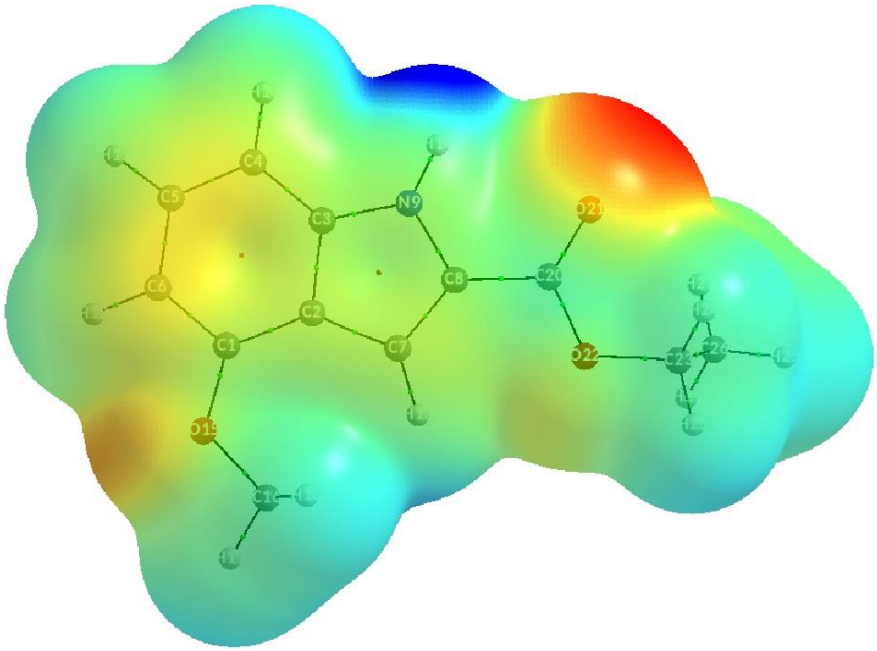

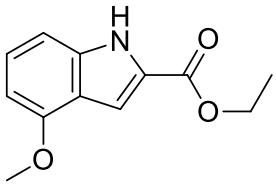

4-OMe BT

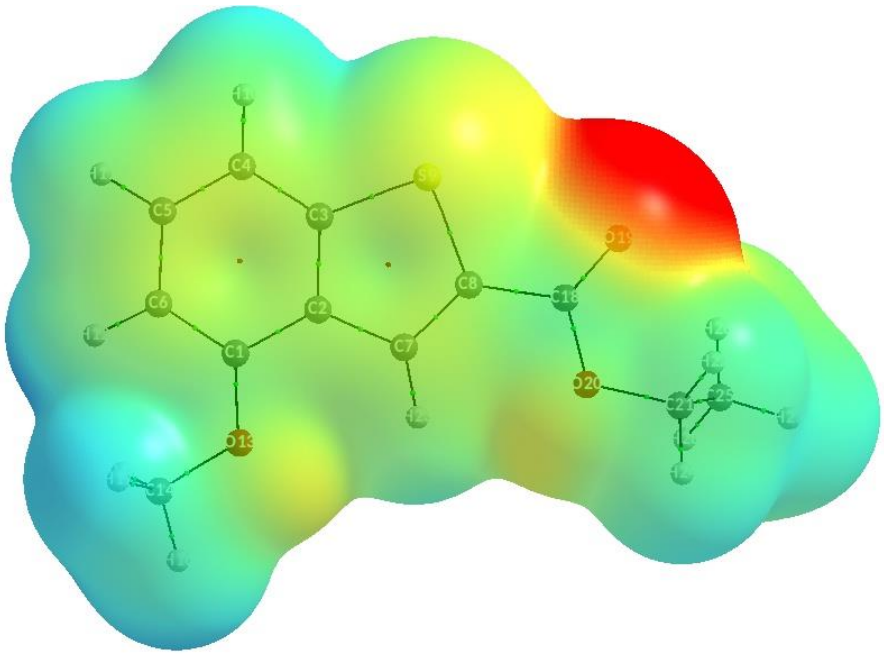

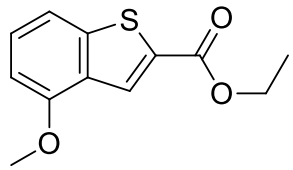

7-OMe BI

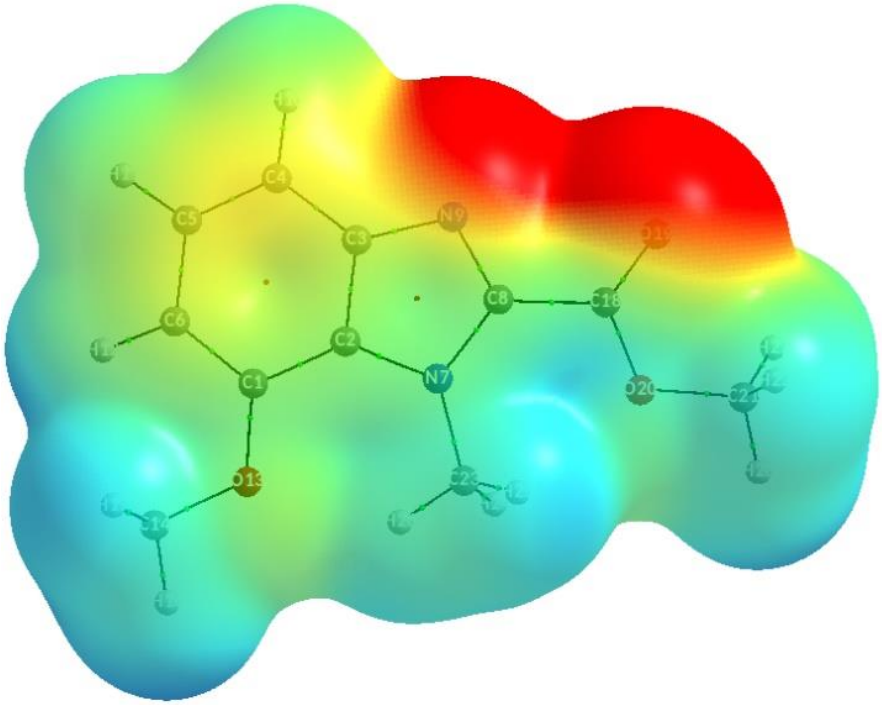

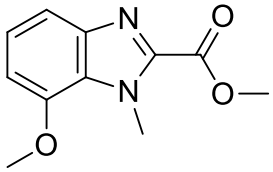

4-OMe BO

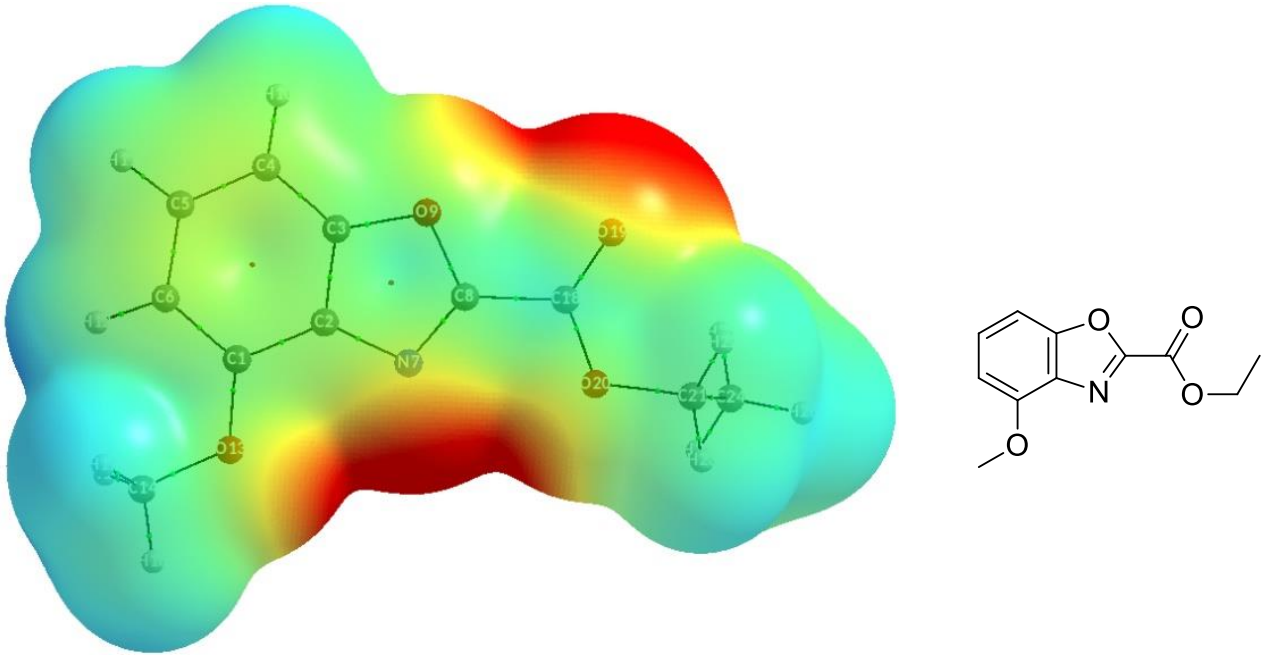

Figure 86: Generated ESP maps of the five heterocycles with a methoxy substituent

Table 4: ESP energy values for the carbonyl carbon and oxygen atoms for the C2-ester of each heterocycle.

ESP Carbonyl carbon (Hartree)	Maximum	Minimum	Average	Average (kcal/mol)
4-OMe IM	0.0069	-0.0117	0.0004	0.26
4-OMe IH	0.0122	-0.0093	0.0062	3.89
4-OMe BT	0.0082	-0.0127	0.0018	1.12
7-OMe BI	0.0270	-0.0276	0.0098	6.16
4-OMe BO	0.0177	-0.0185	0.0114	7.17
ESP Carbonyl oxygen (Hartree)	**Maximum**	**Minimum**	**Average**	**Average (kcal/mol)**
4-OMe IM	0.0026	-0.0528	-0.0331	-20.75
4-OMe IH	0.0075	-0.0494	-0.0289	-18.14
4-OMe BT	0.0023	-0.0597	-0.0408	-25.61
7-OMe BI	0.0117	-0.0838	-0.0467	-29.31
4-OMe BO	0.0097	-0.0592	-0.0376	-23.60

The ESP energy values obtained that corresponded with the carbonyl carbon and oxygen atoms of the ester were obtained in Hartree energy units, and the average energy values were converted to kcal/mol. **Table 4** illustrates the values obtained from the ESP calculations.

Analysis of the data indicates that the carbonyl carbon of **4-OMe IM** has the lowest positive ESP value of 0.26 kcal/mol and the oxygen atom has the second highest negative ESP value of -20.75 kcal/mol. The benzothiophene carbonyl carbon has the second most positive value at 1.12 kcal/mol but has an increased negative energy value for the oxygen atom at -25.61 kcal/mol. When comparing the low yields obtained for the amidation of the 2-carboethoxy-3-methyl indole versus the 2-carboethoxy-benzothiophene it is clear that the low electrophilicity of the **4-OMe IM** ester group could be attributed to the lowest ESP value obtained for the carbonyl carbon, hence there is a greater electron density at that specific carbon which in turn would result in a lowering of the electrophilicity of the carbonyl carbon.

The difference between the **4-OMe IM** and **4-OMe IH** is the 3-methyl group, which has a positive inductive effect into the indole heterocycle. This in turn would increase the electron density of the indole and subsequently on the ester group, decreasing the electrophilicity. The ESP energy value for the C3-carbon of both indoles, annotated C7 in the ESP maps, is -5.61 kcal/mol for **4-OMe IH** and -9.77 kcal/mol for **4-OMe IM**, providing evidence that the methyl increases electron density at the C3-carbon and would subsequently have an electronic effect on the pyrrole ring of **4-OMe IM**. Though both indole ester groups indicated a relatively low electrophilicity experimentally, the 2-carboethoxy-3-methyl indole was still less reactive. This was noted as after the same reaction times and conditions, the 2-carboethoxy-3-methyl indole consistently gave lower yields than the 2-carboethoxy-indole analogue. The ESP energy value for the **4-OMe IH** carbonyl carbon is 3.89 kcal/mol, which is 3.63 kcal/mol more than the **4-OMe IM** carbonyl carbon. However, **4-OMe IH** has a higher ESP energy value for the oxygen atom at -18.14 kcal/mol which could explain the lower reactivity of the ester 2-carboethoxy-indole versus the 2-carboethoxy-benzothiophene.

The ESP energy values of **7-OMe BI** and **4-OMe BO** are in correspondence with the experimental data (when considering the amidation reactions) whereby the carbon and oxygen ESP energy values of **7-OMe BI** are 6.16 and -29.31 kcal/mol, and the analogous ESP energy values for **4-OMe BO** are 7.17 and -23.60 kcal/mol. These are the two highest ESP energy values for the carbonyl carbon in comparison to the other three heterocycles, and the oxygen atom values are the lowest and third lowest of the five different heterocycles. This data is in agreement with the experimentally obtained results for the amidation reactions.

With all of the data in hand then, the experimentally observed sequence of C2-ester electrophilicity should be modified slightly as follows:

3-methyl indole < indole ≤ benzothiophene < benzimidazole ≤ benzoxazole

8.4 Conclusions

We set out to investigate whether there is a quantifiable method to determine electrophilicity of the ester groups at the C2-position of each heterocycle. Experimentally we observed that each heterocycle has an effect on the electrophilicity of the C2-ester group, as both indoles and the benzothiophene esters were less electrophilic than the benzimidazole and benzoxazole esters. The ESP energy values of each atom in each heterocycle were calculated, giving us the ability to observe the ESP energy values of the carbon and oxygen atoms in the carbonyl group of each ester. The values are comparable to the experimentally obtained yields when considering the amidation reactions for each heterocycle. The least electrophilic ester was that connected to the 3-methyl indole system, as the ESP energy value for the carbonyl carbon was the least positive, and the carbonyl oxygen was the second highest negative value. A difference between the ESP energy values of the carbonyl atoms between the indole and 3-methyl indole was observed when compared. This indicated that the presence of the methyl group at the C3-position has a significant effect on the electronics of the indole heterocycle, and this in turn is the explanation as to why the ester group is so unreactive. The benzothiophene had the second lowest ESP energy value at the carbonyl carbon but the second lowest ESP energy value for the carbonyl oxygen, thus introducing a new variable to be considered. A clear relationship between electrophilicity of the carbonyl carbon and reactivity cannot be established unambiguously. As expected, the benzoxazole and benzimidazole esters had the highest positive ESP energy values at the carbonyl carbon and the lowest and third lowest ESP energy vales for the oxygen atom. This is computational proof that electrophilicity of the benzoxazole and benzimidazole esters are in fact increased relative to the indoles and benzothiophene esters.

Several insights can be drawn from this. Firstly, that the determination of electrophilicity of these heterocycles is possible within a reasonable computational time frame. In some cases reasonable simplifications to the molecular complexity should be made in order to reduce the number of degrees of freedom, but care should be taken to avoid making simplifications which would significantly influence the electron distribution over the key area under study. Secondly, that the

computational results do, in fact, correlate remarkably well with the experimentally observed results. Thirdly, as is highlighted with the benzothiophene, occasionally the computational results can highlight a new variable which may not be immediately obvious from the usual organic chemists' arrow pushing approach.

8.5 References

1. Sjoberg, P.; Politzer, P. *J. Phys. Chem.* **1990,** *94,* 3959.

2. Frisch, M. J.; Trucks, G. W.; Schlegel, H. B.; Scuseria, G. E.; Robb, M. A.; Cheeseman, J. R.; Scalmani, G.; Barone, V.; Mennucci, G.; Petersson, A.; Nakatsuji, H.; Caricato, M.; Li, X.; Hratchian, H. P.; Izmaylov, A. F.; Bloino, J.; Zheng, G.; Sonnenberg, J. L.; Hada, M.; Ehara, M.; Toyota, K.; Fukuda, R.; Hasegawa, J.; Ishida, M.; Nakajima, T.; Honda, Y.; Kitao, O.; Nakai, H.; Vreven, T.; Jr., J. A. M.; Peralta, J. E.; Ogliaro, F.; Bearpark, M.; Heyd, J. J.; Brothers, E.; Kudin, K. N.; Staroverov, V. N.; Keith, T.; Kobayashi, R.; Normand, J.; Raghavachari, K.; Rendell, A.; Burant, J. C.; Iyengar, S. S.; Tomasi, J.; Cossi, M.; Rega, N.; Millam, J. M.; Klene, M.; Knox, J. E.; Cross, J. B.; Bakken, V.; Adamo, C.; Jaramillo, J.; Gomperts, R.; Stratmann, R. E.; Yazyev, O.; Austin, A. J.; Cammi, R.; Pomelli, C.; Ochterski, J. W.; Martin, R. L.; Morokuma, K.; Zakrzewski, V. G.; Voth, G. A.; Salvador, P.; Dannenberg, J. J.; Dapprich, S.; Daniels, A. D.; Farkas, O.; Foresman, J. B.; Ortiz, J. V.; Cioslowski, J.; Fox, D. J. Gaussian, Inc.: Wallingford CT **2013**.

3. AIMAll (Version 15.05.18), Todd A. Keith, TK Gristmill Software, Overland Park KS, USA, 2016 (aim.tkgristmill.com)

Chapter 9

9.1 Conclusions

This thesis describes the process of choosing PfNMT as an enzymatic target which is necessary for the viability of *Plasmodium falciparum*. This thesis also discusses the mode of action of an existing antiplasmodial series of benzofuran compounds that are efficient inhibitors of PfNMT, and ultimately describes the synthesis of five novel heterocyclic series of compounds that have isostructural similarities to the benzofuran series.

The heterocycles chosen to replace the benzofuran scaffold were indole, 3-methyl indole, 1-methyl benzimidazole, benzoxazole and benzothiophene. From a synthetic point of view, the first challenge of this project was to determine an efficient and effective route to synthesize each heterocycle with the appropriate substituents. That is to say that the heterocycle contained an ester group at the C2-position and a derivatizable oxygen atom at the C4-position (C7-position for the benzimidazole). The second challenge was the incorporation of a methyl group at the C3-position as it was deemed desirable to ascertain the difference in activity of the 3-methyl indole ester and amide analogues, as well as observe any change in activity when comparing the efficacy of compounds of the other heterocyclic series that are structurally analogous to the 3-methyl indole series.

The synthesis of the indole scaffold was effective as it allowed for the direct incorporation of an ester at the C2-position and an oxygen atom at the C4-position via the Knoevenagel condensation Hemetsberger indolization reaction sequence, providing the main indole scaffold in moderate yields. The advantage of the Knoevenagel condensation reaction was that the reaction conditions were mild and that apart from the additive, trifluoroethyl acetate, the starting materials are relatively cheap, easy to come by and the reaction could easily be scaled up. Most of the experimental derivatization reactions were carried out on the indole scaffold to develop the most favourable conditions needed to, firstly, carry out the Mitsunobu reaction of 1-Boc-4-hydroxypiperidine and, secondly, afford transesterification and amidation reactions of the ethyl ester at the C2-position. We discovered that the Mitsunobu reaction occurs flawlessly, but due to the purification issues encountered we changed the R_f value of the coupled product by introducing a Boc group at the indole nitrogen. The follow-up steps involved finding a suitable method for amidation and transesterification. The use of K_3PO_4 as the base and using the aromatic alcohol involved in the transesterification reaction as solvent was deemed the most efficient route for

transesterification. The transesterification reaction did proceed at elevated temperatures due to the low electrophilicity of the indole ester. Amidation was also achieved, albeit at a much higher temperature than transesterification, with the addition of DBU as a proton scavenger. The yields of the esterification and amidation reactions were moderate due to the unreactive nature of the indole ester. Boc deprotection afforded compounds **IH1** – **IH7**.

Synthesis of the 3-methyl indole scaffold was problematic at first as we followed three different synthetic routes before we finally found a suitable and effective method for direct regioselective methylation. The Vilsmeier-Haack formylation reaction followed by the Mozingo reduction was successful in introducing a methyl group, but regioselectivity was problematic as the C7-position on the indole scaffold was preferred.

In order to synthesize the 3-methyl indole scaffold we attempted the ligand-free copper-catalyzed coupling of ethyl isocyanoacetate to 1-(2-bromo-6-(methoxymethoxy)phenyl) -ethanone, but we were unsuccessful as we did not manage to synthesize 1-(2-bromo-6-(methoxymethoxy)phenyl)ethanone, the required bromo acetophenone for the cyclization reaction.

We attempted to utilize the Larock heteroannulation reaction which would also have enabled us to assemble the indole heterocycle with a methyl group incorporated at the C3-position, but the final heteroannulation reaction of the synthesized 2-iodo aniline derivatives with but-2-yn-1-ol proved to be unsuccessful.

Our fortune changed when we discovered literature indicating the regioselective C-3 bromination of indoles that had a similar functional group substitution pattern. Further literature searches indicated that methylation of aryl bromides was possible using a Suzuki-coupling with trimethylboroxine. The bromination was successful and regioselective, and methylation was achieved in relatively high yields. We managed to Boc-protect the 3-methyl indole, debenzylate and couple 1-Boc-4-hydroxypiperidine via the Mitsunobu reaction. Transesterification or amidation reactions were successful but afforded us the desired products in low yields. It would appear that the additional methyl group lowered the reactivity of the ester significantly in comparison to the C3-unsubstituted indole. The final compounds **IM1** – **IM7** were successfully synthesized upon Boc deprotection.

The synthesis of the 1-methyl benzimidazole scaffold was relatively straight forward, whereby subsequent benzylation, methylation and nitro reduction with iron and acetic acid afforded the desired substituted *N*-methyl phenylenediamine, which upon cyclization with trimethyl orthoformate provided the 1-methyl benzimidazole scaffold in relatively high yield. Initially, a

methoxy group was used as protecting group, due to the fact that we used Pd/C with hydrogen to reduce the nitro group and could not use benzyl groups as protecting groups. Various literature procedures suggested that demethylation was quite feasible. However, we did not succeed in the demethylation step and subsequently changed the methyl protecting group to the benzyl group.

C2-functionalisation was initially difficult as carboalkoxylation was never achieved by way of deprotonation of the C2-proton followed by the addition of an alkyl chloroformate as the electrophile. Formylation was achieved by means of deprotonation of the C2-proton followed by quenching with DMF to produce the aldehyde. Direct conversion of the aldehyde to a methyl ester was achieved by way of an oxidative esterification reaction using I_2, KOH and methanol as reagents, affording the esterified product in a high yield. Subsequent debenzylation, Mitsunobu coupling, amidation or transesterification and Boc deprotection afforded the final compounds **BI1** – **BI7**.

The synthesis of the (2-benzyloxy)benzoxazole scaffold was achieved via the same cyclization reaction as that of the 1-methyl benzimidazole, whereby 2-aminoresorcinol was synthesized, ring closed and benzylated. Carbomethoxylation at the C2-position using *n*-BuLi followed by the addition of methyl chloroformate was unsuccessful as the benzoxazole undergoes a ring opening reaction when deprotonated. We followed other procedures that involve cyclodehydration of 2-aminoresorcinol with methyl 2,2,2-trimethoxyacetate and ethyl chlorooxoacetate, but only the reaction with ethyl chlorooxoacetate afforded the desired 2-carboethoxy-4-hydroxy benzoxazole, although in a low yield.

Utilizing Mitsunobu coupling conditions however proved to be very effective in the synthesis of benzoxazoles. A one-pot acylation of 2-aminoresorcinol with ethyl chlorooxoacetate followed by the addition of DEAD and PPh_3 proved to be an efficient route to synthesize the desired 2-carboethoxy-4-hydroxy benzoxazole in a high yield. The subsequent steps involved the Mitsunobu coupling of 1-Boc-4-hydroxypiperidine with the Mitsunobu reagent ADDM, amidation or transesterification, and ultimately Boc-deprotection to afford the benzoxazole final compounds **BO1** – **BO7**.

The benzothiophene heterocycle was synthesized in a quick and high yielding manner. The *ipso*-nucleophilic substitution of *o*-nitrobenzaldehydes has been studied extensively in literature. We synthesized the required 2-hydroxy-6-nitrobenzaldehyde via a Duff reaction using HMTA, followed by benzyl protection, then a base mediated substitution/dehydration reaction with ethyl thioglycolate to afford the desired benzothiophene. The procedure to produce the final compounds **BT1** – **BT7** from this step is the same as for the previous 4 heterocyclic series.

It was observed that amidation or transesterification reactions involving the indole, 3-methyl indole and benzothiophene C2-ester occurred at elevated temperatures relative to the reactions occurring at ambient temperature when carried out on the benzoxazole and benzimidazole C2-ester. Through computational studies generating ESP energy values, we could derive a theoretical trend in reactivity which represents the experimentally observed tend in reactivity. It was observed that the trend in reactivity follows:

3-methyl indole < indole ≤ benzothiophene < benzimidazole ≤ benzoxazole

The compounds were sent in for biological assessment against chloroquine sensitive *P. falciparum* NF54 strain in a wholce cell assay. Most of the compounds showed moderate activity in the low micromolar to submicromolar range. This achieved an improvement in efficacy of up to an order of magnitude compared to the benzofuran molecules which were the inspiration for this project. All but one of the benzoxazole series of compounds were considered inactive, while the 3-methyl indole series was considered the most active in this assay. The efficacy of the indole and benzothiophene compounds was comparable, and the benzimidazole compounds were the least active. In general the compounds containing a naphthyl group exhibited the best activity.

Overall, useful insight has been developed with respect to the synthesis and reactivity of these series of heterocycles. Exploration into the use of computational methods at two different levels has provided important information. Firstly, the use of molecular docking studies into the active site of PvNMT provided a working hypothesis for the development of the series of compounds. This proved valuable, although somewhat limited. As the benzoxazoles clearly illustrate, a good calculated binding energy will not result in an active compound if there is a chemical reactivity problem with the scaffold. Secondly, on a much more refined level, molecular modelling gave a good indicator of potential reactivity which correlated well with experimental findings. In addition to the important experience and insight gained into the synthesis of these five heterocyclic systems, moderate gains in antiplasmodial efficacy were also achieved.

9.2 Future work

In light of the compounds only showing moderate improvement to the benzofuran analogues on which they were based, it could be feasible to synthesize different aromatic ester and amide substituents containing substituted and unsubstituted quinolines and isoquinolines, since the compounds containing a naphthyl group were the most efficacious. Research into derivatizing the C3-position of the benzothiophene is also a possible step in the right direction, as the 3-methyl indoles were the most efficacious, but the benzothiophene analogues were slightly less active.

From a synthetic perspective, the cyclodehydration reaction under Mitsunobu conditions producing the benzoxazole heterocycle is a versatile tool. Employing this procedure to the synthesis of benzimidazoles could prove to be a worthwhile avenue of exploration as it would eliminate the multi-step synthesis of 2-carboalkoxy benzimidazoles. Furthermore, it could potentially give a far greater range of substitution at the C3-position than is currently available.

Chapter 10: Supporting information

10.1 General information regarding to synthesis and characterization

All chemicals used were bought from Merck, Fluka and Aldrich. Tetrahydrofuran (THF) and diethylether (Et_2O) were dried over sodium wire/sand and distilled under nitrogen with benzophenone as an indicator. Dichloromethane (DCM) was distilled over calcium hydride under nitrogen. Other solvents e.g. ethyl acetate, hexane and tri-ethylamine were purified according to standard procedures.[1] The molarity of *n*-BuLi was determined using a method as described in the literature.[2] Reactions requiring anhydrous conditions were performed under nitrogen or argon atmosphere. All ^{1}H and ^{13}C nuclear magnetic resonance spectra were obtained using a 300 MHz Varian VNMRS (75 MHz for ^{13}C), a 400 MHz Varian Unity Inova (100 MHz for ^{13}C) and a 600MHz Varain Unity Inova (150 MHz for ^{13}C). *d*-Chloroform was used as standard solvent. Variable temperature NMR spectroscopy was carried out on a 400 MHz Varian Unity Inova (100 MHz for ^{13}C) using DMSO-*d6* as solvent. Chemical shifts (δ) were recorded using residual chloroform peaks at δ 7.26 in ^{1}H NMR and δ 77.0 in ^{13}C NMR, and residual DMSO peaks at δ 2.50 in ^{1}H NMR and δ 39.51 in ^{13}C NMR. All chemical shifts are reported in ppm and coupling constants, *J*, are given in Hertz (Hz). All spectra were obtained at 25 °C. All NMR spectroscopy and mass spectrometry was performed by the CAF (Central Analytical Facility) Institute at Stellenbosch University. Infrared spectra were obtained using a Nexus Thermo-Nicolet FT-IR using the ATR. LC-MS purity data were obtained at CAF using a Waters Synapt G2 instrument, ESI positive, using a diode array as detection method. Compounds were detected at a wavelength of 280 nm. All chromatography was performed using either (or a combination of) ethyl acetate, methanol, ethanol, triethylamine, acetone and dichloromethane. Thin layer chromatography (TLC) was carried out on aluminium backed Merck silica gel 60 F254 plates. Visualization was achieved with a UV lamp, iodine vapour or by spraying with a Cerium Ammonium Molybdate solution (CAM) or a ninhydrin solution and then heating. All column chromatography was carried out with Merck silica gel 60 (particle size 0.040-0.063 mm).

10.2 Synthesis of compounds pertaining to Chapter 2

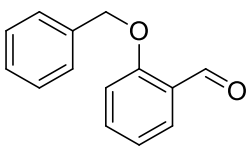

(7) 2-(benzyloxy)benzaldehyde

To a solution of salicylaldehyde (7.71g, 63.2 mmol), Na_2CO_3 (9.38g, 88.5 mmol) in DMF (50 mL) was added 10.5 mL (88.5 mmol) benzyl bromide dropwise at 0°C under an atmosphere of nitrogen. The mixture was stirred at room temperature for 2 hours, where the initial yellow solution turned milky white. The reaction was monitored until complete consumption of starting material was observed on TLC. The mixture was diluted with EtOAc (150 mL) and washed with water (4 x 50 mL), and then washed with brine. The organic phase was dried over $MgSO_4$, filtered and reduced *in vacuo*. The product was crystallized with EtOAc:hexane to provide the product as a white solid. 11.8 g, 88% yield; ^{1}H NMR (400 MHz, CHLOROFORM-*d*) *δ* ppm 5.21 (s, 2 H), 7.07 (d, *J*=8.2 Hz, 2 H), 7.34 – 7.48 (m, 5 H), 7.1 – 7.58 (m, 1 H), 7.88 (dd, *J*=8.0, 1.8 Hz, 1 H), 10.58 (s, 1 H); HRMS–ESI+: m/z $[M+H]^+$ calculated for $C_{14}H_{13}O_2$: 213.0916; found: 213.0920. Characterization data corresponded with literature values.[3, 4]

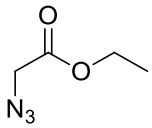

(19) Ethyl 2-azidoacetate

To a mixture of acetone (75 mL) and water (25 mL) was added sodium azide (8.1 g, 124.3 mmol) and ethyl 2-chloroacetate (7 mL, 65.4 mmol) and stirred overnight at room temperature. The heterogeneous mixture was diluted with water (70 mL) and washed with EtOAc (3 x 30 mL). The organic fractions were combined, dried over $MgSO_4$ and the solvent removed *in vacuo* to afford a light yellow liquid. 7.21 g, 85% yield; ^{1}H NMR (400 MHz, CHLOROFORM-*d*) *δ* ppm 1.26 (t, *J*=7.0 Hz, 3 H), 3.81 (s, 2 H), 4.20 (q, *J*=7.0 Hz, 2 H); HRMS–ESI+: m/z $[M+H]^+$ calculated for $C_4H_8N_3O_2$: 130.0572; found: 130.0512. Characterization data corresponded with literature values.[5]

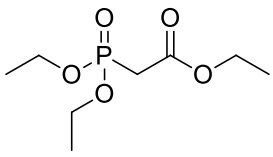

(4) Ethyl 2-(diethoxyphosphoryl)acetate

Ethyl chloroacetate (20.0 mL, 187 mmol) and triethyl phosphite (32.0 mL, 187 mmol) were added in a 100 mL flask, fitted with a condenser and heated to 120 °C for 3 hours, and then at 170 °C overnight under an atmosphere of nitrogen. The

product was purified by distilling off the starting materials at 80 °C under vacuum, leaving the product behind. 14.6 g, 35% yield. ^{1}H NMR (400 MHz, CHLOROFORM-*d*) δ ppm 1.26 (t, *J*=7.0 Hz, 3 H), 1.32 (t, *J*=7.0 Hz, 6 H), 2.86 (d, *J*=21.6 Hz, 2 H), 4.10 – 4.21 (m, 6 H); ^{31}P NMR (162 MHz, CHLOROFORM-*d*, H_3PO_4 reference) *δ* ppm 20.67 (s, 1 P); HRMS–ESI+: m/z $[M+H]^+$ calculated for $C_8H_{18}O_5P$: 225.0892; found: 225.0883; Characterization data corresponded with literature values.[6]

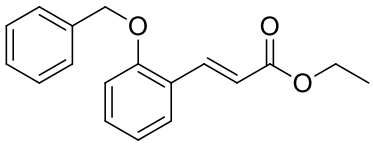

(12) (*E*)-Ethyl 3-(2-(benzyloxy)phenyl)acrylate

To a suspension of NaH (104 mg, 60% dispersion in oil, 2.59 mmol) in THF (13 mL) was added ethyl 2-(diethoxyphosphoryl) acetate **(4)** (581 mg, 2.59 mmol) dropwise at 0 °C under an atmosphere of nitrogen. The mixture was allowed to stir for 1 hour at room temperature, to which a solution of **(7)** (500 mg, 2.34 mmol, dissolved in 2 mL THF) was added at 0 °C. The reaction was stirred overnight, after which the reaction was quenched with aqueous $NaHCO_3$ (10 mL). The product was extracted with EtOAc (2 x 40 mL). The organic fractions were combined and washed with brine, dried over $MgSO_4$, and the solvent reduced *in vacuo*. The product was purified by column chromatography over silica gel (15% EtOAc, 85% hexane) to afford a colourless liquid that solidified to a white solid. 489 mg, 74% yield. R_f: 0.47 (10% EtOAc, 90% hexane). The product has the same R_f value on TLC as the starting material. ^{1}H NMR (400 MHz, CHLOROFORM-*d*) *δ* ppm 1.35 (t, *J*=7.0 Hz, 3 H), 4.27 (q, *J*=7.0 Hz, 2 H), 5.19 (s, 2 H), 6.56 (d, *J*=16.2 Hz, 1 H), 6.94 – 7.01 (m, 2 H), 7.28 – 7.48 (m, 6 H), 7.56 (dd, *J*=7.8, 1.6 Hz, 1 H), 8.12 (d, *J*=16.2 Hz, 1 H); ^{13}C NMR (101 MHz, CHLOROFORM-*d*) *δ* ppm 14.3, 60.3, 70.3, 112.7, 118.8, 121.0, 123.9, 127.1 (2 C), 127.9, 128.6 (2 C), 128.7, 131.3, 136.6, 139.8, 157.3, 167.4; HRMS–ESI+: m/z $[M+H]^+$ calculated for $C_{18}H_{19}O_3$: 283.1334; found: 283.1338. Characterization data corresponded with literature values.[7]

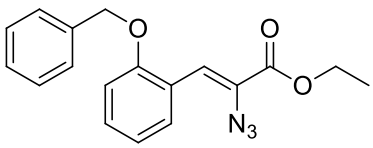

(18) (*Z*)-Ethyl 2-azido-3-(2-(benzyloxy)phenyl)acrylate

<u>Method 1:</u>

To EtOH (60 mL, freshly distilled from Mg/I_2) was added 1.30 g sodium metal (divided in small pieces) under an atmosphere of nitrogen. While stirring, the temperature was kept below 30 °C until the complete dissolution of the sodium metal. 2-(Benzyloxy)benzaldehyde **(7)** (6.00 g, 28.3 mmol) was added to the solution and ethyl trifluoroacetate (6.7 mL, 56.5 mmol) was added via a syringe. The solution was cooled to

-10 °C, and ethyl azidoacetate **(19)** (7.00 g, 56.5 mmol) was added dropwise over a period of 5 minutes. The yellow heterogeneous solution started to become more turbid during the addition of the ethyl azidoacetate. The reaction was stirred at -10 °C for 2 hours while the heterogeneous solution becomes slurry like. The precipitate was filtered with the aid of a vacuum pump and dried under vacuum to afford the desired compound in analytically pure form. 5.03 g, 55% yield.

Method 2:

To a deoxygenated mixture of DMF (5 mL), NaN_3 (173 mg, 2.66 mmol) and (*E*)-Ethyl 3-(2-(benzyloxy)phenyl)acrylate **(12)** (500 mg, 1.77 mmol) was added a pre-dissolved deoxygenated solution of ceric ammonium nitrate (2.43 g, 4.43 mmol, dissolved in 5 mL DMF) dropwise at 0 °C under an atmosphere of nitrogen. The mixture was left to stir overnight at room temperature. The intermediate product was extracted with DCM (50 mL) and washed with water (4 x 50 mL), brine and dried over $MgSO_4$. The solvent was reduced *in vacuo* and dissolved in acetone (4 mL) to which anhydrous sodium acetate was added. The mixture was stirred at room temperature for 6 hours, after which the sodium acetate was filtered off, the solvent reduced and the product purified by column chromatography over silica gel (15% EtOAc, 85% hexane) to afford the product as a white solid. 127 mg, 22% yield.

^{1}H NMR (300 MHz, CHLOROFORM-*d*) δ ppm 1.39 (t, *J*=7.1 Hz, 3 H), 4.36 (q, *J*=7.1 Hz, 2 H), 5.15 (s, 2 H), 6.96 (d, *J*=8.4 Hz, 1 H), 7.03 (t, *J*=7.3 Hz, 1 H), 7.28 – 7.49 (m, 6 H), 7.54 (s, 1 H), 8.24 (dd, *J*=7.8, 1.6 Hz, 1 H); ^{13}C NMR (101 MHz, CHLOROFORM-*d*) δ ppm 14.4, 62.3, 70.6, 112.5, 119.6, 121.0, 122.9, 125.5, 127.1 (2 C), 128.1, 128.8 (2 C), 130.8, 130.9, 137.0, 157.0, 164.0; HRMS–ESI+: m/z $[M+H]^+$ calculated for $C_{18}H_{18}N_3O_3$: 324.1303; found: 324.1348. IR ATR (cm^{-1}): 2118, 1684, 1485, 1242. Characterization data corresponded with literature values.[8]

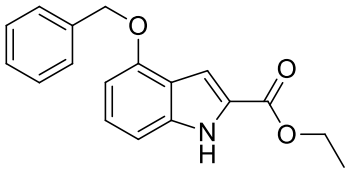

(24) Ethyl 4-(benzyloxy)-1H-indole-2-carboxylate

1,3-dichlorobenzene (7 mL) was heated to 160 °C to which **(18)** (700 mg, dissolved in 1 mL 1,3-dichlorobenzene) was added dropwise under an atmosphere of nitrogen. The slow addition of **(18)** resulted in the evolution of gas from the heated solution. The reaction mixture was stirred for an additional 5 minutes and cooled to room temperature, where the desired product crystallized out of solution. The product was filtered off, and the remaining product dissolved in the mother liquor was purified by column chromatography over silica gel (20% EtOAc, 80% hexane) to afford the product as a white solid. Overall yield of 556 mg, 87%, R_f: 0.39 (15% EtOAc, 85% hexane); ^{1}H NMR (400 MHz,

CHLOROFORM-*d*) *δ* ppm 1.42 (t, *J*=7.1 Hz, 3 H), 4.41 (q, *J*=7.1 Hz, 2 H), 5.23 (s, 2 H), 6.60 (d, *J*=7.8 Hz, 1 H), 7.04 (d, *J*=8.6Hz, 1 H), 7.19 – 7.24 (m, 1 H), 7.33 – 7.48 (m, 4 H), 7.52 (d, *J*=8.2 Hz, 2 H), 8.95 (br. s., 1 H); ^{13}C NMR (CHLOROFORM-*d*) *δ* ppm 14.4, 60.9, 69.9, 101.1, 105.0, 106.5, 119.3, 126.2, 126.3, 127.4, 127.9, 128.5, 137.1, 138.2, 153.7, 162.0; HRMS–ESI+: m/z $[M+H]^+$ calculated for $C_{18}H_{18}NO_3$: 296.1287; found: 296.1283. Mp: 160 – 162 °C; IR ATR (cm^{-1}): 3321, 1682, 1620, 1242, 1195. Characterization data corresponded with literature values.[8,9]

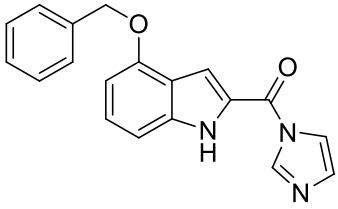

(26) (4-(Benzyloxy)-1*H*-indol-2-yl)(1*H*-imidazol-1-yl)methanone

To a solution of **(24)** (206 mg, 0.699 mmol) in EtOH (10 mL) was added 1M KOH (2.80 mL, 2.80 mmol) and stirred at 70 °C for 3 hours after which no starting material was detected on TLC. The solution was diluted with 15 mL water and acidified with 2M(aq) HCl, after which the product was extracted with EtOAc (2 x 30 mL). The organic phase was washed with brine, dried over $MgSO_4$ and the solvent reduced *in vacuo* to afford the intermediate indole acid as a white solid. The indole acid was dissolved in THF (3 mL) and cooled to 0 °C to which carbonyl diimidazole (136 mg, 0.840 mmol, dissolved in 1 mL THF) was added dropwise. The reaction was stirred for 4 hours, after which the solvent was reduced *in vacuo*. The product was purified by column chromatography over silica gel (30% EtOAc, 70% hexane) to afford the product as a yellow solid. 209 mg, 94% yield over two steps. R_f: 0.33 (40% EtOAc, 60% hexane); ^{1}H NMR (400 MHz, CHLOROFORM-*d*) *δ* ppm 5.24 (s, 2 H), 6.64 (d, *J*=7.8 Hz, 1 H), 7.10 (d, *J*=9.0 Hz, 1 H), 7.23 (s, 1 H), 7.31 – 7.37 (m, 1 H), 7.37 – 7.54 (m, 6 H), 7.75 (s, 1 H), 8.45 (s, 1 H), 9.31 (br. s., 1 H); ^{13}C NMR (101 MHz, DMSO-d_6) *δ* ppm 69.2, 101.3, 105.7, 109.1, 118.5, 118.6, 126.2, 127.5 (s, 2 C), 127.5, 127.8, 128.4 (s, 2 C), 130.3, 137.0, 137.9, 139.8, 153.3, 158.3; HRMS–ESI+: m/z $[M+H]^+$ calculated for $C_{19}H_{16}N_3O_2$: 318.1241; found 318.1241; Mp: decomposition; IR ATR (cm^{-1}): 3325, 3147, 1652, 1615, 1530, 1244, 1084.

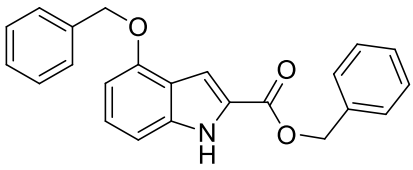

(27) Benzyl 4-(benzyloxy)-1*H*-indole-2-carboxylate

To a mixture of THF and NaH (27.2 mg, 60% dispersion in oil, 0.756 mmol) was added benzyl alcohol (78.0 µL, 0.756 mmol) at 0 °C under an atmosphere of nitrogen. The mixture was stirred for 30 minutes, to which a solution of **(26)** (120 mg, 0.378 mmol, dissolved in 2.5 mL THF) was added dropwise at 0 °C and

heated to 50 °C for 2 hours. Aqueous NH_4Cl (4 mL) was added and the product was extracted with EtOAc (2 x 30 mL). The organic phase was washed with brine, dried over $MgSO_4$ and the solvent reduced *in vacuo*. The product was purified by column chromatography over silica gel (30% EtOAc, 70% hexane) to afford the product as a white solid. 54 mg, 40% yield. R_f: 0.52 (30% EtOAc, 70% hexane); ^{1}H NMR (400 MHz, CHLOROFORM-*d*) δ ppm 5.21 (s, 2 H), 5.39 (s, 2 H), 6.59 (d, *J*=7.8 Hz, 1 H), 7.03 (d, *J*=8.2 Hz, 1 H), 7.19 – 7.26 (m, 1 H), 7.31 – 7.55 (m, 11 H), 8.88 (br. s., 1 H); ^{13}C NMR (101 MHz, CHLOROFORM-*d*) δ ppm 66.6, 69.9, 101.1, 105.0, 107.0, 119.3, 125.8, 126.5, 127.4, 127.9, 128.3, 128.4, 128.5, 128.6, 135.8, 137.0, 138.3, 153.7, 161.7; HRMS–ESI+: m/z $[M+H]^+$ calculated for $C_{23}H_{20}NO_3$: 358.1443; found 358.1436; Mp: 145 – 148 °C; IR ATR (cm-1): 3319, 1697, 1585, 1518, 1351, 1194.

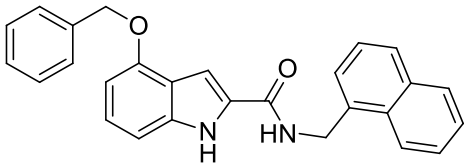

(28) 4-(Benzyloxy)-*N*-(naphthalen-1-ylmethyl)-1*H*-indole-2-carboxamide

To a solution of **(26)** (120 mg, 0.378 mmol) in THF (4 mL) was added naphthalen-1-ylmethanamine (83.1 µL, 0.567 mmol) at 0 °C, stirred at room temperature for 2 hours. The solvent was reduced *in vacuo* and the product was purified by column chromatography over silica gel (40% EtOAc, 60% hexane) to afford the product as a light yellow solid. 105 mg, 68 % yield. R_f: 0.78 (40% EtOAc, 60% hexane); ^{1}H NMR (400 MHz, CHLOROFORM-*d*) δ ppm 5.14 (d, *J*=5.5 Hz, 2 H), 5.16 (s, 2 H), 6.40 (t, *J*=5.1 Hz, 1 H), 6.57 (d, *J*=7.8 Hz, 1 H),6.93 – 6.95 (m, 1 H), 7.07 (d, *J*=8.6 Hz, 1 H), 7.15 – 7.21 (m, 1 H), 7.28 – 7.39 (m, 3 H), 7.41 – 7.49 (m, 3 H), 7.50 – 7.58 (m, 3 H), 7.86 (d, *J*=8.2 Hz, 1 H), 7.89 – 7.95 (m, 1 H), 8.07 – 8.12 (m, 1 H), 9.50 (br. s., 1 H); ^{13}C NMR (101 MHz, CHLOROFORM-*d*) δ ppm 41.9, 69.8, 100.1, 100.9, 105.2, 119.2, 123.4, 125.4, 125.5, 126.1, 126.8, 126.8, 127.5, 127.9, 128.5, 128.8, 128.8, 129.1, 131.4, 133.1, 133.9, 137.0, 137.7, 153.3, 161.2; HRMS–ESI+: m/z $[M+H]^+$ calculated for $C_{27}H_{23}N_2O_2$: 407.1760; found 407.1756; Mp: 202 – 203 °C; IR ATR (cm^{-1}): 3416, 3236, 1640, 1542, 1417, 1354, 1238.

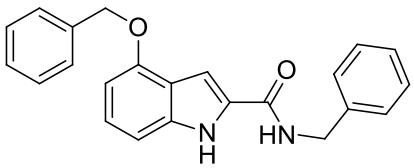

(29) *N*-Benzyl-4-(benzyloxy)-1*H*-indole-2-carboxamide

The reaction, workup and purification procedure of **(28)** was used. **(26)** (120 mg, 0.378 mmol) and benzyl amine (81 µL, 0.756 mmol) was added to THF (4 mL). 102 mg, 76 % yield. R_f: 0.56 (35% EtOAc, 65% hexane); ^{1}H NMR (300 MHz, CHLOROFORM-*d*) δ ppm 4.69 (d, *J*=5.9 Hz, 2 H), 5.20 (s, 2 H), 6.44 (t, *J*=5.5

Hz, 1 H), 6.59 (d, *J*=7.6 Hz, 1 H), 7.02 (d, *J*=2.2 Hz, 1 H), 7.06 (d, *J*=8.4 Hz, 1 H), 7.16 – 7.24 (m, 1 H), 7.29 – 7.53 (m, 10 H), 9.47 (br. s., 1 H); ^{13}C NMR (75 MHz, CHLOROFORM-*d*) *δ* ppm 43.7, 69.9, 100.0, 101.0, 105.3, 119.2, 125.5, 127.5 (2 C), 127.7, 127.9 (2 C), 127.9, 128.5 (2 C), 128.8 (2 C), 129.2, 137.1, 137.8, 137.9, 153.3, 161.4; HRMS–ESI+: m/z $[M+H]^+$ calculated for $C_{23}H_{21}N_2O_2$: 357.1603; found 357.1556; Mp: 174 – 176 °C; IR ATR (cm^{-1}) 3228, 1640, 1585, 1541, 1455, 1355, 1244, 1087.

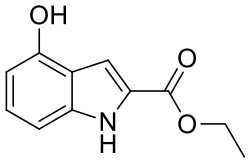

(31) Ethyl 4-hydroxy-1*H*-indole-2-carboxylate

(24) (700 mg, 3.41 mmol) and 70 mg 10% Pd/C was added to MeOH (12 mL) and placed under an atmosphere of H_2 via a balloon. The solution was stirred overnight, after which the solution was filtered through Celite and the solvent reduced *in vacuo*. The compound was purified by column chromatography over silica gel (50% EtOAc, 50% hexane) to afford the product as a white solid. 87%, 423.1 mg. R_f: 0.23 (20 % EtOAc, 80% hexane); ^{1}H NMR (300 MHz, CHLOROFORM-*d*) *δ* ppm 1.43 (t, *J*=7.0 Hz, 3 H), 4.42 (q, *J*=7.0 Hz, 2 H), 5.23 (s, 1 H), 6.53 (dd, *J*=7.6, 0.7 Hz, 1 H), 7.02 (dt, *J*=8.3, 0.8 Hz, 1 H), 7.18 (dd, *J*=8.3, 7.6 Hz, 1 H), 7.34 (dd, *J*=2.2, 1.0 Hz, 1 H), 8.89 (br. s., 1 H); ^{13}C NMR (75 MHz, CHLOROFORM-*d*) *δ* ppm 14.4, 61.1, 104.5, 104.7, 105.3, 118.0, 126.4, 138.5, 150.3, 160.5; HRMS–ESI+: m/z $[M+H]^+$ calculated for $C_{11}H_{12}NO_3$: 206.0818; found: 206.0848; Mp: 156 – 158 °C; IR ATR (cm^{-1}): 3313, 1691, 1585, 1238, 1197, 1020. Characterization data corresponded with literature values.[9]

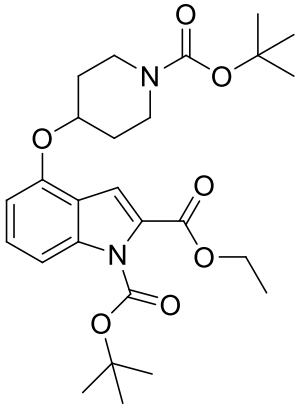

(39) 1-*tert*-Butyl 2-ethyl 4-((1-(*tert*-butoxycarbonyl)piperidin-4-yl)oxy)-1*H*-indole-1,2-dicarboxylate

To a solution of **(31)** (380 mg, 1.85 mmol), PPh_3 (930 mg, 4.62 mmol) and 1-Boc-4-hydroxypiperidine **(32)** (1,21g, 4.62 mmol) in THF (8 mL) was added DBAD (851 mg, 4.62 mmol) dissolved in 2 mL THF dropwise at 0 °C under an atmosphere of nitrogen. The solution was stirred overnight, followed by the removal of the solvent *in vacuo*. The crude product was loaded directly onto silica gel and the intermediate product was isolated together with di-*tert*-butyl hydrazine-1,2-dicarboxylate as co-eluent, (EtOAc 15%, hexane 85% an eluent). The fractions containing the intermediate product were collected, and the solvent reduced *in vacuo* to produce a white solid. The mixture was dissolved in DCM (12 mL) to

which Et_3N (0.5 mL) was added and Boc_2O (2.83 g, 12.2 mmol, dissolved in 3 mL DCM) was added dropwise at 0 °C under an atmosphere of nitrogen. The reaction was stirred overnight, after which the solvent was reduced *in vacuo*. The compound was purified by column chromatography over silica gel (12% EtOAc, 88% hexane) to afford the product as a colourless semi-solid that solidified into a white solid. 859 mg, 95%. R_f: 0.39 (15% EtOAc, 85% hexane) ^{1}H NMR (300 MHz, CHLOROFORM-*d*) δ ppm 1.39 (t, *J*=7.2 Hz, 3 H), 1.48 (s, 9 H), 1.61 (s, 9 H), 1.77 – 1.89 (m, 2 H), 1.89 – 2.00 (m, 2 H), 3.38 - 3.49 (m, 2 H), 3.63 - 3.74 (m, 1 H), 4.37 (q, *J*=7.2 Hz, 2 H), 4.59 – 4.68 (m, 1 H), 6.67 (d, *J*=7.9 Hz, 1 H), 7.24 (d, *J*=0.7 Hz, 1 H), 7.26 – 7.33 (m, 1 H), 7.65 (d, *J*=8.5 Hz, 1 H); ^{13}C NMR (75 MHz, CHLOROFORM-*d*) δ ppm 14.2, 27.7 (s, 3 C), 28.4 (s, 3 C), 30.3 (s, 2 C), 40.3, 61.2, 72.2, 79.5, 84.4, 105.8, 107.7, 112.2, 119.3, 127.7, 129.3, 139.4, 149.2, 151.3, 154.7, 161.6; HRMS–ESI+: m/z $[M+H]^+$ calculated for $C_{26}H_{37}N_2O_7$: 489.2601; found: 489.2589; Mp: 85 – 89 °C; IR ATR (cm^{-1}): 2974, 1743, 1728, 1689, 1364, 1278, 1145, 1035.

Compounds **(48)** and **(49)** were synthesized from **(39)** via the same transesterification procedure. Compound **(39)**, K_3PO_4 (3 equivalents) and the alcohol used for transesterification (20 – 30 equivalents) were placed in a vial, purged with argon, sealed and heated to 80 °C for 10 – 20 hours. The reaction was monitored via TLC using either (15% EtOAc, 85% hexane) or (5% EtOAc, 95% DCM) as mobile phase to determine whether the starting material had been consumed. The K_3PO_4 was filtered off, and the alcohol removed via heating the solution to 50 °C and streaming compressed air over the solution. After the majority of the solvent volume has been evaporated off, the product was purified by column chromatography over silica gel (5% EtOAc, 95% DCM).

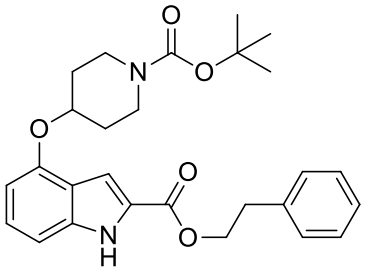

(48) Phenethyl 4-((1-(*tert*-butoxycarbonyl)piperidin-4-yl)oxy)-1*H*-indole-2-carboxylate

(39) (100 mg, 0.205 mmol), 2-phenylethanol (720 µL, 6.15 mmol) and K_3PO_4 (150 mg, 0.701 mmol) was heated to 80 °C. White solid, 37.2 mg, 39% yield, R_f: 0.69 (5% EtOAc, 95% DCM); ^{1}H NMR (300 MHz, CHLOROFORM-*d*) δ ppm 1.54 (s, 9 H), 1.86 – 2.09 (m, 4 H), 3.15 (t, *J*=7.0 Hz, 2 H), 3.43 – 3.56 (m, 2 H), 3.70 – 3.81 (m, 2 H), 4.61 (t, *J*=7.0 Hz), 4.66 – 4.75 (m, 1 H), 6.58 (d, *J*=7.6 Hz, 1 H), 7.05 (d, *J*=8.2 Hz, 1 H), 7.20 – 7.27 (m, 2 H), 7.28 – 7.43 (m, 6 H), 9.09 (br.

s., 1 H); ^{13}C NMR (75 MHz, CHLOROFORM-*d*) *δ* ppm 28.4 (3 C), 30.5 (2 C), 35.3, 40.7, 65.3, 72.0, 79.6, 102.6, 105.0, 106.5, 120.0, 126.0, 126.3, 126.6, 128.5 (2 C), 128.9 (2 C), 137.6, 138.5, 152.0, 154.8, 161.8; HRMS–ESI-: m/z $[M-H]^-$ calculated for $C_{27}H_{31}N_2O_5$: 463.2233; found: 463.2231; Mp: 131 – 134 °C; IR ATR (cm^{-1}): 3314, 2928, 1692, 1666, 1582, 1516, 1355.

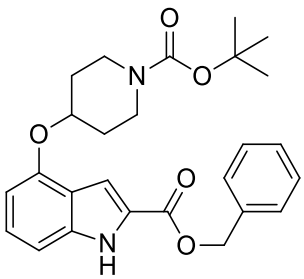

(49) Benzyl 4-((1-(*tert*-butoxycarbonyl)piperidin-4-yl)oxy)-1*H*-indole-2-carboxylate

(39) (100 mg, 0.205 mmol), benzyl alcohol (640 µL, 6.15 mmol) and K_3PO_4 (150 mg, 0.701 mmol) was heated to 80 °C. White solid, 41.3 mg, 45 % yield, R_f: 0.36 (15% EtOAc, 85% hexane); ^{1}H NMR (300 MHz, CHLOROFORM-*d*) *δ* ppm 1.51 (s, 9 H), 1.79 – 2.06 (m, 4 H), 3.39 – 3.52 (m, 2 H), 3.65 – 3.79 (m, 2 H), 4.63 – 4.73 (m, 2 H), 5.42 (s, 2 H), 6.55 (d, *J*=7.6 Hz, 1 H), 7.02 (d, *J*=8.2 Hz, 1 H), 7.18 – 7.25 (m, 1 H), 7.34 – 7.57 (m, 6 H), 9.21 (br. s., 1 H); ^{13}C NMR (75 MHz, CHLOROFORM-*d*) *δ* ppm 28.4 (3 C), 30.4 (2 C), 40.7 (2 C), 66.6, 71.9, 79.5, 102.4, 104.9, 106.8, 120.0, 125.8, 126.3, 128.3 (2 C), 128.3, 128.6 (2 C), 135.7, 138.6, 152.0, 154.8, 161.8; HRMS–ESI-: m/z $[M-H]^-$ calculated for $C_{26}H_{29}N_2O_5$: 449.2076; found: 469.2072; Mp: 147 – 149 °C; IR ATR (cm^{-1}): 3318, 2959, 1702, 1686, 1583, 1518, 1392.

Compounds **(50) – (53)** were synthesized from **(39)** via the same procedure. Compound **(39)** and thearomatic amine used for the amidation reaction (10 equivalents) were placed in a vial, to which was added acetonitrile (1 mL) and DBU (15 µL). The vial was purged with argon, sealed and heated to 140 °C for 10 – 20 hours. The reaction was monitored via TLC using (50% EtOAc, 50% hexane) as mobile phase to determine whether the starting material has been consumed. The product was purified by column chromatography over silica gel (30% EtOAc, 70% hexane to 100% EtOAc).

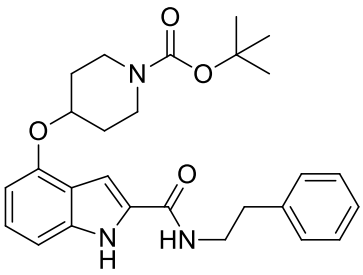

(50) *tert*-Butyl 4-((2-(phenethylcarbamoyl)-1*H*-indol-4-yl)oxy) piperidine-1-carboxylate

(39) (100 mg, 0.205 mmol), 2-phenylethylamine (260 µL, 2.05 mmol), DBU (15 µL, 0.100 mmol) and acetonitrile (1 mL). Yellow solid, 50.3 mg, 53% yield, R_f: 0.56 (30% EtOAc, 70% hexane); ^{1}H

NMR (300 MHz, CHLOROFORM-*d*) δ ppm 1.48 (s, 9 H), 1.75 – 2.08 (m, 4 H), 2.97 (t, *J*=7.0 Hz, 2 H), 3.37 – 3.50 (m, 2 H), 3.67 – 3.80 (m, 4 H,), 4.61 – 4.71 (m, 1 H), 6.20 (t, *J*=6.5 Hz, 1 H), 6.54 (d, *J*=7.6 Hz, 1 H), 6.84 (d, *J*=1.2 Hz, 1 H), 7.04 (d, *J*=8.2 Hz, 1 H), 7.14 – 7.21 (m, 1 H) 7.24 – 7.35 (m, 5 H), 9.23 (br.s, 1 H); ^{13}C NMR (75 MHz, CHLOROFORM-*d*) δ ppm 28.5 (3 C), 30.6 (2 C), 36.0, 40.6 (2 C), 40.9, 72.0, 79.6, 99.5, 102.4, 105.3, 120.0, 125.3, 126.7, 128.8 (2 C), 128.9 (2 C), 129.6, 138.0, 138.8, 151.5, 154.9, 161.6; HRMS–ESI-: m/z $[M-H]^-$ calculated for $C_{27}H_{32}N_3O_4$: 462.2393; found: 462.2391; Mp: 209 – 211 °C; IR ATR (cm^{-1}): 3244, 2924, 1667, 1635, 1555, 1423.

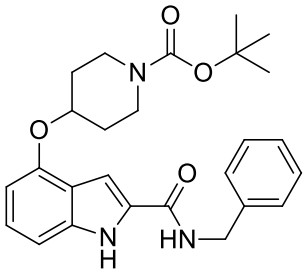

(51) *tert*-Butyl 4-((2-(benzylcarbamoyl)-1*H*-indol-4-yl)oxy) piperidine-1-carboxylate

(39) (100 mg, 0.205 mmol), benzylamine (224 µL, 2.05 mmol), DBU (15 µL, 0.100 mmol) and acetonitrile (1 mL). Yellow solid, 58.6 mg, 64% yield, R_f: 0.47 (30% EtOAc: 70% hexane); ^{1}H NMR (300 MHz, CHLOROFORM-*d*) δ ppm 1.49 (s, 9 H), 1.78 - 1.90 (m, 2 H), 1.90 - 2.02 (m, 2 H), 3.37 – 3.49 (m, 2 H), 3.64 - 3.76 (m, 2 H), 4.61 – 4.69 (m, 1 H), 4.73 (d, *J*=5.9 Hz, 2 H), 6.53 (d, *J*=7.6 Hz, 1 H), 6.87 (t, *J*=5.3 Hz, 1 H), 7.03 (d, *J*=8.2 Hz, 1 H), 7.07 (d, *J*=1.8 Hz, 1 H), 7.10 – 7.18 (m, 1 H), 7.28 – 7.49 (m, 5 H), 10.24 (br. s., 1 H); ^{13}C NMR (75 MHz, CHLOROFORM-*d*) δ ppm 28.4 (3 C), 30.5 (2 C), 40.4 (2 C), 43.6, 71.7, 79.5, 100.0, 102.2, 105.4, 119.9, 125.1, 127.6, 127.8 (2 C), 128.7 (2 C), 129.3, 138.0, 138.3, 151.4, 154.8, 161.7; HRMS–ESI+: m/z $[M+Na]^+$ calculated for $C_{26}H_{31}N_3O_4Na$: 472.2213; found: 472.2177; Mp: 211 – 213 °C; IR ATR (cm^{-1}): 3273, 2923, 1664, 1634, 1552, 1419, 1227

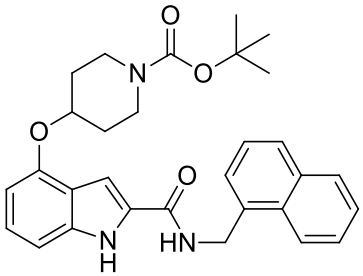

(52) *tert*-Butyl 4-((2-((naphthalen-1-ylmethyl)carbamoyl)-1*H*-indol-4-yl)oxy)piperidine-1-carboxylate

(39) (100 mg, 0.205 mmol), naphthalen-1-ylmethanamine (300 µL, 2.05 mmol), DBU (15 µL, 0.100 mmol) and acetonitrile (0.5 mL). White solid, 64.5 mg, 63% yield, R_f: 0.47 (35% EtOAc, 65% hexane); ^{1}H NMR (300 MHz, CHLOROFORM-*d*) δ ppm 1.48 (s, 9 H), 1.74 – 1.88 (m, 2 H), 1.88 – 2.01 (m, 2 H), 3.34 – 3.45 (m, 2 H), 3.61 – 3.72 (m, 2 H), 4.57 – 4.69 (m, 1 H), 5.15 (d, *J*=5.9 Hz, 2 H), 6.39 (t, J=5.3 Hz, 1 H), 6.53 (d, *J*=7.6 Hz, 1 H), 6.89 (d, *J*=2.3 Hz, 1 H), 7.06 (d, *J*=8.2 Hz, 1 H), 7.14 – 7.22 (m, 1 H), 7.46 – 7.61 (m, 4 H), 7.85 – 7.96

(m, 2 H), 8.08 – 8.15 (m, 1 H), 9.27 (br. s., 1 H); ^{13}C NMR (75 MHz, CHLOROFORM-*d*) *δ* ppm 28.4 (3 C), 30.4 (2 C), 40.6 (2 C), 41.8, 71.7, 79.5, 100.1, 102.2, 105.3, 119.9, 123.4, 125.2, 125.4, 126.0, 126.7, 126.7, 128.7, 128.7, 129.2, 131.4, 133.1, 133.8, 138.2, 151.4, 154.8, 161.5; HRMS–ESI+: m/z $[M+K]^+$ calculated for $C_{30}H_{33}N_3O_3K$: 522.2159; found: 522.2383; Mp: 207 – 209 °C; IR ATR (cm^{-1}): 3408, 3240, 2928, 1701, 1648, 1544, 1415, 1243.

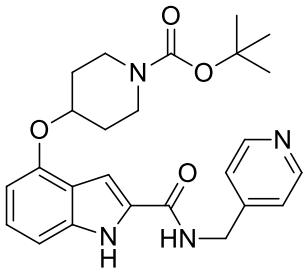

(53) *tert*-Butyl 4-((2-((pyridin-4-ylmethyl)carbamoyl)-1*H*-indol-4-yl)oxy)piperidine-1-carboxylate

(39) (60.0 mg, 0.123 mmol), pyridin-4-ylmethanamine (250 µL, 2.46 mmol) was heated neat to 145 °C. Yellow solid, 39.3 mg, 71% yield, R_f: 0.52 (100% EtOAc); ^{1}H NMR (300 MHz, CHLOROFORM-*d*) *δ* ppm 1.46 (s, 9 H), 1.74 – 1.94 (m, 4 H), 3.37 – 3.48 (m, 2 H), 3.48 – 3.61 (m, 2 H), 4.59 – 4.71 (m, 3 H), 6.48 (d, *J*=7.6 Hz, 1 H), 6.94 (d, *J*=8.2 Hz, 1 H) 7.09 – 7.16 (m, 1 H), 7.20 (d, *J*=1.2 Hz, 1 H), 7.27 (d, *J*=5.3 Hz, 2 H), 7.90 (t, *J*=5.9 Hz, 1 H), 8.51 (d, J=5.3 Hz, 2 H), 10.20 (s, 1 H); ^{13}C NMR (75 MHz, CHLOROFORM-*d*) *δ* ppm 28.4 (3 C), 30.3 (2 C), 40.2 (2 C), 42.2, 71.4, 79.7, 100.9, 102.3, 105.3, 120.0, 122.3 (2 C), 125.3, 129.1, 138.2, 147.9, 149.7 (2 C), 151.4, 154.9, 162.2; HRMS–ESI+: m/z $[M+H]^+$ calculated for $C_{25}H_{31}N_4O_4$: 451.2346; found 451.2351; Mp: 105 – 108 °C; IR ATR (cm^{-1}): 3252, 2923, 1664, 1638, 1550, 1418, 1231.

Compounds **IH1 – IH7** except **IH3** were synthesized from **(48)** – **(53)** via the same procedure. In a small flask was added the Boc-protected compound and DCM (1 mL) followed by the addition of 4M HCl/dioxane (1 mL). The solution was stirred for one to two hours, after which the solvent was reduced *in vacuo*. A small amount of DCM was added followed by the addition of EtOAc which caused the salt to precipitate out of solution. The solvent was reduced *in vacuo* and the product dried under vacuum.

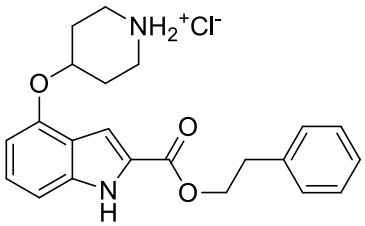

(IH1) 4-((2-(Phenethoxycarbonyl)-1*H*-indol-4-yl)oxy)piperidin-1-ium chloride

25.5 mg, 79% yield, white powder. ^{1}H NMR (400 MHz, DMSO-d_6) *δ* ppm 1.91 – 2.02 (m, 2 H), 2.12 – 2.21 (m, 2 H), 3.05 (t, *J*=6.8 Hz, 2 H), 3.07 – 3.15 (m, 2 H), 3.21 – 3.30 (m, 2 H), 4.48 (t, *J*=6.8 Hz, 2 H), 4.78 – 4.85 (m, 1 H), 6.65

(d, *J*=7.8 Hz, 1 H), 7.05 (d, *J*=8.2 Hz, 1 H), 7.13 (d, *J*=1.2 Hz, 1 H), 7.14 – 7.20 (m, 1 H), 7.19 – 7.37 (m, 5 H), 9.24 (br. s., 2 H), 11.92 (s, 1 H); ^{13}C NMR (101 MHz, DMSO-d_6) δ ppm 27.0 (2 C), 34.5, 40.2 (2 C), 64.9, 68.8, 102.3, 105.1, 105.9, 118.9, 125.7, 126.0, 126.4, 128.4 (2 C), 128.9 (2 C), 137.9, 139.0, 150.8, 161.0; HRMS-TOF MS ES+: m/z $[M+H]^+$ calculated for $C_{22}H_{25}N_2O_3$: 365.1865; found: 365.1859; Purity: >99%; Mp: 215 – 217 °C; IR ATR (cm^{-1}): 3191, 2927, 1712, 1581, 1526, 1349, 1240, 1189.

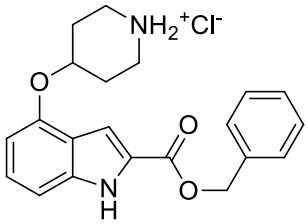

(IH2) 4-((2-((Benzyloxy)carbonyl)-1*H*-indol-4-yl)oxy)piperidin-1-ium chloride

34.2 mg, 96% yield, white powder. ^{1}H NMR (400 MHz, DMSO-d_6) δ ppm 1.89 – 2.02 (m, 2 H), 2.09 – 2.23 (m, 2 H), 3.03 – 3.18 (m, 2 H), 3.19 – 3.32 (m, 2 H), 4.76 – 4.87 (m, 1 H), 5.37 (s, 2 H), 6.65 (d, *J*=7.8 Hz, 1 H), 7.06 (d, *J*=8.2 Hz, 1 H), 7.14 – 7.21 (m, 1 H), 7.22 (d, *J*=1.2 Hz, 1 H), 7.32 – 7.52 (m, 5 H), 9.12 (br. s, 1 H), 9.32 (br. s, 1 H), 11.98 (br. s., 1 H); ^{13}C NMR (101 MHz, DMSO-d_6) δ ppm 26.9 (2 C), 65.7, 68.8, 102.3, 105.4, 105.9, 118.9, 125.8, 125.9, 128.0 (2 C), 128.1 (2 C), 128.5, 136.1, 139.1, 150.8, 160.9 (missing carbon of piperidine ring behind DMSO signal); HRMS-TOF MS ES+: m/z $[M+H]^+$ calculated for $C_{21}H_{23}N_2O_3$: 351.1709; found: 351.1714; Purity: >99%; Mp: decomposition; IR ATR (cm^{-1}): 3206, 2943, 1709, 1580, 1524, 1342, 1234, 1192.

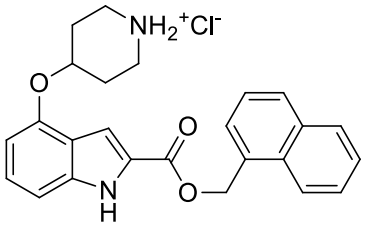

(IH3) 4-((2-((Naphthalen-1-ylmethoxy)carbonyl)-1*H*-indol-4-yl)oxy)piperidin-1-ium chloride

(39) (100 mg, 0.205 mmol), K_3PO_4 (150 mg, 0.742 mmol) and naphthalen-1-ylmethanol (158 mg, 1.00 mmol) was added to a vial and the mixture stirred at 100 °C overnight. The mixture was dissolved in DCM (3 mL) and the K_3PO_4 filtered off. The solvent was reduced *in vacuo* and the crude product dissolved in DCM (1 mL) to which 4M HCl/dioxane (1 mL) was added and stirred for 2 hours. The solvent was reduced *in vacuo* and the product was purified by column chromatography over silica gel (100% DCM to 10% MeOH, 90% DCM) to afford the product as a white solid. 20.4 mg, 23% yield over two steps. ^{1}H NMR (400 MHz, DMSO-d_6) δ ppm 1.83 – 1.98 (m, 2 H), 2.06 – 2.18 (m, 2 H), 3.01 – 3.12 (m, 2 H), 3.17 – 3.30 (m, 2 H), 4.75 – 4.83 (m, 1 H), 5.85 (s, 2 H), 6.63 (d, *J*=7.4 Hz, 1 H), 7.04 (d, *J*=8.2 Hz, 1 H), 7.13 – 7.19 (m, 2 H), 7.52 – 7.66 (m, 3 H), 7.71 (d, *J*=7.3 Hz, 1 H), 7.96 – 8.03 (m, 2 H), 8.14 (d, *J*=8.6 Hz, 1 H), 8.77 (br. s, 1 H),

8.98 (br. s, 1 H), 11.96 (s, 1 H); ^{13}C NMR (101 MHz, DMSO-d_6) δ ppm 27.1 (2 C), 40.2 (2 C), 64.2, 68.9, 102.3, 105.5, 105.9, 118.9, 123.6, 125.4, 125.8, 125.9, 126.1, 126.7, 127.3, 128.6, 129.0, 131.1, 131.6, 133.3, 139.2, 150.9, 161.0; HRMS-TOF MS ES+: m/z $[M+H]^+$calculated for $C_{25}H_{25}N_2O_3$: 401.1865; found: 401.1867; Purity: >99%; Mp: 211 – 214 °C; IR ATR (cm^{-1}): 3224, 2929, 1713, 1581, 1514, 1345, 1233, 1186.

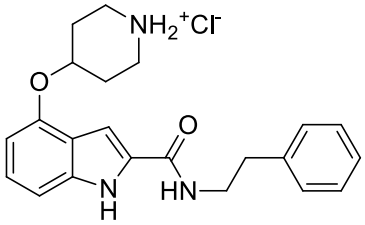

(IH4) 4-((2-(Phenethylcarbamoyl)-1*H*-indol-4-yl)oxy)piperidin-1-ium chloride

23.1 mg, 81% yield, yellow solid. ^{1}H NMR (400 MHz, DMSO-d_6) δ ppm 1.88 – 1.99 (m, 2 H), 2.13 – 2.23 (m, 2 H), 2.87 (t, *J*=7.4 Hz, 2 H), 3.06– 3.18 (m, 2 H), 3.19 – 3.33 (m, 2 H), 3.47 – 3.54 (m, 2 H), 4.74 – 4.82 (m, 1 H), 6.61 (d, *J*=7.4 Hz, 1 H), 7.02 (d, *J*=8.2 Hz, 1 H), 7.05 – 7.10 (m, 1 H), 7.16 – 7.33 (m, 6 H), 8.60 (t, *J*=5.5 Hz, 1 H), 9.00 (br. s., 1 H), 9.06 (br. s., 1 H), 11.58 (s, 1 H); ^{13}C NMR (101 MHz, METHANOL-d_4) δ ppm 28.5 (2 C), 36.9, 42.0 (2 C), 42.4, 69.7, 102.0, 104.0, 107.2, 121.3, 126.1, 127.4, 129.6 (2 C), 130.0 (2 C), 131.5, 140.1, 140.7, 152.1, 164.0; HRMS-TOF MS ES+: m/z $[M+H]^+$calculated for $C_{22}H_{26}N_3O_2$: 364.2025; found: 364.2018; Purity: 91.3%; Mp: 87 – 89 °C; IR ATR (cm^{-1}): 3251, 2927, 1619, 1554, 1508, 1343, 1243.

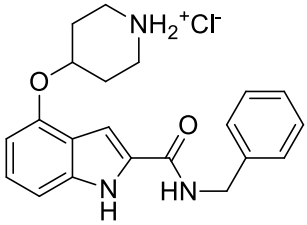

(IH5) 4-((2-(Benzylcarbamoyl)-1*H*-indol-4-yl)oxy)piperidin-1-ium chloride

43.4 mg, 86% yield, yellow solid. ^{1}H NMR (400 MHz, DMSO-d_6) δ ppm 1.88 – 2.05 (m, 2 H), 2.08 – 2.27 (m, 2 H), 3.04 – 3.16 (m, 2 H), 3.18 – 3.31 (m, 2 H), 4.49 (d, *J*=5.9 Hz, 2 H), 4.72 – 4.86 (m, 1 H), 6.62 (d, *J*=7.4 Hz, 1 H), 7.00 – 7.13 (m, 2 H), 7.20 – 7.41 (m, 6 H), 9.11 (t, *J*=5.9Hz, 1 H), 9.28 (br. s., 2 H), 11.67 (br. s., 1 H); ^{13}C NMR (101 MHz, DMSO-d_6) δ ppm 27.2 (2 C), 40.4 (2 C), 42.1, 69.0, 100.3, 102.1, 105.8, 119.1, 124.2, 126.8, 127.3 (2 C), 128.3 (2 C), 130.5, 138.2, 139.7, 150.6, 161.0; HRMS-TOF MS ES+: m/z $[M+H]^+$calculated for $C_{21}H_{24}N_3O_2$: 350.1869; found: 350.1855; Purity: >99%; Mp: decomposition; IR ATR (cm^{-1}): 3243, 2933, 1656, 1548, 1421, 1288, 1230.

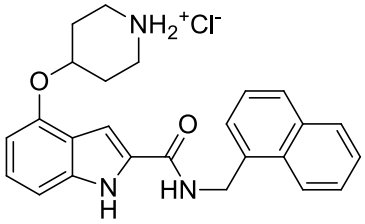

(IH6) 4-((2-((Naphthalen-1-ylmethyl)carbamoyl)-1*H*-indol-4-yl)oxy)piperidin-1-ium chloride

54.7 mg, 97% yield, yellow solid. ^{1}H NMR (400 MHz, DMSO-d_6) δ ppm 1.86 – 2.03 (m, 2 H), 2.10 – 2.27 (m, 2 H), 3.10 (br. s., 2 H), 3.22 (br. s., 2 H), 4.72 – 4.84 (m, 1 H), 4.97 (d, *J*=4.7Hz, 2 H), 6.61 (d, *J*=7.4 Hz, 1 H), 7.01 – 7.13 (m, 2 H), 7.34 (s, 1 H), 7.43 – 7.61 (m, 4 H), 7.84 (d, *J*=8.2 Hz, 1 H), 7.95 (d, *J*=8.6 Hz, 1 H), 8.22 (d, *J*=8.2 Hz, 1 H), 9.13 (t, *J*=5.66 Hz, 1 H), 9.29 (br. s., 2 H), 11.71 (s, 1 H); ^{13}C NMR (101 MHz, DMSO-d_6) δ ppm 27.7 (2 C), 40.7 (2 C), 40.9, 69.4, 100.9, 102.5, 106.3, 119.5, 124.0, 124.7, 125.9, 126.0, 126.2, 126.7, 128.0, 129.0, 130.9, 131.4, 133.7, 135.1, 138.6, 151.0, 161.3; HRMS-TOF MS ES+: m/z $[M+H]^+$ calculated for $C_{25}H_{26}N_3O_2$: 400.2025; found: 400.2014; Purity: 95.5%; Mp: 202 – 204 °C; IR ATR (cm^{-1}): 3243, 2933, 1656, 1548, 1421, 1288.

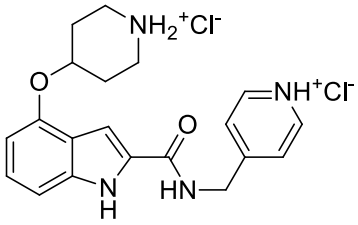

(IH7) 4-((4-(Piperidin-1-ium-4-yloxy)-1*H*-indole-2-carboxamido)methyl)pyridin-1-ium chloride

26.3 mg, 80% yield, yellow solid. ^{1}H NMR (600 MHz, DMSO-d_6) δ ppm 1.98 (br. s, 2 H), 2.19 (br. s., 2 H), 3.11 (br. s., 2 H), 3.24 (br. s., 3 H), 4.76 (d, *J*=5.3 Hz, 2 H), 4.82 (br. s., 1 H), 6.64 (d, *J*=7.6 Hz, 1 H), 7.04 (d, *J*=8.2 Hz, 1 H), 7.08 – 7.14 (m, 1 H), 7.41 (s, 1 H), 7.98 (d, *J*=5.3 Hz, 2 H), 8.86 (d, *J*=5.3 Hz, 2 H), 9.31 (br. s., 1 H), 9.47 (br. s., 1 H), 9.54 (t, *J*=5.3 Hz, 1 H), 11.75 (br. s., 1 H); ^{13}C NMR (151 MHz, DMSO-d_6) δ ppm 27.2 (2 C), 40.4 (2 C), 41.8, 69.0, 101.2, 102.1, 105.8, 119.0, 124.5, 124.8 (2 C), 129.7, 138.3, 141.5 (2 C), 150.6, 159.9, 161.5; HRMS-TOF MS ES+: m/z $[M+H]^+$calculated for $C_{20}H_{23}N_4O_2$: 352.1899; found: 352.1879; Purity: 96.5%; Mp: 219 – 221 °C; IR ATR (cm^{-1}): 3047, 2927, 1634, 1555, 1509, 1417, 1245.

10.3 Synthesis of compounds pertaining to Chapter 3

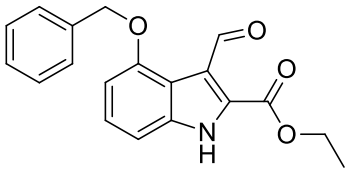

(54) Ethyl 4-(benzyloxy)-3-formyl-1*H*-indole-2-carboxylate

To a solution of DCM (3 mL) and DMF (260 µL, 3.36 mmol) $POCl_3$ (104 µL, 1.12 mmol) was added dropwise at 0°C under an atmosphere of nitrogen. The solution was allowed to stir for 10 minutes followed by the dropwise addition of **(24)** (300 mg, 1.02 mmol dissolved in 1 mL DCM) resulting in the clear solution turning yellow. The mixture was allowed to stir overnight at room temperature. 2M aqueous NaOH (3mL) was added to a vigorously stirring solution and the products were extracted with DCM (2 x 20 mL). The organic phase was dried over $MgSO_4$, and the solvent reduced *in vacuo*. The product was purified by column chromatography over silica gel (15% EtOAc, 85% hexane) to afford the product as a white powder. 41 mg, 13% yield. R_f: 0.43 (15% EtOAc, 85% hexane); ^{1}H NMR (400 MHz, CHLOROFORM-*d*) δ ppm 1.46 (t, *J*=7.2 Hz, 3 H), 4.50 (q, *J*=7.2 Hz, 2 H), 5.29 (s, 2 H), 6.77 (d, *J*=7.8 Hz, 1 H), 7.08 (d, *J*=8.2 Hz, 1 H), 7.28 – 7.37 (m, 2 H), 7.37 – 7.44 (m, 2 H), 7.55 – 7.60 (m, 2 H), 9.38 (br. s., 1 H), 10.84 (s, 1 H); ^{13}C NMR (101 MHz, CHLOROFORM-*d*) δ ppm 14.2, 62.2, 70.5, 104.5, 105.1, 115.7, 117.0, 127.2 (2 C), 127.4, 127.8, 128.5 (2 C), 129.0, 136.7, 136.9, 154.5, 160.7, 187.4; HRMS-TOF MS ES+: m/z $[M+H]^+$ calculated for $C_{19}H_{18}NO_4$: 324.1236; found: 324.1222; Mp: 145 – 146 °C; IR ATR (cm^{-1}): 3459, 3448, 1709, 1652, 1584, 1513, 1380, 1297, 1222, 1088.

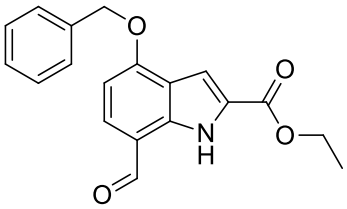

(**54A) Ethyl 4-(benzyloxy)-7-formyl-1*H*-indole-2-carboxylate**

(54A) was the major product obtained during the formylation of **(24)** to produce **(54)**. 203 mg, 62% yield. R_f: 0.33 (15% EtOAc, 85% hexane) ^{1}H NMR (400 MHz, CHLOROFORM-*d*) δ ppm 1.41 (t, *J*=7.1 Hz, 3 H), 4.41 (q, *J*=7.1 Hz, 2 H), 5.31 (s, 2 H), 6.69 (d, *J*=8.2 Hz, 1 H), 7.32 – 7.51 (m, 6 H), 7.68 (d, *J*=8.2 Hz, 1 H), 9.94 (s, 1 H), 10.53 (br. s., 1 H); ^{13}C NMR (101 MHz, CHLOROFORM-*d*) δ ppm 14.4, 61.1, 70.4, 101.6, 106.5, 116.2, 119.2, 127.3 (2 C), 127.9, 128.3, 128.7 (2 C), 135.1, 135.9, 136.0, 159.2, 161.1, 190.8; HRMS-TOF MS ES+: m/z $[M+H]^+$ calculated for $C_{19}H_{18}NO_4$: 324.1236; found: 324.1245; Mp: 110 – 112 °C; IR ATR (cm^{-1}): 3460, 3448, 1708, 1652, 1585, 1513, 1365, 1297, 1222, 1071.

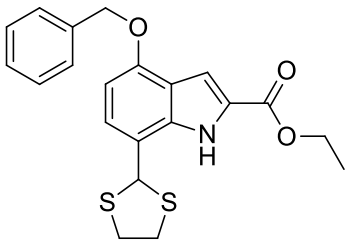

(55A) Ethyl 4-(benzyloxy)-7-(1,3-dithiolan-2-yl)-1*H*-indole-2-carboxylate

(54A) (136 mg, 0.385 mmol), ethane-1,2-dithiol (32.5 µL, 0.423 mmol), *p*TsOH (4 mg) and silica gel (7 mg) was added to THF (2 mL) and stirred at 40 °C overnight. The mixture was filtered, and the solvent reduced *in vacuo*. The product was purified by column chromatography over silica gel (15% EtOAc, 85% hexane) to afford the product as a white powder. 136.7 mg, 81% yield. R_f: 0.39 (20% EtOAc, 80% hexane), ^{1}H NMR (400 MHz, CHLOROFORM-*d*) *δ* ppm 1.41 (t, *J*=7.0 Hz, 3 H), 3.37 – 3.47 (m, 2 H), 3.55 – 3.66 (m, 2 H), 4.40 (q, *J*=7.2 Hz, 2 H), 5.22 (s, 2 H), 5.93 (s, 1 H), 6.46 (d, *J*=7.8 Hz, 1 H), 7.23 (d, *J*=8.2 Hz, 1 H), 7.30 – 7.52 (m, 6 H), 9.51 (br. s., 1 H), ^{13}C NMR (101 MHz, CHLOROFORM-*d*) *δ* ppm 14.4, 40.0 (2 C), 55.9, 60.9, 69.9, 100.6, 106.5, 112.8, 120.2, 126.3, 126.6, 127.3 (2 C), 127.9, 128.5 (2 C), 135.7, 136.9, 154.3, 161.8; HRMS-TOF MS ES+: m/z $[M+H]^+$ calculated for $C_{21}H_{22}NO_3S_2$: 400.1041; found: 400.1045; Mp: 162 – 164°C; IR ATR (cm^{-1}): 3316, 1686, 1518, 1199, 1171, 1065.

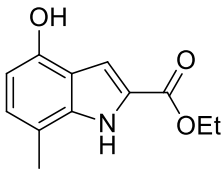

(56A) Ethyl 4-hydroxy-7-methyl-1H-indole-2-carboxylate

To a mixture of EtOAc (4ml) and (**55A**) (63.3 mg, 0.158 mmol) was added Raney Nickel (2g, stored under EtOH), and heated to 57 °C for 1.5 hours, after which the starting material had disappeared when monitored by of means of TLC. The mixture was filtered through a plug of Celite and washed with hot EtOAc, and the solvent removed *in vacuo* to produce the product as a white solid without further purification. 27.1 mg, 78% yield. R_f: 0.16 (20% EtOAc, 80% hexane); ^{1}H NMR (400 MHz, CHLOROFORM-*d*) *δ* ppm 1.43 (t, J=7.2 Hz, 3 H), 2.44 (s, 3 H), 4.43 (q, J=7.2 Hz, 2 H), 6.45 (d, J=7.8 Hz, 1 H), 6.95 (d, J=7.8 Hz, 1 H), 7.34 (d, J=2.0 Hz, 1 H), 8.80 (br. s., 1 H); ^{13}C NMR (101 MHz, CHLOROFORM-*d*) *δ* ppm 14.4, 16.0, 61.1, 104.4, 105.9, 113.6, 117.5, 126.1, 126.4, 138.0, 148.5, 162.0.

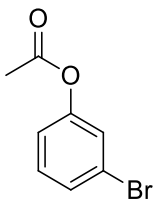

(62) 3-Bromophenyl acetate

To a solution of 3-bromophenol (1.23 mL, 11.6 mmol) and DMAP (10 mg) in DCM (30mL) was added acetic anhydride (1.64 mL, 17.3 mmol) at 0 °C and stirred for 4 hours. The solvent was reduced *in vacuo*, and the product was purified by column chromatography over silica gel (20% EtOAc, 80% hexane) to afford the products as a colourless

liquid. 2.48 g, >99% yield. R_f: 0.71 (20% EtOAc, 80% hexane), ^{1}H NMR (300 MHz, CHLOROFORM-*d*) *δ* ppm 2.30 (s, 3 H), 7.03 – 7.08 (m, 1 H), 7.22 – 7.29 (m, 1 H), 7.29 – 7.31 (m, 1 H), 7.36 – 7.40 (m, 1 H); ^{13}C NMR (75 MHz, CHLOROFORM-*d*) *δ* ppm 21.0, 120.4, 122.3, 125.1, 129.0, 130.4, 151.1, 168.9; Characterization data corresponded with literature values.[10]

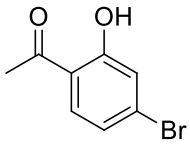

(64) 1-(4-Bromo-2-hydroxyphenyl)ethanone

In a flask was placed **(62)** (2.48 g, 11.6 mmol) and $AlCl_3$ (2.32 g, 17.4 mmol) and the resulting mixture was heated to 140 °C for 2 hours. The mixture was cooled down and 5% HCl solution was added, resulting in the solid material dissolving. The mixture was added to 100 mL DCM and washed with 2 x 40 mL $NaHCO_3$ solution. The organic phase was washed with brine, dried over $MgSO_4$ and the solvent reduced *in vacuo.* The product was purified by column chromatography over silica gel (20% EtOAc, 80% hexane) to afford the products as a white solid. 1.17 g, 47% yield. R_f: 0.63 (20% EtOAc, 80% hexane); ^{1}H NMR (300 MHz, CHLOROFORM-*d*) *δ* ppm 2.62 (s, 3 H), 7.03 – 7.08 (m, 1 H), 7.17 – 7.21 (m, 1 H), 7.56 – 7.61 (m, 1 H), 12.35 (s, 1 H); ^{13}C NMR (75 MHz, CHLOROFORM-*d*) *δ* ppm 26.6, 118.6, 121.6, 122.5, 130.8, 131.6, 162.8, 203.9. Characterization data corresponded with literature values.[11]

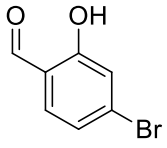

(66) 4-Bromo-2-hydroxybenzaldehyde

3-bromophenol (580 mg, 3.35 mmol), TBAB (4.32 mg), dioxane (432 µL) and 40% NaOH solution (1.34 mL) were mixed together at 0 °C, followed by the dropwise addition of $CHCl_3$ (348 µL, 4.35 mmol) under an atmosphere of nitrogen. The reaction was heated to 50 °C and stirred for 5 hours. The reaction was acidified and extracted with DCM (2 x 50 mL). The organic phase was dried over $MgSO_4$ and the solvent was reduced *in vacuo*. The product was purified by column chromatography over silica gel (30% EtOAc, 70% hexane) to afford the product as a white solid. 182 mg, 26% yield. R_f: 0.65, ^{1}H NMR (300 MHz, CHLOROFORM-*d*) *δ* ppm 6.07 (br. s., 1 H), 6.90 (dd, *J*=8.4, 2.4 Hz, 1 H), 7.15 (d, *J*=2.3 Hz, 1 H), 7.88 (d, *J*=8.7 Hz, 1 H), 10.22 (s, 1 H); ^{13}C NMR (101 MHz, CHLOROFORM-*d*) *δ* ppm 115.3, 120.1, 125.7, 128.9, 131.5, 163.5, 191.1; Characterization data corresponded with literature values.[12]

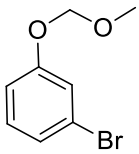

(67) 1-bromo-3-(methoxymethoxy)benzene

To a mixture of NaH (509 mg, 60% dispersion in oil, 12.72 mmol) in THF (18 mL) was added 3-bromophenol (1.23 mL, 11.6 mmol) dropwise at 0 °C and stirred for 30 minutes at 0 °C under an atmosphere of nitrogen. Chloromethyl methyl ether (1.14 mL, 15.0 mmol) was added and stirred for 4 hours. The reaction was quenched with aqueous NH_4Cl (15 mL) and stirred for 10 minutes. The product was extracted with 2 x 50 mL EtOAc, the organic phase was washed with brine and dried over $MgSO_4$. The solvent was reduced *in vacuo* and the product purified by column chromatography over silica gel (30% EtOAc, 70% hexane) to afford the product as a colourless oil. 977 mg, 39 % yield. R_f: 0.67 (15% EtOAc, 85% hexane); ^{1}H NMR (300 MHz, CHLOROFORM-*d*) δ ppm 3.49 (s, 3 H), 5.17 (s, 2 H), 6.96 – 7.01 (m, 1 H), 7.14 – 7.17 (m, 2 H), 7.22 – 7.25 (m, 1 H); ^{13}C NMR (75 MHz, CHLOROFORM-*d*) δ ppm 56.1, 94.4, 115.0, 119.6, 122.7, 124.9, 130.5, 158.0; Characterization data corresponded with literature values.[13]

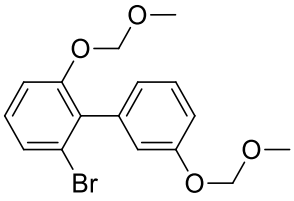

(69) 2-Bromo-3',6-bis(methoxymethoxy)-1,1'-biphenyl

To a solution of 2,2,6,6-tetramethylpiperidine (247 µL, 1.45 mmol) in THF (2.5 mL) was added *n*-BuLi (495 µL, 1.15 mmol) dropwise at -78 °C, after which the solution was warmed to 0 °C and stirred for 30 minutes. The solution was cooled to -100 °C and **(67)** (200 mg, 0.966 mmol, dissolved in 500 µL THF) was added to the solution dropwise and stirred for 2 hours at -100 °C, after which dimethylacetamide (180 µL, 1.93 mmol) was added. The solution was warmed to 0 °C and stirred for an additional hour. The reaction was quenched with water (4 mL) and extracted with EtOAc (2 x 30 mL). The organic phase was washed with brine, dried over $MgSO_4$ and the solvent reduced *in vacuo*. The product was purified by column chromatography over silica gel (15% EtOAc, 85% hexane) to afford the product as a colourless oil. 32 mg, 9% yield. R_f: 0.47 (15% EtOAc, 85% hexane), ^{1}H NMR (300 MHz, CHLOROFORM-*d*) δ ppm 3.34 (s, 3 H), 3.51 (s, 3 H), 5.06 (s, 2 H), 5.21 (d, *J*=2.2 Hz, 2 H), 6.93 (dt, *J*=7.6, 1.2 Hz, 1 H), 6.98 (dd, *J*=2.5, 1.5 Hz, 1 H), 7.07 (ddd, *J*=8.3, 2.6, 1.0 Hz, 1 H), 7.13 – 7.21 (m, 2 H), 7.31 – 7.39 (m, 2 H); ^{13}C NMR (75 MHz, CHLOROFORM-*d*) δ ppm 56.0, 56.0, 94.7, 94.7, 114.1, 115.3, 118.2, 123.6, 124.5, 126.2, 128.8, 129.3, 132.8, 138.8, 155.3, 156.9; Mass spectrometry did not indicate a molecular ion.

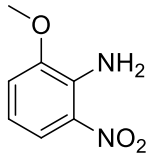

(71) 2-Methoxy-6-nitroaniline

To a mixture of 2-amino-3-nitrophenol (1.50 g, 9.73 mmol) and K_2CO_3 (2.69 g, 19.46 mmol) in DMF (18 mL) was added methyl iodide (750 µL, 12.05 mmol) at 0 °C under an atmosphere of nitrogen. The reaction was stirred at room temperature overnight. The reaction mixture was then diluted with EtOAc (100 mL), and the organic phase was washed with water (4 x 80 mL) followed by a wash with brine. The organic phase was dried over $MgSO_4$ and the solvent reduced *in vacuo*. The product was purified by column chromatography over silica gel (20% EtOAc, 80% hexane) to afford an orange solid. 1590 mg, 97% yield. R_f: 0.35 (20% EtOAc, 80% hexane) ^{1}H NMR (300 MHz, CHLOROFORM-*d*) *δ* ppm 3.88 (s, 3 H), 6.43 (br. s, 2 H), 6.57 (dd, *J*=8.9, 7.6 Hz, 1 H), 6.87 (d, *J*=7.6 Hz, 1 H), 7.69 (dd, *J*=8.9, 1.2 Hz, 1 H); ^{13}C NMR (75 MHz, CHLOROFORM-*d*) *δ* ppm 56.1, 113.2, 114.5, 117.1, 131.4, 137.0, 148.0. Characterization data corresponded with literature values.[17]

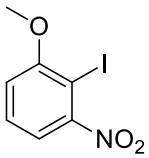

(72) 2-Iodo-1-methoxy-3-nitrobenzene

(71) (250 mg, 1.49 mmol) was added to DMSO (7 mL) and 30% aqueous H_2SO_4 (7 mL) and heated to 50 °C for 2 hours. The solution was cooled to 0 °C and $NaNO_2$ (154 mg, 2.24 mmol, dissolved in 1 mL water) was added dropwise with vigorous stirring. The solution turned clear and was stirred for an additional hour at 0 °C. KI (742 mg, 4.47 mmol, dissolved in 1 mL water) was added dropwise. The evolution of gas was observed. The reaction was stirred for 1 hour, after which another portion of KI (742 mg) was added. The solution was stirred overnight, followed by the addition of EtOAc (40 mL), after which the organic phase was washed with 10% $Na_2S_2O_4$ (30 mL), water (3 x 40 mL) and brine. The organic phase was dried over $MgSO_4$ and the solvent reduced *in vacuo*. The product was purified by column chromatography over silica gel (20% EtOAc, 80% hexane) to afford the product as a yellow solid. 337 mg, 81 % yield. R_f: 0.44 (20% EtOAc, 80% hexane) ^{1}H NMR (300 MHz, CHLOROFORM-*d*) *δ* ppm 3.97 (s, 3 H), 6.97 – 7.03 (m, 1 H), 7.27 – 7.32 (m, 1 H), 7.40 – 7.48 (m, 1 H); ^{13}C NMR (75 MHz, CHLOROFORM-*d*) *δ* ppm 57.2, 79.9, 105.0, 113.4, 116.8, 130.0, 159.6; Characterization data corresponded with literature values.[14]

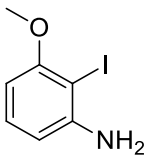

(73) 2-Iodo-3-methoxyaniline

To an open flask was added **(72)** (200 mg, 0.717 mmol), glacial acetic acid (1.50 mL), EtOH (1.50 mL), water (0.750 mL) and iron powder (200 mg, 3.56 mmol). The mixture was sonicated at 30 °C for 3 hours. The solution turned from red to dark yellow. The iron powder was removed via a magnet. The mixture was diluted with EtOAc (50 mL) and the organic phase washed with 2M aqueous KOH (2 x 30 mL) solution. The organic phase was dried over $MgSO_4$, and the solvent reduced *in vacuo*. The product was purified by column chromatography over silica gel (20% EtOAc, 80% hexane) to afford a yellow liquid. 168 mg, 94% yield. R_f: 0.67 (20% EtOAc, 80% hexane); ^{1}H NMR (300 MHz, CHLOROFORM-*d*) *δ* ppm 3.86 (s, 3 H), 4.24 (br. s., 2 H), 6.23 (dd, *J*=8.1, 0.9 Hz, 1 H), 6.42 (dd, *J*=8.1, 1.2 Hz, 1 H), 7.04 – 7.13 (m, 1 H); ^{13}C NMR (75 MHz, CHLOROFORM-*d*) *δ* ppm 56.2, 75.8, 100.3, 107.7, 129.4, 148.2, 158.6; Characterization data corresponded with literature values.[15]

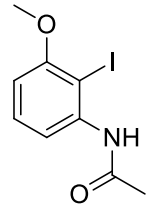

(74) *N*-(2-Iodo-3-methoxyphenyl)acetamide

To a solution of **(73)** (168 mg, 0.676 mmol) in DCM (3 mL) was added acetic anhydride (95.8 µL, 1.01 mmol) dropwise at 0 °C under an atmosphere of nitrogen. After the solution was stirred for four hours, a saturated solution of aqueous NH_4Cl (3 mL) was added and stirred for 10 minutes. The product was extracted with EtOAc (2 x 30 mL), after which the organic phase was washed with brine, dried over $MgSO_4$ and the solvent reduced *in vacuo*. The product was purified by column chromatography over silica gel (30% EtOAc, 70% hexane) to afford a yellow solid. 115 mg, 58% yield. R_f: 0.27 (30% EtOAc, 70% hexane); ^{1}H NMR (300 MHz, CHLOROFORM-*d*) *δ* ppm 2.28 (s, 3 H), 3.91 (s, 3 H), 6.62 (d, *J*=8.4 Hz, 1 H), 7.26 – 7.35 (m, 1 H), 7.63 (br. s., 1 H), 7.91 (d, *J*=7.9 Hz, 1 H); ^{13}C NMR (101 MHz, CHLOROFORM-*d*) *δ* ppm 25.0, 56.6, 77.2, 106.7, 114.4, 130.3, 139.6, 158.2, 168.3, Mp: 72 – 73 °C; IR ATR (cm^{-1}): 3234, 2922, 1704, 1573, 1465, 1366, 1245, 1366, 1018.

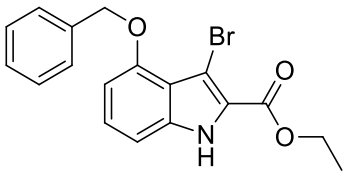

(75) Ethyl 4-(benzyloxy)-3-bromo-1*H*-indole-2-carboxylate

To a solution of **(24)** (1.14 g, 3.87 mmol) in DMF (15 mL) was added NBS (178 mg, 4.25 mmol, dissolved in 2 mL DMF) dropwise and stirred for 1 hour at 0 °C. The reaction mixture was diluted with EtOAc (100 mL), and washed with water (4 x 100 mL), followed by a wash with brine. The organic

layer was dried over $MgSO_4$ and reduced *in vacuo*. The compound was purified by column chromatography over silica gel (25% EtOAc, 75% hexane) to afford the product as a white solid. 1.17 g, 80 % yield. R_f: 0.44 (25% EtOAc, 75% hexane); ^{1}H NMR (300 MHz, CHLOROFORM-*d*) *δ*ppm 1.46 (t, *J*=7.04 Hz, 3 H), 4.45 (q, *J*=7.19 Hz, 2 H), 5.26 (s, 2 H), 6.61 (dd, *J*=7.78, 0.6 Hz, 1 H), 7.01 (dd, *J*=8.36, 0.7 Hz, 1 H), 7.24 (dd, *J*=8.36, 7.78 Hz, 1 H), 7.30 – 7.45 (m, 3 H), 7.57 – 7.64 (m, 2 H), 8.98 (br. s., 1 H) ^{13}C NMR (75 MHz, CHLOROFORM-*d*) *δ* ppm 14.4, 61.4, 70.2, 95.9, 102.2, 105.2, 118.0, 123.3, 127.1 (2 C), 127.2, 127.7, 128.4 (2 C), 136.9, 137.2, 154.2, 161.1; HRMS–ESI+: m/z $[M+H]^+$ calculated for $C_{18}H_{17}NO_3Br$: 374.0392; found: 374.0398; Mp: 164 – 166 °C; IR ATR (cm^{-1}): 3307, 1676, 1576, 1507, 1249, 1199, 1099.

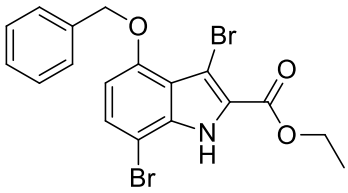

Ethyl 4-(benzyloxy)-3,7-dibromo-1*H*-indole-2-carboxylate

Compound **(77)** was formed as a byproduct during the bromination of **(24)** to produce **(75)** and isolated after purification of another reaction starting with 1.40 g of **(24)**. 310 mg, 14 % yield. R_f: 0.41 (25% EtOAc, 75% hexane); ^{1}H NMR (300 MHz, CHLOROFORM-*d*) *δ* ppm 1.47 (t, *J*=7.2 Hz, 3 H), 4.48 (q, *J*=7.2 Hz, 2 H), 5.23 (s, 2 H), 6.52 (d, *J*=8.4 Hz, 1 H), 7.28 – 7.45 (m, 4 H), 7.51 – 7.65 (m, 2 H), 9.00 (br. s., 1 H); ^{13}C NMR (75 MHz, CHLOROFORM-*d*) *δ* ppm 14.3, 61.5, 70.3, 96.3, 96.6, 103.6, 118.5, 123.9, 127.0 (2 C), 127.8, 128.4 (2 C), 128.8, 135.0, 136.4, 153.6, 160.4; HRMS–ESI+: m/z $[M+H]^+$ calculated for $C_{18}H_{16}NO_3Br_2$: 451.9497; found: 451.9502; Mp:145 – 148°C; IR ATR (cm^{-1}): 3275, 1688, 1513, 1330, 1262, 1235, 1190, 1101.

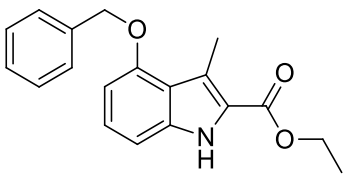

(76) Ethyl 4-(benzyloxy)-3-methyl-1*H*-indole-2-carboxylate

In a flask containing **(75)** (1.00g, 4.74 mmol), K_2CO_3 (1.97 g, 14.2 mmol), $Pd(PPh_3)_4$ (548 mg, 0.474 mmol) and trimethylboroxine (729 µL, 5.21 mmol), was added 24 mL dioxane under an atmosphere of nitrogen and stirred at 110 °C for 6 h followed by stirring at room temperature overnight. The reaction mixture was filtered through a plug of Celite and the solvent reduced *in vacuo*. The compound was purified by column chromatography over silica gel (15% EtOAc, 85% hexane) to afford the product as a white solid. 725 mg, 87%. R_f: 0.37 (15% EtOAc, 85% hexane); ^{1}H NMR (300 MHz, CHLOROFORM-*d*) *δ* ppm 1.43 (t, *J*=7.0 Hz, 3 H), 2.84 (s, 3 H), 4.42 (q, *J*=7.0 Hz, 2 H), 5.22 (s, 2 H), 6.54 (d, *J*=7.8 Hz, 1 H), 6.97 (dd, *J*=8.3, 0.7Hz, 1 H), 7.16 – 7.22 (m, 1 H), 7.33 – 7.46 (m, 3 H), 7.50 – 7.56 (m, 2 H), 8.63 (br. s., 1 H); ^{13}C NMR (75

MHz, CHLOROFORM-*d*) *δ* ppm 12.4, 14.5, 60.6, 69.9, 100.6, 104.9, 119.0, 121.5, 122.3, 126.4, 127.3 (2 C), 127.8, 128.6 (2 C), 137.2, 137.7, 155.7, 162.7; HRMS–ESI+: m/z $[M+H]^+$ calculated for $C_{19}H_{20}NO_3$: 310.1443; found: 310.1445; Mp: 149 – 150 °C; IR ATR (cm^{-1}): 3323 2916, 1661, 1351, 1246, 1198, 1099.

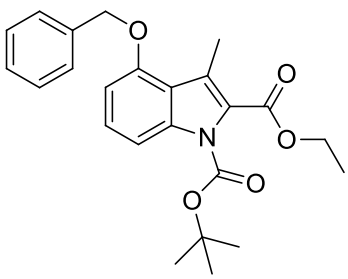

(77) 1-*tert*-Butyl 2-ethyl 4-(benzyloxy)-3-methyl-1*H*-indole-1,2-dicarboxylate

To a solution of **(76)** (826 mg, 2.67 mmol) and DMAP (20 mg, 0.164 mmol) in DCM (10 mL) was added Boc_2O (680 mg, 3.20 mmol, dissolved in 2 mL DCM) dropwise and stirred for 3 hours. The solvent was reduced *in vacuo* and the product purified by column chromatography over silica gel (10% EtOAc, 90% hexane) to afford the product as a white solid. 1.09 g, 99% yield. R_f: 0.43 (10% EtOAc, 90% hexane); ^{1}H NMR (300 MHz, CHLOROFORM-*d*) *δ* ppm 1.41 (t, *J*=7.1 Hz, 3 H), 1.64 (s, 9 H), 2.60 (s, 3 H), 4.41 (q, *J*=7.2 Hz, 2 H), 5.19 (s, 2 H), 6.72 (d, *J*=7.9 Hz, 1 H), 7.26 – 7.32 (m, 1 H), 7.32 – 7.53 (m, 5 H), 7.71 (d, *J*=8.4 Hz, 1 H); ^{13}C NMR (75 MHz, CHLOROFORM-*d*) *δ* ppm 11.9, 14.2, 27.9 (3 C), 61.1, 70.0, 84.1, 104.6, 107.9, 119.0, 123.6, 125.7, 127.2 (2 C), 127.4, 127.8, 128.5 (2 C), 136.8, 138.3, 149.5, 154.6, 162.7.

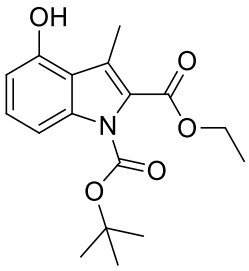

(78) Ethyl 4-hydroxy-3-methyl-1*H*-indole-2-carboxylate

(77) (1090 mg, 2.66 mmol) and Pd/C (10%, 245 mg, 0229 mmol) was placed in a flask, evacuated and purged with hydrogen from a balloon, to which was added EtOH (10 mL) and stirred overnight at room temperature under an atmosphere of hydrogen. The mixture was filtered through a plug of Celite and the solvent reduced *in vacuo*. The product was purified by column chromatography over silica gel (30% EtOAc, 70% hexane) to afford the product as a white solid. 296 mg, 36% yield. R_f: 0.50 (30% EtOAc, 70% hexane); ^{1}H NMR (300 MHz, CHLOROFORM-*d*) *δ* ppm 1.41 (t, *J*=7.2 Hz, 3 H), 1.62 (s, 9 H), 2.60 (s, 3 H), 4.43 (q, *J*=7.1 Hz, 2 H), 6.58 (dd, *J*=7.8, 0.7 Hz, 1 H), 6.73 (s, 1 H), 7.09 – 7.19 (m, 1 H), 7.58 (dd, *J*=8.4, 0.7 Hz, 1 H); ^{13}C NMR (75 MHz, CHLOROFORM-*d*) *δ* ppm 11.6, 14.2, 28.0 (3 C), 61.5, 84.3, 107.1, 108.5, 118.0, 124.4, 125.4, 127.7, 138.8, 149.7, 152.2, 163.5.

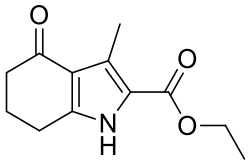

(80) Ethyl 3-methyl-4-oxo-4,5,6,7-tetrahydro-1*H*-indole-2-carboxylate

(76) (50 mg, 0.162 mmol) and Pd/C (10%, 10 mg, 0.009 mmol) was placed in a flask, evacuated and purged with hydrogen from a balloon, after which DMF/EtOH (3 mL, 50:50) was added. The mixture was stirred overnight under hydrogen atmosphere. The mixture was filtered through a plug of Celite, and the solvent reduced *in vacuo*. The product was purified by column chromatography over silica gel (25% EtOAc, 75% hexane) to afford the product as a white powder. 36 mg, >99% yield. R_f: 0.46 (25% EtOAc, 75% hexane); ^{1}H NMR (300 MHz, CHLOROFORM-*d*) δ ppm 1.34 (t, *J*=6.9 Hz, 3 H), 2.03 – 2.17 (m, 2 H), 2.38 – 2.50 (m, 2 H), 2.58 (s, 3 H), 2.76 – 2.91 (m, 2 H), 4.31 (q, *J*=7.0 Hz, 2 H), 10.29 (br. s., 1 H); ^{13}C NMR (75 MHz, CHLOROFORM-*d*) δ ppm 11.5, 14.4, 23.0, 23.4, 38.9, 60.5, 119.6, 120.3, 128.5, 145.5, 162.3, 195.4; HRMS–ESI+: m/z $[M+H]^+$ calculated for $C_{12}H_{16}NO_3$: 222.1130; found: 222.1089; Mp: 162 – 165 °C; IR ATR (cm^{-1}): 3155, 1686, 1635, 1511, 1319, 1263, 1177, 1098; Characterization data corresponded with literature values.[16]

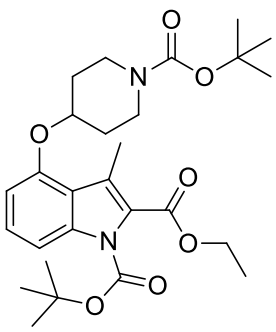

(79) 1-*tert*-Butyl 2-ethyl 4-((1-(*tert*-butoxycarbonyl)piperidin-4-yl)oxy)-3-methyl-1*H*-indole-1,2-dicarboxylate

(78) (238 mg, 0.745 mmol), PPh_3 (294 mg, 1.12 mmol) and 1-Boc-4-hydroxypiperdine were dissolved in THF (4.7 mL) after which DBAD (258 mg, 1.12 mmol, dissolved in 1mL THF) was dropwise at 0 °C under an atmosphere of nitrogen, and stirred overnight. The solvent was reduced *in vacuo* and the product purified by column chromatography over silica gel (15% EtOAc, 85% hexane) to afford the product as a semi solid. 352 mg, 94% yield. R_f: 0.44 (15% EtOAc:85% hexane); ^{1}H NMR (400 MHz, CHLOROFORM-*d*) δ ppm 1.38 (t, *J*=7.0 Hz, 3 H), 1.45 (s, 9 H), 1.59 (s, 9 H), 1.79 – 1.90 (m, 2 H), 1.90 – 2.01 (m, 2 H), 2.55 (s, 3 H), 3.43 – 3.53 (m, 2 H), 3.55 – 3.66 (m, 2 H), 4.37 (q, *J*=7.3 Hz, 2 H), 4.61 – 4.69 (m, 1 H), 6.62 (d, *J*=8.2 Hz, 1 H), 7.19 – 7.29 (m, 1 H), 7.64 (d, *J*=8.2 Hz, 1 H); ^{13}C NMR (75 MHz, CHLOROFORM-*d*) δ ppm 12.0, 14.0, 27.7 (3 C), 28.2 (3 C), 30.1 (2 C), 40.1 (2 C), 60.9, 71.4, 79.3, 83.9, 105.0, 107.4, 119.3, 123.2, 125.6, 127.2, 138.4, 149.2, 152.8, 154.5, 162.5; HRMS-TOF MS ES+: m/z $[M+H]^+$ calculated for $C_{27}H_{39}N_2O_7$: 503.2757; found: 503.2758; IR ATR (cm^{-1}): 2978, 1723, 1692, 1592, 1214, 1156, 1096, 1024.

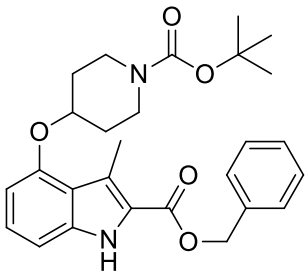

(81) Benzyl 4-((1-(*tert*-butoxycarbonyl)piperidin-4-yl)oxy)-3-methyl-1*H*-indole-2-carboxylate

(79) (80 mg, 0.159 mmol), K_3PO_4 (119 mg, 0.48 mmol) and benzyl alcohol (500 µL, 4.85 mmol) were added to a vial. The vial was sealed and the mixture stirred at 120 °C for 10 hours. The K_3PO_4 was filtered off, and the alcohol removed via heating the solution to 50 °C and streaming compressed air over the solution. After the majority of the solvent volume had been evaporated off, the product was purified by column chromatography over silica gel (5% EtOAc, 95% DCM) to afford the product as a white solid. 28 mg, 38% yield. R_f: 0.61 (5% EtOAc, 95% DCM) (^{1}H NMR (300 MHz, CHLOROFORM-*d*) *δ* ppm 1.53 (s, 9 H), 1.85 – 2.06 (m, 4 H), 2.85 (s, 3 H), 3.56 (s, 2 H), 3.59 – 3.70 (m, 2 H), 4.64 – 4.75 (m, 1 H), 5.40 (s, 2 H), 6.45 (d, *J*=8.2 Hz, 1 H), 6.90 (d, *J*=8.2 Hz, 1 H), 7.13 – 7.20 (m, 1 H), 7.28 – 7.52 (m, 5 H), 8.73 (br. s., 1 H); ^{13}C NMR (75 MHz, CHLOROFORM-*d*) *δ* ppm 12.5, 28.4 (3 C), 30.2 (2 C), 40.3 (2 C), 66.3, 71.2, 79.6, 101.1, 104.5, 119.4, 121.9, 121.9, 126.5 (2 C), 126.9, 128.3, 128.6 (2 C), 135.9, 137.9, 154.0, 154.8, 162.2; HRMS-TOF MS ES+: m/z $[M+Na]^+$ calculated for $C_{27}H_{32}N_2O_5Na$: 488.2287; found: 488.2231; Mp: 121 – 124 °C, IR ATR (cm^{-1}): 3337, 2928, 1668, 1580, 1511, 1422, 1248, 1229, 1090.

Compounds **(82)** – **(85)** were synthesized via the same procedure. Compound **(79)** and the aromatic amine used for the amidation reaction (30 equivalents) were placed in a vial. The vial was purged with argon, sealed and heated to 140 °C for 30 hours. The reaction was monitored via TLC using (50% EtOAc, 50% hexane) as mobile phase to determine whether the starting material has been consumed. The product was purified by column chromatography over silica gel (30% EtOAc, 70% hexane to 100% EtOAc).

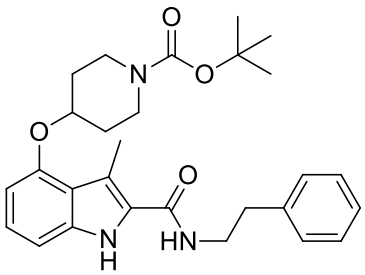

(82) *tert*-Butyl 4-((3-methyl-2-(phenethylcarbamoyl)-1*H*-indol-4-yl)oxy)piperidine-1-carboxylate

21 mg, 34% yield, yellow solid. R_f: 0.35 (30% EtOAc, 70% hexane); ^{1}H NMR (300 MHz, CHLOROFORM-*d*) *δ* ppm 1.51 (s, 9 H), 1.83 – 1.95 (m, 2 H), 1.95 – 2.07 (m, 2 H), 2.59 (s, 3 H), 2.99 (t, *J*=6.7 Hz, 2 H), 3.41 – 3.54 (m, 2 H), 3.62 – 3.74 (m, 2 H), 3.83 (q, *J*=6.5 Hz, 2 H), 4.64 – 4.72 (m, 1 H), 6.04 (t, *J*=5.3 Hz, 1 H), 6.46 (d, *J*=7.6 Hz, 1 H), 6.97 (d, *J*=7.6 Hz, 1

H), 7.09 – 7.16 (m, 1 H), 7.23 – 7.40 (m, 5 H), 9.29 (br. s, 1 H); ^{13}C NMR (75 MHz, CHLOROFORM-*d*) *δ* ppm 12.1, 28.4 (3 C), 30.4 (2 C), 35.6, 40.6 (2 C), 40.8, 71.5, 79.6, 101.2, 104.7, 112.5, 119.2, 125.1, 126.4, 126.7 (2 C), 128.5, 128.8 (2 C), 137.1, 138.7, 153.5, 154.8, 162.6; HRMS-TOF MS ES+: m/z $[M+H]^+$ calculated for $C_{28}H_{36}N_3O_4$: 478.2706; found: 478.2710; Mp: 168 – 170 °C, IR ATR (cm^{-1}): 3253, 2929, 1681, 1627, 1545, 1422, 1259, 1098.

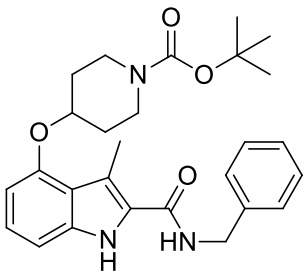

(83) *tert*-Butyl 4-((2-(benzylcarbamoyl)-3-methyl-1*H*-indol-4-yl)oxy)piperidine-1-carboxylate

17 mg, 28% yield, yellow solid. R_f: 0.29 (30% EtOAc, 70% hexane); ^{1}H NMR (300 MHz, CHLOROFORM-*d*) *δ* ppm 1.48 (s, 9 H), 1.82 – 2.02 (m, 4 H), 2.79 (s, 3 H), 3.42 – 3.55 (m, 2 H), 3.57 – 3.71 (m, 2 H), 4.63 – 4.75 (m, 3 H), 6.38 (t, *J*=5.3 Hz, 1 H), 6.46 (d, *J*=7.6 Hz, 1 H), 6.93 (d, *J*=8.2 Hz, 1 H), 7.09 – 7.16 (m, 1 H), 7.25 – 7.41 (m, 5 H), 9.28 (s, 1 H); ^{13}C NMR (75 MHz, CHLOROFORM-*d*) *δ* ppm 12.7, 28.5 (3 C), 30.4 (2 C), 40.4 (2 C), 43.8, 71.4), 79.7, 101.4, 104.8, 113.0, 119.3, 125.3, 126.2, 127.6 (2 C), 128.6, 128.9 (2 C), 137.2, 138.2, 153.6, 154.9, 162.7; HRMS-TOF MS ES+: m/z $[M+Na]^+$ calculated for $C_{27}H_{33}N_3O_4Na$: 486.2369; found: 486.2361; Mp: 171 – 174 °C, IR ATR (cm^{-1}): 3282, 2932, 1694, 1633, 1542, 1462, 1255, 1231, 1091.

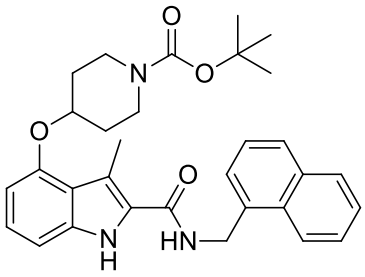

(84) *tert*-Butyl 4-((3-methyl-2-((naphthalen-1-ylmethyl)carbamoyl)-1*H*-indol-4-yl)oxy)piperidine-1-carboxylate

30 mg, 37% yield, yellow solid. R_f: 0.54 (40% EtOAc, 60% hexane); ^{1}H NMR (400 MHz, CHLOROFORM-*d*) *δ* ppm 1.46 (s, 9 H), 1.80 – 1.90 (m, 2 H), 1.90 – 2.02 (m, 2 H), 2.66 (s, 3 H), 3.40 – 3.52 (m, 2 H), 3.54 – 3.65 (m, 2 H), 4.63 – 4.69 (m, 1 H), 5.16 (d, *J*=5.5 Hz, 2 H), 6.28 (t, *J*=5.1 Hz, 1 H), 6.45 (d, *J*=7.8 Hz, 1 H), 6.95 (d, *J*=8.2 Hz, 1 H), 7.09 – 7.15 (m, 1 H), 7.44 – 7.61 (m, 4 H), 7.86 (d, *J*=8.2 Hz, 1 H), 7.89 – 7.93 (m, 1 H), 8.11 (d, *J*=8.2 Hz, 1 H), 9.05 (br. s, 1 H); ^{13}C NMR (101 MHz, CHLOROFORM-*d*) *δ* ppm 12.5, 28.4 (3 C), 30.3 (2 C), 40.6 (2 C), 42.1, 71.3, 79.6, 101.4, 104.7, 113.0, 119.3, 123.3, 125.3, 125.4, 126.1, 126.2, 126.6, 126.7, 128.8, 128.9, 131.3, 133.3, 134.0, 137.1, 153.5, 154.8, 162.3; HRMS-TOF MS ES+: m/z $[M+Na]^+$ calculated for $C_{31}H_{35}N_3O_4Na$: 536.2525; found: 536.2541, Mp: 220 – 224 °C, IR ATR (cm^{-1}): 3287, 2922, 1682,1617, 1540, 1505, 1426, 1365, 1230, 1092.

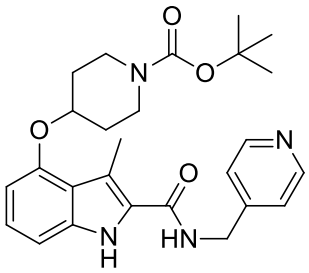

(85) *tert*-Butyl 4-((3-methyl-2-((pyridin-4-ylmethyl)carbamoyl)-1*H*-indol-4-yl)oxy)piperidine-1-carboxylate

16.2 mg, 29% yield, yellow solid. R_f: 0.50 (5% MeOH, 95% DCM); ^{1}H NMR (300 MHz, CHLOROFORM-*d*) δ ppm 1.48 (s, 9 H), 1.82 – 2.06 (m, 4 H), 2.84 (s, 3 H), 3.42 - 3.55 (m, 2 H), 3.59 - 3.71 (m, 2 H), 4.64 – 4.76 (m, 3 H), 6.46 (d, *J*=7.6 Hz, 1 H), 6.59 (t, *J*=5.9 Hz, 1 H), 6.91 (d, *J*=8.2 Hz, 1 H), 7.09 – 7.16 (m, 1 H), 7.27 (d, *J*=5.9 Hz, 2 H), 8.56 (d, *J*=5.9 Hz, 2 H), 9.38 (br. s, 1 H); ^{13}C NMR (75 MHz, CHLOROFORM-*d*) δ ppm 13.1, 28.8 (3 C), 30.8 (2 C), 40.6 (2 C), 42.9, 71.9, 80.1, 101.8, 105.1, 106.6, 119.7, 122.6 (2 C), 126.0, 126.1, 137.8, 148.0, 150.4 (2 C), 154.0, 155.2, 163.3; HRMS-TOF MS ES+: m/z $[M+H]^+$ calculated for $C_{26}H_{33}N_4O_4$: 465.2502; found: 465.2492; Mp: 196 – 199 °C, IR ATR (cm^{-1}): 3290, 2929, 1698, 1636, 1553, 1408, 1349, 1253, 1091.

Compounds **IM2** and **IM4 – IM7** were synthesized via the same procedure. In a small flask was added the Boc-protected compound **(81)** – **(85)** separately dissolved in DCM (1 mL) followed by the addition of 4M HCl/dioxane (1 mL). The solution was stirred for one hour, after which the solvent was reduced *in vacuo*. A small amount of DCM was added followed by the addition of EtOAc which caused the salt to precipitate out of solution. The solvent was reduced *in vacuo* and the product dried under vacuum.

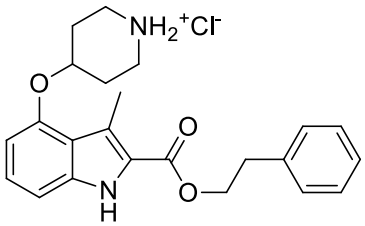

(IM1) 4-((3-Methyl-2-(phenethoxycarbonyl)-1*H*-indol-4-yl)oxy)piperidin-1-ium chloride

In a vial was added **(79)** (80 mg, 0.159 mmol), K_3PO_4 (110 mg, 0.518 mmol) and 2-phenyl ethanol (400 µL, 1.00 mmol) and stirred neat at 100 °C overnight. The mixture was dissolved in DCM (3 mL) and the K_3PO_4 filtered of. The solvent was reduced *in vacuo* and the crude residue redissolved in DCM (1 mL) to which 4M HCl/dioxane (1 mL) was added and stirred for 2 hours. The solvent was reduced *in vacuo* and the product was purified by column chromatography over silica gel using gradient elution (100% DCM to 10% MeOH, 90% DCM) to afford the product as a white solid. 12.3 mg, 19% yield over two steps. ^{1}H NMR (400 MHz, DMSO-d_6) δ ppm 1.89 – 2.02 (m, 2 H), 2.10 – 2.23 (m, 2 H), 2.67 (s, 3 H), 3.06 (t, *J*=6.8 Hz, 2 H), 3.08 – 3.24 (m, 4 H), 4.50 (t, *J*=6.8 Hz,

2 H), 4.76 – 4.84 (m, 1 H), 6.55 (d, *J*=7.8 Hz, 1 H), 6.97 (d, *J*=8.2 Hz, 1 H), 7.08 – 7.14 (m, 1 H), 7.19 – 7.38 (m, 5 H), 8.87 – 9.20 (m, 2 H), 11.42 (s, 1 H); ^{13}C NMR (101 MHz, DMSO-d_6) δ ppm 12.1, 27.0 (2 C), 34.5, 40.3 (2 C), 64.7, 68.6, 101.1, 105.5, 118.4, 119.0, 122.0, 125.8, 126.4, 128.4 (2 C), 128.9 (2 C), 138.1, 138.3, 152.8, 161.8; HRMS-TOF MS ES+: m/z $[M+H]^+$ calculated for $C_{23}H_{27}N_2O_3$: 379.2022; found: 379.2013; Purity: 77.1%; Mp: 188 – 191 °C, IR ATR (cm^{-1}): 3345, 2926, 1681, 1615, 1579, 1453, 1356, 1243, 1087.

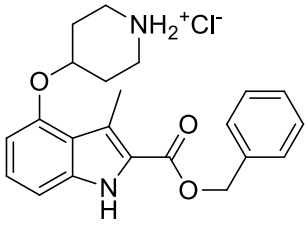

(IM2) 4-((2-((Benzyloxy)carbonyl)-3-methyl-1*H*-indol-4-yl)oxy) piperidin-1-ium chloride

28 mg, 38% yield, white powder. ^{1}H NMR (400 MHz, DMSO-d_6) δ ppm 1.91 – 2.02 (m, 2 H), 2.11 – 2.21 (m, 2 H), 2.72 (s, 3 H), 3.06 – 3.23 (m, 4 H), 4.75 – 4.83 (m, 1 H), 5.35 (s, 2 H), 6.53 (d, *J*=7.8 Hz, 1 H), 6.96 (d, *J*=8.2 Hz, 1 H),7.09 – 7.15 (m, 1 H), 7.29 – 7.51 (m, 5 H), 8.95 – 9.35 (m, 2 H), 11.47 (s, 1 H); ^{13}C NMR (101 MHz, DMSO-d_6) δ ppm 12.2, 26.8 (2 C), 40.1 (2 C), 65.4, 68.3, 101.1, 105.6, 118.4, 119.5, 121.7, 125.9, 127.9 (2 C), 128.0, 128.5 (2 C), 136.3, 138.3, 152.7, 161.5; HRMS-TOF MS ES+: m/z $[M+H]^+$ calculated for $C_{22}H_{25}N_2O_3$: 365.1865; found: 365.1859; Purity: > 98%; Mp: 220 – 222 °C, IR ATR (cm^{-1}): 3178, 2956, 1702, 1577, 1353, 1240, 1084.

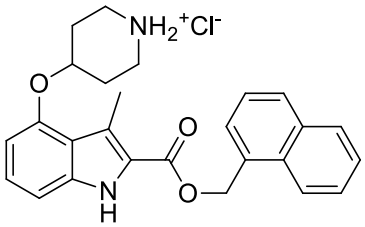

(IM3) 4-((3-Methyl-2-((naphthalen-1-ylmethoxy)carbonyl)-1*H*-indol-4-yl)oxy)piperidin-1-ium chloride

In a vial was added **(79)** (57 mg, 0.114 mmol), K_3PO_4 (88.0 mg, 0.426 mmol) and naphthalen-1-yl-methanol (242 mg, 1.53 mmol) and stirred at 100 °C overnight. The mixture was dissolved in DCM (3 mL) and the K_3PO_4 filtered off. The solvent was reduced *in vacuo* and the crude dissolved in DCM (1 mL) to which 4M HCl/dioxane (1 mL) was added and stirred for 2 hours. The solvent was reduced *in vacuo* and the product was purified by column chromatography over silica gel using a gradient elution (100% DCM to 10% MeOH,90% DCM) to afford the product as a white solid. 25.1 mg, 49% yield. ^{1}H NMR (400 MHz, DMSO-d_6) δ ppm 1.88 – 2.00 (m, 2 H), 2.07 – 2.20 (m, 2 H), 2.68 (s, 3 H), 3.02 – 3.20 (m, 4 H), 4.73 – 4.84 (m, 1 H), 5.83 (s, 2 H), 6.53 (d, *J*=7.8 Hz, 1 H), 6.96 (d, *J*=8.2 Hz, 1 H), 7.07 – 7.14 (m, 1 H), 7.50 – 7.66 (m, 3 H), 7.71 (d, *J*=6.6 Hz, 1 H), 7.93 – 8.03 (m, 2 H), 8.16 (d, *J*=8.2 Hz, 1 H), 8.96 (br. s, 2 H), 11.45 (s, 1 H); ^{13}C NMR (101 MHz, DMSO-d_6) δ ppm 12.6, 27.4 (2 C), 40.7 (2 C), 64.3, 69.0, 101.6, 106.0, 118.9, 120.0, 122.2, 124.1, 125.9, 126.3, 126.5,

127.1, 127.8, 129.0, 129.4, 131.5, 132.2, 133.7, 138.8, 153.2, 162.1; HRMS-TOF MS ES+: m/z $[M+H]^+$ calculated for $C_{26}H_{27}N_2O_3$: 415.2022; found: 415.2010; Purity: > 98%; Mp: 197 – 200 °C, IR ATR (cm^{-1}): 3338, 2927, 1682, 1578, 1509, 1357, 1254, 1086.

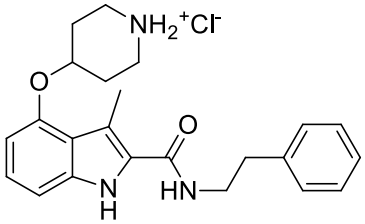

(IM4) 4-((3-Methyl-2-(phenethylcarbamoyl)-1*H*-indol-4-yl)oxy)piperidin-1-ium chloride

13.3 mg, 73 %, yellow solid. ^{1}H NMR (400 MHz, DMSO-d_6) δ ppm 1.89 – 2.02 (m, 2 H), 2.08 – 2.24 (m, 2 H), 2.66 (s, 3 H), 2.86 (t, *J*=7.4 Hz, 2 H), 3.05 – 3.27 (m, 4 H), 3.46 – 3.53 (m, 2 H), 4.73 – 4.81 (m, 1 H), 6.51 (d, *J*=7.8 Hz, 1 H), 6.92 (d, *J*=8.2 Hz, 1 H), 7.01 – 7.08 (m, 1 H), 7.13 – 7.32 (m, 5 H), 8.12 (t, *J*=5.3 Hz, 1 H), 8.94 – 9.23 (m, 2 H), 11.37 (s, 1 H); ^{13}C NMR (101 MHz, DMSO-d_6) δ ppm 12.0, 26.9 (2 C), 35.1, 40.2 (2 C), 40.5, 68.2, 101.1, 105.2, 114.1, 118.4, 124.3, 126.1, 126.5, 128.3 (2 C), 128.6 (2 C), 137.2, 139.5, 152.4, 161.9; HRMS-TOF MS ES+: m/z $[M+H]^+$ calculated for $C_{23}H_{28}N_3O_2$: 378.2182; found: 378.2174; Purity: 98.0%; Mp: 125 – 129 °C, IR ATR (cm^{-1}): 3267, 2923, 1618, 1560, 1506, 1453, 1354, 1249, 1086.

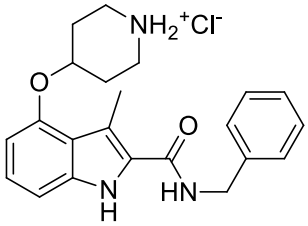

(IM5) 4-((2-(Benzylcarbamoyl)-3-methyl-1*H*-indol-4-yl)oxy)piperidin-1-ium chloride

9.1 mg, 62% yield, yellow solid. ^{1}H NMR (400 MHz, DMSO-d_6) δ ppm 1.90 – 2.05 (m, 2 H), 2.08 – 2.26 (m, 2 H), 2.72 (s, 3 H), 3.15 (br. s., 4 H), 4.49 (d, *J*=5.5 Hz, 1 H), 4.80 (br. s., 1 H), 6.54 (d, *J*=7.4 Hz, 1 H), 6.94 (d, *J*=8.2 Hz, 1 H), 7.00 – 7.12 (m, 1 H), 7.19 – 7.42 (m, 5 H), 8.60 (t, *J*=5.7 Hz, 1 H), 8.90 – 9.25 (m, 2 H), 11.42 (s, 1 H); ^{13}C NMR (101 MHz, DMSO-d_6) δ ppm 12.1, 26.8 (2 C), 40.2 (2 C), 42.2, 68.2, 101.2, 105.2, 114.5, 118.5, 124.4, 126.3, 126.5, 127.4 (2 C), 128.2 (2 C), 137.2, 139.6, 152.4, 161.9; HRMS-TOF MS ES+: m/z $[M+H]^+$ calculated for $C_{22}H_{26}N_3O_2$: 364.2025; found: 364.2032; Purity: 97.7%; Mp: 128 – 131 °C, IR ATR (cm^{-1}): 3316, 2923, 1619, 1585, 1506, 1453, 1356, 1250, 1086.

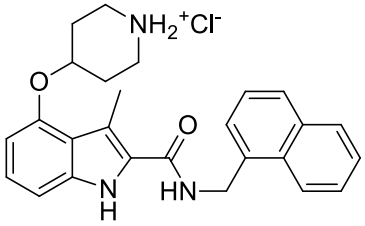

(IM6) 4-((3-Methyl-2-((naphthalen-1-ylmethyl)carbamoyl)-1*H*-indol-4-yl)oxy)piperidin-1-ium chloride

9.1 mg, 62 % yield, yellow solid. ^{1}H NMR (400 MHz, DMSO-d_6) δ ppm 1.91 – 2.01 (m, 2 H), 2.10 – 2.22 (m, 2 H), 2.72 (s, 3 H), 3.09–3.26 (m, 4 H), 4.75 – 4.83 (m, 1 H), 4.96 (d, *J*=5.5 Hz, 2 H), 6.54 (d, *J*=7.8 Hz, 1 H), 6.92 (d, *J*=8.2 Hz, 1 H), 7.02 – 7.09 (m, 1 H), 7.47 – 7.62 (m, 4 H), 7.88 (d, *J*=8.2 Hz, 1 H), 7.94 – 7.99 (m, 1 H), 8.19 (d, *J*=7.8 Hz, 1 H), 8.49 (t, *J*=5.7 Hz, 1 H), 8.68 – 9.02 (m, 2 H), 11.30 (s, 1 H); ^{13}C NMR (101 MHz, DMSO-d_6) δ ppm 12.1, 26.8 (2 C), 40.2 (2 C), 40.3, 68.2, 101.2, 105.1, 114.9, 118.5, 123.5, 124.5, 125.4, 125.6, 125.8, 126.1, 126.2, 127.5, 128.5, 130.9, 133.3, 134.6, 137.2, 152.4, 161.8; HRMS-TOF MS ES+: m/z $[M+H]^+$calculated for $C_{26}H_{28}N_3O_2$: 414.2182; found: 414.2185; Purity: 96.4%; Mp: 227 – 230 °C, IR ATR (cm^{-1}): 3268, 2924, 1614, 1537, 1505, 1439, 1358, 1249, 1105.

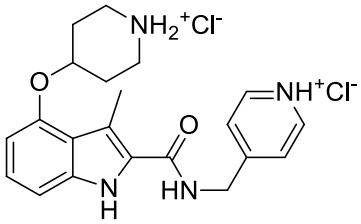

(IM7) 4-((3-methyl-4-(piperidin-1-ium-4-yloxy)-1*H*-indole-2-carboxamido)methyl)pyridin-1-ium chloride

8 mg, 57% yield, yellow solid. ^{1}H NMR (400 MHz, DMSO-d_6) δ ppm 1.93 – 2.04 (m, 2 H), 2.12 – 2.24 (m, 2 H), 2.73 (s, 3 H), 3.15 (br. s., 4 H), 4.74 (d, *J*=5.9 Hz, 2 H), 4.81 (br. s., 1 H), 6.56 (d, *J*=7.8 Hz, 1 H), 6.95 (d, *J*=8.2 Hz, 1 H), 7.06 – 7.12 (m, 1 H), 7.96 – 8.05 (m, 2 H), 8.82 – 8.90 (m, 2 H), 9.11 – 9.34 (m, 3 H), 11.76 (s, 1 H); ^{13}C NMR (101 MHz, DMSO-d_6) δ ppm 12.6, 27.3 (2 C), 42.4 (2 C), 43.5, 68.8, 101.7, 105.7, 116.1, 118.9, 125.3, 125.3 (2 C), 126.0, 137.9, 142.1 (2 C), 153.0, 160.5, 162.9; HRMS-TOF MS ES+: m/z $[M+H]^+$ calculated for $C_{21}H_{25}N_4O_2$: 365.1978; found: 365.1982; Purity: >98%; Mp: decomposition, IR ATR (cm^{-1}): 3257, 2924, 2609, 1637, 1612, 1543, 1504, 1248.

10.4 Synthesis of compounds pertaining to Chapter 4

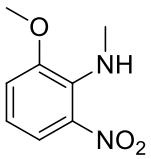

(86) 2-Methoxy-*N*-methyl-6-nitroaniline

To a mixture of NaH (130 mg, 60% dispersion in oil, 3.27 mmol) in THF (10 mL) was added (**71)** (500 mg, 2.97 mmol, dissolved in 2 mL THF) dropwise at -10 °C under an atmosphere of nitrogen. The mixture was stirred for 30 minutes after which MeI (203.5 µL, 3.27 mmol) was added. The mixture was allowed to reach room temperature and stirred overnight. The mixture was quenched with water (10 mL) and the product was extracted with EtOAc (2 x 60 mL) and washed with brine. The organic phase was dried over $MgSO_4$ and the solvent was removed *in vacuo*. The product was purified by column chromatography over silica gel (20% EtOAc, 80% hexane) to afford a red solid. 301 mg, 56% yield. R_f: 0.63 (20% EtOAc, 80% hexane) ^{1}H NMR (300 MHz, CHLOROFORM-*d*) *δ* ppm 3.17 (s, 3 H), 3.84 (s, 3 H), 6.57 – 6.65 (m, 1 H), 6.90 (dd, *J*=7.8, 1.4 Hz, 1 H), 7.55 (br. s., 1 H), 7.66 – 7.71 (m, 1 H); ^{13}C NMR (75 MHz, CHLOROFORM-*d*) *δ* ppm 33.9, 56.3, 115.4, 115.8, 118.6, 134.7, 139.5, 150.8. Characterization data corresponded with literature values.[17]

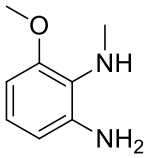

(87) 6-Methoxy-*N*^{1}-methylbenzene-1,2-diamine

(86) (350 mg, 1.92 mmol) was placed in a flask with Pd/C (204 mg, 10%, 0191 mmol). The flask was evacuated and purged with hydrogen from a balloon, after which EtOH (6 mL) was added. The reaction was monitored via TLC until complete disappearance of the starting material (3-4 hours). The mixture was filtered through a plug of Celite and the solvent reduced *in vacuo*. The product was purified by column chromatography over silica gel (20% EtOAc, 80% hexane) to afford a red solid. 289 mg, 98% yield. R_f: 0.29 (20% EtOAc, 80% hexane) ^{1}H NMR (300 MHz, CHLOROFORM-*d*) *δ* ppm 2.70 (s, 3 H), 3.75 (br. s, 3 H), 3.82 (s, 3 H), 6.36 (dd, *J*=8.1, 1.2 Hz, 1 H), 6.41 (dd, *J*=8.1, 1.3 Hz, 1 H), 6.82 – 6.89 (m, 1 H); ^{13}C NMR (75 MHz, CHLOROFORM-*d*) *δ* ppm 34.3, 55.6, 101.0, 108.9, 123.5, 125.4, 141.7, 153.1 Characterization data corresponded with literature values.[17]

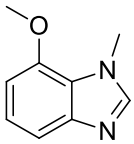

(88) 7-Methoxy-1-methyl-1*H*-benzo[*d*]imidazole

In an open 10 mL round bottom flask was added **(87)** (464 mg, 3.05 mmol), trimethyl orthoformate (400 µL, 3.65 mmol) and a *p*TsOH (5 mg). The mixture was heated to 115 °C for 40 minutes. The solution was diluted with DCM (2 mL) and was purified by column chromatography over silica gel (5% MeOH, 95% DCM) to afford a brown solid. 405 mg, 82% yield. R_f: 0.41 (5% MeOH, 95% DCM); ^{1}H NMR (400 MHz, CHLOROFORM-*d*) δ ppm 3.92 (s, 3 H), 4.02 (s, 3 H), 6.67 (d, *J*=8.2 Hz, 1 H), 7.11 – 7.17 (m, 1 H), 7.38 (d, *J*=8.2 Hz, 1 H), 7.69 (s, 1 H); ^{13}C NMR (101 MHz, CHLOROFORM-*d*) δ ppm 33.8, 55.4, 103.3, 112.9, 122.3, 124.2, 143.6, 145.8, 147.5; HRMS-TOF MS ES+: m/z $[M+H]^+$ calculated for $C_9H_{11}N_2O$: 163.0871; found: 163.0831; Characterization data corresponded with literature values.[17]

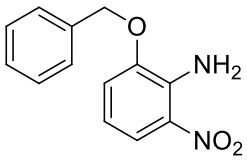

(91) 2-(Benzyloxy)-6-nitroaniline

To a solution of 2-amino-3-nitrophenol (1.00 g, 6.48 mmol) in DMF (15mL) was added K_2CO_3 (1.34g, 9.72 mmol) at -10 °C, followed by the addition of benzyl bromide (1.00 mL, 8.42 mmol) under an atmosphere of nitrogen. The mixture was stirred at -10 °C for 8 hours to prevent *N*-alkylation. The mixture was added to EtOAc (100mL) and was washed with water (4 x 100 mL) followed by a wash with brine. The organic phase was dried over $MgSO_4$, and the solvent reduced *in vacuo*. The product was purified by column chromatography over silica gel using a gradient elution (10% EtOAc, 90% hexane to 30% EtOAc, 70% hexane gradient) to afford a red oil. 1.55 g, 98% yield. R_f: 0.55 (20% EtOAc:80% hexane) ^{1}H NMR (300 MHz, CHLOROFORM-*d*) δ ppm 5.13 (s, 2 H), 6.51 (br. s, 2 H), 6.59 (dd, *J*=8.9, 7.8 Hz, 1 H), 6.97 (dd, *J*=7.8, 0.9 Hz, 1 H), 7.34 – 7.51 (m, 5 H), 7.75 (dd, *J*=8.9, 1.2 Hz, 1 H); ^{13}C NMR (75 MHz, CHLOROFORM-*d*) δ ppm 71.1, 114.4, 114.8, 117.5, 127.6 (2 C), 128.4, 128.7 (2 C), 131.6, 135.7, 137.1, 147.1

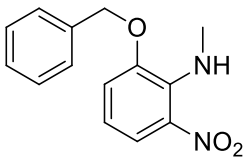

(92) 2-(Benzyloxy)-*N*-methyl-6-nitroaniline

To a mixture of NaH (144 mg, 60% dispersion in oil, 3.59 mmol) in THF (14 mL) was added **(91)** (800 mg, 3.27 mmol, dissolved in 2 mL THF) dropwise at -10 °C under an atmosphere of nitrogen. The mixture was stirred for 30 minutes to which MeI (224 µL, 3.59 mmol) was added. The mixture was allowed to reach room temperature and left

stirring overnight. The mixture was quenched with water (10 mL) and the product was extracted with EtOAc (2 x 60 mL). The organic phase was washed with brine, dried over $MgSO_4$ and the solvent was removed *in vacuo*. The product was purified by column chromatography over silica gel (15% EtOAc, 85% hexane) to afford a red solid. 820 mg, 97% yield. R_f: 0.59 (15% EtOAc, 85% hexane) ^{1}H NMR (300 MHz, CHLOROFORM-*d*) *δ* ppm 3.15 (s, 3 H), 5.07 (s, 2 H), 6.59 (dd, *J*=8.7, 7.8 Hz, 1 H), 6.99 (dd, *J*=7.8, 1.4 Hz, 1 H), 7.35 – 7.49 (m, 5 H), 7.73 (dd, *J*=8.7, 1.4 Hz, 1 H); ^{13}C NMR (75 MHz, CHLOROFORM-*d*) *δ* ppm 34.0, 71.8, 115.2, 117.5, 118.9, 127.6 (2 C), 128.2, 128.6 (2 C), 134.7, 135.9, 139.6, 149.6, HRMS-TOF MS ES+: m/z $[M+H]^+$ calculated for $C_{14}H_{15}N_2O_3$: 259.1083; found: 259.1076.

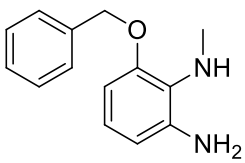

(93) 6-(Benzyloxy)-*N*^{1}-methylbenzene-1,2-diamine

In an open flask was added **(92)** (820 mg, 3.17 mmol), glacial acetic acid (6.6 mL), EtOH (6.6 mL), water (3.3 mL) and iron powder (880 mg, 15.9 mmol). The mixture was subjected to sonication at 30 °C for 3 hours, turning the red solution to dark yellow. The iron powder was removed via a magnet. The mixture was diluted with EtOAc (100 mL) and washed with a 2M KOH solution (2 x 60 mL). The organic phase was dried over $MgSO_4$, and the solvent reduced *in vacuo*. The product was purified by column chromatography over silica gel (50% EtOAc, 50% hexane) to afford a yellow oil. 520 mg, 72% yield. R_f: 0.28 (50% EtOAc, 50% hexane) ^{1}H NMR (300 MHz, CHLOROFORM-*d*) *δ* ppm 2.82 (s, 3 H), 3.98 (s, 3 H), 5.17 (s, 2 H), 6.47 – 6.59 (m, 2 H), 6.93 – 7.04 (m, 1 H), 7.41 – 7.65 (m, 5 H); ^{13}C NMR (75 MHz, CHLOROFORM-*d*) *δ* ppm 34.1, 70.1, 102.2, 108.9, 123.3, 125.5, 127.2 (2 C), 127.6, 128.2 (2 C), 137.0, 141.8, 152.1, HRMS-TOF MS ES+: m/z $[M+H]^+$ calculated for $C_{14}H_{17}N_2O$: 229.1341; found: 229.1345; Characterization data corresponded with literature values.[18]

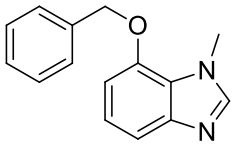

(94) 7-(Benzyloxy)-1-methyl-1*H*-benzo[*d*]imidazole

In an open 10 mL round bottom flask was added **(93)** (956 mg, 4.19 mmol), trimethyl orthoformate (550 µL, 5.02 mmol) and *p*TsOH (20 mg). The mixture was heated to 100 °C for 40 minutes. The solution was diluted with DCM (2 mL) and purified by column chromatography over silica gel (100% EtOAc) to afford a white solid. 967 mg, 97% yield. R_f: 0.56 (100% EtOAc); ^{1}H NMR (400 MHz, CHLOROFORM-*d*) *δ* ppm 4.04 (s, 3 H), 5.19 (s, 2 H), 6.78 (d, *J*=8.2 Hz, 1 H), 7.12 – 7.18 (m, 1 H), 7.34 – 7.50 (m, 6 H), 7.71 (s, 1 H); ^{13}C NMR (101

MHz, CHLOROFORM-*d*) *δ* ppm 33.9, 70.4, 104.6, 113.3, 122.4, 124.4, 127.4 (2 C), 128.0, 128.6 (2 C), 136.7, 143.8, 146.0, 146.6; HRMS-TOF MS ES+: m/z $[M+H]^+$ calculated for $C_{15}H_{15}N_2O$: 239.1184; found: 239.1135; Mp: 114 – 116 °C; IR ATR (cm^{-1}): 3092, 2866, 1620, 1586, 1499, 1378, 1286, 1259, 1077.

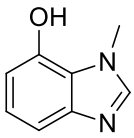

(89) 1-Methyl-1*H*-benzo[*d*]imidazol-7-ol

(94) (1.25 g, 5.26 mmol) was placed in a flask with Pd/C (56 mg, 10%, 0.053 mmol). The flask was evacuated and purged with hydrogen from a balloon, after which EtOH (16 mL) was added. The reaction was stirred overnight, after which the reaction mixture was filtered through a pad of Celite, and the solvent reduced *in vacuo*. The product was purified by column chromatography over silica gel (5% MeOH, 95% DCM%) to afford a light pink solid. 508 mg, 65% yield. R_f: 0.38 (5% MeOH, 95% DCM); ^{1}H NMR (400 MHz, DMSO-d6) *δ* ppm 4.00 (s, 3 H), 6.60 (d, J=7.4 Hz, 1 H), 6.87 – 6.97 (m, 1 H), 7.06 (d, J=7.8 Hz, 1 H), 7.98 (s, 1 H), 9.93 (br. s., 1 H); ^{13}C NMR (101 MHz, DMSO-d6) *δ* ppm 33.2, 107.3, 110.5, 122.0, 123.7, 144.3, 145.0, 145.9; HRMS-TOF MS ES+: m/z $[M+H]^+$ calculated for $C_8H_9N_2O$: 149.0715; found: 149.0683; Mp: decomposition; IR ATR (cm^{-1}): 2953, 1624, 1593, 1499, 1456, 1290, 1270, 1059.

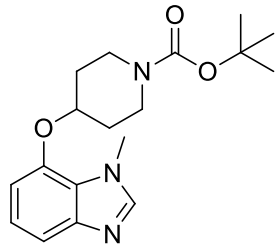

(90) *tert*-Butyl 4-((1-methyl-1*H*-benzo[*d*]imidazol-7-yl)oxy)piperidine-1-carboxylate

136 (508 mg, 3.43 mmol), 1-Boc-4-hydroxypiperidine (1.38 mg, 6.86 mmol) and PPh_3 (1.80 g, 6.86 mmol) were dissolved in THF (40 mL). To this solution was added DBAD (1.58 g, 6.86 mmol) dissolved in THF (4 mL) dropwise at 0 °C under an atmosphere of nitrogen. The reaction was stirred overnight at room temperature. The solvent was reduced and the product was purified by column chromatography over silica gel (20% acetone, 80% DCM) to afford a white solid. 1.18 g, 98% yield. R_f: 0.33 (20% acetone: 80% DCM); ^{1}H NMR (300 MHz, CHLOROFORM-*d*) *δ* ppm 1.39 – 1.46 (m, 9 H), 1.70 – 1.84 (m, 2 H), 1.89 – 2.01 (m, 2 H), 3.31 – 3.41 (m, 2 H), 3.56 – 3.67 (m, 2 H), 3.96 (s, 3 H), 6.61 (d, *J*=7.9 Hz, 1 H), 7.01 – 7.08 (m, 1 H), 7.29 (dd, *J*=8.2, 0.6 Hz, 1 H), 7.63 (s, 1 H); ^{13}C NMR (75 MHz, CHLOROFORM-*d*) *δ* ppm 28.1 (3 C), 30.2 (2 C), 33.8, 40.4 (2 C), 72.1, 79.4, 105.0, 112.7, 122.1, 124.6, 143.7, 144.6, 145.9, 154.4; HRMS-TOF MS ES+: m/z

$[M+H]^+$calculated for $C_{18}H_{26}N_3O_3$: 332.1974; found: 332.1913; Mp: 130 – 133 °C; IR ATR (cm^{-1}): 2928, 1688, 1619, 1497, 1422, 1280, 1229, 1165, 1080.

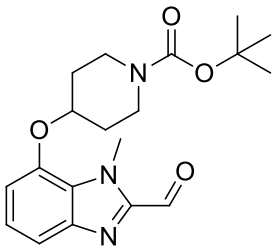

(98) *tert*-Butyl 4-((2-formyl-1-methyl-1*H*-benzo[*d*]imidazol-7-yl)oxy)piperidine-1-carboxylate

To a solution of THF (1.5 mL) and **(90)** (50 mg, 0.151 mmol) was added *n*-BuLi (1.7 M in hexanes, 98 µL, 0.166 mmol) at -78 °C under an atmosphere of argon, turning the solution yellow. The solution was left stirring at -78 °C for 30 minutes, followed by the addition of DMF (100 µL, 0314 mmol) turning the solution light yellow. The reaction was left stirring at -78 °C for 30 minutes, followed by the addition of aqueous $NaHCO_3$ solution (0.50 mL). The mixture was added to EtOAc (30 mL) and water (30 mL) and the organic layer was separated after which the aqueous phase was washed with EtOAc (30 mL). The organic fractions were combined and washed with brine. The organic phase was dried over $MgSO_4$, and the solvent reduced *in vacuo*. The product was purified by column chromatography over silica gel (40% EtOAc, 60% hexane) to afford a yellow solid. 29 mg, 54% yield. R_f: 0.25 (40% EtOAc, 60% hexane); ^{1}H NMR (300 MHz, CHLOROFORM-*d*) *δ* ppm 1.48 (s, 9 H), 1.80 – 1.93 (m, 2 H), 2.03 (s, 2 H), 3.36 – 3.46 (m, 2 H), 3.65 – 3.79 (m, 2 H), 4.42 (s, 3 H),4.63 – 4.74 (m, 1 H), 6.80 (d, *J*=7.9 Hz, 1 H), 7.18 – 7.26 (m, 1 H), 7.46 (dd, *J*=8.3, 0.7 Hz, 1 H), 10.07 (s, 1 H); ^{13}C NMR (75 MHz, CHLOROFORM-*d*) *δ* ppm 28.4 (3 C), 30.4 (2 C), 34.1, 40.7 (2 C), 73.0, 79.8, 108.0, 114.6, 124.1, 127.7, 144.8, 145.7, 146.0, 154.7, 184.9.

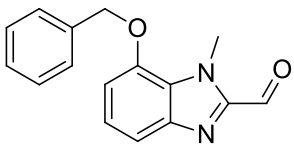

(99) 7-(Benzyloxy)-1-methyl-1*H*-benzo[*d*]imidazole-2-carbaldehyde

To a solution of **(94)** (600 mg, 2.52 mmol) in THF (12 mL) was added *n*-BuLi (1.6M in hexanes ,1.73 mL, 2.77 mmol) dropwise at -78 °C under an atmosphere of argon, and stirred at -78 °C for 30 minutes, after which DMF (253 µL, 3.28 mmol) was added dropwise, and stirred for 30 minutes, after which the solution was left to reach 0 °C. The reaction was quenched with a solution of aqueous $NaHCO_3$ (5 mL), diluted with water (15 mL) and the product extracted with EtOAc (2 x 30 mL). The organic phase was washed with brine, dried with $MgSO_4$, and reduced *in vacuo*. The product was purified by column chromatography over silica gel (50% EtOAc, 50% hexane) to afford a yellow solid. 460 mg, 69% yield. R_f: 0.73 (50% EtOAc, 50% hexane); ^{1}H NMR (300 MHz, CHLOROFORM-*d*)

δ ppm 4.40 (s, 3 H), 5.22 (s, 2 H), 6.89 (d, *J*=7.8 Hz, 1 H), 7.22 – 7.29 (m, 1 H), 7.37 – 7.49 (m, 5 H), 7.51 (d, *J*=8.4 Hz, 1 H), 10.09 (s, 1 H); ^{13}C NMR (75 MHz, CHLOROFORM-*d*) *δ* ppm 34.0, 70.8, 107.5, 114.8, 124.2, 127.2, 127.4 (2 C), 128.3, 128.7 (2 C), 136.1, 144.6, 146.0, 147.4, 184.8; HRMS-TOF MS ES+: m/z $[M+H+MeOH]^+$ calculated for $C_{17}H_{19}N_2O_3$: 299.1396; found: 229.1344; Mp: 88 – 90 °C; IR ATR (cm^{-1}): 3002, 2362, 1699, 1687, 1581, 1471, 1264, 1195, 1090.

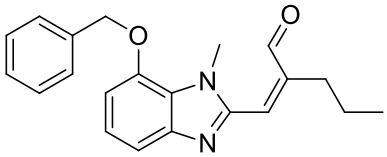

(107) (Z)-2-((7-(Benzyloxy)-1-methyl-1*H*-benzo[*d*]imidazol-2-yl)methylene)pentanal

Compound **(107)** was a byproduct formed during the synthesis of **(99)**. R_f: 0.83 (50% EtOAc, 50% hexane) ^{1}H NMR (400 MHz, CHLOROFORM-*d*) *δ* ppm 0.98 (t, *J*=7.4 Hz, 3 H), 1.50 – 1.63 (m, 2 H), 3.00 – 3.11 (m, 2 H), 4.16 (s, 3 H), 5.23 (s, 2 H), 6.82 (d, *J*=8.2 Hz, 1 H), 7.13 (s, 1 H), 7.16 – 7.21 (m, 1 H), 7.36 – 7.53 (m, 6 H), 9.66 (s, 1 H); HRMS-TOF MS ES+: m/z $[M+H]^+$ calculated for $C_{21}H_{23}N_2O_2$: 335.1760; found: 335.1695.

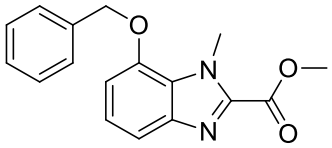

(110) Methyl 7-(Benzyloxy)-1-methyl-1*H*-benzo[*d*]imidazole-2-carboxylate

(99) (42.3 mg, 0.159 mmol) was dissolved in MeOH (2.1 mL) and cooled to 0 °C. KOH (23.0 mg, 0.412 mmol, dissolved in 0.50 mL MeOH) was added to the solution, followed by the dropwise addition of I_2 (52.7 mg, 0.208 mmol, dissolved in 0.50 mL MeOH). The reaction was left to warm up to room temperature and stirred overnight. The mixture was diluted with EtOAc (50 mL) and washed with 2 x 30 mL water. The organic phase was washed with brine, dried with $MgSO_4$, and reduced *in vacuo*. The product was purified by column chromatography over silica gel (50% EtOAc, 50% hexane) to afford a white solid. 37 mg, 79% yield. R_f: 0.55 (50% EtOAc, 50% hexane); ^{1}H NMR (300 MHz, CHLOROFORM-*d*) *δ* ppm 4.03 (s, 3 H), 4.42 (s, 3 H), 5.21 (s, 2 H), 6.86 (d, *J*=7.8 Hz, 1 H), 7.18 – 7.25 (m, 1 H), 7.37 – 7.51 (m, 6 H); ^{13}C NMR (75 MHz, CHLOROFORM-*d*) *δ* ppm 34.8, 52.7, 70.8, 106.6, 114.6, 123.8, 126.8, 127.5 (2 C), 128.2, 128.7 (2 C), 136.2, 140.6, 143.5, 147.0, 160.3; HRMS-TOF MS ES+: m/z $[M+H]^+$ calculated for $C_{17}H_{17}N_2O_3$: 297.1239; found: 297.1182; Mp: 78 – 82 °C; IR ATR (cm^{-1}): 3366, 2953, 1713, 1593, 1468, 1247, 1096.

(111) Methyl 7-hydroxy-1-methyl-1*H*-benzo[*d*]imidazole-2-carboxylate

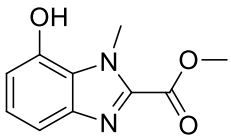

(110) (350 mg, 1.18 mmol) and Pd/C (10%, 22 mg, 0.0206 mmol) was placed in a flask, evacuated and purged with hydrogen from a balloon after which MeOH (6 mL) was added and the reaction was stirred overnight. The mixture was filtered through a plug of Celite and the solvent reduced *in vacuo*. The product was purified by column chromatography over silica gel (70% EtOAc, 30% hexane) to afford a white solid. 224 mg, 92% yield. R_f: 0.37 (70% EtOAc, 30% hexane); ^{1}H NMR (300 MHz, CHLOROFORM-*d*) *δ* ppm 3.87 (s, 3 H), 4.31 (s, 3 H), 6.62 (d, *J*=7.6 Hz, 1 H), 6.88 – 6.97 (m, 1 H), 7.15 (d, *J*=8.2 Hz, 1 H), 9.45 (s, 1 H); ^{13}C NMR (101 MHz, DMSO-d_6) *δ* ppm 34.2, 52.4, 109.4, 111.6, 123.7, 125.8, 140.6, 143.3, 145.5, 160.1; HRMS-TOF MS ES+: m/z $[M+H]^+$ calculated for $C_{10}H_{11}N_2O_3$: 207.0770; found: 207.0727; Mp: 202 – 204 °C; IR ATR (cm-1): 2951, 1723, 1597, 1471, 1281, 1242, 1127, 1072.

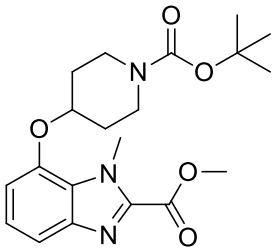

(112) Methyl 7-((1-(*tert*-butoxycarbonyl)piperidin-4-yl)oxy)-1-methyl-1*H*-benzo[*d*]imidazole-2-carboxylate

(111) (224 mg, 1.09 mmol), PPh_3 (429 mg, 1.64 mmol) and 1-Boc-4-hydroxypiperidine (329 mg, 1.63 mmol) were dissolved in THF (6mL). The solution was cooled to 0 °C and DBAD (376 mg, 1.63 mmol, dissolved in 1 mL THF) was added dropwise under an atmosphere of nitrogen. The reaction was stirred overnight at room temperature. The solvent was reduced *in vacuo* and the product was purified by column chromatography over silica gel (50% EtOAc, 50% hexane) to afford a white solid. 321 mg, 76% yield. R_f: 0.41 (50% EtOAc, 50% hexane); ^{1}H NMR (300 MHz, CHLOROFORM-*d*) *δ* ppm 1.41 (s, 9 H), 1.72 – 1.87 (m, 2 H), 1.91 – 2.05 (m, 2 H), 3.28 – 3.41 (m, 2 H), 3.59 – 3.68 (m, 2 H), 3.94 (s, 3 H), 4.37 (s, 3 H), 4.56 – 4.65 (m, 1 H), 1 H), 6.69 (d, *J*=7.8 Hz, 1 H), 7.07 – 7.14 (m, 1 H), 7.36 (d, *J*=8.2 Hz, 1 H);^{13}C NMR (75 MHz, CHLOROFORM-*d*) *δ* ppm 28.2 (3 C), 30.2 (2 C), 34.6, 40.5 (2 C), 52.5, 72.7, 79.6, 107.0, 114.1, 123.5, 127.0, 140.4, 143.5, 145.0, 154.5, 160.1; HRMS-TOF MS ES+: m/z $[M+H]^+$ calculated for $C_{20}H_{28}N_3O_5$: 390.2029; found: 390.1953; Mp: 85 – 88 °C; IR ATR (cm^{-1}): 2948, 1728, 1682, 1583, 1482, 1422, 1231, 1167, 1077, 1022.

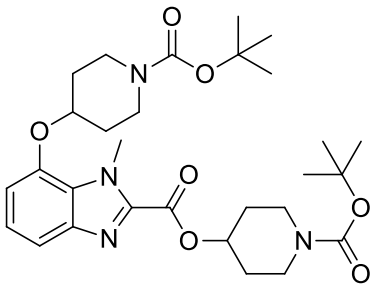

(113) 1-(*tert*-Butoxycarbonyl)piperidin-4-yl 7-((1-(*tert*-butoxycarbonyl)piperidin-4-yl)oxy)-1-methyl-1*H*-benzo[*d*]imidazole-2-carboxylate

(113) was the byproduct that formed during the synthesis of **(112)**. 72 mg, 12% yield, white solid. R_f: 0.54 (50% EtOAc, 50% hexane); ^{1}H NMR (300 MHz, CHLOROFORM-*d*) *δ* ppm 1.43 – 1.53 (m, 18 H), 1.79 – 1.95 (m, 4 H), 1.97 – 2.11 (m, 4 H), 3.06 – 3.19 (m, 2 H), 3.36 – 3.48 (m, 2 H), 3.64 – 3.76 (m, 2 H), 3.92 – 4.03 (m, 2 H), 4.43 (s, 3 H), 4.62 – 4.70 (m, 1 H), 5.15 – 5.25 (m, 1 H), 6.77 (d, *J*=7.9 Hz, 1 H), 7.15 – 7.22 (m, 1 H), 7.47 (d, *J*=7.9 Hz, 1 H); ^{13}C NMR (75 MHz, CHLOROFORM-*d*) *δ* ppm 28.3 (s,6 C), 30.3 (2 C), 30.6 (2 C), 34.9, 40.6 (2 C), 41.5 (2 C), 72.5, 72.8, 79.7, 79.7, 107.2, 114.5, 123.6, 127.2, 140.9, 143.7, 145.1, 154.6, 159.4; HRMS-TOF MS ES+: m/z $[M+H]^+$ calculated for $C_{29}H_{43}N_4O_7$: 559.3132; found: 559.3154, Loss of compound prevented full characterization.

Compounds **(114)** – **(116)** were synthesized via the same procedure. Compound **(102)**, K_3PO_4 (3 equivalents) and the aromatic alcohol used for the transesterification reaction (20 – 30 equivalents) were placed in a flask and stirred under nitrogen at room temperature for 12 – 20 hours. The reaction was monitored via TLC using (5% EtOAc, 95% DCM) as mobile phase to determine whether the starting material had been consumed. The K_3PO_4 was filtered off, and the alcohol removed via heating the solution to 50 °C and streaming compressed air over the solution. After the majority of the solvent volume has been evaporated off, the product was purified by column chromatography over silica gel (5% EtOAc, 95% DCM).

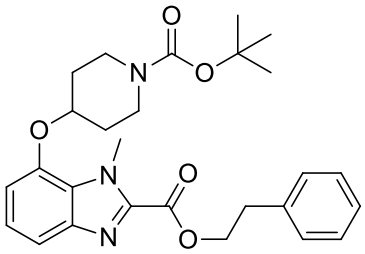

(114) Phenethyl-7-((1-(*tert*-butoxycarbonyl)piperidin-4-yl)oxy)-1-methyl-1*H*-benzo[*d*]imidazole-2-carboxylate

36 mg, 50% yield, brown semi-solid. R_f: 0.55 (50% EtOAc: 50% hexane); ^{1}H NMR (300 MHz, CHLOROFORM-*d*) *δ* ppm 1.49 (s, 9 H), 1.81 – 1.95 (m, 2 H), 1.99 – 2.11 (m, 2 H), 3.18 (t, *J*=7.6 Hz, 2 H), 3.36 – 3.48 (m, 2 H), 3.66 – 3.77 (m, 2 H), 4.40 (s, 3 H), 4.60 – 4.74 (m, 3 H), 6.78 (d, *J*=7.6 Hz, 1 H), 7.16 – 7.23 (m, 1 H), 7.23 – 7.35 (m, 5 H), 7.48 (d, *J*=8.2 Hz, 1 H);^{13}C NMR (75 MHz, CHLOROFORM-*d*) *δ* ppm 28.5 (3 C), 30.5 (2 C), 34.8, 35.1, 40.7 (2 C), 66.4, 72.9, 79.9, 107.3,

114.5, 123.7, 126.8, 127.3, 128.6 (2 C), 129.0 (2 C), 137.1, 141.0, 143.8, 145.3, 154.7, 159.9; HRMS-TOF MS ES+: m/z $[M+H]^+$ calculated for $C_{27}H_{34}N_3O_5$: 480.2498; found: 480.2515; IR ATR (cm^{-1}): 2961, 2926, 1718, 1688, 1585, 1465, 1422, 1229, 1084, 1023.

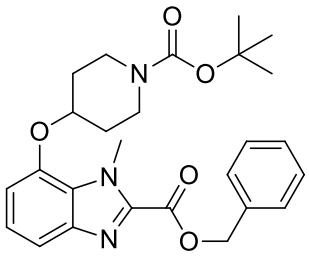

(115) benzyl 7-((1-(*tert*-Butoxycarbonyl)piperidin-4-yl)oxy)-1-methyl-1*H*-benzo[*d*]imidazole-2-carboxylate

38 mg, 52% yield, white solid. R_f: 0.53 (40% EtOAc, 60% hexane); ^{1}H NMR (300 MHz, CHLOROFORM-*d*) *δ* ppm 1.48 (s, 9 H), 1.80 – 1.93 (m, 2 H), 1.98 – 2.10 (m, 2 H), 3.36 – 3.47 (m, 2 H), 3.65 – 3.77 (m, 2 H), 4.43 (s, 3 H), 4.63 – 4.73 (m, 1 H), 5.48 (s, 2 H), 6.77 (d, J=7.9 Hz, 1 H), 7.15 – 7.22 (m, 1 H), 7.31 – 7.55 (m, 6 H); ^{13}C NMR (75 MHz, CHLOROFORM-d) δ ppm 28.4 (3 C), 30.4 (2 C), 34.9, 40.8 (2 C), 67.6, 73.0, 79.9, 107.3, 114.5, 123.7, 127.3, 128.5, 128.6 (2 C), 128.8 (2 C), 135.3, 140.8, 143.8, 145.3, 154.7, 159.9; HRMS-TOF MS ES+: m/z $[M+H]^+$ calculated for $C_{26}H_{32}N_3O_5$: 466.2342; found: 466.2325; Mp: 145 – 148 °C, IR ATR (cm^{-1}): 2957, 2926, 1725, 1686, 1589, 1466, 1422, 1233, 1021.

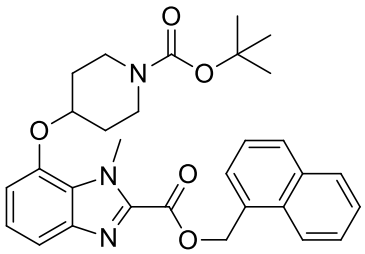

(116) Naphthalen-1-ylmethyl 7-((1-(*tert*-butoxycarbonyl) piperidin-4-yl)oxy)-1-methyl-1*H*-benzo[*d*]imidazole-2-carboxylate

45 mg, 57% yield, yellow solid. R_f: 0.56 (50% EtOAc, 50% hexane); ^{1}H NMR (300 MHz, CHLOROFORM-*d*) *δ* ppm 1.46 (s, 9 H), 1.77 – 1.92 (m, 2 H), 1.96 – 2.13 (m, 2 H), 3.34 – 3.47 (m, 2 H), 3.64 – 3.78 (m, 2 H), 4.41 (s, 3 H), 4.61 – 4.71 (m, 1 H), 5.95 (s, 2 H), 6.76 (d, *J*=7.6 Hz, 1 H), 7.13 – 7.20 (m, 1 H), 7.42 – 7.63 (m, 4 H), 7.72 (d, *J*=7.0 Hz, 1 H), 7.83 – 7.94 (m, 2 H), 8.19 (d, *J*=8.2 Hz, 1 H); ^{13}C NMR (75 MHz, CHLOROFORM-*d*) *δ* ppm 28.4 (3 C), 30.3 (2 C), 34.8, 40.6 (2 C), 65.7, 72.8, 79.8, 107.2, 114.4, 123.4, 123.6, 125.2, 125.9, 126.6, 127.2, 127.9, 128.6, 129.4, 130.6, 131.5, 133.7, 140.8, 143.7, 145.1, 154.7, 159.8; HRMS-TOF MS ES+: m/z $[M+H]^+$ calculated for $C_{30}H_{34}N_3O_5$: 516.2498; found: 516.2410; Mp: 134 – 137 °C, IR ATR (cm^{-1}): 2969, 2930, 1724, 1676, 1583, 1477, 1418, 1220, 1088, 1019.

Compounds **(117)** – **(120)** were synthesized via the same procedure. Compound **(102)** and the aromatic amine used for the amidation reaction (10 equivalents) were dissolved in THF (1 mL) and stirred under nitrogen at room temperature for 12 – 20 hours. The reaction was monitored via TLC using (50% EtOAc, 50% hexane) mobile phase to determine whether the starting material had been consumed. The product was purified by column chromatography over silica gel (50% EtOAc, 50% hexane – 100% EtOAc).

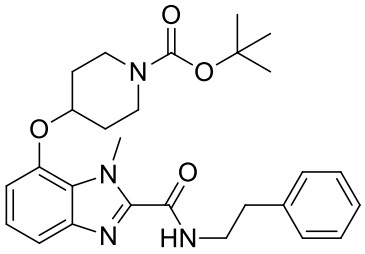

(117) *tert*-Butyl 4-((1-methyl-2-(phenethylcarbamoyl)-1*H*-benzo[*d*]imidazol-7-yl)oxy)piperidine-1-carboxylate

47 mg, 81% yield, yellow solid. R_f: 0.53 (40% EtOAc: 60% hexane); ^{1}H NMR (300 MHz, CHLOROFORM-*d*) *δ* ppm 1.50 (s, 9 H), 1.81 – 1.96 (m, 2 H), 1.99 – 2.11 (m, 2 H), 2.96 (t, *J*=7.3 Hz, 2 H), 3.39 – 3.50 (m, 2 H), 3.66 – 3.78 (m, 4 H), 4.52 (s, 3 H), 4.63 – 4.74 (m, 1 H), 6.76 (d, *J*=7.6 Hz, 1 H), 7.14 – 7.21 (m, 1 H), 7.21 – 7.38 (m, 6 H), 7.88 (t, *J*=5.9 Hz, 1 H); ^{13}C NMR (75 MHz, CHLOROFORM-*d*) *δ* ppm 28.5 (3 C), 30.5 (2 C), 34.9, 35.9, 40.6 (2 C), 40.8, 72.9, 79.8, 106.7, 113.2, 123.5, 126.5, 127.4, 128.6 (2 C), 128.8 (2 C), 138.7, 143.1, 143.4, 145.5, 154.7, 159.8; HRMS-TOF MS ES+: m/z $[M+H]^+$ calculated for $C_{27}H_{35}N_4O_4$: 479.2658; found: 479.2668; Mp: 84 – 86 °C, IR ATR (cm^{-1}): 2930, 2865, 1671, 1529, 1422, 1231, 1166, 1085, 1023.

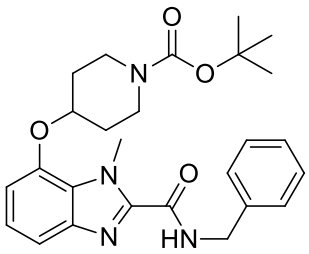

(118) *tert*-Butyl 4-((2-(benzylcarbamoyl)-1-methyl-1*H*-benzo[*d*]imidazol-7-yl)oxy)piperidine-1-carboxylate

51mg, 90% yield, whitesolid. R_f: 0.58 (40% EtOAc: 60% hexane); ^{1}H NMR (300 MHz, CHLOROFORM-*d*) *δ* ppm 1.50 (s, 9 H), 1.82 – 1.96 (m, 2 H), 1.99 – 2.11 (m, 2 H), 3.38 – 3.52 (m, 2 H), 3.67 – 3.78 (m, 2 H), 4.54 (s, 3 H), 4.60 – 4.74 (m, 3 H), 6.76 (d, *J*=7.6 Hz, 1 H), 7.13 – 7.21 (m, 1 H), 7.22 – 7.44 (m, 6 H), 8.17 (t, *J*=5.9 Hz, 1 H); ^{13}C NMR (75 MHz, CHLOROFORM-*d*) *δ* ppm 28.5 (3 C), 30.5 (2 C), 34.9, 40.8 (2 C), 43.4, 72.9, 79.8, 106.8, 113.2, 123.6, 127.4, 127.6, 127.9 (2 C), 128.7 (2 C), 137.7, 143.1, 143.3, 145.5, 154.7, 159.7; HRMS-TOF MS ES+: m/z $[M+H]^+$ calculated for $C_{26}H_{33}N_4O_4$: 465.2502; found: 465.2518; Mp: 68 – 71 °C, IR ATR (cm^{-1}): 2928, 2872, 1671, 1529, 1422, 1231, 1166, 1086, 1024.

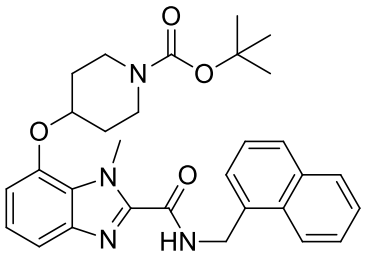

(119) *tert*-Butyl 4-((1-methyl-2-((naphthalen-1-ylmethyl) carbamoyl)-1*H*-benzo[*d*]imidazol-7-yl)oxy)piperidine-1-carboxylate

73 mg, 92% yield, light brown solid. R_f: 0.63 (40% EtOAc, 60% hexane); ^{1}H NMR (300 MHz, CHLOROFORM-*d*) *δ* ppm 1.50 (s, 9 H), 1.83 – 1.95 (m, 2 H), 1.97 – 2.10 (m, 2 H), 3.38 – 3.49 (m, 2 H), 3.65 – 3.78 (m, 2 H), 4.58 (s, 3 H), 4.63 – 4.74 (m, 1 H), 5.10 (d, *J*=5.9 Hz, 2 H), 6.74 (d, *J*=7.6 Hz, 1 H), 7.10 – 7.20 (m, 1 H), 7.21 – 7.29 (m, 1 H), 7.41 – 7.60 (m, 4 H), 7.78 – 7.95 (m, 2 H), 8.03 (br. s., 1 H), 8.11 (d, *J*=7.6 Hz, 1 H); ^{13}C NMR (75 MHz, CHLOROFORM-*d*) *δ* ppm 28.4 (3 C), 30.4 (2 C), 34.9, 40.7 (2 C), 41.4, 72.8, 79.8, 106.7, 113.1, 123.4, 123.5, 125.4, 125.9, 126.6, 126.7, 127.4, 128.7, 128.8, 131.4, 132.9, 133.9, 143.1, 143.2, 145.5, 154.7, 159.4; HRMS-TOF MS ES+: m/z $[M+H]^+$ calculated for $C_{30}H_{35}N_4O_4$: 515.2658; found: 515.2648; Mp: 90 – 92 °C, IR ATR (cm^{-1}): 2927, 2866, 1676, 1528, 1423, 1231, 1167, 1087, 1023.

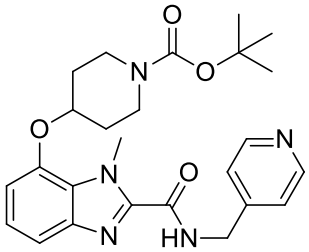

(120) *tert*-Butyl 4-((1-methyl-2-((pyridin-4-ylmethyl)carbamoyl)-1*H*-benzo[*d*]imidazol-7-yl)oxy)piperidine-1-carboxylate

48 mg, 92% yield, yellow solid. R_f: 0.63 (40% EtOAc, 60% hexane); ^{1}H NMR (300 MHz, CHLOROFORM-*d*) *δ* ppm 1.47 (s, 9 H), 1.79 – 1.93 (m, 2 H), 1.98 – 2.10 (m, 2 H), 3.36 – 3.47 (m, 2 H), 3.64 – 3.76 (m, 2 H), 4.51 (s, 3 H), 4.57 – 4.73 (m, 3 H), 6.76 (d, *J*=7.6 Hz, 1 H), 7.13 – 7.22 (m, 1 H), 7.22 – 7.35 (m, 3 H), 8.35 (br. s., 1 H), 8.47 – 8.63 (m, 2 H); ^{13}C NMR (75 MHz, CHLOROFORM-*d*) *δ* ppm 28.4 (3 C), 30.4 (2 C), 34.9, 40.8 (2 C), 42.1, 72.9, 79.9, 106.9, 113.2, 122.3, 123.8 (2 C), 127.5, 142.8, 143.1, 145.6, 147.0, 150.0 (2 C), 154.7, 160.0; HRMS-TOF MS ES+: m/z $[M+H]^+$ calculated for $C_{25}H_{32}N_5O_4$: 466.2454; found: 466.2473; Mp: 153 – 155 °C, IR ATR (cm^{-1}): 3322, 2930, 2855, 1684, 1661, 1531, 1414, 1231, 1165, 1085.

Compounds **BI1** – **BI7** were synthesized via the same procedure. In a small flask was added the Boc-protected compounds **(114)** – **(120)** separately dissolved in DCM (1 mL) followed by the addition of 4M HCl/dioxane (1 mL). The solution was stirred for one hour, after which the solvent was reduced *in vacuo*. A small amount of DCM was added followed by the addition of EtOAc which caused the salt to precipitate out of solution. The solvent was reduced *in vacuo* and the product dried under vacuum.

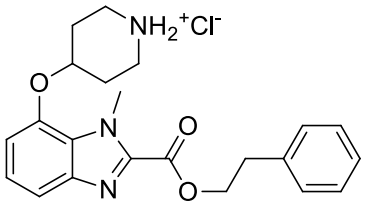

(BI1) 4-((1-Methyl-2-(phenethoxycarbonyl)-1*H*-benzo[*d*]imidazol-7-yl)oxy)piperidin-1-ium chloride

26 mg, 83% yield, yellow solid. ^{1}H NMR (600 MHz, DMSO-d_6) δ ppm 1.97 – 2.07 (m, 2 H), 2.18 – 2.27 (m, 2 H), 3.05 – 3.16 (m, 4 H), 3.21 (br. s., 2 H), 4.30 (s, 3 H), 4.59 (t, *J*=6.7 Hz, 2 H), 4.90 (br. s., 1 H), 7.07 (d, *J*=7.6 Hz, 1 H), 7.20 – 7.39 (m, 7 H), 9.25 (br. s., 1 H), 9.44 (br. s., 1 H); ^{13}C NMR (151 MHz, DMSO-d_6) δ ppm 26.7 (2 C), 34.1, 34.8, 40.2 (2 C), 66.3, 70.2, 108.2, 112.6, 124.6, 126.0, 126.5, 128.4 (2 C), 128.9 (2 C), 137.6, 140.4, 141.3, 144.9, 158.5; HRMS-TOF MS ES+: m/z $[M+H]^+$ calculated for $C_{22}H_{26}N_3O_3$: 380.1974; found: 380.1966; Purity: 98.6%; Mp: 179 – 182 °C, IR ATR (cm^{-1}): 2960, 2568, 1749, 1614, 1491, 1257, 1098, 1022

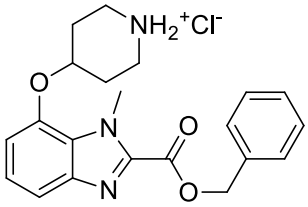

(BI2) 4-((2-((Benzyloxy)carbonyl)-1-methyl-1*H*-benzo[*d*]imidazol-7-yl)oxy)piperidin-1-ium chloride

28 mg, 87% yield, yellow solid. ^{1}H NMR (600 MHz, DMSO-d_6) δ ppm 1.92 – 2.08 (m, 2 H), 2.13 – 2.29 (m, 2 H), 3.12 (br. s., 2 H), 3.22 (br. s., 2 H), 4.36 (s, 3 H), 4.87 – 4.92 (m, 1 H), 5.44 (s, 2 H), 7.07 (d, *J*=8.2 Hz, 1 H), 7.24 – 7.30 (m, 1 H), 7.35 (d, *J*=8.2 Hz, 1 H), 7.37 – 7.55 (m, 5 H), 9.12 – 9.47 (m, 2 H); ^{13}C NMR (151 MHz, DMSO-d_6) δ ppm 26.7 (2 C), 34.9, 40.2 (2 C), 67.2, 70.1, 108.2, 112.6, 124.6, 126.1, 128.4, 128.5 (2 C), 128.5 (2 C), 135.2, 140.3, 141.3, 144.9, 158.5; HRMS-TOF MS ES+: m/z $[M+H]^+$ calculated for $C_{21}H_{24}N_3O_3$: 366.1818; found: 366.1812; Purity: >98%; Mp: 134 – 137 °C, IR ATR (cm^{-1}): 3372, 2715, 1752, 1619, 1493, 1249, 1105, 1022

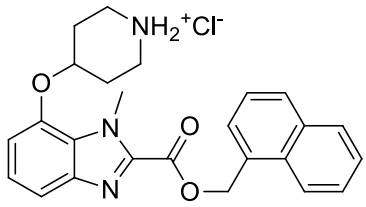

(BI3) 4-((1-Methyl-2-((naphthalen-1-ylmethoxy)carbonyl)-1*H*-benzo[*d*]imidazol-7-yl)oxy)piperidin-1-ium chloride

38 mg, 95% yield, orange solid. ^{1}H NMR (600 MHz, DMSO-d_6) δppm 1.95 – 2.05 (m, 2 H), 2.16 – 2.26 (m, 2 H), 3.11 (br. s., 2 H), 3.21 (br. s., 2 H), 4.35 (s, 3 H), 4.85 – 4.91 (m, 1 H), 5.89 (s, 2 H), 7.04 (d, *J*=7.6 Hz, 1 H), 7.21 – 7.27 (m, 1 H), 7.29 (d, *J*=8.2 Hz, 1 H), 7.53 – 7.65 (m, 3 H), 7.75 (d, *J*=7.0 Hz, 1 H), 7.97 – 8.04 (m, 2 H), 8.17 (d, *J*=8.2 Hz, 1 H), 9.09 – 9.43 (m, 2 H); ^{13}C NMR (151 MHz, DMSO-d_6) δ ppm 26.7 (2 C), 34.8, 40.2 (2 C), 65.6, 70.1, 108.1, 112.8, 123.8, 124.4, 125.4, 126.1, 126.2, 126.8, 128.1, 128.6, 129.4, 130.7, 131.2, 133.3, 140.4, 141.6, 144.9, 158.7; HRMS-TOF MS ES+: m/z $[M+H]^+$ calculated for $C_{25}H_{26}N_3O_3$: 416.1974; found: 416.1985; Purity:

95.3%; Mp: 125 – 128 °C, IR ATR (cm^{-1}): 3382, 2962, 2806, 1741, 1616, 1496, 1347, 1267, 1232, 1094.

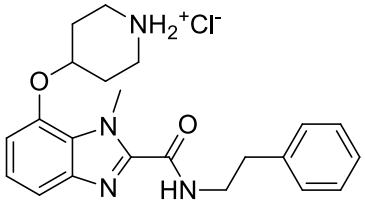

(BI4) 4-((1-Methyl-2-(phenethylcarbamoyl)-1*H*-benzo[*d*]imidazol-7-yl)oxy)piperidin-1-ium chloride

35 mg, 87% yield, yellow solid. ^{1}H NMR (600 MHz, DMSO-d_6) δ ppm 1.98 – 2.06 (m, 2 H), 2.18 – 2.26 (m, 2 H), 2.88 (t, *J*=7.3 Hz, 2 H), 3.12 (br. s., 2 H), 3.21 (br. s., 2 H), 3.53 (q, *J*=7.0 Hz, 2 H), 4.33 (s, 3 H), 4.85 – 4.90 (m, 1 H), 7.01 (d, *J*=7.6 Hz, 1 H), 7.18 – 7.32 (m, 7 H), 9.07 – 9.20 (m, 2 H), 9.40 (br. s., 1 H); ^{13}C NMR (151 MHz, DMSO-d_6) δ ppm 26.7 (2 C), 34.5, 34.8, 40.2 (2 C), 40.4, 69.9, 107.5, 112.1, 124.0, 126.1, 126.1, 128.3 (2 C), 128.6 (2 C), 139.2, 141.3, 143.6, 145.0, 158.5; HRMS-TOF MS ES+: m/z $[M+H]^+$ calculated for $C_{22}H_{27}N_4O_2$: 379.2134; found: 379.2126; Purity: >98%; Mp: 204 – 207 °C, IR ATR (cm^{-1}): 2924, 2788, 1683, 1489, 1340, 1279.

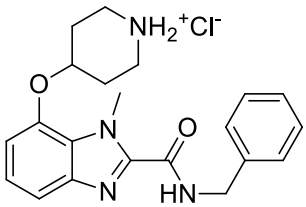

(BI5) 4-((2-(Benzylcarbamoyl)-1-methyl-1*H*-benzo[*d*]imidazol-7-yl)oxy)piperidin-1-ium chloride

39 mg, 89% yield, red brown solid. ^{1}H NMR (600 MHz, DMSO-d_6) δ ppm 1.98 – 2.05 (m, 2 H), 2.19 – 2.26 (m, 2 H), 3.11 (br. s., 2 H), 3.21 (br. s., 2 H), 4.37 (s, 3 H), 4.48 (d, *J*=6.4 Hz, 2 H), 4.86 – 4.91 (m, 1 H), 7.02 (d, *J*=7.6 Hz, 1 H), 7.22 – 7.27 (m, 2 H), 7.29 – 7.40 (m, 5 H), 9.19 (br. s., 1 H), 9.46 (br. s., 1 H), 9.62 (t, *J*=6.2 Hz, 1 H); ^{13}C NMR (151 MHz, DMSO-d_6) δ ppm 26.7 (2 C), 34.6, 40.2 (2 C), 42.3, 69.9, 107.6, 112.1, 124.1, 126.1, 126.9, 127.4 (2 C), 128.3 (2 C), 138.9, 141.2, 143.5, 145.0, 158.6; HRMS-TOF MS ES+: m/z $[M+H]^+$ calculated for $C_{21}H_{25}N_4O_2$: 367.1979; found: 367.1974; Purity: 98.4%; Mp: 196 – 198 °C, IR ATR (cm^{-1}): 3458, 2929, 1682, 1486, 1294, 1252, 1092.

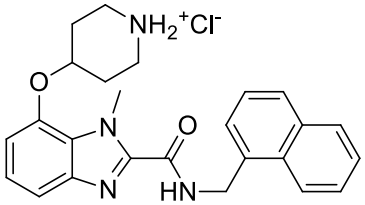

(BI6) 4-((1-Methyl-2-((naphthalen-1-ylmethyl)carbamoyl)-1*H*-benzo[*d*]imidazol-7-yl)oxy)piperidin-1-ium

62 mg, 97 % yield, ^{1}H NMR (600 MHz, DMSO-d_6) δ ppm 1.96 – 2.06 (m, 2 H), 2.20 (br. s., 2 H), 3.12 (br. s., 2 H), 3.23 (br. s., 2 H), 4.38 (s, 3 H), 4.87 (br. s., 1 H), 4.95 (d, *J*=6.4 Hz, 2 H), 6.98 (d, *J*=7.6 Hz, 1 H), 7.16 – 7.23 (m, 1

H), 7.29 (d, *J*=8.2 Hz, 1 H), 7.45 – 7.50 (m, 1 H), 7.51 – 7.57 (m, 2 H), 7.57 – 7.62 (m, 1 H), 7.86 (d, *J*=8.2 Hz, 1 H), 7.96 (d, *J*=7.6 Hz, 1 H), 8.26 (d, *J*=8.2 Hz, 1 H), 8.89 (br. s, 1 H), 9.15 (br. s, 1 H), 9.52 (t, *J*=5.9 Hz, 1 H); ^{13}C NMR (151 MHz, DMSO-d_6) δ ppm 26.7 (2 C), 34.4, 40.1 (2 C), 40.2, 69.8, 107.4, 112.3, 123.4, 123.7, 125.3, 125.4, 125.7, 126.2, 126.2, 127.5, 128.4, 130.7, 133.2, 133.9, 141.8, 143.5, 144.8, 158.9; HRMS-TOF MS ES+: m/z $[M+H]^+$ calculated for $C_{25}H_{27}N_4O_2$: 415.2134; found: 415.2131; Purity: 96.9%; Mp: 124 – 127 °C, IR ATR (cm^{-1}): 3376, 2953, 1678, 1533, 1488, 1351, 1253, 1116, 1083.

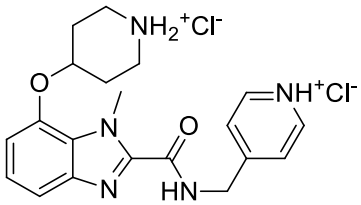

(BI7) 4-((1-Methyl-7-(piperidin-1-ium-4-yloxy)-1*H*-benzo[*d*]imidazole-2-carboxamido)methyl)pyridin-1-ium chloride

37 mg, 83% yield, brown solid. ^{1}H NMR (600 MHz, DMSO-d_6) δ ppm 1.97 – 2.09 (m, 2 H), 2.23 (br. s., 2 H), 3.11 (br. s., 2 H), 3.20 (br. s., 2 H), 4.34 (s, 3 H), 4.77 (d, *J*=5.9 Hz, 2 H), 4.89 (br. s., 1 H), 7.03 (d, *J*=7.6 Hz, 1 H), 7.17 – 7.30 (m, 1 H), 7.33 (d, *J*=8.2 Hz, 1 H), 8.03 (d, *J*=5.9 Hz, 2 H), 8.89 (d, *J*=5.9 Hz, 2 H), 9.38 (br. s., 1 H), 9.55 (br. s., 1 H), 9.87 (t, *J*=5.6 Hz, 1 H);^{13}C NMR (151 MHz, DMSO-d_6) δ ppm 26.7 (2 C), 34.5, 40.1 (2 C), 42.1, 70.0, 107.7, 112.5, 124.0, 125.1 (2 C), 126.5, 141.2 (2 C), 142.0, 143.0, 145.0, 159.6, 159.8; HRMS-TOF MS ES+: m/z $[M+H]^+$ calculated for $C_{20}H_{24}N_5O_2$: 366.1930; found: 366.1927; Purity: 97.8%; Mp: 212 – 214 °C, IR ATR (cm^{-1}): 3390, 2929, 1667, 1638, 1523, 1505, 1467, 1260, 1096, 998.

10.5 Synthesis of compounds pertaining to Chapter 5

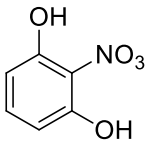

(122) 2-Nitroresorcinol

(122) was synthesized according to a modified literature procedure. [19] Resorcinol (5.00 g, 0.05 mol) was added to H_2SO_4 (36 mL). The solution warmed up resulting in complete dissolution of the resorcinol, and was stirred for 30 minutes, after which white resorcinol•$2H_2SO_4$ precipitated out of solution. A precooled solution of HNO_3 (70%, 2.84 g, 0.05mmol) and H_2SO_4 (9.09 g, 0.09 mmol) was added to the mixture dropwise at 0 °C under vigorous stirring until complete solubilization was observed. Crushed ice (40 g) was added to the

mixture, and the product was purifed via steam distillation. The collected distillate fractions were combined and the product was extracted with DCM (3 x 80mL) to produce analytically pure 3-nitroresorcinol. 1.23g, 16% yield. ^{1}H NMR (300 MHz, CHLOROFORM-*d*) *δ* ppm 6.62 (d, *J*=8.4 Hz, 2 H), 7.44 (t, *J*=8.4 Hz, 1 H), 10.66 (s, 2 H); ^{13}C NMR (75 MHz, CHLOROFORM-*d*) *δ* ppm 109.4, 123.9, 138.9, 156.2 Characterization data corresponded with literature values.[20]

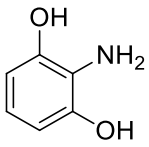

(123) 2-Aminoresorcinol

(122) (1.23 g, 7.19 mmol) was dissolved in MeOH (10 mL) followed by the addition of Pd/C (10%, 100 mg, 0.09 mmol). The flask was purged with hydrogen from a balloon, and the mixture was stirred under an atmosphere of hydrogen until the starting material has disappeared as monitored via TLC. The mixture was filtered through a plug of Celite, and the solvent was reduced *in vacuo*. The product was purified by column chromatography over silica gel (100% EtOAc) to afford a dark yellow solid. 863 mg, 87% yield. ^{1}H NMR (300 MHz, CHLOROFORM-*d,* CD_3OD-*d*) *δ* ppm 6.31 (d, *J*=7.9 Hz, 2 H), 6.44 – 6.51 (m, 1 H); ^{13}C NMR (75 MHz, CHLOROFORM-*d,* CD_3OD-*d*) *δ* ppm 106.8, 118.4, 121.6, 145.6.

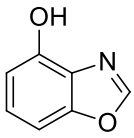

(124) Benzo[*d*]oxazol-4-ol

To a 10 mL round bottom flask was added **(123)** (100 mg, 0.800 mmol), *p*TsOH (5 mg) and triethyl orthoformate (300 µL, 2.72 mmol) and heated to 100 °C while stirring slowly for 30 minutes. The solution was diluted with DCM (2 mL) and the product was purified by column chromatography over silica gel (50% EtOAc, 50% hexane) to afford a pink solid. 96 mg, 88% yield. R_f: 0.76 (50% EtOAc, 50% hexane); ^{1}H NMR (300 MHz, DMSO-d_6) *δ* ppm 6.77 (d, *J*=7.8 Hz, 1 H), 7.14 (d, *J*=8.1 Hz, 1 H), 7.17 – 7.26 (m, 1 H), 8.55 (s, 1 H), 10.34 (s, 1 H); ^{13}C NMR (75 MHz, DMSO-d_6) *δ* ppm 101.6, 110.2, 126.1, 128.6, 149.8, 151.2, 152.1 Characterization data corresponded with literature values.[21]

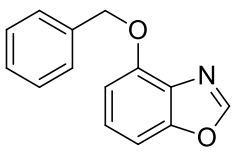

(125) 4-(Benzyloxy)benzo[*d*]oxazole

To DMF (4 mL) in a flask was added **(124)** (96 mg, 0.710 mmol), K_2CO_3 (195 mg, 1.41 mmol) followed by the addition of benzyl bromide (126 µL, 1.06 mmol) at 0 °C under an atmosphere of nitrogen. The mixture was stirred for 1.5 hours. The mixture was added to EtOAc (50 mL), and the organic layer was washed with water (4 x 40 mL), followed

by a wash with brine. The organic phase was dried over $MgSO_4$, and the solvent evaporated *in vacuo*. The product was purified by column chromatography over silica gel (20% EtOAc, 80% hexane) to afford a light yellow solid. 159 mg, quantitative. R_f: 0.66 (20% EtOAc, 80% hexane); ^{1}H NMR (300 MHz, CHLOROFORM-*d*) *δ* ppm 5.43 (s, 2 H), 6.87 (dd, *J*=7.8, 1.1 Hz, 1 H), 7.20 (dd, *J*=9.4, 7.2 Hz, 1 H), 7.24 – 7.31 (m, 1 H), 7.31 – 7.42 (m, 3 H), 7.48 – 7.55 (m, 2 H), 8.02 (s,1 H); ^{13}C NMR (75 MHz, CHLOROFORM-*d*) *δ* ppm 71.2, 103.8, 108.5, 126.1, 127.4 (2 C), 127.9, 128.5 (2 C), 129.9, 136.7, 150.9, 151.0, 151.6; HRMS-TOF MS ES+: m/z $[M+H]^+$ calculated for $C_{14}H_{12}NO_2$: 226.0868; found: 226.0865; Mp: 71 – 73 °C; IR ATR (cm^{-1}): 3128, 2872, 1615, 1496, 1305, 1275, 1069.

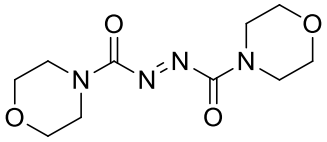

(ADDM) Azodicarbonyldimorpholide

To a solution of diethyl ether (30 mL) and morpholine (2.50 mL, 2.87 mmol) was added diethylazodicarboxylate (1.79 ml, 11.5 mmol) dropwise at 0 °C, and stirred for 30 minutes, afterwhich light orange precipitate fell out of solution. The precipitate was filtered, washed with diethyl ether and dried under vacuum to afford the product as a light orange solid. 2.63 g, 89% yield. ^{1}H NMR (300 MHz, CHLOROFORM-*d*) *δ* ppm 3.58 – 3.66 (m, 1 H), 3.68 – 3.80 (m, 3 H), 3.81 – 3.86 (m, 1 H); ^{13}C NMR; (75 MHz, CHLOROFORM-*d*) *δ* ppm 43.7, 45.2, 66.4, 66.5, 110.0, 159.7.

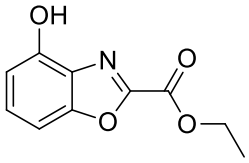

(130) Ethyl 4-hydroxybenzo[*d*]oxazole-2-carboxylate

Method 1:[22] To a solution of **(123)** (450 mg, 3.60 mmol) in pyridine (18 mL) was added ethyl chlorooxoacetate (1.57 mL, 14.0 mmol) at 0 °C under an atmosphere of nitrogen. The solution was heated to 100 °C and stirred overnight. The solution was diluted with 100 mL EtOAc and the organic layer was washed with water (3 x 60 mL) followed by a wash with brine. The organic phase was dried over $MgSO_4$, and the solvent reduced *in vacuo*. The product was purified by column chromatography over silica gel (40% EtOAc, 60% hexane) to afford a white solid. 189 mg, 25% yield. R_f: 0.51 (40% EtOAc, 60% hexane)

Method 2: This method is a modified literature procedure.[23] To a solution of **(123)** (783 mg, 6.26 mmol) in THF (30 mL) and Et_3N (12.5 mmol, 1.75 mL) was added ethyl chlorooxoacetate (770 µL, 6.89 mmol) at -10 °C. The mixture was stirred and allowed to warm to room temperature.

The reaction was monitored by TLC and was completed in 2 hours. *N*-acylated product R_f: 0.75 (60% EtOAc: 40% hexane). The resulting dark brown solution was cooled down to 0 °C followed by the addition of THF (50 mL) and PPh_3 (4.38 g, 16.7 mmol). DEAD (1070 µL, 6.88 mmol) was added dropwise, and the solution turned yellow. The reaction was monitored by TLC and was completed in 3 hours. The solvent was reduced *in vacuo*, and the product was purified by column chromatography over silica gel (40% EtOAc, 60% hexane) to afford a white solid. 1.02 g, 84% yield over two steps. R_f: 0.52 (40% EtOAc, 60% hexane); ^{1}H NMR (300 MHz, DMSO-d_6) δ ppm 1.37 (t, *J*=7.1 Hz, 3 H), 4.43 (q, *J*=7.1 Hz, 2 H), 6.84 (d, *J*=8.1 Hz, 1 H), 7.25 (d, *J*=8.1 Hz, 1 H), 7.34 – 7.42 (m, 1 H), 10.80 (s, 1 H); ^{13}C NMR (75 MHz, CHLOROFORM-*d*) δ ppm 13.9, 62.5, 101.9, 110.9, 129.1, 129.4, 150.8, 151.0, 151.8, 155.8; HRMS-TOF MS ES+: m/z $[M+H]^+$ calculated for $C_{10}H_{10}NO_4$: 208.0610; found: 208.0616; Mp 131 – 134 °C; IR ATR (cm^{-1}): 3440, 2916, 1717, 1686, 1551, 1375, 1270, 1159, 1017.

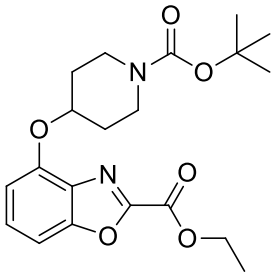

(140) Ethyl 4-((1-(*tert*-butoxycarbonyl)piperidin-4-yl)oxy) benzo[*d*]oxazole-2-carboxylate

To a solution of **(130)** (217 mg, 1.05 mmol), PPh_3 (466 mg, 1.78 mmol) and 1-Boc 4-hydroxypiperidine (358 mg, 1.78 mmol) in THF (6 mL) was added diazene-1,2-diylbis(morpholinomethanone) (ADDM) (456 mg, 1.78 mmol, dissolved in 1 mL DCM) dropwise at 0 °C under an atmosphere of nitrogen. The solution was taken off the ice and stirred at room temperature overnight. The solvent was reduced *in vacuo*, and the product was purified by column chromatography over silica gel (40% EtOAc, 60% hexane) to afford a white solid. 323 mg, 79% yield. R_f: 0.62 (40% EtOAc, 60% hexane); ^{1}H NMR (300 MHz, CHLOROFORM-*d*) δ ppm 1.45 – 1.51 (m, 12 H), 1.78 – 1.93 (m, 2 H), 1.96 – 2.08 (m, 2 H), 3.26 – 3.37 (m, 2 H), 3.77 – 3.89 (m, 2 H), 4.55 (q, *J*=7.1 Hz, 2 H), 4.95 – 5.05 (m, 1 H), 6.89 (d, *J*=7.6 Hz, 1 H), 7.22 – 7.26 (m, 1 H), 7.37 – 7.45 (m, 1 H); ^{13}C NMR (75 MHz, CHLOROFORM-*d*) δ ppm 14.1, 28.4 (3 C), 30.6 (2 C), 40.7 (2 C), 63.1, 74.1, 79.6, 104.1, 110.5, 128.8, 131.2, 150.6, 151.4, 152.5, 154.8, 156.4; HRMS-TOF MS ES+: m/z $[M+H]^+$ calculated for $C_{20}H_{27}N_2O_6$: 391.1869; found: 391.1868; Mp: 112 – 114 °C; IR ATR (cm^{-1}): 2936, 1739, 1545, 1418, 1269, 1159, 1081.

Compounds **(141)** – **(143)** were synthesized via the same procedure. Compound **(140)**, K_3PO_4 (3 equivalents) and the aromatic alcohol used for the transesterification reaction (20 – 30

equivalents) were placed in a flask and stirred under nitrogen at room temperature for 12 – 20 hours. The reaction was monitored via TLC using (5% EtOAc, 95% DCM) as mobile phase to determine whether the starting material had been consumed. The K_3PO_4 was filtered off, and the alcohol removed via heating the solution to 50 °C and streaming compressed air over the solution. After the majority of the solvent volume had been evaporated off, the product was purified by column chromatography over silica gel (5% EtOAc, 95% DCM).

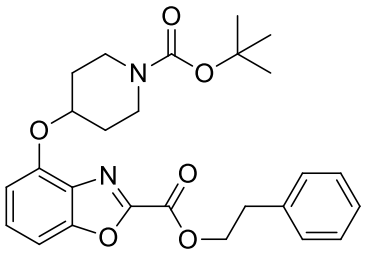

(141) Phenethyl4-((1-(*tert*-butoxycarbonyl)piperidin-4-yl)oxy)benzo[*d*]oxazole-2-carboxylate

44 mg, 45% yield, white solid. R_f: 0.56 (30% EtOAc, 70% hexane); ^{1}H-NMR (300 MHz, CHLOROFORM-*d*) *δ* ppm 1.47 (s, 9 H), 1.79 – 1.94 (m, 2 H), 1.98 – 2.12 (m, 2 H), 3.15 (t, *J*=7.3 Hz, 2 H), 3.28– 3.41 (m, 2 H), 3.78 – 3.92 (m, 2 H), 4.66 (t, *J*=7.3 Hz, 2 H), 5.00 – 5.09 (m, 1 H), 6.92 (d, *J*=7.6 Hz, 1 H), 7.20 – 7.38 (m, 6 H), 7.39 – 7.46 (m, 1 H); ^{13}C NMR (75 MHz, CHLOROFORM-*d*) *δ* ppm 28.4 (3 C), 30.6 (2 C), 34.9, 40.9 (2 C), 67.2, 74.2, 79.6, 104.1, 110.8, 126.8, 128.6 (2 C), 128.8, 128.9 (2 C), 131.1, 136.8, 150.6, 151.2, 152.5, 154.8, 156.3; HRMS-TOF MS ES+: m/z $[M+H]^+$ calculated for $C_{26}H_{31}N_2O_6$: 467.2182; found: 467.2170; Mp: 114 – 117 °C, IR ATR (cm^{-1}): 2970, 1734, 1685, 1614, 1409, 1324, 1149, 1081, 1026.

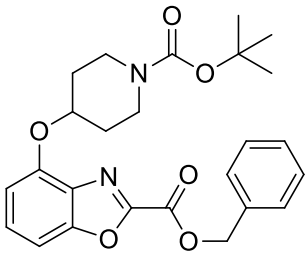

(142) Benzyl 4-((1-(*tert*-butoxycarbonyl)piperidin-4-yl)oxy) benzo[*d*]oxazole-2-carboxylate

17 mg, 24% yield, white solid. R_f: 0.77 (30% EtOAc, 70% hexane); ^{1}H NMR (300 MHz, CHLOROFORM-*d*) *δ* ppm 1.47 (s, 9 H), 1.77 – 1.91 (m, 2 H), 1.95 – 2.08 (m, 2 H), 3.25– 3.36 (m, 2 H), 3.77 – 3.88 (m, 2 H), 4.97 – 5.06 (m, 1 H), 5.50 (s, 2 H), 6.89 (d, *J*=8.2 Hz, 1 H), 7.20 – 7.28 (m, 1 H), 7.35 – 7.55 (m, 6 H); ^{13}C NMR (75 MHz, CHLOROFORM-*d*) *δ* ppm 28.4 (3 C), 30.6 (2 C), 40.5 (2 C), 68.4, 74.2, 79.6, 104.1, 110.6, 128.7 (2 C), 128.8, 128.9 (2 C), 131.2, 134.5, 150.6, 151.1, 152.5, 154.8, 156.3; Missing carbon signal, suspected to be merged with signals located between 128.8 ppm – 129.0 ppm; HRMS-TOF MS ES+: m/z $[M+H]^+$ calculated for $C_{25}H_{29}N_2O_6$: 453.2026; found: 453.2006; Mp: 118 – 120 °C, IR ATR (cm^{-1}): 2972, 1738, 1686, 1613, 1430, 1323, 1149, 1079, 1027.

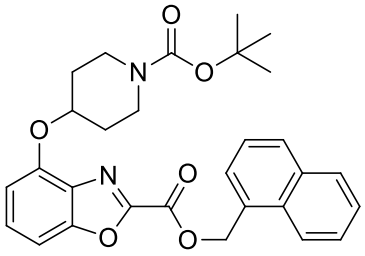

(143) Naphthalen-1-ylmethyl 4-((1-(*tert*-butoxycarbonyl) piperidin-4-yl)oxy)benzo[*d*]oxazole-2-carboxylate

41 mg, 53% yield, white solid. R_f: 0.80 (5% EtOAc: 95% DCM) ^{1}H NMR (300 MHz, CHLOROFORM-*d*) δ ppm 1.48 (s, 9 H), 1.75 – 1.89 (m, 2 H), 1.94 – 2.04 (m, 2 H), 3.21 – 3.35 (m, 2 H), 3.75 – 3.88 (m, 2 H), 4.97 – 5.06 (m, 1 H), 5.96 (s, 2 H), 6.87 (d, *J*=8.2 Hz, 1 H), 7.19 (d, *J*=8.2 Hz, 1 H), 7.34 – 7.41 (m, 1 H), 7.45 – 7.63 (m, 3 H), 7.71 (d, *J*=6.5 Hz, 1 H), 7.87 – 7.93 (m, 2 H), 8.15 (d, *J*=8.2 Hz, 1 H); ^{13}C NMR (75 MHz, CHLOROFORM-*d*) δ ppm 28.4 (3 C), 30.6 (2 C), 40.7 (2 C), 66.6, 74.3, 79.5, 104.0, 110.8, 123.4, 125.2, 126.0, 126.8, 128.3, 128.7, 128.8, 129.8, 129.9, 131.1, 131.6, 133.7, 150.5, 151.0, 152.5, 154.8, 156.3; HRMS-TOF MS ES+: m/z $[M+H]^+$ calculated for $C_{29}H_{31}N_2O_6$: 503.2182; found: 503.2171; Mp: 129 – 132 °C, IR ATR (cm^{-1}): 2959, 1727, 1686, 1546, 1472, 1362, 1269, 1159, 1070, 1016.

Compounds **(144)** – **(147)** were synthesized via the same procedure. Compound **(140)** and the respected amine (10 equivalents) were dissolved in THF (1 mL) and stirred under nitrogen at room temperature for 12 – 20 hours. The reaction was monitored via TLC using (50% EtOAc, 50% hexane) mobile phase to determine whether the starting material had been consumed. The product was purified by column chromatography over silica gel (50% EtOAc, 50% hexane – 100% EtOAc)

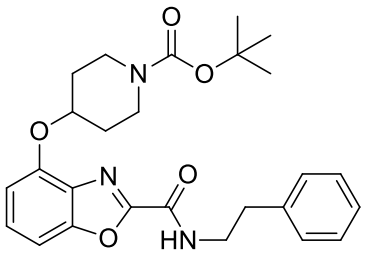

(144) *tert*-Butyl 4-((2-(phenethylcarbamoyl)benzo[*d*]oxazol-4-yl)oxy)piperidine-1-carboxylate

51 mg, 91% yield, yellow solid. R_f: 0.71 (50% EtOAc, 50% hexane); ^{1}H NMR (300 MHz, CHLOROFORM-*d*) δ ppm 1.44 – 1.56 (m, 9 H), 1.76 – 1.92 (m, 2 H), 1.95 – 2.10 (m, 2 H), 2.98 (t, *J*=7.3 Hz, 2 H), 3.25 – 3.38 (m, 2 H), 3.72 – 3.89 (m, 4 H), 4.86 – 4.95 (m, 1 H), 6.90 (d, *J*=8.2 Hz, 1 H), 7.19 – 7.43 (m, 8 H); ^{13}C NMR (75 MHz, CHLOROFORM-*d*) δ ppm 28.4 (3 C), 30.6 (2 C), 35.5, 40.7 (2 C), 40.9, 74.1, 79.6, 104.5, 110.6, 126.7, 127.9, 128.7 (4 C), 130.6, 138.2, 149.9, 152.8, 154.1, 154.7, 155.5; Missing carbon signal, suspected to be merged with signal located at 128.7 ppm; HRMS-TOF MS ES+: m/z $[M+H]^+$ calculated for $C_{26}H_{32}N_3O_5$:

466.2342; found: 466.2338; Mp: 71 – 73 °C, IR ATR (cm^{-1}): 3313, 2930, 1681, 1617, 1553, 1496, 1423, 1364, 1265, 1165, 1067, 1022.

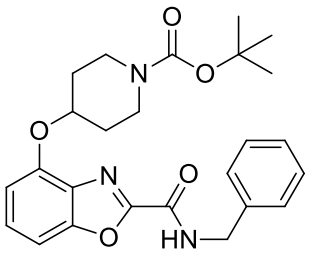

(145) *tert*-Butyl 4-((2-(benzylcarbamoyl)benzo[*d*]oxazol-4-yl)oxy) piperidine-1-carboxylate

52 mg, 96% yield, yellow solid. R_f: 0.65 (50% EtOAc, 50% hexane); ^{1}H NMR (300 MHz, CHLOROFORM-*d*) *δ* ppm 1.46 (s, 9 H), 1.77 – 1.89 (m, 2 H), 1.94– 2.05 (m, 3 H), 3.24 – 3.34 (m, 2 H), 3.75 – 3.86 (m, 2 H), 4.67 (d, *J*=6.5 Hz, 2 H), 4.73 – 4.84 (m, 1 H), 6.88 (d, *J*=7.6 Hz, 1 H), 7.23 – 7.27 (m, 1 H), 7.27 – 7.40 (m, 6 H), 7.66 (t, *J*=5.9 Hz, 1 H); ^{13}C NMR (75 MHz, CHLOROFORM-*d*) *δ* ppm 28.3 (3 C), 30.5 (2 C), 40.6 (2 C), 43.7, 74.0, 79.6, 104.4, 110.1, 127.8, 128.0 (3 C), 128.7 (2 C), 130.6, 136.9, 149.9, 152.7, 154.1, 154.7, 155.4; Missing carbon signal, suspected to be merged with signal located at 128.0 ppm; HRMS-TOF MS ES+: m/z $[M+Na]^+$ calculated for $C_{25}H_{29}N_3O_5Na$: 474.2005; found: 474.2001; Mp: 148 – 151 °C, IR ATR (cm^{-1}): 3374, 2969, 1689, 1618, 1550, 1419, 1266, 1234, 1165, 1082.

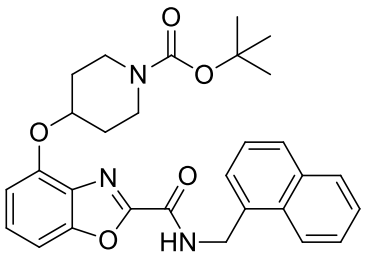

(146) *tert*-Butyl 4-((2-((naphthalen-1-ylmethyl)carbamoyl) benzo[*d*]oxazol-4-yl)oxy)piperidine-1-carboxylate

51 mg, 86% yield, yellow solid. R_f: 0.32 (35% EtOAc, 65% hexane); ^{1}H NMR (300 MHz, CHLOROFORM-*d*) *δ* ppm 1.41 – 1.51 (m, 9 H), 1.73– 1.85 (m, 2 H), 1.91 – 2.02 (m, 2 H), 3.18 – 3.29 (m, 2 H), 3.72 – 3.84 (m, 2 H), 4.77 – 4.87 (m, 1 H), 5.14 (d, *J*=5.9 Hz, 2 H), 6.85 (d, *J*=7.6 Hz, 1 H), 7.25 (d, *J*=8.2 Hz, 1 H), 7.30 – 7.64 (m, 6 H), 7.82 – 7.93 (m, 2 H), 8.09 (d, *J*=7.6 Hz, 1 H); ^{13}C NMR (75 MHz, CHLOROFORM-*d*) *δ* ppm 28.4 (3 C), 30.6 (2 C), 40.8 (2 C), 41.9, 74.0, 79.7, 104.5, 110.0, 123.4, 125.4, 126.2, 126.9, 127.2, 128.1, 128.9, 129.1, 130.7, 131.4, 132.3, 133.9, 150.0, 152.8, 154.1, 154.8, 155.2; HRMS-TOF MS ES+: m/z $[M+Na]^+$ calculated for $C_{29}H_{31}N_3O_5Na$: 524.2162; found: 524.2145; Mp: 84 – 87 °C, IR ATR (cm^{-1}): 3299, 2933, 1682, 1617, 1551, 1499, 1423, 1364, 1267, 1165, 1078.

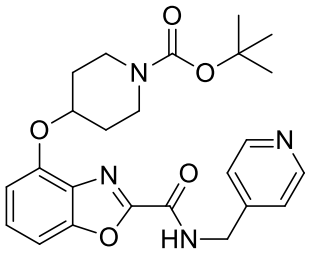

(147) *tert*-Butyl 4-((2-((pyridin-4-ylmethyl)carbamoyl) benzo[*d*]oxazol-4-yl)oxy)piperidine-1-carboxylate

66 mg, 95% yield, yellow solid. R_f: 0.54 (100% EtOAc); ^{1}H NMR (300 MHz, CHLOROFORM-*d*) *δ* ppm 1.46 (s, 9 H), 1.76 – 1.91 (m, 2 H), 1.95 – 2.06 (m, 2 H), 3.25 – 3.36 (m, 2 H), 3.74 – 3.86 (m, 2 H), 4.69 (d, *J*=6.5 Hz, 2 H), 4.81 – 4.90 (m, 1 H), 6.89 (d, *J*=8.2 Hz, 1 H), 7.22 – 7.31 (m, 3 H), 7.35 – 7.42 (m, 1 H), 7.96 (t, *J*=6.5 Hz, 1 H), 8.57 (d, *J*=5.3 Hz, 2 H); ^{13}C NMR (75 MHz, CHLOROFORM-*d*) *δ* ppm 28.3 (3 C), 30.5 (2 C), 40.5 (2 C), 42.4, 73.9, 79.7, 104.5, 110.0, 122.4 (2 C), 128.3, 130.6, 146.2, 150.0, 150.0 (2 C), 152.8, 153.7, 154.7, 155.8; HRMS-TOF MS ES+: m/z $[M+H]^+$ calculated for $C_{21}H_{29}N_4O_5$: 453.2138; found: 453.2136; Mp: 188 – 192 °C, IR ATR (cm^{-1}): 3400, 2929, 1699, 1680, 1605, 1548, 1412, 1234, 1164, 1079.

Compounds **BI1** – **BI7** were synthesized via the same procedure. In a small flask was added the Boc-protected compound **(141)** – **(147)** separately and DCM (1 mL) followed by the addition of 4M HCl/dioxane (1 mL). The solution was stirred for one hour, after which the solvent was reduced *in vacuo*. A small amount of DCM was added followed by the addition of EtOAc which caused the salt to precipitate out of solution. The solvent was reduced *in vacuo* and the product dried under vacuum.

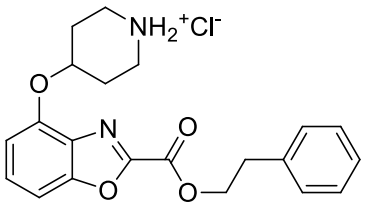

(BO1) 4-((2-(phenethoxycarbonyl)benzo[*d*]oxazol-4-yl)oxy) piperidin-1-ium chloride

37 mg, 98% yield, white solid. ^{1}H NMR (600 MHz, DMSO-d_6) *δ* ppm 1.92 – 2.02 (m, 2 H), 2.15 – 2.29 (m, 2 H), 3.05 – 3.14 (m, 4 H), 3.23 – 3.30 (m, 2 H), 4.61 (t, *J*=7.0 Hz, 2 H), 5.02 – 5.07 (m, 1 H), 7.16 (d, *J*=8.2 Hz, 1 H), 7.20 – 7.36 (m, 5 H), 7.45 (d, *J*=8.2 Hz, 1 H), 7.49 – 7.57 (m, 1 H), 9.24 (br. s., 1 H); ^{13}C NMR (151 MHz, DMSO-d_6) *δ* ppm 27.1 (2 C), 34.1, 40.4 (2 C), 66.7, 70.8, 104.5, 110.3, 126.6, 128.4 (2 C), 128.9 (2 C), 129.2, 130.5, 137.4, 149.6, 151.2, 151.8, 155.6; HRMS-TOF MS ES+: m/z $[M+H]^+$ calculated for $C_{21}H_{23}N2O_4$: 367.1658; found: 367.1663; Purity: >95%; Mp: 184– 186 °C, IR ATR (cm^{-1}): 2958, 2731, 1740, 1609, 1494, 1263, 1142, 1084.

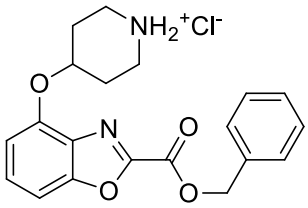

(BO2) 4-((2-((Benzyloxy)carbonyl)benzo[*d*]oxazol-4-yl)oxy) piperidin-1-ium chloride

9.8 mg, 69% yield, white solid. ^{1}H NMR (600 MHz, DMSO-d_6) δ ppm 1.91 – 2.00 (m, 2 H), 2.16 – 2.24 (m, 2 H), 3.05 – 3.13 (m, 2 H), 3.21 – 3.29 (m, 2 H), 4.99 – 5.05 (m, 1 H), 5.46 (s, 2 H), 7.16 (d, *J*=8.2 Hz, 1 H), 7.38 – 7.48 (m, 4 H), 7.48 – 7.56 (m, 3 H), 9.21 (br. s., 1 H); ^{13}C NMR (151 MHz, DMSO-d_6) δ ppm 27.1 (2 C), 40.4 (2 C), 67.8, 70.7, 104.5, 110.2, 128.6 (3 C), 128.7 (2 C), 129.2, 130.6, 134.8, 149.6, 151.2, 151.8, 155.6; Missing carbon signal, suspected to be merged with signal located at 128.6 ppm; HRMS-TOF MS ES+: m/z $[M+H]^+$ calculated for $C_{20}H_{21}N_2O_4$: 353.1501; found: 353.1491; Purity: >95%; Mp: 189 – 192 °C, IR ATR (cm^{-1}): 2930, 2676, 1741, 1616, 1541, 1497, 1320, 1271, 1178, 1070.

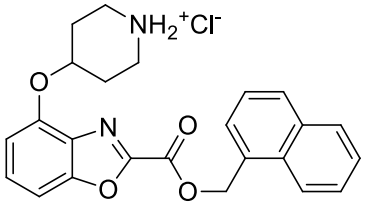

(BO3) 4-((2-((Naphthalen-1-ylmethoxy)carbonyl) benzo[*d*]oxazol-4-yl)oxy)piperidin-1-ium chloride

27 mg, 75% yield, white solid. ^{1}H NMR (600 MHz, DMSO-d_6) δ ppm 1.87 – 1.98 (m, 2 H), 2.14 – 2.22 (m, 2 H), 3.02 – 3.11 (m, 2 H), 3.19 – 3.28 (m, 2 H),4.97 – 5.03 (m, 1 H), 5.93 (s, 2 H), 7.14 (d, *J*=8.2 Hz, 1 H), 7.42 (d, *J*=8.8 Hz, 1 H), 7.48 – 7.53 (m, 1 H), 7.53 – 7.66 (m, 3 H), 7.74 (d, *J*=7.0 Hz, 1 H), 7.99 – 8.04 (m, 2 H), 8.18 (d, *J*=8.2 Hz, 1 H), 9.17 (br. s., 2 H); ^{13}C NMR (151 MHz, DMSO-d_6) δ ppm 27.1 (2 C), 40.4 (2 C), 66.2, 70.7, 104.5, 110.1, 123.7, 125.4, 126.2, 126.9, 128.3, 128.6, 129.2, 129.6, 130.3, 130.5, 131.2, 133.3, 149.5, 151.2, 151.8, 155.6; HRMS-TOF MS ES+: m/z $[M+H]^+$ calculated for $C_{24}H_{23}N_2O_4$: 403.1658; found: 403.1655; Purity: >95%; Mp: 168 – 170 °C, IR ATR (cm^{-1}): 2930, 2798, 1734, 1620, 1543, 1504, 1325, 1276, 1181, 1142, 1074.

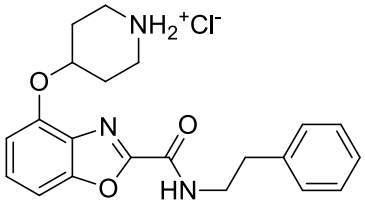

(BO4) 4-((2-(Phenethylcarbamoyl)benzo[*d*]oxazol-4-yl)oxy) piperidin-1-ium chloride

39 mg, 89% yield, white solid. ^{1}H NMR (600 MHz, DMSO-d_6) δ ppm 1.91 – 1.99 (m, 2 H), 2.18 – 2.24 (m, 2 H), 2.89 (t, *J*=7.3 Hz, 2 H), 3.06 – 3.14 (m, 2 H), 3.28 (br. s., 2 H), 3.53 (q, *J*=7.0 Hz, 2 H), 5.03 – 5.09 (m, 1 H), 7.14 (d, *J*=8.2 Hz, 1 H), 7.19 – 7.22 (m, 1 H), 7.23 – 7.27 (m, 2 H), 7.27 – 7.32 (m, 2 H), 7.42 (d, *J*=8.2 Hz, 1 H), 7.45 – 7.49 (m, 1 H), 9.07 (br. s., 1 H), 9.18 (br. s., 1 H), 9.35 (t, *J*=5.9 Hz, 1 H); ^{13}C NMR (151 MHz, DMSO-d_6) δ ppm 27.2 (2 C), 34.7, 40.6 (2 C), 40.7, 70.7, 104.3, 109.8, 126.2, 128.1, 128.3

(2 C), 128.6 (2 C), 130.0, 139.1, 149.2, 151.8, 154.4, 154.9; HRMS-TOF MS ES+: m/z $[M+H]^+$ calculated for $C_{21}H_{24}N_3O_3$: 366.1818; found: 366.1824; Purity: >98%; Mp: 220 – 223 °C, IR ATR (cm^{-1}): 3390, 2931, 1673, 1617, 1557, 1496, 1267, 1193, 1071.

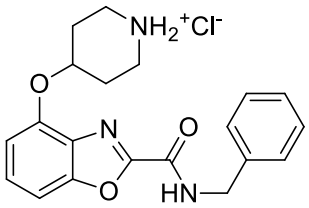

(BO5) 4-((2-(Benzylcarbamoyl)benzo[*d*]oxazol-4-yl)oxy)piperidin-1-ium chloride

44 mg, 97% yield, yellow solid. ^{1}H NMR (600 MHz, DMSO-d_6) δ ppm 1.92 – 2.01 (m, 2 H), 2.18 – 2.26 (m, 2 H), 3.06 – 3.14 (m, 2 H), 3.24 – 3.31 (m, 2 H), 4.48 (d, *J*=6.4 Hz, 2 H), 5.05 – 5.11 (m, 1 H), 7.14 (d, *J*=8.2 Hz, 1 H), 7.23 – 7.28 (m, 1 H), 7.30 – 7.39 (m, 4 H), 7.42 (d, *J*=8.2 Hz, 1 H), 7.44 – 7.49 (m, 1 H), 9.23 (br. s., 1 H), 9.34 (br. s., 1 H), 9.85 (t, *J*=6.4 Hz, 1 H); ^{13}C NMR (151 MHz, DMSO-d_6) δ ppm 27.2 (2 C), 40.7 (2 C), 42.6, 70.8, 104.3, 109.8, 126.9, 127.4 (2 C), 128.2, 128.3 (2 C), 130.1, 138.7, 149.2, 151.9, 154.4, 155.1; HRMS-TOF MS ES+: m/z $[M+H]^+$ calculated for $C_{20}H_{22}N_3O_3$: 352.1616; found: 352.1653; Purity: >98%; Mp: 102 – 105 °C, IR ATR (cm^{-1}): 3380, 2929, 1674, 1616, 1556, 1496, 1267, 1071.

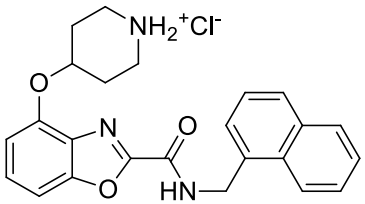

(BO6) 4-((2-((Naphthalen-1-ylmethyl)carbamoyl) benzo[*d*]oxazol-4-yl)oxy)piperidin-1-ium chloride

42 mg, 92% yield, yellow solid. ^{1}H NMR (600 MHz, DMSO-d_6) δ ppm 1.91 – 2.00 (m, 2 H), 2.18 – 2.25 (m, 2 H), 3.02 – 3.13 (m, 2 H), 3.26 (br. s., 2 H), 4.96 (d, *J*=5.9 Hz, 2 H), 5.04 – 5.09 (m, 1 H), 7.14 (d, *J*=8.2 Hz, 1 H), 7.41 – 7.44 (m, 1 H), 7.45 – 7.51 (m, 2 H), 7.52 – 7.57 (m, 2 H), 7.57 – 7.61 (m, 1 H), 7.86 (d, *J*=8.2 Hz, 1 H), 7.96 (d, *J*=8.2 Hz, 1 H), 8.24 (d, *J*=8.8 Hz, 1 H), 9.23 (br. s., 1 H), 9.34 (br. s., 1 H), 9.91 (t, *J*=6.2 Hz, 1 H); ^{13}C NMR (151 MHz, DMSO-d_6) δ ppm 27.2 (2 C), 40.7, 40.7 (2 C), 70.7, 104.3, 109.8, 123.4, 125.4, 125.5, 125.8, 126.3, 127.6, 128.2, 128.5, 130.1, 130.7, 133.2, 133.6, 149.2, 151.9, 154.4, 155.2; HRMS-TOF MS ES+: m/z $[M+H]^+$ calculated for $C_{24}H_{24}N_3O_3$: 402.1818; found: 402.1817; Purity: >93.1%; Mp: 230 – 232 °C, IR ATR (cm^{-1}): 3380, 2929, 1674, 1616, 1556, 1496, 1267, 1071.

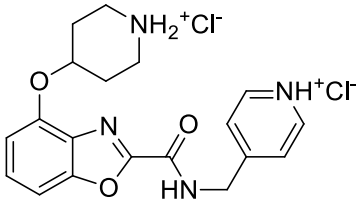

(BO7) 4-((4-(Piperidin-1-ium-4-yloxy)benzo[*d*]oxazole-2-carboxamido)methyl)pyridin-1-ium chloride

53 mg, 94% yield, yellow solid. ^{1}H NMR (600 MHz, DMSO-d_6) δ ppm 1.95 – 2.04 (m, 2 H), 2.18 – 2.28 (m, 2 H), 3.06 – 3.18 (m, 2 H), 3.26 (br. s., 2 H), 4.77 (d, *J*=5.9 Hz, 2 H), 5.07 – 5.16 (m, 1 H), 7.17 (d, *J*=8.2 Hz, 1 H), 7.43 (d, *J*=8.2 Hz, 1 H), 7.46 – 7.52 (m, 1 H), 8.01 (d, *J*=5.9 Hz, 2 H), 8.86 (d, *J*=5.9 Hz, 2 H), 9.40 (br. s., 1 H), 9.64 (br. s, 1 H), 10.11 (t, *J*=6.2 Hz, 1 H); ^{13}C NMR (151 MHz, DMSO-d_6) δ ppm 27.2 (2 C), 40.7 (2 C), 42.2, 70.8, 104.2, 109.7, 124.9 (2 C), 128.4, 130.0, 141.7 (2 C), 149.3, 151.9, 153.9, 155.7, 158.5; HRMS-TOF MS ES+: m/z $[M+H]^+$ calculated for $C_{19}H_{21}N_4O_3$: 353.1614; found: 353.1614; Purity: 96.7%; Mp: 239 – 241 °C, IR ATR (cm^{-1}): 3382, 2692, 1694, 1602, 1518, 1259, 1070.

10.6 Synthesis of compounds pertaining to Chapter 6

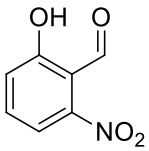

(160) 2-Hydroxy-6-nitrobenzaldehyde

3-nitrophenol (1.00 g 7.19 mmol) was placed in a vial and combined with hexamethylenetetramine (1.21 g, 8.59 mmol) and 5.00 mL trifluoroacetic acid. The vial was flushed with argon, sealed, and the solution was stirred at 90 °C for 12 hours. The reaction mixture was poured onto 50 mL ice-water and extracted with 2 x 50 mL EtOAc. The organic fractions were combined, washed with brine, dried over $MgSO_4$, and the solvent reduced *in vacuo*. The product was purified by column chromatography over silica gel (20% EtOAc, 80% hexane) to afford the product as a yellow solid. 354 mg, 29% yield. R_f: 0.59 (20% EtOAc, 80% hexane); ^{1}H NMR (300 MHz, CHLOROFORM-*d*) δ ppm 7.28 – 7.34 (m, 1 H), 7.54 – 7.60 (m, 1 H), 7.60 – 7.67 (m, 1 H), 10.33 (s, 1 H), 12.11 (br. s., 1 H); ^{13}C NMR (75 MHz, CHLOROFORM-*d*) δ ppm 112.3, 116.0, 124.2, 135.9, 163.1, 163.3, 193.8; Characterization data corresponded with available literature values.[24]

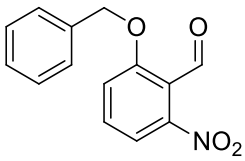

(161) 2-(Benzyloxy)-6-nitrobenzaldehyde

In DMF (4 mL) was added **(160)** (354 mg, 2.12 mmol), benzyl bromide (0.760 mL, 6.36 mmol) and K_2CO_3 (440 mg, 3.18 mmol) at 0 °C under an atmosphere of nitrogen. The reaction mixture was warmed to room temperature and stirred overnight. The reaction mixture was dissolved in EtOAc (60 mL), and washed with water (4 x 50 mL) followed by a wash with brine. The organic layer was dried over $MgSO_4$, filtered and reduced *in vacuo*. The product was purified by column chromatography over silica gel (50% EtOAc, 50% hexane) to afford the product as a yellow solid. Quantitative, 557 mg. R_f: 0.23 (20% EtOAc, 80% hexane); ^{1}H NMR (400 MHz, CHLOROFORM-*d*) *δ* ppm 5.23 (s, 2 H), 7.29 (d, *J*=8.2 Hz, 1 H), 7.34 – 7.43 (m, 5 H), 7.45 (d, *J*=8.2 Hz, 1 H), 7.54 – 7.60 (m, 1 H), 10.45 (s, 1 H); ^{13}C NMR (101 MHz, CHLOROFORM-*d*) *δ* ppm 71.5, 115.8, 117.6, 121.1, 127.2 (2 C), 128.6, 128.9 (2 C), 133.4, 135.0, 148.7, 158.8, 187.6; Characterization data corresponded with available literature values.[24]

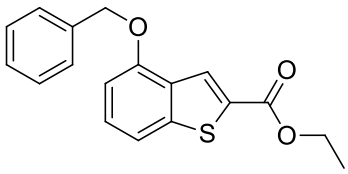

(163) Ethyl 4-(benzyloxy)benzo[*b*]thiophene-2-carboxylate

In a Schlenk flask was added **(161)** (557 mg, 2.17 mmol), K_2CO_3 (361 mg, 2.61 mmol) and DMF (4.5 mL). Ethyl thioglycolate (250 µL, 2.27 mmol) was added dropwise at 0 °C under an atmosphere of nitrogen, upon which the initial yellow solution turned light yellow. The mixture was stirred at 0 °C for 30 minutes, then heated to 50 °C for 48 hours. The mixture was diluted with EtOAc (60 mL), and washed with water (4 x 50 mL) followed by a wash with brine. The organic fraction was dried over $MgSO_4$, and the solvent reduced *in vacuo*. The product was purified by column chromatography over silica gel (5% EtOAc, 95% hexane) to afford the product as a yellow solid. 644 mg, 95% yield. R_f: 0.45 (5% EtOAc, 95% hexane); ^{1}H NMR (300 MHz, CHLOROFORM-*d*) *δ* ppm 1.43 (t, *J*=7.0 Hz, 3 H), 4.42 (q, *J*=7.0 Hz, 2 H), 5.22 (s, 2 H), 6.82 (d, *J*=7.0 Hz, 1 H), 7.32 – 7.55 (m, 7 H), 8.31 (s, 1 H); ^{13}C NMR (75 MHz, CHLOROFORM-*d*) *δ* ppm 14.3, 61.4, 70.0, 105.3, 115.0, 127.3 (2 C), 127.4, 128.0, 128.1, 128.5 (2 C), 130.1, 132.1, 136.4, 143.7, 155.2, 162.7; HRMS-TOF MS ES+: m/z $[M+H]^+$ calculated for $C_{18}H_{17}O_3S$: 313.0898; found: 313.0888; IR ATR (cm^{-1}): 2926, 1704, 1564, 1519, 1285, 1233, 1151, 1021.

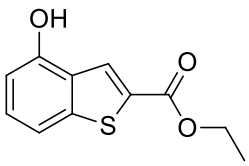

(164) Ethyl 4-hydroxybenzo[*b*]thiophene-2-carboxylate

To a solution of **(163)** (630 mg, 2.02 mmol) in MeOH (6 mL) was added Pd/C (10%, 170 mg, 0.159 mmol), after which the flask was purged with hydrogen from a balloon, stirred under an atmosphere of hydrogen for 12 hours. The mixture was filtered through a plug of Celite and the solvent removed *in vacuo*. The product was purified by column chromatography over silica gel (30% EtOAc, 70% hexane) to afford the product as a yellow solid. 314 mg, 68% yield. R_f: 0.43 (30% EtOAc, 70% hexane); ^{1}H NMR (300 MHz, CHLOROFORM-*d*) *δ* ppm 1.43 (t, *J*=7.0 Hz, 3 H), 4.43 (q, *J*=7.0 Hz, 2 H), 5.73 (s, 1 H), 6.77 (d, *J*=7.0 Hz, 1 H), 7.29 – 7.36 (m, 1 H), 7.43 (d, *J*=8.2 Hz, 1 H), 8.32 (d, *J*=1.2 Hz, 1 H); ^{13}C NMR (75 MHz, CHLOROFORM-*d*) *δ* ppm 14.3, 61.7, 109.2, 110.0, 115.2, 126.9, 128.3, 132.1, 144.1, 152.3, 163.1; HRMS-TOF MS ES+: m/z $[M+Na]^+$calculated for $C_{11}H_{10}O_3SNa$: 245.0249; found: 245.0254; Mp: 154 – 156 °C; IR ATR (cm^{-1}): 3376, 1692, 1564, 1527, 1332, 1279, 1218, 1149.

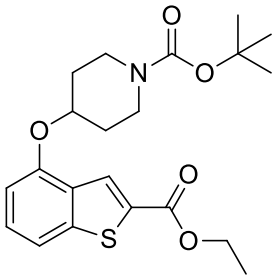

(165) *tert*-butyl 4-((2-(ethoxycarbonyl)benzo[*b*]thiophen-4-yl)oxy)piperidine-1-carboxylate

(164) (314 mg, 1.41 mmol), PPh_3 (629 mg, 2.40 mmol) and 1-Boc-4-hydroxypiperidine (483 mg, 2.40 mmol) were dissolved in THF (9 mL) under an atmosphere of nitrogen. To this solution was added DBAD (553 mg, 2.4 mmol, dissolved in 1 mL THF) dropwise at 0 °C. The solution was stirred overnight at room temperature, after which the solvent was removed *in vacuo*, and the product was purified by column chromatography over silica gel (20% EtOAc, 80% hexane) to afford the product as a colorless semisolid that solidified over time into a white solid. 571 mg, 99% yield. R_f: 0.48 (20% EtOAc, 80% hexane); ^{1}H NMR (300 MHz, CHLOROFORM-*d*) *δ* ppm 1.36 (t, *J*=7.0 Hz, 3 H), 1.44 (s, 9 H), 1.74 – 1.87 (m, 2 H), 1.87 – 1.97 (m, 2 H), 3.34 – 3.45 (m, 2 H), 3.61 – 3.72 (m, 2 H), 4.34 (q, *J*=7.0 Hz, 2 H), 4.56 – 4.66 (m, 1 H), 6.70 (d, *J*=7.0 Hz, 1 H), 7.24 – 7.31 (m, 1 H), 7.34 (d, *J*=8.2 Hz, 1 H), 8.14 (s, 1 H); ^{13}C NMR (75 MHz, CHLOROFORM-*d*) *δ* ppm 14.1, 28.2 (3 C), 30.1 (2 C), 40.3 (2 C), 61.2, 72.0, 79.3, 106.2, 114.7, 127.0, 127.9, 130.6, 131.9, 143.7, 153.5, 154.5, 162.5; HRMS-TOF MS ES+: m/z $[M+Na]^+$ calculated for $C_{21}H_{27}NO_5SNa$: 428.1508; found: 428.1515; Mp: 64 – 67 °C; IR ATR (cm^{-1}): 2947, 1716, 1696, 1681, 1562, 1416, 1253, 1230, 1150, 1023.

Compounds **(166)** – **(168)** were synthesized via the same procedure. Compound **(165)**, K_3PO_4 (3 equivalents) and the aromatic alcohol used for the transesterification reaction (26 equivalents) were placed in a flask and stirred under nitrogen at 70 °C for 12 – 20 hours. The reaction was monitored via TLC using 5% EtOAc, 95% DCM as mobile phase to determine whether the starting material had been consumed. The K_3PO_4 was filtered off, and the alcohol removed via heating the solution to 50 °C and streaming compressed air over the solution. After the majority of the solvent volume had been evaporated off, the product was purified by column chromatography over silica gel (5% EtOAc, 95% DCM).

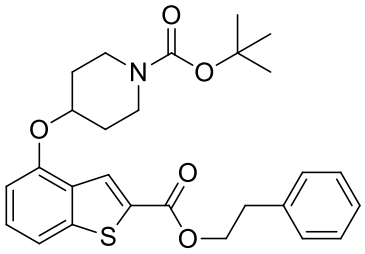

(166) *tert*-Butyl 4-((2-(phenethoxycarbonyl)benzo[*b*]thiophen-4-yl)oxy)piperidine-1-carboxylate

53 mg, 88% yield, clear semi-solid. R_f: 0.50 (20% EtOAc, 80% hexane); ^{1}H NMR (400 MHz, CHLOROFORM-*d*) δ ppm 1.50 (s, 9 H), 1.84 – 1.94 (m, 2 H), 1.94 – 2.04 (m, 2 H), 3.11 (t, *J*=7.0 Hz, 2 H), 3.43– 3.52 (m, 2 H), 3.65 – 3.74 (m, 2 H), 4.56 (t, *J*=7.2 Hz, 2 H), 4.65 – 4.74 (m, 1 H), 6.78 (d, *J*=7.4 Hz, 1 H), 7.23 – 7.35 (m, 5 H), 7.35 – 7.40 (m, 1 H), 7.41 – 7.44 (m, 1 H), 8.19 (d, *J*=0.8 Hz, 1 H); ^{13}C NMR (75 MHz, CHLOROFORM-*d*) δ ppm 28.4 (3 C), 30.3 (2 C), 35.2, 40.3 (2 C), 65.9, 72.2, 79.7, 106.4, 115.0, 126.6, 127.5, 128.2, 128.5 (2 C), 129.0 (2 C), 130.9, 131.8, 137.6, 144.0, 153.7, 154.8, 162.6; HRMS-TOF MS ES+: m/z $[M+Na]^+$ calculated for $C_{27}H_{31}NO_5SNa$: 504.1821; found: 504.1829; IR ATR (cm^{-1}): 2930, 1691, 1564, 1454, 1231, 1152, 1028.

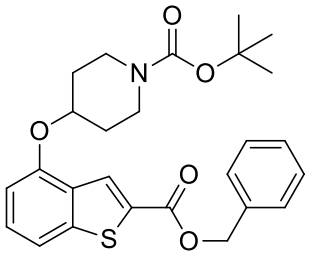

(167) *tert*-Butyl 4-((2-((benzyloxy)carbonyl)benzo[*b*]thiophen-4-yl)oxy)piperidine-1-carboxylate

35 mg, 51% yield, clear semi-solid. R_f: 0.57 (20% EtOAc, 80% hexane); ^{1}H NMR (300 MHz, CHLOROFORM-*d*) δ ppm 1.50 (s, 9 H), 1.81 – 1.93 (m, 2 H), 1.93 – 2.05 (m, 2 H), 3.38 – 3.50 (m, 2 H), 3.67 – 3.78 (m, 2 H), 4.63 – 4.73 (m, 1 H), 5.40 (s, 2 H), 6.77 (d, *J*=7.6 Hz, 1 H), 7.32 – 7.51 (m, 7 H), 8.24 (s, 1 H); ^{13}C NMR (75 MHz, CHLOROFORM-*d*) δ ppm 28.4 (3 C), 30.3 (2 C), 40.4 (2 C), 67.0, 72.4, 79.6, 106.4, 114.9, 127.7, 128.2 (3 C), 128.3, 128.6 (2 C), 130.8, 131.6, 135.7, 144.1, 153.8, 154.7, 162.6; Missing carbon signal, suspected to be merged with signal located at 128.3 ppm; HRMS-TOF MS ES+: m/z $[M+Na]^+$ calculated for $C_{26}H_{29}NO_5SNa$: 490.1664; found: 490.1663; IR ATR (cm^{-1}): 2930, 1688, 1564, 1418, 1229, 1151, 1027.

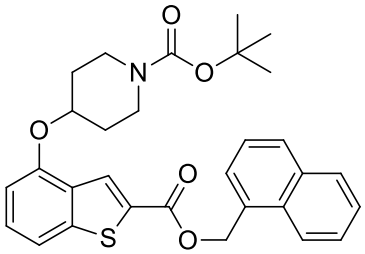

(168) *tert*-Butyl 4-((2-((naphthalen-1-ylmethoxy)carbonyl) benzo[*b*]thiophen-4-yl)oxy)piperidine-1-carboxylate

46 mg, 61% yield, clear solid. R_f: 0.65 (30% EtOAc, 70% hexane); ^{1}H NMR (300 MHz, CHLOROFORM-*d*) *δ* ppm 1.50 (s, 9 H), 1.79 – 1.91 (m, 2 H), 1.91 – 2.05 (m, 2 H), 3.37 – 3.48 (m, 2 H), 3.65 – 3.76 (m, 2 H), 4.61 – 4.70 (m, 1 H), 5.86 (s, 2 H), 6.72 – 6.78 (m, 1 H), 7.31 – 7.41 (m, 2 H), 7.47 – 7.65 (m, 3 H), 7.67 (d, *J*=6.5 Hz, 1 H), 7.87 – 7.94 (m, 2 H), 8.15 (d, *J*=8.2 Hz, 1 H), 8.22 (s, 1 H); ^{13}C NMR (75 MHz, CHLOROFORM-*d*) *δ* ppm 28.4 (3 C), 30.3 (2 C), 40.6 (2 C), 65.4, 72.4, 79.6, 106.4, 114.9, 123.5, 125.2, 126.0, 126.6, 127.5, 127.8, 128.2, 128.7, 129.4, 130.8, 131.1, 131.5, 131.6, 133.7, 144.1, 153.7, 154.7, 162.6; HRMS-TOF MS ES+: m/z $[M+Na]^+$ calculated for $C_{30}H_{31}NO_5SNa$: 540.1821; found: 540.1813;Mp: 86 – 89 °C, IR ATR (cm^{-1}): 2926, 1686, 1564, 1418, 1227, 1150, 1025.

Compounds **(169)** – **(172)** were synthesized via the same procedure. Compound **165** and the respected amine (20 equivalents) were stirred under nitrogen at 145 °C for 12 – 20 hours. The reaction was monitored via TLC using (50% EtOAc, 50% hexane) mobile phase to determine whether the starting material had been consumed. The product was purified by column chromatography over silica gel using a gradient elution (50% EtOAc, 50% hexane – 100% EtOAc)

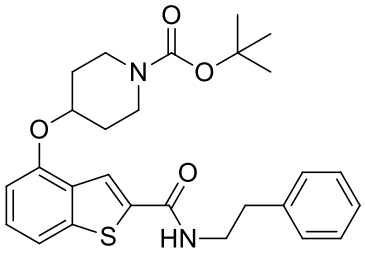

(169) *tert*-Butyl 4-((2-(phenethylcarbamoyl)benzo[*b*]thiophen-4-yl)oxy)piperidine-1-carboxylate

55 mg, 77% yield, white solid. R_f: 0.53 (35% EtOAc, 65% hexane); ^{1}H NMR (300 MHz, CHLOROFORM-*d*) *δ* ppm 1.51 (s, 9 H), 1.80–1.92 (m, 2 H), 1.92 – 2.04 (m, 2 H), 2.97 (t, *J*=7.0 Hz, 2 H), 3.40 – 3.53 (m, 2 H), 3.65 – 3.78 (m, 4 H), 4.63 – 4.72 (m, 1 H), 6.36 (t, *J*=5.9 Hz, 1 H), 6.78 (d, *J*=7.6 Hz, 1 H), 7.23 – 7.39 (m, 6 H), 7.42 (d, *J*=7.6 Hz, 1 H), 7.85 (s, 1 H); ^{13}C NMR (75 MHz, CHLOROFORM-*d*) *δ* ppm 28.4 (3 C), 30.3 (2 C), 35.7, 40.4 (2 C), 41.3, 72.1, 79.7, 106.5, 115.0, 121.6, 126.6, 127.4, 128.7 (2 C), 128.8 (2 C), 131.1, 137.1, 138.7, 142.6, 153.2, 154.8, 162.2; HRMS-TOF MS ES+: m/z $[M+Na]^+$ calculated for $C_{27}H_{32}N_2O_4SNa$: 503.1981; found: 503.1989; Mp: 75 – 78 °C, IR ATR (cm^{-1}): 3309, 2930, 1668, 1630, 1497, 1422, 1256, 1164, 1027.

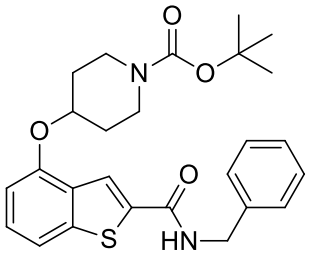

(170) *tert*-Butyl 4-((2-(benzylcarbamoyl)benzo[*b*]thiophen-4-yl)oxy)piperidine-1-carboxylate

46 mg, 67% yield, white solid. R_f: 0.45 (35% EtOAc, 65% hexane); ^{1}H NMR (300 MHz, CHLOROFORM-*d*) δ ppm 1.48 (s, 9 H), 1.78 – 1.91 (m, 2 H), 1.91 – 2.04 (m, 2 H), 3.36 – 3.47 (m, 2 H), 3.65 – 3.76 (m, 2 H), 4.65 – 4.70 (m, 3 H), 6.52 (t, *J*=5.3 Hz, 1 H), 6.77 (d, *J*=8.2 Hz, 1 H), 7.28 – 7.47 (m, 7 H), 7.92 (s, 1 H); ^{13}C NMR (75 MHz, CHLOROFORM-*d*) δ ppm 28.4 (3 C), 30.4 (2 C), 40.7 (2 C), 44.1, 72.3, 79.7, 106.4, 115.0, 121.8, 127.5, 127.7, 128.0 (2 C), 128.8 (2 C), 131.1, 136.8, 137.9, 142.7, 153.3, 154.8, 162.1; HRMS-TOF MS ES+: m/z $[M+Na]^+$ calculated for $C_{26}H_{30}N_2O_4SNa$: 489.1824; found: 489.1818; Mp: 196 – 198 °C, IR ATR (cm^{-1}): 3307, 2963, 1663, 1644, 1552, 1424, 1255, 1083, 1028.

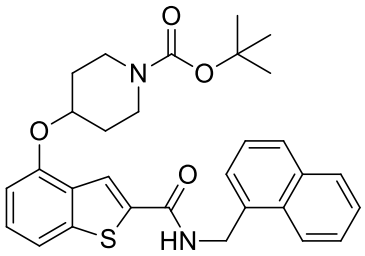

(171) *tert*-Butyl 4-((2-((naphthalen-1-ylmethyl)carbamoyl) benzo[*b*]thiophen-4-yl)oxy)piperidine-1-carboxylate

38 mg, 50% yield, yellow solid. R_f: 0.54 (35% EtOAc, 65% hexane); ^{1}H NMR (300 MHz, CHLOROFORM-*d*) δ ppm 1.47 (s, 9 H), 1.73 – 1.86 (m, 2 H), 1.86 – 2.00 (m, 2 H), 3.29 – 3.43 (m, 2 H), 3.60 – 3.75 (m, 2 H), 4.58 – 4.67 (m, 1 H), 5.11 (d, *J*=5.3 Hz, 2 H), 6.62 (t, *J*=5.3 Hz, 1 H), 6.74 (d, *J*=7.6 Hz, 1 H), 7.28 – 7.35 (m, 1 H), 7.37 – 7.49 (m, 2 H), 7.49 – 7.60 (m, 3 H), 7.82 – 7.93 (m, 3 H), 8.07 – 8.15 (m, 1 H); ^{13}C NMR (75 MHz, CHLOROFORM-*d*) δ ppm 28.4 (3 C), 30.3 (2 C), 40.6 (2 C), 42.3, 72.2, 79.6, 106.3, 114.9, 121.8, 123.5, 125.4, 126.0, 126.7, 127.0, 127.4, 128.7, 128.7, 131.0, 131.4, 133.1, 133.8, 136.8, 142.7, 153.3, 154.7, 162.0; HRMS-TOF MS ES+: m/z $[M+Na]^+$ calculated for $C_{30}H_{32}N_2O_4SNa$: 539.1981; found: 539.1992; Mp: 205 – 207 °C, IR ATR (cm^{-1}): 3316, 2936, 1664, 1638, 1551, 1435, 1276, 1161, 1025.

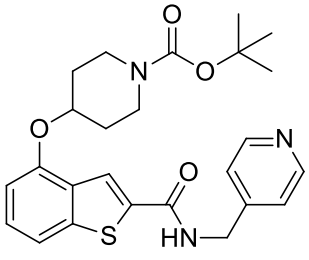

(172) *tert*-Butyl 4-((2-((pyridin-4-ylmethyl)carbamoyl) benzo[*b*]thiophen-4-yl)oxy)piperidine-1-carboxylate

58 mg, 83% yield, white solid. R_f: 0.49 (100% EtOAc); ^{1}H NMR (300 MHz, CHLOROFORM-*d*) δ ppm 1.45 (s, 9 H), 1.70 – 1.94 (m, 4 H), 3.42 (br. s., 4 H), 4.58 – 4.70 (m, 3 H), 6.72 (d, *J*=7.6 Hz, 1 H), 7.24 (d, *J*=5.9

Hz, 2 H), 7.28 – 7.34 (m, 1 H), 7.41 (d, *J*=8.2 Hz, 1 H), 8.13 (s, 1 H), 8.18 – 8.25 (m, 1 H), 8.47 (d, *J*=5.9 Hz, 2 H); ^{13}C NMR (75 MHz, CHLOROFORM-*d*) *δ* ppm 28.4 (3 C), 30.1 (2 C), 40.0 (2 C), 42.6, 71.4, 79.8, 106.2, 115.0, 122.0, 122.6 (2 C), 127.4, 131.2, 137.1, 142.9, 147.9, 149.6 (2 C), 153.2, 154.7, 162.8; HRMS-TOF MS ES+: m/z $[M+H]^+$ calculated for $C_{25}H_{30}N_3O_4S$: 468.1957; found: 468.1955; Mp: 85 – 87 °C, IR ATR (cm^{-1}): 3306, 2930, 1685, 1648, 1542, 1417, 1232, 1163, 1027.

Compounds **BT1 – BT7** were synthesized via the same procedure. In a small flask was added the Boc-protected compound **(166)** – **(172)** seperately and DCM (1 mL) followed by the addition of 4M HCl/dioxane (1 mL). The solution was stirred for one hour, after which the solvent was reduced *in vacuo*. A small amount of DCM was added followed by the addition of EtOAc which caused the salt to precipitate out of solution. The solvent was reduced *in vacuo* and the product dried under vacuum.

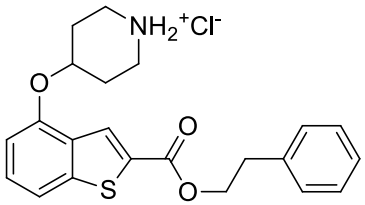

(BT1) 4-((2-(Phenethoxycarbonyl)benzo[*b*]thiophen-4-yl)oxy) piperidin-1-ium chloride

41 mg, 89% yield, white solid. ^{1}H NMR (400 MHz, DMSO-d_6) *δ* ppm 1.94 – 2.05 (m, 2 H), 2.15 – 2.26 (m, 2 H), 3.04 (t, *J*=6.8 Hz, 2 H), 3.08 – 3.16 (m, 2 H), 3.23 – 3.32 (m, 2 H), 4.50 (t, *J*=6.8 Hz, 2 H), 4.85 – 4.95 (m, 1 H), 7.08 (d, *J*=7.8 Hz, 1 H), 7.24 (dq, *J*=8.5, 4.2 Hz, 1 H), 7.31 (d, *J*=4.3 Hz, 4 H), 7.44 – 7.50 (m, 1 H), 7.61 (d, *J*=8.2 Hz, 1 H), 8.09 (s, 1 H), 9.28 (br. s., 2 H); ^{13}C NMR (101 MHz, DMSO-d_6) *δ* ppm 26.8 (2 C), 34.4, 65.8, 69.4, 107.2, 115.3, 126.5, 126.9, 128.4 (2 C), 129.0 (2 C), 129.8, 131.3, 137.8, 142.9, 153.0, 161.7; Missing carbon signal, suspected to be merged with *d*DMSO solvent signal located at 40.2 ppm; HRMS-TOF MS ES+: m/z $[M+H]^+$ calculated for $C_{22}H_{24}NO_3S$: 382.1477; found: 382.1477; Purity: 99.2%; Mp: 226 – 228 °C, IR ATR (cm^{-1}): 2938, 2712, 1705, 1584, 1456, 1234, 1062, 989.

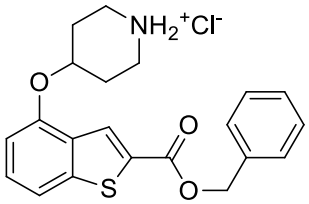

(BT2) 4-((2-((Benzyloxy)carbonyl)benzo[*b*]thiophen-4-yl)oxy) piperidin-1-ium chloride

30 mg, 98% yield, white solid. ^{1}H NMR (400 MHz, DMSO-d_6) *δ* ppm 1.92 – 2.03 (m, 2 H), 2.13 – 2.25 (m, 2 H), 3.05 – 3.16 (m, 2 H), 3.21 –

3.32 (m, 2 H), 4.87 – 4.93 (m, 1 H), 5.39 (s, 2 H), 7.08 (d, *J*=7.8 Hz, 1 H), 7.34 – 7.45 (m, 3 H), 7.45 – 7.52 (m, 3 H), 7.62 (d, *J*=8.2 Hz, 1 H), 8.18 (d, *J*=0.8 Hz, 1 H), 9.03 (br. s., 1 H), 9.24 (br. s., 1 H); ^{13}C NMR (101 MHz, DMSO-d_6) δ ppm 26.8 (2 C), 66.7, 69.4, 107.2, 115.4, 127.1, 128.1 (2 C), 128.3, 128.6 (2 C), 129.1, 129.9, 131.2, 135.7, 143.0, 153.1, 161.7; Missing carbon signal, suspected to be merged with *d*DMSO solvent signal located at 40.2 ppm; HRMS-TOF MS ES+: m/z $[M+H]^+$ calculated for $C_{21}H_{22}NO_3S$: 368.1324; found: 368.1320; Purity: >98%; Mp: 204 – 206 °C, IR ATR (cm^{-1}): 2934, 2727, 1705, 1564, 1239, 1068, 1029.

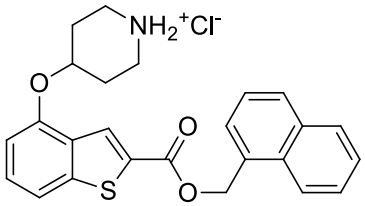

(BT3) 4-((2-((Naphthalen-1-ylmethoxy)carbonyl) benzo[*b*]thiophen-4-yl)oxy)piperidin-1-ium chloride

39 mg, 95% yield, white solid. ^{1}H NMR (400 MHz, DMSO-d_6) δ ppm 1.90 – 2.03 (m, 2 H), 2.11 – 2.23 (m, 2 H), 3.10 (br. s., 2 H), 3.25 (br. s., 2 H), 4.84 – 4.91 (m, 1 H), 5.86 (s, 2 H), 7.07 (d, *J*=8.2 Hz, 1 H), 7.44 – 7.50 (m, 1 H), 7.51 – 7.67 (m, 4 H), 7.69 (d, *J*=7.0 Hz, 1 H), 7.95 – 8.03 (m, 2 H), 8.13 – 8.20 (m, 2 H), 9.01 (br. s., 1 H), 9.23 (br. s., 1 H); ^{13}C NMR (101 MHz, DMSO-d_6) δ ppm 26.8 (2 C), 65.2, 69.4, 107.2, 115.4, 123.6, 125.4, 126.1, 126.7, 127.1, 127.5, 128.6, 129.1, 129.2, 129.8, 131.1, 131.1, 131.2, 133.3, 143.0, 153.0, 161.6; Missing carbon signal, suspected to be merged with *d*DMSO solvent signal located at 40.2 ppm; HRMS-TOF MS ES+: m/z $[M+H]^+$ calculated for $C_{25}H_{24}NO_3S$: 418.1477; found: 418.1478; Purity: >98%; Mp: 208 – 210 °C, IR ATR (cm^{-1}): 2937, 2714, 1704, 1564, 1239, 992.

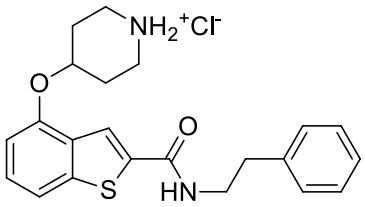

(BT4) 4-((2-(Phenethylcarbamoyl)benzo[*b*]thiophen-4-yl)oxy) piperidin-1-ium chloride

42 mg, 87% yield, yellow solid. ^{1}H NMR (400 MHz, DMSO-d_6) δ ppm 1.92 – 2.03 (m, 2 H), 2.15 – 2.26 (m, 2 H), 2.88 (t, *J*=7.6 Hz, 2 H), 3.09 – 3.18 (m, 2 H), 3.27 – 3.35 (m, 2 H), 3.45 – 3.53 (m, 2 H), 4.84 – 4.92 (m, 1 H), 7.04 (d, *J*=7.8 Hz, 1 H), 7.18 – 7.34 (m, 5 H), 7.36 – 7.42 (m, 1 H), 7.56 (d, *J*=8.2 Hz, 1 H), 8.20 (s, 1 H), 8.95 – 9.11 (m, 3 H); ^{13}C NMR (151 MHz, DMSO-d_6) δ ppm 27.0 (2 C), 35.1, 40.4 (2 C), 40.9, 69.5, 107.0, 115.2, 121.0, 126.1, 127.4, 128.3 (2 C), 128.6 (2 C), 130.7, 138.8, 139.4, 141.8, 152.5, 161.3; HRMS-TOF MS ES+: m/z $[M+H]^+$ calculated for $C_{22}H_{25}N_2O_2S$: 381.1637; found: 381.1635; Purity: 97.6%; Mp: 204 – 208 °C, IR ATR (cm^{-1}): 3261, 2925, 1619, 1547, 1463, 1253, 1032.

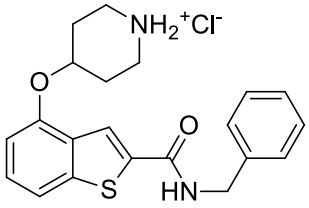

(BT5) 4-((2-(Benzylcarbamoyl)benzo[*b*]thiophen-4-yl)oxy) piperidin-1-ium chloride

35 mg, 88% yield, yellow solid. ^{1}H NMR (600 MHz, DMSO-d_6) δ ppm 1.95 – 2.02 (m, 2 H), 2.17 – 2.23 (m, 2 H), 3.12 (br. s., 2 H), 3.27 – 3.35 (m, 2 H), 4.49 (d, *J*=5.9 Hz, 2 H), 4.89 (br. s., 1 H), 7.04 (d, *J*=7.6 Hz, 1 H), 7.23 – 7.27 (m, 1 H), 7.30 – 7.37 (m, 4 H), 7.37 – 7.41 (m, 1 H), 7.56 (d, *J*=8.2 Hz, 1 H), 8.35 (s, 1 H), 9.22 (br. s., 2 H), 9.52 (t, *J*=6.2 Hz, 1 H); ^{13}C NMR (151 MHz, DMSO-d_6) δ ppm 27.0 (2 C), 40.3 (2 C), 42.6, 69.4, 107.1, 115.2, 121.4, 126.8, 127.4 (2 C), 127.5, 128.3 (2 C), 130.8, 138.6, 139.3, 141.9, 152.6, 161.4; HRMS-TOF MS ES+: m/z $[M+H]^+$ calculated for $C_{21}H_{23}N_2O_2S$: 367.1480 found: 367.1494; Purity: >98%; Mp: 217 – 219 °C, IR ATR (cm^{-1}): 3278, 2928, 1625, 1544, 1463, 1300, 1253, 993.

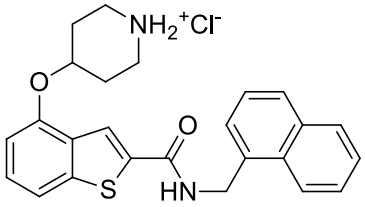

(BT6) 4-((2-((Naphthalen-1-ylmethyl)carbamoyl) benzo[*b*]thiophen-4-yl)oxy)piperidin-1-ium chloride

31 mg, 93% yield, yellow solid. ^{1}H NMR (600 MHz, DMSO-d_6) δ ppm 1.92 – 2.01 (m, 2 H), 2.15 – 2.22 (m, 2 H), 3.06 – 3.15 (m, 2 H), 3.24– 3.33 (m, 2 H), 4.84 – 4.90 (m, 1 H), 4.97 (d, *J*=5.9 Hz, 2 H), 7.04 (d, *J*=7.6 Hz, 1 H), 7.37 – 7.41 (m, 1 H), 7.47 – 7.52 (m, 1 H), 7.52 – 7.61 (m, 4 H), 7.87 (d, *J*=8.2 Hz, 1 H), 7.96 (d, *J*=8.2 Hz, 1 H), 8.21 (d, *J*=8.8 Hz, 1 H), 8.36 (s, 1 H), 9.21 (br. s., 2 H), 9.52 (t, *J*=5.9 Hz, 1 H); ^{13}C NMR (151 MHz, DMSO-d_6) δ ppm 27.0 (2 C), 40.3 (2 C), 40.8, 69.4, 107.1, 115.2, 121.5, 123.5, 125.4, 125.7, 125.8, 126.3, 127.5, 127.6, 128.5, 130.7, 130.9, 133.3, 134.3, 138.5, 141.9, 152.6, 161.4; HRMS-TOF MS ES+: m/z $[M+H]^+$ calculated for $C_{25}H_{25}N_2O_2S$: 417.1637 found: 417.1622; Purity: >98%; Mp: decomposition, IR ATR (cm^{-1}): 2930, 1638, 1552, 1464, 1298, 1257, 995.

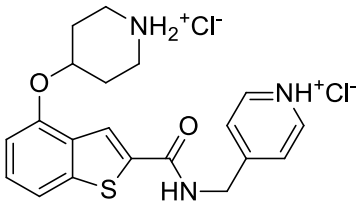

(BT7) 4-((4-(Piperidin-1-ium-4-yloxy)benzo[*b*]thiophene-2-carboxamido)methyl)pyridin-1-ium chloride

52 mg, 96% yield, yellow solid. ^{1}H NMR (600 MHz, DMSO-d_6) δ ppm 1.98 – 2.06 (m, 2 H), 2.15 – 2.24 (m, 2 H), 3.12 (br. s., 2 H), 3.31 – 3.39 (m, 2 H), 4.75 (d, *J*=5.9 Hz, 2 H), 4.89 – 4.96 (m, 1 H), 7.07 (d, *J*=8.2 Hz, 1 H), 7.37 – 7.44 (m, 1 H), 7.58 (d, *J*=8.2 Hz, 1 H), 8.00 (d, *J*=5.9 Hz, 2 H), 8.55 (s, 1 H), 8.86 (d, *J*=6.4 Hz,

2 H), 9.36 (br. s., 1 H), 9.39 (br. s., 1 H), 10.06 (t, *J*=5.9 Hz, 1 H); ^{13}C NMR (151 MHz, DMSO-d_6) δ ppm 26.9 (2 C), 40.2 (2 C), 42.2, 69.3, 107.2, 115.3, 122.5, 124.9, 127.8, 130.8, 137.5, 141.7, 142.0, 152.7, 159.4, 162.1; HRMS-TOF MS ES+: m/z $[M+H]^+$ calculated for $C_{20}H_{22}N_3O_2S$: 368.1433 found: 368.1427; Purity: >98%; Mp: 151– 154 °C, IR ATR (cm^{-1}): 3379, 2925, 1637, 1541, 1463, 1300, 1254, 993.

10.7 Crystal structure data

Data collection and refinement details:

Single crystals of diffraction quality were obtained, mounted in oil and data were collected using a Bruker SMART Apex III X-ray diffractometer equipped with a Mo fine-focus sealed tube (λ = 0.71073 Å). Data collections were performed at 298 K using an Oxford Cryostream cryostat (700 series Cryostream Plus) attached to the diffractometer. Reduction of data, adsorption corrections as well as unit cell determination was carried out using Bruker diffraction software APEXIII.[25,26] All structures were solved using SHELXS-97 and refined using SHELXL-97[27] within the X-Seed[28,29] graphical user interface. Non-hydrogen atoms were refined anisotropically and hydrogen atoms were placed on calculated positions, except those on oxygen and nitrogen atoms, which were located using electron density maps. Figures were generated using POVRay[30] within the X-Seed graphical user interface.

Table 5: Crystallographic data for **(54A)** Ethyl 4-(benzyloxy)-7-formyl-1*H*-indole-2-carboxylate

Molecular formula	$C_{76}H_{68}N_4O_{16}$
Mr/g mol^{-1}	1293.40
Temperature/K	100
Crystal system	Orthorhombic P
Space group	*Pbca*
a/ Å	13.148(1)
b/ Å	19.150(7)
c/ Å	25.118(4)
Σ/∀	90.00
T/∀	90.00
Y/∀	90.00
V / Å^3	6324.70
Z	4
µ/mm^{-1}	0.096
R_1 [I > 2′(I)]	0.0661
wR_2 (F^2)	0.1757

Table 6: Crystallographic data for **(107)** (Z)-2-((7-(Benzyloxy)-1-methyl-1*H*-benzo[*d*]imidazol -2-yl)methylene)pentanal

Molecular formula	$C_{21}H_{22}N_2O_2$
Mr/g mol^{-1}	334.42
Temperature/K	298(2)
Crystal system	Triclinic P
Space group	*P 1*
a/ Å	7.614(6)
b/ Å	10.621(3)
c/ Å	11.927(3)
Σ/∀	87.62(6)
T/∀	72.28(8)
Y/∀	84.09(1)
V / Å^3	913.98
Z	2
µ/mm^{-1}	0.08
R_1 [I > 2′(I)]	0.0813
wR_2 (F^2)	0.3010

Table 7: Crystallographic data for **(130)** Ethyl 4-hydroxybenzo[d]oxazole-2-carboxylate

Molecular formula	$2(C_{10}H_9NO_2)$
Mr/g mol^{-1}	826.74
Temperature/K	298(2)
Crystal system	Orthorhombic P
Space group	*Pnma*
a/ Å	10.087(8)
b/ Å	6.656(2)
c/ Å	14.426(8)
Σ/∀	90.00
T/∀	90.00
Y/∀	90.00
V / Å^3	968.71
Z	4
μ/mm^{-1}	0.11
R_1 [I > 2′(I)]	0.0444
wR_2 (F^2)	0.1454

10.8 Whole cell testing

The test samples were tested in triplicate on one or two separate occasions against chloroquine sensitive (CQS) strain of *Plasmodium falciparum* (NF54). Continuous *in vitro* cultures of asexual erythrocyte stages of *P. falciparum* were maintained using a modified method of Trager and Jensen (1976).[31] Quantitative assessment of antiplasmodial activity *in vitro* was determined via the parasite lactate dehydrogenase assay using a modified method described by Makler (1993). The test samples were prepared to a 20 mg/mL stock solution in 100% DMSO and sonicated to enhance solubility. Samples were tested as a suspension if not completely dissolved. Stock solutions were stored at -20 °C. Further dilutions were prepared on the day of the experiment. Chloroquine (CQ) and artesunate was used as the reference drug in all experiments. A full dose-response was performed for all compounds to determine the concentration inhibiting 50% of parasite growth (EC_{50}–value). Test samples were tested at a starting concentration of 100 μg/mL, which was then serially diluted 2-fold in complete medium to give 10 concentrations; with the lowest concentration being 0.2 μg/mL. The same dilution technique was used for all samples. The EC_{50}–values were obtained using a non-linear dose-response curve fitting analysis via Graph Pad Prism software.

10.9 Electrostatic potential energy values of each atom per heterocycle

4-OMe IM Atom Label	ESP Max IDS(A)	ESP Min IDS(A)	ESP Avg IDS(A)	ESP Avg in kcal/mol
C1	0.00023	-0.02322	-0.01466	-9.20
C2	-0.01166	-0.02166	-0.01873	-11.75
C3	0.02674	-0.02306	-0.01544	-9.69
C4	0.03410	-0.02688	-0.01354	-8.50
C5	0.01358	-0.02693	-0.01545	-9.69
C6	0.01445	-0.02631	-0.01423	-8.93
C7	-0.00994	-0.01971	-0.01556	-9.77
C8	-0.00159	-0.01914	-0.01191	-7.47
N9	0.04060	-0.01540	-0.00288	-1.81
H10	0.03686	-0.00692	0.01402	8.80
H11	0.02027	-0.00742	0.00996	6.25
H12	0.02708	-0.00459	0.01452	9.11
H13	0.05414	-0.00372	0.03437	21.57
O14	0.00341	-0.02207	-0.01367	-8.58
C15	0.02631	-0.00166	0.01508	9.46
H16	0.02408	0.00276	0.01797	11.28
H17	0.02719	-0.00202	0.01834	11.51
H18	0.02421	0.00206	0.01791	11.24
C19	0.00691	-0.01175	0.00041	0.26
O20	0.00262	-0.05275	-0.03307	-20.75
O21	0.00557	-0.02163	-0.00972	-6.10
C22	0.02095	-0.01700	0.01104	6.93
H23	0.01823	-0.02431	0.00641	4.03
H24	0.02347	-0.00080	0.01622	10.18
C25	0.02040	-0.02061	0.00333	2.09
H26	0.00657	-0.02730	-0.00103	-0.65
H27	0.02017	0.00080	0.01262	7.92
H28	0.01546	-0.00754	0.00782	4.91
C29	-0.00346	-0.01971	-0.00735	-4.61
H30	0.00720	-0.01852	-0.00159	-1.00
H31	0.00460	-0.01735	-0.00366	-2.30
H32	0.00716	-0.01771	-0.00178	-1.11
				0.00
Total	0.05414	-0.05275	-0.00001	-0.01

4-OMe IH Atom Label	ESP Max IDS(A)	ESP Min IDS(A)	ESP Avg IDS(A)	ESP Avg in kcal/mol
C1	0.00517	-0.02336	-0.01491	-9.35
C2	0.00458	-0.02079	-0.01353	-8.49
C3	0.02304	-0.02130	-0.01236	-7.75
C4	0.04354	-0.02612	-0.01221	-7.66
C5	0.01230	-0.02707	-0.01597	-10.02
C6	0.00872	-0.02716	-0.02015	-12.64
C7	0.01023	-0.01582	-0.00895	-5.61
C8	0.00495	-0.01480	-0.00629	-3.95
N9	0.04411	-0.00970	0.00286	1.80
H10	0.04173	-0.00551	0.01619	10.16
H11	0.01908	-0.00810	0.00852	5.35
H12	0.01301	-0.02025	-0.00002	-0.01
H13	0.03200	-0.00911	0.01466	9.20
H14	0.06080	0.00379	0.04108	25.78
O15	0.00618	-0.03416	-0.02146	-13.47
C16	0.02985	-0.00553	0.01449	9.09
H17	0.02935	0.00261	0.01824	11.45
H18	0.02929	0.00255	0.01805	11.32
H19	0.02599	-0.00492	0.01690	10.61
C20	0.01220	-0.00931	0.00620	3.89
O21	0.00755	-0.04941	-0.02891	-18.14
O22	0.01048	-0.01882	-0.00844	-5.29
C23	0.02436	-0.01470	0.01424	8.93
H24	0.02177	-0.02100	0.01018	6.39
H25	0.02692	0.00275	0.01967	12.34
C26	0.02392	-0.01026	0.00689	4.32
H27	0.00981	-0.02211	0.00264	1.66
H28	0.02329	0.00417	0.01559	9.78
H29	0.01896	-0.00428	0.01124	7.05
				0.00
Total	0.06080	-0.04941	0.00118	0.74

4-OMe BT Atom Label	ESP Max DS(A)	ESP Min IDS(A)	ESP Avg IDS(A)	ESP Avg in kcal/mol
C1	0.01112	-0.01355	-0.00568	-3.57
C2	-0.00701	-0.01307	-0.01086	-6.81
C3	0.00747	-0.01598	-0.01209	-7.59
C4	0.01866	-0.01865	-0.00922	-5.78
C5	0.02288	-0.01856	-0.00713	-4.47
C6	0.02247	-0.01691	-0.00489	-3.07
C7	-0.00351	-0.01484	-0.01009	-6.33
C8	0.00080	-0.01870	-0.00968	-6.08
S9	0.02143	-0.03599	-0.01397	-8.76
H10	0.02458	-0.00206	0.01481	9.29
H11	0.02674	0.00031	0.01694	10.63
H12	0.03510	0.00458	0.02310	14.49
O13	0.01113	-0.02184	-0.01110	-6.96
C14	0.03193	0.00237	0.02033	12.76
H15	0.03183	0.00963	0.02413	15.14
H16	0.03180	0.00346	0.02311	14.50
H17	0.03165	0.01034	0.02412	15.14
C18	0.00821	-0.01266	0.00179	1.12
O19	0.00231	-0.05969	-0.04082	-25.61
O20	0.00660	-0.02212	-0.01170	-7.34
C21	0.02087	-0.01580	0.01108	6.96
H22	0.01813	-0.02618	0.00602	3.78
H23	0.01778	-0.01253	0.00385	2.41
H24	0.02360	-0.00173	0.01607	10.09
C25	0.02003	-0.01593	0.00315	1.98
H26	0.00538	-0.02656	-0.00192	-1.20
H27	0.01999	0.00022	0.01230	7.72
H28	0.01559	-0.00789	0.00776	4.87
				0.00
Total	0.03510	-0.05969	0.00015	0.09

7-OMe BI Atom Label	ESP Max IDS(A)	ESP Min IDS(A)	ESP Avg IDS(A)	ESP Avg in kcal/mol
C1	0.01022	-0.01633	-0.00479	-3.01
C2	0.01146	-0.01627	-0.00531	-3.33
C3	-0.00360	-0.03536	-0.01998	-12.54
C4	0.00745	-0.03300	-0.02073	-13.01
C5	0.01685	-0.02599	-0.01447	-9.08
C6	0.01833	-0.02190	-0.00818	-5.13
N7	0.02396	-0.00157	0.00627	3.94
C8	0.02682	-0.03611	-0.00062	-0.39
N9	-0.00239	-0.08445	-0.04977	-31.23
H10	0.01115	-0.03243	-0.00326	-2.04
H11	0.02038	-0.00726	0.00983	6.17
H12	0.03371	0.00195	0.02045	12.83
O13	0.01343	-0.01123	0.00004	0.03
C14	0.03340	0.00947	0.02288	14.36
H15	0.03074	0.01138	0.02502	15.70
H16	0.03513	0.01248	0.02732	17.14
H17	0.03134	0.01136	0.02513	15.77
C18	0.02696	-0.02764	0.00982	6.16
O19	0.01170	-0.08376	-0.04671	-29.31
O20	0.02631	-0.00839	0.00563	3.53
C21	0.02716	-0.02507	0.01722	10.81
H22	0.02370	-0.02405	0.01521	9.55
C23	0.02682	0.00457	0.01696	10.64
H24	0.02569	0.00210	0.01842	11.56
H25	0.02836	0.00711	0.02225	13.96
H26	0.02421	-0.00103	0.01697	10.65
H27	0.02367	-0.02311	0.01365	8.57
H28	0.03312	0.01268	0.02524	15.84
				0.00
Total	0.03513	-0.08445	0.00079	0.49

4-OMe BO Atom Label	ESP Max IDS(A)	ESP Min IDS(A)	ESP Avg IDS(A)	ESP Avg in kcal/mol
C1	0.01222	-0.03025	-0.00400	-2.51
C2	0.01075	-0.03047	-0.00606	-3.80
C3	0.01154	-0.00927	-0.00208	-1.30
C4	0.02112	-0.01431	-0.00521	-3.27
C5	0.02562	-0.01429	-0.00402	-2.52
C6	0.02536	-0.01355	-0.00276	-1.73
N7	0.01155	-0.06463	-0.03720	-23.35
C8	0.01555	-0.01579	0.00685	4.30
O9	0.01335	-0.05333	-0.01734	-10.88
H10	0.02699	0.00038	0.01517	9.52
H11	0.02944	0.00339	0.01972	12.37
H12	0.03636	0.00658	0.02465	15.47
O13	0.01203	-0.05794	-0.02374	-14.90
C14	0.03285	-0.00575	0.01859	11.66
H15	0.03243	0.00786	0.02390	15.00
H16	0.02946	-0.00520	0.02002	12.56
H17	0.03257	0.00917	0.02392	15.01
C18	0.01774	-0.01852	0.01142	7.17
O19	0.00969	-0.05919	-0.03761	-23.60
O20	0.01325	-0.06001	-0.02169	-13.61
C21	0.02352	-0.01804	0.01236	7.75
H22	0.02076	-0.02137	0.00982	6.16
H23	0.02398	-0.00651	0.01589	9.97
C24	0.02279	-0.01332	0.00569	3.57
H25	0.00853	-0.02281	0.00170	1.07
H26	0.02244	0.00313	0.01435	9.01
H27	0.01497	-0.01009	0.00767	4.82
				0.00
Total	0.03636	-0.06463	-0.00099	-0.62

10.10 References

1. Perrin, D. D.; Armarego, W. L. F., In *Purification of Laboratory Chamicals;* 1988, 391.

2. Burchat, A. F.; Chong, J. M.; Nielsen, N. *J. Organomet. Chem.* **1997,** *542,* 281.

3. Mori, K.; Kawasaki, T.; Sueoka, S.; Akiyama, T. *Org. Lett.* **2010,** *12,* 1732.

4. Kobayashi, T.; Komatsu, T.; Kamiya, M.; Campos, C.; Gonzalez-Gaitan, M.; Terai, T.; Hanaoka, K.; Nagano, T.; Urano, Y. *J. Am. Chem. Soc.* **2012,** *134,* 11153.

5. Shi, F.; Waldo, J. P.; Chen, Y.; Larock, R. C. *Org. Lett.* **2008,** *10,* 2409.

6. Kiddle, J.; Gurley, A. *Phosphorus Sulfur Silicon Relat. Elem.* **2000,** *160,* 195.

7. Nakamura, K.; Ohmori, K.; Suzuki, K. *Chem. Commun.* **2015,** *51,* 7012.

8. Henn, L.; Hickey, D. M. B.; Moody, C. J.; Rees, C. W. *J. Chem. Soc., Perkin Trans. 1.* **1984,** 2189.

9. Sheng, C.; Xu, H.; Wang, W.; Cao, Y.; Dong, G.; Wang, S.; Che, X.; Ji, H.; Miao, Z.; Yao, J.; Zhang, W. *Eur. J. Med. Chem.* **2010,** *45,* 3531.

10. Gondo, K.; Oyamada, J.; Kitamura, T. *Org. Lett.* **2015,** *17,* 4778.

11. Yoo, S.; Lee, S.; Kim, S.; Lee, S. *Bioorg. Med. Chem.* **1997,** *5,* 445.

12. Matsumura, K.; Ono, M.; Kitada, A.; Watanabe, H.; Yoshimura, M.; Iikuni, S.; Kimura, H.; Okamoto, Y.; Ihara, M.; Saji, H. *J. Med. Chem.* **2015,** *58,* 7241.

13. Kaiser, F.; Schwink, L.; Velder, J.; Schmalz, H. G. *J. Org. Chem.* **2002,** *67,* 9248.

14. Banwell, M. G.; Jones, M. T.; Loong, D. T. J.; Lupton, D. W.; Pinkerton, D. M.; Ray, J. K.; Willis, A. C. *Tetrahedron* **2010,** *66,* 9252.

15. Wu, W.; Li, Z.; Zhou, G.; Jiang, S. *Tetrahedron Lett.* **2011,** *52,* 2488.

16. Elliott, L. D.; Berry, M.; Orr-Ewing, A. J.; Booker-Milburn, K. I. *J. Am. Chem. Soc.* **2007,** *129,* 3078.

17. Zhou, J.; Jin, J.; Zhang, Y.; Yin, Y.; Chen, X.; Xu, B. *Eur. J. Med. Chem.* **2013,** *68,* 222.

18. Gamble, A. B.; Garner, J.; Gordon, C. P.; O'Conner, S. M. J.; Keller, P. A. *Synth. Commun.* **2007,** *37,* 2777.

19. Schaffrath, R. E. *J. Chem. Educ.* **1970,** *47,* 224.

20. Cozza, G.; Gianoncelli, A.; Bonvini, P.; Zorzi, E.; Pasquale, R.; Rosolen, A.; Pinna, L. A.; Meggio, F.; Zagotto, G.; Moro, S. *ChemMedChem.* **2011,** *6,* 2273.

21. Buckman, B. O.; Nicholas, J. B.; Emayan, K.; Seiwert, S. D. *Lysophosphatidic acid receptor antagonists* **2013,** .

22. Teno, N.; Gohda, K.; Wanaka, K.; Tsuda, Y.; Akagawa, M.; Akiduki, E.; Araki, M.; Masuda, A.; Otsubo, T.; Yamashita, Y. *Bioorg. Med. Chem.* **2015,** *23,* 3696.

23. Wang, F.; Hauske, J. R. *Tetrahedron Lett.* **1997,** *38,* 6529.

24. Simonetti, S. O.; Larghi, E. L.; Kaufman, T. S. *Org. Biomol. Chem.* **2016,** *14,* 3333.

25. SMART Data Collection Software, Version 5.629; Bruker AXS Inc.: Madison, WI, **2003**.

26. SADABS Version 2.05; Bruker AXS Inc.: Madison, WI, **2002**.

27. Sheldrick, G.M., Acta Crystallogr. Sect. A: Found. Crystallogr., **2008**, *64*, 112.

28. Barbour, L.J., Supramol. Chem. **2001**, *1*, 189.

29. Atwood, J.L., Barbour, l.J., Cryst. Growth & Des., **2003**, *3*, 3.

30. POV-Ray, Version 3.6, Persistance of Vision Raytracer Pty. Ltd.: Williamstone, **2004**.

31. Trager, W.; Jensen, J. B. Science **1976**, *193*, 673.